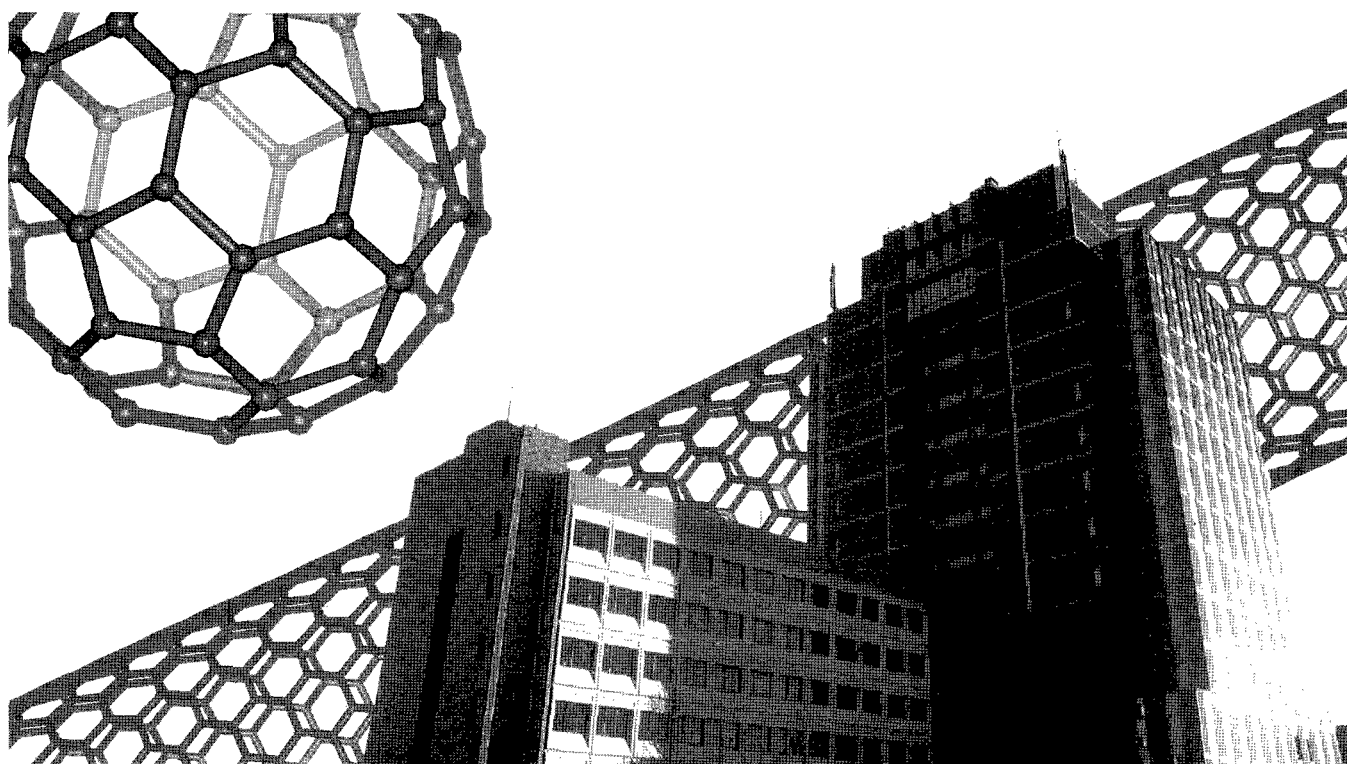


Abstract  
The 34<sup>th</sup> Fullerene-Nanotubes General Symposium

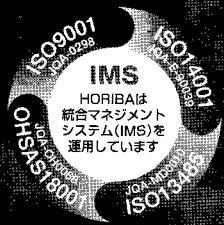
第34回フラーレン・ナノチューブ  
総合シンポジウム

講演要旨集



March 3-5, 2008 Nagoya, Aichi  
平成20年3月3日～5日 名城大学

The Fullerenes and Nanotubes Research Society  
フラーレン・ナノチューブ学会



ハイテクの一步先に、いつも。

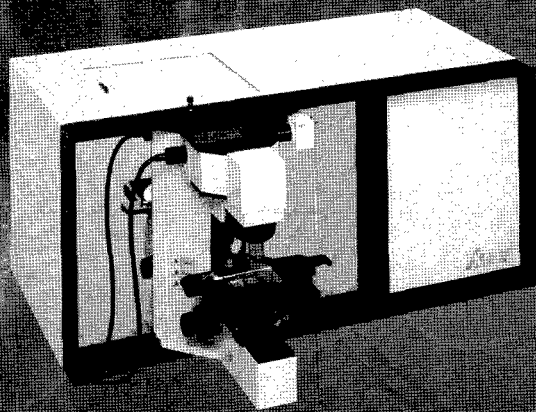
# HORIBA

Explore the future

## CNTの測定にはデファクトスタンダードの LabRamHR-800が最適

～RBM/フォトルミネッセンスを同スポットで測定～

### 顕微レーザーラマン分光測定装置 LabRamシリーズ



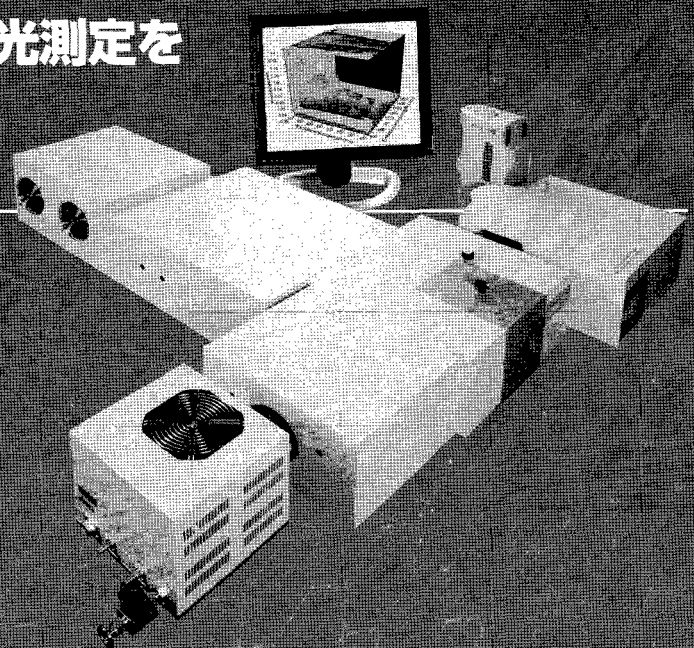
- ・244nm～1064nmのレーザーによる測定が可能
- ・焦点距離800nmの分光器により高分解能測定を実現

## SWCNTの近赤外領域の蛍光測定を 大幅にスピードアップ

～ナノテクリサーチに～

### 近赤外対応蛍光分光測定装置 SPEX NanoLogシリーズ

- ・InGaAsアレイ検出器による高感度測定
- ・高速・高分解能マトリックスマッピング
- ・モジュールユニットだからアプリケーションに  
応じた各種NIR検出器の組み合わせも可能



# HORIBA JOBIN YVON

株式会社堀場製作所

科学システム営業部 03-3861-8234

本社 〒601-8510 京都市南区吉祥院宮の東町2 TEL(075)313-8121

- 仙台(022)308-7890 ●つくば(0298)56-0521 ●東京(03)3861-8231
- 横浜(045)451-2091 ●名古屋(052)936-5781 ●大阪(06)6390-8011
- 広島(082)288-4433 ●愛媛(0897)34-8143 ●福岡(092)472-5041

製品の詳しい情報は

<http://www.jyhoriba.jp>

<http://www.horiba.co.jp> e-mail:info@horiba.co.jp

Abstract  
The 34<sup>th</sup> Fullerene-Nanotubes General Symposium

第 34 回 フラーレン・ナノチューブ  
総合シンポジウム

講演要旨集

The Fullerenes and Nanotubes Research Society

The Chemical Society of Japan

The Japan Society of Applied Physics

The Electrochemical Society of Japan

The Society of Polymer Science, Japan

主催：フラーレン・ナノチューブ学会

共催：日本化学会

協賛：応用物理学会・電気化学会・高分子学会

Date: March 3<sup>rd</sup>(Mon) – 5<sup>th</sup>(Wed), 2008

Place: Meijo University

1-501 Shiogamaguchi, Tempaku-ku, Nagoya 468-8502

TEL: 052-832-1151

Presentation: Special Lecture (25 min presentation, 5min discussion)

General Lecture (10 min presentation, 5min discussion)

Poster Preview (1 min presentation, no discussion)

日時：平成 20 年 3 月 3 日(月)～5 日(水)

場所：名城大学

〒468-8502 愛知県名古屋市中区天白区塩釜口 1-501

TEL：052-832-1151

発表時間：特別講演 (発表 25 分・質疑応答 5 分)

一般講演 (発表 10 分・質疑応答 5 分)

ポスタープレビュー (発表 1 分・質疑応答 なし)

展示団体御芳名(アイウエオ順、敬称略)

IOP英国物理学会出版局  
(株)アインテスラ  
アクセルリス(株)  
(株)アドサイエンス  
(株)アルバック  
(株)エリオニクス  
サイバネットシステム(株)  
(株)島津製作所  
ナカライテスク(株)  
日本エマソン(株)ブランソン事業本部  
日本電子(株)  
(株)堀場製作所  
(株)マイクロフェーズ  
(株)名城ナノカーボン  
(有)イーアンドティー

広告掲載団体御芳名(アイウエオ順、敬称略)

アクセルリス(株)	(財)名古屋大学出版会
(株)アドサイエンス	名古屋バルブ・フィティング(株)
(株)ATR	日本エマソン(株)ブランソン事業本部
エムエス機器(株)	日本電子(株)
(株)エリオニクス	日本分光(株)
(株)岡村製作所	日本分析工業(株)
オザワ科学(株)	(有)菱田商店
(株)サイエンスラボラトリーズ	ブルカー・ダルトニクス(株)
(株)産業タイムズ社	フロンティアカーボン(株)
(株)三洋商事	(株)フロンティア出版
三洋貿易(株)	(株)堀場製作所
シグマ アルドリッチ ジャパン(株)	(株)マシナックス
(株)島津製作所	(株)マツボー
スペクトラ・フィジックス(株)	(株)名城ナノカーボン
住友商事(株)	(株)UBE科学分析センター
(株)十合	理科研(株)
東洋炭素(株)	
東レ(株)	
ナカライテスク(株)	

## Contents

Time Table	.....	i
Chairperson	.....	iii
Program	Japanese .....	iv
	English .....	xv
Abstracts	Special lecture .....	1
	General lecture .....	9
	Poster preview .....	51
Author Index	.....	201

## 目次

早見表	.....	i
座長一覽	.....	iii
プログラム	和文 .....	iv
	英文 .....	xv
講演予稿	特別講演 .....	1
	一般講演 .....	9
	ポスター発表 .....	51
発表索引	.....	201

# プログラム早見表

各項目敬称略

	3月3日(月)	3月4日(火)	3月5日(水)	
9:00	特別講演1(岡本 稔治) 9:00~9:30	特別講演3(Dean Ho) 9:00~9:30	特別講演5(Nikos Tagmatarchis) 9:00~9:30	9:00
9:30	一般講演4件 (ナノチューブの物性) 9:30~10:30	一般講演4件 (金属内包フラーレン) 9:30~10:30	一般講演4件 (ナノチューブの生成と精製) 9:30~10:30	9:30
10:30	休憩 10:30~10:45			10:30
10:45	一般講演4件 (ナノチューブの物性) 10:45~11:45	一般講演4件 (フラーレン固体とフラーレンの化学) 10:45~11:45	特別講演6(松尾 豊) 10:45~11:15	10:45
11:15	昼食 11:45~13:00		一般講演4件 (ナノチューブの精製と応用) 11:15~12:15	11:15
12:15			昼食 12:15~13:30	12:15
13:00	特別講演2(栗野 祐二) 13:00~13:30	授賞式 13:00~13:30		
13:30	一般講演5件 (ナノチューブの物性) 13:30~14:45	特別講演4(西堀 英治) 13:30~14:00	特別講演7(田原 修一) 13:30~14:00	13:30
14:00		一般講演4件 (内包ナノチューブ・ナノホーン) 14:00~15:00	ポスタープレビュー 1分×50件 14:00~15:00	14:00
14:45	休憩 14:45~15:00			
15:00	一般講演5件 (ナノチューブの物性) 15:00~16:15	休憩 15:00~15:15	ポスターセッション 15:00~16:20	15:00
16:15		一般講演3件 (ナノ炭素科学) 15:15~16:00		16:20
16:20	ポスタープレビュー 1分×50件 16:15~17:15	ポスタープレビュー 1分×50件 16:00~17:00		
17:15	ポスターセッション 17:15~18:35	ポスターセッション 17:00~18:20		
18:35				

**3月3日(月)**  
チュートリアル 103講義室  
15:00~16:30  
講師 片浦弘道先生  
(独)産業技術総合研究所

18:30~懇親会

特別講演 発表25分 質疑5分  
一般講演 発表10分 質疑5分  
ポスタープレビュー 発表1分 質疑なし

# TIME TABLE

	Mon. Mar. 3	Tue. Mar. 4	Wed. Mar. 5	
9:00	Special Lecture(Y.Okamoto) 9:00~9:30	Special Lecture(D.Ho) 9:00~9:30	Special Leture(N.Tagmatarchis) 9:00~9:30	9:00
9:30	General Lecture[4] (Properties of Nanotubes) 9:30~10:30	General Lecture[4] (Metallofullerenes) 9:30~10:30	General Lecture[4] (Formation and Purification of Nanotubes) 9:30~10:30	9:30
10:30	Break 10:30~10:45			10:30
10:45	General Lecture[4] (Properties of Nanotubes) 10:45~11:45	General Lecture[4] (Fullerene Solids and Chemistry of Fullerenes) 10:45~11:45	Special Lecture(Y.Matsuo) 10:45~11:15	10:45
11:45	Lunch 11:45~13:00		General Lecture[4] (Purification and Applications of Nanotubes) 11:15~12:15	11:15
12:15			Lunch 12:15~13:30	
13:00	Special Lecture(Y.Awano) 13:00~13:30	Awards Ceremony 13:00~13:30		
13:30	General Lecture[5] (Properties of Nanotubes) 13:30~14:45	Special Lecture(E.Nishibori) 13:30~14:00	Special Lecture(S.Tahara) 13:30~14:00	13:30
14:00		General Lecture[4] (Endohedral Nanotubes· Nanohorns) 14:00~15:00	Poster Preview 1min × [50] 14:00~15:00	14:00
14:45	Break 14:45~15:00			
15:00	General Lecture[5] (Properties of Nanotubes) 15:00~16:15	Break 15:00~15:15	Poster Session 15:00~16:20	15:00
16:15		General Lecture[3] (Science of Nanocarbons) 15:15~16:00		
16:20	Poster Preview 1min × [50] 16:15~17:15	Poster Preview 1min × [50] 16:00~17:00		16:20
17:15	Poster Session 17:15~18:35	Poster Session 17:00~18:20		
18:35				

### 18:30~Banquet

**Mon. Mar. 3**  
**Tutorial Room103**  
**15:00~16:30**  
**Dr. Hiromichi Kataura**

Special Lectures 25min presentation, 5min discussion  
 General Lectures 10min presentation, 5min discussion  
 Poster Previews 1min presentation, No discussion

# 座長一覽

3月3日(月)

(敬称略)

	時 間	座 長
特 別 講 演(岡本)	9:00 ~ 9:30	宮本 良之
一 般 講 演	9:30 ~ 10:30	大野 雄高
一 般 講 演	10:45 ~ 11:45	坂東 俊治
特 別 講 演(栗野)	13:00 ~ 13:30	片浦 弘道
一 般 講 演	13:30 ~ 14:45	谷垣 勝己
一 般 講 演	15:00 ~ 16:15	菅井 俊樹
ポスタープレビュー	16:15 ~ 17:15	是常 隆
ポスターセッション	17:15 ~ 18:35	西出 大亮

3月4日(火)

	時 間	座 長
特 別 講 演(Ho)	9:00 ~ 9:30	大澤 映二
一 般 講 演	9:30 ~ 10:30	山本 和典
一 般 講 演	10:45 ~ 11:45	竹延 大志
特 別 講 演(西堀)	13:30 ~ 14:00	中村 新男
一 般 講 演	14:00 ~ 15:00	北浦 良
一 般 講 演	15:15 ~ 16:00	小塩 明
ポスタープレビュー	16:00 ~ 17:00	安坂 幸師
ポスターセッション	17:00 ~ 18:20	前田 優

3月5日(水)

	時 間	座 長
特 別 講 演(Tagmatarchis)	9:00 ~ 9:30	篠原 久典
一 般 講 演	9:30 ~ 10:30	稲熊 正康
特 別 講 演(松尾)	10:45 ~ 11:15	齋藤 毅
一 般 講 演	11:15 ~ 12:15	藤ヶ谷 剛彦
特 別 講 演(田原)	13:30 ~ 14:00	湯田坂 雅子
ポスタープレビュー	14:00 ~ 15:00	柳 和宏
ポスターセッション	15:00 ~ 16:20	若林 知成



3月3日(月)

特別講演 発表25分・質疑応答5分  
一般講演 発表10分・質疑応答5分  
ポスタープレビュー 発表1分・質疑応答なし

特別講演(9:00-9:30)

- 1S-1 燃料電池触媒のin silico設計  
○岡本穂治 1

一般講演(9:30-10:30)

ナノチューブの物性

- 1-1 金属ナノチューブにおけるラマンG-bandスペクトルのソフト化  
○齋藤理一郎、佐々木健一、佐藤健太郎、朴珍成 9
- 1-2 単層カーボンナノチューブの電場変調吸収スペクトル  
○岸田英夫、長澤嘉明、今村禎允、中村新男 10
- 1-3 孤立垂直配向単層カーボンナノチューブのバンドル化に伴う蛍光発光強度の増大  
○加藤俊顕、畠山力三 11
- 1-4 単一カーボンナノチューブ分光による多励起子再結合過程と励起子微細構造  
○松田一成、井上匡志、村上陽一、丸山茂夫、金光義彦 12

☆☆☆☆☆☆ 休憩 (10:30-10:45) ☆☆☆☆☆☆

一般講演(10:45-11:45)

ナノチューブの物性

- 1-5 Polyfluoreneを使って、収集された半導体SWNTの光学・電気特性  
○カザウイサイ、イザルニコラ、畠賢治、岡崎俊也、斎藤毅、佐藤雄太、末永和知、二見能資、南信次 13
- 1-6 ボロンドープカーボンナノチューブの三次元効果  
○是常隆、斎藤晋 14
- 1-7 ホウ酸・メタノール溶液から合成したホウ素ドープMWNTにおける電気伝導率の上昇  
○石井聡、渡邊徹、津田俊輔、山口尚秀、高野義彦 15
- 1-8 カーボンナノチューブ超伝導研究の最近の進展  
○春山純志、丸山茂夫、篠原久典 16

☆☆☆☆☆☆ 昼食 (11:45-13:00) ☆☆☆☆☆☆

特別講演(13:00-13:30)

- 1S-2 カーボンナノチューブのLSIビア配線応用  
○粟野祐二 2

一般講演(13:30-14:45)

ナノチューブの物性

- 1-9 金属単結晶表面上におけるカーボンナノチューブの局所電子状態  
○金有洙、Hyung-Joon Shin、Sylvain Clair、川合真紀 17
- 1-10 Ag(100)単結晶表面上におけるカーボンナノチューブのバンドギャップモジュレーション  
○シンヒョンジェン、クレアシルバイン、金有洙、川合真紀 18
- 1-11 グラフェンおよびナノチューブ上における酸素原子拡散に関する電子状態計算  
○河合孝純、宮本良之 19
- 1-12 単層カーボンナノチューブの電界電子放出特性に及ぼすエミッタモルフォロジー効果  
○白鳥洋介、古市考次、野田優、杉目恒志、辻佳子、張正宜、丸山茂夫、山口由岐夫 20
- 1-13 金属ナノチューブの非接触磁気抵抗  
○大島勇吾、鈴木宏貴、岩佐義宏、野尻浩之 21

☆☆☆☆☆☆ 休憩 (14:45-15:00) ☆☆☆☆☆☆

## 一般講演(15:00-16:15)

## ナノチューブの物性

1-14	カーボンナノチューブの熱伝導への周囲材料の影響:分子動力学シミュレーション ○塩見淳一郎、丸山茂夫	22
1-15	比表面積測定によるSWNTの純度および割合の評価 ○二葉ドン、後藤潤大、山田健郎、保田諭、湯村守雄、飯嶋澄男、畠賢治	23
1-16	カーボンナノチューブ分散阻害剤のカイラリティ依存性 ○齋藤浩、佐野正人	24
1-17	電気化学によるカーボンナノチューブの直径選択的切断方法 ○大森滋和、齋藤毅、大嶋哲、湯村守雄、飯嶋澄男	25
1-18	5-7員環の対によるカーボンナノチューブの曲げ変形 ○若生啓、小田竜樹、橋勝、小島謙一	26

## ポスタープレビュー(16:15-17:15)

## ポスターセッション(17:15-18:35)

## ナノチューブの生成と精製

1P-1	炭素透過法を用いたCNT成長 ○日方威、林和彦、水越朋之、櫻井芳昭、石神逸男、青木学聡、瀬木利夫、松尾二郎	51
1P-2	SiC表面分解法による放射状に配向したCNT粉末の合成 ○吉川和男、山本元弘、楠美智子	52
1P-3	窒素雰囲気中アーク放電法により作製した孤立分散単層カーボンナノチューブからの発光 ○水沢崇志、鈴木信三、岡崎俊也、阿知波洋次	53
1P-4	レーザーアブレーションおよびACCVDによる単層カーボンナノチューブの生成 ○児玉真一、池田篤、榊尾祐樹、村上哲史、若林知成	54
1P-5	Synthesis and Applications of Novel Vanadium Oxide Nanotubes ○Abhishek Kumar, Nikhil Dhawan	55
1P-6	高真空アルコールガスソース法により作製したカーボンナノチューブの成長時間変化 ○谷奥健次、白岩倫行、丸山隆浩、成塚重弥	56
1P-7	Patterned growth of CNTs through AFM nano-lithography ○邱建超、吉村雅満、上田一之	57
1P-8	アルコールCCVD法によるCNT合成における金属触媒粒子のカイラリティ選択性 ○鈴木祥吾、佐藤英樹、畑浩一、梶原和夫	58
1P-9	Taマスクを用いてSiC表面分解法で作製したカーボンナノチューブパターンのTEM観察 ○穂積葉子、山本陽、森みどり、丸山隆浩、成塚重弥、楠美智子	59
1P-10	金担持触媒上でのナノチューブの成長とメカニズム ○吉原直記、吾郷浩樹、辻正治	60

## その他

1P-11	一層、二層そして三層グラフェンのG'バンドラマンスペクトル ○朴珍成、Alfonso Reina Cecco、齋藤理一郎、Jing Kong、Gene Dresselhaus、and Mildred S. Dresselhaus	61
-------	---	----

## ナノチューブの応用

1P-12	Influence of Cathode-Anode Distance on Field Emission Properties for Bulky CNT Emitters ○Huarong Liu, Shigeki Kato, Yahachi Saito	62
1P-13	高配向・高密度カーボンナノチューブ膜の電気二重層キャパシタへの応用 ○加藤治夫、楠美智子、杉本重幸、杉原邦浩、柴田典義	63
1P-14	多層カーボンナノチューブの金属表面への溶接過程その場観察 ○安坂幸師、中原仁、齋藤弥八	64
1P-15	可溶化カーボンナノチューブを素材とするPET上でのハニカム構造体形成 ○若松信雄、高森久義、藤ヶ谷剛彦、中嶋直敏	65
1P-16	カーボンナノチューブへのメタン吸着の電界放出顕微鏡法による研究 ○山下徹也、安坂幸師、中原仁、齋藤弥八	66
1P-17	透明導電性カーボンナノチューブ薄膜上での骨芽細胞様細胞の培養 ○赤坂司、横山敦郎、松岡真琴、阿部薫明、宇尾基弘、佐藤義倫、田路和幸、橋本剛、亘理文夫	67

## 3月3日(月)

- 1P-18 単一カーボンナノチューブからの電界放出のその場観察透過電子顕微鏡法  
○奥村健介、安坂幸師、齋藤弥八 68
- 1P-19 ALDを用いたバイオセンサ用カーボンナノチューブFETの作成  
○中島康宏、大野雄高、岸本茂、大河内美奈、本多裕之、水谷孝 69
- 1P-20 カーボンナノチューブ電界放出エミッタの電子光学的評価  
○河野匠、安坂幸師、中原仁、齋藤弥八 70

### ナノチューブの物性

- 1P-21 Studying the Same-Handedness in Double-Walled Carbon Nanotubes Using the Dispersion-Augmented Density Functional Tight Binding Method  
○Stephan Irle, Raviprasad Krishnamurthy, Keiji Morokuma 71
- 1P-22 複合(DNA/SWCNT)薄膜の電子物性  
○丸山有成、本橋寛、田中雅之、周虎、小林昭子、緒方啓典 72
- 1P-23 グラフェンにおけるエッジ状態の超伝導  
○佐々木健一、鈴木雅裕、齋藤理一郎、大成誠一郎、田仲由喜夫 73
- 1P-24  $C_{99}N$ フラレンを内包した単層カーボンナノチューブと二層カーボンナノチューブの電気輸送特性  
○李永峰、金子俊郎、西垣昭平、畠山力三 74
- 1P-25 Embedding of Carbon Nanotubes on Silicon substrates for use in Solar Cells  
○Abhishek Kumar, Nikhil Dhawan 75
- 1P-26 12相交流アーク放電法によるシングルウォールカーボンナノチューブの合成  
○松浦次雄、近藤幸江、真木教雄、井藤有美、松本和憲、田村奈美子、平祐樹、江原遼一 76
- 1P-27 カーボンナノチューブ端の電子状態と分子動力学シミュレーション  
○坂下浩史、小田竜樹、藤間信久 77
- 1P-28 カーボンナノチューブにおける朝永ラッティンジャー液体から超伝導相への相転移の観察  
○松平将治、春山純志、村田尚義、八木優子、Erik Einarsson、丸山茂夫、菅井俊樹、篠原久典 78
- 1P-29 ナノチューブ表面の局所変形を利用したカルベン化学修飾の協同現象  
○湯村尚史、Miklos Kertesz 79

### 金属内包フラレン

- 1P-30  $Ce_2@C_{78}$ およびそのケイ素化体における内包金属原子の配向  
○山田道夫、若原孝次、土屋敬広、前田優、赤阪健、与座健治、溝呂木直美、永瀬茂 80
- 1P-31 スカンジウムカーバイド内包フラレンの $^{13}C$  NMR研究  
○山崎裕子、中嶋康二、若原孝次、土屋敬広、前田優、赤阪健、Markus Waelchli、溝呂木直美、永瀬茂 81
- 1P-32  $La@C_{82}$ とシクロペンタジエン誘導体の反応  
○佐藤悟、前田優、稲田浩司、山田道夫、土屋敬広、石塚みどり、長谷川正、赤阪健、加藤立久、溝呂木直美、永瀬茂 82
- 1P-33 STM探針からの電子注入による金属内包フラレン $Ce_2@C_{80}$ の重合反応  
○大橋一範、福井信志、赤地祐彦、赤地孝夫、梅本久、伊藤靖浩、菅井俊樹、北浦良、篠原久典 83
- 1P-34 金属内包フラレン $Sc_3N@C_{70}$ 相対安定性  
○鄭紅、徐謙、趙翔 84
- 1P-35 エルビウム金属カーバイド内包フラレン( $Er_2C_2$ ) $@C_{2n}$ の蛍光特性におけるケージサイズ依存性  
○赤地祐彦、伊藤靖浩、岡崎俊也、大野雄高、水谷孝、北浦良、菅井俊樹、篠原久典 85

### 内包ナノチューブ

- 1P-36 収差補正電子顕微鏡によるフラレンの配向決定  
○佐藤雄太、末永和知、大窪清吾、岡崎俊也、飯島澄男 86
- 1P-37 金属酸化物によるコーティングBNナノチューブの新合成法  
○Yang Huang、板東義雄、Chengchun Tang、Chunyi Zhi、寺尾剛、Dmitri Golberg 87
- 1P-38 単層カーボンナノチューブ内へのポリインの吸蔵量解析  
○村上哲史、若林知成 88
- 1P-39 in-situ X線回折法によるナノピーポッド生成反応の追跡  
○加藤祐子、北浦良、青柳忍、西堀英治、伊藤靖浩、坂田誠、篠原久典 89
- 1P-40 ナノテンプレート反応による金属ナノワイヤー内包カーボンナノチューブの創製  
○今津直樹、北浦良、小林慶太、篠原久典 90

## 3月3日(月)

- 1P-41** 高充填銅ナノワイヤー内包カーボンナノチューブ形成条件の最適化  
○小塩明、水野直樹、鬼頭大信、小海文夫 91
- 1P-42** 塩化エルビウムナノワイヤーを内包したカーボンナノチューブの合成と評価  
○小川大輔、北浦良、小林慶太、齋藤毅、大島哲、篠原久典 92
- 1P-43** カーボンナノチューブ内部での触媒金属からの単層カーボンナノチューブ生成  
○伊豆好史、塩見淳一郎、丸山茂夫 93

### ナノホーン

- 1P-44** SWNH as an Effective Delivery System for Macromolecule Anti-cancer Drugs  
○Xu Jianxun, Yudasaka Masako, Zhang Minfang, Iijima Sumio 94
- 1P-45** カーボンナノホーンの内部に閉じ込められた酸化ガドリニウム  
○弓削亮太、湯田坂雅子、市橋鋭也、宮脇仁、吉武務、飯島澄男 95
- 1P-46** ナノホーンで作製したペレットの電気抵抗率の圧縮圧力効果  
○福永雄平、原田学、坂東俊治、飯島澄男 96
- 1P-47** ZnPc-ナノホーン-蛋白質ナノハイブリッドを用いた光線力学治療のモウスモデル評価  
○張民芳、湯田坂雅子、村上達也、安嶋久美子、サンダナヤカ、伊藤攻、土田邦博、飯島澄男 97
- 1P-48** 触媒層形成法と導電性材料混合による直接メタノール型燃料電池性能への影響  
○和泉勇毅、篠原賢司、山本真伸、桶真一郎、滝川浩史、榊原敏洋、菅原秀一、青柳伸宜、大川隆、吉川和男、三浦光治、伊藤茂生、山浦辰雄 98
- 1P-49** 加熱によるナノホーンの孔の開閉  
ファンジン、○湯田坂雅子、宮脇仁、弓削亮太、河合孝純、飯島澄男 99
- 1P-50** カーボンナノホーンの静脈内投与毒性  
宮脇仁、○湯田坂雅子、張民芳、飯島澄男 100

3月4日(火)

特別講演 発表25分・質疑応答5分  
一般講演 発表10分・質疑応答5分  
ポスタープレビュー 発表1分・質疑応答なし

特別講演(9:00-9:30)

- 2S-3 Applications of Nanodiamond Hydrogels Toward Biology and Medicine  
Houjin Huang, Erik Pierstorff, Eiji Osawa, and Dean Ho 3

一般講演(9:30-10:30)

金属内包フラーレン

- 2-1 アルカンチオール自己組織化単分子膜上のLu@C<sub>82</sub>におけるトンネル分光マッピング  
○安武裕輔、河野馨士朗、小林昇洋、岩本全央、梅本久、伊藤靖浩、沖本治哉、篠原久典、真島豊 27
- 2-2 Lu内包フラーレンにおける電荷移動量の推定  
○宮崎隆文、隅井良平、梅本久、沖本治哉、菅井俊樹、篠原久典、日野照純 28
- 2-3 Pr<sub>2</sub>@C<sub>80</sub>とLaPr@C<sub>80</sub>の<sup>13</sup>C NMRの研究  
○伊藤学、長岡志保、兒玉健、三宅洋子、鈴木信三、菊地耕一、阿知波洋次 29
- 2-4 金属カーバイド内包フラーレンSc<sub>2</sub>C<sub>2</sub>@C<sub>82</sub>(C<sub>2v</sub>)の構造  
○中嶋康二、山崎裕子、若原孝次、土屋敬広、前田優、赤阪健、Markus Waelchli、与座健治、溝呂木直美、永瀬茂 30

☆☆☆☆☆☆ 休憩 (10:30-10:45) ☆☆☆☆☆☆

一般講演(10:45-11:45)

フラーレン固体とフラーレンの化学

- 2-5 フラーレン成長における原子状炭素挿入反応の発見  
○尾形照彦、三重野哲、紫尾雄岳、豊谷仁男 31
- 2-6 Chemical modification on a non-IPR metallofullerene: La<sub>2</sub>@C<sub>72</sub>  
○Xing Lu、二川秀史、土屋敬広、前田優、赤阪健、溝呂木直美、永瀬茂 32
- 2-7 水素分子内包C<sub>60</sub>の物理物性  
○谷垣勝己、良知健、熊代良太郎、村田靖次郎、小松紘一、垣内徹、澤博、小濱芳允、泉澤徹、阿竹徹 33
- 2-8 二次元C<sub>60</sub>ポリマーの圧力誘起構造相転移  
○山上雄一郎、斎藤晋 34

☆☆☆☆☆☆ 昼食 (11:45-13:00) ☆☆☆☆☆☆

☆☆☆☆☆☆ 授賞式 (13:00-13:30) ☆☆☆☆☆☆

特別講演(13:30-14:00)

- 2S-4 放射光粉末回折データの系統的解析に基づく金属内包フラーレンの構造  
○西堀英治 4

一般講演(14:00-15:00)

内包ナノチューブ・ナノホーン

- 2-9 ナノメートルサイズの空孔を通過する単一炭化水素鎖の画像化  
○田中隆嗣、越野雅至、ソリン・ニクラス、磯部寛之、中村栄一 35
- 2-10 Pd内包カーボンナノチューブの合成とプローブ顕微鏡探針への応用  
○坂本友和、邱建超、田仲圭、吉村雅満、上田一之 36
- 2-11 共鳴ラマンおよび光学発光分光によるポリイン分子の電子構造  
○若林知成 37
- 2-12 アミノ基で連結したカーボンナノホーンとポルフィリンの光誘起電荷分離過程  
○伊藤攻、アツラ サンダナヤカ、荒木保幸、田中隆嗣、磯部寛之、中村栄一、湯田坂雅子、飯島澄男 38

☆☆☆☆☆☆ 休憩 (15:00-15:15) ☆☆☆☆☆☆

3月4日(火)

一般講演(15:15-16:00)

ナノ炭素科学

- 2-13 グラフェンナノリボンのノンコリニア磁気相図  
○澤田啓介、石井史之、斎藤峯雄、岡田晋、河合孝純 39
- 2-14 フラーレン煤の熱処理とランタンカーバイドを内包した多重カーボンナノカプセルの生成  
○山本和典、若原孝次、赤阪健 40
- 2-15 単分散一桁ナノダイヤモンドを結晶成長核とするCVDダイヤモンド薄膜(1)種付け手法の予備検討  
○稲葉智雄、多羅尾隆、川部雅章、Oliver A. Williams、大澤映二 41

ポスタープレビュー(16:00-17:00)

ポスターセッション(17:00-18:20)

ナノチューブの生成と精製

- 2P-1 高真空中アルコールガスソース法による単層カーボンナノチューブ成長への酸化アルミニウムバッファ層の影響  
○白岩倫行、沼尾茂悟、大石修、西信之、丸山隆浩、成塚重弥 101
- 2P-2 金属触媒を担持したゼオライトを用いて合成した単層カーボンナノチューブの分散と分離  
○橋本正博、前田優、長谷川正、神田信、土屋敏広、若原孝次、赤阪健、宮内雄平、丸山茂夫、Jing Lu、永瀬茂 102
- 2P-3 密度勾配遠心分離法において金属・半導体カーボンナノチューブに付着した界面活性剤・密度勾配剤の除去法  
○柳和宏、宮田耕充、佐藤雄太、劉崢、末永和知、石田敬雄、片浦弘道 103
- 2P-4 テレセントリック光学システムを用いた垂直配向CNTフォレストの成長の制御と評価  
○保田諭、二葉ドン、湯村守雄、飯島澄男、畠賢治 104
- 2P-5 FT-IRによるアルコールCVDのガス分析  
○島津智寛、鈴木義信、大島久純、丸山茂夫 105
- 2P-6 MgO基板上への2層および3層カーボンナノチューブの成長  
○内藤亮治、村上俊也、長谷部祐樹、木曾田賢治、西尾弘司、一色俊之、播磨弘 106
- 2P-7 両親媒性オリゴペプチドを利用したカーボンナノチューブの精製  
○増原真也、山本淳、三浦陽介、前田寧、小野慎 107
- 2P-8 Toward Single Structure of SWNTs: Simultaneous Enrichment in (n,m) and the Optical Purity of SWNTs through Extraction with Carbazole-Bridged Chiral Diporphyrin Nanotweezers  
○Xiaobin Peng、Naoki Komatsu、Takahide Kimura、Atsuhiko Osuka 108
- 2P-9 ACCVD法での白金触媒を使った細い直径を持つSWNTs生成に及ぼす炭素供給量の影響  
○浦田圭輔、鈴木信三、長澤浩、阿知波洋次 109
- 2P-10 レーザ蒸発法による選択的金属単層カーボンナノチューブの合成  
○鶴岡泰広、阿知波洋次 110
- 2P-11 アーク放電法によるSWCNT薄膜の作製  
○李振華、汪華鋒、井上栄、安藤義則 111

ナノチューブの応用

- 2P-12 Nitrogen and oxygen plasma functionalization of carbon nanotubes for photovoltaic device application  
○Golap Kalita、Sudip Adhikari、Hare Ram Aryal、Rakesh Afre、Tetsuo Soga、Maheshwar Sharon、Masayoshi Umeno 112
- 2P-13 アルカリハロゲンプラズマイオン照射によるナノpn接合ダイオードの形成  
○宍戸淳、加藤俊顕、大原渡、畠山力三、田路和幸 113
- 2P-14 カーボンナノチューブ・UV硬化性樹脂複合体の特性とナノインプリントによるパターンニング  
○藤ヶ谷剛彦、福丸貴弘、中嶋直敏 114
- 2P-15 開口処理による単層カーボンナノチューブの比表面積の増加と電気化学キャパシタンスの改善  
○イザディナジャファバディアリ、畠賢治、平岡樹、山田健郎、二葉ドン、保田諭、棚池修、羽鳥浩章、湯村守雄、飯島澄男 115
- 2P-16 SWCNTとフラーレンから作成した光起電力セル  
○倉本竜典、新井徹、信國真吾、下手義和、森口哲次 116
- 2P-17 片持ち梁ナノチューブの高感度な光学的振動検出  
○深見瞬、秋田成司 117
- 2P-18 Density increase of well-dispersed single-walled carbon nanotubes by laser trapping  
○Thomas Rodgers、Satoru Shoji、Satoshi Kawata 118
- 2P-19 カーボンナノチューブに吸着した耐熱性タンパク質へのマイクロ波の影響  
○堀口拓一、佐野正人 119

## 3月4日(火)

- 2P-20 CNT-FETバイオセンサー感度の絶縁膜厚依存性  
○阿部益宏、村田克之、安宅龍明、松本和彦 120
- 2P-21 表面修飾したSWCNTsのFET特性  
○熊代良太郎、小松直也、齋藤達也、赤阪健、前田優、小林長夫、谷垣勝己 121

### ナノチューブの物性

- 2P-22 グラフェンアドアトムとその集合体の原子構造  
○橋知史、斎藤峯雄 122
- 2P-23 単層カーボンナノチューブの励起子における環境効果  
○佐藤健太郎、齋藤理一郎、Jie Jiang、Gene Dresselhaus、Mildred S. Dresselhaus 123
- 2P-24 ポリフルオレンで選択的に孤立分散した半導体カーボンナノチューブのドーピング過程と吸収・発光スペクトル変化  
○南信次、二見能資、カザウイ・サイ 124
- 2P-25 走査型ゲート顕微鏡を用いたカーボンナノチューブ電界効果型トランジスタの振動ゲートに対する応答  
○畑晃輔、中山善萬、秋田成司 125
- 2P-26 単層カーボンナノチューブにおける3次非線形光学応答と位相緩和時間  
○市田正夫、清原由美江、齋藤伸吾、宮田耕充、片浦弘道、安藤弘明 126
- 2P-27 マルチバッキングゲートのカーボンナノチューブ2重接合型量子ドットの制御  
○水野智行、牧英之、鈴木哲、小林慶裕、佐藤徹哉 127
- 2P-28 Siナノチューブの物質設計:新しい多層ナノチューブ  
○岡田晋 128
- 2P-29 多層カーボンナノチューブのラマンスペクトルに及ぼす直径の影響  
○二井裕之、住山芳行、中川浜三、國重敦弘 129
- 2P-30 金属および半導体単層カーボンナノチューブの共鳴ラマン分光  
○宮田耕充、柳和宏、真庭豊、片浦弘道 130

### 金属内包フラーレン

- 2P-31 フェニルクロロジアジリンを用いたLa@C<sub>82</sub>とLa<sub>2</sub>@C<sub>80</sub>の化学修飾  
○榎春香、石塚みどり、土屋敬広、赤阪健、Zdenek Slanina、Michael T. H. Liu、溝呂木直美、永瀬茂 131
- 2P-32 フラーレンへのナイトレンの環状付加と分子内転位  
○岡田光了、仲程司、森田弘之、吉村敏章、石塚みどり、土屋敬広、前田優、藤原尚、赤阪健、Xingfa Gao、永瀬茂 132
- 2P-33 Li内包[60]フラーレンのHPLC精製  
○酒井健、岡田洋史、山下冬子、表研次、笠間泰彦、横尾邦義、小野昭一、飛田博実、畠山力三、都田昌之 133
- 2P-34 内包されたSc<sub>2</sub>C<sub>2</sub>部位を導線構造としたSc<sub>2</sub>C<sub>2</sub>@C<sub>84</sub>の電気伝導特性。第一原理計算による解析  
○白井信志、井上鑑孝 134
- 2P-35 N@C<sub>60</sub>の光物性  
○二川秀史、松永洋一郎、赤阪健、加藤立久、荒木保幸、伊藤攻、阿多誠文、Klaus-Peter Dinse 135
- 2P-36 窒素原子内包フラーレンの高純度合成  
○西垣昭平、金子俊郎、畠山力三 136

### 炭素ナノ粒子

- 2P-37 多価イオンを利用した、原子1層グラフェンの同定  
○宮本良之、Hong Zhang 137
- 2P-38 炭化フェリチン作製における処理温度の影響  
富永昌人、○宮原勝也、中尾航大、谷口功 138
- 2P-39 塩素末端ポリイン:生成およびキャラクタリゼーション  
○和田資子、若林知成 139
- 2P-40 ポリインのラマンスペクトルにおける共鳴効果  
○阿弥曜平、若林知成 140
- 2P-41 アセトニトリル中におけるグラファイトのレーザーアブレーションにより生成するシアノポリイン  
○長谷場誉樹、榎原良彦、若林知成 141
- 2P-42 液体窒素中におけるグラファイトのレーザーアブレーションにより生成するジシアノポリイン  
○榎原良彦、長谷場誉樹、若林知成 142

## 3月4日(火)

### フラーレンの化学

- 2P-43** フレロイドおよびメタノフラーレンと各種ジエンとのDiels-Alder反応における速度論的研究  
○周参見恭範、北村啓、小久保研、大島巧 143
- 2P-44**  $\beta$ -カロテン退色法を用いる水溶性フラーレン誘導体と天然抗酸化物の抗酸化能評価  
○都賀谷京子、後藤忠示、小久保研、青島央江、大島巧 144
- 2P-45** ITO電極上における[70]フラーレン誘導体の光電気化学特性  
○一木孝彦、松尾豊、中村栄一 145
- 2P-46** フラーレンコバルトジチオレン錯体の合成と物性  
○丸山優史、松尾豊、中村栄一 146
- 2P-47** フラーレンと芳香族化合物のヒドロアリール化と続くFriedel-Craftsアセチル化反応  
○遠近真矢、薛維依、加藤万依、小久保研、大島巧 147
- 2P-48** フラーレン二重膜ベシクルの表面化学修飾と水透過性の制御  
○本間達也、原野幸治、磯部寛之、中村栄一 148
- 2P-49** フラーレン水溶液の一重項酸素発生効率と光照射による細胞毒性  
○飯泉陽子、岡崎俊也、張民芳、湯田坂雅子、飯島澄男 149
- 2P-50** 銅触媒下でのHuisgen付加環化反応を用いたフラーレン-糖複合体の合成  
○張家銘、ソリンニクラス、ウェルツダニエル、磯部寛之、シーバーガーピーター、中村栄一 150



3月5日(水)

特別講演 発表25分・質疑応答5分  
一般講演 発表10分・質疑応答5分  
ポスタープレビュー 発表1分・質疑応答なし

特別講演(9:00-9:30)

- 3S-5 Chemical Modification of Carbon Nanohorns  
○Nikos Tagmatarchis 5

一般講演(9:30-10:30)

ナノチューブの生成と精製

- 3-1 きわめて細い直径をもつ単層カーボンナノチューブの共鳴ラマン  
○阿知波洋次、鶴岡泰広、浦田圭輔 42
- 3-2 金触媒における炭素材料の成長機構  
○高木大輔、小林慶裕、日比野浩樹、鈴木哲、本間芳和 43
- 3-3 ACCVDによる垂直配向SWNT合成のアセチレンを用いた増進  
○項榮、大川潤、張正宜、Erik Einarsson、宮内雄平、村上陽一、丸山茂夫 44
- 3-4 新規炭素構造体の発見:自己組織的に形成された多層グラフェンと配向ナノチューブの複合構造  
○近藤大雄、佐藤信太郎、川端章夫、栗野祐二 45

☆☆☆☆☆☆ 休憩 (10:30-10:45) ☆☆☆☆☆☆

特別講演(10:45-11:15)

- 3S-6 フラーレン金属錯体の電子的・光電気化学的機能  
○松尾豊 6

一般講演(11:15-12:15)

ナノチューブの精製と応用

- 3-5 酸化における2層カーボンナノチューブの安定性  
○吉田宏道、菅井俊樹、篠原久典 46
- 3-6 ゲル電気泳動による単層カーボンナノチューブの金属・半導体分離  
○田中文字、金赫華、宮田耕充、片浦弘道 47
- 3-7 カーボンナノチューブ-polybenzimidazole複合体の新機能開発  
○岡本稔、藤ヶ谷剛彦、中嶋直敏 48
- 3-8 化学機械研磨により内層を利用した低温成長CNTビアの抵抗値の低減  
○石丸研太郎、横山大輔、岩崎孝之、佐藤信太郎、百島孝、二瓶瑞久、栗野祐二、川原田洋 49

☆☆☆☆☆☆ 昼食 (12:15-13:30) ☆☆☆☆☆☆

特別講演(13:30-14:00)

- 3S-7 NECのナノテクノロジー研究への取り組み  
○田原修一 7

ポスタープレビュー(14:00-15:00)

ポスターセッション(15:00-16:20)

ナノチューブの生成と精製

- 3P-1 低圧力気相化学成長法による単層カーボンナノチューブの低温度成長特性  
○吉田寛、浅倉理啓、渡部秀、塩川高雄、石橋幸治 151
- 3P-2 単層カーボンナノチューブの長い成長持続時間に有効な触媒径  
○内田貴司、酒井裕司、山崎明、小林慶裕 152
- 3P-3 反射高速電子回折によるカーボンナノチューブの化学気相成長過程の研究  
○永津秀俊、安坂幸師、中原仁、齋藤弥八 153
- 3P-4 デイップコートした(Fe,Co)Mo触媒によるカーボンナノチューブの化学気相成長  
○石塚大祐、柳井貴幸、奥山博基、内田勝美、岩田展幸、矢島博文、山本寛 154

## 3月5日(水)

3P-5	密度勾配超遠心法による二層カーボンナノチューブの分離 ○伊奈真吾、柳和宏、宮田耕充、真庭豊、片浦弘道	155
3P-6	垂直配向単層カーボンナノチューブ高速成長のその場観察及び速度解析 ○長谷川馨、野田優、丸山茂夫、山口由岐夫	156
3P-7	カーボンナノチューブ高速成長の鍵:エチレンの気相熱分解 ○伊藤龍平、野田優、大沢利男、丸山茂夫、山口由岐夫	157
3P-8	両親媒性オリゴペプチドのカーボンナノチューブとの相互作用 ○小野慎、山本淳、増原真也、三浦陽介、前田寧、日高貴志夫、宮本博光	158
3P-9	高密度触媒微粒子による垂直長尺カーボンナノチューブ成長 ○加藤良吾、真木翼、岩崎孝之、川原田洋	159
3P-10	ディップコートした(Fe,Co)Pt触媒によるカーボンナノチューブの化学気相成長 ○園村拓也、石塚大祐、奥山博基、岩田展幸、山本寛	160
3P-11	ACCV法による垂直配向カーボンナノチューブ合成におけるエタノール流量の影響 ○大川潤、シャンロン、丸山茂夫	161
3P-12	界面処理をしたゼオライトを用いた触媒担持化学的気相成長法による極めて細い単層カーボンナノチューブの成長 ○小林慶太、北浦良、篠原久典	162

### ナノチューブの応用

3P-13	カーボンナノチューブ量子ドットのテラヘルツ量子応答 ○豊川聖子、布施智子、河野行雄、山口智弘、石橋幸治	163
3P-14	耐熱性キチナーゼによる単層カーボンナノチューブの分散 ○田中丈士、朴恵卿、金赫華、今中忠行、片浦弘道	164
3P-15	GaAs/AlGaAs2次元電子ガス基板上に作製したカーボンナノチューブ単電子トランジスタ ○巻幡光俊、森貴洋、山口智弘、青柳克信、石橋幸治	165
3P-16	酸性化に基づく単層カーボンナノチューブの酸化に対するカルボキシメチルセルロース被覆の抑制効果 ○石井亨、内田勝美、石井忠浩、矢島博文	166
3P-17	光学顕微鏡下におけるマイクロ流体チップ内でのカーボンナノチューブの操作と観察 ○猪股直生、山西陽子、新井史人	167
3P-18	二層カーボンナノチューブの精製と物理化学的特性に関する研究 ○前田範子、内田勝美、石井忠浩、矢島博文	168
3P-19	ランダムネットワークSWNT-FETにおける中性Arビーム照射の効果 ○佐藤俊介、森貴洋、大村一夫、石橋幸治	169
3P-20	負電荷を付加したカーボンナノチューブにおけるイオン透過機構の理論的解析 ○炭竈享司、齊藤真司、大峰巖	170

### ナノチューブの物性

3P-21	SWNTの低エネルギー照射損傷の回復過程 ○山谷憲司、鈴木哲、本間芳和、小林慶裕	171
3P-22	FH-arc放電法によるSWNTsの合成およびラマン分光評価 ○陳ベイベイ、井上栄、橋本剛、安藤義則	172
3P-23	単層カーボンナノチューブを介した長距離電子伝達系 ○斎藤毅、松浦宏治、大嶋哲、大森滋和、湯村守雄、飯島澄男	173
3P-24	SEM画像による多層カーボンナノチューブの直径評価 ○川元亨、中川浜三、村中隆、國重敦弘、住山芳行	174
3P-25	高フォトンフルーエンスにおけるカーボンナノチューブからの蛍光飽和挙動:モット濃度近傍での励起子消滅 ○村上陽一、河野淳一郎	175
3P-26	カーボン13ナノチューブの成長と評価 ○山崎信之、橋場亮、大家学、落合勇一、山口智弘、石橋幸治	176
3P-27	垂直配向カーボンナノチューブの偏光ラマン分光 ○張正宜、宮内雄平、エリック エイナルソン、丸山茂夫	177
3P-28	分子動力学法による単層カーボンナノチューブにおけるフォノン緩和 ○西村峰鷹、塩見淳一郎、丸山茂夫	178
3P-29	原子間力顕微鏡によるパリスティック伝導時のSWNT表面電位評価 ○宮戸祐治、小林圭、松重和美、山田啓文	179

## 3月5日(水)

3P-30	ナノビーボッドから作製した2層カーボンナノチューブのラマン散乱:発光スペクトルとの比較 ○鄭淳吉、岡崎俊也、岸直希、中西毅、坂東俊治、Zujin Shi、飯島澄男	180
<b>その他</b>		
3P-31	カーボンナノチューブ合成基板表面上での細胞挙動 富永昌人、○永石祥一朗、吉坂菜希紗、熊谷エツ子、原田信志、谷口功	181
3P-32	SiC表面分解法による廃棄物SiC粉末からのCNT粉末の合成 ○森下敬之、市川明博、山本元弘、笹井亮、楠美智子	182
3P-33	リチウムイオン二次電池負極材としてのカーボンナノウォール ○北田典央、吉村博史、棚池修、小林健一、小島謙一、橘勝	183
3P-34	膨潤化による薄層グラファイトの作製 ○平郡論、木全希、小林本忠	184
3P-35	扁平化カーボンナノコイルとフィールドエミッタへの応用 ○篠原雄一郎、細川雄治、横田真志、桶真一郎、滝川浩史、藤村洋平、山浦辰雄、伊藤茂生、三浦光治、吉川和男、伊奈孝、岡田文男	185
3P-36	チタン電極に接合した電界下グラフェン薄膜の第一原理電子状態計算 ○大淵真理、伊藤正勝	186
3P-37	カーボンナノチューブと籠状炭素から成る多孔質炭素の合成 ○坂本雄司、猪俣克也、大竹芳信	187
3P-38	フラーレンおよびフラーレン誘導体の抗菌活性 ○青島央江、小久保研、白川翔吾、伊藤雅之、山名修一、大島巧	188
<b>フラーレン生成・高次フラーレン</b>		
3P-39	アステロイド衝突の爆発反応による炭素クラスター合成(モデル実験) ○三重野哲、長谷川直	189
3P-40	原子空孔を持つフラーレンのエネルギー論と電子状態 ○岡田晋	190
<b>フラーレン固体</b>		
3P-41	電子デバイス用C <sub>60</sub> 薄膜のモルフォロジー ○相模寛之、大泉春菜、才田守彦、表研次、溝渕裕三、笠間泰彦、横尾邦義、小野昭一、大東弘二、古賀啓子、古川猛夫	191
3P-42	ヘリウムをインターカレートしたC <sub>60</sub> 固体の高圧下の構造 ○川崎晋司、原武司、金森祐輔、岩田篤志	192
3P-43	C <sub>60</sub> を分散させたポラスカーボンの電気二重層キャパシタ容量 ○森俊介、川下雄大、川崎晋司	193
3P-44	光・電子線照射C <sub>60</sub> の電気伝導特性 ○千葉康人、都司一、上野岬、青木伸之、尾上順、落合勇一	194
3P-45	水素化によるフラーレン材料のホール輸送特性の改良:C <sub>60</sub> H <sub>4</sub> に関する理論的研究 ○徳永健、川畑弘、松重和美	195
3P-46	可溶性n型半導体C60MC12を用いた有機TFTの作製評価 ○坂口幸一、近松真之、板倉篤志、吉田郵司、阿澄玲子、八瀬清志	196
3P-47	可溶性C <sub>60</sub> 誘導体を用いた高性能n型有機薄膜トランジスタ ○近松真之、板倉篤志、坂口幸一、吉田郵司、阿澄玲子、八瀬清志	197
3P-48	GPaオーダーで圧縮したC <sub>60</sub> 圧粉体への自由電子レーザー照射効果 ○岩田展幸、安藤慎悟、野苺家亮、飯尾靖也、山本寛	198
3P-49	溶液中でのC <sub>60</sub> 結晶成長とC <sub>60</sub> 圧粉体への自由電子レーザー照射効果 ○飯尾靖也、安藤慎悟、野苺家亮、岩田展幸、山本寛	199
3P-50	超伝導相ナトリウム添加フラーレン化合物Na <sub>x</sub> C <sub>60</sub> の磁氣的性質 ○木全希、平郡論、小林本忠	200

March 3rd, Monday

**Special lecture : 25 min (Presentation) + 5 min (discussion)**  
**General lecture : 10 min (Presentation) + 5 min (discussion)**  
**Poster preview : 1 min (Presentation), no discussion**

**Special lecture (9 : 00-9 : 30)**

- 1S-1 In silico catalyst design for fuel cells  
○Yasuharu Okamoto 1

**General lecture (9 : 30-10 : 30)**

**Properties of Nanotubes**

- 1-1 Phonon softening effect on Raman G-band spectra of metallic single wall carbon nanotubes  
○Riichiro Saito, Ken'ichi Sasaki, Kentaro Sato, Jin Sung Park 9
- 1-2 Electroabsorption spectroscopy in single wall carbon nanotubes  
○Hideo Kishida, Yoshiaki Nagasawa, Sadanobu Imamura, Arao Nakamura 10
- 1-3 Photoluminescence brightening through the direct transition from isolated to bundled freestanding single-walled carbon nanotubes  
○Toshiaki Kato, Rikizo Hatakeyama 11
- 1-4 Multiexciton recombinations and exciton fine structures studied by a single carbon nanotube photoluminescence spectroscopy  
○Kazunari Matsuda, Tadashi Inoue, Yoichi Murakami, Shigeo Maruyama, and Yoshihiko Kanemitsu 12

☆☆☆☆☆☆ Coffee Break (10 : 30-10 : 45) ☆☆☆☆☆☆

**General lecture (10 : 45-11 : 45)**

**Properties of Nanotubes**

- 1-5 Optical and electrical properties of semiconducting SWNT extracted using polyfluorene  
○S. Kazaoui, N. Izard, K. Hata, T. Okazaki, T. Saito, Y. Sato, K. Suenaga, Y. Futami, N. Minami 13
- 1-6 Three dimensional effects in the boron-doped carbon nanotubes  
○Takashi Koretsune, Susumu Saito 14
- 1-7 Conductivity Enhancement of Boron-Doped MWNTs Synthesized from Methanol Solution Containing Boric Acid  
○Satoshi Ishii, Tohru Watanabe, Shunsuke Tsuda, Takahide Yamaguchi, Yoshihiko Takano 15
- 1-8 Recent progress of study of carbon-nanotube superconductivity  
○Junji Haruyama, Shigeo Maruyama, Hisanori Shinohara 16

☆☆☆☆☆☆ Lunch Time (11 : 45-13 : 00) ☆☆☆☆☆☆

**Special lecture (13 : 00-13 : 30)**

- 1S-2 Carbon nanotube LSI via interconnects  
○Yuji Awano 2

**General lecture (13 : 30-14 : 45)**

**Properties of Nanotubes**

- 1-9 Local electronic structure of a carbon nanotube on metal surface  
○Yousoo Kim, Hyung-Joon Shin, Sylvain Clair, Maki Kawai 17
- 1-10 Long-ranged bandgap modulation of SWCNT on Ag (100)  
○Hyung-Joon Shin, Sylvain Clair, Yousoo Kim, Maki Kawai 18
- 1-11 First Principles Calculations for Electronic Properties of Diffusing Oxygen Atoms on the Surface of Graphene and Nanotubes  
○Takazumi Kawai, Yoshiyuki Miyamoto 19
- 1-12 Field Emission Properties of Single-Walled Carbon Nanotubes with a Variety of Emitter-Morphologies  
○Yosuke Shiratori, Koji Furuichi, Suguru Noda, Hisashi Sugime, Yoshiko Tsuji, Zhengyi Zhang, Shigeo Maruyama, Yukio Yamaguchi 20
- 1-13 Magnetoresistance of the Metallic Nanotubes observed by Contactless Method  
○Yugo Oshima, Hirota Suzuki, Yoshihiro Iwasa, Hiroyuki Nojiri 21

March 3rd, Monday

☆☆☆☆☆☆ Coffee Break (14 : 45-15 : 00) ☆☆☆☆☆☆

**General lecture (15 : 00-16 : 15)**

**Properties of Nanotubes**

- 1-14 Influence of surrounding materials on heat conduction of carbon nanotubes : Molecular dynamics simulations 22  
○Junichiro Shiomi, Shigeo Maruyama
- 1-15 Specific Surface Area Measurement for Purity and SWNT Selectivity Analysis 23  
○Don N. Futaba, Jundai Gotou, Takeo Yamada, Satoshi Yasuda, Motoo Yumura, Sumio Iijima and Kenji Hata
- 1-16 Chirality Dependence on Destabilizing Agents Added to CMC-stabilized Carbon Nanotube Dispersions 24  
○Hiroshi Saito, Masahito Sano
- 1-17 Electrochemical and Diameter-selective Cutting of Carbon Nanotubes 25  
○Shigekazu Ohmori, Takeshi Saito, Satoshi Ohshima, Motoo Yumura, Sumio Iijima
- 1-18 Bending deformation of carbon nanotubes caused by a five-seven pair couple defect 26  
○Kei Wako, Tatsuki Oda, Masaru Tachibana, Kenichi Kojima

**Poster Preview (16 : 15-17 : 15)**

**Poster Session (17 : 15-18 : 35)**

**Formation and Purification of Nanotubes**

- 1P-1 Growth of Carbon Nanotubes by Carbon Transmission Method 51  
○Takeshi Hikata, Kazuhiko Hayashi, Tomoyuki Mizukoshi, Yoshiaki Sakurai, Itsuo Ishigami, Takaaki Aoki, Toshio Seki, Jiro Matsuo
- 1P-2 Synthesis of Radially-Aligned Carbon Nanotube Powder by SiC Surface Decomposition Method 52  
○Kazuo Yoshikawa, Motohiro Yamamoto, Michiko Kusunoki
- 1P-3 Photoluminescence of mono-dispersed single-walled carbon nanotubes made by using arc-burning method in nitrogen gas atmosphere 53  
○Takashi Mizusawa, Shinzo Suzuki, Toshiya Okazaki, Yohji Achiba
- 1P-4 Production of SWNTs by Laser Ablation and ACCVD 54  
○Shin-ichi Kodama, Atsushi Ikeda, Yuki Masuo, Tetsushi Murakami, Tomonari Wakabayashi
- 1P-5 Synthesis and Applications of Novel Vanadium Oxide Nanotubes 55  
○Abhishek Kumar, Nikhil Dhawan
- 1P-6 Time Dependence of Carbon Nanotube Growth by Gas Source Method using Alcohol in High Vacuum 56  
○Kenji Tanioku, Tomoyuki Shiraiwa, Takahiro Maruyama, Shigeya Naritsuka
- 1P-7 Patterned growth of CNTs through AFM nano-lithography 57  
○Chien-Chao Chiu, Masamichi Yoshimura, Kazuyuki Ueda
- 1P-8 A Study on Chirality-Selectivity of Metal Catalyst Particles in CNT Synthesis by Alcohol-CCVD 58  
○Shogo Suzuki, Hideki Sato, Koichi Hata, Kazuo Kajiwara
- 1P-9 TEM observation of Carbon Nanotube Pattern fabricated on SiC (000-1) using Ta mask 59  
○Yoko Hozumi, Yo Yamamoto, Midori Mori, Takahiro Maruyama, Shigeya Naritsuka, Michiko Kusunoki
- 1P-10 Growth mechanism of carbon nanotubes over gold-supported catalysts 60  
○Naoki Yoshihara, Hiroki Ago, Masaharu Tsuji

**Miscellaneous**

- 1P-11 G' band Raman Spectrum of Single, Double, and Triple Layer Graphene 61  
○Jin Sung Park, Alfonso Reina Cecco, Riichiro Saito, Jing Kong, Gene Dresselhaus, and Mildred S. Dresselhaus

**Applications of Nanotubes**

- 1P-12 Influence of Cathode-Anode Distance on Field Emission Properties for Bulky CNT Emitters 62  
○Huarong Liu, Shigeki Kato, Yahachi Saito
- 1P-13 Applications of vertically well-aligned CNT films in capacitors 63  
○Haruo Kato, Michiko Kusunoki, Shigeyuki Sugimoto, Kunihiko Sugihara, Noriyoshi Shibata
- 1P-14 In-situ observation of welding process of a multi-walled carbon nanotube to metal surface 64  
○Koji Asaka, Hitoshi Nakahara, Yahachi Saito
- 1P-15 Formation of Honeycomb Structure on PET Using Soluble Carbon Nanotube 65  
○Nobuo Wakamatsu, Hisayoshi Takamori, Tsuyohiko Fujigaya, Naotoshi Nakashima

## March 3rd, Monday

- 1P-16** Investigation of Methane Adsorption on MWNTs Using Field Emission Microscopy (FEM)  
○Tetsuya Yamashita, Koji Asaka, Hitoshi Nakahara, Yahachi Saito 66
- 1P-17** Culture of osteoblast-like cells on transparent conductive thin films with carbon nanotubes  
○Tsukasa Akasaka, Atsuro Yokoyama, Makoto Matsuoka, Shigeaki Abe, Motohiro Uo, Yoshinori Sato, Kazuyuki Tohji, Takeshi Hashimoto, Fumio Watari 67
- 1P-18** In situ TEM study on field emission property of an isolated CNT  
○Kensuke Okumura, Koji Asaka, Yahachi Saito 68
- 1P-19** Fabrication Process of Carbon Nanotube FETs Using ALD Passivation for Biosensors  
○Yasuhiro Nakashima, Yutaka Ohno, Shigeru Kishimoto, Mina Okochi, Hiroyuki Honda, Takashi Mizutani 69
- 1P-20** Electron Optical Evaluation of Carbon Nanotube Field-Emitter  
○Takumi Kono, Koji Asaka, Hitoshi Nakahara, Yahachi Saito 70

### Properties of Nanotubes

- 1P-21** Studying the Same-Handedness in Double-Walled Carbon Nanotubes Using the Dispersion-Augmented Density Functional Tight Binding Method  
○Stephan Irlé, Raviprasad Krishnamurthy, Keiji Morokuma 71
- 1P-22** Electronic properties of hybrid (DNA/SWCNT) thin film  
○Yusei Maruyama, Satoru Motohashi, Masayuki Tanaka, Biao Zhou, Akiko Kobayashi, Hironori Ogata 72
- 1P-23** Theory of superconductivity by the edge states in graphene  
○Ken-ichi Sasaki, Masahiro Suzuki, Riichiro Saito, Seiichiro Onari, Yukio Tanaka 73
- 1P-24** Electrical transport properties of azafullerene C<sub>59</sub>N encapsulated single- and double-walled carbon nanotubes  
○Y. F. Li, T. Kaneko, S. Nishigaki, and R. Hatakeyama 74
- 1P-25** Embedding of Carbon Nanotubes on Silicon substrates for use in Solar Cells  
○Abhishek Kumar, Nikhil Dhawan 75
- 1P-26** Synthesis of single-walled carbon nanotubes by arc plasma reactor with twelve-phase alternating current discharge  
○T. Matsuura, Y. Kondo, N. Maki, Y. Ito, K. Matsumoto, N. Tamura, Y. Taira, R. Ehara 76
- 1P-27** Electronic structures at edges of carbon nanotube and molecular dynamics simulations  
○Hirofumi Sakashita, Tatsuki Oda, Nobuhisa Fujima 77
- 1P-28** Phase transition from Tomonaga-Luttinger liquid states to superconductive phase in carbon nanotubes.  
○Masaharu Matsudaira, Junji Haruyama, Naoyoshi Murata, Yuko Yagi, Erik Einarsson, Shigeo Maruyama, Toshiki Sugai, Hisanori Shinohara 78
- 1P-29** Cooperative behaviors in carbene additions through local modifications of nanotube surface  
○Takashi Yumura, Miklos Kertesz 79

### Metallofullerenes

- 1P-30** Location of the Metal Atoms in Ce<sub>2</sub>@C<sub>78</sub> and Its Bis-silylated Derivative  
○Michio Yamada, Takatsugu Wakahara, Takahiro Tsuchiya, Yutaka Maeda, Takeshi Akasaka, Kenji Yoza, Naomi Mizorogi, Shigeru Nagase 80
- 1P-31** <sup>13</sup>C NMR Spectroscopic Study of <sup>13</sup>C-enriched Carbide-encapsulated Scandium Metallofullerenes  
○Yuko Yamazaki, Koji Nakajima, Takatsugu Wakahara, Tsuchiya Takahiro, Yutaka Maeda, Takeshi Akasaka, Markus Waelchli, Naomi Mizorogi, Shigeru Nagase 81
- 1P-32** Reaction of La@C<sub>82</sub> with Cyclopentadiene Derivatives  
○Satoru Sato, Yutaka Maeda, Koji Inada, Michio Yamada, Takahiro Tsuchiya, Midori O. Ishitsuka, Tadashi Hasegawa, Takeshi Akasaka, Tatsuhisa Kato, Naomi Mizorogi, Shigeru Nagase 82
- 1P-33** STM-tip Current Induced Polymerization of Ce<sub>2</sub>@C<sub>80</sub> Metallofullerenes  
○Kazunori Ohashi, Nobuyuki Fukui, Masahiro Akachi, Takao Akachi, Hisashi Umemoto, Yasuhiro Ito, Toshiki Sugai, Ryo Kitaura, Hisanori Shinohara 83
- 1P-34** Relative Stability of Metallofullerenes Sc<sub>3</sub>N@C<sub>70</sub>  
○Hong ZHENG, Qian XU, Xiang ZHAO 84
- 1P-35** Cage Size Dependence on Photoluminescence Properties of Erbium-Metal-Carbide Metallofullerenes : (Er<sub>2</sub>C<sub>2</sub>) @C<sub>2n</sub>  
○Masahiro Akachi, Yasuhiro Ito, Toshiya Okazaki, Yutaka Ohno, Takashi Mizutani, Ryo Kitaura, Toshiki Sugai, Hisanori Shinohara 85

### Endohedral Nanotubes

- 1P-36** Orientation of individual fullerenes inside carbon nanotubes determined by aberration-corrected electron microscopy  
○Yuta Sato, Kazu Suenaga, Shingo Okubo, Toshiya Okazaki, Sumio Iijima 86

## March 3rd, Monday

<b>1P-37</b>	Coating of BN nanotubes with metal oxides using novel ethanol-thermal method ○Yang Huang, Yoshio Bando, Chengchun Tang, Chunyi Zhi, Takeshi Terao and Dmitri Golberg	87
<b>1P-38</b>	Adsorption Efficiency of Polyynes into Single-Wall Carbon Nanotubes ○Tetsushi Murakami, Tomonari Wakabayashi	88
<b>1P-39</b>	Direct Observation on Formation Process of Nanopeapods by in-situ X-ray diffraction Measurements ○Yuko Kato, Ryo Kitaura, Shinobu Aoyagi, Eiji Nishibori, Yasuhiro Ito, Makoto Sakata, Hisanori Shinohara	89
<b>1P-40</b>	Fabrication of Metal-Nanowire in Carbon Nanotube Via Nano-Template Reaction ○Naoki Imazu, Ryo Kitaura, Keita Kobayashi, Hisanori Shinohara	90
<b>1P-41</b>	Optimization of Conditions for Formation of Carbon Nanotubes Filled Perfectly with Copper Nanowire ○Akira Koshio, Naoki Mizuno, Hironobu Kito, Fumio Kokai	91
<b>1P-42</b>	Synthesis and Characterization of Carbon Nanotubes Encapsulating Erbium-Chloride Nanowires ○Daisuke Ogawa, Ryo Kitaura, Keita Kobayashi, Takeshi Saito, Satoshi Ohshima, H. Shinohara	92
<b>1P-43</b>	Nucleation of an SWNT from a catalytic metal cluster inside a carbon nanotube template : MD simulations of DWNT formation ○Yoshifumi Izu, Junichiro Shiomi and Shigeo Maruyama	93

### Nanohorns

<b>1P-44</b>	SWNH as an Effective Delivery System for Macromolecule Anti-cancer Drugs ○Xu Jianxun, Yudasaka Masako, Zhang Minfang, Iijima Sumio	94
<b>1P-45</b>	Gd oxide particles confined inside single-wall carbon nanohorns ○Ryota Yuge, Masako Yudasaka, Toshinari Ichihashi, Jin Miyawaki, Tsutomu Yoshitake, Sumio Iijima	95
<b>1P-46</b>	Effect of compression pressure on the electrical resistivity for the pellet formed from nanohorns ○Yuhei Fukunaga, Manabu Harada, Sunji Bandow, Sumio Iijima	96
<b>1P-47</b>	Anticancer Effect of ZnPc-Nanohorn-Protein in vivo ○Minfang Zhang, Masako Yudasaka, Tatsuya Murakami, Kumiko Ajima, A. D. Sandanayaka, Osamu Ito, Kunihiro Tsuchida, Sumio Iijima	97
<b>1P-48</b>	Influence of formation technique of catalyst layer and addition of conductive material on performance of direct methanol fuel cell ○yuuki izumi, kennzi shinohara, masanobu yamamoto, shinnichirou oke, hirofumi takikawa, ikuo sakakibara, syuuichi sugawara, nobuyoshi aoyagi, takashi ookawa, kazuo yoshikawa, mituharu miura, shigeo ito, tatuo yamaura	98
<b>1P-49</b>	Close-open-close evolution of holes in single-wall carbon nanohorns caused by heat treatment Jing Fan, ○Masako Yudasaka, Jin Miyawaki, Ryouta Yuge, Takazumi Kawai, Sumio Iijima	99
<b>1P-50</b>	Intravenous Toxicity of Single-Walled Carbon Nanohorns Jin Miyawaki, ○Masako Yudasaka, Minfang Zhang, Sumio Iijima	100

March 4th, Tuesday

Special lecture: 25 min (Presentation) + 5 min (discussion)

General lecture: 10 min (Presentation) + 5 min (discussion)

Poster preview: 1 min (Presentation), no discussion

**Special lecture (9 : 00-9 : 30)**

- 2S-3 Applications of Nanodiamond Hydrogels Toward Biology and Medicine  
*Houjin Huang, Erik Pierstorff, Eiji Osawa, and Dean Ho* 3

**General lecture (9 : 30-10 : 30)**

**Metallofullerenes**

- 2-1 Scanning Tunneling Spectroscopy Mapping of a Single Lu@C<sub>82</sub> on Alkanethiol Self Assembled Monolayer  
○Yuhusuke Yasutake, Keijiro Kono, Norihiro Kobayashi, Masachika Iwamoto, Hisashi Umemoto, Yasuhiro Ito, Haruya Okimoto, Hisanori Shinohara, Yutaka Majima 27
- 2-2 Estimation of the amounts of transferred electron in Lu-entrapped Metallofullerenes  
○Takafumi Miyazaki, Ryohei Sumii, Hisashi Umemoto, Haruya Okimoto, Toshiki Sugai, Hisanori Shinohara, Shojun Hino 28
- 2-3 <sup>13</sup>C NMR Study of Pr<sub>2</sub>@C<sub>80</sub> and LaPr@C<sub>80</sub>  
○Manabu Ito, Shiho Nagaoka, Takeshi Kodama, Yoko Miyake, Shinzo Suzuki, Koichi Kikuchi, Yohji Achiba 29
- 2-4 Structure of metal-carbide endohedral metallofullerene Sc<sub>2</sub>C<sub>2</sub>@C<sub>82</sub>(C<sub>2v</sub>)  
○Koji Nakajima, Yuko Yamazaki, Takatsugu Wakahara, Takahiro Tsuchiya, Yutaka Maeda, Takeshi Akasaka, Markus Waelchli, Kenji Yoza, Naomi Mizorogi, Shigeru Nagase 30

☆☆☆☆☆☆ Coffee Break (10 : 30-10 : 45) ☆☆☆☆☆☆

**General lecture (10 : 45-11 : 45)**

**Fullerene Solids and Chemistry of Fullerenes**

- 2-5 Discovery of the atomic-carbon-insertion reactions for fullerene growth  
○Teruhiko Ogata, Tetsu Mieno, Yutaka Shibi, Yoshio Tatamitani 31
- 2-6 Chemical modification on a non-IPR metallofullerene : La<sub>2</sub>@C<sub>72</sub>  
○Xing Lu, Hidefumi Nikawa, Takahiro Tsuchiya, Yutaka Maeda, Takeshi Akasaka, Naomi Mizorogi and Shigeru Nagase 32
- 2-7 Physical Properties of H<sub>2</sub> Endohedral C<sub>60</sub>  
○Katsumi Tanigaki, Takeshi Rachi, Ryotaro Kumashiro, Yasujiro Murata, Koichi Komatsu, Toru Kakiuchi, Hiroshi Sawa, Yoshimitsu Kohama, Satoru Izumisawa, Hitoshi Kawaji, Tooru Atake 33
- 2-8 Pressure-Induced Structural Phase Transition of Two-dimensionally polymerized C<sub>60</sub>  
○Yuichiro Yamagami, Susumu Saito 34

☆☆☆☆☆☆ Lunch Time (11 : 45-13 : 00) ☆☆☆☆☆☆

☆☆☆☆☆☆ Awards Ceremony (13 : 00-13 : 30) ☆☆☆☆☆☆

**Special lecture (13 : 30-14 : 00)**

- 2S-4 The structures of endohedral metallofullerene by the systematic structural studies from SR powder diffraction data  
○Eiji Nishibori 4

**General lecture (14 : 00-15 : 00)**

**Endohedral Nanotubes·Nanohorns**

- 2-9 Imaging of Transportation of Single Hydrocarbon Chain through Nano-sized Pore  
○Takatsugu Tanaka, Masanori Koshino, Niclas Solin, Hiroyuki Isobe, Eiichi Nakamura 35
- 2-10 Synthesis of Pd-filled CNTs for the tip of SPM  
○Tomokazu Sakamoto, Chien-Chao Chiu, Kei Tanaka, Masamichi Yoshimura, Kazuyuki Ueda 36
- 2-11 Electronic Structure of Polyyne Molecules by Resonance Raman and Optical Emission Spectroscopy  
○Tomonari Wakabayashi 37
- 2-12 Photoinduced Charge-Separation of Carbon Nanohorns with Porphyrin Connected via Amino Group  
○Osamu Ito, Atula Sandanayaka, Yasuyuki Araki, Takatsugu Tanaka, Hiroyuki Isobe, Ei-ichi Nakamura, Masako Yudasaka, Sumio Iijima 38



March 4th, Tuesday

☆☆☆☆☆☆☆ Coffee Break (15 : 00-15 : 15) ☆☆☆☆☆☆☆

**General lecture (15 : 15-16 : 00)**

**Science of Nanocarbons**

- 2-13 Non-collinear Magnetic Phase Diagram of Graphene Nanoribbons 39  
○Keisuke Sawada, Fumiyuki Ishii, Mineo Saito, Susumu Okada, Takazumi Kawai
- 2-14 High temperature treatment of carbon fullerene soot and formation of multi-shell carbon nano-capsules filled with La carbide 40  
○Kazunori Yamamoto, Takatsugu Wakahara, Takeshi Akasaka
- 2-15 Monodisperse Single-Nano Diamond Particles as Seeding for CVD Diamond Thin Films. 1. A New Seeding Technique 41  
○Sachio Inaba, Takashi Tarao, Masaaki Kawabe, Oliver A. Williams, Eiji Osawa

**Poster Preview (16 : 00-17 : 00)**

**Poster Session (17 : 00-18 : 20)**

**Formation and Purification of Nanotubes**

- 2P-1 Effect of Al oxide buffer layer on SWNT growth using alcohol gas source in high vacuum 101  
○Tomoyuki Shiraiwa, Shigenori Numao, Osamu Oishi, Nobuyuki Nishi, Takahiro Maruyama, Shigeo Naritsuka
- 2P-2 Dispersion and Separation of Single-Walled carbon nanotubes prepared by using metal-catalysts supported on Zeolite 102  
○Masahiro Hashimoto, Yutaka Maeda, Tadashi Hasegawa, Makoto Kanda, Takahiro Tsuchiya, Takatsugu Wakahara, Takeshi Akasaka, Yuhei Miyauchi, Shigeo Maruyama, Jing Lu, Shigeru Nagase
- 2P-3 A protocol to remove surfactants and gradient media from metallic and semiconducting single-wall carbon nanotubes in density gradient separations 103  
○Kazuhiro Yanagi, Yasumitsu Miyata, Yuta Sato, Zheng Liu, Kazutomo Suenaga, Takeo Ishida, Hiromich Kataura
- 2P-4 Diagnostics and Control of Growth of Vertical-aligned Carbon Nanotube Forest by Using a Telecentric Optical System 104  
○Satoshi Yasuda, Don N. Futaba, Motoo Yumura, Sumio Iijima, Kenji Hata
- 2P-5 FT-IR Gas Analysis for Alcohol Catalytic Chemical Vapor Deposition 105  
○Tomohiro Shimazu, Yoshinobu Suzuki, Hisayoshi Oshima, Shigeo Maruyama
- 2P-6 Growth of double- and triple-walled carbon nanotube on MgO substrate 106  
○Ryoji Naito, Toshiya Murakami, Yuki Hasebe, Kenji Kisoda, Koji Nishio, Toshiyuki Isshiki, Hiroshi Harima
- 2P-7 Purification of Carbon Nanotubes by Amphiphilic Oligopeptides 107  
○Shinya Masuhara, Atsushi Yamamoto, Yosuke Miura, Yasushi Maeda, Shin Ono
- 2P-8 Toward Single Structure of SWNTs : Simultaneous Enrichment in (n, m) and the Optical Purity of SWNTs through Extraction with Carbazole-Bridged Chiral Diporphyrin Nanotweezers 108  
○Xiaobin Peng, Naoki Komatsu, Takahide Kimura, Atsuhiko Osuka
- 2P-9 Effect of density of carbon supply on the synthesis of small diameter SWNTs by ACCVD method using platinum as catalyst 109  
○Keisuke Urata, Sinzo Suzuki, Hiroshi Nagasawa, and Yohji Achiba
- 2P-10 Toward the selective production of metallic SWNT by the laser ablation method 110  
○Yasuhiro Tsuruoka, Yohji Achiba
- 2P-11 The synthesis of the single-walled carbon nanotubes films by DC arc discharge 111  
○Zhh. Li, Hf. Wang, S. Inoue Y. Ando

**Applications of Nanotubes**

- 2P-12 Nitrogen and oxygen plasma functionalization of carbon nanotubes for photovoltaic device application 112  
○Golap Kalita, Sudip Adhikari, Hare Ram Aryal, Rakesh Afre, Tetsuo Soga, Maheshwar Sharon, Masayoshi Umeno
- 2P-13 Formation of nano pn junction diode via alkali-halogen plasma ion irradiation 113  
○Jun Shishido, Toshiaki Kato, Wataru Oohara, Rikizo Hatakeyama, Kazuyuki Tohji
- 2P-14 Novel Carbon Nanotubes/Photopolymer Nanocomposites with High Conductivity and Application to Nanoimprint Photolithography 114  
○Tsuayohiko Fujigaya, Takahiro Fukumaru, Naotoshi Nakashima
- 2P-15 Increase of surface area of super-growth single-walled carbon nanotubes via opening, resulting in improved electrochemical capacitance 115  
○Ali Izadi-Najafabadi, Kenji Hata, Tatsuki Hiraoka, Takeo Yamada, Don N. Futaba, Satoshi Yasuda, Osamu Tanaike, Hiroaki Hatori, Motoo Yumura, Sumio Iijima

## March 4th, Tuesday

<b>2P-16</b>	Photovoltaic cell made of single wall carbon nanotubes and fullerenes ○Tatsunori Kuranoto, Toru Arai, Shingo Nobukuni, Yoshikazu Shimote, Tetsuji Moriguchi	116
<b>2P-17</b>	Precise Optical Detection of Mechanical Vibration of Cantilevered Carbon Nanotubes in Air ○Shun Fukami, Seiji Akita	117
<b>2P-18</b>	Density increase of well-dispersed single-walled carbon nanotubes by laser trapping ○Thomas Rodgers, Satoru Shoji, Satoshi Kawata	118
<b>2P-19</b>	Effects of Microwave Radiation on Heat-resistive Proteins Adsorbed on Carbon Nanotubes ○Hirokazu Horiguchi, Masahito Sano	119
<b>2P-20</b>	Dependence on Insulator thickness for sensitivity of Carbon Nanotube Field-Effect Transistor Biosensor ○Masuhiro Abe, Katsuyuki Murata, Tatsuki Ataka, Kazuhiko Matsumoto	120
<b>2P-21</b>	FET Properties of Exohedrally Modified SWCNTs ○Ryotaro Kumashiro, Naoya Komatsu, Tatsuya Saito, Takeshi Akasaka, Yutaka Maeda, Nagao Kobayashi, Katsumi Tanigaki	121

### Properties of Nanotubes

<b>2P-22</b>	Atomic structures of graphene adatom and its aggregation ○Tomofumi Hashi, Mineo Saito	122
<b>2P-23</b>	Environmental effect on excitons of single wall carbon nanotubes ○Kentaro Sato, Riichiro Saito, Jie Jiang, Gene Dresselhaus, Mildred S. Dresselhaus	123
<b>2P-24</b>	Spectroscopically probed doping processes in semiconducting single-wall carbon nanotubes selectively isolated using polyfluorene ○Nobutsugu Minami, Yoshisuke Futami, Said Kazaoui	124
<b>2P-25</b>	Response of Carbon Nanotube Field Effect Transistors to Vibrating Gate Using Scanning Gate Microscopy ○Kosuke Hata, Yoshikazu Nakayama, Seiji Akita	125
<b>2P-26</b>	Third-order nonlinear optical properties and phase relaxation time in single-walled carbon nanotubes ○Masao Ichida, Yumie Kiyohara, Shingo Saito, Yasumitsu Miyata, Hiromichi Kataura, Hiroaki Ando	126
<b>2P-27</b>	Multi-backgate control of carbon nanotube double quantum dot ○Tomoyuki Mizuno, Hideyuki Maki, Satoru Suzuki, Yoshihiro Kobayashi, Tetsuya Sato	127
<b>2P-28</b>	Design of Si Nanotube : New Multi-shell Nanotubes ○Susumu Okada	128
<b>2P-29</b>	Influence of Diameter on the Raman Spectra of Multi-Walled Carbon Nanotubes ○Hiroyuki Nii, Yoshiyuki Sumiyama, Hamazo Nakagawa, Atsuhiko Kunishige	129
<b>2P-30</b>	Resonance Raman spectroscopy of metallic and semiconducting single-wall carbon nanotubes ○Yasumitsu Miyata, Kazuhiro Yanagi, Yutaka Maniwa, Hiromichi Kataura	130

### Metallofullerenes

<b>2P-31</b>	Chemical Derivatization of La@C <sub>82</sub> and La <sub>2</sub> @C <sub>80</sub> with Phenylchlorodiazirine ○Haruka Enoki, Midori O. Ishitsuka, Takahiro Tsuchiya, Takeshi Akasaka, Zdenek Slanina, Michael T. H. Liu, Naomi Mizorogi, Shigeru Nagase	131
<b>2P-32</b>	[2+1] Cycloaddition of Nitrene onto [60]fullerene : Interconversion between an Aziridinofullerene and an Azafulleroid ○Mitsunori Okada, Tsukasa Nakahodo, Hiroyuki Morita, Toshiaki Yoshimura, Midori O. Ishitsuka, Takahiro Tsuchiya, Yutaka Maeda, Hisashi Fujihara, Takeshi Akasaka, Xingfa Gao, Shigeru Nagase	132
<b>2P-33</b>	HPLC Purification of Li Endohedral [60]Fullerene ○Takeshi Sakai, Hiroshi Okada, Fuyuko Yamashita, Kenji Omote, Yasuhiko Kasama, Kuniyoshi Yokoo, Shoichi Ono, Hiromi Tobita, Rikizo Hatakeyama, Masayuki Toda	133
<b>2P-34</b>	Electron Transport Properties of Sc <sub>2</sub> C <sub>2</sub> @C <sub>84</sub> Using the Encapsulated Sc <sub>2</sub> C <sub>2</sub> Moiety as an Electric lead, First-Principle Study ○Shinji Usui, Noritaka Inoue	134
<b>2P-35</b>	Photophysical Properties of N@C <sub>60</sub> ○Hidefumi Nikawa, Yoichiro Matsunaga, Takeshi Akasaka, Tatsuhisa Kato, Yasuyuki Araki, Osamu Ito, Masafumi ATA, Klaus-Peter Dinse	135
<b>2P-36</b>	Synthesis of High Purity Nitrogen Atom Encapsulated Fullerenes ○Shohei Nishigaki, Toshiro Kaneko, Rikizo Hatakeyama	136

### Carbon Nanoparticles

<b>2P-37</b>	Detection of single atomic layer of graphene by highly charged ion ○Yoshiyuki Miyamoto, Hong Zhang	137
--------------	---	-----

## March 4th, Tuesday

<b>2P-38</b>	Effect of heat-treatment temperature on preparation of carbonized ferritin <i>Masato Tominaga, ○Katsuya Miyahara, Kota Nakao, Isao Taniguchi</i>	138
<b>2P-39</b>	Chlorine-End-Capped Polyynes : Formation and Characterization <i>○Yoriko Wada, Tomonari Wakabayashi</i>	139
<b>2P-40</b>	Resonance Effects in the Raman Spectra of Polyynes <i>○Yohei Ami, Tomonari Wakabayashi</i>	140
<b>2P-41</b>	Cyanopolyynes Formed by Laser Ablation of Graphite in Acetonitrile <i>○Takaki Haseba, Yoshihiko Kashihara, Tomonari Wakabayashi</i>	141
<b>2P-42</b>	Dicyanopolyynes Formed by Laser Ablation of Graphite in Liquid Nitrogen <i>○Yoshihiko Kashihara, Takaki Haseba, Tomonari Wakabayashi</i>	142
<b>Chemistry of Fullerenes</b>		
<b>2P-43</b>	Kinetic study in Diels-Alder reactions of fulleroids and methanofullerenes with various 1, 3-dienes <i>○Yasunori Susami, Hiroshi Kitamura, Ken Kokubo, Takumi Oshima</i>	143
<b>2P-44</b>	Evaluation of Antioxidant Activity of Water-Soluble Fullerene Derivatives and Natural Antioxidants by $\beta$ -Carotene Bleaching Assay <i>○Kyoko Togaya, Tadashi Goto, Ken Kokubo, Hisae Aoshima, Takumi Oshima</i>	144
<b>2P-45</b>	Photoelectrochemical Properties of [70]fullerene derivatives on ITO <i>○Takahiko Ichiki, Yutaka Matsuo, Eiichi Nakamura</i>	145
<b>2P-46</b>	Synthesis and Property of Fullerene Cobalt Dithiolene Complexes <i>○Masashi Maruyama, Yutaka Matsuo, Eiichi Nakamura</i>	146
<b>2P-47</b>	Hydroarylation of Fullerene with Aromatic Compound and Subsequent Friedel-Crafts Acetylation Reaction <i>○Shinya Tochika, Yui Sol, Mai Kato, Ken Kokubo and Takumi Oshima</i>	147
<b>2P-48</b>	Surface Functionalization of Fullerene Bilayer Vesicles and Study of Water Permeability <i>○Tatsuya Homma, Koji Harano, Hiroyuki Isobe, Eiichi Nakamura</i>	148
<b>2P-49</b>	Singlet Oxygen Generation Efficiencies of Water-Soluble Fullerenes and Their Photo-Induced Cytotoxicity <i>○Yoko Iizumi, Toshiya Okazaki, Minfang Zhang, Masako Yudasaka, Sumio Iijima</i>	149
<b>2P-50</b>	Synthesis of Fullerene Glycoconjugates via a Copper-Catalyzed Huisgen Cycloaddition Reaction <i>○Kaimei Cho, Niclas Solin, Daniel B. Werz, Hiroyuki Isobe, Peter H. Seeberger, Eiichi Nakamura</i>	150

March 5th, Wednesday

Special lecture: 25 min (Presentation) + 5 min (discussion)  
General lecture: 10 min (Presentation) + 5 min (discussion)  
Poster preview: 1 min (Presentation), no discussion

**Special lecture (9 : 00-9 : 30)**

- 3S-5 Chemical Modification of Carbon Nanohorns 5  
○Nikos Tagmatarchis

**General lecture (9 : 30-10 : 30)**

**Formation and Purification of Nanotubes**

- 3-1 Intensity enhancement of intermediate frequency Raman mode (IFM) by the presence of very small diameter SWNTs 42  
○Yohji Achiba, Yasuhiro Tsuruoka, Keisuke Urata
- 3-2 Mechanism of Gold-Catalyzed Carbon Material Growth 43  
○Daisuke Takagi, Yoshihiro Kobayashi, Hiroki Hibino, Satoru Suzuki, Yoshikazu Homma
- 3-3 Acetylene Assisted Fast Growth of Vertically Aligned Single Walled Carbon Nanotubes in Alcohol Catalytic Chemical Vapor Deposition 44  
○Rong Xiang, Jun Okawa, Zhengyi Zhang, Erik Einarsson, Yohei Miyauchi, Yoichi Murakami, Shigeo Maruyama
- 3-4 Discovery of Novel Carbon Structure : Graphene Multi-Layers Spontaneously Formed on the Top of Aligned Carbon Nanotubes 45  
○Daiyu Kondo, Shintaro Sato, Akio Kawabata, Yuji Awano

☆☆☆☆☆☆ Coffee Break (10 : 30-10 : 45) ☆☆☆☆☆☆

**Special lecture (10 : 45-11 : 15)**

- 3S-6 Electronic and Photo-electrochemical Functions of Fullerene-Metal Complexes 6  
○Yutaka Matsuo

**General lecture (11 : 15-12 : 15)**

**Purification and Applications of Nanotubes**

- 3-5 Stability of Double Wall Carbon Nanotubes on Oxidation 46  
○Hiromichi Yoshida, Toshiki Sugai, Hisanori Shinohara
- 3-6 Separation of Metallic and Semiconducting Single-Wall Carbon Nanotubes by Gel Electrophoresis 47  
○Takeshi Tanaka, Hehua Jin, Yasumitsu Miyata, Hiromichi Kataura
- 3-7 The New Feature Development of Carbon Nanotubes-Polybenzimidazole Composite 48  
○Minoru Okamoto, Tsuyohiko Fujigaya, Naotoshi Nakashima
- 3-8 Reduction of low-temperature-growth-CNT via resistances using inner layers by Chemical Mechanical Polishing 49  
○Kentaro Ishimaru, Daisuke yokoyama, Takayuki Iwasaki, Shintaro Sato, Takashi Hyakushima, Mizuhisa Nihei, Yuji Awano and Hiroshi Kawarada

☆☆☆☆☆☆ Lunch Time (12 : 15-13 : 30) ☆☆☆☆☆☆

**Special lecture (13 : 30-14 : 00)**

- 3S-7 Review of Nanotechnology R&D in NEC 7  
○Shuichi Tahara

**Poster Preview (14 : 00-15 : 00)**

**Poster Session (15 : 00-16 : 20)**

**Formation and Purification of Nanotubes**

- 3P-1 Growth characteristics of single-walled carbon nanotubes at low temperature by low-pressure chemical vapor deposition 151  
○Hiroshi Yoshida, Masahiro Asakura, Shu Watanabe, Takao Shiokawa, and Koji Ishibashi
- 3P-2 Effective catalyst diameter for extended growth duration of single-walled carbon nanotubes 152  
○Takashi Uchida, Hiroshi Sakai, Akira Yamazaki, Yoshihiro Kobayashi
- 3P-3 RHEED Study on Growth Process of Carbon Nanotubes by Chemical Vapor Deposition 153  
○Hidetoshi Nagatsu, Koji Asaka, Hitoshi Nakahara, Yahachi Saito

## March 5th, Wednesday

<b>3P-4</b>	Carbon Nanotube Growth with Dipped (Fe, Co) Mo Catalysts by Chemical Vapor Deposition ○Daisuke Ishizuka, Takayuki Yanai, Hiroki Okuyama, Katsumi Uchida, Nobuyuki Iwata, Hirofumi Yajima, Hiroshi Yamamoto	154
<b>3P-5</b>	Sorting of double-walled carbon nanotubes using density-gradient ultracentrifugation. ○Shingo Ina, Kazuhiro Yanagi, Yasumitsu Miyata, Yutaka Maniwa, Hiromichi Kataura	155
<b>3P-6</b>	In-situ Monitoring and Kinetic Analysis of Millimeter-Thick Single-Walled Carbon Nanotube Growth ○Kei Hasegawa, Suguru Noda, Shigeo Maruyama and Yukio Yamaguchi	156
<b>3P-7</b>	Crucial Role of Gas-Phase Pyrolysis of Ethylene in Rapid Growth of Carbon Nanotubes ○Ryuhei Ito, Suguru Noda, Toshio Osawa, Shigeo Maruyama, Yukio Yamaguchi	157
<b>3P-8</b>	Interaction of Amphiphilic Oligopeptides with Carbon Nanotubes ○Shin Ono, Atsushi Yamamoto, Shin-ya Masuhara, Yosuke Miura, Yasushi Maeda, Kishio Hidaka, Hiromitsu Miyamoto	158
<b>3P-9</b>	Growth of super-long straight CNTs by highly dense catalyst particles ○Ryogo Kato, Tasuku Maki, Takayuki Iwasaki, Hiroshi Kawarada	159
<b>3P-10</b>	Chemical Vapor Deposition of Carbon Nanotubes with dip-coated (Fe, Co) Pt catalysts ○Takuya Sonomura, Daisuke Ishizuka, Hiroki Okuyama, Nobuyuki Iwata, Hiroshi Yamamoto	160
<b>3P-11</b>	Effect of flow rate of ethanol on growth dynamics of VA-SWNT -Transition from no-flow CVD to normal ACCVD- ○Jun Okawa, Rong Xiang, Shigeo Maruyama	161
<b>3P-12</b>	Growth of Very-Thin Single-Wall Carbon Nanotubes by Catalyst-supported Chemical Vapor Deposition Using Surface-Treated Zeolites ○Keita Kobayashi, Ryo Kitaura, Hisanori Shinohara	162

### Applications of Nanotubes

<b>3P-13</b>	Quantum response of carbon nanotube quantum dots to terahertz wave ○Seiko Toyokawa, Tomoko Fuse, Yukio Kawano, Tomohiro Yamaguchi, Koji Ishibashi	163
<b>3P-14</b>	Dispersion of Single-Wall Carbon Nanotubes by Thermostable Chitinases ○Takeshi Tanaka, Hyekeyeong Park, Hehua Jin, Tadayuki Imanaka, Hiromichi Kataura	164
<b>3P-15</b>	Carbon nanotube single electron transistors on a GaAs/AlGaAs 2-dimensional electron gas wafer ○Mitsutoshi Makihata, Takahiro Mori, Tomohiro Yamaguchi, Yoshinobu Aoyagi, Koji Ishibashi	165
<b>3P-16</b>	Inhibitory Effect of Carboxymethylcellulose Wrapping on the Oxidation of Single-walled Carbon Nanotubes Induced by Acidification ○Toru Ishii, Katsumi Uchida, Tadahiro Ishii, Hirofumi Yajima	166
<b>3P-17</b>	Manipulation and Observation of Carbon Nanotubes in Microfluidic Chip Under Optical Microscope ○Naoki Inomata, Yoko Yamanishi, Fumihito Arai	167
<b>3P-18</b>	Purification and Physicochemical Properties of Double-Walled Carbon Nanotubes ○Noriko Maeda, Katsumi Uchida, Tadahiro Ishii, Hirofumi Yajima	168
<b>3P-19</b>	Effects of the neutral Ar beam irradiation to the random-network single-walled carbon nanotube field effect transistors ○Shunsuke Sato, Takahiro Mori, Kazuo Omura, Koji Ishibashi	169
<b>3P-20</b>	Theoretical Analysis on Ion Permeation Mechanism through an Anion-Doped Carbon Nanotube ○Takashi Sumikama, Shinji Saito, Iwao Ohmine	170

### Properties of Nanotubes

<b>3P-21</b>	Recovery process of low-energy irradiation damage of SWNTs ○Kenji Yamaya, Satoru Suzuki, Yoshikazu Homma, Yoshihiro Kobayashi	171
<b>3P-22</b>	Synthesis of SWNTs by FH-arc method and evaluation of SWNTs by Raman spectroscopy ○Beibei Chen, Sakae Inoue, Takeshi Hashimoto, Yoshinori Ando	172
<b>3P-23</b>	Long-range Electron Transfer through a Single-walled Carbon Nanotube Sheet ○Takeshi Saito, Koji Matsuura, Satoshi Ohshima, Shigekazu Ohmori, Motoo Yumura, Sumio Iijima	173
<b>3P-24</b>	Diameter evaluation of multi-walled carbon nanotubes using SEM images ○Tohru Kawamoto, Hamazo Nakagawa, Takashi Muranaka, Atsuhiko Kunishige, and Yoshiyuki Sumiyama	174
<b>3P-25</b>	Saturation of Photoluminescence from Carbon Nanotubes at High Laser Intensities : Exciton-Exciton Annihilation near the Mott Density ○Yoichi Murakami, Junichiro Kono	175
<b>3P-26</b>	Growth and characteristics of <sup>13</sup> C enriched carbon nanotubes ○Nobuyuki Yamazaki, Ryo Hashiba, Manabu Oie, Yuichi Ochiai, Tomohiro Yamaguchi, Koji Ishibashi	176
<b>3P-27</b>	Polarized Raman Spectroscopy of Vertically Aligned Single-walled Carbon Nanotubes ○Zhengyi Zhang, Yuhei Miyauchi, Erik Einarsson, Shigeo Maruyama	177

## March 5th, Wednesday

<b>3P-28</b>	Molecular dynamics of phonon relaxation of an SWNT ○ <i>Minetaka Nihsimura, Junichiro Shiomi, Shigeo Maruyama</i>	178
<b>3P-29</b>	Surface Potential Investigations of Ballistic Conduction in SWNTs by Atomic Force Microscopy ○ <i>Yuji Miyato, Kei Kobayashi, Kazumi Matsushige, Hirofumi Yamada</i>	179
<b>3P-30</b>	Raman Scattering Studies on Nanopeapod-Derived Double-Walled Carbon Nanotubes : Comparisons with Photoluminescence Spectra ○ <i>Soon-Kil Joung, Toshiya Okazaki, Naoki Kishi, Takeshi Nakanishi, Shunji Bandow, Zujin Shi, Sumio Iijima</i>	180
<b>Miscellaneous</b>		
<b>3P-31</b>	Behaviors of cells cultured on carbon nanotube-synthesized substrate surface <i>Masato Tominaga, Shouichiro Nagaishi, Nagisa Yoshizaka, Estuko Kumagai, Shinji Harada, Isao Taniguchi</i>	181
<b>3P-32</b>	Synthesis of Carbon Nanotube Particles from Used SiC Powder by SiC Surface Decomposition Method ○ <i>Takayuki Morishita, Akihiro Ichikawa, Motohiro Yamamoto, Ryo Sasai, Michiko Kusunoki</i>	182
<b>3P-33</b>	Carbon nanowalls as a negative electrode in lithium-ion secondary battery ○ <i>Norihiro Kitada, Hirofumi Yoshimura, Osamu Tanaike, Ken-ichi Kobayashi, Kenichi Kojima, Masaru Tachibana</i>	183
<b>3P-34</b>	Synthesis of Thin Graphite by Exfoliation Technique ○ <i>Satoshi Heguri, Nozomu Kimata, Mototada Kobayashi</i>	184
<b>3P-35</b>	Flattened Carbon Nanocoil and application to field emitter ○ <i>Yuichiro Shinohara, Yuji Hosokawa, Masashi Yokota, Shinichiro Oke, Hirofumi Takikawa, Youhei Fujimura, Tatsuo Yamaura, Shigeo Itoh, Koji Miura, Kazuo Yoshikawa, Takashi Ina, Fumio Okada</i>	185
<b>3P-36</b>	Ab-initio study on the electronic structure of few-layer graphene films connected to a titanium electrode under an electric field ○ <i>Mari Ohfuchi, Masakatsu Ito</i>	186
<b>3P-37</b>	Preparation of porous carbons composed of carbon nanotube and fullerene-like carbon by carbonization of Fe-containing phenol formaldehyde resin ○ <i>Yuji Sakamoto, Katsuya Inomata, Yoshinobu Otake</i>	187
<b>3P-38</b>	Antimicrobial activity of fullerene and its derivatives ○ <i>Hisae Aoshima, Ken Kokubo, Shogo Shirakawa, Masayuki Ito, Shuichi Yamana, Takumi Ohshima</i>	188
<b>Formation of Fullerenes·Higher Fullerenes</b>		
<b>3P-39</b>	Production of carbon clusters by collisional explosion-reaction of asteroids in space (model experiment) ○ <i>Tetsu Mieno, Sunao Hasegawa</i>	189
<b>3P-40</b>	Energetics and Electronic Structures of Fullerenes with Vacancies ○ <i>Susumu Okada</i>	190
<b>Fullerene Solids</b>		
<b>3P-41</b>	Morphological Study of C <sub>60</sub> Thin Films for Electronic Device Application ○ <i>Hiroyuki Sagami, Haruna Oizumi, Morihiko Saida, Kenji Omote, Yuzo Mizobuchi, Yasuhiko Kasama, Kuniyoshi Yokoo, Shoichi Ono, Hiroji Ohigashi, Keiko Koga, Takeo Furukawa</i>	191
<b>3P-42</b>	Helium intercalated C <sub>60</sub> solid under high pressure ○ <i>Shinji Kawasaki, Takeshi Hara, Yusuke Kanamori, Atsushi Iwata</i>	192
<b>3P-43</b>	Electric double-layer capacitances of the C <sub>60</sub> dispersed porous carbons ○ <i>Shunsuke Mori, Takehiro Kawashita, Shinji Kawasaki</i>	193
<b>3P-44</b>	Electronic transport properties of photo- and electron-beam-irradiated C <sub>60</sub> ○ <i>Yasuto Chiba, Hajime Tsuji, Misaki Ueno, Nobuyuki Aoki, Jun Onoe, Yuichi Ochiai</i>	194
<b>3P-45</b>	Modification of Hole-Transport Property of Fullerene Materials by Hydrogenation : A DFT Study on C <sub>60</sub> H <sub>4</sub> ○ <i>Ken Tokunaga, Hiroshi Kawabata, Kazumi Matsushige</i>	195
<b>3P-46</b>	Fabrication of C <sub>60</sub> MC <sub>12</sub> Films for Solution-Processed n-type Organic Thin Film Transistors ○ <i>Koichi Sakaguchi, Masayuki Chikamatsu, Atsushi Itakura, Yuji Yoshida, Reiko Azumi, Kiyoshi Yase</i>	196
<b>3P-47</b>	High Performance N-Type Organic Thin-Film Transistors Based on Soluble C <sub>60</sub> Derivatives ○ <i>M. Chikamatsu, A. Itakura, K. Sakaguchi, Y. Yoshida, R. Azumi, K. Yase</i>	197
<b>3P-48</b>	Effect of Free Electron Laser Irradiation on Pressed C <sub>60</sub> Powder at the Order of GPa ○ <i>Nobuyuki Iwata, Shingo Ando, Ryo Nokariya, Yasunari Iio, Hiroshi Yamamoto</i>	198
<b>3P-49</b>	C <sub>60</sub> Crystal Growth and Free Electron Laser Irradiation Effect on Pressed C <sub>60</sub> Powder in Solution ○ <i>Yasunari Iio, Shingo Ando, Ryo Nokariya, Nobuyuki Iwata, Hiroshi Yamamoto</i>	199

**March 5th, Wednesday**

**3P-50** Magnetic Properties of superconducting sodium fulleride  $\text{Na}_x\text{C}_{60}$   
○*Nozomu Kimata, Satoshi Heguri, Mototada Kobayasi*

200

特別講演  
**Special Lecture**

**1S - 1 ~ 1S - 2**

**2S - 3 ~ 2S - 4**

**3S - 5 ~ 3S - 7**



## In silico catalyst design for fuel cells

○Yasuharu Okamoto<sup>1,2,3</sup>

<sup>1</sup>Nano Electronics Research Laboratories, NEC Corporation 34 Miyukigaoka, Tsukuba, Ibaraki, 305-8501, Japan

<sup>2</sup>Institute for Solid State Physics, University of Tokyo, 5-5-5, Kashiwanoha, Kashiwa 277-8581, Japan

<sup>3</sup>CREST, Japan Science and Technology Agency, 4-1-8 Honcho Kawaguchi, Saitama, Japan

Oxygen-reduction reactions (ORR) are basic reactions in electrochemistry and are closely related to the cathodic reactions in proton exchange membrane fuel cells (PEMFCs), where one O<sub>2</sub> molecule is reduced to two H<sub>2</sub>O molecules on Pt or Pt alloy particles that act as electrocatalysts. Minimizing Pt particle size has been a key to the development of electrocatalysts for PEMFCs because it helps make the best use of the precious metals such as Pt by maximizing the surface-to-volume ratio of the particles, and the minimum Pt particle size is currently 2 nm (about 300 atoms). Calculations based on density-functional theory (DFT) have suggested that the minimum size of the Pt particles could be further reduced to 1.5 nm (about 150 atoms) [1]. The further reduction of particle size deserves consideration because the behavior of adsorption energies on an atom or clusters comprising only a few atoms is quite different from that on clusters comprising dozens of atoms.

In this study, DFT calculations were done to find metal dimers that catalyze O<sub>2</sub> reduction [2]. A metal dimer embedded in a graphite sheet with a six-membered-ring carbon vacancy was treated as a model electrocatalyst structure. First, dimers suitable in terms of stability and electrocatalysis were selected from among Ni<sub>2</sub>, Ru<sub>2</sub>, Pd<sub>2</sub>, Pt<sub>2</sub>, and Au<sub>2</sub>. Under the assumption that the efficiency of electrocatalysis is estimated by the O<sub>2</sub> and O adsorption energies on the dimers, Pt<sub>2</sub> and Pd<sub>2</sub> were selected. Then a series of first-principles molecular dynamics (FPMD) simulations was performed to confirm electrocatalysis of Pt<sub>2</sub> with regard to O<sub>2</sub> reduction. Pathways that lead to H<sub>2</sub>O are normal and favorable, while pathways that lead to HOOH are unfavorable. It was found that O<sub>2</sub>(ads), OOH(ads), O(ads), and OH(ads) can be respectively reduced to OOH(ads), HOOH, OH(ads), and H<sub>2</sub>O. It was noted that HOOH formation on the Pt<sub>2</sub> is quite different from the ORR on Pt(111) where an FPMD simulation of ORR on Pt(111)/H<sub>2</sub>O interface showed that OOH(ads) spontaneously and immediately decomposed into O(ads) and OH(ads) after the first reduction of O<sub>2</sub>(ads) to OOH(ads) completed [3]. This difference was attributed to the bond breaking reaction energy of OOH(ads) → OH(ads) + O(ads): The reaction on Pt<sub>2</sub> is endothermic, while that on Pt(111) is exothermic. Further improvements in the catalyst model are needed if we are to find a pathway from HOOH to H<sub>2</sub>O or to cause 4e<sup>-</sup> reduction from O<sub>2</sub> to H<sub>2</sub>O without intermediate formation of HOOH.

[1] Y. Okamoto, *Chem. Phys. Lett.*, **429**, 209 (2006).

[2] Y. Okamoto, *J. Phys. Chem. C*. (in press).

[3] Y. Okamoto, unpublished.

Corresponding Author: Yasuharu Okamoto

TEL: +81-298-50-1571, FAX: +81-298-856-6137, E-mail: [y-okamoto@df.jp.nec.com](mailto:y-okamoto@df.jp.nec.com)

### Carbon nanotube LSI via interconnects

Yuji Awano

*MIRAI-Selete, Fujitsu Limited, Fujitsu Laboratories Ltd  
Morinosato-Wakamiya 10-1, Atsugi 243-0197, Japan*

Carbon nanotubes (CNTs) offer unique properties such as highest current density, ultra-high thermal conductivity, ballistic transport along the tube and extremely high mechanical strength with high aspect ratio of more than 1000. Because of these remarkable properties, they have been expected for use as future wiring materials to solve several serious problems of conventional Cu interconnects, for examples, electro-migration, high resistance, heat removal and fabrication of a small-sized via in future LSIs. In this paper, we report present status of Multi-walled CNT (MWNT) growth technologies and the potential of metallic CNT vias. In particular, we demonstrate our original catalytic nano-particle technique for the diameter and density control growth of MWNTs. We were able to lower the MWNT growth temperature to 400°C, which meets the requirement to avoid thermal damage to LSIs. We have succeeded in forming a 40-nm-diameter via with the MWNT density of 9E11/cm<sup>2</sup>, which is the highest density ever reported. The electrical properties of the CNT vias fabricated by our damascene process which is mostly compatible with conventional Cu interconnects are also discussed. From the temperature dependence of via resistance, we discuss the possibility of ballistic transport in CNT vias. Our low-temperature planar CNT via technologies are very promising for the achievement of low-resistance scaled-down CNT vias in future LSIs beyond hp32nm technology node.

This work was partly completed as part of the MIRAI Project supported by NEDO.

#### References:

1. Y. Awano, S. Sato, D. Kondo, M. Ohfuti, A. Kawabata, M. Nihei and N. Yokoyama, Phys. Stat. Sol. (a) 203, No. 14, pp. 361 1-3616 (2006)
2. M. Nihei, T. Hyakushima, S. Sato, T. Nozue, M. Norimatsu, M. Mishima, T. Murakami, D. Kondo, A. Kawabata, M. Ohfuti and Y. Awano, Proceedings of IEEE International Interconnect Technology Conference (IITC), June 4-6, 2007.

**E-mail:** y.awano@jp.fujitsu.com

**Tel&Fax:** +81-46-250-8186/-8844

**Applications of Nanodiamond Hydrogels Toward Biology and Medicine****Houjin Huang<sup>1,2</sup>, Erik Pierstorff<sup>1,2</sup>, Eiji Osawa<sup>3</sup>, and Dean Ho<sup>1,2,4\*</sup>**<sup>1</sup>*Department of Biomedical Engineering, Northwestern University, Evanston, Illinois, USA*<sup>2</sup>*Department of Mechanical Engineering, Northwestern University, Evanston, Illinois, USA*<sup>3</sup>*Nanocarbon Research Institute Asama Research Extension Center, Shinshu University, Japan*<sup>4</sup>*Robert H. Lurie Comprehensive Cancer Center, Chicago, Illinois, USA**\* Corresponding Author: d-ho@northwestern.edu*

Nanodiamonds serve as a versatile class of nanomaterials with significant advantages that can be applied toward drug delivery and cellular interrogation with unprecedented capabilities. Their high surface area-to-volume ratio enables therapeutic loading capacities that are several times higher than existing methodologies (e.g. liposomes, polymersomes), and their aspect ratios and stability confer an innate biocompatibility to the diamond particles that generate an amenable response when interfaced with surrounding biological material. This study demonstrates the application of nanodiamonds toward the treatment of cancer and inflammation using multiple form factors that include particle, film, and device-based methodologies. Because of the unique nature of the onset and progression of diseases that include cancer, inflammation, etc., a suite of strategies that include widespread (particle), as well as localized (device, film) drug elution enable versatile clinical responses. Therefore, this work aims to realize nanodiamonds as foundational materials for nanoscale medicine.

Chemotherapeutic-functionalized nanodiamond particles were fabricated through the interaction of Doxorubicin hydrochloride (Dox) with water-suspended nanodiamonds. Dox is a clinically relevant chemotherapeutic that displays a systemic, or generalized form of activity that induces apoptosis, or cell death in healthy as well as diseased cells. Therefore, the ability to deliver Dox in a controlled manner may result in increased treatment efficacy with reduced patient side effects. We have demonstrated the ability to controllably switch Dox release and adsorption, and therefore functionality via controlled interactions with the nanodiamond surface. Furthermore, as Dox is a cytotoxic element with a DNA fragmentation-based readout, laddering assays confirmed the ability of the nanodiamonds to preserve and facilitate drug delivery and activity upon multiple cell lines including Raw 264.7 murine macrophages as well as the HT-29 human colorectal cancer cell line. Comprehensive examination of cellular reaction toward bare nanodiamonds served as a biocompatibility assessment, where inflammatory gene expression levels of interleukin 6 (IL-6), inducible nitric oxide synthase (iNOS), and tumor necrosis factor alpha (TNFalpha) were quantified via real time polymerase chain reaction (RT-PCR). As inflammation can generate complications against chemotherapy by supporting the spread of cancer, or counteracting therapeutic activity, the observed maintain basal levels of these signaling elements confirmed the biocompatibility of the nanodiamonds.

We have also utilized poly-L-lysine, a cationic protein, to template the deposition of nanodiamond thin films to serve as localized drug delivery platforms. Dexamethasone (Dex) is a potent anti-inflammatory that was used to functionalize the diamond films. Through a binding process with a cytoplasmic glucocorticoid receptor, a subsequent nuclear translocation of the receptor-drug complex enables the suppression of inflammatory gene expression. Following the characterization of multi-layered nanodiamond-drug hybrids, RT-PCR studies demonstrated a potent reduction in the expression of IL-6, iNOS, and TNFalpha levels. Furthermore, basal expression levels of cells cultured on glass and bare diamond films revealed no increase in inflammatory gene expression, further confirming the innate biocompatibility of the nanodiamond films. Subsequent studies will be elucidated to explore opportunities in using vapor-deposited polymers to package the nanodiamond matrices to generate tangible drug delivery devices for applications in directed and sustained therapeutic efficacy. These capabilities are expected to impact a broad range of medical fields including cancer, cardiovascular medicine, orthopedics, neurosurgery, and beyond. This in turn confirms the importance of the introduction of nanodiamonds as a transforming technology for nano-engineered medicine.

**The structures of endohedral metallofullerene by the systematic structural studies from SR powder diffraction data.**

○Eiji Nishibori

<sup>1</sup>*Department of Applied Physics, Nagoya University, Nagoya 464-8603, Japan*

Endohedral metallofullerenes have attracted much interest during past decades due to their characteristic structural and electrical properties [1]. The recent findings of various kinds of metal carbide encapsulated fullerenes by <sup>13</sup>C-NMR and X-ray analysis have provided further information on the characterization of endohedral metallofullerenes. Importantly, several kinds of di-metallofullerenes have been re-characterized as C<sub>2</sub> encapsulated metallofullerenes, (M<sub>x</sub>C<sub>2</sub>)@C<sub>n</sub>, since the discovery and synthesis of C<sub>2</sub>-encapsulated metallofullerenes. Furthermore, the recent experimental results of ion mobility, UV-vis-NIR absorption, and <sup>13</sup>C-NMR studies for metallofullerenes have indicated that many of di- and tri-metallofullerenes have possibilities of C<sub>2</sub> encapsulation.

The precise structural information has provided the basis for understanding the physical properties and growth mechanism of metal-carbide endohedral metallofullerenes. An X-ray structural study is suitable for the structural characterization of endohedral metallofullerene. Several structures of C<sub>2</sub> endohedral metallofullerenes such as (Sc<sub>2</sub>C<sub>2</sub>)@C<sub>84</sub>, (Sc<sub>2</sub>C<sub>2</sub>)@C<sub>82</sub>(III), (Sc<sub>3</sub>C<sub>2</sub>)@C<sub>80</sub>, and (Y<sub>2</sub>C<sub>2</sub>)@C<sub>82</sub>(III), have been determined by the X-ray structural analysis. The positions of encapsulated atoms from these results always have shown a complicated multiple disorder structure. The disorder structure prevents a determination of precise structural information.

Under these circumstances, the systematic structural studies have to be done for revealing precise structural information, which will provide a clear understanding of structural differences. Recently, we have carried out the series of structural study for (M<sub>x</sub>C<sub>2</sub>)@C<sub>n</sub> metallofullerenes by using synchrotron X-ray powder diffraction data at SPring-8. The structures of more than ten kinds for (M<sub>x</sub>C<sub>2</sub>)@C<sub>n</sub> metallofullerenes will be presented.

[1] H. Shinohara, *Rep. Prog. Phys.*, **63**, (2000), 843-892..

Corresponding Author: Eiji Nishibori

TEL: +81-52-789-3702, FAX: +81-52-789-3724, E-mail: eiji@mcr.nuap.nagoya-u.ac.jp

## Chemical Modification of Carbon Nanohorns

Nikos Tagmatarchis

Theoretical and Physical Chemistry Institute, National Hellenic Research Foundation, 48  
Vassileos Constantinou Avenue, Athens 116 54, Hellas

tagmatar@eie.gr

Carbon nanohorns (CNHs) represent a largely unexplored carbon allotrope within the family of fullerenes and nanotubes. The unique structural features of CNHs include the presence of five 5-membered rings at one terminal tip forming a highly strained cone. Three are the critical points that differentiate CNHs from nanotubes, namely, i) purity, due to the absence of any transition metal nanoparticles during production, ii) heterogeneous surface structure, due to highly-strained conical-ends and iii) aggregation in spherical superstructures, typically ranging between 50-100 nm.<sup>1</sup>

The chemistry of CNHs has been only recently started to emerge, while their chemical modification is expected not only to advance their manipulation by introducing the desired solubility but also to fundamentally contribute on the study of their solution properties.

Herein, I will present recent results from our group on the chemical modification of CNHs. Briefly, CNHs can be functionalized by i) covalent attachment of organic units onto their skeleton<sup>2-7</sup>, and ii) non-covalent supramolecular, van der Waals, pi-pi stacking and/or coulombic electrostatic interactions with aromatic planar and/or charged organic moieties<sup>8-10</sup>. Moreover, functionalization of CNHs can be performed either at the highly-strained conical-tips or at the side-walls.<sup>11-14</sup>

## References

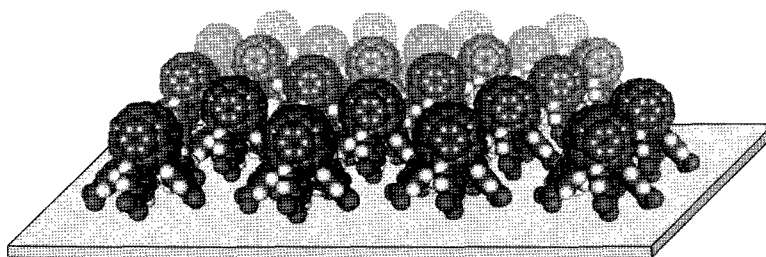
- 1 S. Iijima, M. Yudasaka, R. Yamada, S. Bandow, K. Suenega, F. Kokai, K. Takahashi, *Chem. Phys. Lett.* **1999**, 309, 165.
- 2 N. Tagmatarchis, A. Maigné, M. Yudasaka, S. Iijima, *Small* **2006**, 2, 490.
- 3 I. D. Petsalakis, G. Pagona, G. Theodorakopoulos, N. Tagmatarchis, M. Yudasaka, S. Iijima, *Chem. Phys. Lett.* **2006**, 429, 194.
- 4 G. Pagona, G. Rotas, I. D. Petsalakis, G. Theodorakopoulos, A. Maigné, J. Fan, M. Yudasaka, S. Iijima, N. Tagmatarchis, *J. Nanosci. Nanotech.* **2007**, 7, 3468.
- 5 G. Mountrichas, S. Pispas, N. Tagmatarchis, *Chem. Eur. J.* **2007**, 13, 7595.
- 6 I. D. Petsalakis, G. Pagona, G. Theodorakopoulos, N. Tagmatarchis, M. Yudasaka, S. Iijima, *Chem. Phys. Lett.* **2006**, 429, 194.
- 7 I. D. Petsalakis, G. Pagona, N. Tagmatarchis, G. Theodorakopoulos, *Chem. Phys. Lett.* **2007**, 448, 115.
- 8 G. Pagona, A. S. D. Sandanayaka, Y. Araki, J. Fan, N. Tagmatarchis, M. Yudasaka, S. Iijima, O. Ito, *J. Phys. Chem. B* **2006**, 110, 20729.
- 9 G. Pagona, J. Fan, A. Maigné, M. Yudasaka, S. Iijima, N. Tagmatarchis, *Diam. Relat. Mater.* **2007**, 16, 1150.
- 10 G. Pagona, A. S. D. Sandanayaka, A. Maigné, J. Fan, G. C. Papavassiliou, I. D. Petsalakis, B. R. Steele, N. Tagmatarchis, M. Yudasaka, S. Iijima, O. Ito, *Chem. Eur. J.* **2007**, 13, 7600.
- 11 G. Pagona, N. Tagmatarchis, J. Fan, M. Yudasaka, S. Iijima, *Chem. Mater.* **2006**, 18, 3918.
- 12 A. S. D. Sandanayaka, G. Pagona, N. Tagmatarchis, M. Yudasaka, S. Iijima, Y. Araki, O. Ito, *J. Mater. Chem.* **2007**, 17, 2540.
- 13 G. Pagona, A. S. D. Sandanayaka, Y. Araki, J. Fan, N. Tagmatarchis, G. Charalambidis, A. G. Coutsolelos, B. Boitrel, M. Yudasaka, S. Iijima, O. Ito, *Adv. Funct. Mater.* **2007**, 17, 1705.
- 14 G. Mountrichas, N. Tagmatarchis, S. Pispas, *J. Nanosci. Nanotechn.* **2008**, In press.

## Electronic and Photo-electrochemical Functions of Fullerene-Metal Complexes

Yutaka Matsuo

*Nakamura Functional Carbon Cluster Project, ERATO, Japan Science and Technology  
Agency, Hongo, Bunkyo-ku, Tokyo 113-0033, Japan*

Conversion from solar energy to electric energy is most important issue for life and many efforts have been devoted to create the solar cells. Fullerene is one of intriguing materials to construct photocurrent conversion cells, because it shows multiple redox events and long-lived excited state upon photo-absorption. We have reported the synthesis of transition metal-penta(organo)[60]fullerene complexes  $M(C_{60}R_5)L_n$  ( $M$  = metal atoms;  $R$  = Me, Ph, *etc.*;  $L$  = organic ligands). A series of iron complexes, buckyferrocenes  $Fe(C_{60}R_5)Cp$  is a compact and rigid donor-acceptor system, which undergoes reversible multiple reduction and oxidation on the fullerene and ferrocene parts. It should be noted that if these unique materials can be immobilized at an electrode surface, many intriguing devices should be created. We herein report on preparation self-assembled monolayers (SAMs) of buckyferrocenes on indium tin oxide (ITO) electrodes (Figure 1), and discuss photocurrent generation properties of this SAMs.



**Figure 1.** Self-assembled monolayer of buckyferrocenes.

Corresponding Author: Yutaka Matsuo

E-mail: matsuo@chem.s.u-tokyo.ac.jp; TEL/FAX: +81-3-5841-1476

URL: <http://www.chem.s.u-tokyo.ac.jp/users/erato/index-e.html>

#### Review of Nanotechnology R&D in NEC

Shuichi Tahara ○

*NEC Corporation, Nano Electronics Labs.*

*34 Miyukigaoka, Tsukuba, Ibaraki, Japan*

In order to build a convenient IT Society, NEC has grappled with R&D for nanotechnology as a fundamental technology for advanced IT/NW system, and has worked on the development of high-performance and energy-conscious devices with nanotechnology. And also, NEC has made significant accomplishments in the field of nanotechnology since the late 1980's. These include discovering a carbon nanotube (CNT), the solid-state devices for quantum computers and so on. In this presentation, I would like to introduce some of our nanotechnology – future LSI technology, CNT application, Si photonics for IT/NW breakthrough, and the vision and value of nanotechnology in NEC.

**E-mail : [tahara@aj.jp.nec.com](mailto:tahara@aj.jp.nec.com)**

**Tel : 029-850-1154 & Fax : 0298-56-6135**

一般講演  
**General Lecture**

**1 - 1 ~ 1 - 18**

**2 - 1 ~ 2 - 15**

**3 - 1 ~ 3 - 8**



## Phonon softening effect on Raman G-band spectra of metallic single wall carbon nanotubes

R. Saito<sup>○</sup>, K. Sasaki, K. Sato, J. S. Park

*Department of Physics, Tohoku University and CREST JST, Sendai 980-8578*

In the metallic single wall carbon nanotubes, one of the two G-band Raman spectra is known to be soft which is now generally understood by Kohn Anomaly. Recently, Farhat et al. reported Raman spectroscopy of individual metallic carbon nanotube in which the G<sup>+</sup> band becomes soft and level crossing between G<sup>+</sup> and G<sup>-</sup> Raman signal is observed as a function of the Fermi energy position. Further the Raman spectral width depends on the Fermi energy position, too. The experimental results clearly show that the electron-phonon interaction gives a finite life time of carrier and that we expect both the frequency shift and spectra broadening effect by the electron-phonon interaction when the Fermi energy matches to the Dirac cone, K point in the two dimensional Brillouin zone.

In order to investigate the phonon softening effect, we calculated the phonon self energy due to the electro-phonon interaction in which the real part of the self energy gives the frequency shift of the phonon and the imaginary part of the self energy gives the broadening of the phonon spectra. The electro-phonon interaction is calculated by the extended tight-binding calculation method which reproduced well the chirality and diameter dependence of resonance Raman intensities. The calculated phonon spectra as a function of the Fermi energy reproduce well the experimental results of phonon softening phenomena.

This work is partially supported by MEXT grant, (No. 16076201).

References: [1] H. Farhat et al., Phys. Rev. Lett., 99, 145506 (2007).

Corresponding Author: Riichiro Saito

E-mail: rsaito@flex.phys.tohoku.ac.jp

Tel&Fax: 022-795-7754, 6445

## Electroabsorption spectroscopy in single wall carbon nanotubes

○Hideo Kishida, Yoshiaki Nagasawa, Sadanobu Imamura, and Arao Nakamura

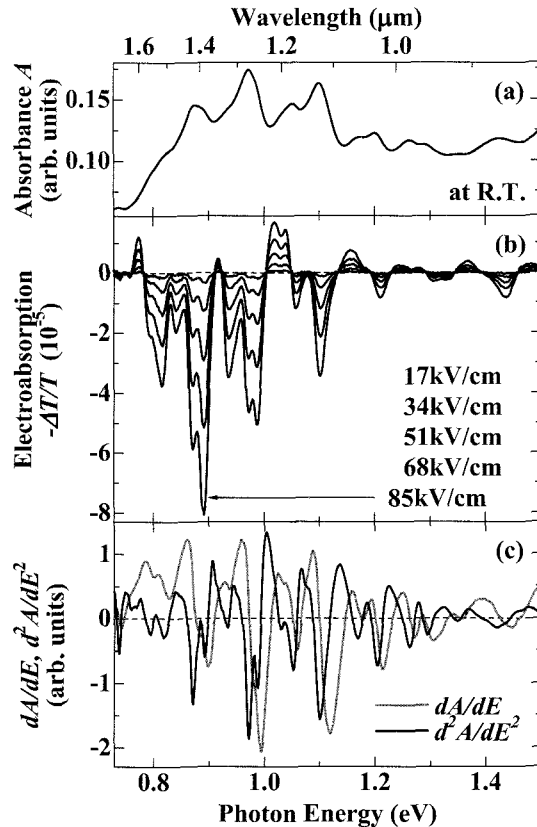
*Department of Applied Physics, Nagoya University, Nagoya 464-8603 Japan*

We have performed electroabsorption (EA) spectroscopy on micelle-wrapped single-wall carbon nanotubes (SWNT) to clarify the excited-level structure. In EA experiments, the change of absorption induced by applied electric field is measured. The electric field mixes one-photon allowed states and two-photon allowed states, so that the two-photon allowed states can be observed in the absorption measurement.

The sample was thin films of SWNT(HiPco)/SDBS embedded in gelatin. The film was formed onto an ITO/SiO<sub>2</sub> substrate, and then a semitransparent Al electrode was fabricated on the film. We applied alternating electric field (electric field 17~85kV/cm, frequency  $f=1$ kHz) between the two electrodes and measured the change of absorption using the lock-in method.

In fig.(a), we show the absorption spectra in the  $E_{11}$  region. In fig. (b), we show the EA spectra and their electric-field dependence. The intensities of EA signals are proportional to the square of the electric field. The shapes of EA spectra are not dependent on the intensity of electric field. These facts indicate that the EA signals come from electric field effects on discrete levels such as exciton levels. Most of the peaks and valleys seen in the EA spectra are reproduced by the second derivative curves (fig.(c)) of the absorption spectra. Second-derivative-like EA spectra are obtained in the case that there are two nearly degenerate discrete levels. Therefore, we assigned one to one-photon allowed “bright” exciton and the other to two-photon allowed “dark” exciton.

**Corresponding Author:** H. Kishida,  
**E-mail:** kishida@nuap.nagoya-u.ac.jp



## Photoluminescence brightening through the direct transition from isolated to bundled freestanding single-walled carbon nanotubes

○T. Kato and R. Hatakeyama

*Department of Electronic Engineering, Tohoku University, Sendai 980-8579, Japan*

Photoluminescence (PL) brightening is clearly observed as a result of the direct transition from isolated to bundled morphology in the case of using vertically-, and individually-freestanding single-walled carbon nanotubes (SWNTs) as a starting material prepared by diffusion-plasma chemical vapor deposition. Figure 1 shows the time trace of photoluminescence excitation (PLE) map from as-grown freestanding SWNTs. With an increase in the passage time after the growth, the intensity of (6,5) and (7,6) peaks drastically decrease, and in contrast, originally-broad peak intensities become obviously strong. This increment of quantum yield of SWNTs PL is explained in terms of the exciton energy transfer through the tube bundles. Since the low quantum yield of individual SWNTs PL is considered to be the critical disadvantage restricting their industrial application, the bundle engineering with standing nanotubes will be a potential candidate for realizing the superior optoelectronic device fabrication.

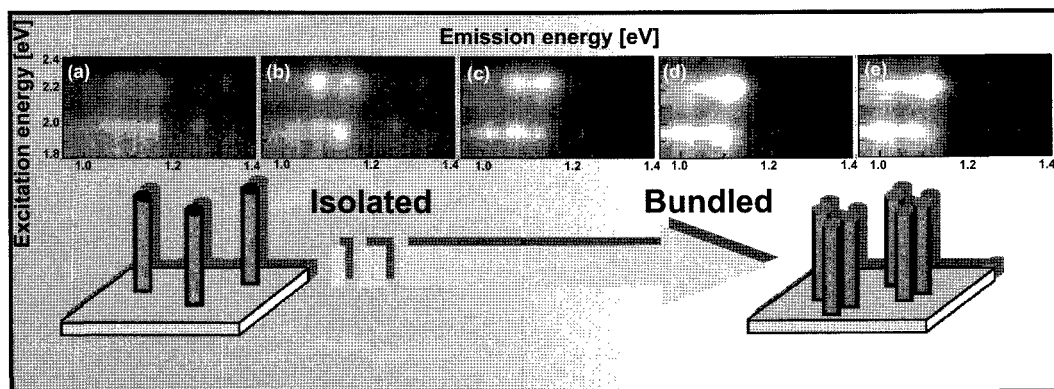


Figure 1: Time evolution of the PLE map measured just after the growth (a), at 1h (b), 3.5h (c), 7.5h (d), and 10h (e), respectively. All data are plotted on the same color scale.

**Corresponding Author T. Kato**

**E-mail: kato12@ecei.tohoku.ac.jp**

**Tel&Fax: +81-22-795-7046 / +81-22-263-9225**

## Multiexciton recombinations and exciton fine structures studied by a single carbon nanotube photoluminescence spectroscopy

○Kazunari Matsuda<sup>1</sup>, Tadashi Inoue<sup>1</sup>, Yoichi Murakami<sup>2</sup>, Shigeo Maruyama<sup>2</sup>,  
and Yoshihiko Kanemitsu<sup>1</sup>

<sup>1</sup>*Institute for Chemical Research, Kyoto University, Gokasho Uji, Kyoto, Japan*

<sup>2</sup>*Department of Mechanical Engineering, The University of Tokyo, 7-3-1, Hongo, Bunkyo, Tokyo, Japan*

The electronic properties of single-walled carbon nanotubes (SWNTs) have attracted a great deal of attention. The characteristic optical properties of SWNTs are determined by the dynamics of excitons with extremely large binding energies due to the strong Coulomb interaction. It is also expected that the strong Coulomb interaction would enhance the many body effects of excitons. The spectroscopic observation of a single carbon nanotube is a useful to understand the dynamics and many body effects of excitons in SWNTs [1-3].

We studied the temperature and excitation power dependence of photoluminescence (PL) spectra from spatially isolated single SWNTs using a single nanotube spectroscopy [3]. It is found that the linewidth of the observed narrow PL spectrum corresponding to homogeneous linewidth (Fig. 1(a)) arises from the exciton-dephasing with consideration of exciton lifetime of 30 ps [4]. The PL linewidth linearly decreases with decreasing temperature, which implies that the exciton-dephasing is dominated by the interaction between the exciton and the phonon mode with very low energy. In the high excitation conditions using femtosecond laser pulses, the homogeneous linewidth broadens nonlinearly with an increase in excitation intensity as shown in Fig. 1(b). Our observation suggests that the broadening of homogeneous linewidth arises from the annihilation of excitons through a rapid Auger recombination process. The multiexciton dynamics and exciton fine structures will be discussed.

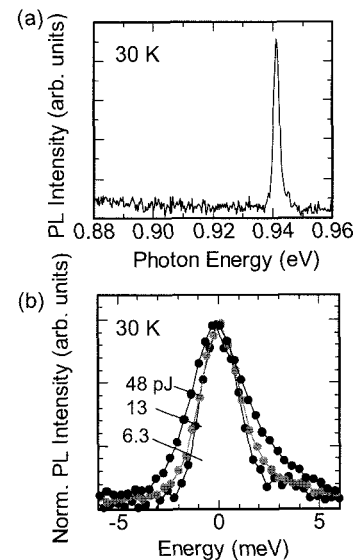


Fig.1 (a) and (b) PL spectra of a single carbon nanotube at 30 K.

### References

- [1] K. Matsuda, Y. Kanemitsu, K. Irie, T. Saiki, T. Someya, Y. Miyauchi, and S. Maruyama, *Appl. Phys. Lett.* **86**, 123116 (2005).
- [2] T. Inoue, K. Matsuda, Y. Murakami, S. Maruyama, and Y. Kanemitsu, *Phys. Rev. B* **73**, 233401 (2006).
- [3] K. Matsuda, T. Inoue, Y. Murakami, S. Maruyama, and Y. Kanemitsu, *Phys. Rev. B* **77**, 033406 (2008).
- [4] H. Hirori, K. Matsuda, Y. Miyauchi, S. Maruyama, and Y. Kanemitsu, *Phys. Rev. Lett.* **97**, 257401 (2006).

Corresponding Author: Kazunari Matsuda

TEL: +81-774-38-4515, FAX: +81-774-38-4515, E-mail: matsuda@scl.kyoto-u.ac.jp

## Optical and electrical properties of semiconducting SWNT extracted using polyfluorene

○S. Kazaoui<sup>1</sup>, N. Izard<sup>1</sup>, K. Hata<sup>1</sup>, T. Okazaki<sup>1</sup>, T. Saito<sup>1</sup>, Y. Sato<sup>1</sup>, K. Suenaga<sup>1</sup>,  
Y. Futami<sup>2</sup>, N. Minami<sup>2</sup>

<sup>1</sup>Research Center for Advanced Carbon Materials, AIST, Tsukuba 305-8565, Japan

<sup>2</sup>Nanotechnology Research Institute, AIST, Tsukuba 305-8565, Japan

The production of pure semiconducting single-wall carbon nanotubes (s-SWNT) is essential in several areas such as basic research, standardization and applications (FET transistors, optoelectronic devices, sensors). Significant progresses were already achieved using for instance DNA, density-gradient concentration and polymer wrapping to extract s-SWNT from “as-produced SWNT powders”.

Very recently, s-SWNT were extracted with polyfluorene (such as Poly(9,9-di-*n*-octyl-fluorenyl-2,7-diyl)) in toluene solution assisted by sonication/centrifugation methods [1], using the conditions we have already described for poly(phenylene-vinylene) (MEHPPV) and polythiophene (P3OT) [2].

In this study, we have optimized the centrifugation conditions in order to selectively extract near-armchair semiconducting while totally discarding metallic nanotubes. Clear evidences were obtained by photoluminescence (Fig.1), optical absorption (Fig. 2), Raman as well as by electrical measurements. At this symposium, very interesting optical and electrical properties from such pure semiconducting SWNT will be presented.

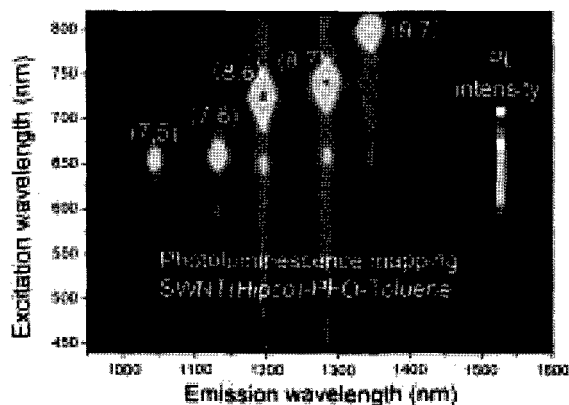


Fig. 1: Photoluminescence map of SWNT(HiPco)-PFO

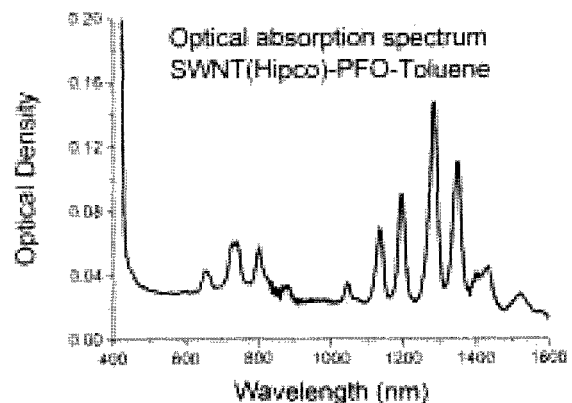


Fig. 2: Optical absorption of SWNT(HiPco)-PFO

[1] (a) Nish et al. *Nature Nanotechnology* 2, 640 (2007) (b) Chen et al. *Nano Letters* 7, 3013 (2007).

[2] (a) S. Kazaoui et al, *Appl. Phys. Lett.* **87**, 211914 (2005), (b) *J. Appl. Phys.* **98**, 084314 (2005).

**Corresponding Author:** S. Kazaoui (カザウイ)

**E-mail:** [s-kazaoui@aist.go.jp](mailto:s-kazaoui@aist.go.jp), **Tel:** 029-861-4838, **Fax:** 029-861-4851

## Three dimensional effects in the boron-doped carbon nanotubes

○Takashi Koretsune and Susumu Saito

*Department of Physics, Tokyo Institute of Technology  
2-12-1 Oh-okayama, Meguro-ku, Tokyo 152-8551*

Carbon nanotubes are considered to be attractive materials for nanoscale electronic device in the next generations. To control the transport properties including superconductivity[1], boron doping will play an important role. So far, we have clarified the effect of boron doping in the isolated single walled carbon nanotubes[2]. However, to discuss the experimental situation and the possibility of superconductivity, it is inevitable to consider the three dimensionality such as bundles of the carbon nanotubes or multiwalled carbon nanotubes. Thus we study the effect of inter-layer interaction in the bundled or multiwalled carbon nanotubes using the density functional theory.

Here, we take (10,0) carbon nanotubes as a typical semiconductor tube and consider the bundles of (10,0) carbon nanotubes. It is found that the peak of the density of states in the isolated carbon nanotubes will remain in the bundles of carbon nanotubes though its height is decreased by three dimensional effect. We discuss the change of the Fermi level density of states by the inter-layer interaction. We also consider the double-walled carbon nanotube, (10,0)@(19,0), where borons are doped only in the inner tube and discuss the charge transfer effect.

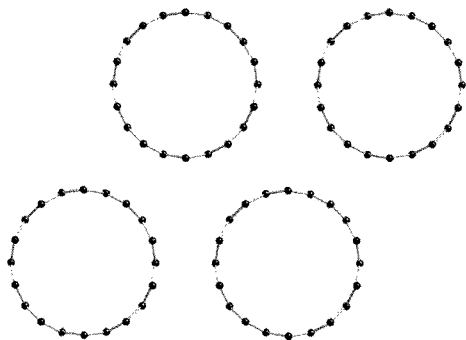
### References:

- [1] I. Takesue et al., Phys. Rev. Lett. **96** 057001 (2006)  
[2] T. Koretsune and S. Saito, submitted.

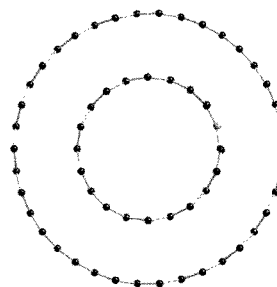
**Corresponding Author:** Takashi Koretsune

**E-mail:** koretune@stat.phys.titech.ac.jp

**Tel:** 03-5734-2387



**Fig 1 Bundle of carbon nanotubes studied.**



**Fig 2 Double walled carbon nanotube studied.**

## Conductivity Enhancement of Boron-Doped MWNTs Synthesized from Methanol Solution Containing Boric Acid

○ Satoshi Ishii, Tohru Watanabe, Shunsuke Tsuda, Takahide Yamaguchi, and  
Yoshihiko Takano

*Nano System Functionality Center, National Institute for Materials Science, 1-2-1,  
Sengen, Tsukuba, Ibaraki 305-0047, Japan*

Carbon nanotubes (CNTs) with high conductivity are required for a variety of applications, such as a conducting film, an electrically-conductive coating, a probe of SPM, and nanowirings inside LSI, while increasing the conductivity of the CNTs has not been realized yet by chirality control.

In this study, we have introduced conduction carriers into multi-walled carbon nanotubes (MWNTs) by boron-doping to enhance the conductivity. When considering boron-doped diamond<sup>[1,2]</sup> and graphite<sup>[3]</sup>, the boron was expected to provide the conduction carriers effectively for the carbon allotropes. We have synthesized boron-doped MWNTs by our CVD method which uses a methanol solution of boric acid as a source material. The boron-doped MWNTs were synthesized from the source solution containing 1.0 atm% and 2.0 atm% of the boron.

Figure 1 shows Raman spectra of the boron-doped MWNTs. A position of a G-band shifts systematically to higher Raman shift side with increasing a boron concentration. This indicates that a carbon site was substituted by the doped boron in the MWNTs. On the other hand, broadenings of both the G and D-bands were originated from inhomogeneity of the boron and defects in the MWNTs.

Figure 2 shows temperature dependence of normalized conductivity  $\sigma/\sigma_{RT}$  of the boron-doped MWNTs, where  $\sigma_{RT}$  is the conductivity at room temperature. The conductivity of each individual MWNT was measured by four-point method from room temperature to 2 K. The four electrodes were fabricated on a target individual MWNT by using electron beam lithography technique. The  $\sigma/\sigma_{RT}$  was enhanced over wide temperature range by increasing the boron concentration. The doped boron provides the conduction carriers for the MWNT effectively increasing the conductivity.

**References:** [1] E. Ekimov et al., *Nature* **428**, 542 (2004).

[2] Y. Takano et al., *Appl. Phys. Lett.* **85**, 2851 (2004).

[3] M. Endo et al., *Phys. Rev. B* **58**, 8991 (1998).

**Corresponding Author:** Satoshi Ishii

**E-mail:** [ISHII.Satoshi@nims.go.jp](mailto:ISHII.Satoshi@nims.go.jp) **Tel:** +81-29-859-2644 **Fax:** +81-29-859-2601

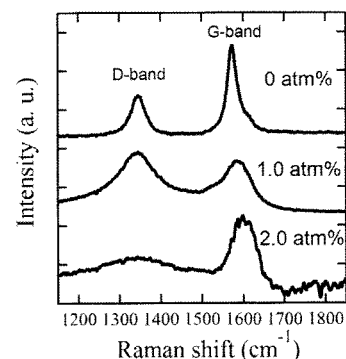


Fig. 1 Raman spectra of MWNTs.

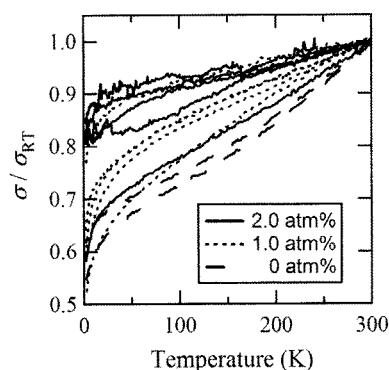


Fig. 2 Temperature dependence of  $\sigma/\sigma_{RT}$ .

## Recent progress of study of carbon-nanotube superconductivity

○J.Haruyama<sup>1,4</sup>, S.Maruyama<sup>2</sup>, H.Shinohara<sup>3,4</sup>

<sup>1</sup>*Aoyama Gakuin University, 5-10-1 Fuchinobe, Kanagawa 229-8558, Japan*

<sup>2</sup>*Tokyo University, 7-3-1 Hongo, Bunkyo-ku, Tokyo 113-0033, Japan*

<sup>3</sup>*Nagoya University, Furo-cho, Chigusa, Nagoya 464-8602, Japan*

<sup>4</sup>*JST-CREST, 4-1-8 Hon-machi, Kawaguchi, Saitama 332-0012, Japan*

**Abstract:** Superconductivity (SC) in carbon nanotubes (CNTs) is quite interesting issue from many standpoints; e.g., 1. From physics of one-dimensional (1D) SC, 2. from electron correlation in 1D conductors, 3. as recently found carbon-related new-superconductor family (CaC<sub>6</sub> and boron-doped diamond), and 4. From possibility of high-T<sub>c</sub> SC (~40K). We reported SC in arrays of multi-walled CNTs (MWNTs) for resistance drop with the highest T<sub>c</sub> = 12K [1] and its correlation with contact structures between metal electrode and MWNTs. After then, based on the report, many theories for the CNT-SC have been proposed and are attracting considerable attention; e.g., 1. Carrier doping effect in MWNTs and phase transitions [2], 3. Carrier doping effect in (10,10) single-walled CNTs [3], and 4. Correlation between SC and edge state [4].

Here, we have had progress in the experiments after reporting ref.[1]. In the talk, I will introduce recent some experimental results of the MWNT-SC; i.e., 1. Meissner effect with T<sub>c</sub> = ~20K in the honey comb array structure of alumina template [5], 2. Interplay between SC and Tomonaga-Luttinger liquid states in partially end-bonded MWNTs [6], 3. Confirmation of presence of boron in the MWNTs by NMR [6]. Moreover, I will briefly talk about Meissner effect found in sheets of boron-doped single-walled CNTs synthesized in controlled doping manner [7].

SC in CNTs is promising. Realizing higher T<sub>c</sub> is highly expected.

### References

- [1] I. Takesue, J. Haruyama et al., **Phys.Rev.Lett.** 96, 057001 (2006)
- [2] E. Perfetto and J. Gonzalez, **Phys.Rev.B** 74, 201403(R) (2006)
- [3] T. Koretsune and S. Saito, To be published in **Phys.Rev.B**
- [4] K. Sasaki, R. Saito et al., **J. Phys. Soc. Jpn.** 76, 033702 (2007)
- [5] N. Murata, J. Haruyama, M. Matsudaira, Y. Yagi, E. Einarsson, S. Chiashi, S. Maruyama, T. Sugai, N. Kishi, H. Shinohara et al., **Phys.Rev.B** 71, 081744 (2007)
- [6] M. Matsudaira, J. Haruyama, N. Murata, Y. Yagi, E. Einarsson, S. Maruyama, T. Sugai, H. Shinohara, To be published in **Physica E** (In submission to Phys.Rev.Lett.)
- [7] K. McGuire, M. S. Dresselhaus, A. M. Rao et al., **Carbon** 43, 219 (2005)

**Corresponding Author: Junji Haruyama**

**E-mail: J-haru@ee.aoyama.ac.jp**

**Tel&Fax: 042-759-6256 (Fax: 6524)**



## Local electronic structure of a carbon nanotube on metal surface

○Yousoo Kim<sup>1</sup>, Hyung-Joon Shin<sup>1,2</sup>, Sylvain Clair<sup>1,#</sup> and Maki Kawai<sup>1,2</sup>

<sup>1</sup>RIKEN, 2-1 Hirosawa, Wako, Saitama 351-0198, Japan

<sup>2</sup>Department of Advanced Materials Science, The University of Tokyo, Chiba 277-8561, Japan

# Present address: INRS-EMT, Université du Québec, 1650 Boul. Lionel-Boulet, Varennes, QC, Canada J3X 1S2

### Abstract:

The scanning tunneling microscopy (STM) study shows that the nature of the interface between a nanotube and a metal surface induces a charge transfer that directly rules the doping level of nanotubes. Whereas it is known that SWCNT on Au(111) are p-doped, we found that it is possible to produce n-doped SWCNT on Cu(111). Additionally, we show that the reconstruction pattern of the Au(111) surface is responsible for periodic oscillations in the electronic structure of adsorbed nanotubes.

The early STM experiments on SWCNT have provided highly valuable details on their structure and their related electronic properties. However, little attention was given to the effect of the adsorption to a metal substrate, and basically only Au(111) surfaces were used. Here we propose systematic investigations on the interaction of a SWCNT with the well defined Au(111) and Cu(111) metal surfaces. The nanotubes were deposited in situ via a vacuum-compatible dry contact transfer (DCT) technique which provides surfaces free of impurities as shown in Fig.1.

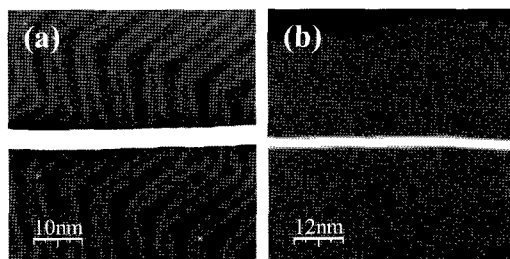


Fig.1 STM images of a single CNTs adsorbed on (a) Au(111) and (b) Ag(100) single crystal surfaces.

### References:

1. C. Rabot, S. Clair, Y. Kim, and Maki Kawai, Jpn. J. Appl. Phys. **46** (2007) 5572-76.
2. S. Clair, C. Rabot, Y. Kim, and Maki Kawai, J. Vac. Sci. Tech. B **25** (2007) 1143-1146.

**Corresponding Author : Yousoo Kim**

**E-mail : ykim@riken.jp**

**Tel&Fax : +81-48-467-4073, +81-48-462-4663**

**Long-Ranged Bandgap Modulation of SWCNT on Ag(100)**○Hyung-Joon Shin<sup>1</sup>, Sylvain Clair<sup>1</sup>, Yousoo Kim<sup>1</sup>, and Maki Kawai<sup>1,2</sup><sup>1</sup>*Surface Chemistry Laboratory, RIKEN, 2-1 Hirosawa, Wako, Saitama 351-0198 Japan.*<sup>2</sup>*Department of Advanced Materials, University of Tokyo, 5-1-5 Kashiwanoha, Kashiwa, Chiba 277-8651, Japan.*

When metal/single-walled carbon nanotube (SWCNT) interface is formed, charge transfer between metal and SWCNT occurs and the position of SWCNT Fermi-level is shifted by local electrostatic potential perturbation. Most STM or STS of SWCNT have been measured on Au (111) surface so far, and the Fermi-level shifts of about 0.2eV to the valence band on gold have been reported experimentally and theoretically [1, 2]. In this study, we investigated the electronic structure of SWCNT on Ag (100) surface by STM and STS at low temperature (4.7K). Ultra-clean SWCNT on silver surface were prepared by dry contact transfer (DCT) technique [3]. The STS results showed that the Fermi-level of SWCNT was shifted to the conduction band, since the work function of Ag (100) (4.4eV) is much smaller than that of Au (111) (5.3eV) and that of SWCNT (4.8 ~ 5.0eV). In addition, we observed that the periodic modulation developed on semiconducting (6, 2) SWCNT over whole length (~300nm). Interestingly, we could observe bandgap modulation of same period from spatially-resolved STS mapping. Considering the chirality and unit cell of SWCNT, the period of modulation showed a good epitaxial relationship between SWCNT and Ag (100) in this configuration. The amount of charge transfer depends on the atomic distance between carbon and silver atom. Thus, the shift of bandgap might be enhanced for the atoms having a good epitaxial relationship. At the peak positions of the height profile, the bandgap was shifted downwards (to the valence band), which implies that carbon and silver atoms have a better epitaxial configuration at these locations.

[1] J.W.G. Wildöer, L.C. Venema, A.G. Rinzler, R.E. Smalley, and C. Dekker. *Nature* 391, 59 (1998)[2] Y. Xue and S. Datta, *Phys. Rev. Lett.* 83, 4844 (1999).[3] P.M. Albrecht and J.W. Lyding, *Appl. Phys. Lett.* 83, 5029 (2003).

Hyung-Joon Shin

hjshin@riken.jp

Tel:+81-48-46-9174 Fax: +81-48-462-4663

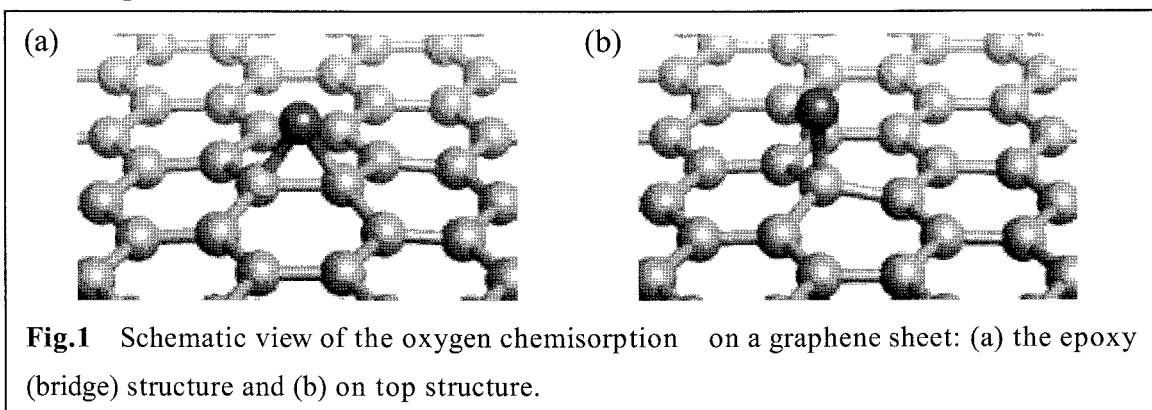
## First Principles Calculations for Electronic Properties of Diffusing Oxygen Atoms on the Surface of Graphene and Nanotubes

○Takazumi Kawai and Yoshiyuki Miyamoto

*Nano Electronics Research Laboratories, NEC Corporation  
34, Miyukigaoka, Tsukuba, Ibaraki 305-8501, JAPAN*

Recent experiments showed the potential ability of graphene not only nanotubes as a electronic devices with small size and high performance[1]. However, it is well-known that the behavior of oxygen drastically change the electronic properties of such devices due to the high accumulation of electrons and further destruction of graphitic sp<sup>2</sup> network. Thus, the properties of oxygen atoms on the graphitic surface is one of the most important issue for future device applications of nano graphitic materials.

Here, we performed first principles calculations for oxygen diffusion on the surface of graphene. The epoxy (bridge) position (Fig.1(a)) is the most stable for chemisorption, and on top position (Fig.1(b)) has 0.89 eV higher energy than epoxy structure. We found that the insertion of an oxygen atom into a C-C bond does not form the stable structure when a periodic unitcell is used, although the insertion structure was claimed to be stable for cluster calculation[2]. We have also studied oxygen diffusion on carbon nanotubes and will discuss the electronic properties and the chirality dependent anisotropic diffusion.



[1] H.B. Heersche, *et al*, *Nature* **446** (2007) 56.

[2] J.-L. Li, *et al*, *Phys. Rev. Lett.* **96** (2006) 176101.

**Corresponding Author: Takazumi Kawai**

**E-mail: takazumi-kawai@mua.biglobe.ne.jp**

**Tel&Fax: +81-29-850-1554, +81-29-856-6136**

## Field Emission Properties of Single-Walled Carbon Nanotubes with a Variety of Emitter-Morphologies

○Yosuke Shiratori<sup>1</sup>, Koji Furuichi<sup>2</sup>, Suguru Noda<sup>1</sup>, Hisashi Sugime<sup>1</sup>, Yoshiko Tsuji<sup>1</sup>, Zhengyi Zhang<sup>3</sup>, Shigeo Maruyama<sup>3</sup> and Yukio Yamaguchi<sup>1</sup>

<sup>1</sup>*Dept. of Chemical System Engineering, The University of Tokyo, Tokyo 113-8656, Japan*

<sup>2</sup>*DAINIPPON SCREEN MFG. CO., LTD., Kyoto 602-8585, Japan*

<sup>3</sup>*Dept. of Mechanical Engineering, The University of Tokyo, Tokyo 113-8656, Japan*

A number of issues are important for future CNT-FED development: (I) A low-temperature and/or short-time growth directly on cathodes through simple and safe processes, (II) a giant tip-enhancement of an applied field and (III) a uniform spacial current distribution, that is, a large number density of emission sites resulting in a mild current per emitter. We focus here on SWNT-emitters prepared using alcohol catalytic CVD (ACCVD)<sup>1</sup>. Prior to application of ACCVD for device fabrication, suitable catalyst compositions to promote a rapid growth of high quality SWNTs and the FE properties of the obtained SWNTs must be systematically studied. We report field emission properties of SWNT-emitters with different morphologies and discuss their potential for FED-applications.

SWNT-emitters were prepared on Si substrates with Co/Al<sub>2</sub>O<sub>3</sub> layers through ACCVD, which realizes a reaction time of 10 s to grow a 4 μm-thick SWNT film. FE properties of SWNTs are tunable by the morphological control of the top-surface (Fig. 1). For a textured Si cathode with well separated SWNT-bundles (Fig. 1d), the turn-on electric field to extract a current density of 1 μA/cm<sup>2</sup> was 2.4 V/μm, and a current density of 0.8 mA/cm<sup>2</sup> was recorded at 4 V/μm. Large area uniformity of luminescence (0.5 cm<sup>2</sup>) was also obtained. Protrusion of emitters is crucial and the optimization of number density, protrusion length and inter-protrusion distance is necessary for uniform field emission and increased operating life. Texturing of substrates effects a large and selective field enhancement at specific protrusive emitters. Currently, SWNTs prepared from ethanol via a fast and safe process showed field emission characteristics suitable for electron sources.

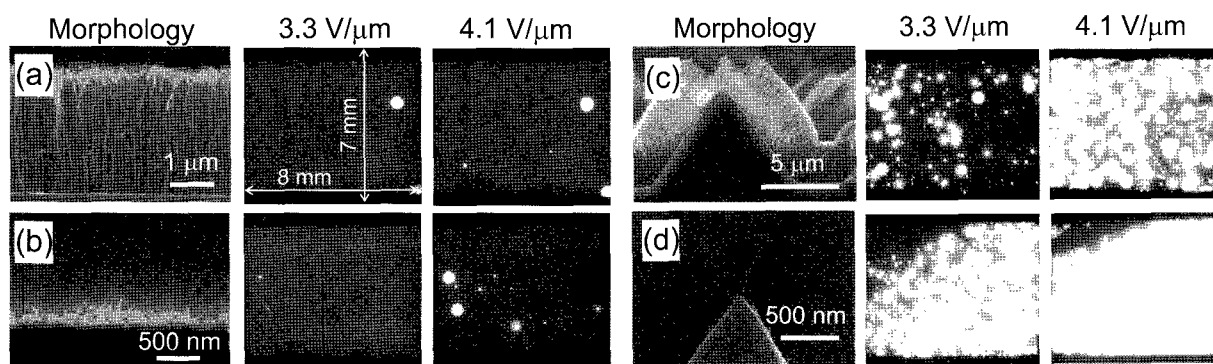


Fig. 1. Cross-sectional SEM micrographs and pictures of luminescence from the rear surface of the anode at 3.3 and 4.1 V/μm; (a) VA-SWNTs, (b) CNT-grass, (c) VA-SWNTs on Si pyramids and (d) free-sanding bundles on Si pyramids.

[1] S. Maruyama, R. Kojima, Y. Miyauchi, S. Chiashi, and M. Kohno: Chem. Phys. Lett. **360** (2002) 229.

Corresponding Author: Yosuke Shiratori and Suguru Noda, TEL: +81-3-5841-7330, FAX: +81-3-5841-7332, E-mail: y-shiratori@chemsys.t.u-tokyo.ac.jp, noda@chemsys.t.u-tokyo.ac.jp

## Magnetoresistance of the Metallic Nanotubes observed by Contactless Method

Yugo Oshima<sup>○</sup>, Hirotaka Suzuki, Yoshihiro Iwasa and Hiroyuki Nojiri

*Institute for Materials Research, Tohoku University, Katahira 2-1-1,  
Aoba, Sendai 980-8577, Japan*

### Abstract:

We have observed the magnetoresistance of the highly-oriented single-wall nanotubes (SWNT) film by contactless method. At 4.2 K, The magnetoresistance increases linearly up to 14 T when the magnetic field is applied along the tube axis. This is different from the results observed in a SWNT film (non-oriented), which shows a negative magnetoresistance or saturation at high magnetic field [1, 2]. In general, the transport properties of the SWNT are difficult to evaluate since there is a high contact resistance between the electrodes and SWNT. Therefore, we have employed the cavity perturbation techniques (contactless method) [3], which eliminate the problems of the contact resistance for the transport measurements of SWNT. Using this technique, no electrode is needed, and we can obtain the high-frequency conductivity of the SWNT by just comparing the Q factor and the resonance frequency of the cavity with and without the sample. We believe that the observed positive magnetoresistance is an intrinsic behavior of the SWNT, which is due to the Aharonov–Bohm effect of the metallic nanotubes. The angular dependence and the temperature dependence will also be presented, and the results are discussed.

### References:

- [1] G. T. Kim *et al.*, Phys. Rev. B **58** (1998) 16064.
- [2] T. Takano *et al.* *to be published*.
- [3] O. Klein *et al.*, Int. J. Inf. Milli. Waves **14** (1993) 2423.

**Corresponding Author: Yugo Oshima**

**E-mail: oshima@imr.tohoku.ac.jp**

**Tel&Fax: +81-(0)22-215-2017, +81-(0)22-215-2016**

## Influence of surrounding materials on heat conduction of carbon nanotubes: Molecular dynamics simulations

○Junichiro Shiomi and Shigeo Maruyama\*

<sup>1</sup>*Department of Mechanical Engineering, The University of Tokyo  
7-3-1 Hongo, Bunkyo-ku, Tokyo 113-8656, Japan*

Characterization of thermal properties of single-walled carbon nanotubes (SWNTs) is a key issue for their prospective electrical and thermal device applications. An SWNT is expected to be a good heat conductor with the extraordinary long phonon mean free paths [1-3]. As a result, phonon transport exhibits complex diffusive-ballistic feature for realistic nanotube-length in many applications even at room temperature. This gives rise to unique steady and unsteady heat conduction characteristics [4-8]. Especially, the length effect of the thermal conductivity or conductance [4,5,8] has caught particular attentions due to its practical importance and there are ongoing discussions on the scattering dynamics of long wave phonons and the effect of low-dimensional confinement.

Although the characteristics of intrinsic heat conduction of SWNTs have been explored extensively for ideal thermal boundary conditions, in practical situations, interfacial heat transfer between SWNTs and heat sinks/sources is expected to determine the overall heat transfer performance. Such interfaces not only give rise to thermal boundary resistances but also influence the intrinsic heat conduction. In a system with significant contribution from ballistic heat transport, the intrinsic phonon distribution function and thus effective heat conduction is expected to depend strongly on the mode-dependent scattering dynamics at the interfaces. In the current study, this aspect is explored by using equilibrium and non-equilibrium molecular dynamics methods. The boundary scattering and its influence on the long wave heat flux correlations is discussed.

- [1]. C. Yu *et.al.*, *Nano Lett.* **5**, (2005) 1842.
- [2]. E. Pop *et.al.*, *Nano Lett.* **6**, (2006) 96.
- [3]. S. Berber, *et.al.*, *Phys. Rev. Lett.* **84**, (2000) 4613
- [4]. S. Maruyama, *Micro. Therm. Eng.* **7**, (2003) 41.
- [5]. N. Mingo and D. A. Broido, *Nano Lett.* **5**, 1221 (2005).
- [6]. J. Shiomi and S. Maruyama, *Phys. Rev. B*, **73**, 205420 (2006)
- [7]. J. Shiomi and S. Maruyama, *Phys. Rev. B*, **74**, 155401 (2006)
- [8]. J. Shiomi and S. Maruyama, *Jpn. J. Appl. Phys.* (in press).

Corresponding Author: Shigeo Maruyama

E-mail: maruyama@photon.t.u-tokyo.ac.jp,

Tel/Fax: +81-3-5800-6983

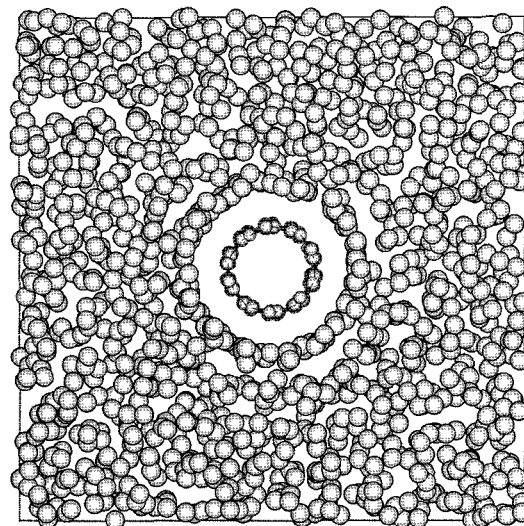


Figure 1. (5, 5) SWNT surrounded by matrix

## Specific Surface Area Measurement for Purity and SWNT Selectivity Analysis

○ Don N. Futaba, Jundai Gotou, Takeo Yamada, Satoshi Yasuda, Motoo Yumura,  
Sumio Iijima and Kenji Hata

*National Institute of Advanced Industrial Science and Technology (AIST), Tsukuba,  
305-8565, Japan*

As the development of carbon nanotube (CNT) technology is reliant upon the availability of CNTs, a great effort has been placed on the improvement of single-walled carbon nanotube (SWNT) synthesis. As a result, a number of groups have reported significant advances in the *efficient* and *highly pure* synthesis of tall SWNT forests (ref) which suggest the possibility for mass production (1-4). However, the techniques for the simple and accurate assessment of the purity and SWNT selectivity trail far behind the ability to synthesize it. Historically, Raman spectroscopy and transmission electron microscopy (TEM) have been the tools which provided qualitative and quantitative assessments. However, both techniques are limited in terms of sampling amount, interpretation, and the need for a skilled operator.

Here, we present the use of specific surface area (SSA) analysis using the Brunauer, Emmett, and Teller (BET) method as a simple and accurate tool of assessing the purity and selectivity of SWNT samples. Sensative to both properties, BET-SSA analysis provides an indispensable tool for the simple, fast and accurate evaluation of macroscopic (10s mg) samplings of SWNTs.

### References:

- [1] K. Hata *et al*, Science, **306**, 1241 (2004).
- [2] G. Zhang, *et al*. Proc. Nat. Am. Soc., **102**, 16141 (2005).
- [3] G. Zhong, T. Iwasaki, J. Robertson, and H. Kawarada, J. Phys. Chem. B, **111**, 1907 (2007).
- [4] S. Noda, *et al*. Jpn. J. Appl. Phys., **46**, L399 (2007).

**Corresponding Author: Don N. Futaba**

**E-mail: d-futaba@aist.go.jp**

**Tel&Fax: (029) 861-5080 ext 44402**

## Chirality Dependence on Destabilizing Agents Added to CMC-stabilized Carbon Nanotube Dispersions

○Hiroshi Saito and Masahito Sano

*Department of Polymer Science and Engineering, Yamagata University 992-8510, Japan*

Dispersing carbon nanotubes (CNTs) in solution is important for both academic and industrial researches and various methods have been reported. One of the common methods is to ultrasonicate CNTs in water with the presence of stabilizing chemicals, such as sodium dodecyl sulfate (SDS) and sodium carboxymethyl cellulose (CMC). We have reported that dispersing efficiency is improved by additions of antifoam agents, such as an oligomer of polyether (PE-M), to the ultrasonicated SDS mixture [1]. PE-M eliminates air bubbles and foams to allow the ultrasonic wave to reach CNT surfaces more efficiently. Also, we have shown that ultrasonication on SDS mixture in air promotes sonochemical reactions of gaseous nitrogen and oxygen with water to yield acid species. This results in lowering of pH, which protonates CNTs with the consequence that absorption and Raman spectroscopic characters of metallic and thick semiconducting CNTs are altered.

PE-M is designed as an antifoaming agent for SDS in water. We have found that although PE-M acts as an antifoaming agent for CMC, it does not improve dispersing CNTs. In fact, continued additions of PE-M destabilized CMC-stabilized CNT dispersion and CNTs coagulated at higher PE-M concentrations. Unlike SDS case, the solution pH remained nearly constant over one hour of ultrasonication. Thus, no protonation of CNTs occurred in the case of CMC.

We have monitored Raman spectra as CMC-stabilized CNT dispersions were destabilized by CMC. Coagulated CNTs were collected by centrifugation and the supernatant was analyzed. Intensities of both RBM and G-bands were reduced because less CNTs could be in the supernatant. Interestingly, each peak in RBM was not reduced uniformly and the reduction rate (the relative reduction of peak intensities at a given CMC concentration) depended on chirality. Also, the line shape around G-band changed depending on the CMC concentration.

[1] H. Saito, M. Sano, "Improved Ultrasonic Dispersion of Carbon Nanotubes", abstract presented at the 32<sup>nd</sup> Fullerene-Nanotubes General Symposium, Nagoya, 2007.

Corresponding Author: Masahito Sano

E-mail: mass@yz.yamagata-u.ac.jp

Tel&Fax: +81-238-26-3072



## Electrochemical and Diameter-selective Cutting of Carbon Nanotubes

○Shigekazu Ohmori<sup>1</sup>, Takeshi Saito<sup>1,2</sup>, Satoshi Ohshima<sup>1</sup>, Motoo Yumura<sup>1</sup>  
and Sumio Iijima<sup>1,3</sup>

<sup>1</sup> *Research Center for Advanced Carbon Materials, AIST, Ibaraki 305-8565 Japan*

<sup>2</sup> *PRESTO, Japan Science and Technology Agency, Kawaguchi 332-0012, Japan*

<sup>3</sup> *Department of Materials Science and Engineering, Meijo Univ., Nagoya 468-8502, Japan*

Carbon nanotubes (CNTs) are expected to be highly potential in various applications such as electronics and nano-medical devices. In these applications, the length of CNTs is one of the most important structural parameters, since it affects on their dispersibility (and processability, as well). Many researchers have been reported mechanical [1] and chemical [2,3] cutting processes of CNTs.

Herein, we report a novel method for cutting single-walled CNTs (SWCNTs) by electrochemical oxidation reaction on the surface of anodic SWCNT electrode. The optimized cutting voltage was estimated to be 10V for the SWCNTs with wide average diameter of 1.8 nm and the cutting reaction could not be observed at below the optimized voltage (see Fig. 1). On the other hand, it has been found that the narrow SWCNTs (mean dia.: ca. 0.9 nm) were cut at lower voltage (4V) than that of the wide ones abovementioned. This result indicates the possibility of the diameter-selective cutting in our electrochemical method.

### References

- [1] Jie Liu, Andrew, et. al., *science*, **280** (1998) 1253.  
[2] Li Qingwen, et. al., *J. Phys. Chem.*, **106** (2002) 11085.  
[3] Z. Gu, et. al., *Nano Letters*, **2** (2002) 1009.

Corresponding author: Takeshi Saito

Tel: +81-29-861-4863, Fax: +81-29-861-3392, E-mail: takeshi-saito@aist.go.jp

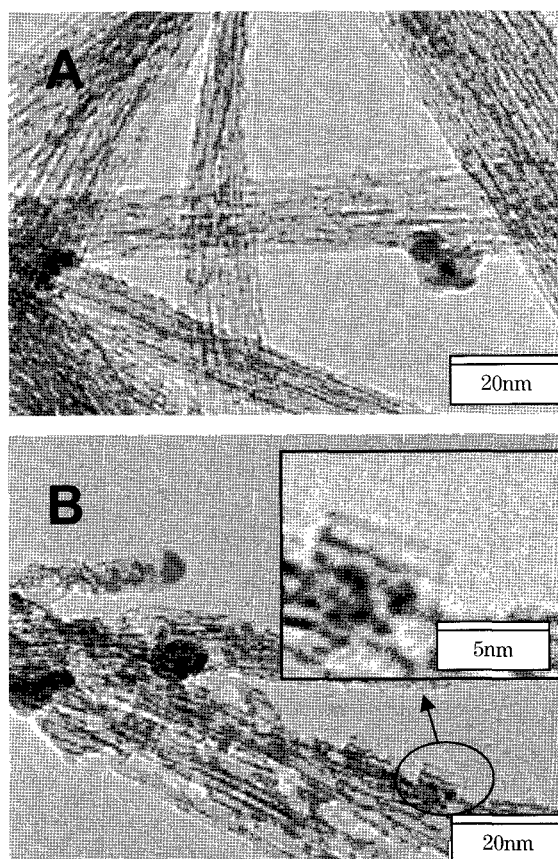


Fig. 1. TEM images of SWCNTs electrochemically treated at A 6V and B 10V.

## Bending deformation of carbon nanotubes caused by a five-seven pair couple defect

○ Kei Wako<sup>1</sup>, Tatsuki Oda<sup>2</sup>, Masaru Tachibana<sup>1</sup>, Kenichi Kojima<sup>1</sup>

<sup>1</sup>Graduate School of Integrated Science, Yokohama City University,  
Yokohama 236-0027, Japan

<sup>2</sup>Graduate School of Natural Science and Technology, Kanazawa University,  
Kanazawa 920-1192, Japan

Carbon nanotubes are promising building blocks for construction of nanosized electronic and electromechanical devices due to their mechanical and electronic properties. Therefore an investigation of plastic deformation and formation of structural defects that are caused by mechanical deformations such as bending deformation is important. Recently, Nakayama *et al.* reported that double-walled carbon nanotubes (DWNTs) were deformed plastically by an application of electric current under bending deformation [1].

We have carried out tight-binding molecular dynamics simulation for the DWNTs under bending deformation in the previous study [2]. As the result, structural defects named 5-7 pair couple defect were formed by atom emission and these defects were thermally and energetically stable. Thus, our results indicate that the 5-7 pair couple defects are responsible for the origin of the plastic deformation. In the present study, to investigate the characteristics of the 5-7 pair couple defect which were formed in single-walled carbon nanotubes (SWNTs), their stable structure and binding energy were analyzed.

Figures 1 (a) and (b) show a removed chain cluster of atoms and a 5-7 pair couple defect in a (8,8) SWNT. For various numbers of removed atoms, stable structure of the defective SWNT was obtained by structural optimization. The bending angles of (8,8) nanotubes are plotted as a function of the number of removed atoms in Fig. 1 (c). Figure 1 (d) shows that the schematic figure of the nanotube with the maximum bending angle and the 5-7 pair couple defects which were formed after removing 14 atoms. Moreover a dependence of bending angles on the diameter of nanotubes was investigated. As results, it was confirmed that the structure of the nanotube with these several kind of defects corresponded to the experimental results.

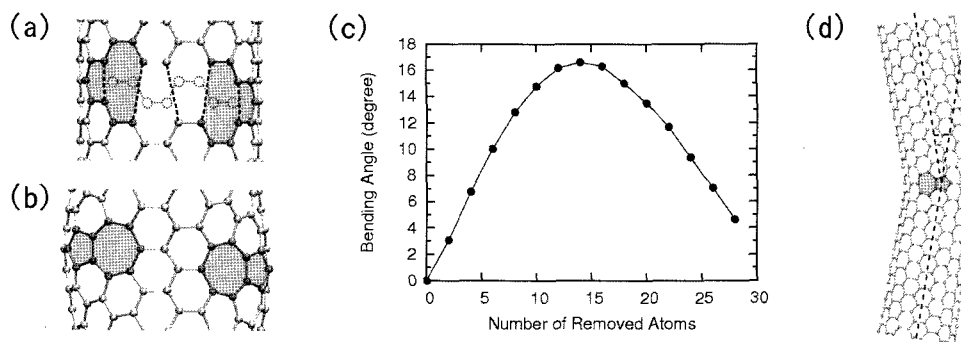


Figure 1: (a) Removing eight atoms and (b) 5-7 pair couple defect in the (8,8) nanotubes, (c) bending angle as a function of the number of removed atoms and (d) stable structure of the (8,8) nanotube that contains the 5-7 pair couple defect which were formed after removing 14 atoms.

[1] Y. Nakayama *et al.* Jpn. J. Appl. Phys. **44**, L720 (2005)

[2] K. Wako, I. Okada, M. Tachibana, K. Kojima, and T. Oda, J. Appl. Phys. **102**, 113522 (2007)

Corresponding Author: Kei Wako TEL: +81-045-787-2171, E-mail: s045913a@yokohama-cu.ac.jp

## Scanning Tunneling Spectroscopy Mapping of a Single Lu@C<sub>82</sub> on Alkanethiol Self Assembled Monolayer

○Y. Yasutake<sup>1</sup>, K. Kono<sup>1</sup>, N. Kobayashi<sup>1</sup>, M. Iwamoto<sup>1</sup>, H. Umemoto<sup>2</sup>,  
Y. Ito<sup>2</sup>, H. Okimoto<sup>2</sup>, H. Shinohara<sup>2,3</sup>, and Y. Majima<sup>1</sup>

<sup>1</sup>*Department of Physical Electronics, Tokyo Institute of Technology, Tokyo 152-8552, Japan*

<sup>2</sup>*Department of Chemistry, Nagoya University, Nagoya 464-8602, Japan*

<sup>3</sup>*Institute for Advanced Research, Nagoya University, Nagoya 464-8602, Japan*

### Abstract:

Endohedral metallofullerenes are one of the candidate materials for nanoelectronics and spintronics applications due to their unique electronic and magnetic properties which associated with the charge transfer interaction between the encapsulated metal atom and a fullerene cage[1]. We demonstrated that single endohedral metallofullerene orientation switching phenomena by introducing alkanethiol self-assembled monolayer(SAM) as interlayer to control the interaction between endohedral metallofullerene and metal substrate.[2, 3] To realize molecular switching device by using endohedral metallofullerene, it is important to characterize the local electrical properties of single endohedral metallofullerenes.

Here, we report the local electrical properties of Lu@C<sub>82</sub> molecule on heptanethiol SAM by scanning tunneling microscopy(STM) images and scanning tunneling spectroscopy(STS) mapping. From high-resolution STM images of Lu@C<sub>82</sub> at 65 K, we observed the stripe structure which indicates that Lu@C<sub>82</sub> molecules on heptanethiol do not rotate freely. Then we measured STS at different 64 points on a single Lu@C<sub>82</sub> molecule on heptanethiol at 65 K. From differential conductance ( $dI/dV$ ) spectra, we observed two peaks centered at -0.5 V and 1.0 V which correspond to HOMO and LUMO energy levels, respectively. HOMO peak intensity shows a spatial dependence. We discuss the relationship between the molecular orientation and the spatial dependence of HOMO peak intensity. By considering the effective applied voltage in double barrier tunnel junction, we also estimate that the intrinsic HOMO-LUMO gap of Lu@C<sub>82</sub> and the Fermi energy level shift of Lu@C<sub>82</sub> on heptanethiol.

### References:

- [1] H. Shinohara, *Rep. Prog. Phys.* **63**,843 (2000).
- [2] Y. Yasutake, Z. Shi, T. Okazaki, H. Shinohara and Y. Majima, *Nano Lett.*, **5**, 1057 (2005).
- [3] Y. Yasutake, Z. Shi, T. Okazaki, H. Shinohara and Y. Majima, *J. Nanosci. Nanotechnol.*, **6**, 3460 (2006).

Corresponding Author: Yuhsuke Yasutake

TEL: +81-3-5734-2673, FAX: +81-3-5734-2673, E-mail: yasutake@nanoele.pe.titech.ac.jp

**Estimation of the amounts of transferred electrons in Lu-entrapped Metallofullerenes**

○Takafumi Miyazaki<sup>1</sup>, Ryohei Sumii<sup>2,3</sup>, Hisashi Umemoto<sup>4</sup>, Haruya Okimoto<sup>4</sup>, Toshiki Sugai<sup>4</sup>,  
Hisanori Shinohara<sup>4</sup>, Shojun Hino<sup>1</sup>,

<sup>1</sup> *Graduate School of Science & Technology, Ehime University*

<sup>2</sup> *Institute for Molecular Science*

<sup>3</sup> *Research Center for Materials Science, Nagoya University*

<sup>4</sup> *Graduate School of Science, Nagoya University*

Ultraviolet photoelectron spectra (UPS) of C<sub>82</sub> endohedral fullerenes containing Lu atom(s) have been measured with synchrotron radiation light source. Principally the spectra are almost identical with those obtained with the endohedral fullerenes with the same cage symmetry. Usually entrapped metal atoms donate electrons and the amounts of transferred electrons have been deduced by either experimentally or theoretically. Lutetium 4f electron levels can be observed in our present UPS. The position of 4f<sub>7/2</sub> level varies from 9.46 eV (Lu<sub>2</sub>C<sub>2</sub>@C<sub>82</sub> isomers), 9.70 eV (Lu<sub>2</sub>@C<sub>82</sub> isomers) to 9.86 eV (Lu@C<sub>82</sub>(I)). This shift is induced by the difference in the charge on Lu atom(s), that is, chemical shift, and can be a good indication for amounts of transferred electrons to the cage.

Corresponding Author : S. Hino, E-mail : hino@eng.ehime-u.ac.jp, phone : 089-927-9924

## 2-3

### $^{13}\text{C}$ NMR Study of $\text{Pr}_2@\text{C}_{80}$ and $\text{LaPr}@\text{C}_{80}$

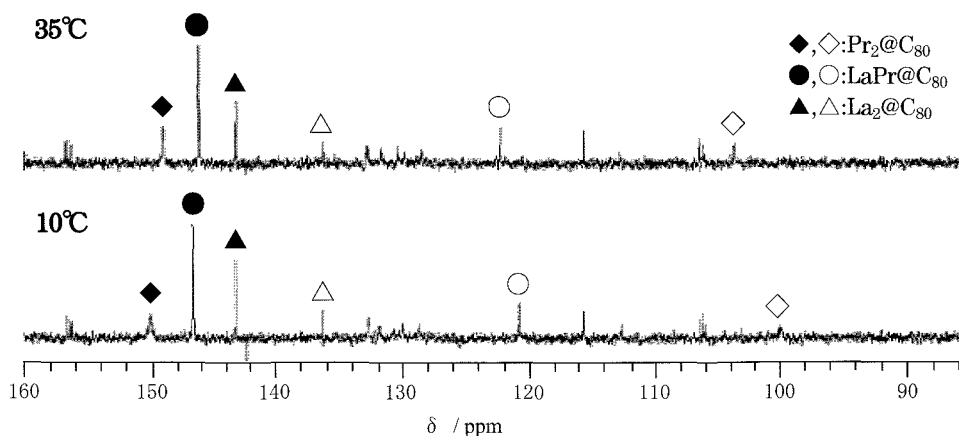
○Manabu Ito<sup>1</sup>, Shiho Nagaoka<sup>1</sup>, Takeshi Kodama<sup>1</sup>, Yoko Miyake<sup>1</sup>,  
Shinzo Suzuki<sup>2</sup>, Koichi Kikuchi<sup>1</sup>, Yohji Achiba<sup>1</sup>

<sup>1</sup>*Department of Chemistry, Tokyo Metropolitan University, Hachioji, 192-0397, Japan*

<sup>2</sup>*Department of Physics, Kyoto Sangyo University, Kamigamo-Motoyama,  
Kita-ku, Kyoto, 603-8555, Japan*

So far, we have studied paramagnetic  $^{13}\text{C}$  NMR shifts of  $\text{Ce}_2@\text{C}_{80}$  and  $\text{CeLa}@\text{C}_{80}$  to clarify a magnetic property of encaged  $\text{Ce}^{3+}$  [1,2], which has a 4f electron. Recently, we have reported  $^{13}\text{C}$  NMR spectra of  $\text{Pr}_2@\text{C}_{80}$  [3], in which  $\text{Pr}^{3+}$  has two 4f electrons, and compared them with those of  $\text{Ce}_2@\text{C}_{80}$  and  $\text{CeLa}@\text{C}_{80}$ . In this study, we report the production and  $^{13}\text{C}$  NMR spectra of  $\text{LaPr}@\text{C}_{80}$ , and analyze the temperature dependence of paramagnetic  $^{13}\text{C}$  NMR shifts of  $\text{Pr}_2@\text{C}_{80}$  and  $\text{LaPr}@\text{C}_{80}$ .

Fig.1 shows the  $^{13}\text{C}$  NMR spectra of  $\text{MM}'@\text{C}_{80}$  ( $\text{M}, \text{M}'=\text{La}, \text{Pr}$ ) in  $\text{CS}_2$ . As shown in Fig.1, the six peaks were assigned to  $\text{La}_2@\text{C}_{80}$ ,  $\text{Pr}_2@\text{C}_{80}$ , and  $\text{LaPr}@\text{C}_{80}$ , respectively. The peaks of  $\text{Pr}_2@\text{C}_{80}$  and  $\text{LaPr}@\text{C}_{80}$  show temperature dependence due to the magnetic moment of encaged  $\text{Pr}^{3+}$ . Detailed analysis of paramagnetic  $^{13}\text{C}$  NMR shift of  $\text{Pr}_2@\text{C}_{80}$  and  $\text{LaPr}@\text{C}_{80}$  will be discussed in the presentation.



**Fig. 1**  $^{13}\text{C}$  NMR spectra of  $\text{MM}'@\text{C}_{80}$  measured at 125 MHz in  $\text{CS}_2$ .

[1] T. Ichikawa et al., The 27<sup>th</sup> Fullerene-Nanotubes General Symposium, 58 (2004).

[2] T. Komaki et al., The 28<sup>th</sup> Fullerene-Nanotubes General Symposium, 128 (2005).

[3] M. Ito et al., The 32<sup>th</sup> Fullerene-Nanotubes General Symposium, 157 (2007).

Corresponding Author: Takeshi Kodama

E-mail: kodama-takeshi@c.metro-u.ac.jp

Tel:+81-42-677-2530, Fax:+81-42-677-2525

## 2-4

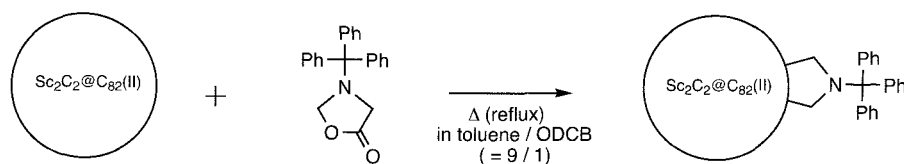
### Structure of metal-carbide endohedral metallofullerene $\text{Sc}_2\text{C}_2@C_{82}(C_{2v})$

○Koji Nakajima<sup>1</sup>, Yuko Yamazaki<sup>1</sup>, Takatsugu Wakahara<sup>1</sup>, Takahiro Tsuchiya<sup>1</sup>,  
Yutaka Maeda<sup>2</sup>, Takeshi Akasaka<sup>1\*</sup>, Markus Waelchli<sup>3</sup>, Kenji Yoza<sup>4</sup>,  
Naomi Mizorogi<sup>5</sup>, and Shigeru Nagase<sup>5</sup>

<sup>1</sup>Center for Tsukuba Advanced Research Alliance, University of Tsukuba, <sup>2</sup>Department of Chemistry, Tokyo Gakugei University, <sup>3</sup>Bruker Biospin K. K., <sup>4</sup>Bruker AXS K. K., <sup>5</sup>Department of Theoretical and Computational Molecular Science, Institute for Molecular Science

Metal-carbide encapsulated metallofullerenes have attracted special interest because of encapsulation of the  $\text{C}_2$  unit together with several metal atoms. Recently, it was revealed that the structure of the dimetallofullerenes such as  $\text{Sc}_2\text{C}_{84}(\text{III})$  and  $\text{Y}_2\text{C}_{84}(\text{III})$  is not normal  $\text{M}_2@C_{84}$  type, but  $\text{M}_2\text{C}_2@C_{82}$  type encapsulated the metal carbide by  $^{13}\text{C}$  NMR spectral determination[1, 2], single crystal[3] and powder X-ray diffraction analyses[4,5]. Moreover, it is confirmed that  $\text{Y}_2\text{C}_{84}(\text{I, II})$  have metal-carbide encapsulated  $\text{Y}_2\text{C}_2@C_{82}$  structures by  $^{13}\text{C}$  NMR spectral determination[2]. However, the structures of  $\text{Sc}_2\text{C}_{84}(\text{I, II})$  have not been verified.

We herein report that the structure of  $\text{Sc}_2\text{C}_{84}(\text{II})$  is also not  $\text{Sc}_2@C_{84}$  but  $\text{Sc}_2\text{C}_2@C_{82}$ , which has the  $C_{82}(C_{2v})$  cage, by means of  $^{13}\text{C}$  NMR spectral analysis and theoretical calculations. We have succeeded in X-ray single-crystal structure analysis of pyrrolidinometallofullerene  $\text{Sc}_2\text{C}_2@C_{82}(\text{II})(\text{CH}_2)_2\text{NTrt}$  (Trt = triphenylmethyl).



[1] Iiduka, Y. et al., *Chem. Commun.* **2006**, 2057-2059. [2] Inoue, T. et al., *J. Phys. Chem. B* **2004**, *108*, 7573-7579. [3] Iiduka, Y. et al., *Angew. Chem. Int. Ed.* **2007**, *46*, 5562-5564. [4] Nishibori, E. et al., *ChemPhysChem* **2006**, *7*, 345-348. [5] Nishibori, E. et al., *Chem. Phys. Lett.* **2006**, *433*, 120-124.

Corresponding Author: Takeshi Akasaka

TEL&FAX: +81-29-853-6409 E-mail: akasaka@tara.tsukuba.ac.jp

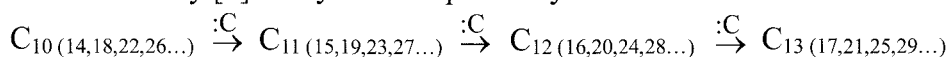
## Discovery of the atomic-carbon-insertion reactions for fullerene growth

○Teruhiko Ogata<sup>1</sup>, Tetsu Mieno<sup>2</sup>, Yutaka Shibi<sup>1</sup>, and Yoshio Tatamitani<sup>1</sup>

<sup>1</sup>Department of Chemistry and <sup>2</sup>Department of Physics, Shizuoka University, Shizuoka 422-8529, Japan

We have synthesized carbon monoxides  $C_nO$  and fullerene  $C_{70}$  from  $C_{60}$  by the atomic-carbon-insertion reactions (ACIRs) Fig.1 [1]. Atomic carbon of  $:C$  “jump” into CC bonds without cleavage of the overall molecular structure and without significant side reactions. The ACIRs seem to be involved in at least two processes of fullerene formation, that is, in the formation of the soot precursors and of the small carbon clusters  $n < 40$ .

For the mass spectrum in the range of 9 to 30 clusters, Cox and co-workers observed a periodic alteration in the ion signal amplitude every four atoms, with maxima at  $n = 11, 15, 19, 23$ , and 27 and minima at  $n = 13, 17, 21, 25$ , and 29. On other hand, Achiba and co-workers observed strong signals at  $n = 10, 14, 18$ , and 22 [3], these preferential evaporations are also observed by the photodissociation which is reminiscent of the Hückel rule  $4n+2$  for aromaticity [4]. They are interpreted by the ACIRs as follows:



Many authors suggest that the precursor of the fullerenes are soot [2b,3b,5]. Achiba and co-workers found that the mass spectra of fullerenes, emerge at lowest fluence, were observed even if only soot targets were exposed by the laser light [3b], and a certain exothermic process occurred related to the formation of fullerenes [3c]. We have efficiently created soot in the photolysis of  $C_3O_2$  at  $1000^\circ C$ , where atomic-carbons were only active chemicals and can cause the ACIRs. The ACIRs are efficient because they are abundant and their activation energy is zero or low. Atomic-carbon has much higher formation enthalpy than  $C_2$  and can release the surplus energy in the formation of the  $sp^2$  bond, which makes the following rearrangements and degradations easier. Therefore, the ACIRs are overwhelmingly efficient especially under rather unfavorable conditions such as the soot formations. These facts strongly suggest that the soot precursors are formed by the ACIRs.

- [1] T. Ogata et al. (a) *JACS*, **117**, 3593 (1995); (b) *J. Chem. Phys.*, **102**, 1493 (1995); (c) 第33回本シポジウム, 3P-28 (2007); (d) Proceedings of CABON 2007 Conference, B083 (2007).  
 [2] Cox and co-workers (a) *JCP*, **81**, 3322 (1984); (b) *ibid.* **88**, 1588 (1988).  
 [3] Achiba & co-workers (a) *JCP*, **106**, 9954(1997); (b) *ibid.* **107**, 8927(1997); (c) *Eur.Phys.J.D*, **16**, 369(2000).  
 [4] M. Pellarin et al., *JCP*, **117**, 3088 (2002).  
 [5] E. Osawa et al., *JPC*, **106**, 7135 (2002).

Corresponding Author: Teruhiko Ogata Tel&Fax: +81-54-238-4935 E-mail: sctogat@ipc.shizuoka.ac.jp

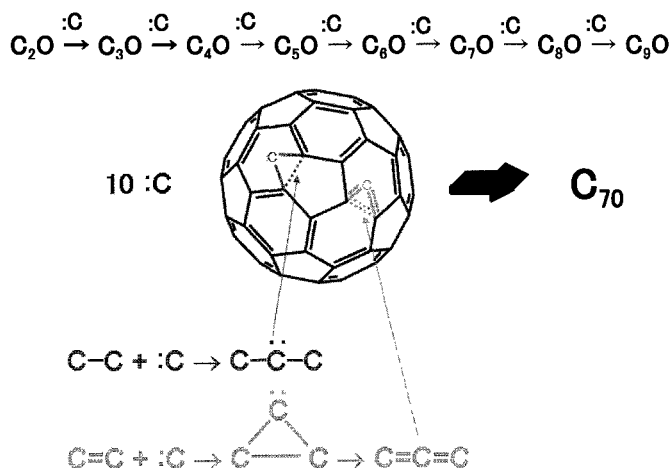


Fig.1. The atomic-carbon-insertion reactions (ACIRs)

## 2-6

### Chemical modification on a non-IPR metallofullerene: $\text{La}_2@C_{72}$

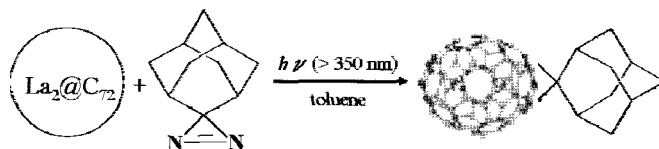
Xing Lu,<sup>†</sup> Hidefumi Nikawa,<sup>†</sup> Takahiro Tsuchiya,<sup>†</sup> Yutaka Maeda,<sup>‡</sup> Takeshi Akasaka,<sup>\*,†</sup> Naomi Mizorogi,<sup>§</sup> and Shigeru Nagase<sup>\*,§</sup>

<sup>†</sup>Center for Tsukuba Advanced Research Alliance, University of Tsukuba, Tsukuba, Ibaraki 305-8577, Japan, email: akasaka@tara.tsukuba.ac.jp,

<sup>‡</sup>Department of Chemistry, Tokyo Gakugei University, Tokyo 184-8501, Japan,

<sup>§</sup>Department of Theoretical and Computational Molecular Science, Institute for Molecular Science, Okazaki 444-8585, Japan.

**Abstract:**  $\text{La}_2@C_{72}$  was previously proposed to have a non-IPR cage structure of either #10611 or #10958 by  $^{13}\text{C}$  NMR measurements.<sup>[1]</sup> Theoretical calculations indicated that the cage of #10611 is energetically more stable,<sup>[2,3]</sup> but unambiguous experimental results are still lacking. In this work, a carbene reagent was adopted to functionalize  $\text{La}_2@C_{72}$ . Monoadducts were successfully isolated and characterized with various kinds of measurements, including single-crystal XRD method, which unambiguously presented that  $\text{La}_2@C_{72}$  takes the  $D_2$  symmetric carbon cage of #10611, with two pairs of fused-pentagons.



#### References

- [1]. Kato, H.; Taninaka, A.; Sugai, T.; Shinohara, H. *J. Am. Chem. Soc.* **2003**, *125*, 7782-7783.
- [2]. Slanina, Z.; Chen, Z.; Schleyer, P. R.; Uhlík, F.; Lu, X.; Nagase, S. *J. Phys. Chem. A* **2006**, *110*, 2231-2234.
- [3]. Popov, A. A.; Dunsch, L. *J. Am. Chem. Soc.* **2007**, *129*, 11835-11849.



## Physical Properties of H<sub>2</sub> Endohedral C<sub>60</sub>

Katsumi Tanigaki<sup>1</sup>, Takeshi Rachi<sup>1</sup>, Ryotaro Kumashiro<sup>1</sup>, Yasujiro Murata<sup>2</sup>, Koichi Komatsu<sup>2</sup>,  
Toru Kakiuchi<sup>3</sup>, Hiroshi Sawa<sup>3</sup>, Yoshimitsu Kohama<sup>4</sup>, Satoru Izumisawa<sup>4</sup>, Hitoshi Kawaji<sup>4</sup>  
and Tooru Atake<sup>4</sup>

<sup>1</sup>*Department of Physics, Graduate of Science, Tohoku University*

<sup>2</sup>*Institute of Chemical Research, Kyoto University*

<sup>3</sup>*Material Structure Science, KEK*

<sup>4</sup>*Materials and Structures Laboratory, Tokyo Institute of Technology*

<sup>1</sup>*6-3 Aoba, Aramaki, Aoba, Sendai 980-8578, Japan*

<sup>2</sup>*Uji, Kyoto 611-0011, Japan*

<sup>3</sup>*1-1, Oho, Tsukuba 305-0801, Japan*

<sup>4</sup>*259 Nagatsuta-cho, Midori-ku, Yokohama 226-8503, Japan*

The physical properties of atoms or molecules encapsulated inside nano-size cages have been one of the very intriguing scientific issues. For performing experiments in order to have reasonable insight to this issue, a large scale synthesis of such materials is needed. Recent success in macroscopic scale production of hydrogen-molecule endohedral C<sub>60</sub> using a molecular surgery method in chemistry has opened a door to a scientifically realistic research stage.

Using this advanced elegant chemical reaction method, pure H<sub>2</sub>@C<sub>60</sub> was prepared in a 10 mg scale, which affords one to carry out specific heat experiments as a function of temperature ranging from 300 K down to 0.085 K using a <sup>3</sup>He/<sup>4</sup>He dilution refrigerator. The excess heat capacity appearing in H<sub>2</sub>@C<sub>60</sub> above 5 K, when it compared to that of C<sub>60</sub>, can successfully be analyzed in terms of the contributions of the localized vibrations and the free rotational motions of the encapsulated hydrogen molecule. In the low temperature region, another heat capacity anomaly was found around 0.6 K with the excess entropy of about 0.75Rln3, and the origin can be rationalized by considering the splitting of the rotational energy level of hydrogen molecule. The results indicate that the rotational ground state ( $J = 1$ ) of the ortho-hydrogen should be split due to the lower symmetry of C<sub>60</sub> than that of the high temperature phase above the rotational phase transition at 260 K. The H<sub>2</sub>@C<sub>60</sub> system has also been tested for observation of superconductivity. These measurements are very important to discuss phonons in solid state physics.

The present work is partially supported by the 21st century COE program "Particle Matter Hierarchy" MEXT Japan, and Center for Interdisciplinary Research Project in Tohoku University. This work was performed by a Grant-in-Aid from the Ministry of Education, Science, Sports and Culture of Japan, No. 15201019, 1771088, 18204030, 18651075 and 19014001.

Corresponding Author: Katsumi Tanigaki

TEL: +81-022-795-6469, FAX: +81-022-795-6470, E-mail: tanigaki@sspns.phys.tohoku.ac.jp

## Pressure-Induced Structural Phase Transition of Two-dimensionally polymerized C<sub>60</sub>

○Yuichiro Yamagami and Susumu Saito

*Department of Physics, Tokyo Institute of Technology  
2-12-1 Oh-okayama, Meguro-ku, Tokyo 152-8551*

Since the discovery of polymerization of solid C<sub>60</sub> (fcc C<sub>60</sub>) [1,2], polymer phases of solid C<sub>60</sub> have attracted a lot of attention. As a polymer phase, three phases proposed by Núñez-Regueiro *et al.* are well known: the 1D orthorhombic, the 2D orthorhombic ('tetragonal'), and the 2D rhombohedral phases [3,4]. These polymer phases are interesting targets for pressurization since there is a possibility that another polymer phase might be synthesized by pressuring one of them. A variety of studies motivated by this idea have been performed [5,6]. Recently, it was reported that a 3D polymer phase was synthesized by pressuring the 2D orthorhombic phase [7]. The single crystal X-ray structure analysis revealed that the product possessed the body-centered orthorhombic lattice, and the structural model derived from the Rietveld refinement was also presented.

In the present work, we first performed the constant-pressure molecular dynamics (MD) study of the 2D orthorhombic phase for pressure range about experimental condition (12, 14, 16, 18, 20, 22, 24, 26, 28 GPa). In all pressure conditions, the 2D orthorhombic phase transformed into a three-dimensional polymer phase. Most of all structures obtained from the MD calculation possess the lattice in which C<sub>60</sub> molecules form the body-centered orthorhombic lattice. Moreover, the lattice constants are all relatively close to the experimental values [7]. In addition, the obtained structures were found to have almost the same covalent-bond network. However, there is a little difference in the bonding pattern of the direction of a short edge of the conventional cell. In the obtained structures, C<sub>60</sub> molecules on a diagonal line of the conventional cell are connected in the same manner as the experimental model, and those on a middle edge are connected with two covalent bonds (horizontal four-membered ring). Furthermore, those on a short edge are also connected with four to six covalent bonds. Next, we performed the LDA analysis for one of the obtained structures. Covalent-bond network of the obtained structure is mostly preserved through the geometry optimization in the LDA. It is also found that the lattice constants are still close to the experimental values. In addition, it is clarified that the obtained structure is metal from the electronic density of states.

[1] A.M. Rao *et al.*, *Science* **259**, 955 (1993).

[2] Y. Iwasa *et al.*, *Science* **264**, 1570 (1994).

[3] C.H. Xu and G.E. Scuseria, *Phys. Rev. Lett.* **74**, 274 (1995).

[4] Núñez-Regueiro, L. Marques, J-L. Hodeau, O. Béthoux, and M. Perroux, *Phys. Rev. Lett.* **74**, 278 (1995).

[5] S. Okada, S. Saito, and A. Oshiyama, *Phys. Rev. Lett.* **83**, 1986 (1999).

[6] D.H. Chi, Y. Iwasa, T. Takano, T. Watanuki, Y. Ohishi, and S. Yamanaka, *Phys. Rev. B* **68**, 153402 (2003).

[7] S. Yamanaka *et al.*, *Phys. Rev. Lett.* **96**, 076602 (2006).

Corresponding Author: Yuichiro Yamagami

TEL: 03-5734-2386, FAX: 03-5734-2739, E-mail: yamagami@stat.phys.titech.ac.jp

## Imaging of Transportation of Single Hydrocarbon Chain through Nano-sized Pore

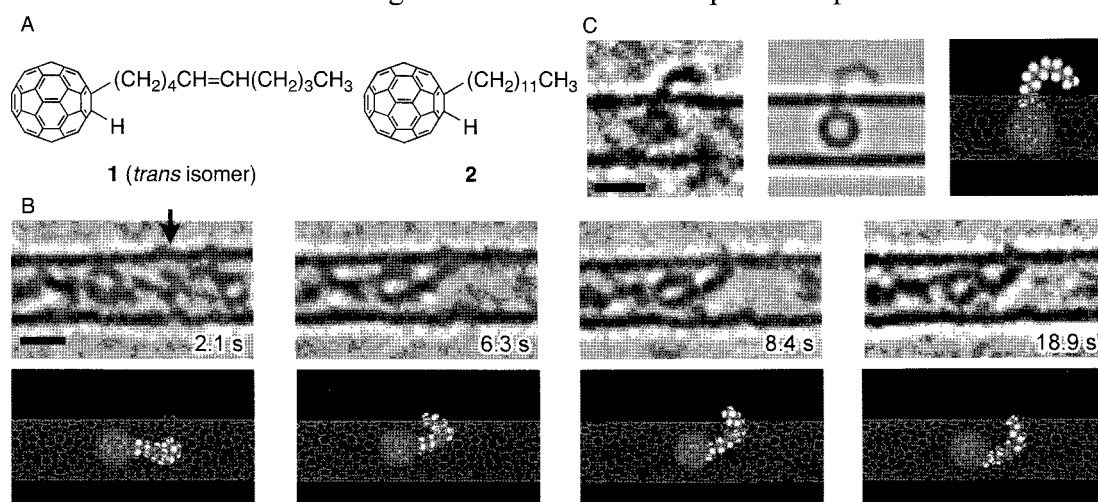
○Takatsugu Tanaka<sup>1</sup>, Masanori Koshino<sup>2</sup>, Niclas Solin<sup>1</sup>,  
Hiroyuki Isobe<sup>1,¶</sup>, Eiichi Nakamura<sup>1,2</sup>

<sup>1</sup>Department of Chemistry, The University of Tokyo, Tokyo 113-0033, Japan

<sup>2</sup>ERATO, Nakamura Functional Carbon Cluster Project, JST, Tokyo 113-0033, Japan

Molecular transport through nano-sized pores in a film, membrane, or wall structure is an event of fundamental importance in a number of physical, chemical, and biological processes. However, there is a lack of experimental methods that can obtain molecular-level information on the structure and orientation of the molecules at the time of transportation, and on the way that molecules interact with pores.

We recently demonstrated that time-resolved, near-atomic resolution imaging by transmission electron microscope (TEM) provides a powerful method to study the structural changes of single organic molecules in motion.<sup>[1]</sup> Here, we report that the TEM methodology can image in what structure and orientation hydrocarbon chains pass through a nano-sized pore on carbon nanotubes (CNTs), and how they interact with the pore. Such information thus far was unavailable for the investigation of molecular transportation phenomena.



**Figure.** (A) The structures of the sample molecules. (B) Sequential TEM images of alkenyl fullerene **1** encapsulated in CNT as a function of time with the corresponding molecular models shown directly below. The figure captions refer to the time after initiation of observation. Scale bar shows 1 nm. The arrow shows the position of the pore on the sidewall of the CNT. (C) TEM image of alkyl fullerene **2** in CNT (shown in left). A simulation and the corresponding model are shown on the right-hand side. Scale bar shows 1 nm.

¶ Present Address: Department of Chemistry, Tohoku University, Aoba-ku, Sendai 980-8578, Japan

References: [1] M. Koshino, *et al.*, *Science* **2007**, 316, 853; N. Solin, *et al.*, *Chem. Lett.* **2007**, 36, 1208.

Corresponding Authors: Hiroyuki Isobe and Eiichi Nakamura

E-mail: isobe@mail.tains.tohoku.ac.jp; nakamura@chem.s.u-tokyo.ac.jp

Tel&Fax: 03-5800-6889

## Synthesis of Pd-filled carbon nanotubes for the tip of SPM

○ Tomokazu Sakamoto<sup>1</sup>, Chien-Chao Chiu<sup>1</sup>, Kei Tanaka<sup>2</sup>, Masamichi Yoshimura<sup>1</sup>,  
Kazuyuki Ueda<sup>1</sup>

1) *Nano High-Tech Research Center, Toyota Technological Institute,  
Nagoya 468-8511, Japan*

2) *Daido Bunseki Research Inc., Nagoya 457-8545, Japan*

Recently growth of metal-filled CNTs has been reported and their characteristics have been investigated<sup>1)</sup>. Since the metal-filled CNT is expected to provide larger radial rigidity, higher mechanical and thermal stability than the conventional hollow nanotube, it would be suitable for the tip of scanning probe microscopy (SPM). Here we report synthesis of Pd-filled CNTs onto the conventional W tip and Si cantilever by microwave plasma enhanced CVD technique.

In order to optimize growth condition, we deposited Pd as a catalyst and Al as a buffer layer on Si wafers and synthesized Pd-filled CNTs by microwave plasma enhanced CVD technique. As seen in Fig.1, the diameter of Pd-filled CNTs depends on the Pd thickness, and minimum diameter of Pd-filled CNTs is approximately 35 nm at the Pd thickness of 7.5 nm. Figure 2 shows TEM image (a) and diffraction pattern (b) of a Pd-filled CNT. It is found that the CNT has graphene sheets of approximately 40-50 layers and the top of the catalyst is covered with amorphous carbon of approximately 3 nm in thickness. The diffraction pattern reveals that the material inside the CNT is a Pd nanowire with fcc structure. Growth of CNTs on scanning probe microscopy (SPM) probes is also presented.

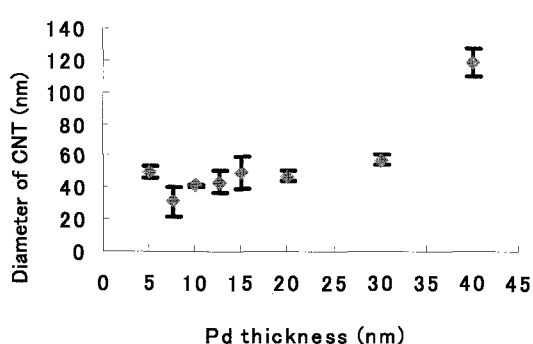


Fig.1: Relationship between the diameter of CNTs and Pd thickness.

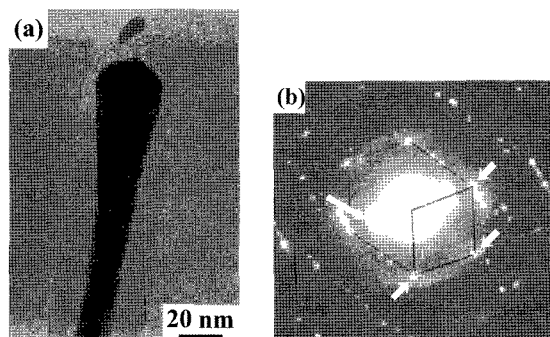


Fig.2: (a) TEM image of Pd-filled CNTs. (b) EDP in the view of Fig.2 (a).

[1] Y. Hayashi, T. Tokunaga, S. Toh, W.-J. Moon, and K. Kaneko: *Diamond Relat. Mater.* **14** (2005) 790.

**Corresponding Author: Tomokazu Sakamoto**

**E-mail: sd04034@toyota-ti.ac.jp**

**Tel: (052)809-1852, Fax: (052)809-1853**

## Electronic Structure of Polyynes Molecules by Resonance Raman and Optical Emission Spectroscopy

Tomonari Wakabayashi

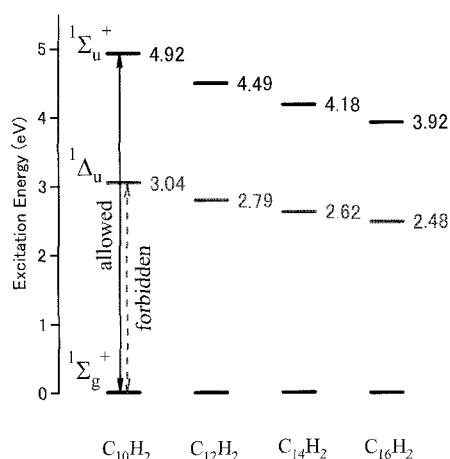
*Department of Chemistry, Kinki University, Higashi-Osaka 577-8502, Japan*

Polyynes, a family of molecules with linear carbon chains in their molecular structures, are model compounds for yet uncharacterized allotrope of carbon, namely, carbyne. Along the sophisticated compounds form chemical synthesis, some simple molecules have become accessible in milligram quantities by laser ablation or arc discharge. In this presentation, recent studies are reviewed focusing on the electronic structure of the linear polyyne molecules and some questions that have emerged from these studies are discussed.

The molecules of interests including  $\text{H}(\text{C}\equiv\text{C})_n\text{H}$ ,  $\text{H}(\text{C}\equiv\text{C})_n\text{C}\equiv\text{N}$ , and  $\text{N}\equiv\text{C}(\text{C}\equiv\text{C})_n\text{C}\equiv\text{N}$  are formed by laser ablation of graphite particles in organic solvents. The hydrogen-capped polyynes,  $\text{H}(\text{C}\equiv\text{C})_n\text{H}$ , are relatively stable under dilute conditions in hexane and subjected to optical spectroscopy, i.e., normal Raman and SERS [1], resonance Raman [2], and laser induced emission spectroscopy [3]. The excitation of the molecule via the allowed electronic transition by uv photon ( $\sim 3.9\text{-}5.0$  eV) is followed by relaxation via Rayleigh and Raman scattering, internal conversion, and so on. As revealed from the weak emission spectra for  $\text{C}_{2n}\text{H}_2$  ( $n=5\text{-}8$ ) as well as the corresponding absorption spectra, the molecule has a low-lying electronic state at  $\sim 2.5\text{-}3.0$  eV above the ground state (see Fig. 1). According to the Herzberg-Teller mechanism, the forbidden transition becomes weakly allowed, when the electronic transition is accompanied by an excitation of the trans-bending vibrational mode of  $\pi_g$  symmetry [3]. The information for the low-lying electronic states of the molecule is demanded for understanding of the optical properties of composite molecules, such as  $\text{C}_{2n}\text{H}_2@\text{SWNTs}$  [4-6].

### References:

- 1) H. Tabata et al., *Carbon* **44**, 3168 (2006).
- 2) T. Wakabayashi et al., *Chem. Phys. Lett.* **433**, 296 (2007).
- 3) T. Wakabayashi et al., *Chem. Phys. Lett.* **446**, 65 (2007).
- 4) D. Nishide et al., *Chem. Phys. Lett.* **428**, 356 (2006).
- 5) D. Nishide et al., *J. Phys. Chem. C* **111**, 5178 (2007).
- 6) L. M. Malard et al., *Phys. Rev. B* **76**, 233412 (2007).



**Figure 1.** Electronic energy levels as revealed from the absorption and emission spectra of  $\text{C}_{2n}\text{H}_2$  in hexane [3].

**Corresponding Author: Tomonari Wakabayashi**

**E-mail: wakaba@chem.kindai.ac.jp**

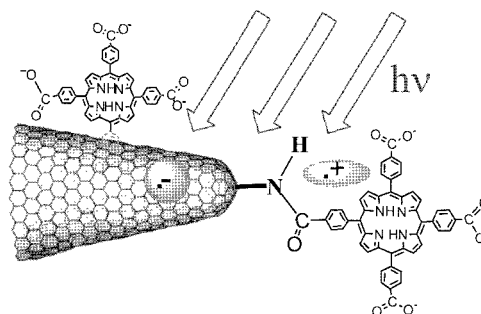
**Tel. 06-6730-5880 (ex. 4101) / FAX 06-6723-2721**

## Photoinduced Charge-Separation of Carbon Nanohorns with Porphyrin Connected via Amino Group

Osamu Ito,<sup>a</sup> Atula Sandanayaka,<sup>a</sup> Yasuyuki Araki,<sup>a</sup> Takatsugu Tanaka,<sup>b</sup> Hiroyuki Isobe,<sup>a,b</sup> Ei-ichi Nakamura,<sup>b</sup> Masako Yudasaka,<sup>c</sup> Sumio Iijima<sup>c,d</sup>

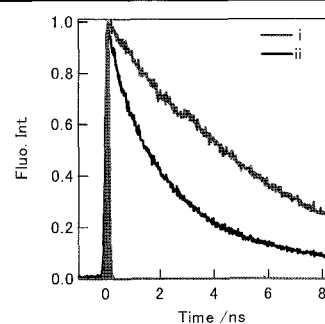
<sup>a</sup>Tohoku University, <sup>b</sup>University of Tokyo, <sup>c</sup>NEC, <sup>d</sup>Meijo University

Carbon nanohorns (CNHs) have been extensively studied, due to their unique properties, including their photo-physical properties dispersed in solutions. Here, we report light induced charge separation processes of amino-substituted CNHs and its adduct with tetracarboxylic porphyrin dispersed in aqueous solution studied by the steady-state and transient spectroscopic methods.<sup>1)</sup> From the fluorescence lifetime measurements of anionic porphyrin ( $H_2P^{4-}$ )

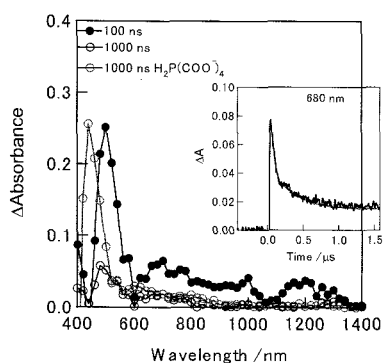


**Fig. 1.** CNH-NH<sub>2</sub>-H<sub>2</sub>P<sup>4-</sup> hybrids.

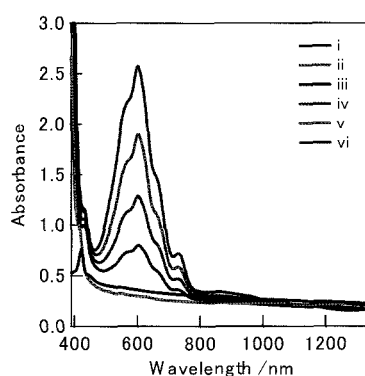
attached on CNH-NH<sub>2</sub> (Fig. 1), appreciable shortening of the fluorescence lifetime of  $H_2P^{4-}$  was observed by the binding and adsorption on CNHs as shown in Fig. 2, suggesting the photoinduced charge separation via the singlet excited state of  $H_2P^{4-}$  to CNH-NH<sub>2</sub>. The transient absorption spectra (Fig. 3) show the absorption peaks due to the radical cation of  $H_2P^{4-}$  in the 600–800 nm regions, in addition to the triplet state of  $H_2P^{4-}$ , which are broadened by strong interaction with CNH-NH<sub>2</sub>. With the steady-light illumination of CNH-NH<sub>2</sub>- $H_2P^{4-}$  in the presence of electron mediator (methyl viologen dication,  $MV^{2+}$ ), the accumulation of  $MV^{•+}$  as electron pool was confirmed by the characteristic 620-nm band in the co-presence of hole transfer reagent (BNAH) as shown in Fig. 4. This observation indirectly supports that charge-separation between the excited singlet state of  $H_2P^{4-}$  and CNH generates respective hole and electron, from which the electron mediates from CNHs to  $MV^{2+}$ , yielding  $MV^{•+}$ , whereas the hole on  $H_2P^{4-}$  mediates to BNAH, retarding back electron transfer processes. Finally, steady-state concentration of  $MV^{•+}$  can be accumulated as electron pool in aqueous solution.



**Fig. 2.**  $H_2P^{4-}$ -fluorescence time profiles of (i)  $H_2P^{4-}$  and (ii) CNH-NH<sub>2</sub>- $H_2P^{4-}$ .



**Fig. 3.** Transient absorption spectra of CNH-NH<sub>2</sub>- $H_2P^{4-}$ .



**Fig. 4.** Accumulation of  $MV^{•+}$  with increase in BNAH (i-vi) by 532-nm light on CNH-NH<sub>2</sub>- $H_2P^{4-}$ .

[1] Pagona, Sandanayaka, Araki, Fan, Tagmatarchis, Yudasaka, Iijima, Ito, *et al*, *Adv. Funct. Mater.* **2007**, *17*, 1705.

\*Corresponding Author:  
Osamu Ito;  
ito@tagen.tohoku.ac.jp

## Non-collinear Magnetic Phase Diagram of Graphene Nanoribbons

K. Sawada<sup>1</sup> ○, F. Ishii<sup>1</sup>, M. Saito<sup>1</sup>, S. Okada<sup>2</sup>, T. Kawai<sup>3</sup>

<sup>1</sup> Graduate School of Natural Science and Technology, Kanazawa University, Kakuma, Kanazawa 920-1192, Japan

<sup>2</sup> Institute of Physics and Center for Computational Sciences, University of Tsukuba, Tennodai, Tsukuba 305-8571, Japan

<sup>3</sup> Fundamental and Environmental Research Laboratories, NEC Corporation, 34 Miyukigaoka, Tsukuba 305-8501, Japan

Recently, graphenes attract much attention as candidates for spintronics materials [1, 2]. One of the reasons is that the flat-band ferromagnetism appears at zigzag edges of graphenes [3]. It was reported that the magnetic ground state of zigzag-edged graphene nanoribbon (ZGNR) has an anti-ferromagnetic (AFM) structure consisting of two ferromagnetic (FM) chains along both edges. Then, theoretical design of the FM states of carbon-based materials is challenged by several groups [4, 5].

In this paper, we clarify that the FM and non-collinear magnetic (NCM) states of ZGNR can be induced by carrier doping, which is achieved by means of the electric field effect method [6]. We have performed non-collinear density-functional calculations and have revealed the magnetic phase diagram of ZGNR, i.e., Fig. 1 shows the relative total energy  $\Delta E$  per the edge-atom which depends on the carrier-doping concentration  $x$  ( $e/\text{Cell}$ ) and the spin-canting angle  $\theta$  between two atoms at both edges (see Fig. 2). We find that the AFM phase ( $\theta = 180^\circ$ ) is transformed into the FM ( $\theta = 0^\circ$ ) phase by either electron ( $x < -0.12$ ) or hole ( $0.12 < x$ ) doping. It should be noticed that NCM states ( $0^\circ < \theta < 180^\circ$ ) appear between the AFM and FM phases.

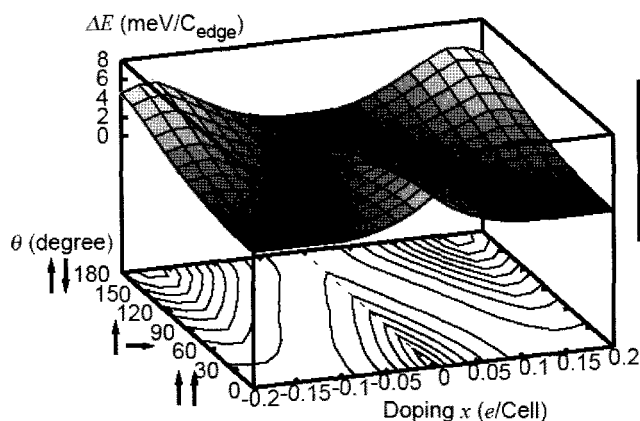


Fig. 1: The magnetic phase diagram of ZGNR.

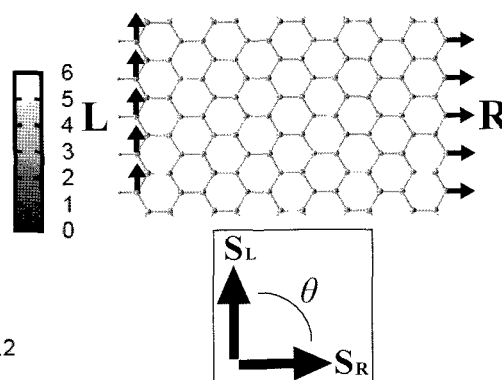


Fig.2: The magnetic structure of ZGNR.

- [1] Y. Son et al., Nature **444**, 347 (2006).
- [2] N. Tombros et al., Nature **448**, 571 (2007).
- [3] M. Fujita et al., J. Phys. Soc. Jpn. **65**, 1920 (1996).
- [4] K. Kusakabe et al., Phys. Rev. B **67**, 092406 (2003).
- [5] S. Okada et al., Phys. Rev. B **74**, 121412(R) (2006).
- [6] K. S. Novoselov et al., Science **306**, 666 (2004).

Corresponding Author: K. Sawada E-mail: sawada@cphys.s.kanazawa-u.ac.jp Tel: 090-8099-3044

## High temperature treatment of carbon fullerene soot and formation of multi-shell carbon nano-capsules filled with La carbide

○Kazunori Yamamoto<sup>a</sup>, Takatsugu Wakahara<sup>b</sup>, Takeshi Akasaka<sup>b</sup>

<sup>a</sup>Nanomaterials Research Group, Quantum Beam Science Directorate,

Japan Atomic Energy Agency, Tokai-mura, Naka-gun, Ibaraki 319-1195, Japan

<sup>b</sup>Center for Tsukuba Advanced Research Alliance, University of Tsukuba, Ibaraki 305-8577, Japan

### Abstract:

There has been great interest in the incorporation of foreign materials into fullerenes, nanotubes, and fullerene-like multi-shell cage structures such as polyhedral nanocapsules.

Fullerenes encapsulating one La atom (called endofullerenes) were discovered in the fullerene soot formed by laser vaporization and following deposition of La with carbon under Ar flow [1]. Soon after the endofullerene soot was produced macroscopically by arc-discharge method [2]. Endofullerenes encapsulating one La atom (such as La@C<sub>82</sub>) formed in the soot were extracted by toluene [1], and well identified after their purification by HPLC [3].

On the other hand, polyhedral nanocapsules containing La element were not found in the fullerene soot, which were discovered in carbonaceous cathode deposits formed by arc-discharge evaporation and following deposition of La with carbon on the cathode surface [4, 5]. Electron diffraction (ED) revealed that the capsules were filled with LaC<sub>2</sub> single crystals, not La metals [5]. Transmission electron microscopy (TEM) characterization showed that the endohedral graphitic nanoparticles were usually seen in the deposit, not in the soot.

In this study, multi-shell single-digit nanoparticles filled with La have been found in La fullerene arc soot synthesized at 35 Torr He, which is lower than the ordinal pressure for the fullerene and nanotube condition. Typical TEM picture of the soot is seen in Figure 1, where most of the single-digit nano-particles contain La. Furthermore, the soot materials have been treated at temperatures between 1000 and 2200°C in vacuum. The modifications resulting from the heat treatment have been followed by TEM and thermogravimetric (TG) measurements. The single-digit nanoparticles have been transformed into larger multi-shell nanoparticles filled with LaC<sub>2</sub>.

### References:

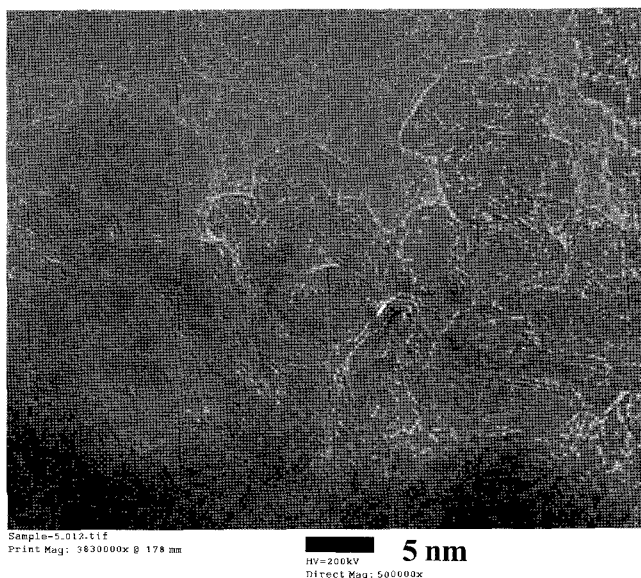
1. Y. Chai, et al., *J Phys Chem.*, **95**, 7564(1991).
2. H. Shinohara, et al., *J Phys Chem.*, **96**, 3571(1992).
3. K. Yamamoto, et al., *J. Phys. Chem.*, **98**, 2008(1994).
4. R. S. Ruoff, et al., *Science*, **259**, 336(1993).
5. M. Tomita, et al., *Jpn. J. Appl. Phys.*, **32**, L280(1993).

**Corresponding Author:** Kazunori Yamamoto

**E-mail:** yamamoto.kazunori@jaea.go.jp

**Tel&Fax:** +81-29-282-6474&+81-29-284-3813.

**Figure 1.** TEM image of multi-shell single-digit nano-particles in La fullerene soot synthesized at 35 Torr He.





## Monodisperse Single-Nano Diamond Particles as Seeding for CVD Diamond Thin Films. 1. A New Seeding Technique

○ Sachio Inaba<sup>#</sup>, Takashi Tarao,<sup>#</sup> Masaaki Kawabe,<sup>#</sup> Oliver A. Williams<sup>§</sup> and Eiji Ōsawa<sup>†</sup>

<sup>#</sup>*Japan Vilene Co., 2-14-5, Soto-Kanda, Chiyoda-ku, Tokyo, Japan*

<sup>§</sup>*Inst. Mater. Res., Hasselt Univ., Wetenschapspark 1, B-3590 Diepenbeek, Belgium*

<sup>†</sup>*NanoCarbon Res. Inst., AREC, Shinshu Univ., 3-15-1 Tokida, Ueda, Nagano 386-8567, Japan*

### Purpose

Being the world's smallest artificial diamond, our single-nano diamond (SND,  $d=4.77\pm 0.76$  nm) particles<sup>1)</sup> obtained by disintegrating crude agglutinates of *detonation nanodiamond* offer the best possible seeding for homoepitaxial growth of CVD diamond films.<sup>2)</sup> Despite vigorous R&D efforts since the breakthrough in CVD diamond growth technique (hot filament) by Sedaka *et al.* in 1982,<sup>3)</sup> no diamond film having acceptable qualities regarding density, transparency, growth rate and surface smoothness has been produced on large scale, primarily because small enough diamond seeds were not available until the SND was *rediscovered* in 2002.<sup>1)</sup> Our first and probably the most important task towards our temporal goals of obtaining good-quality NCD, UNCD films by CVD using SND seeds<sup>3)</sup> is to develop a coating technique capable of reaching a seeding density in the order of  $10^{12}/\text{cm}^2$ .

### Results

*Preparation of nanodiamond colloid having virtually unimodal distribution.* Our SND used to contain 5-10% of double-nano diamond single crystals. Improvements in the purification steps afforded products containing more than 98% of particles having diameters between 4 and 5 nm.

*Dip-coating* of 0.05~0.1% aqueous colloid of SND over silicon wafers on a MicroDip (ND-0408, SDI Co.) at a pulling speed of 0.1 mm/s afforded uniform coating of single layer of SND. Seeding densities of the order of  $10^{11}/\text{cm}^2$  have been achieved. Even by immersion-coating, this level of density could be achieved when SND colloid was used. CVD diamond films grown over such seeded plates were of high quality.<sup>2,4)</sup> However, we soon noticed that these simple coating methods provide too small degree of freedom for precise attenuation of seeding conditions.

*Colloid-jet printing.* It occurred to us that the ink-jet printing technique may be modified for CVD seeding instruments to allow the highest possible seeding density and also to align and orient SND crystals on the surface of substrate. Preliminary examination using an Ink Jet Patterning instrument (NanoPrinter-500D) from MicroJet Co. is giving out promising results. Colloidal solutions of 0.01% SND in ethylene-glycol/ethanol (8:2) mixed solvent and a set of 128 jet-nozzles each having a diameter of 40  $\mu\text{m}$  are being used.

### References

(1) Ōsawa, E. *Gendai Kagaku*, **2007**, Dec. Issue, 52-56; *Pure & Appl. Chem.* in press. (2) Williams, O. A. *et al. Chem. Phys. Lett.* **2007**, *445*, 255-258. (3) Kobashi, K. 'Diamond Films,' Elsevier: Amsterdam, **2005**. (4) Williams, O. A. *Adv. Mater.* in press.

**Corresponding Author** Eiji Ōsawa, [OsawaEiji@aol.com](mailto:OsawaEiji@aol.com), Tel 0268-75-8381, Fax 0268-75-8551

## Intensity enhancement of intermediate frequency Raman mode (IFM) by the presence of very small diameter SWNTs

○Yohji Achiba, Yasuhiro Tsuruoka, and Keisuke Urata

*Department of Chemistry, Tokyo Metropolitan University, Tokyo 192-0397, Japan*

Raman scattering spectroscopy has been established as a powerful tool to clarify the electronic and vibrational properties of SWNTs. As has been well known, there are basically two types of Raman active modes; i.e., radial breathing mode (RBM) and tangential mode (T-mode or G-mode), and the origin of the appearance of these optical phonons has been understood by the first order process of electron-phonon interaction.

Since the first systematic report on the Raman spectrum of SWNTs<sup>[1]</sup>, on the other hand, in addition to these strong RBM and T-mode Raman bands, the appearance of very weak but distinctive Raman bands has been reported in the intermediate frequency region (500-1200 $\text{cm}^{-1}$ ) and these Raman bands have been called as “intermediate frequency mode (IFM)”<sup>[2]</sup>. Usually the intensity of these IFM is less than 10% of those of RBM or T-M. Furthermore, by changing excitation photon energy, the observed frequency of the IFM band changes as a “step-like” behaviors suggesting the excitation of only some SWNTs with specific chiral indices. With use of rather simple theoretical approach, such a behavior has been understood by the Raman scattering caused by the combination of optical and acousticlike phonons<sup>[3,4]</sup>. The previous reports has further indicated that because of the momentum conservation rule, in the case of IFM, only the SWNTs with a zigzag type or near zigzag type should be selectively excited as the candidate for showing experimental IFM bands.

In the present paper, we demonstrate the observation of extraordinary strong IFM Raman bands for the sample containing the SWNTs with very small diameter. Intensity of the IFM bands observed in the present work is almostly the same as the one for the RBM. The diameter distribution of the sample is centered at around 0.6-0.5 nm and very strong RBM of (5,4) and (7,2) were observed by the excitation of 488 nm and 633 nm, respectively. Figure 1 shows the Raman scattering spectrum of the frequency region from 100  $\text{cm}^{-1}$  to 5000  $\text{cm}^{-1}$ . The two bands with a broad feature appearing at 3000-4000  $\text{cm}^{-1}$  are due to fluorescence bands of (5,4) and (6,4) SWNTs. In the spectrum region between 500-2600  $\text{cm}^{-1}$ , there appears at least 6 peaks which are able to be assigned to IFM (shown by arrows). Detailed analysis and discussion will be performed in the symposium.

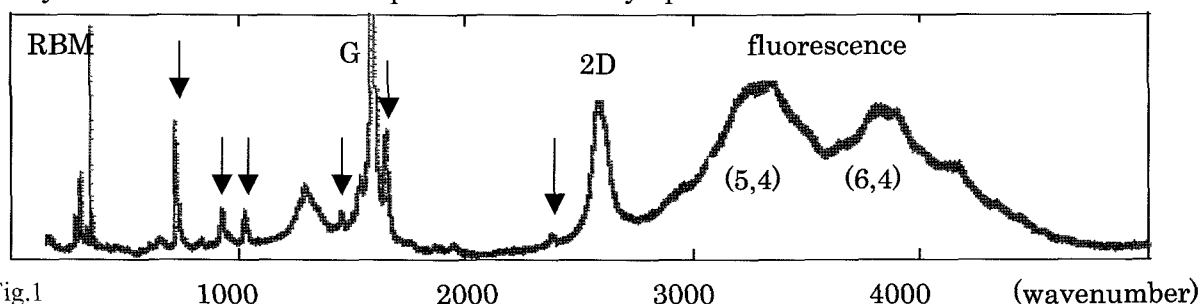


Fig.1

[1] A. M. Rao et al., *Science*, 275, 187 (1997). [2] L. Alvarez et al., *C. P. L.* 316, 186 (2000).

[3] C. Fantini et al., *PRL.*, 93, 87401 (2004). [4] C. Fantini et al., *PRB*72, 85446 (2005).

Corresponding Author: Yohji Achiba

TEL: 042-667-2534, E-mail: achiba-yohji@tmu.ac.jp

## Mechanism of Gold-Catalyzed Carbon Material Growth

○Daisuke Takagi<sup>1,3</sup>, Yoshihiro Kobayashi<sup>2,3</sup>, Hiroki Hibino<sup>2</sup>,  
Satoru Suzuki<sup>2,3</sup>, Yoshikazu Homma<sup>1,3</sup>

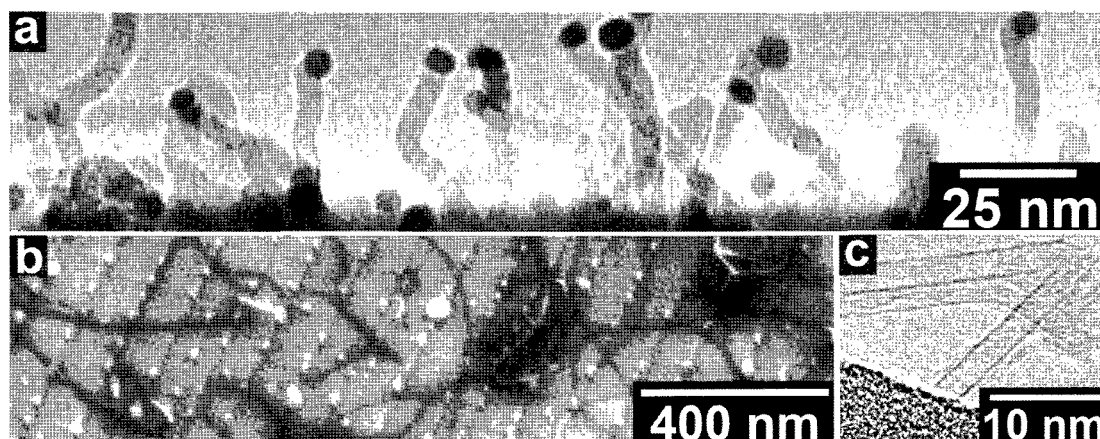
<sup>1</sup>*Department of Physics, Tokyo University of Science, Shinjuku, Tokyo 162-8601, Japan*  
<sup>2</sup>*NTT Basic Research Laboratories, NTT Corporation, Atsugi, Kanagawa 243-0198, Japan*  
<sup>3</sup>*CREST, JST, Chiyoda, Tokyo 102-0075, Japan*

Unlike the iron-group metals, carbon solubility of Au is extremely low in bulk phase. However single-walled carbon nanotube (SWCNT) can be grown from Au catalysts<sup>1</sup>. For the clarification of the SWCNT growth mechanism from metal catalysts, it is necessary to consider the results of Au-catalyzed SWCNT growth. In present report, we discuss the growth mechanism of SWCNT from Au based on the observation of carbon nanowire (CNW) growth.

We synthesized carbon materials by chemical vapor deposition (CVD) with ethanol or methane. Interestingly, Au-catalyzed carbon material growth by CVD undergoes a structural change, either a CNW or a SWCNT, depending on the catalyst particle size.

Figure 1a is the TEM image of carbon materials grown from ~10 nm Au particles. The TEM image reveals that grown materials are wires not tubes. Figure 1b (SEM) and 1c (TEM) are the results for carbon material growth catalyzed by Au particles ~5 nm or smaller. The TEM image (c) reveals that grown materials are SWCNTs.

CNW formation provides insight into carbon material growth mechanism from Au catalysts. In the Au catalyzed semiconductor nanowire growth, Au and source elements of nanowire form eutectic alloy<sup>2,3</sup>. Similarly, CNW formation from Au catalysts means Au can form Au-C eutectic alloy during carbon material growth. When Au catalyst particle size is 10-30 nm, supersaturated carbon atoms form CNW at the catalyst-substrate interface. In contrast, supersaturated carbon atoms in Au catalyst particles 5 nm or less form a carbon cap on the particle surface and the cap leads SWCNT growth<sup>4</sup>. Present results show that nanosized Au have a significant carbon solubility unlike bulk Au. As a result, Au-C alloy is formed and the Au-C causes CNW and SWCNT growth.



**Figure 1.** Carbon material growth from size-controlled Au nanoparticles

[1] D. Takagi, *et al.*, *Nano Lett.*, **2006**, *6*, 2642.

[2] R. S. Wagner, *et al.*, *Appl. Phys. Lett.* **1964**, *4*, 89.

[3] S. Kodambaka, *et al.*, *Science* **2007**, *316*, 729.

[4] D. Takagi, *et al.*, *Nano Lett.*, **2007**, *7*, 2272.

**Corresponding Author: Daisuke Takagi**

TEL: +81-3-5228-8244, FAX +81-3-5261-1023, E-mail: daisuke@will.brl.ntt.co.jp

## Acetylene Assisted Fast Growth of Vertically Aligned Single Walled Carbon Nanotubes in Alcohol Catalytic Chemical Vapor Deposition

○ Rong Xiang, Jun Okawa, Zhengyi Zhang,

Erik Einarsson, Yohei Miyauchi, Yoichi Murakami, Shigeo Maruyama

*Department of Mechanical Engineering, The University of Tokyo*

With an *in situ* optical absorption, [1] we studied the influences of different foreign molecules on the activity of Co/Mo in alcohol catalytic chemical vapor deposition (ACCVD). An interesting growth acceleration phenomenon was observed when acetylene was introduced to growing SWNTs. Fig. 1a shows that growth rate was enhanced almost 10 times in case of only 1% acetylene. However, pure acetylene of same partial pressure deactivated catalysts in a couple of seconds, no matter with or without a cap formed from ethanol. Then, when ethanol was re-supplied, the activity of these partially poisoned catalyst particles could be recovered, as shown in Fig. 1b. Therefore, the importance of ethanol for SWNT growth, not only at the beginning stage, was demonstrated and detailed mechanism is to be discussed. Several other recent results [2, 3] on the growth mechanism and structure control of vertically aligned SWNTs in ACCVD will also be presented.

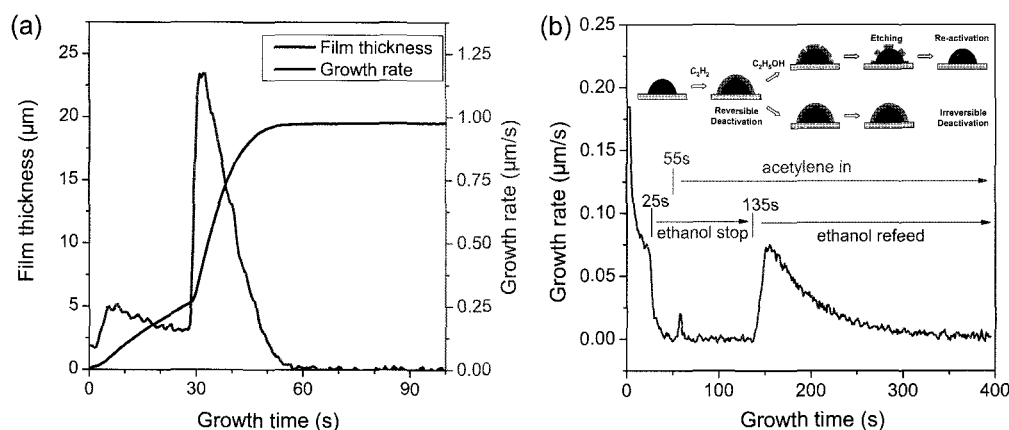


Figure 1. Acetylene assisted ACCVD: (a) a typical growth curve showing growth can be significantly accelerated when acetylene is introduced; (b) a growth started with ethanol and continued by only acetylene, indicating that, without ethanol, catalyst will be deactivated in seconds but this partial poisoned catalyst can be re-activated by ethanol. A possible mechanism was proposed as the inset.

### References

- [1] S. Maruyama, Chem. Phys. Lett. (2004), 403, 320.
- [3] R. Xiang, et al., Jpn. J. Appl. Phys., in press.
- [4] R. Xiang, et al., J. Phys. Chem. C (2008), submitted.

Corresponding author: Shigeo Maruyama E-mail: maruyama@photon.t.u-tokyo.ac.jp, Tel/Fax: +81-3-5800-6983

## Discovery of Novel Carbon Structure: Graphene Multi-Layers Spontaneously Formed on the Top of Aligned Carbon Nanotubes

○Daiyu Kondo, Shintaro Sato, Akio Kawabata, Yuji Awano

*Nanotechnology Research Center, Fujitsu Laboratories Ltd., 10-1 Morinosato-Wakamiya, Atsugi 243-0197, Japan*

Novel carbon structure composed of graphene multi-layers and aligned multi-walled carbon nanotubes (MWNTs) has been discovered. The new structure has graphene multi-layers spontaneously formed on the top of aligned MWNTs, which was obtained by chemical vapor deposition (CVD). The graphene layers are perpendicular to the aligned direction of MWNTs. The obtained structure is clearly different from usual vertically-aligned MWNTs [1], and looks like carbon nanotubes with parasols.

The CVD process was performed in a low-pressure vacuum chamber. As the carbon source, a mixture of acetylene and argon gases was introduced into the CVD chamber, where the substrate was placed. The substrate temperature and total pressure were 510 °C and 1kPa, respectively. As a catalyst, a 2.6-nm-thick cobalt film on a titanium nitride film by the conventional sputtering method was used. Figure 1(a) shows a cross sectional image of the new carbon structure on a silicon substrate by scanning electron microscopy (SEM). A flat structure on vertically aligned MWNT bundles is clearly observed. Analyzing this flat structure by transmission electron microscopy (TEM) in Fig. 1(b), we have found that the flat structure is composed of multiple graphite domains next to each other, whose thickness was estimated to be approximately 18 nm. This thickness can be controlled by the growth condition and catalyst composition. The obtained structure is unique and can be synthesized at low temperature. Therefore, it may find new applications in the electronic industry. Details will be discussed in the presentation. The authors thank Dr. Naoki Yokoyama, Fellow of Fujitsu Laboratories Ltd. for his support and useful suggestions.

### References

[1] S. Sato *et al.*, Chem. Phys. Lett. 402(2005)149.

Corresponding Author: Daiyu Kondo

E-mail: kondo.daiyu@jp.fujitsu.com

Tel&Fax: +81-46-250-8234&+81-46-250-8844

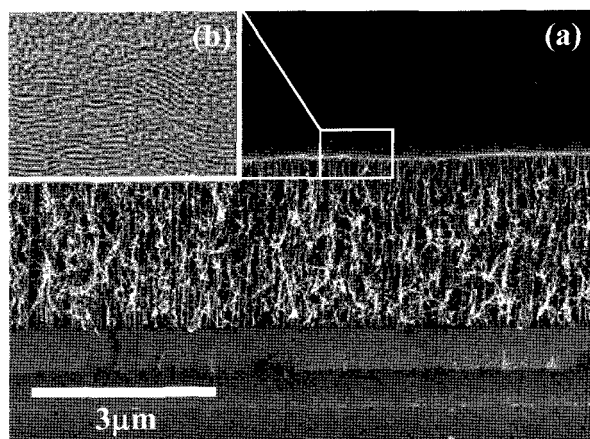


Figure 1 (a) SEM image of the new carbon structure composed of graphene multi-layers and MWNTs; (b) TEM image of the graphene multi-layers.

## Stability of Double Wall Carbon Nanotubes on Oxidation

○Hiromichi Yoshida, Toshiki Sugai, Hisanori Shinohara

*Department of Chemistry & Institute for Advanced Research,  
Nagoya University, Nagoya 464-8602, Japan  
CREST, Japan Science and Technology Agency, c/o Department of Chemistry,  
Nagoya University, Nagoya 464-8602, Japan*

The purification of double-wall carbon nanotubes (DWNTs) is crucial to properly characterize their structural, electronic and magnetic properties. To purify DWNTs produced by the high temperature pulsed arc discharge method (HTPAD) [1], we have utilized a high-temperature oxidation processes together with a reported dispersion technique [2]. In this purification process of carbon nanotubes (CNTs) dependences on the stability of the number of layers and on diameters are important to obtain pure nanotube materials. Here, we have investigated the structural stability of the HTPAD-DWNTs on high-temperature oxidation (i.e., burning) in terms of the number of layers and oxidation temperature.

DWNTs together with the single-wall CNTs (SWNTs) having a maximum diameter of 1.8 nm were synthesized by HTPAD using Ni/Co/Y catalysts. The as-grown material was heated at 360°C and was dispersed into surfactant, which was mixed with fumed silica and dried into a powder. The powder was then refluxed in H<sub>2</sub>O<sub>2</sub>, and oxidized at temperature between 500 and 600°C to remove SWNTs [1]. DWNTs were recovered after elimination of silica. The diameter distribution of such CNTs and the relative abundance of DWNTs and SWNTs were estimated by TEM observation.

Figure 1 shows a TEM image in which most of the thin SWNTs and DWNTs (a,b) are oxidized but thicker SWNTs and DWNTs (c,d) remain; the stability towards the oxidation increases as the diameter of CNTs increase. Figure 2 (a) and (b) present diameter distributions before and after oxidation, respectively. SWNTs with the diameter around 1.4 nm are completely oxidized, whereas SWNTs around 1.0 nm are newly appeared. These thin SWNTs originate from inner layer of thin DWNTs, which are seen in Fig. 1(b). The thicker SWNTs with a diameter around 1.8 nm are enriched by the oxidation, and DWNTs of a similar diameter are twice as abundant as the corresponding SWNTs. The stability of CNTs against oxidation is mainly governed by both the number of layers and the diameters.

[1] T. Sugai et al., *Nano Lett. (Comm.)*, 3, 769 (2003)[2] H. Yoshida et al., *30<sup>th</sup> F&NT symposium*, 2P-22 (2006)**Corresponding Author** : Hisanori ShinoharaE-mail : [noris@cc.nagoya-u.ac.jp](mailto:noris@cc.nagoya-u.ac.jp)

TEL : 052-789-2482 FAX : 052-789-1169

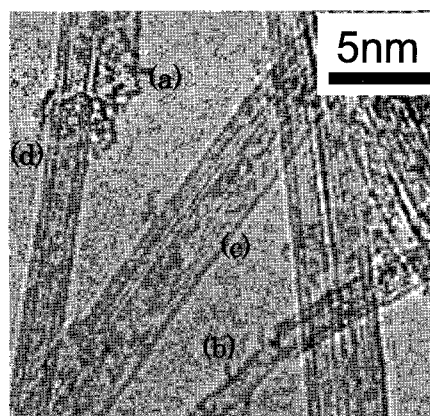
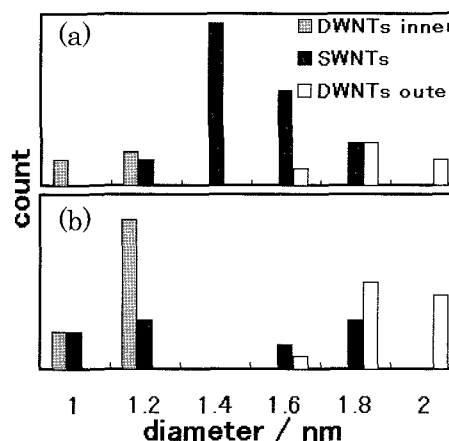


Fig.1 TEM image of purified CNTs

Fig.2 Diameter distribution  
(a) before and (b) after oxidation

## Separation of Metallic and Semiconducting Single-Wall Carbon Nanotubes by Gel Electrophoresis

○ Takeshi Tanaka, Hehua Jin, Yasumitsu Miyata, Hiromichi Kataura

*Nanotechnology Research Institute, National Institute of Advanced Industrial Science and Technology (AIST), 1-1-1 Higashi, Tsukuba, Ibaraki 305-8562, Japan*

As-produced single-wall carbon nanotubes (SWCNTs) contain metallic and semiconducting ones (mSWCNTs and sSWCNTs, respectively). The heterogeneity is one of the most crucial problems preventing application of SWCNTs. There are several reports on the separation of mSWCNTs and sSWCNTs by dielectrophoresis [1], amine extraction [2], ion-exchange chromatography of SWCNTs dispersed by DNA [3], and density-gradient ultracentrifugation [4, 5]. Here we report a novel separation method of mSWCNTs and sSWCNTs by gel electrophoresis. Since the new method is quite simple, quick and scalable, it could be suited for the industrial production. SWCNT dispersion was prepared by a sonication in the presence of detergent, followed by a centrifugation. We first applied the solution to gel electrophoresis (Fig. 1). The mSWCNTs were concentrated in the fractions 3 and 4 and sSWCNTs were in the frac. 1, which means the mSWCNT moved faster. In this case, however, about 90% of the initial SWCNT was left mixed in the frac. 2. We then used SWCNT-dispersed gel as a sample of gel electrophoresis and found a drastic improvement in the separation (Fig. 2). In this method, most of mSWCNTs moved out from the starting gel and formed the frac. 2, while sSWCNTs remained in the gel (frac. 1). As a result, almost all SWCNTs applied to gel electrophoresis were separated into respective electronic type. The principle of the separation is still not clear but is thought to be different from standard gel electrophoresis.

**References:** [1] Krupke et al., *Science* 2003, **301**, 344, [2] Maeda et al., *JACS* 2005, **127**, 10287, [3] Zheng et al., *Nat. Mater.* 2003, **2**, 338, [4] Arnold et al., *Nat. Nanotechnol.* 2006, **1**, 60, [5] Yanagi et al., *The 33<sup>rd</sup> Fullerene-Nanotube General Symposium* 2007, 56.

**Corresponding Author:** T. Tanaka, Tel: 029-861-2903, Fax: 029-861-2786, E-mail: tanaka-t@aist.go.jp

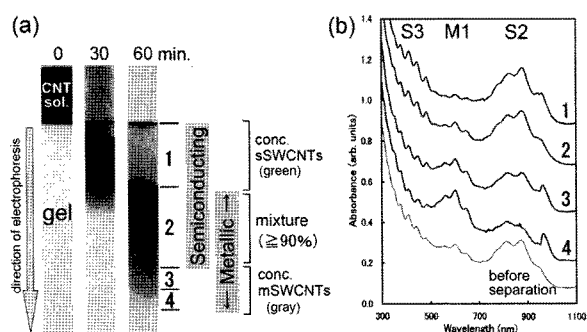


Fig. 1 (a) Separation of the dispersed SWCNT solution by gel electrophoresis. (b) Absorption spectra of fractions after gel electrophoresis.

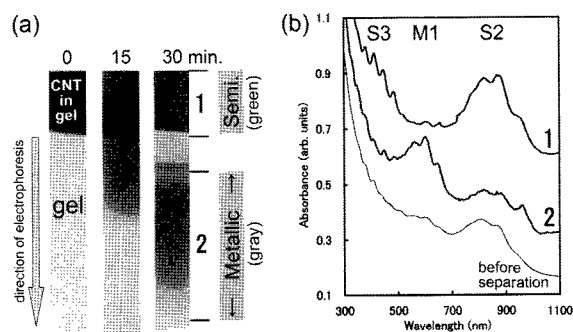


Fig. 2 (a) Separation of SWCNT dispersed in gel by gel electrophoresis. (b) Absorption spectra of fractions after gel electrophoresis.

## The New Feature Development of Carbon Nanotubes-Polybenzimidazole Composite

○Minoru Okamoto, Tsuyohiko Fujigaya and Naotoshi Nakashima

*Department of Applied Chemistry, Graduate School of Engineering  
Kyushu University, Fukuoka, Japan*

Carbon nanotubes (CNTs) have expected in most areas of science and engineering due to their mechanical properties, electrical properties and so on[1]. But, the application of CNTs is limited because they form bundles each other and possess poor solubility in any solvents. Many researches of dispersing CNTs in solvent and preparing CNTs-polymer composites has been reported[2]. In this time, we focus on Polybenzimidazole (PBI) as polymer materials. PBI is used as super engineering plastic because of the heat stability. In addition, PBI is expected to apply for solid polymer electrolyte membrane of fuel cells.

First, we examined if PBI can solubilize CNTs in solvent. CNTs were added to the solution which PBI was dissolved in dimethyl sulfoxide (DMAc). This solution was sonicated to dissolve CNTs, followed by centrifugation. Fig.1 (A) shows the absorption spectra of the suspension after centrifugation. For comparison, the same operation without PBI was carried out and absorption spectra is shown in Fig.1 (B).

In the case of the solution including PBI (Fig.1 (A)), the characteristic spectral features due to dissolved CNTs were clearly observed in the near-IR region. On the other hand, the characteristic absorption due to CNTs was not observed in the absence of PBI (Fig.1 (B)). This means PBI can act as solubilizer for CNTs. It is attributed that the  $\pi$ - $\pi$  interaction between PBI and CNTs plays an important role for debandling of CNTs.

Next, the CNTs-PBI composite films and PBI films were prepared by spreading each solution on a glass plate and the solvent was evaporated, (Fig.2). The tensile strength and Young's modulus of each film was measured, and found that those of CNTs-PBI composite film is about 1.6 times higher than PBI film without CNTs.

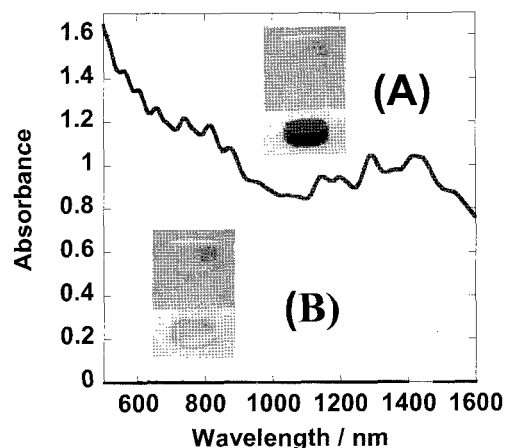


Fig.1 Vis-NIR spectra of CNTs solution (A) with PBI (B) without PBI.

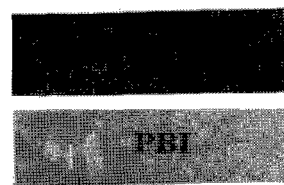


Fig.2 CNTs-PBI composite film and PBI film.

[1] D.Tasis, N. Tagmatarchis, A. Bianco, M. Prato, *Chem. Rev.*, 106, 1105 (2006).

[2] J. N. Coleman, U. Khan, Y. K. Gun'ko, *Adv. Mater.*, 18, 689 (2006).

Corresponding Author: Naotoshi Nakashima

TEL/FAX: +81-92-802-2840, E-mail: E-mail: [nakashima-tcm@mbox.nc.kyushu-u.ac.jp](mailto:nakashima-tcm@mbox.nc.kyushu-u.ac.jp)



## Reduction of low-temperature-growth-CNT via resistances using inner layers by Chemical Mechanical Polishing

○Kentaro Ishimaru<sup>1</sup>, Daisuke Yokoyama<sup>1</sup>, Takayuki Iwasaki<sup>1</sup>, Shintaro Sato<sup>2</sup>,  
Takashi Hyakushima<sup>2</sup>, Mizuhisa Nihei<sup>2</sup>, Yuji Awano<sup>2</sup> and Hiroshi Kawarada<sup>1</sup>

<sup>1</sup>*School of Science and Engineering, Waseda university, Tokyo 169-8555, Japan*

<sup>2</sup>*MIRAI-Selete, Atsugi 243-0197, Japan*

We have grown carbon nanotubes (CNTs) by remote plasma chemical vapor deposition (RP-CVD) lower than 390°C (Fig. 1(a)), which is tolerable temperature for LSI fabrication process, and measured their electrical properties[1]. However, high values of via resistance were observed owing to the surface ununiformity. To overcome this problem, we applied Chemical Mechanical Polishing (CMP) [2] to planarize CNT vias. CNT vias were successfully planarized by CMP (Fig. 1(b)(c)). Since caps of multi-walled MWNTs would be removed by using CMP, carrier conduction should occur on many inner layers as well as the outermost layers. (Fig. 2) Vias planarized by it has much lower resistances than those of without it. In this study, the lowest via resistance at a 2 $\mu$ m via was 16  $\Omega$  without CMP and 0.6  $\Omega$  with CMP, which is close to that of tungsten vias. We also observed ohmic characteristics in temperature dependence.

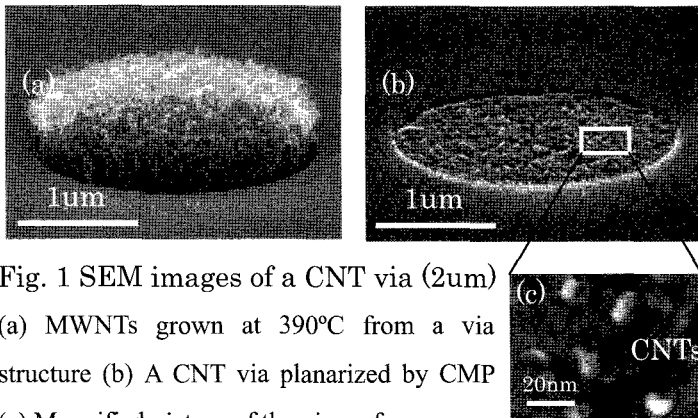


Fig. 1 SEM images of a CNT via (2 $\mu$ m)  
(a) MWNTs grown at 390°C from a via structure  
(b) A CNT via planarized by CMP  
(c) Magnified picture of the via surface

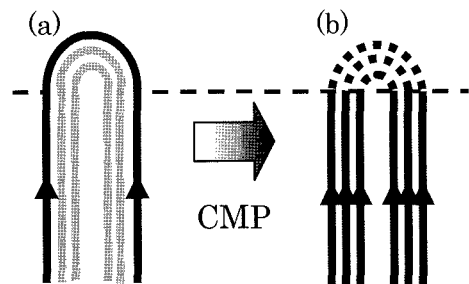


Fig. 2 Carrier paths before and after CMP  
(a) only the outermost layer  
(b) all layer of MWNTs

Acknowledgements: This work was completed as part of the MIRAI Project supported by NEDO.

[1] D. Yokoyama, H. Kawarada, et al., Proc. 32nd Fullerene-Nanotubes General Symp. 3-3(2007)

[2] M. Nihei, et al., IEEE Int Interconnect Technol. Conf. 2007, 204 (2007)

[3] D. Yokoyama, H. Kawarada, et al., Appl. Phys. Lett. 91, 263101(2007)

Corresponding Author: H. Kawarada

E-mail : [kawarada@waseda.ac.jp](mailto:kawarada@waseda.ac.jp) Tel&Fax : +81-3-5286-3391

ポスター発表  
**Poster Preview**

**1P-1 ~ 1P-50**

**2P-1 ~ 2P-50**

**3P-1 ~ 3P-50**

## Growth of Carbon Nanotubes by Carbon Transmission Method

○Takeshi Hikata<sup>1</sup>, Kazuhiko Hayashi<sup>1</sup>, Tomoyuki Mizukoshi<sup>2</sup>,  
Yoshiaki Sakurai<sup>2</sup>, Itsuo Ishigami<sup>2</sup>, Takaaki Aoki<sup>3</sup>, Toshio Seki<sup>3</sup>, and Jiro Matsuo<sup>3</sup>

<sup>1</sup>Sumitomo Electric Industries, Ltd., Osaka 554-0024, Japan

<sup>2</sup>Technology Research Institute of Osaka Prefecture, Osaka 594-1157, Japan

<sup>3</sup>Faculty of Engineering Quantum Science and Engineering Center, Kyoto University,  
Kyoto 606-8501, Japan

Carbon nanotubes (CNTs) have been expected as ideal electric wires with the excellent properties of low resistivity, high strength and light weight. However, it is difficult to fabricate the long length wires because it is difficult to maintain the growth rate of CNTs by covering of unnecessary harmful carbon formed on nano-sized metal particle catalysts in thermal CVD process. We have proposed the Carbon Transmission Method (CTM) for continuous growth of CNT with the concept of the separation between carbon source gas supply and CNT growth as shown in Fig.1. [1] The CTM catalyst foil specimen with thickness of 50 $\mu$ m is composed of Fe filaments through the Ag foil of the separator between the carbon source gas supply (side A) and CNT growth (side B). The both end of Fe filaments in the Ag foil were exposed by chemical etching of Ag with an aqueous solution of NH<sub>3</sub> and H<sub>2</sub>O<sub>2</sub>. The exposed Fe filaments had thickness of sub  $\mu$ m and width of a few  $\mu$ m.

The carbon source mixed gas (CH<sub>4</sub>, H<sub>2</sub> and Ar) was provided on one end of Fe filaments (side A), and Ar gas was provided on the other end of Fe filaments (side B) at 850 °C for 2 hours. As the result of the heat treatment, CNTs were not found at side A in the carbon source mixed gas as shown in Fig.2. In contrast, CNTs with diameter of about 10 - 50 nm were generated at side B as shown in Fig.3. The maximum length was over 100  $\mu$ m.

Next, we carried out the experiment in the same heat treatment condition using an annealed CTM catalyst foil specimen in H<sub>2</sub> gas at 800 °C. As a result, CNTs were not observed at side A and B. It indicates that the reduction of oxide layer on the Fe filaments by H<sub>2</sub> gas leads disappearance of the CNT growth at side B. The oxide layer or the boundary becomes the starting point of CNT growth in Ar gas.

Corresponding Author: Takeshi Hikata /E-mail: hikata-takeshi@sei.co.jp

TEL: +81-6-6466-5790, FAX: +81-6-6466-5705

[1] T.Hikata et al., The 33<sup>rd</sup> Fullerene-Nanotubes General Symposium, 1-11(2007).

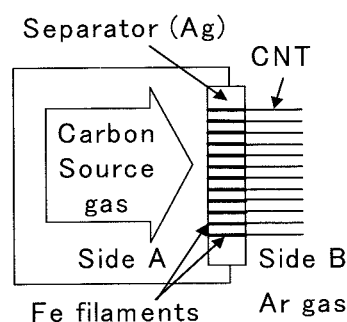


Fig.1 Carbon Transmitting Method

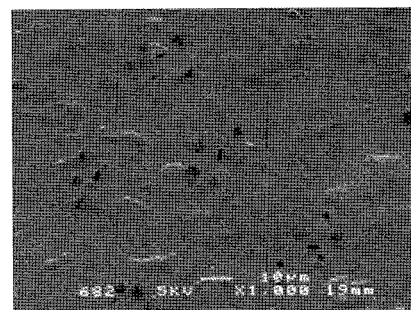


Fig.2 SEM photograph at side A.  
CNTs were not found.



Fig.3 SEM photograph of  
CNTs at side B.

## 1P-2

### Synthesis of Radially-Aligned Carbon Nanotube Powder by SiC Surface Decomposition Method

○Kazuo Yoshikawa<sup>a</sup>, Motohiro Yamamoto<sup>a,b</sup> and Michiko Kusunoki<sup>c</sup>

<sup>a</sup> *Research & Development Div, Tokai Carbon Co.,Ltd. Tokyo 107-8636 Japan.*

<sup>b</sup> *Electro and Material Department, Japan Fine Ceramics Center, Nagoya 456-8587 Japan*

<sup>c</sup> *Division of Environmental Research, EcoTopia Science Institute,  
Nagoya University. Nagoya 464-8602, Japan*

The SiC surface decomposition method is one of the synthetic methods of carbon nanotube (CNT) [1] and the growth mechanism and the characteristics have been reported [2,3]. The CNTs synthesized by this method have unique features, which are highly-aligned, catalysis-free and highly-dense. According to previous reports, the CNTs formed on single crystals of SiC, which is rather expensive, have been investigated as the raw material. In this study, for industrial mass production, we tried to synthesize aligned and high-quality CNT powder using SiC powder, which is relatively low cost.

We revealed that synthesis of CNT powder required appropriate CO gas partial pressure control (the pressure range: 1–100 Pa) and appropriate CO gas fluidization, especially in the process of CNT nanocap formation (the temperature range: 1100–1400 degree Celsius). However, the quality of CNT, which was synthesized by the CO gas controlling method, was not sufficient yet. As a result of investigating the raw material of SiC powder, we found well-crystallized SiC particles provide radially-aligned CNT particles (Fig1).

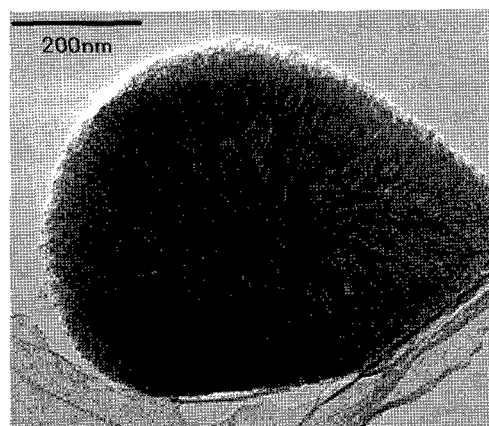


Fig1. TEM image of a radially-aligned CNT particle

#### References:

- [1] M.Kusunoki, M.Rokkaku, T.Suzuki: Appl. Phys. Lett., **71**, 2620 (1997).
- [2] M.Kusunoki, T.Suzuki, T.Hirayama and N.Shibata: Appl. Phys. Lett., **77**, 531 (2000).
- [3] M.Kusunoki, T.Suzuki, C.Honjo, T.Hirayama, N.Shibata: Chem. Phys. Lett., **366**, 458 (2002).

**Corresponding Author:** Motohiro Yamamoto

**E-mail:** myamamoto@jfcc.or.jp

**Tel:** +81-52-871-3500 **Fax:** +81-52-871-3599

## IP-3

### Photoluminescence of mono-dispersed single-walled carbon nanotubes made by using arc-burning method in nitrogen gas atmosphere

○Takashi Mizusawa<sup>1</sup>, Shinzo Suzuki<sup>1</sup>, Toshiya Okazaki<sup>2</sup>, Yohji Achiba<sup>3</sup>

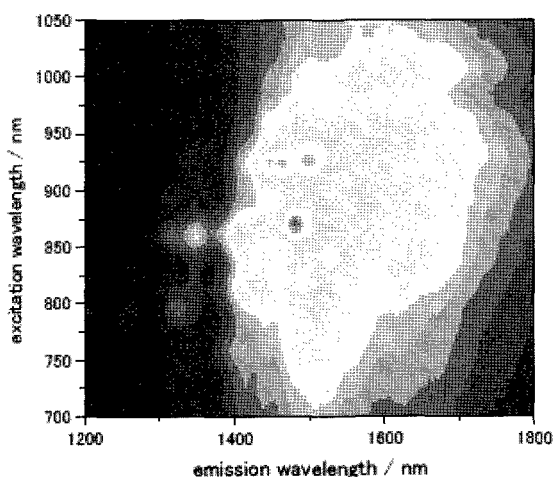
<sup>1</sup>*Department of Physics, Kyoto Sangyo University, Kamigamo-Motoyama, Kita-ku, Kyoto 603-8555, Japan*

<sup>2</sup>*Research Center for Advanced Carbon Materials, AIST, Tsukuba 305-8565, Japan*

<sup>3</sup>*Department of Chemistry, Tokyo Metropolitan University, Hachioji, Tokyo 192-0397, Japan*

**Abstract:** In this presentation, photoluminescence of mono-dispersed carbon nanotubes (SWNTs) made by using arc-burning method in nitrogen gas atmosphere was investigated, since it was suggested that the purity of SWNTs is relatively high, almost comparable to those obtained with laser-ablation method [1]. Typical photoluminescence mapping of mono-dispersed SWNTs in surfactant solution is shown in the figure, demonstrating that the diameter distribution of them is narrow, comparable to those obtained by laser-ablation method [2], though broad background signal can also be seen.

This work was partly supported by the funds of Nippon Sheet Glass Foundation for Material Science and Engineering (NSG Foundation) and the Ministry of Education, Culture, Sports, Science and Technology (MEXT).



#### References:

- [1] S. Suzuki et al., *Eur. Phys. J. D*, **43**, 143-146(2007).
- [2] T. Okazaki et al., *Chem. Phys. Lett.*, **420**, 286(2006).

**Corresponding Author: Shinzo Suzuki**

**E-mail: suzukish@cc.kyoto-su.ac.jp Tel: 075-705-1945 Fax: 075-705-1640**

# 1P-4

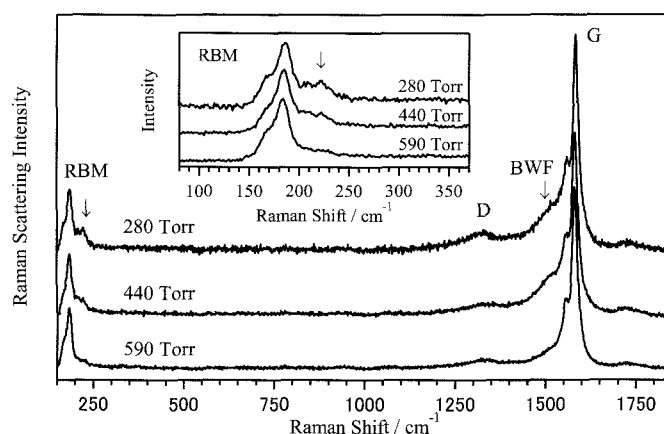
## Production of SWNTs by Laser Ablation and ACCVD

○Shin-ichi Kodama, Atsushi Ikeda, Yuki Masuo, Tetsushi Murakami, and Tomonari Wakabayashi

*Department of Chemistry, Kinki University, Higashi-Osaka 577-8502, Japan*

The purity of single-wall carbon nanotubes (SWNTs) is one of the crucial factors for the study of encapsulation of molecules. Among the possible impurities, amorphous carbon that covers the surface of the nanotubes will affect most seriously to lower the efficiency for encapsulation. The methods to remove amorphous carbon reported so far include heating of the pristine SWNTs in the air, in aqueous hydrogen peroxide, or in boiling water. In this work, we produced SWNTs by both laser ablation and alcohol catalytic CVD (ACCVD) and compared them in view of the quality for molecular encapsulation.

First, in order to refine the experimental conditions for high yields under laser ablation, diameter distributions of SWNTs in the pristine materials were studied by Raman spectroscopy as a function of pressure of the buffer gas. The experimental conditions ( $\sim 1100$  °C, Nd:YAG 1064 nm 0.8 J/pulse at 10 Hz, Ni/Co 0.6/0.6 wt %) were kept throughout the experiments except for the pressure of Ar gas ( $\sim 250$ -610 Torr). Judging from the RBM-frequency regions in the Raman spectra ( $< 300$   $\text{cm}^{-1}$ , inset in Fig. 1), a fraction of SWNTs of smaller diameters decreased by increasing the pressure. The tendency for increasing diameters in average has been reported under higher temperature conditions. Thus, considering the effect of high pressures as confinement of high-temperature particles of carbon and metals, the effective temperature of the precursory particles would be higher under the high pressures. Second, with electron microscope images, the materials from laser ablation contained a substantial amount of amorphous carbon. Finally, the pristine SWNTs were heated at 300 °C in the air and sintered in solutions of molecules, e.g., polyynes  $\text{C}_{2n}\text{H}_2$ , for encapsulation. The Raman spectra of the composite materials were recorded.



**Figure 1.** Raman spectra of pristine SWNTs produced by laser ablation (pressure dependence).

**Corresponding Author: Tomonari Wakabayashi**

**E-mail: wakaba@chem.kindai.ac.jp**

**Tel. 06-6730-5880 (ex. 4101) / FAX 06-6723-2721**

### Synthesis and Applications of Novel Vanadium Oxide Nanotubes

Abhishek Kumar<sup>○</sup>, Nikhil Dhawan<sup>^</sup>

<sup>○</sup> *Materials Science and Engineering Department, Stanford University, California, 94305, USA*  
<sup>^</sup> *Metallurgical Engineering Department, Punjab Engineering College, Chandigarh, INDIA*

The main aim of this work is to produce specialized nanostructures from transition metal oxide for potential applications in electrochemical devices and for catalytic applications. Vanadium oxide nanotubes (VO<sub>x</sub>-NT) have been prepared by mixing hexadecylamine with V<sub>2</sub>O<sub>5</sub>.nH<sub>2</sub>O gels. This procedure was followed by a hydrothermal treatment (150–180°C, 2–7 days), which leads to a large quantity of VO<sub>x</sub>-NT. The structure and morphology of the nanotubes is investigated by SEM and TEM and a model describing nanotubes peculiar morphology has been discussed. The vanadium oxide nanotubes are redox-active and can electrochemically insert lithium reversibly. Further, applications of these transition metal nanotubes in electrical transport and sensor materials have also been outlined.

#### Corresponding Author

Abhishek Kumar [akpec@stanford.edu](mailto:akpec@stanford.edu)  
Materials Science and Engineering Department,  
Stanford University, California 94305, USA  
Tel (650) 644 9442

## 1P-6

### Time Dependence of Carbon Nanotube Growth by Gas Source Method using Alcohol in High Vacuum

○Kenji Tanioku, Tomoyuki Shiraiwa, Takahiro Maruyama, Shigeya Naritsuka

*Department of Materials Science and Engineering, Meijo University,  
1-501 Shiogamaguchi, Tempaku, Nagoya 468-8502*

Carbon nanotubes (CNTs) have been anticipated for use in a lot of future nanodevices. However, the growth mechanism of CNTs has yet to be clarified. Recently, we reported CNT growth by gas source method in an ultra-high vacuum (UHV) chamber [1]. This growth technique enables CNT growth in a high vacuum, which is useful for clarifying the growth mechanism. In this study, we investigated the time dependence of CNT growth using the gas source method.

SiO<sub>2</sub>(100nm)/Si substrates were introduced into a UHV chamber and Co catalysts (~0.1 nm in thickness) were deposited on them by electron beam (EB) evaporation. Then, ethanol gas was supplied onto the substrate surface through a stainless steel nozzle to grow CNTs. Supply of ethanol gas was controlled by monitoring the ambient pressure of the UHV chamber. During the growth, the chamber pressure was kept at  $1 \times 10^{-1}$  Pa. The growth temperature was 700°C, and the growth time was varied from 1 to 60 min. The grown CNTs were analyzed by Raman spectroscopy and scanning electron microscopy (SEM).

Figure 1 shows Raman spectra in the radial breathing mode (RBM) region for CNTs grown at various growth times from 1 to 60 min. When the growth time was 10 min, only RBM peaks from CNTs of less than 1 nm in diameter were observed. As the growth time became longer, CNTs of more than 1 nm in diameter appeared. These results indicate that the small-diameter CNTs are apt to grow faster than the larger-diameter CNTs. From time dependence of the G band intensity, the incubation time was estimated to be about 30 sec. Our results suggest that the growth rate of CNTs is related to the diameter of grown CNTs.

A part of this work was carried out in cooperation with Dr. Uruichi and Prof. Yakushi of the Institute for Molecular Science (IMS), Japan.

#### References

[1] K. Tanioku et al., *Diam. Relat. Mater.*, *in press*.

**Corresponding Author:** Takahiro Maruyama

**TEL:** +81-52-838-2386, **FAX:** +81-52-832-1172,

**E-mail:** takamaru@ccmfs.meijo-u.ac.jp

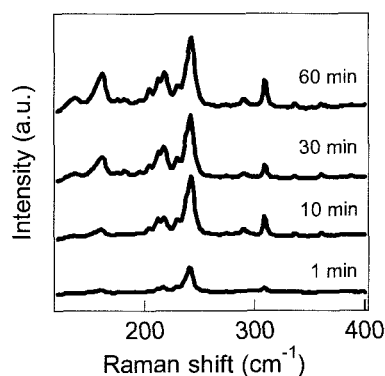


Fig 1



**Patterned growth of CNTs through AFM nano-lithography**Chien-Chao Chiu<sup>○</sup>, Masamichi Yoshimura, Kazuyuki Ueda

*Nano High-Tech Research Center, Toyota Technological Institute, 2-12-1 Hisakata,  
Tempaku, Nagoya 468-8511, Japan*

**Abstract:**

The CNTs have been grown on a patterned Si wafer using an AFM nano-oxidation technique that is an important method to fabricate nano devices. To remove the native oxide layer, a Si wafer was first cleaned by hydrogen fluorides. Nano-oxide films with height of 0.6-4.0 nm were made by changing scan speed 0.5-4.0  $\mu\text{m/s}$  under applying 5-10 V on the sample with respect to a Au coated AFM cantilever using a vector scan mode. Fe film was then coated by arc plasma deposition as a catalyst. After thermal annealing, Fe film on the bare Si area transformed into iron silicides through interfacial reaction, while the reaction was inhibited on the oxide patterned area. High-density CNTs were selectively grown on the extremely thin (1.5 nm-height) nano-oxide area Si by a home-made plasma-enhanced chemical vapor deposition. Figures 1 shows SEM images of a  $\text{SiO}_2$  patterned surface by AFM nano-oxidation(a) and CNT grown on the patterned substrate(b).

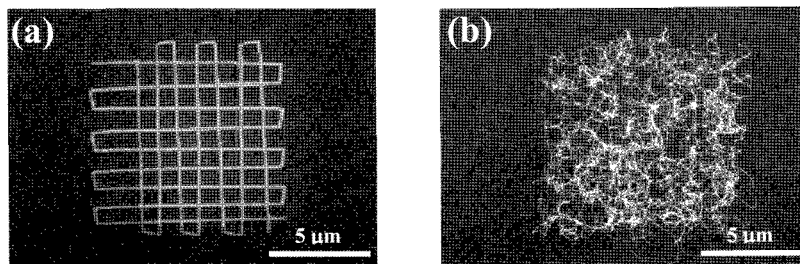


Figure 1. SEM images of (a)  $\text{SiO}_2$  pattern and (b) patterned growth CNTs.

**Reference:** 1. J. A. Dagata and et al., Appl. Phys. Lett. **56** (1990) 2001.

2. C.-C. Chiu and et al., Surf. Coat. Tech. **200** (2006) 3215.

**Corresponding Author: Chien-Chao Chiu**

**E-mail:** [kc@toyota-ti.ac.jp](mailto:kc@toyota-ti.ac.jp)

**Tel:** (052)809-1852, **Fax:** (052)809-1853

## A Study on Chirality-Selectivity of Metal Catalyst Particles in CNT Synthesis by Alcohol-CCVD

○Shogo Suzuki, Hideki Sato, Koichi Hata, and Kazuo Kajiwara

*Department of Electrical and Electronic Engineering, Mie University  
1577 Kurima-machiya-cho, Tsu 514-8507, Japan*

In recent years, the chirality-selective synthesis of carbon nanotubes (CNTs) has been developed for industrial applications [1]. CNTs have metallic or semiconducting properties dependent on their diameters and chiralities. The size and morphology of catalyst nanoclusters play an important role in determining the diameter and chirality of CNTs synthesized by catalytic chemical vapor deposition (CCVD). At present, understanding of catalyst effects on the chirality-selectivity is a major issue to optimize the conditions of CNT synthesis with single chirality by the CCVD method. In this study, quasicrystalline (QC) alloys as catalysts for CNT synthesis were investigated, which possess quasiperiodic structures with classically forbidden symmetry axes [2]. Among QC alloys found so far, two typical QC alloys were chosen as metal catalysts for CNT synthesis, (a) Al-Co-Ni alloy [3] in a decagonal phase with ten-fold symmetry and (b) Al-Cu-Fe alloy in an icosahedral phase with five-fold symmetry.

Al/Co/Ni and Al/Cu/Fe three-layered films (ca. 10 nm in total thickness) were deposited on Si/SiO<sub>2</sub> substrates by sequential electron-beam evaporation so as to become a perfect QC composition [2]. These samples were annealed at 450°C for 1h in a CVD reactor to form nanoclusters with a QC phase, followed by synthesizing CNTs at 700°C for 10 min by alcohol CCVD. These samples were characterized by using SEM, TEM, and resonance Raman spectroscopy. Fig.1 shows cross-sectional SEM images of CNTs synthesized using (a) the Al/Co/Ni film and (b) the Al/Cu/Fe film, and (c) an Al/Co film such as previously described [4]. It was found that vertically aligned CNTs were reproducibly synthesized by using these QC films as catalysts, similar to the Al/Co film. Chirality-selectivity of these samples is to be presented in the symposium.

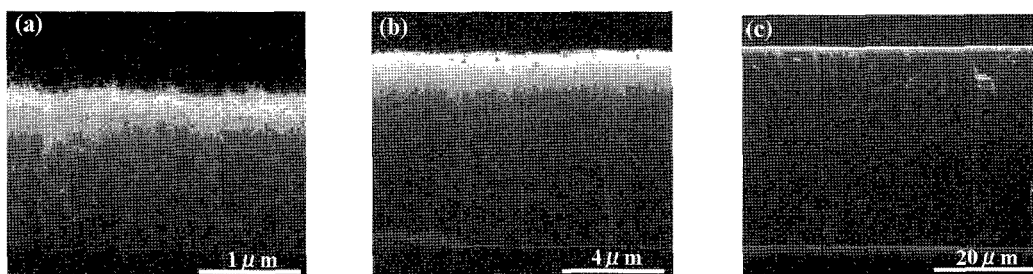


Fig.1 Cross-sectional SEM images of CNTs synthesized using (a) Al/Co/Ni film (with *d*-QC phase), (b) Al/Cu/Fe film (with *i*-QC phase), and (c) a conventional Al/Co film, as catalysts for alcohol CCVD.

- [1] M. Kusunoki et al., Chem. Phys. Lett. **366** (2002) 458.
- [2] Z.M. Stadnik (Ed.), *Physical Properties of Quasicrystals*, Springer, Berlin (1999).
- [3] S. Ohmori et al., Abstracts of the 24<sup>th</sup> Fullerene-Nanotube Symposium 20(P) (Jan. 8-10, 2003) p.41.
- [4] K. Hiasa et al., Abstracts of the 32<sup>nd</sup> Fullerene-Nanotube Symposium 1P-19 (Feb. 13-15, 2007) p.69.

Corresponding Author: Shogo Suzuki

E-mail: shogo@em.elec.mie-u.ac.jp, Tel/Fax: +81 59 231 9404

## TEM observation of Carbon Nanotube Pattern fabricated on SiC(000-1) using Ta mask

○Yoko Hozumi<sup>1</sup>, Yo Yamamoto<sup>2</sup>, Midori Mori<sup>1</sup>, Takahiro Maruyama<sup>1,2</sup>,  
Shigeya Naritsuka<sup>1,2</sup> and Michiko Kusunoki<sup>3</sup>

<sup>1</sup>*Department of Materials Science & Engineering, Meijo University*

<sup>2</sup>*Meijo University 21<sup>st</sup> CENTURY COE program “Nano Factory”*

<sup>3</sup>*Eco Topia Science Institute, Nagoya University*

It has been reported that zigzag-type carbon nanotubes (CNTs) grow after annealing SiC(000-1) substrate above 1300°C in a vacuum [1]. For fabrication of CNT devices, it is necessary to grow CNTs at selected positions on the substrate. The mask patterning technique is a useful way of doing this. However, conventional mask materials, such as SiO<sub>2</sub> or SiN, are unsuitable for selective CNT growth because of low sublimation temperature. To address this, we have been attempting to apply high melting point metal masks. In previous studies, we reported attempts for selective CNT growth using Ti mask. However, some portions of Ti mask melted and evaporated at around 1500 °C [2], therefore, mask material of higher heat-resistance has been desirable. In this study, Ta mask whose melting point is higher than that of Ti was applied for selective CNT growth.

Stripe mask patterns (both width and interval were 10 μm) were fabricated on SiC(000-1) substrates using photolithography technique. They were heated at 1700°C in a vacuum for 30min. After heating, the samples were characterized by scanning electron microscopy (SEM), X-ray photoelectron spectroscopy (XPS), micro Raman spectroscopy and transmission electron microscopy (TEM).

SEM observation and XPS measurement confirmed that, even after heating, Ta mask did not evaporate, maintaining the shape. TEM observation showed that CNTs of more than 200 nm in length grew on the SiC surface at the open area of the mask(Fig. 1(a)). In contrast, SiC did not decompose below most of the mask area (Fig. 1(b)), although CNTs of a few tens of nanometers in length were observed at some portions under the mask areas. These results indicate that Ta mask is more useful to obtain selective CNT growth on SiC substrates than SiN and Ti masks.

A part of this work was supported by “Nanotechnology Network Project” of the Ministry of Education, Culture, Sports, Science and Technology (MEXT), Japan.

### References

- [1] M. Kusuniki et al., Chem. Phys. Lett. 366 (2002) 458.  
[2] Y. Hozumi et al. NT07, P0115 (2007).

**Corresponding Author:** Takahiro Maruyama

**E-mail:** takamaru@ccmfs.meijo-u.ac.jp

**Tel:** +81-52-838-2386, **FAX:** +81-52-832-1172

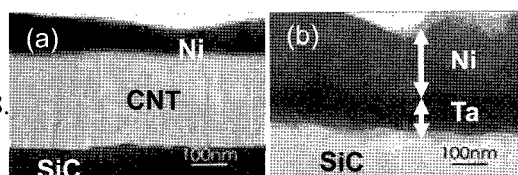


Fig.1 TEM images of (a) CNTs formed in the open area and (b) SiC below the mask area. Ni was deposited on the sample surfaces as a protection layers during the sample preparation for TEM.

## Growth mechanism of carbon nanotubes over gold-supported catalysts

○Naoki Yoshihara,<sup>1</sup> Hiroki Ago,<sup>\*1,2,3</sup> and Masaharu Tsuji<sup>1,2</sup>

<sup>1</sup>Graduate School of Engineering Sciences, Kyushu University, Fukuoka 816-8580, Japan

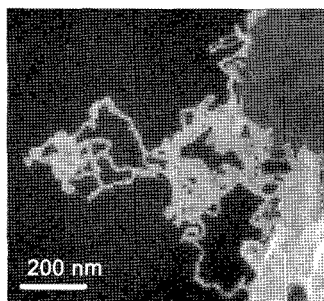
<sup>2</sup>Institute for Materials Chemistry and Engineering, Kyushu University, Japan

<sup>3</sup>PRESTO-JST, Japan

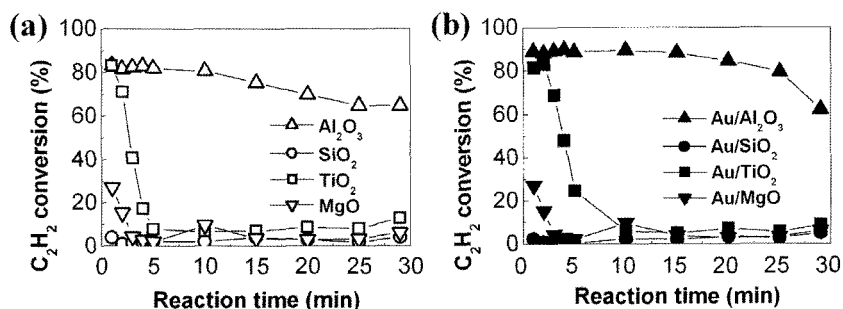
Recently, the growth of carbon nanotubes (CNTs) over gold (Au) catalysts has attracted interest [1,2]. Generally, Au is regarded as an inactive metal with a low catalytic activity and low carbon solubility. Therefore, it is interesting to study the growth mechanism and yield of CNTs over Au catalysts. We previously demonstrated that the analysis of an effluent gas during chemical vapor deposition (CVD) is useful for the understanding of the growth mechanism of CNTs [3]. Here, we investigated the growth of CNTs over Au-supported catalyst by examining various combinations of porous metal oxide supports and hydrocarbon feedstocks, with the aid of the gas analysis [4].

Figure 1 shows a SEM image of the filamentous carbon formed over the Au/Al<sub>2</sub>O<sub>3</sub> catalyst with acetylene (C<sub>2</sub>H<sub>2</sub>) feedstock. The TEM measurements showed that these fibers are multi-walled carbon nanotubes (MWNTs) with diameters of 10-50 nm. These nanotubes are curly and defective, and partly possess a bamboo-shaped structure. The carbon yield was much lower than that of typical Fe-Mo/MgO catalyst. The Au/SiO<sub>2</sub> catalyst also gave MWNTs, but no filamentous carbon was found on the Au/TiO<sub>2</sub> and Au/MgO catalysts.

As shown in Fig. 2a, we found that the Al<sub>2</sub>O<sub>3</sub> and TiO<sub>2</sub> supports decomposed a certain amount of C<sub>2</sub>H<sub>2</sub> feedstock, even without Au. The deposition of the Au onto the Al<sub>2</sub>O<sub>3</sub> and TiO<sub>2</sub> supports slightly increased the C<sub>2</sub>H<sub>2</sub> conversion, but the deposition onto the SiO<sub>2</sub> support showed almost no C<sub>2</sub>H<sub>2</sub> decomposition (Fig. 2b). These results suggest that the nanotube growth is not directly related to the C<sub>2</sub>H<sub>2</sub> decomposition, and we think that interaction between gold and the metal oxide supports is important for the MWNT growth.



**Fig. 1** SEM image of MWNTs grown over Au/Al<sub>2</sub>O<sub>3</sub> catalyst.



**Fig. 2** Time evolution of the C<sub>2</sub>H<sub>2</sub> conversion during the CVD growth over the support materials without Au (a) and Au-supported catalysts (b).

### References:

- [1] S. Y. Lee, M. Yamada, and M. Miyake, *Carbon*, **43**, 2654 (2005).
- [2] D. Takagi, Y. Homma, H. Hibino, S. Suzuki and Y. Kobayashi, *Nano Lett.* **6**, 2642 (2006).
- [3] N. Yoshihara, H. Ago, and M. Tsuji, *J. Phys. Chem. C*, **111**, 11577 (2007).
- [4] N. Yoshihara, H. Ago, and M. Tsuji, *Jpn. J. Appl. Phys.*, in press (2008).

**Corresponding Author:** Hiroki Ago (Tel&Fax: 092-583-7817, E-mail: ago@cm.kyushu-u.ac.jp)

# 1P-11

## G' band Raman Spectrum of Single, Double, and Triple Layer Graphene

\* Jin Sung Park<sup>1)</sup>, Alfonso Reina Cecco<sup>2)</sup>, Riichiro Saito<sup>1)</sup>, Jing Kong<sup>2)</sup>, Gene Dresselhaus<sup>3)</sup>,  
Mildred S. Dresselhaus<sup>2),4)</sup>

<sup>1)</sup>Department of Physics, Tohoku University and CREST JST, Sendai 980-8578, Japan

<sup>2)</sup>Department of Electrical Engineering and Computer Science, <sup>3)</sup>Francis Bitter Magnet Laboratory, <sup>4)</sup>Department of Physics, Massachusetts Institute of Technology, Cambridge, MA 02139-4307, USA

Graphene is the two-dimensional layered hexagonal lattice of carbon atoms. Recently, our collaborators have measured Raman spectra by controlling number of graphene layer from single layer to three layers and with changing excitation laser energy. In the spectra, we observed that the shape and intensity of the G' band depend on number of graphene layer and that the G'/G intensity ratio and G' peak position are changed by excitation laser energy. The G' band peak in single layer becomes strong and sharp comparison to double and triple layers. The integrated G'/G intensity ratio for single layer seems to follow  $(E_{\text{laser}})^{-4}$ . The G' band in graphene is due to two phonons scattering with opposite momentum in the highest optical branch around the K point. By considering the unit cell of double and triple layer graphene, we calculate the electronic structure for each number of layers. As the result, the electronic two linear bands of single graphene layer around Fermi level is split to two (three) bands by the interlayer interaction. This split electronic band plays an important role to determine the G' band shape and intensity in double and triple layers. We will neglect the splitting effect of the phonon branches in two and three graphene layers because of very small splitting of the phonon branches ( $1.5 \text{ cm}^{-1}$ ) [1]. In order to calculate G' band Raman spectrum, we have considered the electron-phonon interaction matrix and electron-photon interaction matrix as nominator of the Raman intensity formula by using extended tight binding model [2].

Reference:

- 1) A. C. Ferrari *et al.*, Phys. Rev. Lett., 97, 187401 (2006)
- 2) Ge. G. Samsonidze, Doctor thesis, MIT, (2006)

\*Email address: [park@flex.phys.tohoku.ac.jp](mailto:park@flex.phys.tohoku.ac.jp)

## Influence of Cathode-Anode Distance on Field Emission Properties for Bulky CNT Emitters

○Huarong Liu<sup>1,2</sup>, Shigeki Kato<sup>3</sup>, Yahachi Saito<sup>1</sup>

<sup>1</sup>Department of Quantum Engineering, Nagoya University, Nagoya 464-8603, Japan

<sup>2</sup>Venture Business Laboratory, Nagoya University, Nagoya 464-8603, Japan

<sup>3</sup>High Energy Accelerator Science Institute (KEK), Ohho1-1, Tsukuba, Ibaraki 305-0801, Japan

The remarkable properties of carbon nanotubes (CNT) make it possible to produce large-area emitters. However, there is an obvious discrepancy in reported field emission (FE) properties of these emitters and it can not be explained by only the adopted CNT geometry [1]. In this paper, the influence of cathode-anode distance (gap) is investigated, and it is shown that the gap can greatly affect the FE properties of bulky emitters.

CNTs produced by arc-discharge technique were fixed on Ti-coated metal substrates by a “rooting” technique [2]. FE tests were conducted at gaps from 0.1 to 0.8 mm in a UHV chamber with a base pressure of  $10^{-9}$  Pa after an aging test. Finally, a test at a gap of 0.8 mm was done again to confirm the FE reproducibility.

A group of emission current density ( $J$ )-applied field ( $E_A$ ) curves are shown in Fig. 2(a) for one typical emitter ( $\sim 1 \text{ mm}^2$ ).  $E_A$ , to obtain a given current, shifts to low field direction with the increase of gap. Fowler-Nordheim (F-N) plots in Fig. 2(b) shows that the increase of gap can enlarge the field enhancement factor ( $\beta$ ). The reason is ascribed to the phenomenon that emission sites can obtain more local electric field with the gap increase.

All the  $J$ - $E_A$  curves and F-N plots can be well normalized, as shown in Fig. 3(a), due to the fact that emission sites are reserved during the gap change. A similar conclusion can also be derived from the F-N theory; it reveals that all the modified F-N plots have the same intercept, as proved by Fig. 3(b).

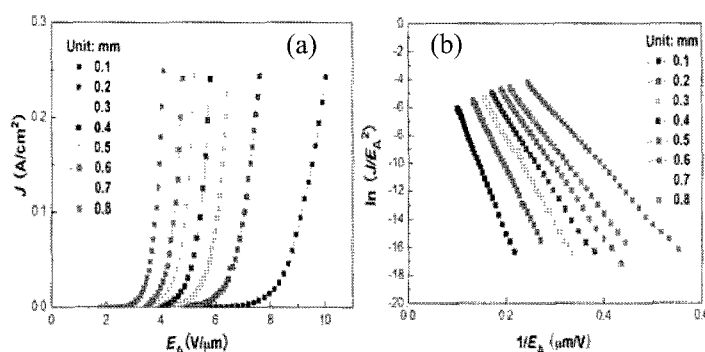


Figure 2. a)  $J$ - $E_A$  curves and (b) F-N plots.

[1] A. Loiseau et al., "Understanding Carbon Nanotubes", Springer, Berlin (2006).

[2] H. Liu, T. Noguchi, S. Kato, presented at the 46th Conference of Vacuum Society of Japan, Tokyo, Japan, 2005.

Corresponding author: Huarong Liu

E-mail:

[liu@surf.nurf.nuqe.nagoya-u.ac.jp](mailto:liu@surf.nurf.nuqe.nagoya-u.ac.jp)

TEL: +81-52-789-3714

FAX: +81-52-789-3703

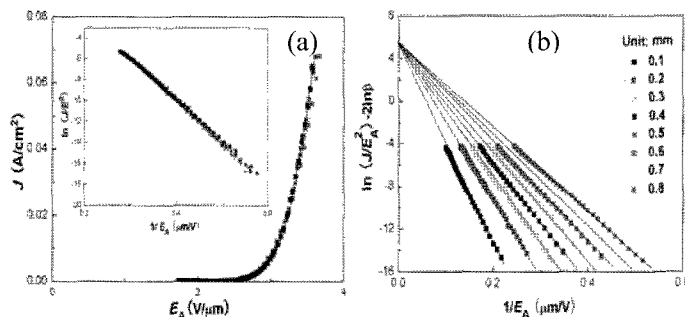


Figure 3. (a) Normalized  $J$ - $E_A$  curves and F-N plots. (b) Modified F-N plots showing the same intercept.

**Applications of vertically well-aligned CNT films to capacitors**

○Haruo Kato, Michiko Kusunoki\*, Shigeyuki Sugimoto\*\*,Kunihiro Sugihara,\*\*  
Noriyoshi Shibata

2-4-1 Mutsuno Atsuta-ku Nagoya,456-8587,Japan Japan Fine Ceramics Center

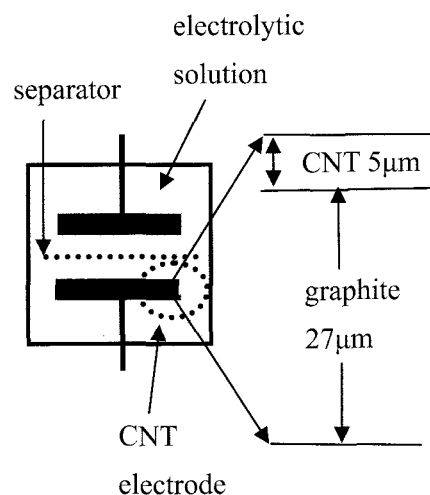
\*Furo-cho Chikusa-ku,Nagoya 464-8603,Japan

Eco Topia Science Institute, Nagoya University

\*\*20-1 Kitasekiyama Odaka-cho Midori-ku. Nagoya459-8522,Japan

Chubu Electric Power Co. ,Inc

**Abstract:** Electric double-layer capacitors are applied as electric sources of electronic devices and are important in terms of energy storage technology. High levels of power density and energy density, and long life spans, are desirable. We achieved high levels of performance in electric double-layer capacitors by controlling the nanostructures of well-aligned and high-density CNT films formed by SiC surface decomposition <sup>1)</sup>. The CNT growth is accompanied by a selective desorption of silicon from the SiC surface leaving free carbon that then forms into nanotubes without the use of catalyst metals. The thin film electrode with vertically aligned zigzag-type CNTs 5μm in length on the graphite layers 27μm in thickness has been developed. This closed-packed CNTs electrode has high conductive pathways and results in low electric resistance. As the results by introducing an electrochemical activation pretreatment, the obtained capacitance of the CNT film was 100F/g and no decrease in degree of capacitance under conditions of higher current density was confirmed in comparison with commercial activated carbon electrode.



**Fig.1** Structure of electric double-layer capacitor developed

**References**

1)M.Kusunoki,M.Rokkaku, and T.Suzuki :Appl.Phys.Lett.71,2620(1997).

**Corresponding Author** Haruo Kato(E-mail: hakato@jfcc.or.jp

Tel +81-52-871-3500 & Fax +81+52-871-3599)

## ***In-situ* observation of welding process of a multi-walled carbon nanotube to metal surface**

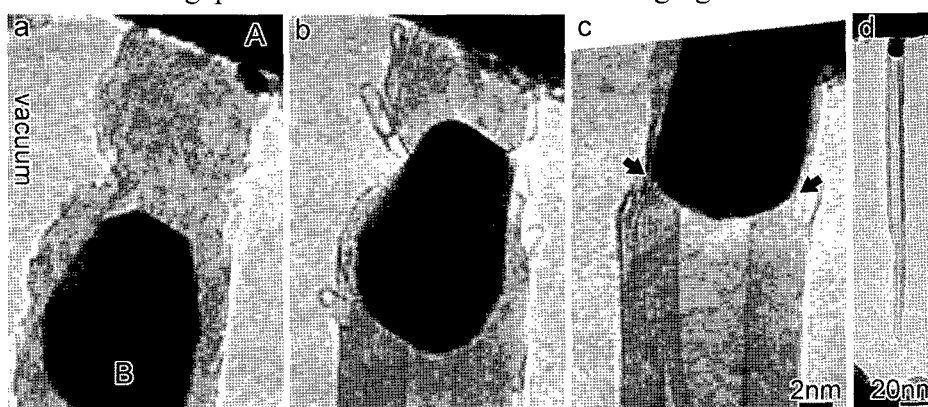
○Koji Asaka, Hitoshi Nakahara, and Yahachi Saito

*Department of Quantum Engineering, Nagoya University, Furo-cho,  
Nagoya 464-8603, Japan*

A single multi-walled carbon nanotube, encapsulating a nanometer-sized platinum particle, was manipulated inside a high-resolution transmission electron microscope combined with a piezo manipulator, and was welded to a platinum surface. The structural dynamics during the welding were *in-situ* observed by high-resolution imaging operated at 120 kV with a television system.

Figures (a)-(c) show time-sequential images of a welding procedure of a single multi-walled carbon nanotube to the platinum surface. In Fig. (a), the dark regions at the top (A) and the bottom (B) are the platinum surface and the platinum particle encapsulated in the nanotube, respectively. The tip of the nanotube is closed and its diameter is 9.1 nm. The surface of the encapsulated particle is surrounded by defined facets. The bright regions are vacuums. First, the tip of the nanotube was fixed tightly with the platinum surface, and a bias voltage was applied from 0 to 2.5 V. At 2.5 V, a current of 100  $\mu$ A passed abruptly through the nanotube. The facets of the particle disappeared and at the same time, the particle started to move toward the platinum surface as seen in Figs. (b). Finally, the particle was bonded to the platinum surface, as shown in Fig. (c). At the junction between the nanotube and the particle, each layer composing the nanotube was directly connected to the particle as shown by arrows in Fig. (c). After the bonding, we retracted the nanotube and formed a single nanotube freestanding on the platinum surface, as shown in Fig. (d).

The single nanotube welded to the platinum surface was used as an emitter for electron field emission and its electron field emission properties were also *in-situ* measured at various gap distances with simultaneous imaging.



Figures (a)-(c) Time-sequential image of a welding procedure of a carbon nanotube. (d) Low magnification image of a single nanotube emitter fabricated by welding. The tip-diameter and the length of the nanotube are 5 nm and 176 nm, respectively.

Corresponding Author: Koji Asaka

E-mail: asaka@nuqe.nagoya-u.a.jp

Tel&Fax: +81-52-789-3714, +81-52-789-3703



## Formation of Honeycomb Structure on PET Using Soluble Carbon Nanotube

○Nobuo Wakamatsu, Hisayoshi Takamori, Tsuyohiko Fujigaya,  
and Naotoshi Nakashima

*Department of Applied Chemistry, Graduate School of Engineering, Kyushu University,  
Fukuoka, Japan*

Potential applications using carbon nanotubes (CNTs) are often limited due to their insolubility in many solvents due to strong intertube van der Waals interactions. Therefore, strategic approaches toward the solubilization of CNTs should be important for the applications of CNTs. We reported the finding that a simple solution casting of carbon nanotubes/lipid complex (complex **1**) produces self-organized honeycomb structures. The mixing of aqueous solution of single-walled carbon nanotubes (SWNTs) with aqueous molecular-bilayers of an artificial ammonium lipid produced a precipitate, which was collected to obtain complex **1** that is soluble in organic solvents. A simple solution casting of the complex **1** was found to produce self-organized honeycomb structures (**Figure 1-a**), whose cell sizes were controllable by changing experimental conditions. The lipid part of complex **1** was easily removed by an “ion exchange” method with maintaining the basic honeycomb structures (**Figure 1-b**). After the ion-exchange, the films with thinner skeletons exhibited dramatic decrease of the surface resistivity.

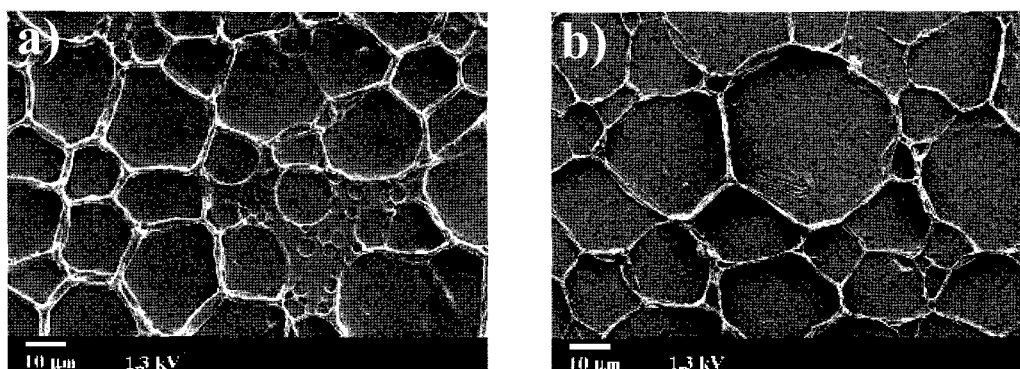


Fig.1. Typical SEM images for the films casting from a chloroform solution of complex **1** before (a) and after (b) the ion exchange.

Corresponding Author: Naotoshi Nakashima

TEL:+81-92-802-2840,FAX:+81-92-802-2840,E-mail:[nakashima-tcm@mbox.nc.kyushu-u.ac.jp](mailto:nakashima-tcm@mbox.nc.kyushu-u.ac.jp)

## Investigation of Methane Adsorption on MWNTs Using Field Emission Microscopy (FEM)

○T.Yamashita, K.Asaka, H. Nakahara, and Y. Saito

*Dept. of Quantum Eng., Nagoya University, Furo-cho, Nagoya 464-8603*

Field emission of electrons from a multiwall carbon nanotube (MWNT) with a closed end occurs preferentially from pentagons at the cap when the nanotube surface is clean. It has been shown that the electron emission is enhanced from the adsorbed molecules when residual gas molecules adsorbed on the surface. In this work, effects of methane adsorption on the surface of MWNTs were studied by field emission microscopy (FEM).

MWNTs produced by arc discharge were attached to a tungsten hairpin by graphi-bond. The base pressure of the FEM chamber was  $\sim 1.0 \times 10^{-7}$  [Pa]. Methane was adsorbed on MWNTs with applying the electric field under the pressure of  $\sim 10^{-6}$  [Pa] for 10 minutes. Adsorption process was also carried out without applying the voltage in order to investigate the effect of an electric field.

Figs. 1(a) and (b) show FEM patterns of a clean surface and methane-adsorbed surface of a MWNT, respectively. A cross-like pattern as indicated by a circle in Fig. 1(b) is observed during the exposure to methane, and we assume that the pattern corresponds to a molecule of methane. Since a methane molecule has the tetrahedral structure, it looks like a cross when the two-fold symmetry axis is normal to the substrate as illustrated in Fig. 2.

Current( $I$ )-voltage( $V$ ) curves before and after methane adsorption are shown in Fig.3. The emission current was remarkably increased after the methane adsorption. The dashed curve in Fig.3 shows an  $I$ - $V$  curve after flashing to desorb adsorbates. The current was decreased after flashing, suggesting that adsorbates were removed. However, FEM patterns did not show the clean surface after the flashing, indicating that some molecules or fragments still remained after the flashing. When MWNTs were exposed to methane gas under no electric field, the MWNT emitter did not show significant change in  $I$ - $V$  curves as well as FEM patterns after the expose to the gas, compared with those before the exposure.

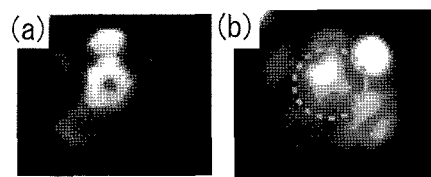


Fig.1 FEM patterns (a) before and (b) after methane exposure

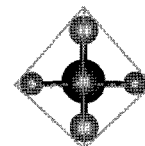


Fig.2 Methane molecule viewed along the 2-fold axis

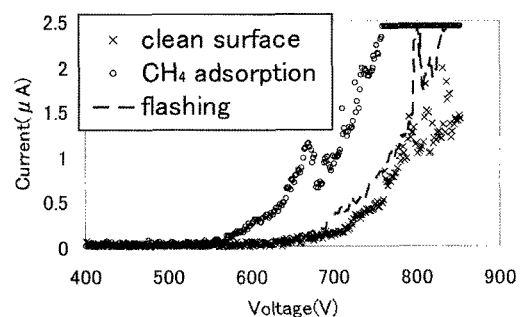


Fig.3 Current-voltage curves

Corresponding author: Tetsuya Yamashita

E-mail: yamashita@surf.nuqe.nagoya-u.ac.jp

TEL: +81-52-789-3714, FAX: +81-52-789-3703

**Culture of Osteoblast-like Cells on Transparent Conductive Thin Films with Carbon Nanotubes**

○Tsukasa Akasaka<sup>1</sup>, Atsuro Yokoyama<sup>1</sup>, Makoto Matsuoka<sup>1</sup>, Shigeaki Abe<sup>1</sup>, Motohiro Uo<sup>1</sup>, Yoshinori Sato<sup>2</sup>, Kazuyuki Tohji<sup>2</sup>, Takeshi Hashimoto<sup>3</sup>, Fumio Watari<sup>1</sup>

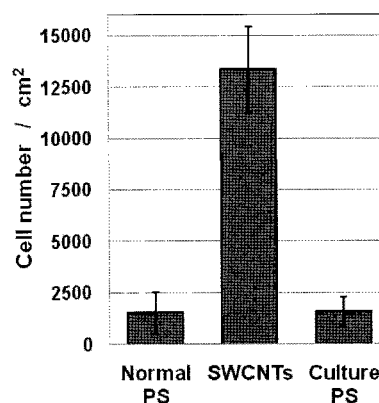
<sup>1</sup>Graduate School of Dental Medicine, Hokkaido University, Sapporo 060-8586, Japan

<sup>2</sup>Graduate School of Environmental Studies, Tohoku University, Sendai 980-8586, Japan

<sup>3</sup>Meijo Nano Carbon Co. Ltd., Nagoya 460-0002, Japan

Although carbon nanotubes (CNTs) have been widely studied, most of the studies focused on the physical and electrical fields, with very few on biomedical applications. Our previous study showed the excellent cell growth on single-walled carbon nanotubes (SWCNTs) and multi-walled carbon nanotubes (MWCNTs) and which implies that CNTs could be suitable scaffold for cell culture [1,2]. However, there is scarce information about cellular response to the culture substrates with CNTs. The aim of the present study was to investigate the cell responses on CNTs coated polystyrene (PS) dishes with the ability of transparent conductive thin film.

On CNTs coated dishes, SaOs2 cells were seeded and cultured in DMEM with 10%FBS for several days. The number of SaOs2 on SWCNTs was greater than that on cell culture PS. In the low concentration of FBS, SWCNTs were more effective in life extension and proliferation than general culture dishes. Hence, SWCNTs thin films may be usable to culture substrate for transfection, ELISA analysis, electrical stimulation, and so on. On the other hand, MWCNTs were advantageous at the points of cell adhesion, cell migration, and alkaline phosphatase activity. These results shows SWCNTs and MWCNTs are suitable and different tools for cell culture.



**Fig.1** Number of SaOs2 cultured on CNTs coated dish in low FBS.

References:

[1] N. Aoki, T. Akasaka, F. Watari, and A. Yokoyama, Dent. Mater. J. 26, 178 (2007). [2] N. Aoki, A. Yokoyama, Y. Nodasaka, T. Akasaka, M. Uo, Y. Sato, K. Tohji, and F. Watari, Chem. Lett. 35, 508 (2006).

Corresponding Author: Tsukasa Akasaka

E-mail: akasaka@den.hokudai.ac.jp, Tel&Fax: 81-11-706-4251

**In Situ TEM Study on Field Emission Property of an Isolated CNT**

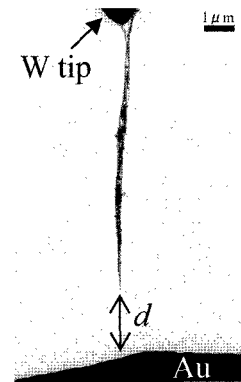
○Kensuke Okumura, Koji Asaka and Yahachi Saito

*Dept. of Quantum Eng., Nagoya University, Nagoya 464-8603, Japan*

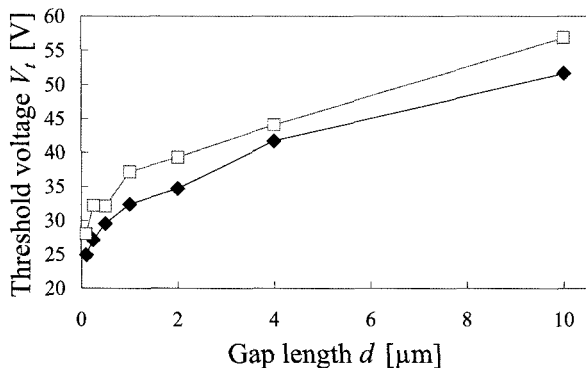
Carbon nanotubes (CNT) are promising candidates for cold cathode electron field emitters because of their excellent electrical conductivity, chemical inertness, mechanical strength and needle-like shape with high aspect ratio that brings about field enhancement on their tips [1]. For the practical use of CNT emitters, the field emission properties of CNTs must be clarified. In this work, the field emission property of the CNT emitter which is an isolated multi-wall nanotube (MWNT) attached to a tungsten needle was studied by in situ transmission electron microscopy (TEM).

A small bundle of MWNTs was attached to the tip of a tungsten needle by electrophoresis. The CNT emitter and a gold anode were mounted in a special sample holder for TEM (Fig.1). The diameter of this MWNT is about 6 nm and the length of the bundle suspended from the W tip is about 8 μm. The distance  $d$  between the CNT emitter and the gold anode was varied between 0.1 μm and 10 μm. The electric voltage was applied from 0 to 100 V, and then it was decreased. The voltage at which the emission current became 10 nA was defined as the threshold voltage  $V_t$ . The field emission measurement was carried out before and after the exposure of the emitter to atmosphere.

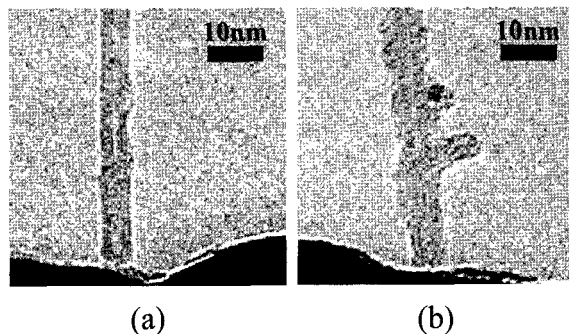
Figure 2 shows that the  $V_t$  against the gap length  $d$ . Before the exposure to air, the  $V_t$  was 52V at  $d=10\mu\text{m}$  and 25V at  $d=0.1\mu\text{m}$ . After the exposure, however, the  $V_t$  increased to 57V at  $d=10\mu\text{m}$  and 30V at  $d=0.1\mu\text{m}$ . This increase in  $V_t$  may result from the degradation of CNT caused by the field emission or the exposure to air (Fig.3).



**Fig.1.** TEM image of the experimental arrangement.



**Fig.2.** Threshold voltage against the gap length before and after the exposure to air.



**Fig.3.** TEM images of the tip of a MWNT (a) before the field emission (FE) and (b) after the FE and exposure to air.

[1] Y.Saito, J.Nanosci. & Nanotech. 3, 39 (2003)  
 Corresponding Author: Kensuke Okumura  
 E-mail: [okumura@surf.nuqe.nagoya-u.ac.jp](mailto:okumura@surf.nuqe.nagoya-u.ac.jp)  
 Tell: 052-789-3714 Fax: 052-789-3703

## Fabrication Process of Carbon Nanotube FETs Using ALD Passivation for Biosensors

<sup>o</sup>Y. Nakashima<sup>1</sup>, Y. Ohno<sup>1</sup>, S. Kishimoto<sup>1,2</sup>, M. Okochi<sup>3</sup>, H. Honda<sup>3</sup>, and T. Mizutani<sup>1</sup>

<sup>1</sup>Dept. of Quantum Eng., Nagoya Univ., Furo-cho, Chikusa-ku, Nagoya 464-8603, Japan

<sup>2</sup>Venture Business Laboratory, Nagoya Univ., Furo-cho, Chikusa-ku, Nagoya 464-8603, Japan

<sup>3</sup>Dept. of Chemical Eng., Nagoya Univ., Furo-cho, Chikusa-ku, Nagoya 464-8603, Japan

Carbon nanotube (CNT) FETs have received much attention for a variety of applications. Among them, CNT-FET sensors are attractive because of their potential for high-sensitive and label-free operations [1, 2]. In order to implement the CNT-FET biosensors, deposition of the passivation film on the device surface is important to suppress the leakage current between electrodes through the electrolyte and to avoid the influence of an environmental charge. However, there is a technical issue that the deposition of the insulator film sometimes causes a decrease of a drain current [3]. In this study, we have applied atomic layer deposition (ALD). It has been confirmed that the ALD is useful for the passivation of the device surface. Biosensor operation was confirmed by CNT-FETs fabricated using the ALD passivation film.

Figure 1 shows a schematic cross section of the fabricated CNT-FETs. Following the fabrication of the back-gate CNT-FETs, HfO<sub>2</sub> film (50 nm) with a large dielectric constant was deposited on the device surface by ALD at 250°C. HfO<sub>2</sub> was chosen as a passivation/top-gate insulator to realize a large transconductance of the device. The step coverage was very good and no leakage current was observed in the HfO<sub>2</sub>-passivated device being immersed in the electrolyte. Finally, a top-gate electrode was formed.

Figure 2 shows the typical  $I_D$ - $V_{BG}$  characteristics of the device before HfO<sub>2</sub> deposition and after top-gate electrode formation. Even though the hysteresis did not decrease by the ALD passivation (not shown), it drastically decreased by the top-gate electrode formation as shown in the figure. This is probably due to that the effect of environmental charge which caused hysteresis was shielded by covering the device surface by the top-gate electrode.

Biosensor measurement was performed by measuring the  $I_D$  when the enzyme Cytochrome c (pI=10.25, 30μmol/ml) containing solution was dropped into the phosphate-buffer (PB) solution (pH=7.0). Figure 3 shows the  $I_D$ - $V_{Gref}$  (reference electrode voltage) characteristics before and after dropping Cytochrome c containing solution. The  $I_D$  increase and the threshold voltage shift of 0.12V were observed, which confirms the detection of the enzyme.

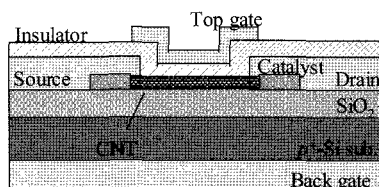


Fig. 1 CNT-FET sensor

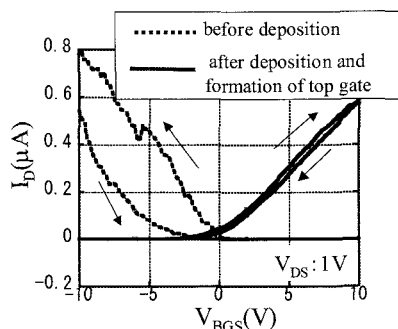


Fig. 2  $I_D$ - $V_{BG}$  characteristics

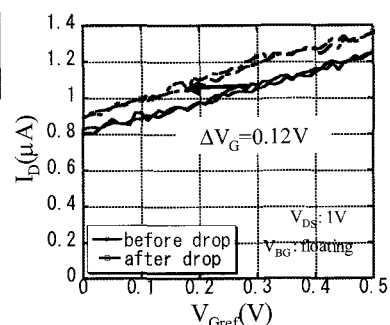


Fig. 3 Sensing experiment

[1] A. Star *et al.*, Nano lett. **3**, 1421 (2003).

[2] A. Kojima *et al.*, Jpn. Appl. Phys. **44**, 1569 (2005).

[3] K. Tani *et al.*, Jpn. Appl. Phys. **45**, 5481 (2006).

Corresponding Author: Yasuhiro Nakashima

E-mail: [nakashima.yasuhiro@ambox.nagoya-u.ac.jp](mailto:nakashima.yasuhiro@ambox.nagoya-u.ac.jp), Phone & Fax: +81-52-789-5455

## Electron Optical Evaluation of Carbon Nanotube Field-Emitter

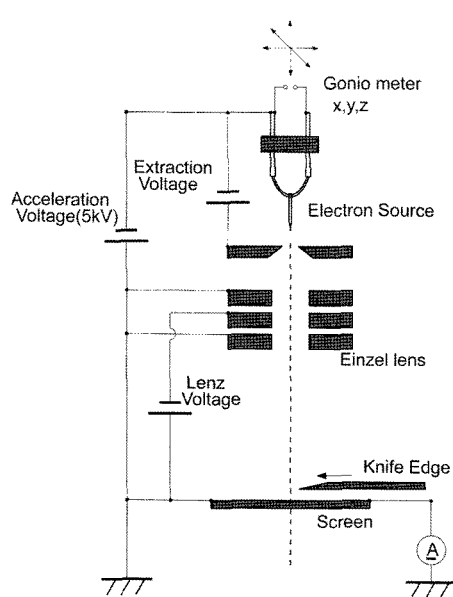
○ T. Kono, K. Asaka, H. Nakahara and Y. Saito

*Dept. of Quantum Eng., Nagoya University, Furo-cho, Nagoya 464-8603*

Carbon nanotubes (CNTs) have high potential for application to electron sources of high resolution electron microscopes. In this work, we investigated current-voltage characteristic and brightness of CNT field-emitters.

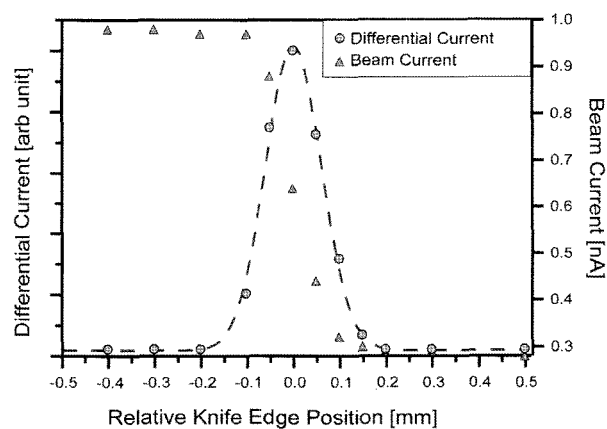
Multi-wall carbon nanotubes produced by arc discharge are glued on top of a tungsten hairpin filament. An electron optical system used in the present experiment is shown in Fig. 1. The position of the CNT emitter relative to the extraction electrode is adjusted by a x-y-z goniometer. An electron beam emitted from CNTs is accelerated by an anode, and focused by an einzel lens to a screen. A knife edge is positioned between the lens and the screen to measure the beam size.

Fig. 2 shows an example of a beam profile. A dashed line is Gaussian fitting for differential current. From FWHM of the Gaussian fitting, a beam size is estimated approximately 0.14 mm. The brightness is calculated as  $0.241 \text{ A/cm}^2 \cdot \text{sr}$ , being much smaller by several orders of magnitude than that



**Fig. 1** Schematic of the experiment

expected from field emission microscopy, presumably due to large aberrations of the lens.



**Fig. 2** An example of a beam profile

Corresponding author: Takumi Kono

E-mail: [takumi@surf.nuqe.nagoya-u.ac.jp](mailto:takumi@surf.nuqe.nagoya-u.ac.jp) TEL: +81-52-789-4659, FAX: +81-52-789-3703

## Studying the Same-Handedness in Double-Walled Carbon Nanotubes Using the Dispersion-Augmented Density Functional Tight Binding Method

○Stephan Irle, Raviprasad Krishnamurthy, Keiji Morokuma

<sup>1</sup>*Institute for Advanced Research and Department of Chemistry, Nagoya University, Nagoya 464-8602, Japan;* <sup>2</sup>*Fukui Institute for Fundamental Chemistry, Kyoto University, Kyoto 606-8106;* <sup>3</sup>*Nanotechnology Victoria, Monash University, Clayton 3800, Victoria, Australia*

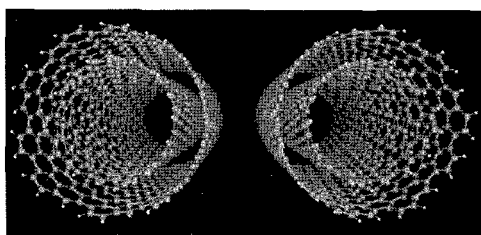


Figure 1. (14,3)@(17,10) (left) and (3,14)@(17,10) right, 30Å models

Prompted by the experimental finding that same-handedness is preferred in double-walled carbon nanotubes (DWNTs) with chiral tube components [1], we have investigated the thermodynamic stabilities of finite-size, hydrogen-terminated 15 Å and 30 Å long as well as infinite-length DWNT model systems. Tested systems were a) right-right (RR) (14,3)@(17,10), b) left-right (LR) (3,14)@(17,10), c) right-left (RL)

(14,3)@(10,17), and d) left-left (LL) (3,14)@(10,17), as well as RL- and RR-combinations of other DWNT systems. As quantum chemical potential we have used the dispersion-augmented density functional tight-binding (DFTB-D) method by Elstner *et al.* [2] We have verified this simple approach which combines quantum chemical potential with a London  $1/R^6$  dispersion term, using MP2/SVP geometry optimized 1-ring model components including computation of larger basis set single-point energies and basis set superposition effects, but did not find any thermodynamic preference for systems either of the DWNT combinations.

As long as the tube diameters are identical, attractive dispersion forces are also identical between the sidewalls so that a continuum model serves in fact as a good description. The origin for same-handedness, if it exists, must stem from the formation process and could be kinetically controlled, rather than originating in a thermodynamic stability preference.

### References:

- [1] Liu, Z.; Suenaga, K.; Yoshida, H.; Sugai, T.; Shinohara, H.; Iijima, S. *Phys. Rev. Lett.* **2005**, *95*, 187406.  
 [2] Elstner, M.; Hobza, P.; Frauenheim, Th.; Suhai, S.; Kaxiras, E. *J. Chem. Phys.* **2001**, *114*, 5149.

### Corresponding Author:

Stephan Irle

E-mail: sirle@iar.nagoya-u.ac.jp

Tel: 052-747-6397/Fax: 052-788-6151

## Electronic properties of hybrid (DNA/SWCNT) thin film

○Yusei Maruyama<sup>1</sup>, Satoru Motohashi<sup>1</sup>, Masayuki Tanaka<sup>1</sup>, Biao Zhou<sup>2</sup>, Akiko Kobayashi<sup>2</sup>,  
Hironori Ogata<sup>1</sup>

<sup>1</sup>*Research Center for Micro/Nano Technology, Hosei University, Midorichou, Koganei, Tokyo  
184-0003, Japan*

<sup>2</sup>*Department of Chemistry, College of Humanities and Sciences, Nihon University,  
Sakurajousui, Setagaya, Tokyo 156-8550, Japan*

It is known that there are some significant interactions between DNA molecules and carbon nanotubes [1,2,3]. In this report, some electronic properties, such as electrical, magnetic and optical, of “hybrid” material (DNA/SWCNT) thin films were measured to identify the electronic interactions between them.

The film was prepared by super-sonication of ss-DNA (calf-thymus) and SWCNT (NANCOS INC.) in ultrapure water for 2 hrs, followed by the evacuation of water. The typical thickness of the film was several tens microns and the appearance was black-metallic- shiny. The morphological study for this material was very preliminary and the SEM image showed just flat view. TEM and STM studies are on the way.

The temperature dependence of magnetism of the film observed by SQUID showed no significant difference from the signal of SWCNT itself. This means that there is no significant magnetic interaction between them or the magnetic impurity in SWCNT sample may mask the effective modulation.

The typical electrical conductivity was 2.5 S/cm at room-temp. and the temperature dependence of the resistivity was best-fitted to the plots of 2-dimensional variable-range hopping regime. This means that the film is essentially metallic 2-dimensional material.

The remarkable modulation due to hybridization in the Raman-scattering spectra of the radial-breathing mode was the reverse in the relative intensity in the lowest wave number region. This result means that the number of thickest “free” tubes was reduced due to hybridization.

- [1] M. Zheng *et al.* *Nature Mater.* 2 (2003) 338.  
[2] N. Nakashima *et al.* *Chem Lett.* 32 (2003) 456.  
[3] M. Iijima *et al.* *Chem. Phys. Lett.* 414 (2005) 520.  
Corresponding Author: Yusei Maruyama  
E-mail: [yusei.maruyama.kd@k.hosei.ac.jp](mailto:yusei.maruyama.kd@k.hosei.ac.jp)  
Tel&Fax: 042-387-5180, 042-387-5121



## Theory of superconductivity by the edge states in graphene

K. Sasaki<sup>1</sup>○, M. Suzuki<sup>1</sup>, R. Saito<sup>1</sup>, S. Onari<sup>2</sup>, Y. Tanaka<sup>2</sup>

<sup>1</sup>*Department of Physics, Tohoku University and CREST, JST, Sendai 980-8576, Japan*

<sup>2</sup>*Department of Applied Physics, Nagoya University, Nagoya 464-8603, Japan*

Superconductivity in graphite intercalation compound (C<sub>6</sub>Ca) and single-wall and multi-wall carbon nanotubes has been attracting much attention due to its high superconducting transition temperature above 10 K [1]. However, the density of states (DOS) near the Fermi energy of graphene is not sufficient to explain the observed high transition temperature. Thus, the mechanism of the superconductivity is an important issue.

The STS measurements [2] show an anomalous DOS near the Fermi level of graphene which is relevant to localized edge states [3]. The edge states significantly enhance the local DOS near the zigzag edge. Thus, it is valuable to examine the effect of the edge states on the superconductivity.

Using the Eliashberg equation, we obtain an appreciable transition temperature for the edge states [4]. We found that the effects of the Coulomb interaction and Fermi energy position are sensitive to the formation of superconducting gap. We report on the calculated STS spectrum near the zigzag edge and discuss the condition for observing the edge state superconductivity.

When the edge states become a superconducting state, a metallic zigzag nanotube having open boundaries can be regarded as a natural Superconductor/Normal metal/Superconductor junction system, in which superconducting states are developed locally at both ends of the nanotube and a normal metal exists in the middle. In this case, a signal of the edge state superconductivity appears as the Josephson current which is sensitive to the bandwidth, the position of the Fermi energy and the length of a nanotube.

[1] Weller *et al.*, *Nature Physics* **1**, 39 (2005); Tang *et al.*, *Science* **292**, 2462 (2001); Takesue *et al.*, *Phys. Rev. Lett.* **96**, 057001 (2006).

[2] Y. Niimi *et al.*, *Appl. Surf. Sci.* **241**, 43 (2005); Y. Kobayashi *et al.*, *Phys. Rev. B* **71**, 193406 (2005).

[3] M. Fujita *et al.*, *J. Phys. Soc. Jpn.* **65**, 1920 (1996).

[4] K. Sasaki *et al.*, *J. Phys. Soc. Jpn.* **76**, 033702 (2007).

Corresponding Author: Ken-ichi Sasaki, E-mail: sasaken@flex.phys.tohoku.ac.jp

## Electrical transport properties of azafullerene C<sub>59</sub>N encapsulated single- and double-walled carbon nanotubes

○Y. F. Li, T. Kaneko, S. Nishigaki and R. Hatakeyama

*Department of Electronic Engineering, Tohoku University, Sendai 980-8579, Japan*

In this work, the electrical transport properties of azafullerene C<sub>59</sub>N encapsulated single- and double-walled carbon nanotubes (SWNTs and DWNTs) are investigated by fabricating them as the channels of field effect transistors (FETs). The synthesis of C<sub>59</sub>N fullerenes is realized by a nitrogen-plasma irradiation method, and they are confirmed by a laser-deposition time-of-flight mass spectrometer. The encapsulation of C<sub>59</sub>N azafullerenes into SWNTs or DWNTs has been prepared by either a vapor reaction method or a plasma irradiation method, which is confirmed in detail by a transmission electron microscope (TEM, Hitachi HF-2000) operated at 200 kV and Raman spectroscopy (Jovin Yvon T-64000) with an Ar laser at 488 nm. The transport properties of azafullerene peapods are studied in both dark and upon light illumination. Compared with *p*-type characteristics of C<sub>60</sub> fullerene encapsulated SWNTs (Fig.1) or DWNTs, our results indicate that *n*-type semiconducting SWNTs (Fig.2) or DWNTs can be formed by the C<sub>59</sub>N fullerene encapsulation, demonstrating electron donor behavior of C<sub>59</sub>N, which is in excellent agreement with a related theoretical predication [1]. The photoinduced transport characteristics of peapods are also investigated, and the distinct response of FET devices to light is reflected in a shift of threshold voltage toward negative voltages. More interestingly, after removing of the light the photoresponse is fully recoverable.

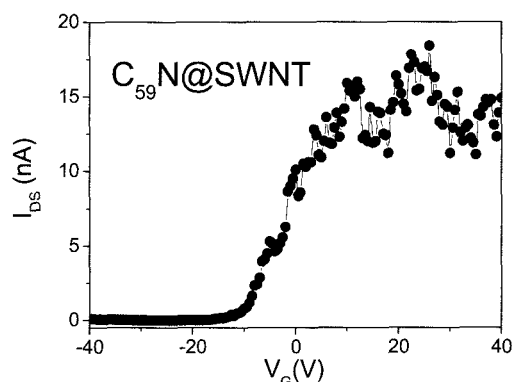
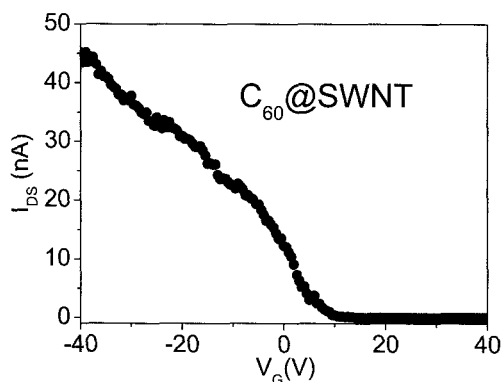


Fig.1 Characteristic of  $I_{DS}$ - $V_G$  for C<sub>60</sub>@SWNT      Fig.2 Characteristic of  $I_{DS}$ - $V_G$  for C<sub>59</sub>@SWNT

( $V_G$ : gate voltage,  $I_{DS}$ : source-drain current)

[1] W. Andreoni, *et al.*, *Chem. Phys. Lett.* **190**, 159 (1992).

Corresponding Author: Yongfeng Li

Tel : 81-22-795-7046, FAX: 81-22-263-9225, E-mail: yfli@plasma.ecei.tohoku.ac.jp

## Embedding of Carbon Nanotubes on Silicon substrates for use in Solar Cells

Abhishek Kumar<sup>○</sup>, Nikhil Dhawan<sup>^</sup>

<sup>○</sup> *Materials Science and Engineering Department, Stanford University, California, 94305, USA*

<sup>^</sup> *Metallurgical Engineering Department, Punjab Engineering College, Chandigarh, INDIA*

### Abstract

Carbon nanotubes bundles were precisely grown atop a p-type silicon wafer that had been treated with catalysts to produce geometries that resemble three-dimensional nano-models to extract more power from the sun. The embedded carbon nanotubes bundles on silicon wafer promise more opportunity for each photon of sunlight to interact with resulting solar cell, as a result of increase of surface area available to produce electricity. The paper discusses morphology and properties of grown nanotubes on silicon wafer along with future prospects of Si-CNTs fabricated solar cells.

Corresponding Author

Abhishek Kumar

[akpec@stanford.edu](mailto:akpec@stanford.edu)

Tel (650) 644 9442

**Synthesis of single-walled carbon nanotubes by arc plasma reactor with twelve-phase alternating current discharge**

○T. Matsuura<sup>1</sup>, Y. Kondo<sup>1</sup>, N. Maki<sup>1</sup>, Y. Ito<sup>1</sup>, K. Matsumoto<sup>2</sup>, N. Tamura<sup>2</sup>, Y. Taira<sup>2</sup>, R. Ehara<sup>2</sup>

<sup>1</sup> *Industrial Technology Center of Fukui Prefecture, Fukui, Japan*

<sup>2</sup> *Department of electronics and informatics, Toyama prefecture university, Toyama, Japan*

**Abstract**

Several methods for synthesis of CNTs such as DC arc-discharge [1, 2], laser ablation and thermal chemical vapor deposition (CVD) have been presented. The DC arc-discharge method can synthesize CNTs in highest quality than the other methods mentioned above. However, its yields are much lower. Up to date, CVD method is the mainstream of mass fabrication of CNTs [3]. In order to avoid the disadvantage of the DC arc-discharge method, the twelve-phase AC arc-discharge method has been developed [4]. In general, multiple-phase AC discharge plasma has unique features as follow [5, 6]; (a) no discharge break in spite of using very low frequency (in this case 60Hz) discharge, (b) rotation of discharge area depend on the frequency of the power source, (c) very low velocity and enriched uniform plasma production in wide space, almost 180mm in diameter, surrounded by multiple electrodes. Single-walled carbon nanotubes (SWCNT) are synthesized in methane gases by using this new type of arc plasma reactor. The felt like SWCNTs shown in Fig.1 are observed in high yield. The structure shown in Fig.2 of the inner diameter and the outer diameter is estimated 3nm and 4nm, respectively. The highest ratio of G-band (1580cm<sup>-1</sup>) and D-band (1360cm<sup>-1</sup>) measured by Raman spectrum shown in Fig. 3 is approximately 14. The catalyst was fed from the carbon electrodes containing 4.2%Atom-Ni and 1%Atom-Y. The effects of substrate temperature, gas pressure, kind of gas were investigated.

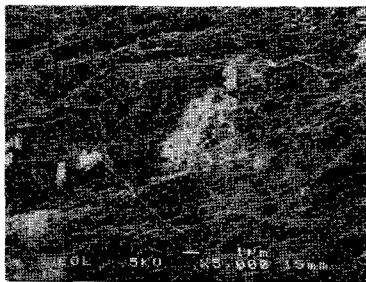


Fig.1 SEM image

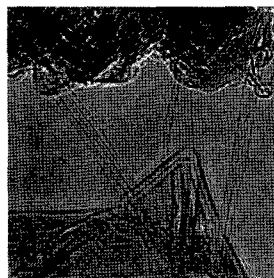


Fig.2TEM image

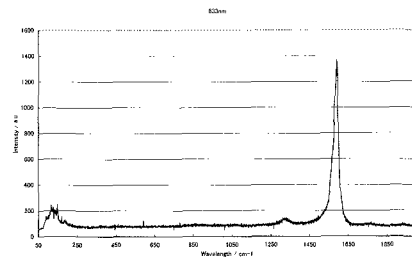


Fig.3 Raman spectrum

**References**

- [1] S. Iijima, Nature, 354, 56 (1991).
- [2] T. W.Ebbesen and P.M.Ajayan, Nature, 358, 220 (1992).
- [3] K. Hata, et al, Science, Vol. 306, 19, Nov. (2004)
- [4] T. Matsuura, et al, 17<sup>th</sup> Int. Sym. on Plasma Che. (2005)
- [5] K. Matsumoto, et al, Proc. 6th International Conference on Reactive Plasma and 23rd Symposium on Plasma Processing (2006)
- [6] T. Matsuura, et al, thin Solid Films, 515, 4240-4246 (2007)

**Corresponding Author: Tsugio Matsuura**

**E-mail: Tsugio\_Matsuura@fklab.fukui.fukui.jp**

**Tel: 0776-55-0664 Fax: 0776-55-0665**

## Electronic structures at edges of carbon nanotube and molecular dynamics simulations

○ Hirofumi Sakashita<sup>1</sup>, Tatsuki Oda<sup>1</sup>, Nobuhisa Fujima<sup>2</sup>

<sup>1</sup>*Graduate School of Natural Science and Technology, Kanazawa University  
Kanazawa, 920-1192, Japan*

<sup>2</sup>*Faculty of Engineering, Shizuoka University, Hamamatsu, 432-8561, Japan*

Cutting surface and edge of carbon materials are important in electronic conductivity and growth of materials, etc. When a catalyst is adsorbed at an edge in a growing carbon nanotube (CNT), we are interested in the change of electronic structure. The catalyst such as iron, nickel and cobalt, usually has a magnetic moment and the magnetism should be taken into account in study of the electronic structure. In investigations of edges for carbon materials, Fujita and his co-workers found that there are localized electronic states which are called 'edge-state'[1] at zigzag edges terminated by single hydrogen atoms. Since this discovery, many theoretical studies have been performed for zigzag edges. Supposing the 'root-growth'[2] model in which the CNT grows up with the catalyst kept on the substrate, we would like to clarify electronic structures at CNT edges.

We have investigated electronic structures at armchair- and zigzag-edges without hydrogen termination and when the iron atom is adsorbed to each edge by using first-principles calculation based on the Kohn-Sham theory. We used a pseudopotential plane wave method and a generalized gradient approximation. We have calculated the armchair- and zigzag-ribbon, CNT(5,5) and (9,0) which have armchair- and zigzag edges at both side, respectively. Furthermore, we have calculated these CNTs which are closed by a half of fullerene C<sub>60</sub> at one side, and adsorbed by an iron atom at the other side.

In armchair edges, the HOMO and LUMO which form  $\pi$ -bondings have weights at the nearest neighbor atom of the edge rather than the edge atom itself. In zigzag edges, both the dangling bond state and  $p_z$  component are clearly spin-polarized around the Fermi level and thus, the edge atoms have a magnetic moment. The spin-polarization of the  $p_z$  component is slightly weakened by the curvature of CNT, compared with results in the zigzag-ribbon.

We will present the atomic and electronic structures in the CNTs which adsorb an iron atom and some of molecular dynamics simulations in growing CNT.

### Reference

- [1] M. Fujita, K. Wakabayashi, K. Nakada, and K. Kusakabe, J. Phys. Soc. Jpn. **65**, 1920 (1996)
- [2] J. Gavillet, A. Loiseau, C. Journet, F. Willaime, F. Ducatelle and J. C. Charlier, Phys. Rev. Lett. **87**, 275504 (2001)

**Corresponding Author** : Hirofumi Sakashita  
**E-mail** : sakasita@cphys.s.kanazawa-u.ac.jp  
**Tel & Fax** +81-76-264-5676, +81-76-264-5740

## Phase transition from Tomonaga-Luttinger liquid states to superconductive phase in carbon nanotubes

○M.Matsudaira<sup>1</sup>, J.Haruyama<sup>1,4</sup>, N.Murata<sup>1</sup>, Y.Yagi<sup>4</sup>, E.Einarsson<sup>2</sup>, S.Maruyama<sup>2</sup>,  
T.Sugai<sup>3,4</sup>, H.Shinohara<sup>3,4</sup>

<sup>1</sup>*Aoyama Gakuin University, 5-10-1 Fuchinobe, Kanagawa 229-8558, Japan*

<sup>2</sup>*Tokyo University, 7-3-1 Hongo, Bunkyo-ku, Tokyo 113-0033, Japan*

<sup>3</sup>*Nagoya University, Furo-cho, Chigusa, Nagoya 464-8602, Japan*

<sup>4</sup>*JST-CREST, 4-1-8 Hon-machi, Kawaguchi, Saitama 332-0012, Japan*

**Abstract:** We have reported superconductivity (SC) in arrays of multi-walled carbon nanotubes (MWNTs) from viewpoints of both abrupt resistance drop with  $T_c = 12\text{K}$  [1] and Meissner effect with  $T_c = \sim 20\text{K}$  [2]. Based on these reports, some theories for the SC have been proposed and are attracting considerable attention [3-5]. One of the very interesting points of the SC is electron correlation in one-dimensional space; i.e., interplay between SC phase (phonon-mediated attractive Coulomb interaction) and Tomonaga-Luttinger liquids (TLL; repulsive Coulomb interaction).

Here, we report the detailed observation of this interplay in relationships of normalized conductance vs.  $eV/kT$  of partially end-bonded MWNTs [6]. We find that the observed results are qualitatively consistent with previous reports of TLL states in CNTs, while a deviation due to emergence of the SC appears at temperatures  $< T_c$  and small  $eV/kT$  values. We interpret this based on carrier-doping and low-energy theory [7]. Half carrier filling and a large electron-phonon coupling parameter may lead to electron coupling with low-energy acoustic phonons and, then, cause transitions from spin-density wave regime to SC phase via TLL states.

### References

- [1] I. Takesue, J. Haruyama et al., **Phys.Rev.Lett.** 96, 057001 (2006)
- [2] N. Murata, J. Haruyama, M. Matsudaira, Y. Yagi, E. Einarsson, S. Chiashi, S. Maruyama, T. Sugai, N. Kishi, H. Shinohara et al., **Phys.Rev.B** 71, 081744 (2007)
- [3] E. Perfetto and J. Gonzalez, **Phys.Rev.B** 74, 201403(R) (2006)
- [4] T. Koretsune and S. Saito, To be published on **Phys.Rev.B**
- [5] K. Sasaki, R. Saito et al., **J. Phys. Soc. Jpn.** 76, 033702 (2007)
- [6] M. Matsudaira, J. Haruyama, N. Murata, Y. Yagi, E. Einarsson, S. Maruyama, T. Sugai, H. Shinohara, To be published on **Physica E** (In submission to Phys.Rev.Lett.)
- [7] D. Loss and T. Martin, **Phys.Rev.B** 50, 12160 (1994-II)

**Corresponding Author: Junji Haruyama**

**E-mail: J-haru@ee.aoyama.ac.jp**

**Tel&Fax: 042-759-6256 (Fax: 6524)**

## Cooperative Behaviors in Carbene Additions through Local Modifications of Nanotube Surface

○Takashi Yumura<sup>1</sup> and Miklos Kertesz<sup>2</sup>

<sup>1</sup>Department of Chemistry and Materials Technology, Kyoto Institute of Technology, Matsugasaki, Sakyo-ku, Kyoto, 606-8585, Japan

<sup>2</sup>Department of Chemistry, Georgetown University, 37<sup>th</sup> and O streets NW Washington DC, 20057 1227, USA

Chemical functionalization in which covalent bonds are formed between adsorbents and a single walled carbon nanotube (SWNT) can modify interesting properties of a SWNT. Up to now, only highly reactive reagents are available to attach covalently into a SWNT surface. For example, Haddon et al. reported that SWNTs treated by nitric-acid were successfully functionalized by divalent carbene-derivatives [1]. Due to their highly chemical reactivities, it is quite difficult to control their adsorption sites.

In order to develop a strategy for site-specific functionalization of a nanotube by carbene ( $\text{CH}_2$ ), we investigated two carbene additions to a (5,5) SWNT by means of density functional theory (DFT) PW91 calculations using periodic boundary conditions [2]. As a result, we found cooperative behaviors in binding sites between the first and second  $\text{CH}_2$  adsorbents through “local” modifications of the SWNT surface induced by covalent bond formation with an inner  $\text{CH}_2$  molecule. In contrast, such local modifications cannot be observed in the case of bond formation between the SWNT and an outer  $\text{CH}_2$  molecule. Thus, the PW91 DFT calculations show that the local modifications, created by the endohedral addition, influence site preferences for second  $\text{CH}_2$  additions, and the effects are limited to the vicinity of the binding site.

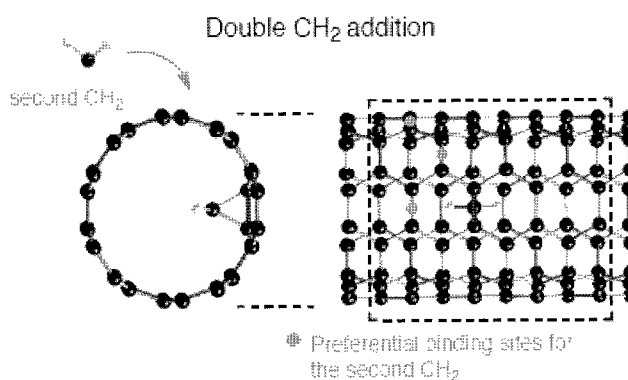


Figure 1 Double  $\text{CH}_2$  addition into a (5,5) nanotube

### References:

[1] Chen, J. et al. *Science*, **1998**, 282, 95.

[2] Yumura, T.; Kertesz, K. *Chem. Mater.* **2007**, 19, 1028.

Corresponding Author: Takashi Yumura

E-mail: yumura@chem.kit.ac.jp, Tel: +82-75-724-7571

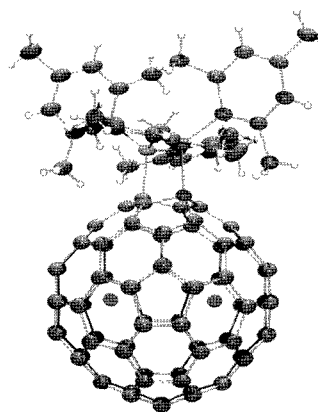
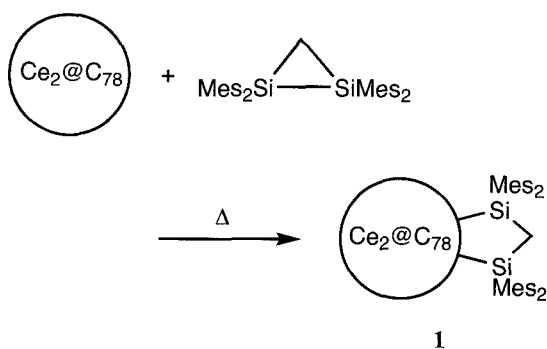
## Location of the Metal Atoms in $Ce_2@C_{78}$ and Its Bis-silylated Derivative

○Michio Yamada,<sup>1</sup> Takatsugu Wakahara,<sup>1</sup> Takahiro Tsuchiya,<sup>1</sup> Yutaka Maeda,<sup>2</sup> Takeshi Akasaka,<sup>1</sup> Kenji Yoza,<sup>3</sup> Naomi Mizorogi,<sup>4</sup> and Shigeru Nagase<sup>4</sup>

<sup>1</sup>Center for Tsukuba Advanced Research Alliance, University of Tsukuba, Tsukuba, Ibaraki 305-8577, Japan, <sup>2</sup>Department of Chemistry, Tokyo Gakugei University, Koganei, Tokyo 184-8501, Japan, <sup>3</sup>Bruker AXS K. K., Yokohama, Kanagawa 221-0022, Japan, <sup>4</sup>Department of Theoretical and Computational Molecular Science, Institute for Molecular Science, Okazaki, Aichi 444-8585, Japan

**Abstract:** Endohedral metallofullerenes have received extensive attention owing to their fascinating structures, properties and chemical reactivities.<sup>1</sup> Especially, considerable interest is now directed toward the dimetallofullerenes such as  $La_2@C_{80}$ <sup>2</sup> and  $Ce_2@C_{80}$ <sup>3</sup> because of the three-dimensional random motion of the two metal atoms inside the fullerene cage. However, the dynamic behavior of the metal atoms in other dimetallofullerenes has not been investigated yet. Herein we report the synthesis and characterization of  $Ce_2@C_{78}$  and its bis-silylated derivative. The location of the metal atoms in  $Ce_2@C_{78}$  and the bis-silylated derivative has been investigated by means of spectroscopic and single-crystal X-ray structural analyses.<sup>4</sup>

### Scheme



**Figure.** ORTEP drawing of 1.

### References:

- (1) *Endofullerenes: A New Family of Carbon Clusters*; Akasaka, T., Nagase, S., Eds.; Kluwer: Dordrecht, The Netherlands, 2002.
- (2) (a) Akasaka, T. et al. *Angew. Chem., Int. Ed. Engl.* **1997**, *109*, 1643. (b) Wakahara, T. et al. *Chem. Commun.* **2007**, 2680.
- (3) Yamada, M. et al. *J. Am. Chem. Soc.* **2005**, *127*, 14570.
- (4) Yamada, M. et al. *Chem. Commun.* **2008**, in press. [Selected as Hot Article and Cover Image]

**Corresponding Author:** Takeshi Akasaka, **E-mail:** akasaka@tara.tsukuba.ac.jp, **Tel&Fax:** +81-298-53-6409



## <sup>13</sup>C NMR Spectroscopic Study of <sup>13</sup>C-enriched Carbide-encapsulated Scandium Metallofullerenes

Yuko Yamazaki,<sup>1</sup> Koji Nakajima,<sup>1</sup> Takatsugu Wakahara,<sup>1</sup> Tsuchiya Takahiro,<sup>1</sup> Yutaka Maeda,<sup>2</sup> Takeshi Akasaka,<sup>\*,1</sup> Markus Waelchli,<sup>3</sup> Naomi Mizorogi,<sup>4</sup> Shigeru Nagase<sup>\*,4</sup>

<sup>1</sup>Center for Tsukuba Advanced Research Alliance, University of Tsukuba, <sup>2</sup>Department of Chemistry, Tokyo Gakugei University, <sup>3</sup>Bruker BioSpin K. K., <sup>4</sup>Department of Theoretical and Computational Molecular Science, Institute for Molecular Science

Much attention has been paid to encapsulation of a metal carbide, since the first isolation and characterization of a metal carbide-encapsulated metallofullerene, Sc<sub>2</sub>C<sub>2</sub>@C<sub>84</sub>, by MEM/Rietveld analysis of synchrotron powder diffraction data.<sup>1</sup> Recently, we have succeeded in determining the structures of Sc<sub>3</sub>C<sub>2</sub>@C<sub>80</sub>(I<sub>h</sub>)<sup>2</sup> and Sc<sub>2</sub>C<sub>2</sub>@C<sub>82</sub>(C<sub>3v</sub>)<sup>3,4</sup> by <sup>13</sup>C NMR spectroscopy and X-ray single-crystal structure analyses, although previously it had been believed that they have the Sc<sub>3</sub>@C<sub>82</sub> and Sc<sub>2</sub>@C<sub>84</sub> structures, respectively. Nishibori and co-workers have applied the MEM/Rietveld method to Y<sub>2</sub>C<sub>2</sub>@C<sub>82</sub>(C<sub>3v</sub>),<sup>5</sup> Sc<sub>2</sub>C<sub>2</sub>@C<sub>82</sub>(C<sub>3v</sub>)<sup>6</sup> and Sc<sub>3</sub>C<sub>2</sub>@C<sub>80</sub>(I<sub>h</sub>).<sup>7</sup> However, it remains an important goal to disclose the electronic properties of their encapsulated C<sub>2</sub> units. Attempts to detect the <sup>13</sup>C NMR signals of the encapsulated C<sub>2</sub> units of metal carbide-metallofullerenes have not been successful so far. The inability to observe the <sup>13</sup>C NMR signals of the C<sub>2</sub> unit has been explained by means of the spin-rotation interaction, because the C<sub>2</sub> unit may rotate inside the carbon cages. It is challenge to observe the <sup>13</sup>C NMR signal of the C<sub>2</sub> unit to disclose its electronic and magnetic property.

We herein report <sup>13</sup>C NMR spectra of Sc<sub>2</sub>C<sub>2</sub>@C<sub>82</sub>(C<sub>3v</sub>) and [Sc<sub>3</sub>C<sub>2</sub>@C<sub>80</sub>(I<sub>h</sub>)]<sup>-</sup> highly enriched in <sup>13</sup>C isotope. <sup>13</sup>C NMR signals of the carbon cages for Sc<sub>2</sub>C<sub>2</sub>@C<sub>82</sub>(C<sub>3v</sub>) and [Sc<sub>3</sub>C<sub>2</sub>@C<sub>80</sub>(I<sub>h</sub>)]<sup>-</sup> were completely assigned by 2D INADEQUATE experiments.

**References:** (1) Wang, C.-R. et al., *Angew. Chem. Int. Ed.* **2001**, *40*, 397. (2) Iiduka, Y. et al., *J. Am. Chem. Soc.* **2005**, *127*, 12500. (3) Iiduka, Y. et al., *Chem. Commun.* **2006**, 2057. (4) Iiduka, Y. et al., *Angew. Chem. Int. Ed.* **2007**, *46*, 5562. (5) Nishibori, E. et al., *ChemPhysChem* **2006**, *7*, 345. (6) Nishibori, E. et al., *Chem. Phys. Lett.* **2006**, *433*, 120. (7) Nishibori, E. *J. Phys. Chem. B.* **2006**, *110*, 19215.

Corresponding author: Takeshi Akasaka

Tel & Fax: +81-29-853-6409

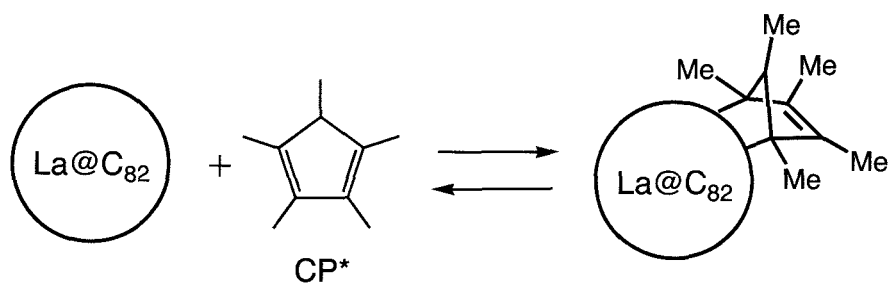
E-mail: akasaka@tara.tsukuba.ac.jp

## Reaction of La@C<sub>82</sub> with Cyclopentadiene Derivatives

○ Satoru Sato,<sup>1</sup> Yutaka Maeda,<sup>2</sup> Koji Inada,<sup>2</sup> Michio Yamada,<sup>1</sup> Takahiro Tsuchiya,<sup>1</sup> Midori O. Ishitsuka,<sup>1</sup> Tadashi Hasegawa,<sup>2</sup> Takeshi Akasaka,<sup>1</sup> Tatsuhisa Kato,<sup>3</sup> Naomi Mizorogi,<sup>4</sup> and Shigeru Nagase<sup>4</sup>

<sup>1</sup>Center for Tsukuba Advanced Research Alliance, University of Tsukuba, Tsukuba, Ibaraki 305-8577, Japan, <sup>2</sup>Department of Chemistry, Tokyo Gakugei University, Koganei, Tokyo 184-8501, Japan, <sup>3</sup>Department of Chemistry, Josai University, Sakado, Saitama 350-0295, Japan, <sup>4</sup>Department of Theoretical and Computational Molecular Science, Institute for Molecular Science, Okazaki, Aichi 444-8585, Japan

It is extremely important to develop a reversible addition reaction of endohedral metallofullerenes, since reversible addition reaction is one of the useful methods for separation and regioselective functionalization of fullerenes by protection of their reactive site. In this context, we reported the reversible and regioselective addition reaction of La@C<sub>82</sub> with cyclopentadiene (CP), in which the kinetic parameters for the retro-reaction of La@C<sub>82</sub>(CP) were determined.<sup>1</sup> In the reversible reaction, substituent effect is one of the important factor of controlling reactivity and stability of the adducts. It has been reported that an adduct of C<sub>60</sub> with 1,2,3,4,5-pentamethylcyclopentadiene (CP\*) is more stable than C<sub>60</sub>(CP).<sup>2</sup> Herein, we report the reversible addition reaction of La@C<sub>82</sub> with CP\* and the stability of its adduct. We will also discuss the kinetical parameter of this addition reaction in detail.



### References:

- [1] Maeda, Y. et al., *J. Am. Chem. Soc.* **2005**, 127, 12190.  
 [2] Meidine, M. F. et al., *J. Chem. Soc., Perkin Trans. 2* **1994**, 1189.

Corresponding Author: Takeshi Akasaka

TEL & FAX: +81-29-853-6409, E-mail: akasaka@tara.tsukuba.ac.jp

## STM-tip Current Induced Polymerization of Ce<sub>2</sub>@C<sub>80</sub> Metallofullerenes

○Kazunori Ohashi<sup>1</sup>, Nobuyuki Fukui<sup>1</sup>, Masahiro Akachi<sup>1</sup>, Takao Akachi<sup>1</sup>,  
Hisashi Umemoto<sup>1</sup>, Yasuhiro Ito<sup>1</sup>, Toshiki Sugai<sup>1</sup>, Ryo Kitaura<sup>1</sup> and Hisanori Shinohara<sup>1,2</sup>

<sup>1</sup>*Department of Chemistry & Institute for Advanced Research,  
Nagoya University, Nagoya 464-8602, Japan*

<sup>2</sup>*CREST, Japan Science and Technology Agency, c/o Department of Chemistry,  
Nagoya University, Nagoya 464-8602, Japan*

Polymerization of C<sub>60</sub> molecules induced by electron/hole injection from an STM tip has been studied previously [1,2]. In these studies, a polymerization mechanism was proposed due to [2+2] cycloaddition with the formation of four-membered ring between adjacent C<sub>60</sub> molecules. However, the detail of the polymerization mechanism has not been clear.

Here, we have studied the polymerization of metallofullerenes such as Ce<sub>2</sub>@C<sub>80</sub>, and Lu<sub>2</sub>@C<sub>76</sub> in reference to that of C<sub>60</sub> induced by electron injection from an STM tip. We also investigated the effect of the reaction temperature. The results indicate that the metallofullerenes are much less easier to polymerize compared to C<sub>60</sub> by the STM-tip current.

The samples were prepared by vacuum sublimation of the metallofullerenes onto Si(111) and Au(111). All the sample preparation and STM measurements were performed under UHV conditions. Figure 1 shows an STM image of a Ce<sub>2</sub>@C<sub>80</sub> thin layer on a Si(111) surface after electron injection at a sample bias voltage of  $V_s = +3.5$  V and a tunneling current of  $I_t = 0.2$  nA for 30 seconds at room temperature. The molecules in dark contrasts represent polymerized Ce<sub>2</sub>@C<sub>80</sub> molecules. The internal images observed in the dark contrasts indicate no free rotation of the molecules is occurring, which is similar to the C<sub>60</sub> case.

We found that the polymerization efficiency of Ce<sub>2</sub>@C<sub>80</sub> is less than that of C<sub>60</sub> and that at a low temperature of 115 K Ce<sub>2</sub>@C<sub>80</sub> are not polymerized. In particular, Lu<sub>2</sub>@C<sub>76</sub> has not shown any STM-tip induced polymerization even at room temperature. The STM-tip current induced polymerization is, therefore, strongly dependent on the type of fullerenes as well as the reaction temperature, suggesting that the configuration of each adjacent fullerene's reactive site and propagation of electrons are crucial for the polymerization reaction.

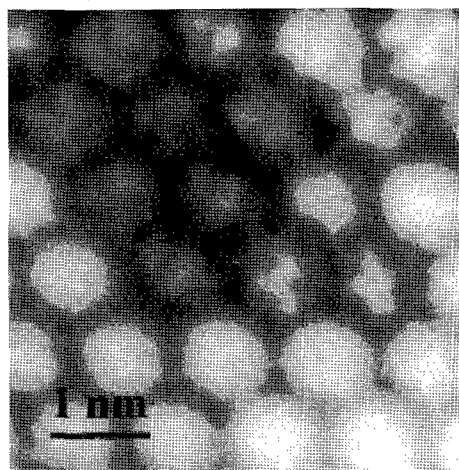


Figure 1: STM image of a Ce<sub>2</sub>@C<sub>80</sub> thin layer on a Si(111) surface after electron injection at  $V_s = +3.5$  V,  $I_t = 0.2$  nA for 30 seconds at room temperature.

[1] R. Nouchi *et al.*, *Phys. Rev. Lett.*, **97**, 196101 (2006).

[2] Y. Nakamura *et al.*, *Surf. Sci.*, **528**, 151 (2003).

Corresponding Author: Hisanori Shinohara

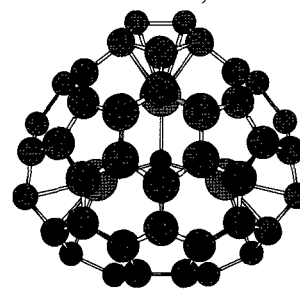
TEL: +81-52-789-2482, FAX: +81-52-789-1169, E-mail: noris@cc.nagoya-u.ac.jp

Relative Stability of Metallofullerenes  $\text{Sc}_3\text{N}@C_{70}$ 

H. Zheng, Q. Xu, X. Zhao

*Department of Chemistry and Institute for Chemical Physics,  
Xi'an Jiaotong University, Xi'an 710049, P. R. China*

To evaluate relative stability of endohedral metallofullerenes  $\text{Sc}_3\text{N}@C_{70}$ , all 8149 isomers of  $C_{70}$  classical fullerenes<sup>[1]</sup> have been calculated at hexa-anion state by AM1 quantum chemical method. Five isomers with lower energies of  $C_{70}^{-6}$ , including the only IPR structure and four non-IPR ones, were re-optimized at B3LYP/6-31G\* and HF/6-31G\* levels of theory, their results reveal good accordance to AM1 method. Then the five lower energy cages were encapsulated with  $\text{Sc}_3\text{N}$  cluster and evaluated at B3LYP/3-21G\* and B3LYP/6-31G\* levels of theory for Carbon atoms, with the effective core potentials for Scandium atoms. All results show that isomer  $\text{Sc}_3\text{N}@C_{70}$ -id133462 (Spiral No. 7854) of  $C_{2v}$  symmetry with 3 adjacent pentagons has the lowest energy and the highest HOMO-LUMO gap of 2.12 eV (6-31G\*). It seems that the encapsulation of  $\text{Sc}_3\text{N}$  cluster can remarkably improve relative stability of  $\text{Sc}_3\text{N}@C_{70}$ -id133462 through localizing three scandium atoms by three pentagon pairs.

Fig. 1:  $\text{Sc}_3\text{N}@C_{70}$ : id133462

According to B3LYP/6-31G\* results, the optimizations of  $C_{70}$  hexa-anions revealed that  $C_{70}^{-6}$ : id1003 (Spiral No. 7957), a structure with two pentagon pairs, played as the second most stable isomer with small relative energy. However, encapsulation of  $\text{Sc}_3\text{N}$  cluster results in a large relative energy of 30.8 kcal/mol. Similarly,  $\text{Sc}_3\text{N}$  encapsulation into the only IPR cage of  $C_{70}$  produces a separation energy of 46.4 kcal/mol to  $\text{Sc}_3\text{N}@$  id133462, while its B3LYP energy of hexa-anion locates only 13.6 kcal/mol higher than that of id133462.

The lowest energy and largest HOMO-LUMO gap indicate the domination state of  $\text{Sc}_3\text{N}@C_{70}$ -id133462 among  $\text{Sc}_3\text{N}@C_{70}$  yields, which is consistent with experiment<sup>[2]</sup>. The  $\text{Sc}_2@C_{70}$  isomers evaluated with entropy analyses have also shown the lower energies and more complex stability property compared with  $\text{Sc}_3\text{N}@C_{70}$  ones. The thermodynamic stabilities of  $\text{Sc}_3\text{N}@C_{70}$  and  $\text{Sc}_2@C_{70}$ <sup>[3]</sup> are discussed as well.

**Reference**

- [1] Fowler, P. W.; Manolopoulos, D.E. *An Atlas of Fullerenes*; Clarendon Press: Oxford, U. K., 1995.  
 [2] Yang, S. F.; Popov, A. A.; Dunsch, L. *Angew. Chem., Int. Ed.* **2007**, *46*, 1256.  
 [3] H. Zheng, X. Zhao, S. Nagase, N. Mizorogi, Q. Xu, manuscript in preparation.

**Corresponding author: X. Zhao,****Email: [xzhao@mail.xjtu.edu.cn](mailto:xzhao@mail.xjtu.edu.cn); Fax: +86-29-82668559**

## Cage Size Dependence on Photoluminescence Properties of Erbium-Carbide Metallofullerenes: $(Er_2C_2)@C_{2n}$

○Masahiro Akachi<sup>1</sup>, Yasuhiro Ito<sup>1</sup>, Toshiya Okazaki<sup>2</sup>, Yutaka Ohno<sup>3</sup>, Takashi Mizutani<sup>3</sup>,  
Ryo Kitaura<sup>1,4</sup>, Toshiki Sugai<sup>1,4</sup> and Hisanori Shinohara<sup>1,4</sup>

<sup>1</sup>*Department of Chemistry & Institute for Advanced Research, Nagoya University, Nagoya 464-8602, Japan*

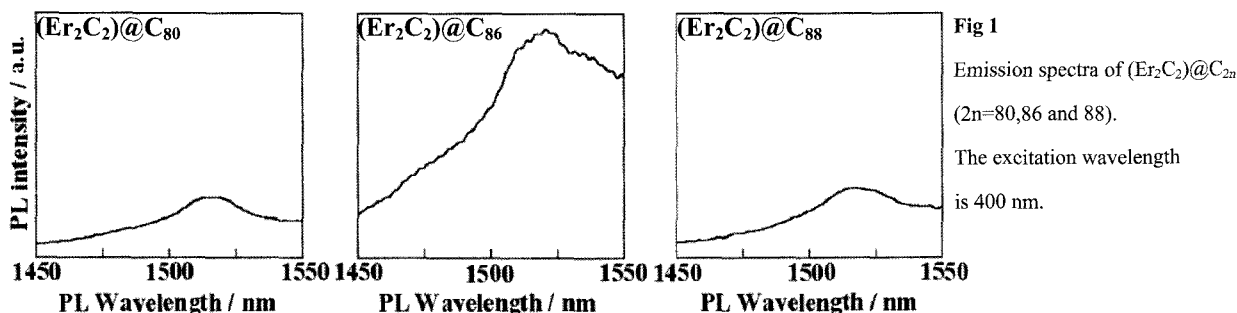
<sup>2</sup>*Reserch Center for Advanced Carbon Materials, National Institute of Advanced Industrial Science and Technology (AIST), Tsukuba 305-8565, Japan*

<sup>3</sup>*Department of Quantum Engineering, Nagoya University, Nagoya 464-8602, Japan*

<sup>4</sup>*CREST, Japan Science and Technology Corporation, c/o Department of Chemistry, Nagoya University, 464-8602, Japan*

We have recently found that an erbium-carbide metallofullerene  $(Er_2C_2)@C_{82}(C_{3v}(8))$  exhibits enhanced photoluminescence (PL) among the several isomers of  $Er_2@C_{82}$  and  $(Er_2C_2)@C_{82}$ [1]. The presence of encapsulated  $C_2$  molecule enhances the PL intensity in  $(Er_2C_2)@C_{82}(C_{3v}(8))$ . In a previous study, we reported the cage size dependence on PL intensities of Er-carbide metallofullerenes with various carbon cages:  $(Er_2C_2)@C_{2n}$  ( $2n=74, 80, 82$  and  $84$ ) together with the relationship between the PL intensities and the HOMO-LUMO gaps[2]. Here, we report PL properties with other erbium-carbide metallofullerenes having higher fullerene cages, i.e.,  $(Er_2C_2)@C_{2n}$  ( $2n=86$  and  $88$ ).

Figure 1 shows emission spectra of  $(Er_2C_2)@C_{2n}$  ( $2n=80, 86$  and  $88$ ) in  $CS_2$  solution at room temperature, which stem from  $f-f$  transitions of  $Er^{3+}$  ( $^4I_{13/2} \rightarrow ^4I_{15/2}$ ) in the carbon cage. The spectral features of these spectra are almost similar to each other, whereas the PL intensities differ from each other. For example, the PL intensity of  $(Er_2C_2)@C_{86}$  is three times stronger than those of  $(Er_2C_2)@C_{80}$  and  $(Er_2C_2)@C_{88}$ . The HOMO-LUMO gap of  $(Er_2C_2)@C_{86}$ , estimated from the absorption onset, is larger than those of other  $(Er_2C_2)@C_{2n}$ . The PL intensities of these higher Er-metallofullerenes also depend on the HOMO-LUMO gap as observed in the  $Er_2@C_{82}$  and  $(Er_2C_2)@C_{82}$  case.



### References

- [1] Y. Ito *et al.*, *ACS Nano*, **1**, 456-461(2007).  
[2] M. Akachi *et al.*, *32<sup>th</sup> Fullerene-Nanotubes General Symposium*, **3P-29** (2007).

**Corresponding Author:** Hisanori Shinohara

**E-mail:** noris@cc.nagoya-u.ac.jp, **Tel&Fax:** +81-52-789-2483&1169

## Orientation of individual fullerenes inside carbon nanotubes determined by aberration-corrected electron microscopy

○Yuta Sato, Kazu Suenaga, Shingo Okubo, Toshiya Okazaki, and Sumio Iijima

*Research Center for Advanced Carbon Materials, National Institute of Advanced Industrial Science and Technology (AIST), Tsukuba 305-8565, Japan*

Single-walled carbon nanotubes (SWNTs) have generally been regarded as almost contrast-less container materials in previous studies on their incorporation of various molecules using transmission electron microscopy (TEM). Recently, however, hexagonal networks of carbon atoms in SWNTs have been directly detected by aberration-corrected TEM,<sup>[1,2]</sup> in which spherical aberration coefficient of the electron lens is reduced to nearly zero in order to improve the spatial resolution. This observation technique should also be able to visualize more detailed structures of encapsulated species inside SWNTs, such as individual fullerene molecules.

Here, time-dependent orientational changes of  $C_{80}(D_{5d})$  and  $Er_3N@C_{80}(I_h)$  fullerenes inside SWNTs were directly observed by aberration-corrected TEM at atomic-level resolution.<sup>[3]</sup> Detailed structure of the ellipsoidal  $C_{80}(D_{5d})$  fullerene (Fig. 1) as well as the endohedral structure of  $Er_3N@C_{80}(I_h)$  was unambiguously identified by TEM images. Even a slight orientational change and/or a slight translational motion of each encapsulated fullerene molecule could be detected with respect to the graphene structure of the outer SWNT by aberration-corrected TEM.

A part of this work was financially supported by the JST-CREST project.

### References

- [1] K. Hirahara *et al.*, *Nano Lett.*, **6**, 1778 (2006).
- [2] K. Suenaga *et al.*, *Nat. Nanotechnol.*, **2**, 358 (2007).
- [3] Y. Sato *et al.*, *Nano Lett.*, **7**, 3704 (2007).

Corresponding Author: Y. Sato (yuta-sato@aist.go.jp).

Tel: +81-29-861-5694, Fax: +81-29-861-4806.

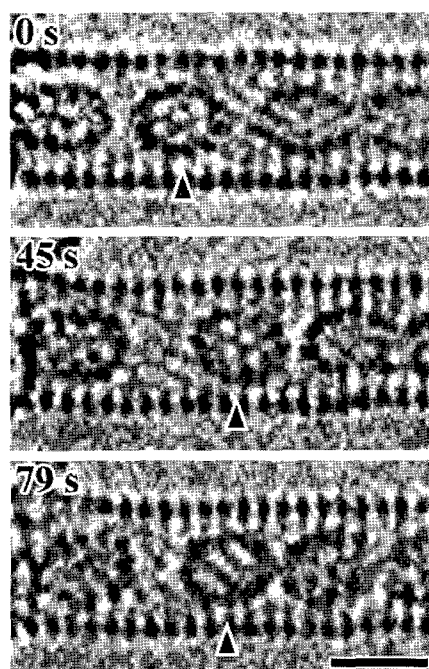


Fig. 1. Sequential TEM images of  $C_{80}(D_{5d})$  fullerenes inside the (18,1) SWNT. Scale bar = 1 nm.

## Coating of BN nanotubes with metal oxides using novel ethanol-thermal method

Yang Huang<sup>1,2</sup>○, Yoshio Bando<sup>1,3,4</sup>, Chengchun Tang<sup>2</sup>, Chunyi Zhi<sup>3</sup>, Takeshi Terao<sup>1,2</sup> and Dmitri Golberg<sup>1,2,4</sup>

<sup>1</sup>*Graduate School of Pure and Applied Sciences, University of Tsukuba, Tennodai 1, Tsukuba, 305-0005, Ibaraki, Japan;*

<sup>2</sup>*Nanoscale Materials Center, National Institute for Materials Science, Namiki 1-1, Tsukuba, 305-0044, Ibaraki, Japan;*

<sup>3</sup>*International Center for Young Scientists (ICYS), Namiki 1-1, Tsukuba, Ibaraki, Japan;*

<sup>4</sup>*World Premier International Center for Materials Nanoarchitectonics (MANA), Namiki 1-1, Tsukuba, Ibaraki, Japan.*

A novel ethanol-thermal method was developed to coat BN nanotubes (BNNTs) with metal oxides. It was confirmed that various oxides, e.g. iron and terbium oxides, could be coated on BNNT surfaces using this method. The coating structures and compositions were investigated by high-resolution transmission electron microscopy (HRTEM), Electron energy loss spectroscopy (EELS) and X-ray diffraction (XRD). It was observed that the coating layers had usually exhibited amorphous or polycrystalline nature, which was found to be advantageous for getting uniform coatings. The influence of experimental conditions on the coating morphology/structure and its mechanism were also discussed. Cathodoluminescence studies show that BNNTs coated with terbium oxide possess the emissions which can be expressed as a superposition of those coming from BNNTs and trivalent Tb. It is envisaged that the present composite nanomaterials may find potential applications in high active catalysts and photoelectrical devices.

**Corresponding Author: Yang Huang**

**E-mail: HUANG.Yang@nims.go.jp**

**Tel:080-5178-8599**

**Fax: 029-851-6280**

## Adsorption Efficiency of Polyynes into Single-Wall Carbon Nanotubes

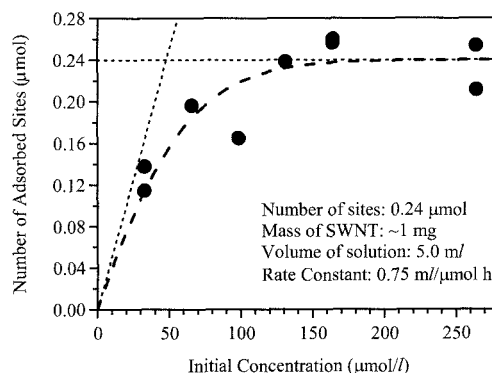
○Tetsushi Murakami and Tomonari Wakabayashi

*Department of Chemistry, Kinki University, Higashi-Osaka 577-8502, Japan*

Polyynes,  $H(C\equiv C)_nH$ , can be accommodated into single-wall carbon nanotubes (SWNTs) and detected by Raman signals for the stretching vibrational modes around  $\sim 2050\text{ cm}^{-1}$  [1,2]. The Raman intensity for  $C_{2n}H_2@SWNT$  is explainable by the resonance effects [3]. However, from the Raman intensity itself, it is difficult to estimate the number of molecules entrapped in the SWNTs.

In order to estimate the number of trapping sites for polyynes in SWNTs, we measured Raman intensity for several samples of  $C_{10}H_2@SWNT$ . A piece of about 1 mg of SWNTs (laser ablation at  $1150\text{ }^\circ\text{C}$ , 500 Torr Ar, Ni/Co 0.6/0.6 wt %) was sintered in solutions of  $C_{10}H_2$  in hexane (0.03 – 0.26 mmol/l, 5.0 ml) and kept at  $80\text{ }^\circ\text{C}$  for 48 hours. After being dried, the Raman spectra of the polyyne-containing SWNTs were measured. The intensity of the polyyne-stretching Raman band at  $2066\text{ cm}^{-1}$  relative to that of a band of SWNTs was plotted as a function of initial concentrations and analyzed as shown in Fig. 1.

At low concentration, most of the polyyne molecules prepared in the solution are adsorbed after a sufficiently long time. Thus, the Raman intensity will increase proportionally to the concentration. At high concentration, most of the trapping sites available in the SWNTs are filled with the molecules. Then, the Raman intensity will saturate. By finding a critical condition where the number of the trapping sites is balanced with the number of the prepared molecules, we made a rough estimation for the upper limit of the adsorption efficiency to be 1 polyyne molecule per  $\sim 3.5 \times 10^2$  carbon atoms in the SWNTs.



**Figure 1.** Adsorption efficiency analysis for the concentration dependence of the Raman intensity of  $\nu_3$  for  $C_{10}H_2@SWNT$ .

### References:

- 1) D. Nishide, H. Dohi, T. Wakabayashi, E. Nishibori, S. Aoyagi, M. Ishida, S. Kikuchi, R. Kitaura, T. Sugai, M. Sakata, H. Shinohara, "Single-Wall Carbon Nanotubes Encaging Linear Chain  $C_{10}H_2$  Polyyne Molecules Inside", *Chem. Phys. Lett.* **428**, 356 (2006).
- 2) D. Nishide, T. Wakabayashi, T. Sugai, R. Kitaura, H. Kataura, Y. Achiba, H. Shinohara, "Raman Spectroscopy of Size-Separated Linear Polyyne Molecules  $C_{2n}H_2$  ( $n=4-6$ ) Encapsulated in Single-Wall Carbon Nanotubes", *J. Phys. Chem. C* **111**, 5178 (2007).
- 3) L. M. Malard, D. Nishide, L. G. Dias, R. B. Capaz, A. P. Gomes, A. Jorio, C. A. Achete, R. Saito, Y. Achiba, H. Shinohara, M. A. Pimenta, "Resonance Raman Study of Polyynes Encapsulated in Single-Wall Carbon Nanotubes", *Phys. Rev. B* **76**, 233412 (2007).

**Corresponding Author: Tomonari Wakabayashi**

**E-mail: wakaba@chem.kindai.ac.jp**

**Tel. 06-6730-5880 (ex. 4101) / FAX 06-6723-2721**



## Direct Observation on Formation Process of Nanopeapods by *in-situ* X-ray Diffraction Measurements

○Yuko Kato<sup>1</sup>, Ryo Kitaura<sup>1</sup>, Shinobu Aoyagi<sup>2</sup>, Eiji Nishibori<sup>2</sup>, Yasuhiro Ito<sup>1</sup>,  
Makoto Sakata<sup>2</sup>, Hisanori Shinohara<sup>1,3\*</sup>

<sup>1</sup>Department of Chemistry, Nagoya University, Nagoya 444-8602, Japan

<sup>2</sup>Department of Applied physics, Nagoya University, Nagoya 444-8602, Japan

<sup>3</sup>Institute for Advanced Research, Nagoya University, and CREST/JST

The so-called nanopeapods have attracted wide range of researchers owing not only to their interesting low-dimensional structure but also to possible applications such as field effect transistors and molecular devices [1]. Observation of formation process and clarifying the formation mechanism of nanopeapods are essential to development of the efficient synthesis method. Transmission electron microscopy (TEM) has generally been used to characterize structures of nanopeapods. However, it is difficult to perform *in-situ* observation of the formation process of nanopeapods by TEM. In addition, TEM provides only local structural information. X-ray diffraction (XRD) is a complementary method, which realizes not only *in-situ* observation but also obtaining bulk structure information. Here, we report direct observation of the fullerene encapsulation process by *in-situ* X-ray diffraction.

SWNTs were prepared by the laser ablation method. C<sub>60</sub> and Ce@C<sub>82</sub> fullerenes were used for encapsulates. Empty SWNTs and fullerenes were mixed in a quartz capillary, which was vacuum-sealed at 400 K to remove adsorbed gases and residual water molecules. *In-situ* X-ray diffraction measurements at high temperatures have been performed every 5 minutes at 723, 773, 823, and 923 K. The x-ray wavelength used in this diffraction studies was 0.8 Å. All the measurements have been done at SP-ring8, BL02B2.

Figure 1 shows XRD patterns of a mixture of SWNTs and C<sub>60</sub>. Left and right figures show the diffraction patterns obtained at 723 K and 823 K, respectively. Due to the encapsulation of C<sub>60</sub> molecules, the intensity of (10) peaks, which are seen around  $2\theta = 3.2$  degree, have significantly decreased. At the same time, a new peak arising from 1-dimensional regulated array of C<sub>60</sub> appears at around  $2\theta = 4.7$  degree.

We will discuss details of the temperature dependence on a fullerene encapsulation rate and a saturated filling ratio.

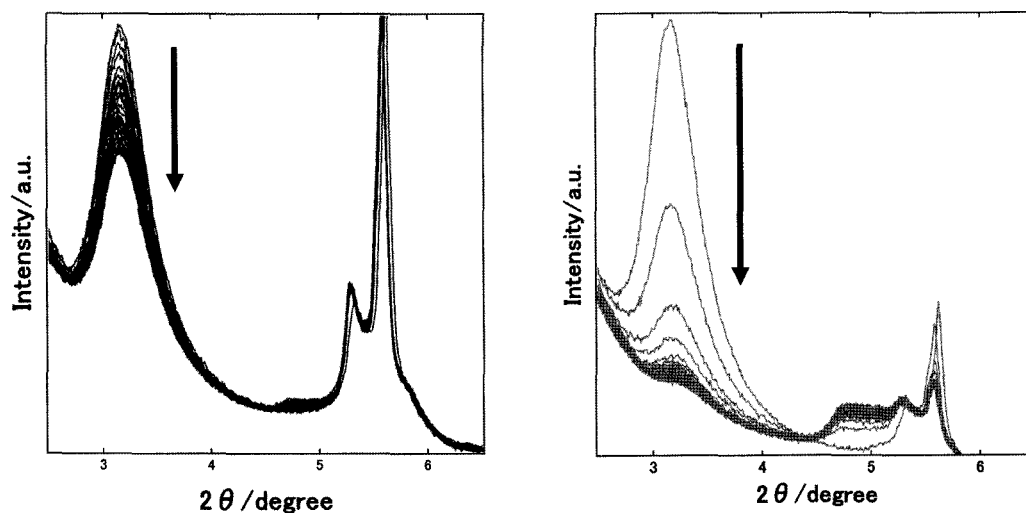


Fig.1. *In-situ* XRD pattern of peapod formation process (Left: 723 K, Right: 823 K)

[1] R.Kitaura, H.Shinohara, *Chem.Asian J.*2006, 1, 646-655

Corresponding Author: Hisanori Shinohara

TEL: +81-52-789-2482, FAX: +81-52-789-1169, E-mail: noris@cc.nagoya-u.ac.jp

## Fabrication of Metal-Nanowire in Carbon Nanotube Via Nano-Template Reaction

○ Naoki Imazu<sup>1</sup>, Ryo Kitaura<sup>1</sup>, Keita Kobayashi<sup>1</sup> and Hisanori Shinohara<sup>1,2</sup>

<sup>1</sup>*Department of Chemistry & Institute for Advanced Research, Nagoya University, Nagoya  
464-8602, Japan*

<sup>2</sup>*CREST, Japan Science and Technology Agency, c/o Department of Chemistry,  
Nagoya University, Nagoya 464-8602, Japan*

Single-wall carbon nanotubes (SWNTs) have an ideal nanometer-scale and one-dimensional internal space where unique low-dimensional nanomaterials can be encapsulated and synthesized. For example, low-dimensional metal halides and metal alloy crystals have been synthesized in SWNTs by the liquid phase encapsulation method<sup>[1,2]</sup>.

For further exploring novel low-dimensional nanomaterials in carbon nanotubes, we have developed a Nano-Template Reaction technique to fabricate metal nanowires by using SWNTs and metallofullerenes. In this reaction, to create low-dimensional metal nanowires, we have utilized well-aligned one-dimensional array of metallofullerenes (Gd@C<sub>82</sub>) in SWNTs (i.e., peapod). We have found that the one-dimensional array of Gd@C<sub>82</sub> was converted effectively to Gd-metal nanowires by high-temperature heat treatment. A similar heat treatment has already been reported for C<sub>60</sub> array in SWNTs, which results in formation of double-wall carbon nanotubes (DWNTs)<sup>[3]</sup>.

We have characterized the Gd-nanowire by high resolution transmission electron microscopy (HRTEM) and Raman Spectroscopy. Based on HRTEM images (Fig.1) together with the multi-slice image simulation, we suggest that the typical nanowires synthesized here possess a 2 × 2 structure as schematically shown in Fig.2. Interestingly, this structure does not correspond to any of bulk Gd crystal structures ever reported. Furthermore, other types of Gd-nanowire structures have also been easily observed by HRTEM. In this presentation, we will discuss detailed structures of these Gd nanowires encapsulated in SWNTs.

### References:

- [1] R. Meyer, et.al., *Science* **289**, 1324(2000).
- [2] R. Carter, et.al., *Phys.Rev.Lett.* **96**, 215501(2006).
- [3] S. Bandow, et.al., *Chem. Phys. Lett.* **337**, 48(2001).

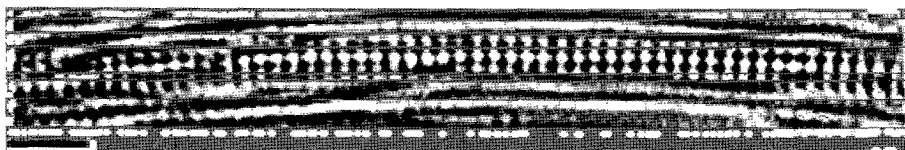


Figure.1 HRTEM image of  
Gd-nanowire@CNT (Scale bar: 2 nm)

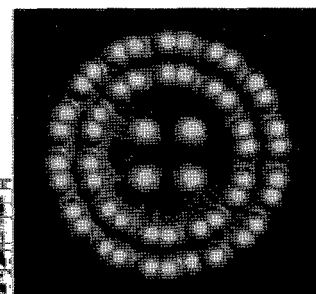


Figure.2 Structure model  
of Gd-nanowire@CNT

Corresponding Author: Hisanori Shinohara  
TEL: +81-52-789-2482, FAX: +81-52-789-1169  
E-mail: [noris@cc.nagoya-u.ac.jp](mailto:noris@cc.nagoya-u.ac.jp)

## Optimization of Conditions for Formation of Carbon Nanotubes Filled Perfectly with Copper Nanowire

○Akira Koshio, Naoki Mizuno, Hironobu Kito, and Fumio Kokai

*Division of Chemistry for Materials, Graduate School of Engineering, Mie University,  
1577 Kurimamachiya-cho, Tsu, Mie 514-8507, Japan*

Copper nanowires (CuNWs) have been extensively studied as a material for next generation electronic nanodevices. However, some problems related to quality, such as stability, crystallinity, and long one-dimensional growth, still remain. The hybridization of CuNWs and carbon nanotubes has been tried as one of the ideas for improving the quality of CuNWs. Arc discharge is believed to be one of the better methods for formation of CuNW-filled multi-wall carbon nanotubes (CuNW@MWNTs). We have recently reported that perfectly filled CuNW@MWNTs can be produced at more than 90% of the filling rate by using the hydrogen arc discharge method. In this study we investigated the effect of a copper content in an electrode and the arc current on the yield and the filling rate.

CuNW@MWNTs were produced by the conventional DC arc discharge. A hole (3 mm diameter) was drilled in the center of a graphite anode (5 mm diameter) and filled with a mixture of graphite and copper powder. The graphite powder and copper powder were mixed by choosing a copper/graphite atomic ratio of 0-100%. A 20 mm in diameter graphite rod was used for the cathode. The two electrodes were set vertically in a vacuum chamber. Hydrogen gas was filled up the chamber at a pressure of 0.1 MPa and was flowed at 500 ml/min during arc vaporization. Arc discharge was maintained at 50-90 A for 1 min.

The yield and filling rate of the CuNW@MWNTs were very low in the case of low copper content (Fig. 1(a)). SEM observation revealed that the yield and the filling rate of CuNW@MWNTs increased gradually with the copper content in the anode (Fig. 1(b)). In the case of copper content of 100% CuNW@MWNTs were included in soot that was deposited in the largest quantities on the inner wall of the chamber (Fig. 1(c)). Figure 1(d) shows that the obtained CuNW@MWNTs had 10-45 nm diameters and the filling rate of the MWNTs was extremely high. Many TEM observations clarified that more than 90% of the as-prepared MWNTs were filled perfectly with CuNWs. The CuNW@MWNTs consists of less than 10-nanotube layers and fcc copper crystals inside the MWNT in a long-range order. The distance between the lattice fringes of the filled copper crystals was measured at about 0.21 nm, which is identical to the d-spacing of the (111) atomic plane of copper.

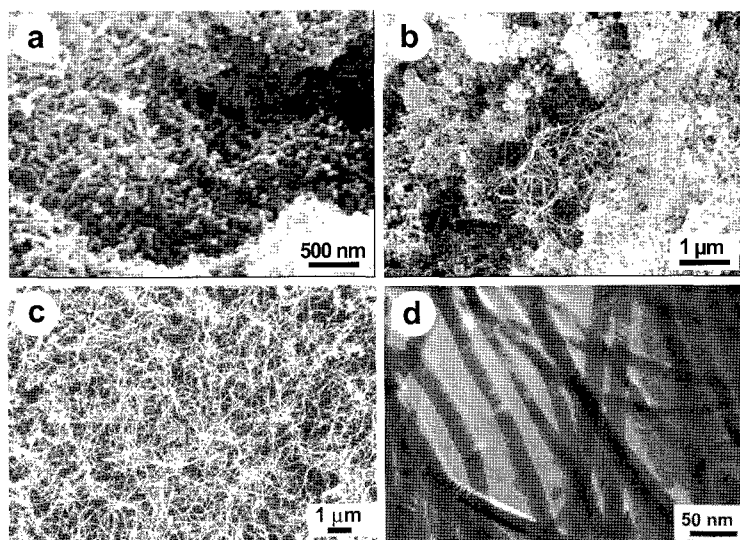


Fig. 1 SEM images of the chamber soot obtained by using the anodes including copper of (a) 10, (b) 70 and (c) 100%. (d) TEM image of CuNW@MWNTs corresponding to (c).

**Corresponding Author:** Akira Koshio

**E-mail:** koshio@chem.mie-u.ac.jp

**Tel & Fax:** +81-59-231-5370

## Synthesis and Characterization of Carbon Nanotubes Encapsulating Erbium-Chloride Nanowires

○D. Ogawa<sup>1</sup>, R. Kitaura<sup>1</sup>, K. Kobayashi<sup>1</sup>, T. Saito<sup>2,3</sup>, S. Ohshima<sup>2</sup>, and H. Shinohara<sup>1,4</sup>

<sup>1</sup>*Department of Chemistry & Institute for Advanced Research, Nagoya University, Nagoya 464-8602, Japan*

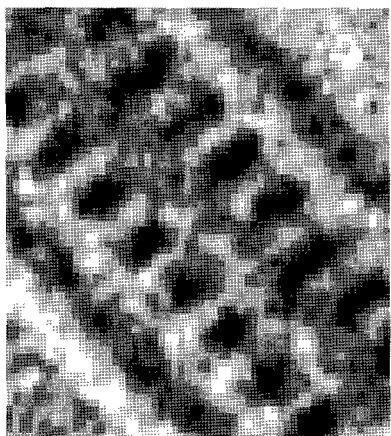
<sup>2</sup>*Research Center for Advanced Carbon Materials, AIST, Tsukuba 305-8565, Japan*

<sup>3</sup>*PRESTO, Japan Science and Technology Agency, Kawaguchi 332-0012, Japan*

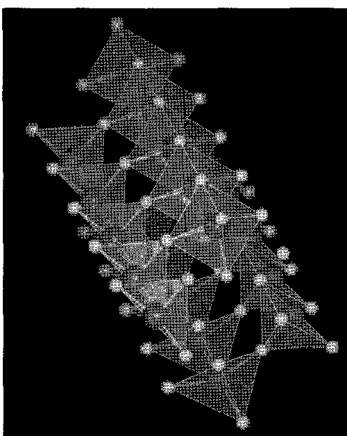
<sup>4</sup>*CREST, Japan Science and Technology Corporation, c/o Department of Chemistry, Nagoya University, Nagoya 464-8602, Japan*

Carbon nanotubes (CNTs) encapsulating metal compounds nanowire (MNW-CNTs) have attracted wide interests because such CNTs may exhibit novel electronic and magnetic properties due to unique low-dimensional structures as well as the possible presence of charge transfer between CNTs and encapsulated nanowires. In this respect, high filling ratio of nanowires is essential to explore properties of MNW-CNTs. Here, we report synthesis of MNW-CNTs of high-filling-ratios and structural characterization of encapsulated nanowires based on TEM observations together with simulated annealing calculations of the observed TEM images.

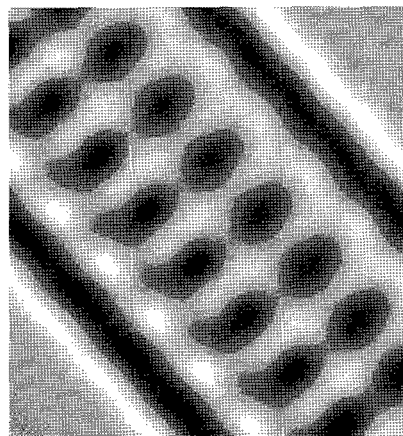
Cap-opened CNTs and  $\text{ErCl}_3$  were high-temperature heat treated at  $800\text{ }^\circ\text{C}$  under a vacuum of  $10^{-4}$  Pa. The sample was then washed in ethanol by ultrasonication and dried at  $80\text{ }^\circ\text{C}$ . Figure 1 shows a TEM image of  $\text{ErCl}_3$ @CNTs. Based on the TEM images, the filling ratio is estimated as high as 90 %, and the mean length of  $\text{ErCl}_3$  nanowire is ca. 50 nm. Minimization of the coulomb interaction energy exerted in the nanowires by a simulated annealing calculation, we have constructed a structure model of  $\text{ErCl}_3$  nanowire as shown in Fig.2. This simulated structure model well reproduces the observed TEM images (Fig. 3). We will also discuss the magnetic property of these novel CNT materials.



**Fig. 1** HR-TEM image  
of MNW-CNTs



**Fig. 2** A structure model  
of  $\text{ErCl}_3$  nanowire



**Fig. 3** The result of TEM  
the image simulation

**Corresponding Author:** Shinohara Hisanori

**E-mail:** nori@nano.chem.nagoya-u.ac.jp

**Tel:** (+81) 52-789-2482, **Fax:** (+81) 52-789-1169

## Nucleation of an SWNT from a catalytic metal cluster inside a carbon nanotube template: MD simulations of DWNT formation

○Yoshifumi Izu, Junichiro Shiomi and Shigeo Maruyama

*Department of Mechanical Engineering, The University of Tokyo  
7-3-1 Hongo, Bunkyo-ku, Tokyo 113-8656, Japan*

Molecular encapsulation in the hollow space of a carbon nanotube has attracted interests with various potential applications. The filling technique has also opened a path to realize controlled chemical reaction in nanoscale chamber for atomic scale selectivity. Experiments have been reported on formation of DWNT from C<sub>60</sub> fullerenes peapods [1] and ferrocene filled SWNT [2, 3]. The reports demonstrate that the growth mechanism of the inner tube depends on filler precursor.

In this work, we perform MD simulations of the nucleation process of SWNTs from a catalytic metal cluster inside an SWNT template to gain understanding in the growth mechanism. The methodology is inherited from the previous works on nucleation of SWNTs from isolated catalytic metal clusters [4]. As an initial condition, a Ni cluster with dissolved carbon atoms is placed in a rigid carbon nanotube. By supplying carbon atoms to the metal cluster, with keeping the number of free carbon atoms constant, nucleation of the inner SWNT was observed. Figure 1 shows the nucleation process at different time of the reaction. Once the open surface of the metal cluster is covered with carbon atoms, the feed carbon atoms are adsorbed onto Ni atoms adjacent to the outer-tube wall. Eventually, the supersaturated carbon atoms inside the metal cluster surface lifts off and the cap can be recognized together with the tubal structure. Dependence of the phenomena on the metal-cluster size and outer-tube diameter will be discussed.

[1] S. Bandow, et al Phys. Chem. Lett., 337 (2001) 48. [2] L. Guan, et al., Carbon 43 (2005) 2780. [3] H. Shiozawa, et al., phys.stat.sol.(b) 244 (2007) 4102. [4] Y. Shibuta and S. Maruyama, Chem. Phys. Lett., 382 (2003) 381.

Corresponding author: Shigeo Maruyama E-mail: maruyama@photon.t.u-tokyo.ac.jp, Tel/Fax: +81-3-5800-6983

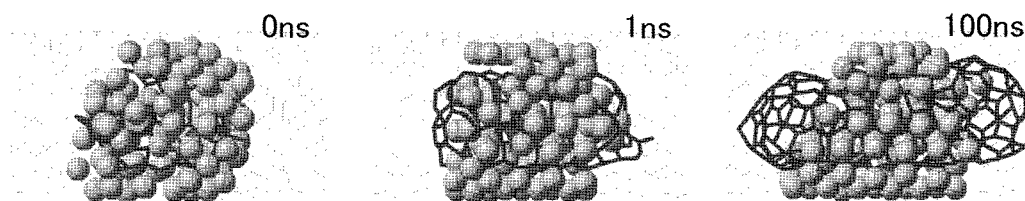


Fig. 1 Nucleation process from a catalytic metal cluster inside carbon nanotube

## SWNH as an Effective Delivery System for Macromolecule Anti-cancer Drugs

O Xu Jianxun,<sup>1</sup> Yudasaka Masako,<sup>1</sup> Zhang Minfang,<sup>1</sup> Iijima Sumio<sup>1,2</sup>

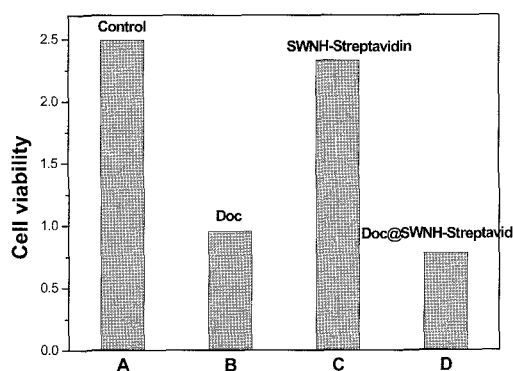
<sup>1</sup>JST/SORST, c/o NEC, 34 Miyukigaoka, Tsukuba, Ibaraki 305-8501, Japan

<sup>2</sup>Meijo University, 1-501 Shiogamaguchi, Tenpaku-ku, Nagoya 468-8502, Japan

Single Wall Carbon Nanohorn (SWNH) is a new kind of nano-carbon material, which has horn-like structure with 2~5 nm diameter. Usually about 2,000 SWNHs assemble to form an spherical aggregate with diameter of around 80~100 nm.<sup>1</sup> The SWNH aggregate emerges as an attractive candidate for a drug delivery system (DDS). It is specially promising to carry an anticancer drug, many of which are water insoluble macromolecules and highly toxic, to make them effectively delivered, and released in a controlled way.

In this study, we incorporated Docetaxel (Doc), an anticancer drug used for stomach cancer, breast cancer, non-small cell lung cancer and so on, into hydrogen peroxide treated SWNHs by modified nano-precipitation method. The weight percent of incorporated Doc is around 28%. Taking advantage of those carboxylic groups on SWNHs, we firstly introduced amine-PEO3-biotin to the conjugate to improve the hydrophilicity, which was identified by energy dispersive x-ray analysis. Then, streptavidin, a small protein, was attached on the complex due to the high affinity between streptavidin and biotin. The weight percent of streptavidin is estimated roughly to be 25%.

Furthermore, we investigated the anticancer effectiveness of Doc@SWNH-Streptavidin using a stomach cancer cell line. The cytotoxicity experiment was conducted using WST-1 reagent (Figure 1). The cells were incubated with Doc, SWNH-Streptavidin and Doc@SWNH-Streptavidin (~3 ug/ml) respectively for two days. We found that the viability of the cells with Doc@SWNH-Streptavidin decreased dramatically: only 1/3 of that of the cells with SWNH-Streptavidin. These indicate that Doc can be delivered by SWNH-Streptavidin into the cells and the released Doc causes cell death. Thus, we think SWNH-Streptavidin could be an effective DDS.



**Figure 1.** Cytotoxicity experiments using cancer cells incubated with Doc (B), SWNH-Streptavidin (C) and Doc@SWNH-Streptavidin.

### References:

1. S. Iijima, M. Yudasaka, R. Yamada, S. Bandow, K. Suenaga, F. Kokai, K. Takahashi *Chem. Phys. Lett.*, **1999**, 309, 165, and therein cited.

**Corresponding Author:** Xu Jianxun, Yudasaka Masako; **E-mail:** xu@frl.cl.nec.co.jp, yudasaka@frl.cl.nec.co.jp; **Tel:** 029-856-1940; **Fax:** 029-850-1366

## Gd oxide particles confined inside single-wall carbon nanohorns

○Ryota Yuge<sup>1</sup>, Masako Yudasaka<sup>1,2</sup>, Toshinari Ichihashi<sup>1</sup>, Jin Miyawaki<sup>2</sup>, Tsutomu Yoshitake<sup>1</sup>,  
and Sumio Iijima<sup>1,2,3</sup>

<sup>1</sup>NEC, 34 Miyukigaoka, Tsukuba 305-8501, Japan

<sup>2</sup>SORST-JST, 34 Miyukigaoka, Tsukuba 305-8501, Japan

<sup>3</sup>Meijo University, 1-501 Shiogamaguchi, Tenpaku-ku, Nagoya, 468-8502, Japan

Single-wall carbon nanohorns (SWNHs) have inherent hollow spaces, and the holes can be opened easily by the oxidation (SWNHox). Various kinds of materials, such as C<sub>60</sub> [1, 2] and Pt-compound [3], can be incorporated inside SWNHox, however, the incorporated materials are exposed to the surrounding gases, solvents, etc. Recently, experimental results and theoretical calculations indicated that the small-holes can be closed by heat-treatment in Ar atmosphere at 1200°C (SWNHh) [4]. In this study, we confined the Gd particles to inside space of SWNHox, which is a potential contrast agent for magnetic resonance imaging. We also found that Gd compounds moved by capillary suction mechanism during the heat treatments, which was useful to infer the structure of the aggregate of SWNH.

Gd acetate (50 mg) and SWNHox (50 mg) dispersed and stirred in ethanol (20 ml) at room temperature for about 12 hours. The mixture was filtered and washed with ethanol (20 ml) two times to remove the excess Gd acetate existing outside SWNHox and dried for 24 hours in vacuum at 50°C (Gd@SWNHox). The Gd@SWNHox was heat-treated for 3 hours at 1200°C under an Ar atmosphere (760 Torr).

Specific surface area and pore size distribution estimated from N<sub>2</sub>-adsorption isotherm at 77K showed that holes were closed by heat treatment and Gd compounds were confined inside SWNHs. STEM/EELS results indicated that Gd acetate changed to Gd<sub>2</sub>O<sub>3</sub> and moved to tips of sheath of SWNHs and center of SWNH aggregates. Besides these, we also found that Gd<sub>2</sub>O<sub>3</sub> with 10~20 nm sizes near the center of SWNH aggregates. The details are shown in the presentation.

### Reference:

- [1] K. Ajima et al. *Adv. Mater.* **16**, 397 (2004).
- [2] R. Yuge et al. *J. Phys. Chem.* **B109**, 17861(2005).
- [3] K. Ajima et al. *Mol. Pharm.* **2**, 475 (2005)
- [4] J. Miyawaki et al. *J. Phys. Chem.* **C111**, 1553(2007).

Corresponding Author: R. Yuge and M. Yudasaka

TEL: +81-29-850-1566, FAX: +81-29-856-6137

E-mail: [ryuge@frl.cl.nec.co.jp](mailto:ryuge@frl.cl.nec.co.jp), [yudasaka@frl.cl.nec.co.jp](mailto:yudasaka@frl.cl.nec.co.jp)

## Effect of compression pressure on the electrical resistivity for the pellet formed from nanohorns

○ Yuhei Fukunaga, Manabu Harada, Shunji Bandow, Sumio Iijima

Department of Materials Science and Engineering, Meijo University,  
1-501 Shiogamaguchi, Tenpaku, Nagoya 468-8502, Japan

Electrical resistivity for the pellet formed from nanohorns (NHs) became low with increasing the doping rate of boron to the nanohorns [1]. Temperature dependence of the electrical resistivity indicated a feature explainable by the mechanism based on the 3-dimensional variable range hopping conduction (3D-VRH). Characteristic temperature  $T_0$  of 3D-VRH for B-doped NHs closely depended on the doping rate and the electrical resistivity at room temperature ( $\rho_{RT}$ ) decreased with increasing the doping rate (see Fig. 1a).

We consider that the change of  $T_0$  is originated in the increase of the electronic density near the Fermi-level due to substitutional doping of boron to the NH-wall. Similar phenomenon was also observed in B-doped nanotubes [2]. However, the detection of boron in the NH-wall has not been succeeded due to possibly low doping rate ( $< 1000$  ppm atomic). In the present study, we carried out the experiments of pressure-dependence on the electrical resistivity that will tell whether or not the  $T_0$  values depend on the condition of contact between the NH-particles. Experimental results of temperature dependence of  $\rho_{RT}$  with a parameter of the pressure to form pellet are in Fig. 1b and summary of  $T_0$  and  $\rho_{RT}$  is in Fig. 2.

From Fig. 2, it can be found that  $T_0$  is not susceptible to the pressure but strongly depends on the doping rate. Difference is clear as indicated by the arrow-headed bar in Fig. 2. On the other hand,  $\rho_{RT}$  is rapidly decreased with increasing the pressure. These facts also support that the change of  $T_0$  is purely the effect of boron doping and the electronic density certainly increases as a function of the doping rate.

[1] M. Harad et al., The 33<sup>rd</sup> F&NT General Symp. (2007) 1P-34.

[2] S. Bandow et al., *J. Phys. Chem. C* **111**, 11763 (2007).

**Corresponding Author:** Shunji Bandow, **E-mail:** bandow@ccmf.s.meijo-u.ac.jp, **Tel&Fax:** +81-52-834-4001.

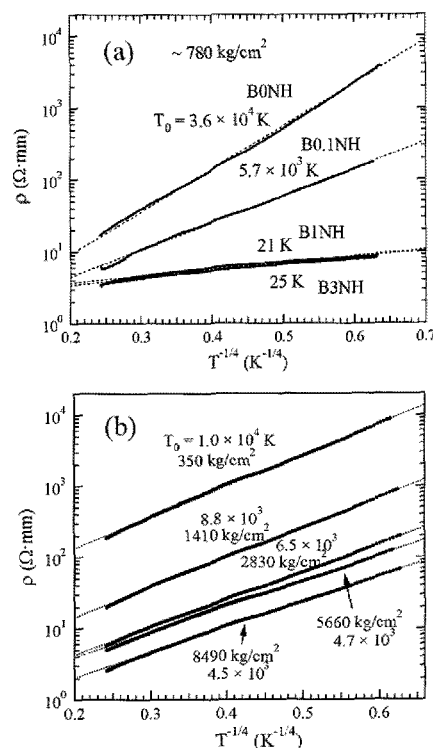


Fig. 1. Temperature dependence of the electrical resistivity for the pellet formed from nanohorns. (a) is for B-doped NHs with different B-doping rate. The pellet was formed with a pressure of  $\sim 780$  kg/cm<sup>2</sup>. (b) is for un-doped NHs, but the pellets were formed at various pressures.

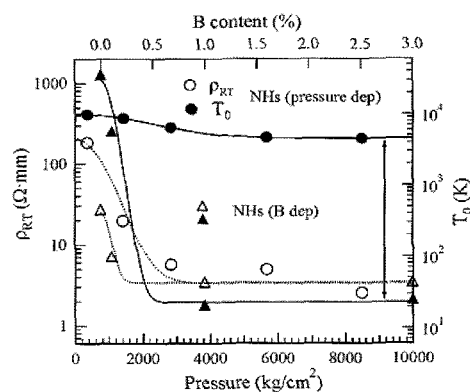


Fig. 2. Pressure dependence of  $\rho_{RT}$  of un-doped NHs (open and closed circles) and doping rate dependence of NHs (open and closed triangles). B content does not mean the doping rate.



**Anti-Cancer Effect of ZnPc-Nanohorn-Protein *in vivo***

OM. Zhang<sup>1</sup>, M. Yudasaka<sup>1,2</sup>, T. Murakami<sup>3</sup>, K. Ajima<sup>1</sup>, A. D. Sandanayaka<sup>4</sup>, O. Ito<sup>4</sup>,

K. Tsuchida<sup>3</sup>, S. Iijima<sup>1,2,5</sup>

<sup>1</sup>*SORST-JST, <sup>2</sup>NEC, 34 Miyukigaoka, Tsukuba, Ibaraki 305-8501, Japan*

<sup>3</sup>*Fijita Health Univ. 1-98 Dengakubo, Kutsukake-cho, Toyoake, Aichi 470-1192, Japan*

<sup>4</sup>*Tohoku Univ. 2-1-1 Katahira, Aoba-ku, Sendai 980-8577, Japan*

<sup>5</sup>*Meijo Univ. 1-501 Shiogamaguchi, Tenpaku-ku, Nagoya 468-8502, Japan*

Recently, we fabricated a nanohorn-based hybrid as a drug delivery system for photodynamic therapy (PDT): a photosensitizer, zinc phthalocyanine (ZnPc) was loaded on single-wall carbon nanohorn (SWNH) with hole-opened (SWNHox) and SWNHox was modified with a protein of bovine serum albumin (BSA). We previously showed that the ZnPc-SWNHox-BSA was taken up by the cultured rat cancer cells and destructed the cells when the 670-nm laser was irradiated. The efficiency of ZnPc-SWNHox-BSA on killing cancer cells was higher than the intact ZnPc was used [1]. We expected the similar PDT advantage of ZnPc-SWNHox-BSA over ZnPc would appear *in vivo*, and carried out the animal (mouse) testing as presented in this report.

We subcutaneously transplanted the cultured rat cancer cells to nude mice, and bred the mice under appropriate conditions. The ZnPc-SWNHox-BSA was prepared by the same method as we previously reported [1]: SWNHox was prepared by light-assisted oxidation [2], ZnPc was loaded on SWNHox, and BSA was attached to the –COOH groups of SWNHox [2]. ZnPc and ZnPc-SWNHox-BSA were dispersed in PBS with a sonicator, and the obtained homogeneous-dispersions were intratumorally injected to the tumors of the mice. The tumor sizes and mouse-body weights were measured everyday after intratumoral injection. We found that the tumor volumes increased with days irrespective of the specimens injected into tumors when the laser was not irradiated, suggesting that ZnPc or ZnPc-SWNHox-BSA did not have any anticancer effects. However, when the 670-nm laser was irradiated on the tumors, the tumor growth was suppressed, exhibiting the PDT effect of ZnPc and ZnPc-SWNHox-BSA. It was also found that the PDT effect of ZnPc-SWNHox-BSA was much stronger than ZnPc. The reason for this is discussed in the talk.

[1] Zhang, M.; Yudasaka, M.; Ajima, J.; Iijima, S. The 33<sup>st</sup> F-NT symposium.

[2] Zhang, M.; Yudasaka, M.; Ajima, K.; Miyawaki, J.; Iijima, S. *ACS NANO*, 1, 265-272 (2007).

Corresponding Authors: Minfang Zhang, Masako Yudasaka

Email: [minfang@frl.cl.nec.co.jp](mailto:minfang@frl.cl.nec.co.jp), [yudasaka@frl.cl.nec.co.jp](mailto:yudasaka@frl.cl.nec.co.jp)

Tel +81-29-8501190, Fax: +81-29-8501366

## Influence of formation technique of catalyst layer and addition of conductive material on performance of direct methanol fuel cell

○Y. Izumi<sup>1</sup>, K. Shinohara<sup>1</sup>, M. Yamamoto<sup>1</sup>, S. Oke<sup>1</sup>, H. Takikawa<sup>1</sup>,  
T. Sakakibara<sup>2</sup>, S. Sugawara<sup>2</sup>, N. Aoyagi<sup>3</sup>, T. Okawa<sup>3</sup>,  
K. Yoshikawa<sup>4</sup>, K. Miura<sup>4</sup>, S. Itoh<sup>5</sup>, and T. Yamaura<sup>5</sup>

<sup>1</sup>Department of Electrical and Electronic Engineering, Toyohashi University of Technology

<sup>2</sup>ENAX Inc., <sup>3</sup>Daiken Chemical Co., Ltd., <sup>4</sup>Tokai Carbon Co., Ltd., <sup>5</sup>Futaba Corporation

Direct methanol fuel cells (DMFC) are very promising power sources for portable applications and high efficiency due to simple handling and processing of fuel. In order to increase the output power of DMFC, it has been used that the catalyst which contained Pt/Ru supported on an arc-soot (AS)<sup>(1)</sup> which was synthesized by twin-torch-arc apparatus. This research discussed fabrication process of the membrane and electrode assembly (MEA) such as formation of the catalyst layer, selection of a carbon paper, and addition of a conductive material.

The catalyst layer was formed by dry squeegee technique. A dry catalyst powder of catalysts was putted on a carbon paper, it was smoothed out, and Nafion solution was dropped onto the catalyst powder to fix the catalyst powder and the carbon paper. The output power in case of the dry squeegee technique was applied to formation of catalyst layer was twice as high as that in case of a conventional technique was applied (Fig.1).

In this research, carbon nano-balloon (CNB)<sup>(2)</sup> was mixed in catalyst to decrease MEA resistance. Resistance and particle size of CNB (0.091 mΩcm, 24 nm) was 1/50 and 1/2 as low and small as AS, respectively. It is shown in Fig. 2, at a CNB content of 25 wt.%, output power has a maximum (10 mW) and MEA resistance has a minimum (36 mΩ). In case of CNB content was greater than 25 wt.%, increasing CNB content caused increasing current course, because CNB had smaller particle size than Pt/Ru particles.

This work has been partly supported by the Research Center for Future Vehicle from Toyohashi University of Technology and the Global COE Program "Frontiers of Intelligent Sensing" from the Ministry of Education, Culture, Sports, Science and Technology.

### References

- [1] K. Higashi, *et al.*, *Appl. Plasma Sci.*, **13**, 99 (2005)  
[2] H. Niwa, *et al.*, *New Diamond Frontier Carbon Tech.*, **15**, 73 (2005)

Corresponding author: S. Oke.

Tel: +81-532-44-6728, fax: +81-532-44-675727, e-mail: oke@eee.tut.ac.jp.

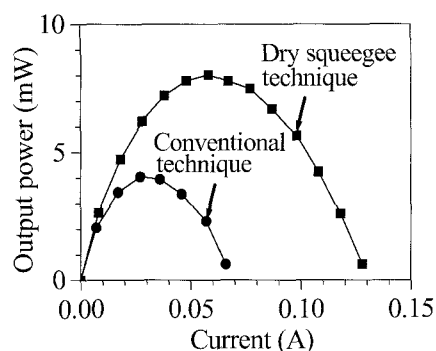


Fig. 1 Comparison of the formation techniques of catalyst layer of MEA.

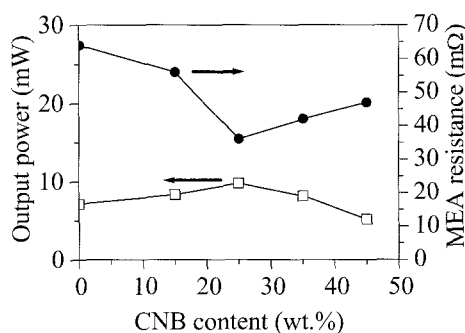


Fig. 2 Variations of output power and MEA resistance with CNB content in catalyst.

## Close-Open-Close Evolution of Holes in Single-Wall Carbon Nanohorns Caused by Heat Treatment

○ Jing Fan<sup>1</sup>, Masako Yudasaka<sup>1,2</sup>, Jin Miyawaki<sup>1</sup>, Ryota Yuge<sup>2</sup>,  
Takazumi Kawai<sup>2</sup>, and Sumio Iijima<sup>1,2,3</sup>

1) SORST/JST, NEC Corporation, 34 Miyukigaoka, Tsukuba 305-8501, Japan

2) NEC Corporation, 34 Miyukigaoka, Tsukuba 305-8501, Japan

3) Meijo University, 1-501 Shiogamaguchi, Tenpaku-ku, Nagoya 468-8502, Japan

Our previous experimental results and theoretical calculations indicated that the holes at the tips of single-wall carbon nanohorns (SWNH) could be closed by the heat treatment at 1200°C in Ar atmosphere [1]. We also found that the hole closing exhibited the close-open-close evolution during the heating when the hole sizes were about 0.7 nm [2]. When the hole sizes were smaller or larger, the close-open-close evolution did not appear, that is, the holes were closed and never re-opened [2]. The mechanism of these changes were investigated precisely, and presented in this report.

To open the holes, SWNHs were oxidized in flowing air by slow combustion method [3] (SWNHox) with various target temperatures (Tox 300~ 500 °C). For closing the holes, SWNHox was heat-treated at 1200°C in Ar for 0~ 3 h. The hole closing was examined by measuring xylene-adsorption quantity using thermogravimetric equipment [4].

The holes with sizes of about 0.7 nm that exhibited the close-open-close evolution by the 1200°C heat treatment were opened by the oxidation at Tox of 400 and 450°C. We stopped the heat treatment at 18 minute when the holes were closed, and at 198 minutes when the hole were re-opened, and the structures of these two types of SWNHox were examined. The transmission electron microscopy observation did not show any appreciable structure changes caused by the heat treatment, indicating that the close-open-close evolution did not accompany any overall structure-changes. IR spectrum and TPD mass-spectrum measurements indicated that the oxygenated groups existing at the edges of holes of SWNHox were removed within the 18-minute of the heat treatment. We inferred from these data that the first quick-closing was oxygen mediated, the quickly-closed tips took an unstable structure, and this structural instability induced the re-opening. Using the oxygen mediated closing model, we could explain the mechanism of the simple thermal-closing of the holes with smaller or larger sizes.

### References:

- [1] J. Miyawaki et al. *J. Phys. Chem. C* **111** (2007) 1553-5.
- [2] J. Fan et al. *The 33 rd F-NT symposium*.
- [3] J. Fan et al. *J. Phys. Chem. B* **110** (2006) 1587-91.
- [4] M. Yudasaka et al. *J. Phys. Chem. B* **109** (2005) 3809-13.

Corresponding Author: Yudasaka Masako

E-mail: yudasaka@frl.cl.nec.co.jp Tel:+0081-29-850-1190; Fax: +0081-29-850-1366.

**Intravenous Toxicity of Single-Walled Carbon Nanohorns**

Jin Miyawaki<sup>1,2</sup>, Masako Yudasaka<sup>1,3</sup>, Minfang Zhang<sup>1</sup>, Sumio Iijima<sup>1,3,4</sup>

<sup>1</sup>JST/SORST, c/o NEC, 34 Miyukigaoka, Tsukuba, Ibaraki 305-8501, Japan

<sup>2</sup>Current address: Institute for Materials Chemistry and Engineering, Kyushu University, 6-1 Kasugakoen, Kasuga, Fukuoka 816-8580, Japan

<sup>3</sup>NEC, 34 Miyukigaoka, Tsukuba, Ibaraki 305-8501, Japan

<sup>4</sup>Meijo University, 1-501 Shiogamaguchi, Tempaku, Nagoya 468-8502, Japan

Comprehensive *in vivo* and *in vitro* toxicity assessments showed low acute toxicity of as-grown single-walled carbon nanohorns (SWNHs) [1]. When hole-openings are introduced at tips and topological defects in sidewalls, SWNHs become to carry various drugs inside internal hollow spaces. Therefore, we proactively investigated intravenous toxicities of hole-opened single-walled carbon nanohorns (SWNHs) toward their biomedical applications. To investigate influence of physicochemical properties on the toxicities, we prepared three samples; hole-opened SWNHs by light-assisted H<sub>2</sub>O<sub>2</sub> oxidation (LAOx) [2] and slow combustion in air (SC) [3] methods, and the LAOx-SWNHs chemically-modified with a protein, bovine serum albumin (BSA).

Irrespective of the hole-opening methods or chemical modification with BSA, all mice ( $n = 5$  for each group) received a single intravenous dose (6 or 8 mg/kg) of nanohorns dispersed in PBS survived the 2-26 week test periods and showed normal body weight gain. Black pigmentations were histopathologically observed in lumen of lung blood vessels, hepatic Kupffer cells, and spleen for all animals, but induced no toxicological lesions.

In the pulmonary vessels, the pigmentations accompanied vessel-wall thickenings for SC-SWNH; both levels of the pigmentation and the wall thickening were time-dependently reduced. We did not observe such wall thickenings for animals in the LAOx-SWNH and BSA-SWNH groups. BSA-SWNHs seemed to be taken up by cells, most likely pulmonic macrophages, at longer observation periods. On the other hand, there was no difference in the level and morphology of pigmentations in the liver and the spleen for any group. The detail will be discussed in the presentation.

[1] J. Miyawaki, *et al.*, *ACS Nano*, *in press*. [2] M. Zhang, *et al.*, *ACS Nano*, **1**, 265 (2007). [3] J. Fan, *et al.*, *J. Phys. Chem. B*, **110**, 1587 (2006).

Corresponding Author: Jin Miyawaki and Masako Yudasaka

E-mail: miyawaki@cm.kyushu-u.ac.jp, yudasaka@frl.cl.nec.co.jp TEL: +81-29-856-1940, FAX: +81-29-850-1366

## Effect of Al oxide buffer layer on SWNT growth using alcohol gas source in high vacuum

○Tomoyuki Shiraiwa<sup>1</sup>, Shigenori Numao<sup>2</sup>, Osamu Oishi<sup>2</sup>, Nobuyuki Nishi<sup>2</sup>  
Takahiro Maruyama<sup>1</sup> and Shigeya Naritsuka<sup>1</sup>

<sup>1</sup>Department of Materials Science and Engineering, Meijo University,  
1-501 Shiogamaguchi, Tempaku, Nagoya 468-8502, Japan

<sup>2</sup>Institute for Molecular Science, 38 Nishigo-Naka, Myodaiji, Okazaki 444-8585, Japan

Recently, the growth mechanism of carbon nanotube (CNT) has been investigated using *in situ* observation techniques, such as transmission electron microscopy (TEM) and X-ray photoelectron spectroscopy (XPS) [1, 2]. To clarify this growth mechanism, we have developed single-walled carbon nanotube (SWNT) growth in a high vacuum chamber using gas source method [3]. However, the yield of grown SWNT was not sufficient for *in situ* observation. In this study, we attempted to increase the yield of SWNT using Al oxide buffer layer and investigated the mechanism.

For the purpose of TEM observation, 200-mesh Mo grids were used as substrates. Firstly, the grids were introduced into an ultra-high vacuum (UHV) chamber and Al buffer layers were deposited on them using a pulsed arc plasma gun. The Al thickness was varied from 0 to 30 nm. Once the grids were exposed to air for oxidation of the Al layer, they were introduced into the chamber again, and Co (thickness ~0.1 nm) was deposited by an e-beam evaporator. Then, they were heated to the growth temperature (typically 700°C), and ethanol gas (pressure:  $1.0 \times 10^{-1}$  Pa) was supplied to grow SWNTs. The grown SWNTs were characterized by scanning electron microscopy (SEM), TEM and Raman spectroscopy (Ar laser: 514.5 nm).

Fig. 1 shows an SEM image of SWNTs grown on 30 nm Al<sub>2</sub>O<sub>x</sub>/Mo grid at 700°C. High-density vertically aligned CNTs were observed on the grid. From TEM observation, it was found that most of the grown CNTs were SWNTs. As the Al<sub>2</sub>O<sub>x</sub> thickness was reduced, the yield of SWNTs decreased, showing web-like structures. In addition, Co catalyst size seemed to decrease as the Al buffer thickness increased. This suggests that the increase of the SWNT yield was partly due to the increase of Co nanoparticles with 1-2 nm in diameter by suppression of Co coalescence. These results indicate that the support of Al oxide layer is effective for high-density SWNTs growth.

A part of this work was supported by “Nanotechnology Network Project” of the Ministry of Education, Culture, Sports, Science and Technology (MEXT), Japan.

### References

- [1] S. Hofmann et al., *Nano Lett.* **7** (2007) 602.
- [2] F. Maeda et al., *Jpn. J. Appl. Phys.* **46** (2007) L148.
- [3] K. Tanioku et al., *Diam. Relat. Mater.* *in press*.

**Corresponding Author:** Takahiro Maruyama

**E-mail:** takamaru@ccmfs.meijo-u.ac.jp

**Tel:** +81-52-838-2386, **Fax:** +81-52-832-1172

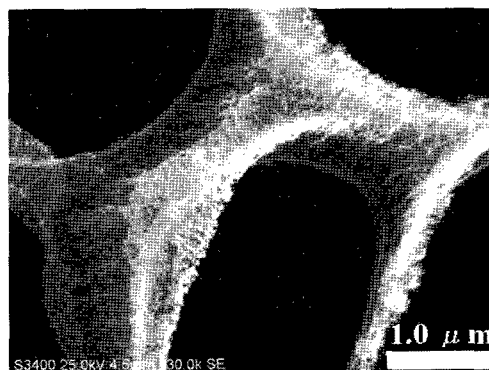


Fig. 1 SEM image of SWNTs grown on 30 nm Al<sub>2</sub>O<sub>x</sub>/Mo grid.

### **Dispersion and Separation of Single-Walled Carbon Nanotubes prepared by using metal-catalysts supported on Zeolite**

○Masahiro Hashimoto,<sup>1</sup> Yutaka Maeda,<sup>1,2</sup> Tadashi Hasegawa,<sup>1</sup> Makoto Kanda,<sup>3</sup> Takahiro Tsuchiya,<sup>3</sup> Takatsugu Wakahara,<sup>3</sup> Takeshi Akasaka,<sup>3</sup> Yuhei Miyauchi,<sup>4</sup> Shigeo Maruyama,<sup>4</sup> Jing Lu,<sup>5</sup> Shigeru Nagase,<sup>6</sup>

<sup>1</sup>*Department of Chemistry, Tokyo Gakugei University, Koganei, Tokyo 184-8501, Japan,*  
<sup>2</sup>*PRESTO, Japan Science and Technology Agency, Chiyoda, Tokyo 102-0075, Japan,*  
<sup>3</sup>*Center for Tsukuba Advanced Research Alliance, University of Tsukuba, Tsukuba 305-8577, Japan,*  
<sup>4</sup>*Graduate School of Engineering, The University of Tokyo, Tokyo 113-8656, Japan,*  
<sup>5</sup>*Department of Physics, Peking University, Beijing 100871, People's Republic of China,*  
<sup>6</sup>*Department of Theoretical Molecular Science, Institute for Molecular Science, Okazaki 444-8585, Japan*

It is remarkable that a diameter selective synthesis of highly pure SWNTs has been achieved by temperature-controlled CVD of an alcohol on metal supported Zeolite [1]. In past several purification methods, removal of metal catalysts and Zeolite from SWNTs under severe purification conditions was required. However, SWNTs may be damaged under the conditions. Recently, an effective exfoliation method of SWNTs in organic solvents with an amine as a dispersion reagent [2] and a convenient amine-assisted separation method for SWNTs that makes metallic SWNTs enriched remarkably in a simple way [3] have been developed.

We report here purification of SWNTs, produced by the CVD method of an alcohol on metal supported Zeolite, was simply achieved through the dispersion-centrifugation process. The purified SWNTs were characterized on the basis of visible-near infrared absorption, photoluminescence and Raman spectroscopic analyses, and scanning electron microscopy observation. Moreover, selective extraction of metallic SWNTs was also accomplished by an optimized amine-assisted separation method.

[1] Murakami, Y. *et al.*, *Chem. Phys. Lett.* **2003**, 374, 53.

[2] Maeda, Y. *et al.*, *J. Phys. Chem. B* **2004**, 108, 18395.

[3] Maeda, Y. *et al.*, *J. Am. Chem. Soc.* **2005**, 127, 10287.

**Corresponding Author** Tadashi Hasegawa

**E-mail** tadashi@u-gakugei.ac.jp

**Tel&Fax** +81-42-329-7496

## A protocol to remove surfactants and gradient media from metallic and semiconducting single-wall carbon nanotubes in density gradient separations

○K. Yanagi<sup>1,4</sup>, Y. Miyata<sup>1,4</sup>, Y. Sato<sup>2</sup>, Z. Liu<sup>2</sup>, K. Suenaga<sup>2</sup>, T. Ishida<sup>3</sup>, H. Kataura<sup>1,4</sup>

<sup>1</sup>Nanotechnology Institute, <sup>2</sup>Research Center for Advanced Carbon Materials, <sup>3</sup>Advanced Manufacturing Research Institute, National Institute of Advanced Industrial Science and Technology (AIST), and <sup>4</sup>JST-CREST.

**Abstract:** Highly purified metallic and semiconducting single-wall carbon nanotubes (SWCNTs) can be obtained from density gradient centrifugations [Fig. 1(a)],<sup>1</sup> however, the estimated high purity has been derived from the ratio of metallic and semiconducting nanotubes. In a sample solution obtained just after the centrifugations, not only SWCNTs but also surfactants and gradient media exist, thus in this context the purity of SWCNTs is not high. Removal of surfactants and gradient media is important to correctly investigate the intrinsic characteristics of SWCNTs with a single electronic type. Here we propose the following removal protocol; filtration with centrifugations, methanol and HCl washing. In a sample, which is not sufficiently rinsed after centrifugations, the amount of residual metals was estimated to be approximately 30 % [Fig.1 (b)], suggesting the presence of sodium and other contaminants originated from the surfactants and gradient media. In a sample purified through our removal protocol, however, it became less than 1 %. HR-TEM images indicated that the presence of contaminants was small. X-ray photoelectron spectra showed that the carbon content of a sample after the removal processes is nearly 99 %.

**References:** [1] Arnold et al., Nature Nano. 1 (2006) 60. Yanagi et al., submitted in 2007.

**Corresponding**

**Author;** KY, e-mail; k-yanagi@aist.go.jp,

**Tel&Fax** 029-861-3132

**& 2786**

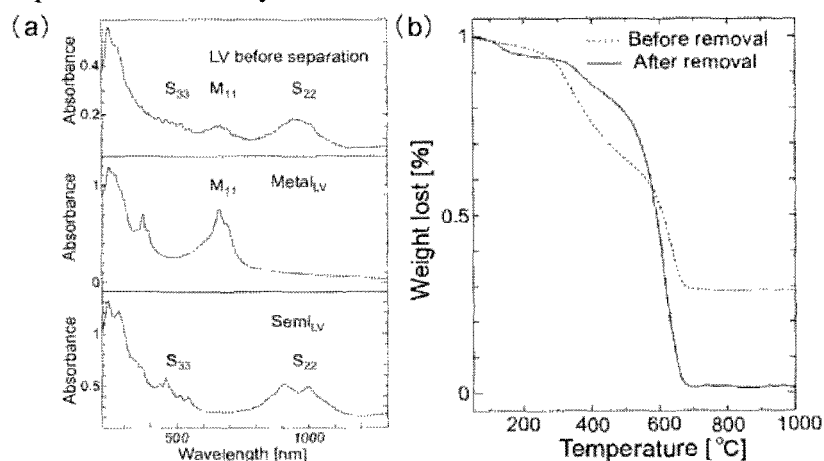


Fig. 1 (a) Absorption spectra of pristine (top), metallic (center) and semiconducting SWCNTs (bottom). (b) The results of thermogravimetric analysis of SWCNTs before and after our removal procedures.

### Diagnosics and Control of Growth of Vertical-aligned Carbon Nanotube Forest by Using a Telecentric Optical System

○Satoshi Yasuda, Don N. Futaba,  
Motoo Yumura, Sumio Iijima, and Kenji Hata

<sup>1</sup>*Reserach Center for Advanced Carbon Materials, National Institute of Advanced Industrial Science and Technology (AIST), Tsukuba, 305-8576, Japan*

The carbon nanotube (CNT) forest with properties of high-purity, vertical alignment, and millimeter-scale height has shown exceptional promise as a new industrial material for various applications spanning actuators, energy storage, to sensors.[1,2] Therefore, understanding the growth mechanism and controlling the growth progression becomes paramount to fully realize the potential for these applications. For that purpose, a monitoring system which possesses ease of use, accuracy and wide range is needed. A number of groups have previously reported *in situ* measurement systems based on optical interference and absorption, diffraction, and projection [3-6]. However, conventional measurement methods were insufficient to accurately measure the growth kinetics for a wide range of growths due to limited resolution and limited field of view. Further the measurement system required periodic adjustment of the optical system and sometimes complex analysis of the raw data.

Here we report a simple *in situ* height measurement system for CNT forests which possesses both high resolution and large field of view. Employing a telecentric optical system operating with a infinite focal distance, this system is free of the need for periodic adjustment to the working distance.

We made it possible to measure the growth curve easily with much higher precision compared with the conventional measurement system. This system enabling *in situ* measurement can monitor the measurement point consecutively, so we have elucidated the existence of various growth curves of forest that have not been verified so far.

- [1] K. Hata, D. N. Futaba, K. Mizuno, T. Namai, M. Yumura, and S. Iijima, *Scinece* 2004, **306**, 1362
- [2] D. N. Futaba, K. Hata, T. Yamada, T. Hiraoka, Y. Hayamizu, Y. Kakudate, O. Tanaike, H. Hatori, M. Yumura, and S. Iijima, *Nature Material* 2006, **5**, 987
- [3] D. B. Geohegan, A. A. Puzos, I. N. Ivanov, S. Jesse, and G. Eres, *Appl. Phys. Lett.*, 2003, **83**, 1851
- [4] S. Maruyama, E. Einarsson, Y. Murakami, T. Edamura, *Chem. Phys. Lett.*, 2005, **403**, 320
- [5] L. M. Dell'Acqua-Bellavitis, J. D. Ballard, P. M. Ajayan, and R. W. Siegel, *Nano lett.* 2004, **4**, 1613
- [6] I. Gunjishima, T. Inoue, and A. Okamoto, *Jpn. J. Appl. Phys.*, 2007, **46**, 3149

Corresponding Author: Kenji Hata

TEL: +81-29-861-4656 , FAX: +81-29-861-4851, E-mail: kenji-hata@aist.go.jp



## FT-IR Gas Analysis for Alcohol Catalytic Chemical Vapor Deposition

Tomohiro Shimazu<sup>1</sup>, Yoshinobu Suzuki<sup>1</sup>, Hisayoshi Oshima<sup>1</sup>, and Shigeo Maruyama<sup>2</sup>

<sup>1</sup>Reserch Laboratories, DENSO CORPORATION  
500-1 Minamiyama, Komenoki, Nisshin-shi, Aichi 470-0111, Japan  
<sup>2</sup>Department of Mechanical Engineering, The University of Tokyo  
7-3-1 Hongo, Bunkyo-ku, Tokyo 113-8656, Japan

### Abstract

Alcohol catalytic chemical vapor deposition (ACCVD) has become a popular CVD method for growth of high-purity single walled carbon nanotube (SWNT) films due to the low cost and easy-handling of a non-hazardous CVD gas source. [1] At CVD temperatures, ethanol mainly decomposes into ethylene and water. [2] These thermally generated molecules could affect SWNT growth. However, there are few gas analysis studies for ACCVD.

In this study, we have investigated gas molecules behavior during ACCVD using Fourier Transfer infrared spectroscopy (FT-IR: Otsuka electronics IG-1000). FT-IR cell was inserted between a reactor tube and a vacuum pump. SWNT synthesis was performed by using ethanol as the carbon source and Co/Mo bimetal as the catalyst. Growth temperature was 1113 K.

The time dependence of gas molecule intensities is shown in Fig.1. In order to distinguish catalytic decomposed molecule intensities from thermally decomposed molecule intensities, the intensities obtained in the presence of catalyst were subtracted from those obtained in the absence of catalyst. In the early stage, ethanol was consumed and ethylene and water were generated. After a few minutes, ethanol was reached to zero, and ethylene and water were changed from generation mode to consumption mode. The consumption mode was continued during growth period. This mode would be caused by deposition and etching of carbon on the substrate and/or synthesized SWNT surface.

We will discuss this behavior of gas molecules with time dependence of SWNT film thickness and weight.

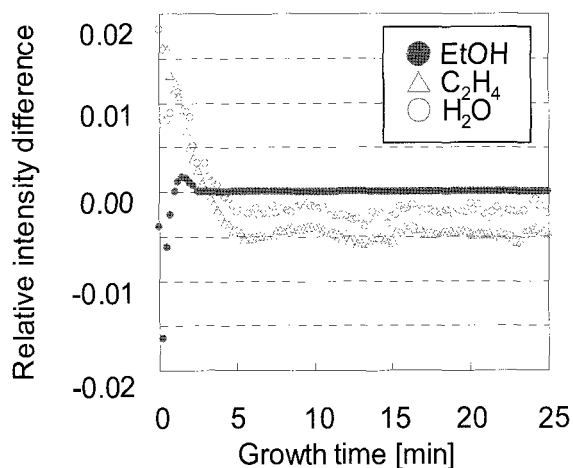


Fig.1 FT-IR intensity difference of with and without catalysts for ethanol, ethylene, and water as function of growth time. Each intensity is normalized by the intensity of ethanol at 2.7 kPa at RT.

**References:** [1] S. Maruyama et al. *Chem. Phys. Lett.*, **360**, 229(2002); [2] J. Herzler et al. *J. Phys. Chem.*, **101**, 5500 (1997)

**Corresponding Author:** Hisayoshi Oshima

**E-mail:** hoosima@rlab.denso.co.jp **Tel.:** +81-561-75-1860 **Fax.:** +81-561-75-1193

## Growth of double- and triple-walled carbon nanotube on MgO substrate

○Ryoji Naito<sup>1</sup>, Toshiya Murakami<sup>1</sup>, Yuki Hasebe<sup>1</sup>, Kenji Kisoda<sup>2</sup>, Koji Nishio<sup>1</sup>,  
Toshiyuki Isshiki<sup>1</sup> and Hiroshi Harima<sup>1</sup>

<sup>1</sup>Department of Electronics, Kyoto Institute of Technology, Kyoto 606-8585, Japan

<sup>2</sup>Physics Department, Wakayama University, Wakayama 640-8510, Japan

Selective growth of carbon nanotubes with desired chirality and wall number is a key issue for future industrial applications. We have recently reported that high purity double-walled carbon nanotubes (DWNT) can be grown with a post-growth purification process by chemical vapor deposition (CVD), using a mixed catalyst on MgO at optimized composition.[1] We developed here a direct synthetic method of DWNT and triple walled nanotubes (TWNT) without such post-growth purification process.

Using Co or Fe catalyst loaded on MgO (100) by dip-coating, carbon nanotubes were grown by CVD at 850°C with ethanol as a carbon source. As seen in a typical TEM image of the as-grown sample, Fig.1, the product was dominated by DWNT (~65%) and TWNT (~35%), while single-walled ones (SWNT) were hardly observed. Tube diameters of the DWNT were distributed in 0.6-3.2 nm (inner tube) and 1.2-4.0 nm (outer tube). Figure 2 shows their Raman spectra (top two traces) comparing with those of high-purity SWNT grown on Si/SiO<sub>2</sub> [2, 3] and DWNT grown on MgO powder.[1] The band shape of radial breathing mode (RBM) and G band of the as-grown samples looks very similar to those of DWNT reference. Recalling that DWNT and TWNT has much lower Raman scattering efficiency compared to SWNT,[1] the Raman spectra also support that DWNT and TWNT were selectively grown on MgO substrate without post-growth purification.

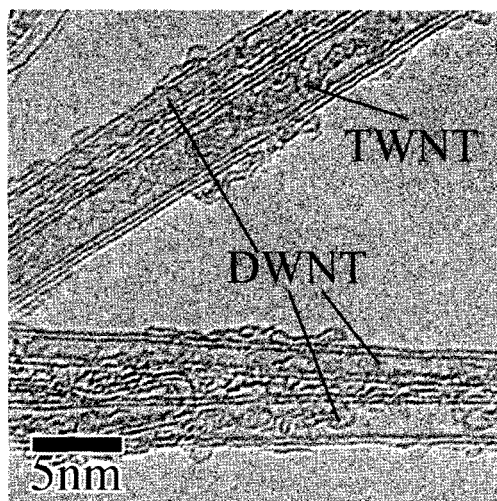


Fig. 1 TEM image

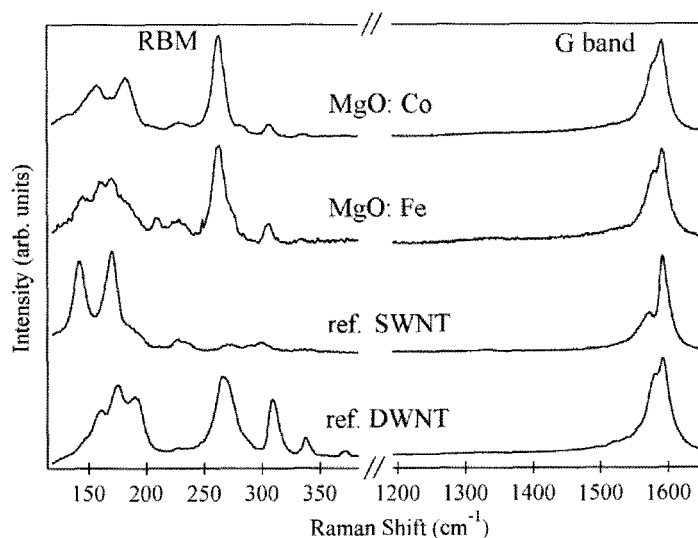


Fig. 2 Raman spectra (532 nm exc.)

[1] T. Murakami, *et al.*, submitted to "J. Appl. Phys."

[2] T. Murakami, *et al.*, J. Appl. Phys. **100** (2006) 094303.

[3] T. Murakami, *et al.*, Jpn. J. Appl. Phys. in press.

Corresponding Author: R. Naito, TEL: +81-75-724-7421, E-mail: m7621018@edu.kit.ac.jp

## Purification of Carbon Nanotubes by Amphiphilic Oligopeptides

○ Shinya Masuhara<sup>1</sup>, Atsushi Yamamoto<sup>1</sup>, Yousuke Miura<sup>1</sup>,  
Yasushi Maeda<sup>2</sup>, and Shin Ono<sup>1</sup>

<sup>1</sup>Graduate School of Science and Engineering, University of Toyama, Toyama  
930-8555, Japan

<sup>2</sup>Graduate School of Engineering, University of Fukui, Fukui 910-8507, Japan

The development of a non-destructive method for purification of carbon nanotubes (CNTs) is needed for their industrial applications. For this purpose, we have designed some amphiphilic oligopeptides which can disperse CNTs in water. The result of dispersion experiment, pep-2 was demonstrated to effectively disperse CNTs in water comparing to other peptides. If pep-2 interacts with CNTs but not with amorphous carbons and metallic catalysts, the dispersion procedure with pep-2 can be used as a method for purification of CNTs without damaging them. In this study, a raw CNT material (MER Co., Tucson USA) containing amorphous carbons and metallic catalysts was dispersed into water and the properties of the dispersed CNTs were evaluated by scanning electron microscopy (SEM), Raman spectroscopy, thermogravimetric analysis (TGA), UV/Vis/NIR spectroscopy, and elemental analysis.

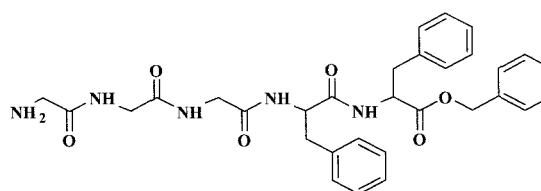
To prepare the CNT-dispersed aqueous solutions, raw CNTs (40 mg) were added to 0.1 wt% pep-2 aqueous solution (40 ml), and the mixture was sonicated in water using bath and tip-type sonicators in an ice bath. After centrifugation, the supernatant was collected to remove insoluble materials. By adding methanol, black materials came out from the supernatant, followed by washing with methanol and water to remove an excess of adsorbed peptides on the surface of CNTs. Finally, recovered CNTs were collected by lyophilization. As a result, 3.6 mg of recovered CNTs was obtained from the 40 mg of raw material.

Comparison of SEM images of the raw and recovered CNTs showed disappearance of most of the amorphous carbons that existed in the raw CNTs. This morphological observation indicates that the raw CNTs can be purified to some extent by dispersing with pep-2. It was thought that amorphous carbons were selectively removed by dispersing with pep-2. Detailed properties of the recovered CNTs estimated by Raman spectroscopy, TGA, UV/Vis/NIR spectroscopy, and elemental analysis will be discussed.

Corresponding Author : Shin Ono

E-mail : shinono@eng.u-toyama.ac.jp

Tel&Fax : +81-76-445-6845



Structure of pep-2.

## Toward Single Structure of SWNTs: Simultaneous Enrichment in $(n,m)$ and the Optical Purity of SWNTs through Extraction with Carbazole-Bridged Chiral Diporphyrin Nanotweezers

○Xiaobin Peng<sup>1</sup>, Naoki Komatsu<sup>1</sup>, Takahide Kimura<sup>1</sup>, Atsuhiro Osuka<sup>2</sup>

<sup>1</sup>Department of Chemistry, Shiga University of Medical Science, Otsu 520-2192, Japan

<sup>2</sup>Department of Chemistry, Graduate School of Science, Kyoto University, Sakyo-ku, Kyoto 606-8502, Japan

We have obtained optically active SWNTs through chiral molecular recognition of carbon nanotubes with chiral porphyrin nanotweezers.<sup>[1,2]</sup> In the studies, we found that changing the spacer in chiral nanotweezers is effective to enhance the optical activity of SWNTs. Here, we designed and synthesized 3,6-carbazole-bridged chiral diporphyrin to discriminate both  $(n,m)$  and helicity of SWNTs.

Figure 1 shows the absorption spectra of the as-received and extracted SWNTs. It shows clearly that (7,5) and (8,4)-SWNTs, having quite similar diameters, were enriched significantly after the extraction, which is also supported by Raman spectra.

As shown in Figure 2, the CD spectra of the extracted SWNTs were symmetrical, indicating that the extracted SWNTs are optically active. Only two dominant CD peaks were observed at 374 and 639 nm, which correspond to  $E_{33}$ , and  $E_{22}$  transitions of the (7,5)-SWNTs. These results indicate that one stereoisomer of (7,5)-SWNTs was preferentially extracted through the extraction with the carbazole-bridged chiral diporphyrin nanotweezers, which is significant progress towards SWNTs with single structure.

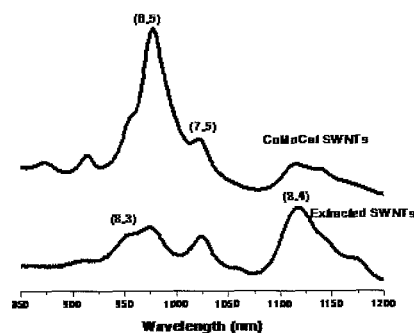


Fig. 1 Absorption spectra of as-received and extracted SWNTs dispersed in  $D_2O$ /SDBS solutions.

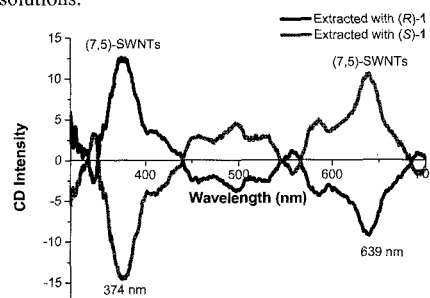


Fig. 2 CD spectra of the extracted SWNTs in  $D_2O$ /SDBS solutions

**References:** [1] X. Peng, N. Komatsu, *et al*, *Nat. Nanotechnol.* **2007**, 2, 361-365. [2] X. Peng, N. Komatsu, T. Kimura, A. Osuka, *J. Am. Chem. Soc.* **2007**, 129, 15947-15953.

**Corresponding Author:** Xiaobin Peng, **E-mail:** xiaobin@belle.shiga-med.ac.jp

**Tel:** +81-77-548-2102, **Fax:** +81-77-548-2405

## Effect of density of carbon supply on the synthesis of small diameter SWNTs by ACCVD method using platinum as catalyst

○Keisuke Urata<sup>1</sup>, Sinzo Suzuki<sup>2</sup>, Hiroshi Nagasawa<sup>3</sup>, and Yohji Achiba<sup>1</sup>

<sup>1</sup>Department of Chemistry, Tokyo Metropolitan University, Tokyo 192-0397, Japan

<sup>2</sup>Department of Physics, Kyoto Sangyo University, Kyoto 603-8555, Japan

<sup>3</sup>Nitta Haas Inc., Tokyo 104-0061, Japan,

Controlling the diameter or diameter distribution of single wall carbon nanotubes (SWNTs) is important subject for application of SWNTs. It is well known that ambient temperature, carbon source materials, and the kind of catalyst are important parameters for controlling the production of SWNTs. We have reported the synthesis of SWNTs with small diameter and narrow diameter distribution by using platinum metal as catalyst and porous glass (PG) as support material [1,2]. Platinum catalyst gives SWNTs with small diameter, and their diameter distribution changes by the density of carbon supply.

The SWNTs samples were synthesized by ACCVD method using ethanol as carbon source, and platinum catalyst was deposited on PG. In the present work, the ambient temperature and the inner pressure of ethanol were systematically changed in order to synthesize the smaller and the narrower diameter distributions of SWNTs. The obtained SWNTs were characterized by TEM, Raman spectroscopy, and fluorescence spectroscopy. Typical example of Raman spectra is shown in Fig.1. It was found that as the ethanol pressure decreases, the diameter distribution of SWNTs shifts to smaller one, especially the Raman peaks at  $311\text{cm}^{-1}$  (assigned to (6,5) tube) and  $370\text{cm}^{-1}$  (assigned to (5,4) tube) increase significantly. In the high frequency region, it was found that D-band,  $G^+$  and  $G^-$  band also systematically change, depending on the ethanol pressure. Furthermore, it was also found that relative ratio of these peaks and diameter distribution of SWNTs change by changing ambient temperature and pore size of porous glass.

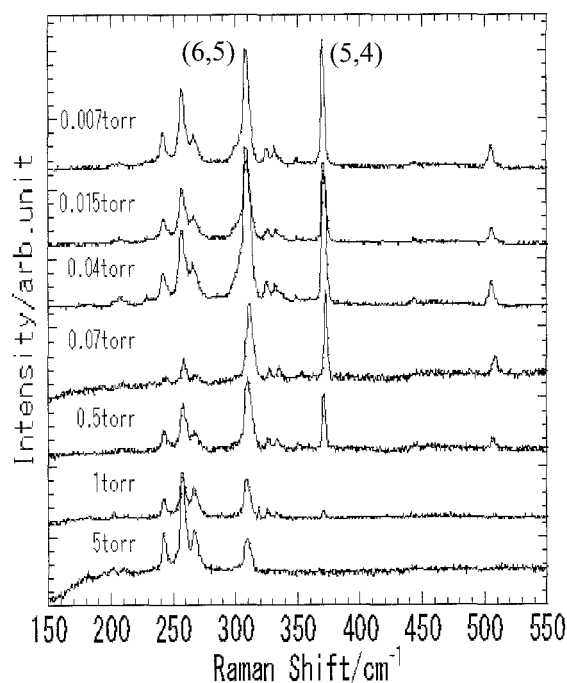


Figure.1.: Raman spectra of SWNTs synthesized at 800 °C with different pressure of ethanol (488nm excitation).

**References:**[1] Y. Aoki et al., Chem. Lett., **562**, 34(2005)

[2] K. Urata et al., The 33<sup>th</sup> Fullerene-Nanotubes General Symposium, 1P-21 (2007).

**Corresponding Author:** Yohji Achiba

**E-mail:** [achiba-yohji@c.metro-u.ac.jp](mailto:achiba-yohji@c.metro-u.ac.jp), TEL:042-677-2534

## Toward the selective production of metallic SWNT by the laser ablation method

○Yasuhiro Tsuruoka and Yohji Achiba,

*Department of Chemistry, Tokyo Metropolitan University, Tokyo 192-0397, Japan*

Selecting catalyst and ambient gas properly are well known to control diameters of SWNTs in laser ablation process. Actually, relatively small and narrow diameter distribution can be realized by laser ablation method with Rh/Pd catalyst combined by N<sub>2</sub> gas atmosphere. Furthermore, in the laser ablation experiments, we were able to make the condition such that the laser-generated plume have different temperature experience during traveling inside the furnace, and deposits somewhere in the downstream area to continue the growth of the tubes up to several  $\mu$  m. [1].

In the present work, we prepared SWNTs by combining He gas and Rh/Pd catalyst by changing the position of the laser ablation target inside a furnace as well as by collecting soot at different positions. Figure 1 shows Raman spectra of the sample obtained by collecting the soot deposited at five different places in the downstream area of the furnace. For example, the sample 1 is the soot collected at relatively upstream position in comparison with the one of the sample 5, and thus the annealing temperature for the sample 1 is reasonably thought to be higher than that of the sample 5. As shown in Fig. 1, the resulting chirality distribution of the (7,7), (8,5) and (9,3) tubes changes significantly, most probably reflecting the difference in the annealing temperature. More detailed results and discussion will be shown in the symposium.

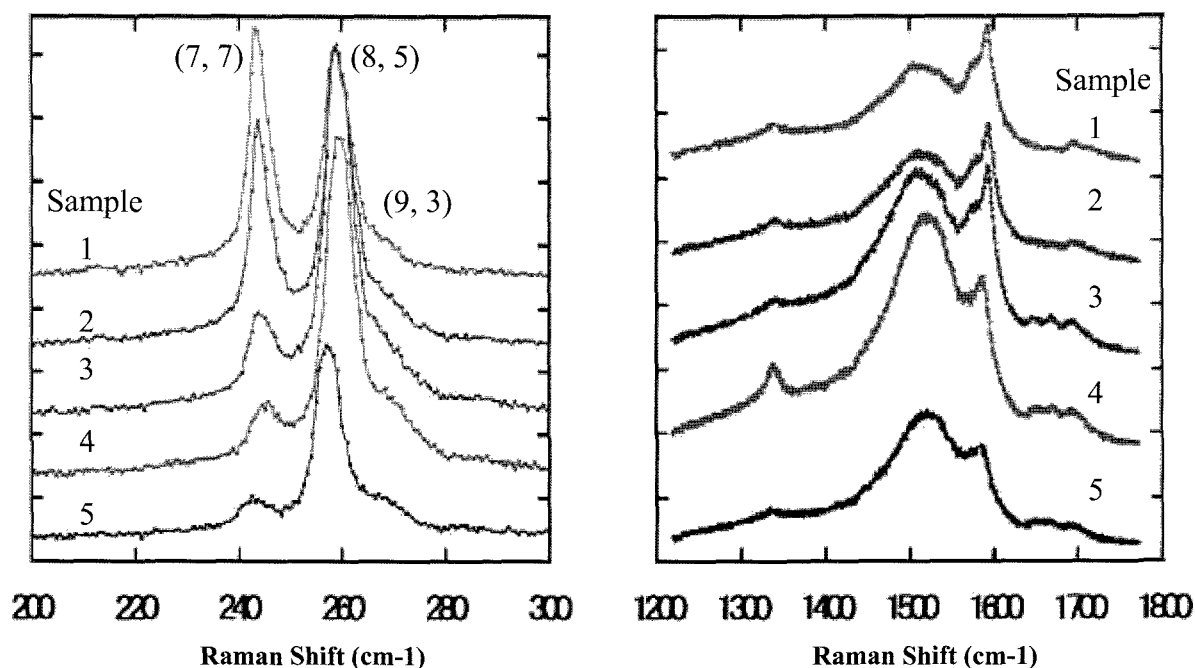


Fig. 1. Raman spectra of deposited soot at 488nm

[1] T.Nakayama et al., The 33<sup>th</sup> Fullerene-Nanotubes General Symposium, 1P-25 (2007)

Corresponding Author: Yohji Achiba

TEL: 042-667-2534, E-mail: [achiba-yohji@c.metro-u.ac.jp](mailto:achiba-yohji@c.metro-u.ac.jp)

## Synthesis of single-walled carbon nanotubes films by DC arc discharge

○Z. Li, H. Wang, S. Inoue, Y. Ando

21<sup>st</sup> COE Program "Nano Factory", Department of Materials Science & Engineering,  
Meijo University, Shiogamaguchi 1-501, Tenpaku-ku, Nagoya 468-8502, Japan

Single-walled carbon nanotubes (SWNTs) films were synthesized with various catalysts by DC arc discharge using two graphite plates fixed on the anode and cathode, respectively [1][2]. Raman spectroscopy, thermal gravimetric analysis (TGA) and scanning electron microscopy (SEM) were used to characterize quality, purity and morphology of SWNTs films. Based on results of these analyses, we have got properties-controlled films by varying catalysts, atmospheres, distance between two plates, current and evaporation time of arc discharge. As an example, when Mo and Fe used as catalyst, Ar and H<sub>2</sub> as buffer gas, a kind of semitransparent SWNTs film (Fig. 1 Macroscopic image) has been made by this method, and the net of sparse SWNTs bundles (Fig. 2 SEM image) was formed on this film. Moreover, the synthesized SWNTs films can easily be stuck on the other substrate, so that these films will be a good candidate in many applications such as composites, field emission, fuel cell and sensors.

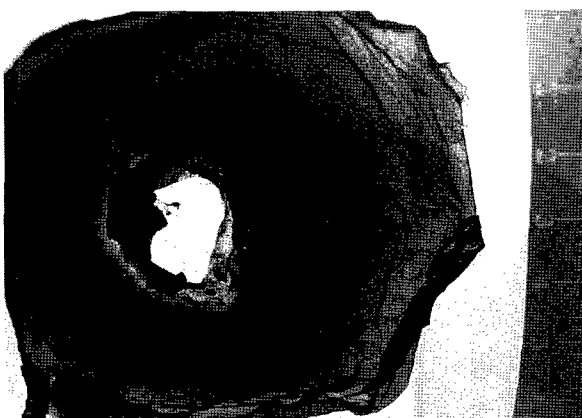


Fig. 1 Macroscopic image of SWNTs film

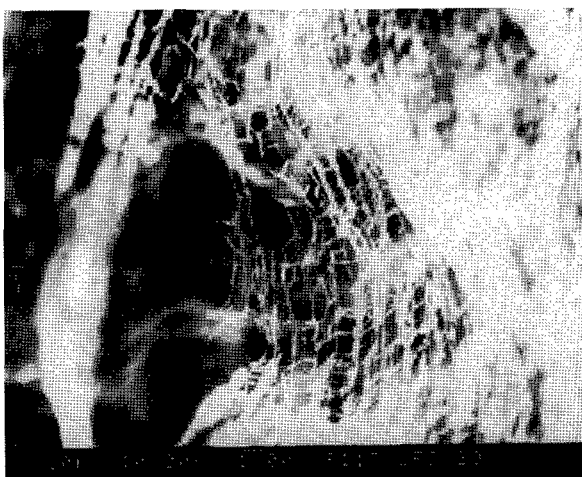


Fig. 2 SEM image of SWNTs film

References: [1] X. Zhao, S. Inoue, M. Jinno, T. Suzuki, Y. Ando, *Chem. Phys. Lett.* 373 (2003) 266.

[2] C. Journet, W.K. Maser, P. Bernier, A. Loiseau, M.L. Chapelle, S. Lefrant, P. Deniard, R. Lee, J.E. Fischer, *Nature* 388 (1997) 756.

Corresponding Author: Zhenhua Li

Tel:+81-52-838-2409, Fax:+81-52-832-1170

E-mail: zhhli@ccmfs.meijo-u.ac.jp

### **Nitrogen and oxygen plasma functionalization of carbon nanotubes for photovoltaic device application**

○Golap Kalita <sup>a,\*</sup>, Sudip Adhikari <sup>a</sup>, Hare Ram Aryal <sup>a</sup>, Rakesh Afre <sup>b</sup>, Tetsuo Soga <sup>b</sup>,  
Maheshwar Sharon <sup>c</sup>, Masayoshi Umeno <sup>a</sup>

<sup>a</sup> *Department of Electrical and Electronics Engineering, Chubu University, 1200 Matsumoto-cho,  
Kasugai-shi 487-8501, Japan*

<sup>b</sup> *Department of Environmental Technology and Urban planning, Nagoya Institute of Technology, Nagoya  
4668555, Japan*

<sup>c</sup> *Nanotechnology Research Center, Birla College, Kalyan- 421304, India.*

#### **Abstract**

Surface wave assisted microwave (SW-MW) plasma was used for surface modification of multiwalled carbon nanotubes (MWCNTs). CNTs were treated with nitrogen and oxygen microwave plasma in order to functionalize covalently their side walls. X-ray photoelectron spectroscopy (XPS) study shows surface modification with nitrogen and oxygen containing different functional groups. Transmission electron microscope (TEM) study shows induced defect in the side walls of nanotubes, without destruction of multi layer structure of the CNTs. Functionalized CNTs shows very good dispersion in organic solvent. Functionalized CNTs were incorporated in organic heterojunction photovoltaic device and enhancement in device performance was observed. Details study of CNTs functionalization via SW-MW plasma will be discussed.

#### **References**

- [1] J. Chen, M. A. Hamon, H. Hu, Y. Chen, A. M. Rao, P.C. Eklund and R. C. Haddon, *Science* 282 (1998) 95.
- [2] M. Zhang, L. Su and L.Mao, *Carbon* 44 (2006) 276–283.
- [3] A. Felten, C. Bittencourt, J.J. Pireaux, G.V. Lier, J.C. Chalier, *J. Appl. Phys.* 98 (2005) 074308.
- [4] B. Pradhan, S. K. Batabyal and A.J. Pal, *Appl. Phys. Lett.* 88 (2006) 093106.

#### **Corresponding Author**

Golap Kalita

E-mail golapkalita@yahoo.co.in

Phone No. : +81-568-51-1111 Fax No. : +81-568-51-1478



## Formation of nano pn junction diode via alkali-halogen plasma ion irradiation

○ J. Shishido<sup>1</sup>, T. Kato<sup>1</sup>, W. Oohara<sup>1</sup>, R. Hatakeyama<sup>1</sup>, and K. Tohji<sup>2</sup>

<sup>1</sup>Department of Electronic Engineering, Tohoku University, Sendai 980-8579, Japan

<sup>2</sup>Graduate School of Environmental Studies, Tohoku University, Sendai 980-8579, Japan

Single-Walled carbon nanotubes (SWNTs) have a strong potential in fabricating novel nano electronic devices in combination with other foreign molecules and atoms, owing to their unique one-dimensional structure and electronic properties. Up to now, our group has demonstrated electrical features of SWNTs can drastically be modified by alkali-metal encapsulation, and hence air-stable n-type semiconducting behavior can be realized [1]. This result motivates us to develop a nano-pn junction diode by encapsulating both electron donor and acceptor in a same individual SWNT. According to the measurement of transport properties of ion-irradiated SWNTs, it is found that halogen atoms filled in SWNTs play a role as an electron acceptor, and extremely enhance p-type characteristics. Furthermore, when both alkali (Cs) and halogen (I) atoms are encapsulated in SWNT, a diode-like electrical property can be observed. In addition to this diode like behavior, an interesting characteristic is also observed for Cs/I encapsulated SWNTs as shown in Fig. 1(a). This characteristic is known as a unique character of the p-n junction structure [2]. Furthermore, negative differential resistance (NDR) properties are also observed at a low temperature condition (Fig. 1(b)). These results indicate that the p-n junctions in SWNTs tend to be created by means of selective doping of electron donors and acceptors with the advanced plasma technology.

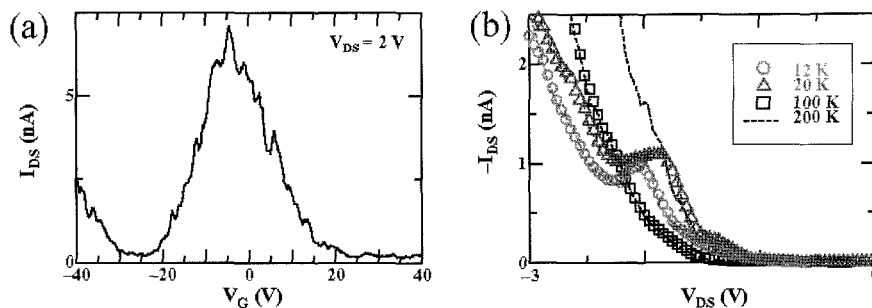


Fig.1 Source-drain current ( $I_{DS}$ ) vs gate voltage ( $V_G$ ) characteristic (a) and NDR properties (b) of Cs/I filled SWNTs under the FET configuration.

[1] T. Izumida et al., Appl. Phys. Lett. **89**, 093121 (2006) .

[2] C. Zhou et al., Science **290**, 1552 (2000).

Corresponding: J. Shishido, [shishido@plasma.ecei.tohoku.ac.jp](mailto:shishido@plasma.ecei.tohoku.ac.jp),

TEL: +81-22-795-7046, FAX: +81-22-263-9225

## Novel Carbon Nanotubes/Photopolymer Nanocomposites with High Conductivity and Application to Nanoimprint Photolithography

○Tsuyohiko Fujigaya, Takahiro Fukumaru, and Naotoshi Nakashima

Department of Applied Chemistry, Graduate School of Engineering, Kyushu University,  
744 Motoooka, Nishi-ku, Fukuoka 819-0395, Japan

### Abstract:

We fabricated the composites of SWNTs and UV-curable monomer **1** (Figure 1) by in situ photopolymerization and

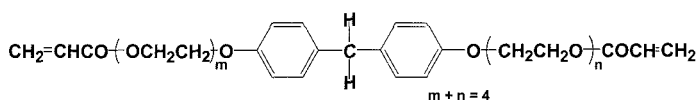


Figure 1. Chemical structure of monomer **1**

found that composite films exhibit extremely high electrical conductivity and low percolation threshold compared to other SWNT/polymer composite. We considered that this results were the consequence of the stable dispersion of SWNT by monomer **1**. The degree of dispersion of SWNT in the film was estimated by UV-near IR absorption spectroscopy and transmission electron microscopy (TEM) technique and found that the SWNT was dispersed homogeneously in the film. Nice 2D patterns of composites are successfully fabricated by using nanoimprint lithography (Figure 2) [1]. The results

clearly indicate the high processability of the composite. Conceptually, the combination of SWNTs and UV cure monomer can be applied in a wide range of lithographic techniques such as ink jet printing and laser stereolithography. The same procedure might be also applicable for the multi-walled carbon nanotubes.

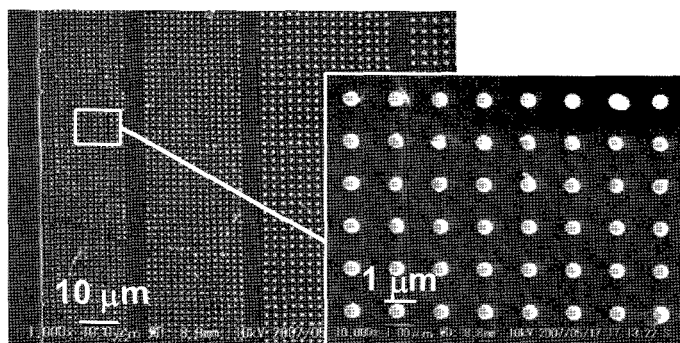


Figure 2. SEM images of nanoimprint patterns fabricated by PDMS stamps.

**References:**[1]T. Fujigaya, S. Haraguchi, T. Fukumaru, N. Nakashima., *Adv. Mater.*, in press.

**Corresponding Author** Naotoshi Nakashima

**E-mail** nakashima-tcm@mbox.nc.kyushu-u.ac.jp

**Tel&Fax** +81-92-802-2840

### Increase of surface area of super-growth single-walled carbon nanotubes via opening, resulting in improved electrochemical capacitance

○Ali Izadi-Najafabadi<sup>1,3</sup>, Kenji Hata<sup>1</sup>, Tatsuki Hiraoka<sup>1</sup>, Takeo Yamada<sup>1</sup>, Don N. Futaba<sup>1</sup>, Satoshi Yasuda<sup>1</sup>, Osamu Tanaike<sup>2</sup>, Hiroaki Hatori<sup>2</sup>, Motoo Yumura<sup>1</sup> and Sumio Iijima<sup>1,3</sup>

<sup>1</sup>*Research Center for Advanced Carbon Materials, National Institute of Advanced Industrial Science and Technology (AIST), Tsukuba 305-8565, Japan*

<sup>2</sup>*Energy Technology Research Institute, National Institute of Advanced Industrial Science and Technology (AIST), Tsukuba 305-8569, Japan*

<sup>3</sup>*21<sup>st</sup> Century COE, Nano-factory, Department of Material Science and Engineering, Meijo University, Nagoya 468-8502, Japan*

High specific surface area (SSA) materials are of huge importance given that all reactions in solid phase take place at the surface. Having a theoretical maximum SSA of 1315 m<sup>2</sup>/g, as-grown single-walled carbon nanotubes (outer surface only) are often overlooked when compared to high SSA materials such as activated carbon having an SSA of 2000 m<sup>2</sup>/g. However theoretically the surface area of SWNTs can be doubled by utilizing the internal area of the tubes.

Here utilizing the highest SSA as-grown SWNT forests (1299 m<sup>2</sup>/g) [1, 2], an opening process, capable of almost doubling the SSA is presented. The opened SWNT forests are then utilized as electrode materials for electrochemical capacitors. Their capacitance performance is enhanced on the same order of magnitude as the increase in SSA.

[1] K. Hata, D. N. Futaba, K. Mizuno, T. Namai, M. Yumura and S. Iijima, *Science*, **306**, 1362 (2004)

[2] D. N. Futaba, K. Hata, T. Yamada, T. Hiraoka, Y. Hayamizu, Y. Kakudate, O. Yanaike, H. Hatori, M. Yumura and S. Iijima, *Nat. Mater.*, **5** (12), 987 (2006)

Corresponding Author: Kenji Hata

TEL: +81-298-861-6763, FAX: +81-298-61-4654, E-mail: [kenji-hata@aist.go.jp](mailto:kenji-hata@aist.go.jp)

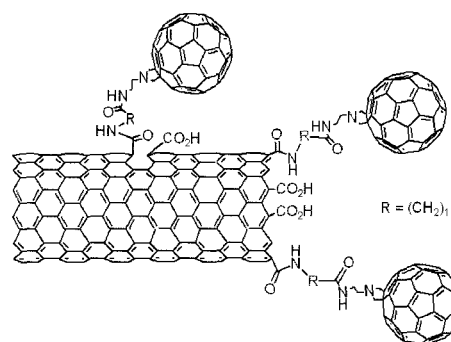
## Photovoltaic cell made of single wall carbon nanotubes and fullerenes

○Tatsunori Kuramoto, Toru Arai, Shingo Nobukuni, Yoshikazu Shimote, Tetsuji Moriguchi

*Department of Applied Chemistry, Faculty of Engineering,  
Kyushu Institute of Technology, Kitakyushu 804-8550, Japan*

Carbon nanotubes and fullerenes have been applied to photo devices[1-3]. In this study, we synthesized the functionalized single wall carbon nanotubes (SWNT-[C<sub>60</sub>]<sub>n</sub>) which were covalently linked to fullerenes with linkers.

SWNT-[C<sub>60</sub>]<sub>n</sub> were deposited on a ITO glass by the electrodeposition method in which Kamat et al. reported the deposition of the SWNTs[4]. That is, SWNT-[C<sub>60</sub>]<sub>n</sub> were suspended in THF with the aid of tetraoctylammonium bromide and were deposited (Fig.1).



Using the SWNT-[C<sub>60</sub>]<sub>n</sub> film on ITO as working electrode, counter electrode was Pt plate or Pt coated ITO, and an acetonitrile solution of 0.05 M iodine / 0.5 M sodium iodine was applied as the electrolyte. SWNT-[C<sub>60</sub>]<sub>n</sub> were excited with Xe light. Fig.2 shows the photoresponse of SWNT-[C<sub>60</sub>]<sub>n</sub> film in a photoelectrochemical cell. These results indicate the successful injection of electrons from the excited SWNT-[C<sub>60</sub>]<sub>n</sub> to the ITO electrode.

The photocurrent density-voltage characteristics were measured with a sandwich cell (5 x 5 mm, data not shown). The observed photocurrent density was very low (for instance, ~3.1 μA/cm<sup>2</sup>). We will present the photocurrent density-voltage profiles and the reaction mechanisms.

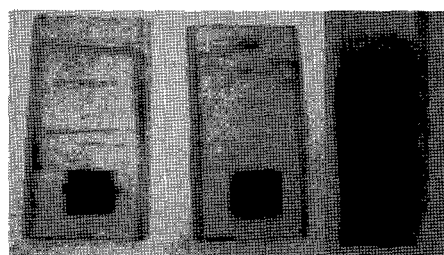


Fig.1. SWNT-[C<sub>60</sub>]<sub>n</sub> were deposited on ITO glasses by electrodeposition.

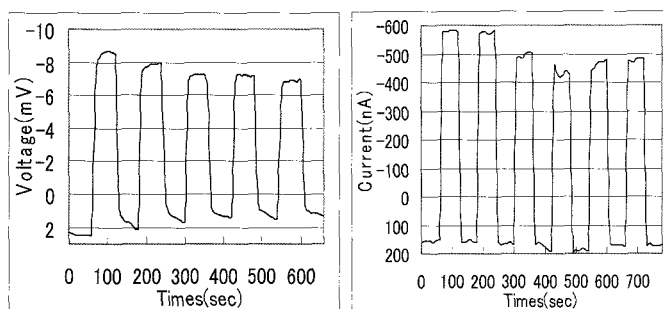


Fig.2. Photovoltage(left) and photocurrent(right) on-off cycles of SWNT-[C<sub>60</sub>]<sub>n</sub>. It is excited with Xe light. The counter electrode is Pt plate, and the electrolyte is 0.05 M I<sub>2</sub>/0.5 M NaI in acetonitrile.

[1] S. Barazzouk, S. Hotchandani, K. Vinodgopal, and P. V. Kamat, *J. Phys. Chem. B* **2004**, 108, 17015.

[2] T. Umeyama, M. Fujita, N. Tezuka, Naoki. Kadota, Y. Matano, K. Yoshida, S. Isoda, and H. Imahori, *J. Phys. Chem. C* **2007**, 111, 11484.

[3] T. Hasobe, S. Fukuzumi, and P. V. Kamat, *J. Phys. Chem. B* **2006**, 110, 25477.

[4] P. V. Kamat, K. G. Thomas, S. Barazzouk, G. Girishkumar, K. Vinodgopal, and D. Meisel, *J. Am. Chem. Soc.* **2004**, 126, 10757.

Corresponding Author: Toru Arai, Tel&Fax: +81-93-884-3303, E-mail: arai@che.kyutech.ac.jp

## Precise Optical Detection of Mechanical Vibration of Cantilevered Carbon Nanotubes in Air

○Shun Fukami<sup>1</sup> and Seiji Akita<sup>1,2</sup>

<sup>1</sup>*Department of Physics and Electronics, Graduate School of Engineering, Osaka Prefecture University, 1-1 Gakuen-cho, Naka-ku, Sakai, Osaka 599-8531, Japan.*

<sup>2</sup>*CREST, Japan Science and Technology Agency*

Mechanical vibration of cantilevered carbon nanotubes (CNT) enables highly sensitive mass measurement with high sensitivity of  $10^{-21}$  g order in a vacuum. In order to apply this method to biological samples, the measurements in air and in liquid are needed. In this study, we have demonstrated the optical detection of mechanical vibration of cantilevered carbon nanotubes in air.

A cantilevered multiwalled carbon nanotube (MWNT) array on the knife-edge was prepared by electrophoresis method. The MWNTs used here were synthesized by CVD and were about 50 nm in diameter. A nanotube array was set on a stage with a piezo device and was then oscillated mechanically by applying an AC voltage to the piezo device. The nanotube cantilever was irradiated by a laser beam with the wavelength of 532 nm under the condition of dark-field illumination. Scattered light by a certain MWNT was collected to a single mode optical fiber with a core diameter of 3.3  $\mu\text{m}$ , which act as an aperture, by using an optical microscope as schematically shown in Fig. 1. At the resonant frequency, the signal becomes minimal because the nanotube cantilever vibration and the vibration amplitude are related to the signal intensity.

Figures 2(a) and 2(b) show, respectively, optical microscope images of the off-resonant and resonant MWNT with the length of 10  $\mu\text{m}$ . Figure 2(c) shows an SEM image of the MWNT. As shown in Figs. 2(a) and 2(b), the vibration of the MWNT is hardly detected from the original optical images. On the other hand, as shown in Fig. 3, the oscillation frequency dependence of the signal intensity is clearly detected by using the detection system used in this experiment. The resonant frequency of the MWNT is  $\sim 151$  kHz and Q factor calculated from the frequency dependence is about 113. Thus, we have successfully detected the vibration of nanotube cantilever in air using the optical detection system.

**Corresponding Author:** Seiji Akita,  
E-mail: akita@pe.osakafu-u.ac.jp, Tel&Fax: 072-254-9265

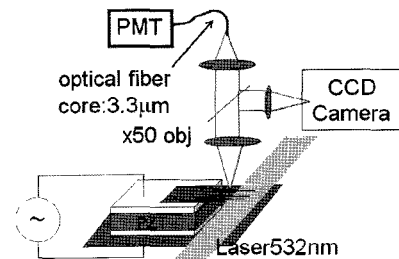


Fig.1 Schematic diagram of the optical detection system.

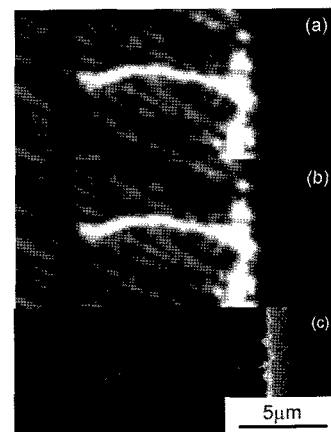


Fig.2 Optical and SEM images of the MWNT cantilever: (a) off-resonance, (b) resonance, and (c) SEM image.

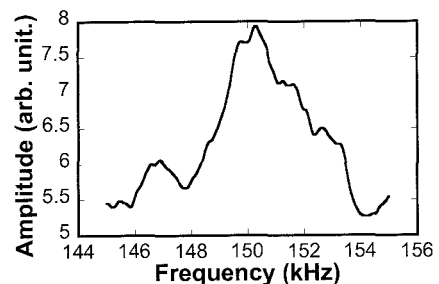


Fig. 3 Frequency-amplitude curve.

### Density increase of well-dispersed single-walled carbon nanotubes by laser trapping

Thomas Rodgers <sup>o</sup>, Satoru Shoji, & Satoshi Kawata

*LaSIE, Department of Applied Physics, Graduate School of Engineering, Osaka University, 2-1 Yamadaoka, Suita, Osaka 565-0871*

Aggregation of individual single walled carbon nanotubes (SWCNTs) in highly focussed laser light was observed by Raman scattering[1]. Nanotubes produced by the high pressure carbon monoxide (HiPCO) method were dispersed in an aqueous surfactant solution by sonication, and ultracentrifugation was used to ensure a high ratio of individual, debundled SWCNTs. Laser light of 633nm was focused through a high numerical aperture ( $NA = 1.35$ ) lens to achieve the high optical field gradient required for optical trapping and aggregation[2]. We observe the dynamics of the radial breathing mode (RBM) Raman scattering signal from the confocal volume of the optical trap, and show that there are distinct fluctuations in the RBM amplitudes. These correspond to transient but significant density increases of nanotubes in the focal volume. We discuss the independent behaviour of the observable RBMs, with respect to the wavelength of the trapping laser and the metallic/semiconducting nature of the corresponding CNTs. This experimental technique has great potential in the application to post-production processing of carbon nanotubes, such as substrate patterning[3] and chirality purification[4], due to its minimal reliance on the chemical modification of SWCNTs[5].

- [1] H. Lopez et al *In-situ Raman Spectroscopy of Optically Trapped Single-Walled Carbon Nanotubes* for the MAR05 Meeting of The American Physical Society (abstract), 2005
- [2] K. Svoboda and S. Block *Optical trapping of metallic Rayleigh particles* Optics Letters Vol. 19 No. 13, 1994
- [3] J. Zhang et al *Multidimensional manipulation of carbon nanotube bundles with optical tweezers*, Applied Physics Letters **88** 053123 (2006)
- [4] S. Tan et al *Optical Trapping of Single Walled Carbon Nanotubes* Nano Letters Vol 4, No 8 2004
- [5] J. Plewa et al *Processing Carbon Nanotubes with Optical Tweezers*, Optics Express **12** 1978, 2004

**Correspondence should be addressed to:**

**Thomas Rodgers**

**thomas@ap.eng.osaka-u.ac.jp**

**Tel/Fax: 06 6879 7846**

### Effects of Microwave Radiation on Heat-resistant Proteins Adsorbed on Carbon Nanotubes

○Hirokazu Horiguchi and Masahito Sano

*Department of Polymer Science and Engineering, Yamagata University 992-8510, Japan*

Carbon nanotubes (CNTs) are heated efficiently by microwave radiation. We have shown that this high heating capability of microwave radiation is quite useful for CNT chemistry. For instance, transitional oil bath heating of the CNT reaction mixture during an amidation reaction gave the maximum yield of 50 % after one week refluxing. Microwave heating of the same mixture increased the yield to nearly 100 % within 30 min irradiation [1]. Also, microwave heating of CNTs has a property that CNTs are heated much faster than the surrounding medium even in solution or bulk. Thus, Pt-salt was reduced only at the surfaces of CNTs to afford Pt-nanoparticles [2] and elastic response was improved in CNT/polymer composites by local melting of polymer on CNT surfaces [3].

In everyday life, we are constantly irradiated by microwave radiation. A cellular phone communicates using nearly 1 W microwave power with a local station which radiates about 30 W. Most IC chips in electronic devices operate at microwave frequencies also. Considering the high efficiency of microwave heating, these situations raise a question of what happens if the substances interacting with CNTs are bio-related. Recently, CNTs are actively studied for medical applications such as DDS, cell scaffolds and artificial joints. Other than those cases that CNTs are intentionally incorporated into bodies, they can be inhaled accidentally during ordinary handling. Thus, it is of great importance to know what level of microwave radiation affects living bodies with CNTs inside.

We have reported that, a red blood cell protein, hemoglobin (Hb) adsorbs specifically on CNTs [4]. As a primary study, the effect of microwave was investigated on Hb/CNT system. We have found that denaturation is clearly enhanced by 5 W power for 25 sec irradiation with the presence of CNTs. In this case, the average temperature of the mixture was about 40 °C and this means that water temperature near CNTs might be still higher. Because Hb denatures easily by heat, this estimate may contain those Hbs that are denatured by heated water rather than CNTs. To see the effect of CNT more directly, a mitochondrial protein, cytochrome-c (Cyt-c) was investigated in this study. Cyt-c is stable against heat and has a reversible folding/unfolding transition at 67 °C. Similar to Hb, Cyt-c possesses heme group that can be used to follow its state by spectroscopy. We show that it takes more microwave power to affect Cyt-c/CNT than Hb/CNT, although their difference is small. The spectra of radiated Cyt-c/CNT indicate that irreversible changes have occurred on Cyt-c upon irradiation, which suggest that the first order structure may be destroyed. The study shows that a local phone station may be hazardous for living bodies with CNTs inside.

[1] K. Kubota, M. Sano, T. Masuko, *Jpn. J. Appl. Phys.* **44**, 465 (2005). [2] S. Yoshida, M. Sano, *Chem. Phys. Lett.* **433**, 97-100 (2006). [3] S. Yoshida, T. Mitsumata, M. Sano, *Chem. Lett.* **35**, 262-263 (2006). [4] K. Kato, M. Sano, *Chem. Lett.* **35**, 1062-1063 (2006).

Corresponding Author: Masahito Sano

E-mail: mass@yz.yamagata-u.ac.jp

Tel&Fax: +81-238-26-3072

## Dependence on Insulator thickness for sensitivity of Carbon Nanotube Field-Effect Transistor Biosensor

Masuhiko Abe<sup>1,2</sup>, Katsuyuki Murata<sup>1,2</sup>, Tatsuaki Ataka<sup>1,2</sup>, and Kazuhiko Matsumoto<sup>2,3,4</sup>

<sup>1</sup>Olympus Corporation, Japan, <sup>2</sup>New Energy and Industrial Technology Development Organization, Japan, <sup>3</sup>National Institute of Advanced Industrial Science and Technology, Japan, <sup>4</sup>Osaka University, Japan

A carbon nanotube field-effect transistor (CNT-FET) should be able to detect living biological molecules with high sensitivity. The structure of the CNT-FET device significantly affects the performance of the sensor. In this study, we compared a sensitivity of the CNT-FET biosensors which differs the thickness of the insulator

The metal gateless type CNT-FETs were used for the biosensor (see figure 1). Antibodies were immobilized on the sensing area of the CNT-FET, and the electron charges of the antigens trapped by the antibodies were detected. Silicon nitride was used as an insulator in the sample CNT-FET. The silicon nitride layer was covered with a waterproof resist. Three kinds of CNT-FETs were

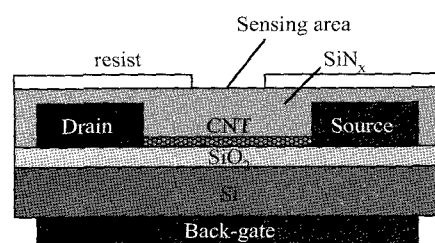


Figure 1. Metal gateless type CNT-FET.

used, which the thicknesses of the insulator were 20 nm, 50 nm, and 80 nm, respectively. Pig serum albumin (PSA) and anti pig serum albumin (a-PSA) were used for the measurement, where PSA and a-PSA are an antigen and a corresponding antibody. For the measurement, a silicone rubber wall was placed on the sensor, where a solution of Tris buffer (pH 8.0) containing PSA was poured. The dependence of the drain current on the PSA concentration was measured.

Figure 2 shows the drain current-top gate voltage curves of biosensors onto which the Tris buffer was poured. Back-gate voltage was controlled, and at a drain voltage of +1 V, a top gate voltage of +1 V, a drain current was same for three biosensors. The transconductance,  $G_m$ , became larger as the thickness of the insulator became thinner. This suggests that the CNT-FET biosensor becomes more sensitive as the thickness of the insulator becomes thinner. The results of the biosensing will be discussed at the presentation.

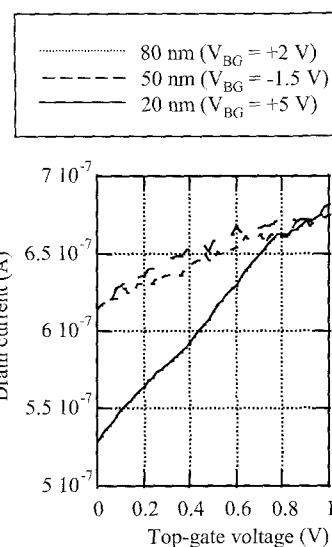


Figure 2. Drain current-Top gate voltage curves of the CNT-FET biosensors.

Corresponding Author: Masuhiko Abe

E-mail: masuhiko\_abe@ot.olympus.co.jp



### FET Properties of Exohedrally Modified SWCNTs

○Ryotaro Kumashiro<sup>1</sup>, Naoya Komatsu<sup>1</sup>, Tatsuya Saito<sup>1</sup>, Takeshi Akasaka<sup>2</sup>, Yutaka Maeda<sup>3,4</sup>,  
Nagao Kobayashi<sup>5</sup>, and Katsumi Tanigaki<sup>1</sup>

<sup>1</sup> *Department of Physics, Graduate School of Science, Tohoku University, Sendai, Japan*

<sup>2</sup> *Center for Tsukuba, Advanced Research Alliance, University of Tsukuba, Tsukuba, Japan*

<sup>3</sup> *Department of Chemistry, Tokyo Gakugei University, Tokyo, Japan*

<sup>4</sup> *PRESTO, Japan Science and Technology Agency, Saitama, Japan*

<sup>5</sup> *Department of Chemistry, Graduate School of Science, Tohoku University, Sendai, Japan*

**Abstract:** Semiconducting single-walled carbon nanotubes (SWCNTs) are promising as electronic materials for nano-scale devices in the future, and the electronic properties of SWCNTs are of significantly fundamental and practical interests. It is well known that the field effect transistors (FETs) fabricated by semiconducting SWCNTs show high performance in terms of the mobility. However, it is also known that some serious problems in CNTs-FETs exist, such as control in the carriers, atmospheric effects, and so on. Semiconducting CNTs have both holes and electrons as carrier, therefore, CNTs-FETs usually exhibit ambipolar charge transport. For applying CNTs to electronic device materials, it is necessary to control the carriers. A carrier doping could exohedrally be possible when the SWCNTs surface is chemically modified. With such chemical modifications, the charge transfer from the exohedral functional groups to SWCNTs will be expected, and this could modify the electronic states of SWCNTs. We have reported the FET properties of SWCNTs exohedrally modified by organic molecule chemisorption, and demonstrated that ambipolar character can be converted to n-type ones[1]. However, because of ununiformity of the surface modification of SWCNTs, the confirmation of charge transfer from the exohedral functional groups to SWCNTs is extremely difficult. In this study, we will report the FET properties of SWCNTs exohedrally modified by Si-containing organic molecules. We used the organic molecule-physisorbed SWCNTs to make clear the effect of exohedrally modification, and it was shown that an n-type character can be enhanced by physisorption also in a similar manner to the chemisorbed ones. We will also discuss the possibility of charge transfer by using spectroscopic methods.

[1] R. Kumashiro et al., J. Phys. Chem. Solids, in press.

**Corresponding Author:** Ryoraro Kumashiro

**E-mail:** rkuma@sspns.phys.tohoku.ac.jp

**Tel&Fax:** +81-22-795-6468 (tel), +81-22-795-6470 (fax)

## Atomic structures of graphene adatom and its aggregation

Tomofumi Hashi<sup>○</sup> and Mineo Saito

*Graduate School of Natural Science and Technology, Kanazawa University, Kakuma,  
Kanazawa 920-1192, Japan*

Graphenes as well as carbon nanotubes recently attract much attention since they are candidates for nano device materials. For achieving nano devices, control of defects is very important as in the case of silicon technology. However, understanding of even fundamental defects such as vacancies and adatoms is still insufficient. In this study, we study atomic structures and energetics of graphene adatom and its aggregation by performing first principles calculations.

The most stable site of adatom is found to be situated on the bond center of graphene sheet. The diffusion barrier is estimated to be very small (0.33 eV), which is consistent with experimental results that interstitial defects in graphite

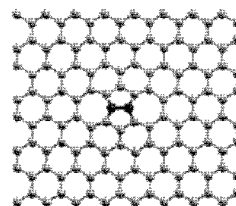


Fig 1

diffuses at temperatures lower the room temperature. As for the dimer of adatoms, two pentagons are formed, so this configuration is very stable (Fig. 1). The energy of the dissociation of the dimer into two adatoms is very large (5.5 eV), indicating that this dimer is very stable. Therefore this dimer is expected to be experimentally detected under some experimental conditions. We find that a line defect in which dimers are arranged in a straight line is found to be more stable than the isolated dimer. This line defect in carbon nanotube are found to be ferromagnetic and is thus useful[1]. To clarify whether this line defect is spontaneously formed by aggregation of adatoms as a result of diffusion of adatoms, we determine stable atomic structures of tetramers. The two dimers arranged in a straight line is very stable but we find that another structure of the tetramer is more stable. Therefore we conclude that the line defect is not formed by thermal diffusion, thus another approach is necessary to form the line defect.

[1] S. Okada et al., Phys. Rev. B 74, 121412(R) (2006).

Mineo Saito

E-mail: m-saito@cphys.s.kanazawa-u.ac.jp Tel&Fax:0298-76-3815

### Environmental effect on excitons of single wall carbon nanotubes

○Kentaro Sato,<sup>1</sup> Riichiro Saito,<sup>1</sup> Jie Jiang,<sup>2</sup> Gene Dresselhaus,<sup>3</sup> Mildred S. Dresselhaus<sup>4</sup>

<sup>1</sup>*Department of Physics, Tohoku Univ. and CREST JST, Sendai, 980-8578*

<sup>2</sup>*Department of Physics, NC State Univ., Raleigh, North Carolina 27695-7518, USA*

<sup>3</sup>*Francis Bitter Magnet Laboratory, Massachusetts Institute of Technology, Cambridge, Massachusetts 02139-4307, USA*

<sup>4</sup>*Department of Physics, Massachusetts Institute of Technology, Cambridge, Massachusetts 02139-4307, USA*

In this paper, we show the diameter dependence of the dielectric constant of single wall carbon nanotubes (SWNTs). The optical transition energies of SWNTs are calculated by solving the Bethe-Salpeter equation in which the one particle energies are given by the extended tight-binding method [1]. As for the surrounding materials of a SWNT, we express the environmental effect on the exciton binding energy by a dielectric constant. In previous paper we used the static dielectric constant (the value is 2.22) in the calculation to reproduce the experimental values of the Raman  $E_{ii}$  or photoluminescence  $E_{ii}$  for SWNT bundle samples [1,2]. For other samples, we need to consider a correction to the environmental effects. To reproduce and evaluate the experimental results, we use the dielectric constant as a linear combination of the screening of nanotubes itself and the surrounding material [3] and adjust the value of dielectric constant. From our calculation the dielectric constant is a function of the diameter and  $E_{ii}$  of SWNT. The calculated results are compared with several experimental results. We also discuss the dependence of the exciton size of the dielectric constant and the diameter of SWNT.

#### References:

- [1] J. Jiang et al., Phys. Rev. B 75, 035407 (2007).
- [2] K. Sato et al., Phys. Rev. B 76, 195446 (2007).
- [3] Y. Miyauchi et al., Chem. Phys. Lett. 442, 394 (2007).

**Corresponding Author: Kentaro Sato**

**E-mail [kentaro@flex.phys.tohoku.ac.jp](mailto:kentaro@flex.phys.tohoku.ac.jp)**

**Tel +81-22-795-6475**

**FAX +81-22-795-6447**

## Spectroscopically probed doping processes in semiconducting single-wall carbon nanotubes selectively isolated using polyfluorene

○Nobutsugu Minami<sup>1</sup>, Yoshisuke Futami<sup>1</sup>, Said Kazaoui<sup>2</sup>

<sup>1</sup>Nanotechnology Research Institute, AIST Central 5, Tsukuba, 305-8565, Japan

<sup>2</sup>Research Center for Advanced Carbon Materials, AIST Central 5, Tsukuba 305-8565, Japan

Absorption (Abs) and photoluminescence (PL) spectroscopy have become indispensable means to probe electronic states of single-wall carbon nanotubes (SWNTs). These spectra, however, have been obscured by a large number of poorly resolved peaks and the considerable background signal even after dispersion using various dispersants, hampering detailed spectral analysis. Very recently, it is shown that the use of polyfluorene (PFO) as a dispersant dissolved in toluene results in the selective isolation and extraction of semiconducting SWNTs (s-SWNTs), leaving very little trace of metallic SWNTs [1, 2]. Remarkably, only s-SWNTs with large chiral angles (near-armchair tubes) are selectively isolated. Moreover, the absorption background supposedly ascribed to carbonaceous impurities and/or  $\pi$ -plasmon has been considerably suppressed. Thus simplified spectral shape has expanded the applicability of optical spectroscopy for the study of various phenomena involving a change in electronic states of SWNTs. Here we report preliminary results of spectroscopic monitoring of doping processes in selectively isolated s-SWNT.

Figures 1 and 2, respectively, show changes in Abs and PL spectra induce by the addition of tetrafluorotetracyanoquinodimethane (TCNQF<sub>4</sub>), a p-dopant, into a HiPco/PFO/toluene solution. It is remarkable that isosbestic points are clearly observed with the increase in TCNQF<sub>4</sub> concentration. The decrease in PL induced by doping is much larger than that in Abs, implying that the underlying mechanisms are different. These and other implications of the observed spectral changes will be discussed in the presentation.

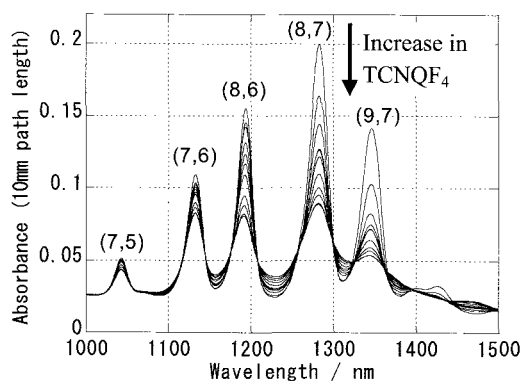


Fig.1 Change in Abs spectra of a HiPco/PFO/toluene solution with an increase in TCNQF<sub>4</sub> concentration from 0 to 150 $\mu$ g/mL.

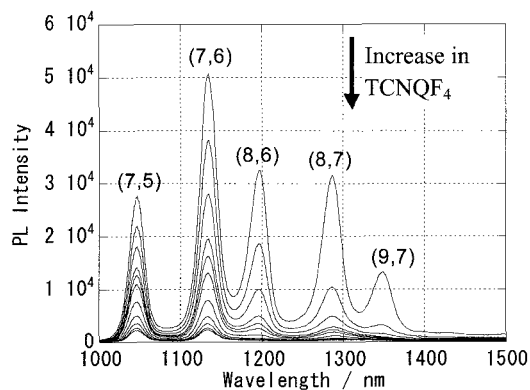


Fig.2 Change in PL spectra of a HiPco/PFO/toluene solution with an increase in TCNQF<sub>4</sub> concentration from 0 to 150 $\mu$ g/mL.  $\lambda_{\text{ex}} = 660\text{nm}$ .

[1] Nish et al., Nature Nanotechnology 2, 640 (2007).

[2] Chen et al., Nano Lett. 7, 3013 (2007).

Corresponding Author: Nobutsugu Minami

TEL: +81-29-861-9385, FAX: +81-29-861-6309, E-mail: [n.minami@aist.go.jp](mailto:n.minami@aist.go.jp)

## Response of Carbon Nanotube Field Effect Transistors to Vibrating Gate Using Scanning Gate Microscopy

○Kosuke Hata<sup>1</sup>, Yoshikazu Nakayama<sup>2,3</sup> and Seiji Akita<sup>1,3</sup>

<sup>1</sup>*Department of Physics and Electronics, Graduate School of Engineering, Osaka Prefecture University, 1-1 Gakuen-cho, Naka-ku, Sakai, Osaka 599-8531, Japan.*

<sup>2</sup>*Department of Mechanical Engineering, Graduate School of Engineering, Osaka University, 2-1 Yamadaoka, Suita, Osaka 565-0871, Japan*

<sup>3</sup>*CREST, Japan Science and Technology Agency*

Combination of carbon nanotube field effect transistor (CNT-FET) sensors and nano-electromechanical systems is expected to be a novel functional force sensing device. Scanning gate microscopy (SGM) is a powerful technique for measuring local electronic properties of these devices because applied voltage cantilever tip acts as a nanoscale local gate. In this report, we have investigated the response of CNT-FET to vibrating gate using a SGM local gate.

We fabricated CNT-FET through conventional photolithography process. The SWNTs were synthesized by low pressure alcohol chemical vapor deposition (ALCVD) method. We performed SGM measurement with non-contact mode at room temperature in air. Lock in amplifier was used here to detect the modulated current signal induced by the cantilever vibration with the amplitude less than 50 nm and the resonant frequency of ~70 kHz (Fig. 1). Topographic image and modulated current image were taken simultaneously.

Figure 2(a) and 2(b) show the topographic and modulated current image induced by the gate vibration with the gate voltage of -1 V, where top and bottom of the images correspond to the source and drain electrodes, respectively. Under this condition, the deep modulation with 2nA was achieved near the source electrodes. This is due to the modulation of the Schottky barrier induced by the gated cantilever vibration. On the contrary, in the cases of the gate voltages of 0 and 1 V, we could not observe clear modulated current images.

In this way, we have succeeded in the detection of the cantilever vibration with the amplitude less than 50 nm and the frequency of 70 kHz using the CNT-FET.

Acknowledgement: We would like to thank Prof. Matsumoto's group in Osaka Univ. for advice for fabricating CNT-FET.

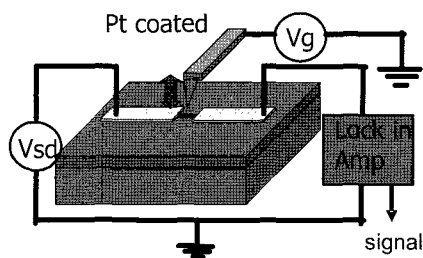


Fig.1 schematic image of circuit

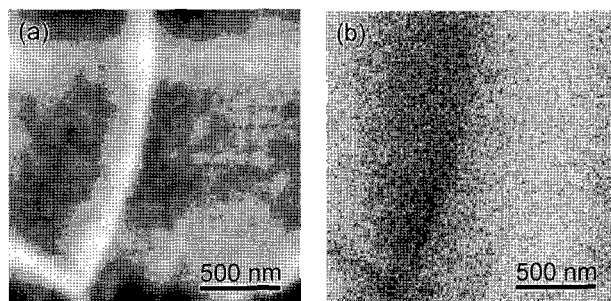


Fig.2 (a) topography and (b) modulated current image.

**Corresponding Author:** Seiji Akita,  
E-mail: akita@pe.osakafu-u.ac.jp, Tel&Fax: 072-254-9265

Third-order nonlinear optical properties and phase relaxation time in single-walled carbon nanotubes

M. Ichida<sup>1,2</sup>, Y. Kiyohara<sup>1</sup>, S. Saito<sup>3</sup>, Y. Miyata<sup>4,5</sup>, H. Kataura<sup>5</sup>, and H. Ando<sup>1,2</sup>

<sup>1</sup>Graduate school of Nature Science, Konan University

<sup>2</sup>Quantum Nano-Technology Laboratory, Konan University

<sup>3</sup>National Institute for Information and Communications Technology

<sup>4</sup>Department of Physics, Tokyo Metropolitan University

<sup>5</sup>Nanotechnology Research Institute, AIST

Phase relaxation time is one of important parameters which govern not only homogeneous line width but also coherent optical phenomena and nonlinear optical properties. In this study, we have measured third-order nonlinear optical properties and phase relaxation time of semiconducting single-walled carbon nanotubes (SWNTs) by Z-scan and two-beam degenerate four-wave mixing (DFWM) [1] methods.

SWNTs (purified HiPco and laser-ablation (LA) tubes) were dispersed in D<sub>2</sub>O with deoxycholic acid. Figure 1 shows the diameter dependence of figure of merit  $\text{Im } \chi^{(3)}/\alpha$ . The absolute value increases with increasing tube diameter for both samples. Comparing the same diameter,  $|\text{Im } \chi^{(3)}/\alpha|$  measured in HiPco sample is smaller than that in LA sample. These results suggest that the value of  $\text{Im } \chi^{(3)}/\alpha$  depends on the population ( $T_1$ ) and phase relaxation ( $T_2$ ) times. Figure 2 shows the time evolutions of DFWM signals for  $k_3$  ( $=2k_1-k_2$ ) and  $k_4$  ( $=2k_2-k_1$ ) directions, where  $k_1$  and  $k_2$  are the wave vectors of incident excitation beams. Both signals shift from  $\tau_d=0$  because of  $T_2$ . Assuming inhomogeneous broadening, the estimated  $T_2$  value is 200 fs which is a good agreement with the homogeneous width measured by single SWNT PL measurements[2].

References

- [1] T. Yajima *et al.*, J. phys. Soc. Jpn. **47**, 1620 (1979).
- [2] T. Inoue, K. Matsuda *et al.*, Phys. Rev. B **73**, 233401 (2006).

Corresponding Author: Masao Ichida, E-mail: [ichida@konan-u.ac.jp](mailto:ichida@konan-u.ac.jp) TEL&FAX: +81-78-435-2679

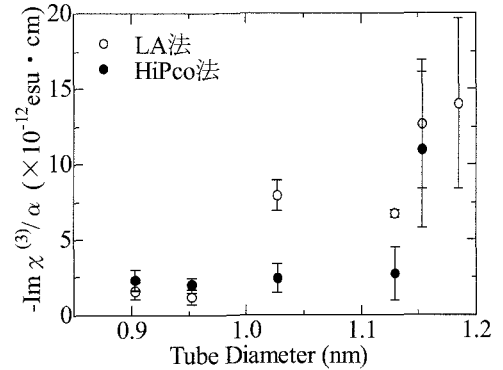


Fig.1:  $\text{Im } \chi^{(3)}/\alpha$  as a function of tube diameter for HiPco and LA samples.

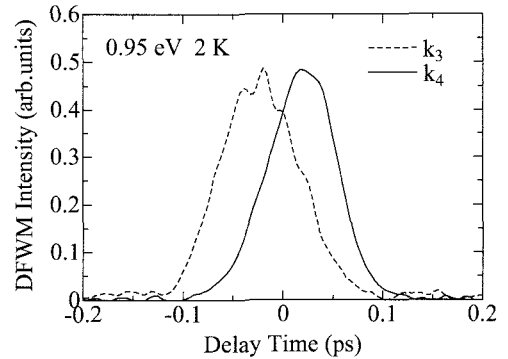


Fig.2: Time evolutions of DFWM Signals for  $k_3$  and  $k_4$  directions

## Multi-backgate control of carbon nanotube double quantum dot

Tomoyuki Mizuno<sup>1</sup>, Hideyuki Maki<sup>2</sup>, Satoru Suzuki<sup>3</sup>, Yoshihiro Kobayashi<sup>3</sup>,  
and Tetsuya Sato<sup>2</sup>

<sup>1</sup> *Department of Integrated Design Engineering, Faculty of Science and Technology,  
Keio University, Hiyoshi, Yokohama 223-8522, Japan*

<sup>2</sup> *Department of Applied Physics and Physico-Informatics, Faculty of Science and Technology,  
Keio University, Hiyoshi, Yokohama 223-8522, Japan*

<sup>3</sup> *NTT Basic Research Laboratories, Nippon Telegraph and Telephone Corporation,  
Morinosato-Wakamiya, Atsugi 243-0198, Japan*

Single walled carbon nanotubes (SWNTs) behave as a quantum dot at low temperatures because of their extremely small diameter of the order of 1 nm. SWNT double quantum dot devices have also been demonstrated [1-4]. In these reports, the devices with multi-topgate structure were fabricated. However, SWNTs in the topgate devices are surrounded by the insulator; therefore, it is difficult to position-selectively create defects, which act as the tunnel barriers, after device fabrication. In this study, we have fabricated the multi-gate device with the back gate structure, in which SWNTs are not surrounded by the insulator. The electronic transport properties of these devices are investigated at low temperature.

Figure 1 shows the schematic side view of the SWNT double quantum dot device. SWNTs were grown by chemical vapor deposition (CVD) method using ethanol on the SiO<sub>2</sub> layer and two Mo gate electrodes (G1 and G2). SWNTs are contacted with Pd electrodes. Gate voltage can be applied to the SWNT through G1, G2 and the Si substrate (BG).

Figure 2 shows experimental charge stability diagrams at 1.7 K for the series double quantum dot at the drain voltage  $V_{ds}$  of 1 mV. In this measurement, three gates (G1, G2 and BG) were used; however, the voltages of G1 and BG were the same. The “honeycomb” shaped array, which indicates the formation of the coupled quantum dots, is observed. Each cell of the honeycomb corresponds to a well-defined electron configuration for the double dot. The smeared shape of the honeycomb indicates that the two quantum dots are strongly coupled [1,4]. From the dimensions of a single cell ( $\Delta V_{g1}$  and  $\Delta V_{g2}$  as illustrated in Figure. 2), the estimated gate capacitances of  $C_{g1}$  and  $C_{g2}$  are 8.9 aF and 1.1 aF, respectively.

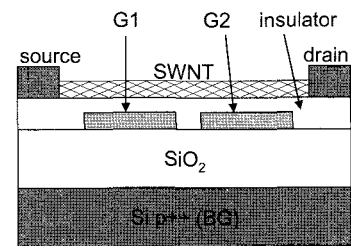


Fig. 1. Schematic view of the fabricated back-gate device with multi-gates (G1, G2 and BG).

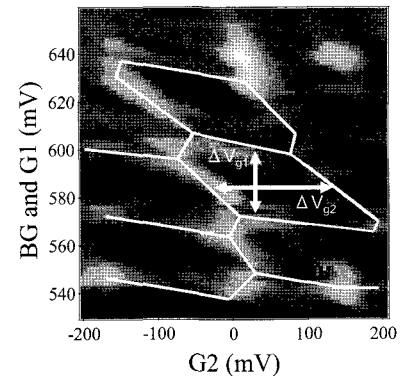


Fig. 2. Experimental charge stability diagram for the series double quantum dot as a function of gate voltages.

[1] N. Mason, M.J.Biercuk, C. M. Marcus, Science, **303**, 655, (2004).

[2] M. R. Graber, et al., Phys Rev B., **74**, 075427, (2006).

[3] H. I. Jorgensen, et al., Appl. Phys. Lett., **89**, 232113, (2006).

[4] Sami Sapmaz, et al., Nano Lett., **6**, 1350, (2006).

Corresponding Author: Hideyuki Maki

E-mail: [maki@appi.keio.ac.jp](mailto:maki@appi.keio.ac.jp), Tel: +81-45-566-1643, FAX: +81-566-1587

## Design of Si Nanotube: New Multi-shalle Nanotubes

Susumu Okada○

*Center for Computational Sciences and Graduate School of Pure & Applied Sciences,  
University of Tsukuba, Tennodai, Tsukuba 305-8577*

Ever since the discovery of nanometer scale tubes of carbon (carbon nanotubes: CNT), much effort has been done to synthesize and design the nano-scale tubular structures consisting of the other chemical elements. Indeed, similar tubular structures with hexagonal network consisting of boron and nitrogen atoms have been experimentally synthesized. The electronic structures of these tubular structures exhibit different characteristics to those in the two-dimensional honeycomb lattice due to the different dimensionality.

In the present work, we explore the possibility of tubular structures of silicon possessing the hexagonal network as in the case of CNT based on the first-principle total-energy calculations. In the case of isolated Si nanotubes (SiNT), the SiNT with cylindrical shape studied here are found to be energetically unstable. Large structural reconstruction takes place on the wall of them to reduce the dangling bond character of the Si atoms. The result is ascribed to the fact that the Si does not possess the planer structures under the usual conditions. However, by encapsulating the SiNT into the CNT, we find that the SiNT keep their cylindrical shape (Fig. 1). The encapsulation results in the energy gain of about 0.5 eV per angstrom. By analyzing the electronic band structures and charge density of the SiNT encapsulated in the CNT, we find that the substantial hybridization of  $\pi$  states of CNT and p states of SiNT and the charge transfer from SiNT to CNT stabilize the new Si-based tubular structure.

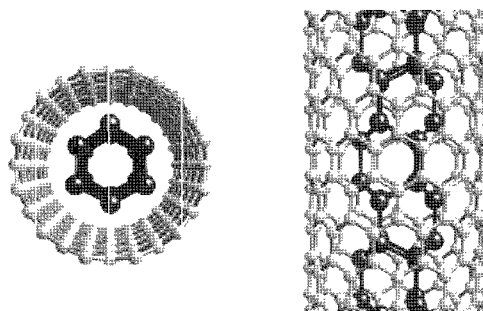


Fig.1: Top and side views of an optimized structure of SiNT@CNT.

**Corresponding Author: Susumu Okada**  
**E-mail: sokada@comas.frsc.tsukuba.ac.jp**  
**Fax: 029-83-5924**



## Influence of Diameter on the Raman Spectra of Multi-Walled Carbon Nanotubes

Hiroyuki Nii<sup>\*1</sup>, Yoshiyuki SUMIYAMA, Hamazo NAKAGAWA, and Atsuhiko KUNISHIGE

*UBE Scientific Analysis Laboratory, Inc., 1978-5 Kogushi, Ube, Yamaguchi 755-8633, Japan*

Raman spectroscopy is an analytical technique largely used to characterize carbon materials. Among them, single-walled carbon nanotubes (SWNTs) have been analyzed both theoretically and experimentally, and the relation between Raman spectra and structure of SWNTs has been well understood [1]. On the other hand, because of the difficulty of the theoretical analysis on multi-walled carbon nanotubes (MWNTs), the Raman spectroscopy of MWNTs has not been well established up to now. For this reason, Raman spectroscopy analysis of MWNTs is mainly used to estimate the crystalline quality using the D-band to G-band intensity ratio, as usually applied to graphite materials. In this study, MWNTs with various diameters produced by Shenzhen Nanotech Port Co., Ltd. have been analyzed with Raman spectroscopy to clarify the influence of diameter on the Raman Spectra of MWNTs.

Figure 1 shows the Raman spectra of MWNTs at 532 nm excitation wavelength. Because Raman peak positions of MWNTs are particularly sensitive to temperature [2], laser power was carefully controlled to minimize laser beam heating effects. Figure 2 shows the diameter dependence of G-band frequencies derived from curve fitting. For the curve fitting, we have used Lorentzian or Breit-Wigner-Fano (BWF) functions for D-band, G-band, and G'-band [3]. Data indicate that G-band frequencies increase with decreasing tube diameter in the region below 20 nm, and that they are almost constant in the region over 20 nm. It was reported that the interlayer spacing of MWNTs increased with decreasing tube diameter [4]. Thus, we believe that G-band frequencies in the region below 20 nm are affected by the interlayer spacing of MWNTs. Moreover, the behavior of G-band frequencies in the region over 20 nm can be explained with the optical penetration depth in graphite [5].

- [1] M. S. Dresselhaus, G. Dresselhaus, R. Saito, and A. Jorio: *Physics Reports* **409** (2005) 47.
- [2] F. Huang, K. Yue, P. Tan, S. Zhang, Z. Shi, X. Zhou, and Z. Gu: *J. Appl. Phys.* **84** (1998) 4022. **61** (2000) 14095.
- [3] A. C. Ferrari and J. Robertson: *Phys. Rev. B* **61** (2000) 14095.
- [4] C.-H. Kiang, M. Endo, P. M. Ajayan, G. Dresselhaus, and M. S. Dresselhaus: *Phys. Rev. Lett.* **81** (1998) 1869.
- [5] A. Gupta, G. Chen, P. Joshi, S. Tadigadapa, and P. C. Eklund: *Nano Lett.* **6** (2006) 2667.

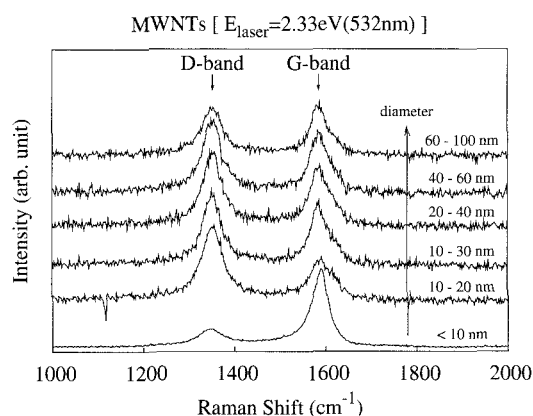


Fig. 1 Raman spectra of multi-walled carbon nanotubes.

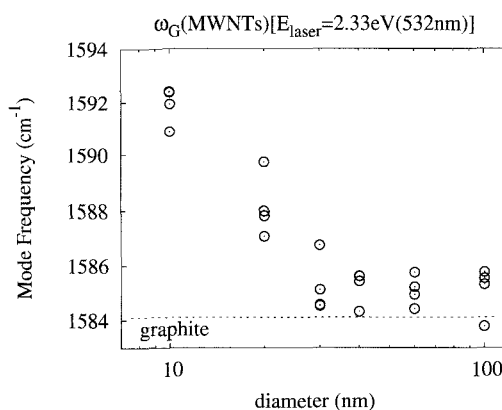


Fig. 2 Diameter dependence for G-band frequencies of multi-walled carbon nanotubes.

<sup>\*1</sup> E-mail address: hiroyuki.nii@ube-ind.co.jp

## Resonance Raman spectroscopy of metallic and semiconducting single-wall carbon nanotubes

○Yasumitsu Miyata<sup>1,2,3</sup>, Kazuhiro Yanagi<sup>2,3</sup>, Yutaka Maniwa<sup>1,3</sup>, Hiromichi Kataura<sup>2,3</sup>

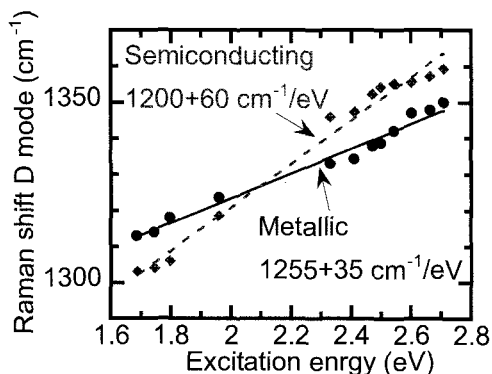
<sup>1</sup>Department of Physics, Tokyo Metropolitan University, 1-1 Minami-Osawa, Hachioji, Tokyo 192-0397, Japan

<sup>2</sup>Nanotechnology Research Institute, AIST, 1-1-1 Higashi, Tsukuba 305-8562, Japan

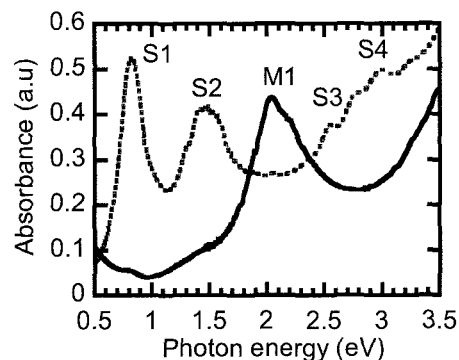
<sup>3</sup>JST-CREST, Kawaguchi 330-0012, Japan

We have measured the resonance Raman spectra of high-purity metallic and semiconducting single-wall carbon nanotubes (SWCNTs) and found a large difference in the Raman frequency of D- and G'- modes. This result strongly suggests an essential difference in the physical properties of them.

In the Raman spectra of SWCNTs, it is known that the disorder-induced mode (D mode) shifts to higher frequency with increasing the laser excitation energy. This behavior can be understood by the double resonance model which is concerning with the electronic band structure and also the phonon dispersion relation.[1,2] In this work, we have measured the D and G' modes for the metallic and the semiconducting SWCNTs varying laser energy from 1.7 to 2.7 eV. The metallic and semiconducting SWCNTs were separated using the density-gradient method [3-5]. In Fig. 1, the D mode frequency was plotted as a function of the laser energy. The slope of fitted line for the semiconducting SWCNT was  $60 \text{ cm}^{-1}/\text{eV}$  while that of the metallic SWCNTs was only  $35 \text{ cm}^{-1}/\text{eV}$ . Interestingly, the two lines are crossing at 2.1 eV that just corresponds to the  $M_{11}$  absorption peak. (See Fig. 2) Similar behaviors were also observed in the G' mode and the other high-frequency mode. We will show the detailed analysis by double resonance model and discuss the difference between metallic and semiconducting SWCNTs.



**Fig. 1.** D mode frequency of metallic and semiconducting SWCNTs plotted as a function of laser energy.



**Fig. 2.** Optical absorption spectra of thin films of metallic (solid line) and semiconducting (dashed line) SWCNTs.

**References:** [1] C. Thomsen et al., Phys. Rev. Lett., 85, 5214 (2000), [2] R. Saito et al., Phys. Rev. Lett., 88, 027401 (2002), [3] M. S. Arnold et al., Nat. Nanotechnol. 1, 60 (2006), [4] K. Yanagi et al., submitted. [5] Y. Miyata et al., J. Phys. Chem. C, accepted.

**Corresponding Author:** Hiromichi Kataura,

**E-mail:** h-kataura@aist.go.jp, **Tel:** +81-29-861-2551, **Fax:** +81-29-861-2786

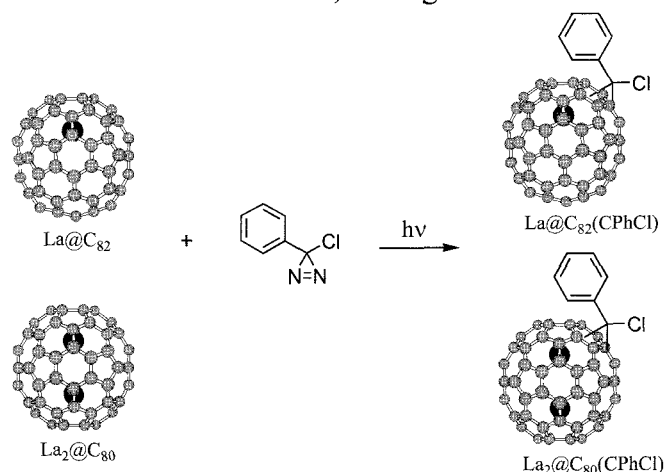
## Chemical Derivatization of La@C<sub>82</sub> and La<sub>2</sub>@C<sub>80</sub> with Phenylchlorodiazirine

○ Haruka Enoki<sup>1</sup>, Midori O. Ishitsuka<sup>1</sup>, Takahiro Tsuchiya<sup>1</sup>, Takeshi Akasaka<sup>1</sup>,  
Zdenek Slanina<sup>1</sup>, Michael T. H. Liu<sup>2</sup>, Naomi Mizorogi<sup>3</sup>, Shigeru Nagase<sup>3</sup>

<sup>1</sup> Center for Tsukuba Advanced Research Alliance, University of Tsukuba, Ibaraki 305-8577, Japan <sup>2</sup> Department of Chemistry, University of Prince Edward Island, Prince Edward Island CIA4P3A, Canada <sup>3</sup> Institute for Molecular Science, Aichi 444-8585, Japan

A chemical derivatization of endohedral metallofullerenes adds new physical and chemical properties to the corresponding metallofullerenes. The structural determination of the functionalized endohedral metallofullerenes is also an important subject, since this can provide useful information for application in material science and biochemistry. Recently, we reported that endohedral metallofullerenes react with adamantylidene carbene (Ad:) to afford the monoadducts regioselectively, La@C<sub>82</sub>(Ad)<sup>[1]</sup>, La<sub>2</sub>@C<sub>78</sub>(Ad)<sup>[2]</sup>, Sc<sub>3</sub>C<sub>2</sub>@C<sub>80</sub>(Ad)<sup>[3]</sup>. Theoretical calculation also suggests that the regioselectivity on carbene addition may be due to the charge density and the local strain of the cage carbons.

Phenylchlorodiazirine has been known to afford phenylchlorocarbene (:CPhCl) upon photoirradiation.<sup>[4]</sup> We carried for the first time the reaction of La@C<sub>82</sub> and La<sub>2</sub>@C<sub>80</sub> with that diazirine and obtained the monoadducts as phenylchlorocarbene derivative. Spectral analysis suggests that La@C<sub>82</sub>(CPhCl) may be a mixture of two inseparable diastereomers having a same addition position of carbene. Meanwhile, the regioselective addition took place to afford La<sub>2</sub>@C<sub>80</sub>(CPhCl).



**References:** [1] (a) Maeda, Y. et al. *J. Am. Chem. Soc.* **2004**, *126*, 6858-6859. (b) Matsunaga, Y. et al. *ITE Lett.* **2006**, *7*, 43-49. [2] Cao, B. et al. *J. Am. Chem. Soc.* in press. [3] Iiduka, Y. et al. *Angew. Chem. Int. Ed.* **2007**, *46*, 5562-5564. [4] *Chemistry of Diazirines*; Liu, M. T. H., Ed., Florida, 1987; Vols 1 & 2.

**Corresponding Author:** Takeshi Akasaka

**E-mail:** akasaka@tara.tsukuba.ac.jp, **Tel&Fax:** +81-29-853-6409

**[2+1] Cycloaddition of Nitrene onto [60]fullerene: Interconversion  
between an Aziridinofullerene and an Azafulleroid**

○Mitsunori Okada<sup>1</sup>, Tsukasa Nakahodo<sup>2</sup>, Hiroyuki Morita<sup>3</sup>, Toshiaki Yoshimura<sup>3</sup>, Midori O. Ishitsuka<sup>1</sup>, Takahiro Tsuchiya<sup>1</sup>, Yutaka Maeda<sup>4</sup>, Hisashi Fujihara<sup>2</sup>, Takeshi Akasaka<sup>1</sup>  
Xingfa Gao<sup>5</sup>, and Shigeru Nagase<sup>5</sup>

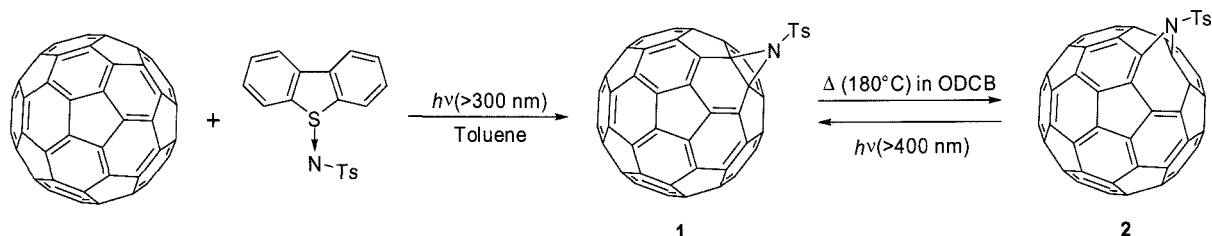
<sup>1</sup>Center for Tsukuba Advanced Research Alliance, University of Tsukuba, Tsukuba, Ibaraki 305-8577, Japan, <sup>2</sup>Department of Applied Chemistry, Kinki University, Kowakae, Higashi-Osaka, Osaka 577-8502, Japan, <sup>3</sup>Department of Applied Chemistry, Graduate School of Science and Engineering University of Toyama, Gofuku, Toyama 930-8555, Japan

<sup>4</sup>Department of Chemistry, Tokyo Gakugei University, Koganei, Tokyo 184-8501, Japan

<sup>5</sup>Department of Theoretical Molecular Science, Institute for Molecular Science, Okazaki, Aichi 444-8585, Japan

In the chemistry of fullerene, the functionalization of fullerenes is one of the most interesting themes regarding to the development of new nanomaterials with the unique properties. Azafulleroids and aziridinofullerenes, including aza-bridged structures, are such examples of modified fullerenes, which are obtained by 1,3-dipolar [3+2] cycloaddition manner of organic azides with crucial problems for toxicity and explosibility.<sup>1</sup> Thus, new useful methods for the preparation of them are expected.

In the course of our study on the development of synthetic methodology for aziridination of [60]fullerene, we carried out the photoreaction of [60]fullerene with sulfilimines. A nitrene generated by photochemical cleavage of the S-N linkage in sulfilimines easily reacted with [60]fullerene to afford the corresponding three-membered aziridinofullerene, exclusively. We also found that aziridinofullerene (**1**) rearranged thermally to azafulleroid (**2**) in high yield, with the fact that **2** rearranges **1** photochemically.<sup>2</sup> Here we report the regioselective aziridination of [60]fullerene and the reversible interconversion between **1** and **2**. The structures of both adducts were successfully determined by single-crystal X-ray analyses.



**References:**

1. J. Averdung, J. Mattay, *Tetrahedron* **1996**, 52, 5407.
2. T. Nakahodo, et al., *Angew. Chem., Int. Ed. in press* (DOI: 10.1002/anie.200704410).

Corresponding Author: Takeshi Akasaka, Tel & Fax: +81-29-853-6409, E-mail akasaka@tara.tsukuba.ac.jp

## HPLC Purification of Li Endohedral [60]Fullerene

○Takeshi Sakai<sup>1</sup>, Hiroshi Okada<sup>1</sup>, Fuyuko Yamashita<sup>1</sup>, Kenji Omote<sup>1</sup>, Yasuhiko Kasama<sup>1</sup>, Kuniyoshi Yokoo<sup>1</sup>, Shoichi Ono<sup>1</sup>, Hiromi Tobita<sup>2</sup>, Rikizo Hatakeyama<sup>3</sup>, and Masayuki Toda<sup>4</sup>

<sup>1</sup>*Ideal Star Inc., Sendai 989-3204, Japan*

<sup>2</sup>*Dept. of Chemistry, Grad. Sch. of Science, Tohoku Univ., Sendai 980-8578, Japan*

<sup>3</sup>*Dept. of Electronic Engineering, Tohoku Univ., Sendai 980-8578, Japan*

<sup>4</sup>*Dept. of Chemistry and Chemical Engineering, Yamagata Univ., Yonezawa 992-8510, Japan*

We have reported efficient synthesis of lithium endohedral fullerene (Li@C<sub>60</sub>) by supplying low energy Li ions together with C<sub>60</sub> molecules on a metal substrate (plasma shower method) and extraction Li@C<sub>60</sub> by precipitation in a solvent [1–2].

HPLC (high performance liquid chromatography) has applied to purify endohedral fullerenes including endohedral [60]fullerene [3–5]. The eluent of aniline was chosen for the purification of both Er@C<sub>60</sub>[3] and Eu@C<sub>60</sub>[4] using a Buckyclutcher-I column. We have tried to apply HPLC purification of Li@C<sub>60</sub>. The poster shows some of experimental results for HPLC purification of Li endohedral [60]fullerene.

1-chloronaphthalene was chosen as extraction solvent and HPLC eluent as a most soluble solvent of the product by the plasma shower method. The chromatogram of the HPLC extract shows two peaks (Fig. 1). The latter peak (peak 2) was assigned as the original fullerene of C<sub>60</sub>. On the other hand, the LDI-TOF mass spectrum of the former peak (peak 1) showed mostly single ion peak of Li@C<sub>60</sub> ( $m/z = 727$ ). However, monomolecular of Li@C<sub>60</sub> was not separated by repetition of the HPLC purification. These results suggest that the interaction between Li@C<sub>60</sub> and C<sub>60</sub> is considerably strong and they form a nano-size cluster in the solution.

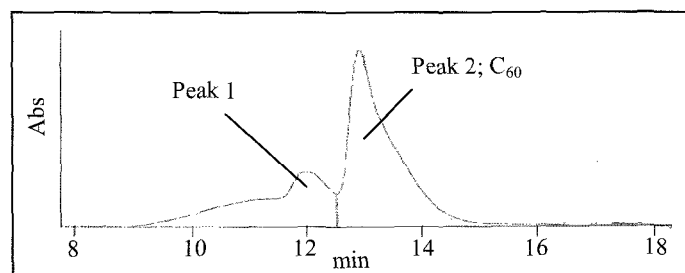


Fig. 1 A chromatogram of extract using a ODS column (0.2mL/min, 391 nm UV detection).

[1] K. Omote et al., *Special Lecture of The 33<sup>rd</sup> Fullerene-Nanotubes General Symposium*, **2S-2** (2007).

[2] H. Okada et al., *The 33<sup>rd</sup> Fullerene-Nanotubes General Symposium*, **1P-13** (2007).

[3] T. Ogawa, T. Sugai, and H. Shinohara, *J. Am. Chem. Soc.*, **122**, 3538 (2000).

[4] T. Inoue, Y. Kubozono, S. Kashino, Y. Takabayashi, K. Fujitaka, M. Hida, M. Inoue, T. Kanbara, S. Emura, and T. Uruga, *Chem. Phys. Lett.*, **316**, 381 (2000).

[5] T. Kanbara, Y. Kubozono, Y. Takabayashi, S. Fujiki, S. Iida, Y. Haruyama, S. Kashino, S. Emura, and T. Akasaka, *Phys. Rev. B*, **64**, 113403 (2001).

Corresponding Author: Hiroshi Okada

TEL: +81-22-303-7336, FAX: +81-22-303-7339, E-mail: [hiroshi.okada@idealstar-net.com](mailto:hiroshi.okada@idealstar-net.com)

## Electron Transport Properties of $\text{Sc}_2\text{C}_2@C_{84}$ Using the Encapsulated $\text{Sc}_2\text{C}_2$ Moiety as an Electric lead, First-Principle Study

○Shinji Usui and Noritaka Inoue

*Cybernet Systems Co., LTD.*

*FUJISOFT Bldg. 3 Kanda-neribeicho, Chiyoda-ku, Tokyo 101-0022 Japan*

Fullerene and its related compounds are active components to establish molecular electronic devices. Endohedral metallo-fullerenes are expected to have distinctive characters of the electron transport properties because of the unique electronic structure of the inside of the carbon shell. In this study, we analyzed the electron transport properties of  $\text{Sc}_2\text{C}_2@C_{84}$ , which has encapsulated  $\text{Sc}_2\text{C}_2$  moiety in the  $C_{84}$  cage, by first-principle calculations.

The model systems to analyze are illustrated in Fig. 1 where a  $\text{Sc}_2\text{C}_2@C_{84}$  is locating between two infinite gold electrodes. Two configurations of the  $C_2$  residue sandwiched by two Sc atoms were analyzed to evaluate the effect of the free movement of the  $C_2$  residue[1]. All of the analyses were performed by Atomistix ToolKit [2-3] which implements nonequilibrium Green's function's (NEGF) technique and density functional theory to calculate electron transport properties of the molecular device.

Fig. 2 shows calculated transmission spectra of two configurations of the  $C_2$  residue, indicating the transmission spectrum is significantly decreased after the rotation of the  $C_2$  residue, in spite of the energy change by the rotation is trivial. The origin of the fall of the transmission around 0.4 eV could be realized by calculating the transmission eigenstate[4], which provide a direct picture of the electronic states that contribute to the transmission. The contour plot of transmission eigenstate (in Fig. 1(a)) at 0.42 eV before  $C_2$  rotation clearly indicates that the back donation like electronic structure between  $\pi^*$  like orbital in the  $C_2$  residue and d-orbital of Sc atoms are important for the transmission. It could be estimated that the formation of the complex between the  $C_2$  residue and Sc atoms were broken by the movement of the  $C_2$  residue and it caused of the decrease of the transmission. The detail analyses will be discussed in the presentation.



Fig. 1 (a) Schematic and (b) graphical plots of  $\text{Sc}_2\text{C}_2@C_{84}$  molecular device. The contour plot in (a) describes a transmission eigenstate at 0.42(eV) before the rotation of the  $C_2$  residue.

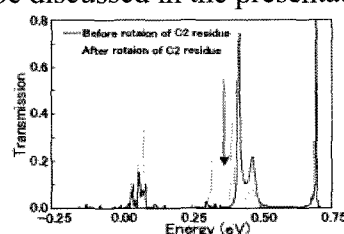


Fig. 2 Transmission spectra of  $\text{Sc}_2\text{C}_2@C_{84}$  molecular device, before rotation of the  $C_2$  residue (black line) and after rotation (gray line)

[1]M. Krause, M. Hulman, H. Kuzmany, O. Dubay, G. Kresse, K. Vietze, G. Seifert, C.R. Wang and H. Shinohara *Phys. Rev. Lett.* **93**, 137403 (2004)

[2]M. Brandbyge, J.-L. Mozos, P. Ordejon, J. Taylor, and K. Stokbro, *Phys. Rev. B* **65**, 165401 (2002)

[3]<http://www.cybernet.co.jp/nanotech/atomistix/>, see also <http://www.atomistix.com>

[4]M. Paulsson and M. Brandbyge, *Phys. Rev. B* **76**, 115117 (2007)

Corresponding Author: Shinji Usui, E-mail: s-usui@cybernet.co.jp, Tel.03-5297-3246, Fax. 03-5297-3637

## Photophysical Properties of N@C<sub>60</sub>

○Hidefumi Nikawa<sup>1</sup>, Yoichiro Matsunaga<sup>1</sup>, Takeshi Akasaka<sup>1</sup>, Tatsuhisa Kato<sup>2</sup>,  
Yasuyuki Araki<sup>3</sup>, Osamu Ito<sup>3</sup>, Masafumi ATA<sup>4</sup>, and Klaus-Peter Dinse<sup>5</sup>

<sup>1</sup>Center for Tsukuba Advanced Research Alliance, University of Tsukuba

<sup>2</sup>Department of Chemistry, Josai University

<sup>3</sup>Institute of Multidisciplinary Research for Advanced Materials, Tohoku University,

<sup>4</sup>National Institute of Advanced Industrial Science and Technology (AIST)

<sup>5</sup>Physical Chemistry III, Darmstadt University of Technology

In 1996, Weidinger and co-workers reported the first synthesis and characterization of N@C<sub>60</sub>.<sup>1</sup> The nitrogen atom encapsulated in C<sub>60</sub> is neutral and locates at the center of the cage without the chemical bonding to the cage. EPR and ENDOR spectra show that the nitrogen atom keeps the atomic ground-state configuration (three electrons in the 2p shell, <sup>4</sup>S<sub>3/2</sub>).<sup>2,3</sup> The complete decoupling of the endohedral spin from the cage causes the exceptionally long spin dechoherence time, even at room temperature in the solid state. Based on these specific properties, N@C<sub>60</sub> has been proposed as the building blocks for logical gates in quantum computing devices.<sup>4,5</sup> However, despite the attractive material, N@C<sub>60</sub> has not yet been fully investigated because of the difficulties in preparation and purification of a large amount of the material.<sup>6,7</sup>

We herein report HPLC purification and photophysical properties of N@C<sub>60</sub>. The multi-step recycling HPLC leads to 100% pure N@C<sub>60</sub> from a crude mixture consisting mostly of empty C<sub>60</sub>. The properties of N@C<sub>60</sub> have been investigated through <sup>13</sup>C NMR spectroscopy, UV-visible absorption spectroscopy and triplet state kinetics by laser flash photolysis experiments.

### References:

- (1) Almeida, T. M.; Pawlik, Th.; Weidinger, A.; Höhne, M.; Alcalá, R.; Spaeth, J.-M. *Phys. Rev. Lett.* **1996**, *77*, 1075.
- (2) Pietzak, B.; Waiblinger, M.; Almeida, T. M.; Weidinger, A.; Höhne, M.; Dietel, E.; Hirsch, A. *Chem. Phys. Lett.* **1997**, *279*, 259.
- (3) Weidinger, A.; Waiblinger, M.; Pietzak, B. Murphy, T. A. *Appl. Phys. A* **1998**, *66*, 287.
- (4) Harneit, W. *Phys. Rev. A* **2002**, *65*, 032322.
- (5) Harneit, W.; Huebener, K.; Naydenov, B.; Schaefer, S.; Scheloske, M. *Phys. Stat. Sol.* **2007**, *244*, 3879.
- (6) Jakes, P.; Dinse, K.-P.; Meyer, C. Harneit, W.; Weidinger, A. *Phys. Chem. Chem. Phys.* **2003**, *5*, 4080.
- (7) Kanai, M.; Porfyraks, K.; Briggs, G. A. D.; Dennis, T. J. S. *Chem. Comm.* **2004**, 210.

**Corresponding Author:** Takeshi Akasaka

**E-mail:** akasaka@tara.tsukuba.ac.jp

**Tel&Fax:** +81-29-853-6409

## Synthesis of High Purity Nitrogen Atom Encapsulated Fullerenes

○S. Nishigaki, T. Kaneko and R. Hatakeyama

*Department of Electronic Engineering, Tohoku University, Sendai 980-8579, Japan*

Many works related to the properties of a nitrogen atom encapsulated fullerene  $C_{60}$  ( $N@C_{60}$ ) are reported [1, 2], but the synthesis of  $N@C_{60}$  with high yield and high purity has not yet been realized. Although  $N@C_{60}$  has been produced by several plasma methods, the purity of  $N@C_{60}$  is extremely low ( $N@C_{60}/C_{60} = 10^{-3} - 10^{-2} \%$ ). The purpose of this research is to elucidate a formation mechanism of  $N@C_{60}$  in order to improve the purity. We reported that the high purity of 0.02 - 0.05 % was achieved using an electron beam superimposed RF discharge plasma and that it was yielded by increasing atomic nitrogen species density in the nitrogen plasma [3].

The schematic of experimental apparatus is shown in Ref.4. The nitrogen plasma is generated by applying an RF power with a frequency of 13.56 MHz to a spiral-shaped RF antenna and controlled by the applied RF power  $P_{RF}$ , a nitrogen gas pressure  $P_{N_2}$ , a substrate potential  $V_{sub}$  and a potential  $V_g$  of a mesh grid (20 meshes/cm), which is set up in the area between the RF antenna and the substrate. The upper side and lower side of the grid are defined as “plasma production area” and “process area”, respectively. The plasma potentials in the two areas are controlled by  $V_g$ , and a potential difference is formed between the areas. The potential difference produces an electron beam from the plasma production area to the process area and the electron beam dissociates nitrogen molecules.  $C_{60}$  is sublimated from an oven and deposited on the water-cooled cylindrical substrate. The nitrogen plasma is continuously irradiated to  $C_{60}$  on the substrate. The  $C_{60}$  compound including  $N@C_{60}$  deposited on the substrate is analyzed by electron spin resonance (ESR) and UV-vis absorption spectroscopy to calculate the purity ( $N@C_{60}/C_{60}$ ).

Figure 1 shows a dependence of the purity of  $N@C_{60}$  on  $P_{RF}$ . It is found that the purity of about 0.08 % is achieved under the condition that the applied RF power is more than 300 W. It is considered that the electron density in the plasma production area and the electron beam density in the process area increase with increasing  $P_{RF}$ . This increased electron beam enhances the production of atomic nitrogen species in the process area, resulting in the improvement of the purity.

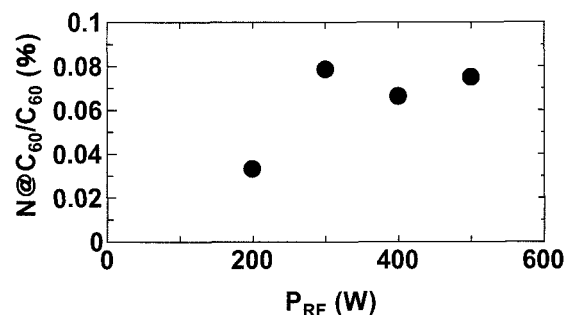


Fig. 1: Dependence of the purity of  $N@C_{60}$  on  $P_{RF}$ .  $P_{N_2} = 0.7$  Pa,  $V_g = 100$  V,  $V_{sub} = 100$  V.

- [1] M. Waiblinger *et al.*, *Phys. Rev. B*, **64**, 159901 (2001).
- [2] S. C. Benjamin *et al.*, *J. Phys.: Condens. Matter*, **18**, S867 (2006).
- [3] S. Nishigaki *et al.*, *Abstract of the 33rd Fullerene-Nanotubes General Symposium*, 209 (2007).
- [4] S. Nishigaki *et al.*, *Abstract of the 32nd Fullerene-Nanotubes General Symposium*, 155 (2007).

Corresponding Author: Shohei Nishigaki

TEL: +81-22-795-7046, FAX: +81-22-263-9225, E-mail: [nishigaki@plasma.ecei.tohoku.ac.jp](mailto:nishigaki@plasma.ecei.tohoku.ac.jp)



## Detection of single atomic layer of graphene by highly charged ion

Yoshiyuki Miyamoto<sup>1</sup>○, Hong Zhang<sup>2</sup>

<sup>1</sup>*Nano Electronics Research Labs., NEC, 34 Miyukigaoka, Tsukuba 305-8501, Japan,*

<sup>2</sup>*School of Physical Science and Technology, Sichuan Uni., Chengdu, 610065, PRC*

**Abstract:** In this paper, we propose a possibility of detecting single-atomic layer of graphene by using high-speed highly charged Ar ion. We have applied the molecular dynamics simulation [1] coupled with the time-dependent density functional theory [2] for an Ar<sup>7+</sup> ion which is passing through a graphene sheet with high kinetic energies. When the kinetic energy of the Ar<sup>7+</sup> ion reached 500 KeV at the moment of passing through a graphene sheet, electronic excitation occurs inside Ar<sup>7+</sup> ion in addition to the charge transfer. Because of the excitation, the penetrated Ar ion can emit lights in an energy range from extreme violet to soft X-ray which was also reported similar experiment using a carbon foil [3].

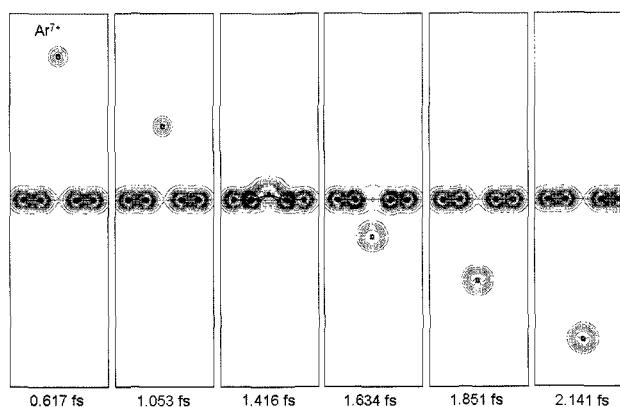


Fig. 1 Charge contour map of Ar<sup>7+</sup> passing through a graphene sheet.

According to the charge density profile around Ar ion (Fig. 1), the oscillation of electron cloud can be seen after passing through a graphene sheet. This picture suggests the intra-ion excitation. This work is supported by the Next Generation Supercomputer Project of the Ministry of Education, Culture, Sports, Science and Technology (MEXT) Japan.

### References:

- [1] O. Sugino and Y. Miyamoto, Phys. Rev. B **59**, 2579 (1999); *ibid*, Phys. Rev. B **66**, 089901(E) (2001).
- [2] E. Runge and E. K. U. Gross, Phys. Rev. Lett. **52**, 997 (1984).
- [3] S. Bashkin, H. Oona, and E. Veje, Phys. Rev. A **25**, 417 (1982).

**Corresponding Author: Yoshiyuki Miyamoto**

**E-mail: y-miyamoto@ce.jp.nec.com**

**Tel&Fax: +81-29-850-1586, +81-29-856-6136**

## Effect of heat-treatment temperature on preparation of carbonized ferritin

Masato Tominaga, ○Katsuya Miyahara, Kota Nakao, and Isao Taniguchi

Graduate School of Science and Technology, Kumamoto University,  
Kumamoto 860-8555, Japan

Ferritin is an iron storage protein, which is consisted of protein shell and ferrihydrite phosphate nanoparticle. The inner and outer diameters of protein shell are ca. 8 and 12 nm, respectively. This protein is a potential candidate for protein engineering of nanomaterial synthesis. In this study, carbonization ferritin was prepared by heat-treatment under a hydrogen gas atmosphere.

Ferritin was immobilized onto 3-aminopropyltrimethoxysilane-modified silicon surface (3-APMS/Si). Carbonized ferritin was prepared by heat-treatment for ferritin on 3-APMS/Si at 200, 400 and 600 °C for 60 min under H<sub>2</sub> gas.

After heat-treatment at 400 and 600 °C, the treated ferritin showed graphite structure by Raman spectroscopic measurements. The results indicated that protein shell was carbonized well. On the other hand, after heat-treatment at 200 °C, graphite structure was not confirmed. Fig. 1 shows tapping-mode AFM image of carbonized ferritin at 400 °C. The size of each carbonization ferritin was evaluated to be approximately 5 nm in diameter, which was similar size to the ferritin core size. Fig. 2 shows XPS spectra of ferritin after heat-treatment at 400 °C. The XPS spectrum for heat-treatment under air gave an iron oxide peak around 711 eV. On the other hand, heat-treatment under H<sub>2</sub> gas did not give any peak corresponding to iron species. The result suggests that ferritin core was covered with the carbon film derived from protein shell.

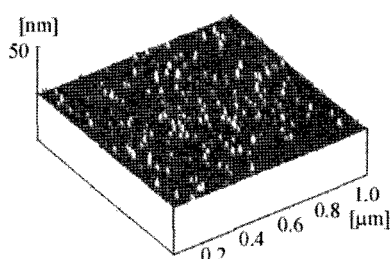


Fig. 1 Tapping-mode AFM image of ferritin after heat-treatment at 400 °C for 60 min under H<sub>2</sub> gas.

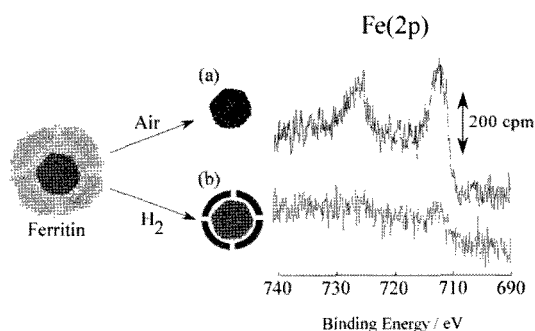


Fig. 2 XPS spectra in the Fe (2p) of ferritin after heat-treatment at 400 °C for 60 min under (a) air and (b) H<sub>2</sub> gas.

Corresponding Author: Masato Tominaga

E-mail: masato@gpo.kumamoto-u.ac.jp

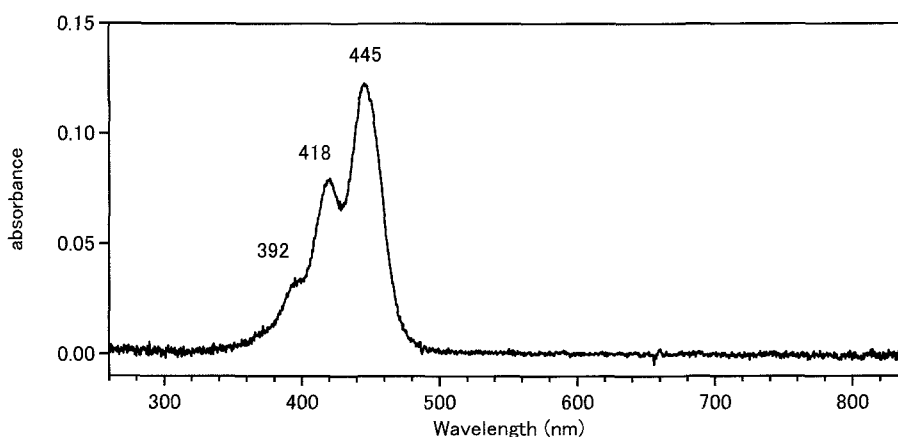
Tel&Fax: 096-342-3656

## Chlorine-End-Capped Polyynes: Formation and Characterization

○Yoriko Wada and Tomonari Wakabayashi

*Department of Chemistry, Kinki University, Higashi-Osaka 577-8502, Japan*

We performed laser ablation of graphite particles in organic solvents composed of carbon and chlorine, e.g., tetrachloroethylene, and analyzed soluble molecules by high performance liquid chromatography. Among many kinds of molecules thus produced then detected by their uv absorption spectra, we found one exhibiting absorption spectra typical for linear-polyynes species. Figure 1 shows uv/vis absorption spectra of the molecule in hexane at room temperature. The observation of a single electronic transition, a band peaking at 445 nm which is accompanied by a few peaks due to a vibrational progression, is compatible with the characteristic features commonly observed for polyynes: a single dipole-allowed electronic transition of  $\pi$ - $\pi^*$  character (*cf.* in the uv region of 227-316 nm for  $\text{HC}_{2n}\text{H}$  of  $n=4-8$  in hexane) with a single vibrational progression for one of the stretching modes of the *sp*-carbon chain (*cf.*  $\sim 2000\text{ cm}^{-1}$  for  $\text{HC}_{2n}\text{H}$ ). The similarity in overall appearance in the absorption spectra indicates that the carrier of the absorption features in Fig. 1 is a symmetric polyyne,  $\text{XC}_{2n}\text{X}$ . Concerning the energy levels, however, some quantitative differences are noticeable. The transition energy ( $\sim 2.8\text{ eV}$ ) and the vibrational frequency ( $\sim 1500\text{ cm}^{-1}$ ) are distinctly lower than those for  $\text{HC}_{2n}\text{H}$ . If we assume the substituents, X, being Cl atoms, the differences would be understood in terms of an electron-induction effect due to the end-capping chlorine atoms, by which the electronic structure and the potential curve thus its vibrational frequency should be modified.



**Figure 1.** Absorption spectra of molecules isolated from laser-ablated graphite in tetrachloroethylene (measurement performed in hexane at room temperature).

**Corresponding Author: Tomonari Wakabayashi**

**E-mail: wakaba@chem.kindai.ac.jp**

**Tel. 06-6730-5880 (ex. 4101) / FAX 06-6723-2721**

## Resonance Effects in the Raman Spectra of Polyynes

○Yohei Ami and Tomonari Wakabayashi

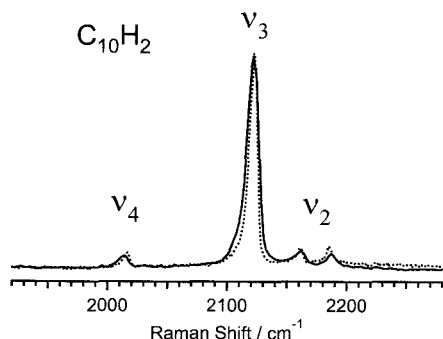
*Department of Chemistry, Kinki University, Higashi-Osaka 577-8502, Japan*

Raman spectroscopy is a powerful tool for the study of vibrational as well as electronic properties of molecules and solids, including fullerenes and nanotubes. Conjugated linear carbon molecules, polyynes, are also characterized by Raman spectroscopy [1,2]. The resonance enhancement of the Raman scattering intensity is advantageous for detection and useful for understanding of the spectral features. We here present theoretical analysis of the Raman scattering intensity for a selected polyynene,  $C_{10}H_2$  [2]. Our study includes 1) experimental excitation curves of the Raman scattering intensity, 2) theoretical analysis of the Franck-Condon overlaps between the excited and the ground states, and 3) a fitting for the excitation curves in terms of the resonance effects. The analysis for polyynene  $C_{10}H_2$  provides us with valuable insights into vibrational as well as electronic properties for polyatomic molecular systems with a linear symmetry.

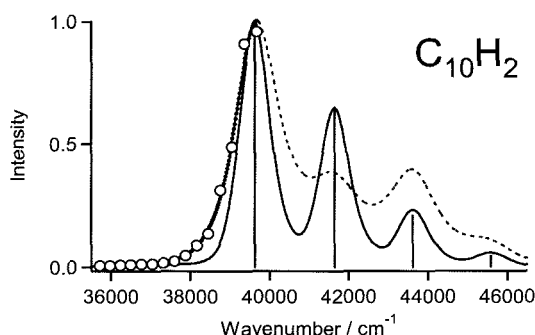
Figure 1 shows typical Raman spectra of  $C_{10}H_2$  in hexane. The band at  $2123\text{ cm}^{-1}$  is attributed to a single-quantum excitation of the symmetric-stretching vibrational mode,  $\nu_3\sigma_g$ , of the carbon chain. The Raman scattering intensity for this mode is increased upon resonance excitation of the dipole-allowed electronic transition,  ${}^1\Sigma_u^+ \leftarrow {}^1\Sigma_g^+$ , in the uv. Figure 2 shows the experimental excitation function of the Raman scattering intensity and the absorption spectra for comparison. Detailed analysis of the excitation profile will be discussed.

**References:**

- 1) H. Tabata, M. Fujii, S. Hayashi, T. Doi, T. Wakabayashi, "Raman and surface-enhanced Raman scattering of a series of size-separated polyynes", *Carbon* **44**, 3168-3176 (2006).
- 2) T. Wakabayashi, H. Tabata, T. Doi, H. Nagayama, K. Okuda, R. Umeda, I. Hisaki, M. Sonoda, Y. Tobe, T. Minematsu, K. Hashimoto, S. Hayashi, "Resonance Raman spectra of polyynene molecules  $C_{10}H_2$  and  $C_{12}H_2$ ", *Chem. Phys. Lett.* **433**, 296-300 (2007).



**Figure 1.** Resonance Raman spectra of  $C_{10}H_2$  in hexane excited with uv laser pulses at 262 nm.



**Figure 2.** Excitation function of the Raman scattering intensity (o), absorption (-), and a fitting curve (...).

**Corresponding Author: Tomonari Wakabayashi**

**E-mail: wakaba@chem.kindai.ac.jp**

**Tel. 06-6730-5880 (ex. 4101) / FAX 06-6723-2721**

## Cyanopolyynes Formed by Laser Ablation of Graphite in Acetonitrile

○Takaki Haseba, Yoshihiko Kashihara, and Tomonari Wakabayashi

*Department of Chemistry, Kinki University, Higashi-Osaka 577-8502, Japan*

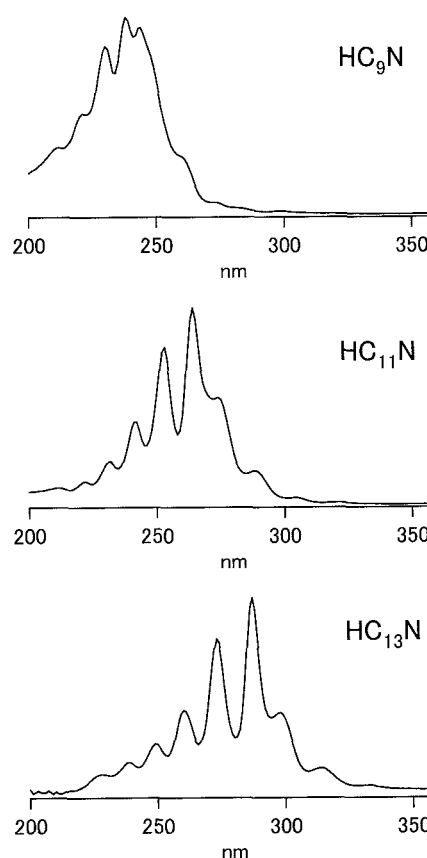
Since the astronomical observation of cyanopolyynes,  $H(C\equiv C)_n C\equiv N$ , in the late '70s [1], there have been a number of reports on spectroscopic investigations for the linear carbon molecules both in the laboratory and in space, mostly by rotational spectroscopy in the radio-frequency ranges. Interests in the optical and electronic properties due to conjugated  $\pi$ -electron systems have emerged recently, especially after the production by laser ablation.

In this work, we produced milligram quantities of cyanopolyynes by laser ablation of graphite particles in acetonitrile. They were separated by using high performance liquid chromatography (HPLC) and detected by uv-absorption spectra. For the studies of the molecular structure and the formation mechanism,  $^{13}C$ -nmr spectra were recorded by using  $^{13}C$ -enriched graphite powders as starting materials.

Figure 1 shows uv absorption spectra of  $HC_9N$ ,  $HC_{11}N$ , and  $HC_{13}N$  in acetonitrile at room temperature. A rich structure in the spectra is attributed to two vibrational progressions, one for the dipole-allowed electronic transition in shorter wavelengths and the other for the forbidden electronic transition in longer wavelengths. In contrast to the case for the symmetric polyynes, e.g.,  $HC_{2n}H$  or  $NC_{2n}N$ , the absorption intensity for the latter progression relative to the former one is two orders of magnitude higher for the asymmetric polyynes of  $HC_{2n+1}N$ .

**Reference:**

- 1) H.W. Kroto, C. Kirby, D.R.M. Walton, L.W. Avery, N.W. Broten, J.M. Macleod, T. Oka, *Astrophys. J.* **219**, L133 (1978).



**Figure 1.** Absorption spectra of monocyanopolyynes.

**Corresponding Author:** Tomonari Wakabayashi

**E-mail:** wakaba@chem.kindai.ac.jp

**Tel.** 06-6730-5880 (ex. 4101) / **FAX** 06-6723-2721

## Dicyanopolyynes Formed by Laser Ablation of Graphite in Liquid Nitrogen

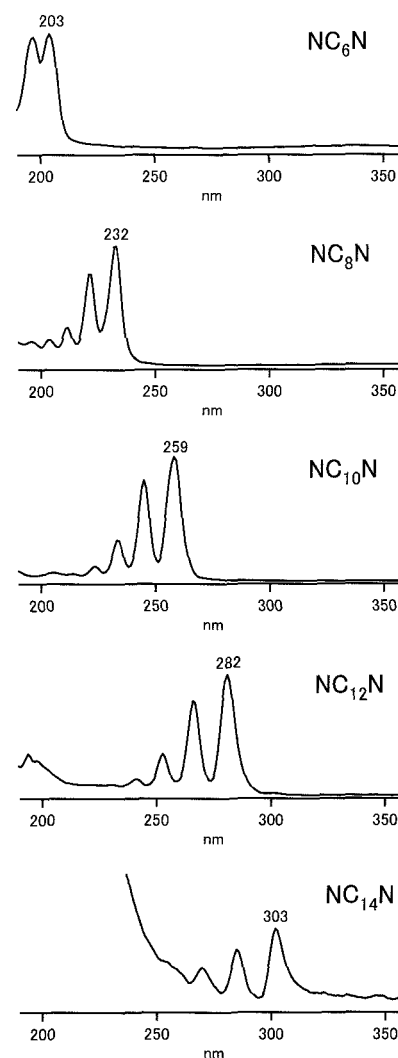
○Yoshihiko Kashihara, Takaki Haseba, and Tomonari Wakabayashi

*Department of Chemistry, Kinki University, Higashi-Osaka 577-8502, Japan*

Dicyanoacetylenes constitute a homologous series of end-capped linear *sp* carbon. Hirsch et al. produced the series of molecules,  $\text{N}\equiv\text{C}(\text{C}\equiv\text{C})_n\text{C}\equiv\text{N}$  of  $n=3-8$ , by vaporization of graphite under Krätschmer-Huffman conditions in the presence of cyanogen  $(\text{CN})_2$  and characterized by uv-absorption and  $^{13}\text{C}$ -nmr spectra [1]. In the present work, we applied laser ablation of graphite particles in liquids to form dicyanopolyynes. In acetonitrile,  $\text{CH}_3\text{CN}$ , the yield of the molecules was less than the series of monocyanopolyynes,  $\text{H}(\text{C}\equiv\text{C})_n\text{C}\equiv\text{N}$ . Therefore, for the purpose of increasing the relative yield of dicyanopolyynes, we performed laser ablation of graphite particles under hydrogen-free conditions, i.e., in liquid nitrogen.

Graphite powders were dispersed in liquid nitrogen and ablated by laser pulses (Nd:YAG 532 nm  $\sim 0.2$  J/pulse, 10 Hz) for 3 hours. The molecules were extracted with acetonitrile. After filtration, we got brown-colored solutions. The chemical species in the solutions were detected by uv absorption spectra upon chromatographic separations.

Figure 1 shows uv absorption spectra of dicyanopolyynes ( $n=2-6$ ) in acetonitrile. The absorption wavelengths systematically shift with the molecular size. The vibrational progression with separations of  $\sim 2000\text{ cm}^{-1}$  is characteristic of symmetric stretching vibration of the *sp* carbon chain. These molecules found to be unstable in solutions at room temperatures. For the study for polymerization, decay curves of the uv absorption intensity were measured for size-separated dicyanopolyne molecules in solution.



**Figure 1.** Absorption spectra of dicyanopolyynes.

**Reference:**

- 1) G. Schermann, T. Grösser, F. Hampel, A. Hirsch, "Dicyanopolyynes: A Homologous Series of End-Capped Linear *sp* Carbon", *Chem. Eur. J.* **3**, 1105-1112 (1997).

**Corresponding Author:** Tomonari Wakabayashi

**E-mail:** wakaba@chem.kindai.ac.jp

**Tel.** 06-6730-5880 (ex. 4101) / **FAX** 06-6723-2721

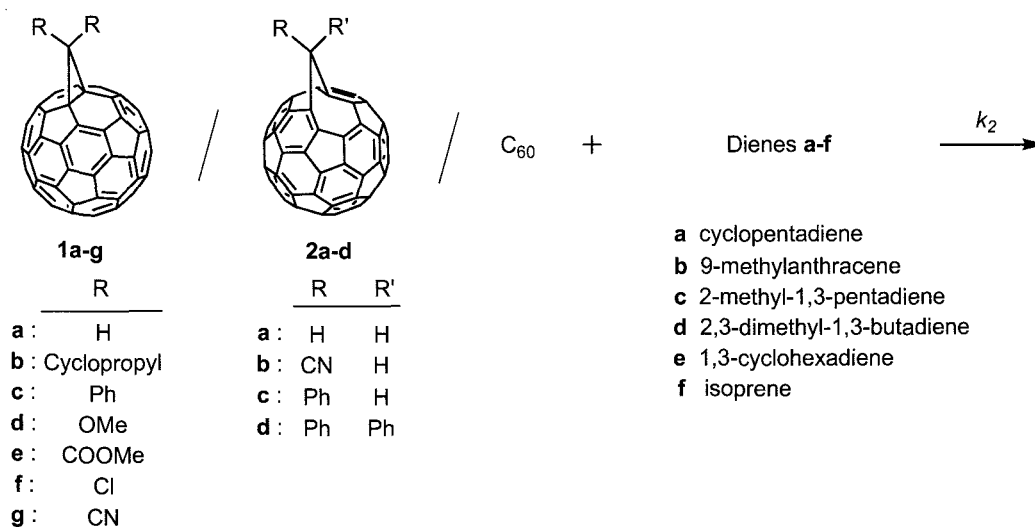
## Kinetic study in Diels-Alder reactions of fulleroids and methanofullerenes with various 1,3-dienes

○Yasunori Susami, Hiroshi Kitamura, Ken Kokubo and Takumi Oshima

*Division of Applied Chemistry, Graduate School of Engineering, Osaka University  
Suita, Osaka 565-0871, Japan*

The 1,3-dipolar cycloaddition reaction of various diazoalkanes with  $C_{60}$  is well known to give the [6,6]closed methanofullerenes **1** and the [5,6]open fulleroids **2** via the nitrogen evolution from the primary adducts pyrazolines.<sup>1</sup> Like the pristine  $C_{60}$ , these two types of fullerene derivatives also exhibit the thermally allowed  $[\pi 2_s + \pi 4_s]$  cycloadditions such as Diels-Alder (DA) reaction.<sup>2</sup> However, a detailed kinetic study of these fullerene derivatives with 1,3-dienes has not been hitherto carried out. Hence, in the present work on the DA reactions of variously substituted 1,3-dienes with **1** and **2** bearing various R and R' substituents at 30°C in toluene, we have investigated the factors controlling the reactivity in comparison with the reactions with  $C_{60}$ .

It was found that the fulleroids **2** were 1.1–165 times more reactive than the methanofullerenes **1** for all the 1,3-dienes tested. The relative rate constants with respect to the DA reaction with  $C_{60}$  were strongly dependent on the steric nature of the 1,3-dienes as well as the substituents R and R' at the methano-bridged carbon atom. These steric effects will be discussed in terms of the difference in the Diels-Alder reaction site of these fullerene derivatives.



[1] Suzuki, T.; Khemani, K. C.; Almarsson, Ö. *Science* **1991**, *254*, 1186–1188.

[2] Pang, L. S. K.; Wilson, M. A. *J. Phys. Chem.* **1993**, *97*, 6761–6763.

Corresponding Author: Takumi Oshima

TEL: +81-6-6879-4591, FAX: +81-6-6879-4593, E-mail: oshima@chem.eng.osaka-u.ac.jp

## Evaluation of Antioxidant Activity of Water-Soluble Fullerene Derivatives and Natural Antioxidants by $\beta$ -Carotene Bleaching Assay

○Kyoko Togaya<sup>1</sup>, Tadashi Goto<sup>1</sup>, Ken Kokubo<sup>1</sup>, Hisae Aoshima<sup>2</sup>, and Takumi Oshima<sup>1</sup>

<sup>1</sup>*Division of Applied Chemistry, Graduate School of Engineering, Osaka University  
Suita, Osaka 565-0871, Japan*

<sup>2</sup>*Vitamin C60 BioResearch Corporation, 1-8-7, Kyobashi, Chuo-ku, Tokyo 104-0031, Japan*

Water-soluble fullerenes are known to behave as potent scavengers for reactive oxygen species (ROS) in cell cultures and can protect human skin keratinocytes from UV irradiation and chemical oxidative damage by *tert*-butyl hydroperoxide [1,2]. Recently, we first evaluated the antioxidant activity of some water-soluble fullerenes such as  $\gamma$ -cyclodextrin-bicapped [60]fullerene ( $\gamma$ -CD/C<sub>60</sub>) and polyvinylpyrrolidone-entrapped [60]fullerene (PVP/C<sub>60</sub>) by  $\beta$ -carotene bleaching assay and found the good inhibitory effects on the oxidative discoloration of  $\beta$ -carotene associated with the spontaneous autoxidation of linoleic acid [3].

In the present study, we investigated the antioxidant activity of water-soluble [60]fullerene derivatives such as epoxides, methanofullerenes, and fulleroid, in comparison with some natural antioxidants. We found that the PVP/C<sub>60</sub>O and PVP/C<sub>60</sub>O<sub>n</sub> showed higher antioxidant activity (%AOA) than PVP/C<sub>60</sub> and some natural antioxidants.

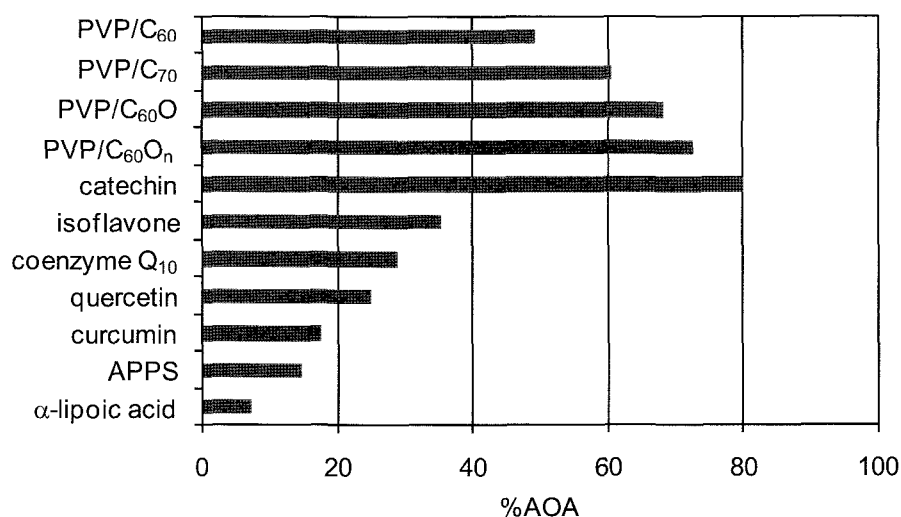


Fig.1 Antioxidant activity (%AOA) of various antioxidants assayed by  $\beta$ -carotene bleaching method.

[1] L. Xiao, H. Takada, K. Maeda, M. Haramoto and N. Miwa, *Biomed. Pharmacother.* **2005**, *59*, 351–358.

[2] L. Xiao, H. Takada, X. H. Gan and N. Miwa, *Bioorg. Med. Chem. Lett.* **2006**, *16*, 1590–1595.

[3] H. Takada, K. Kokubo, K. Matsubayashi and T. Oshima, *Biosci. Biotechnol. Biochem.* **2006**, *70*, 3088–3093.

Corresponding Author: Ken Kokubo

TEL: +81-6-6879-4592, FAX: +81-6-6879-4593, E-mail: kokubo@chem.eng.osaka-u.ac.jp



## Photoelectrochemical Properties of [70]fullerene derivatives on ITO

○ Takahiko Ichiki, Yutaka Matsuo and Eiichi Nakamura

*Department of Chemistry, The University of Tokyo, Hongo, Bunkyo-ku, Tokyo 113-0033,  
Japan*

*Japan Science and Technology Agency, ERATO Nakamura Functional Carbon Cluster  
Project, Hongo, Bunkyo-ku, Tokyo 113-0033, Japan*

Photocurrent conversion system is one of the most important issues and many efforts have been devoted to create more efficient and useful devices. Fullerene is one of promising materials for the purpose because of its special electrochemical properties, such as multiple redox events. Especially, [70]fullerene shows a high performance of optical and electrochemical properties. Previously, we have reported the synthesis and characterizations of tri-adducts of fullerenes and their metal complexes.<sup>1</sup> They show a long-wavelength absorption ( $> 650$  nm) and reversible multiple redox based on the fullerene and metal moieties. It should be noted that if these unique materials can be immobilized on an electrode surface, many intriguing devices should be created.

We will report preparation method of self-assembled monolayers (SAMs) consisting [70]fullerene derivatives on the indium tin oxide (ITO) electrodes (Fig. 1) and their photoelectrochemical properties. Furthermore, we will propose a unique application of these fullerene derivatives.

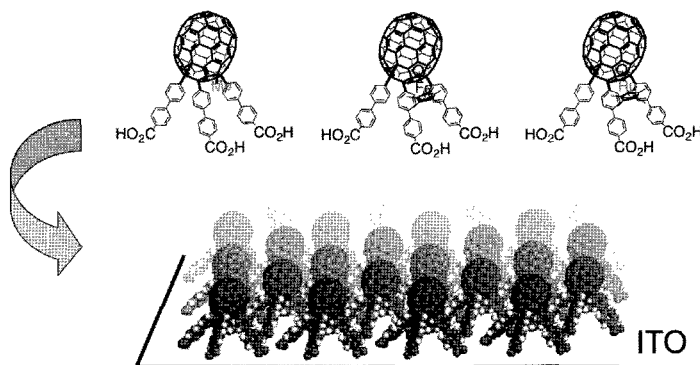


Fig.1. Image of the film preparation on an indium tin oxide (ITO) electrode

[1] a) E. Nakamura, *et al. J. Mater. Chem.* **2002**, *12*, 2109. b) E. Nakamura, *et al. J. Am. Chem. Soc.* **2002**, *124*, 9354.

Corresponding Author: Yutaka Matsuo and Eiichi Nakamura

E-mail: matsuo@chem.s.u-tokyo.ac.jp; nakamura@chem.s.u-tokyo.ac.jp; Tel&Fax: (+81)-3-5841-1476

## Synthesis and Property of Fullerene Cobalt Dithiolene Complexes

○Masashi Maruyama<sup>1</sup>, Yutaka Matsuo<sup>2</sup>, Eiichi Nakamura<sup>1,2</sup>

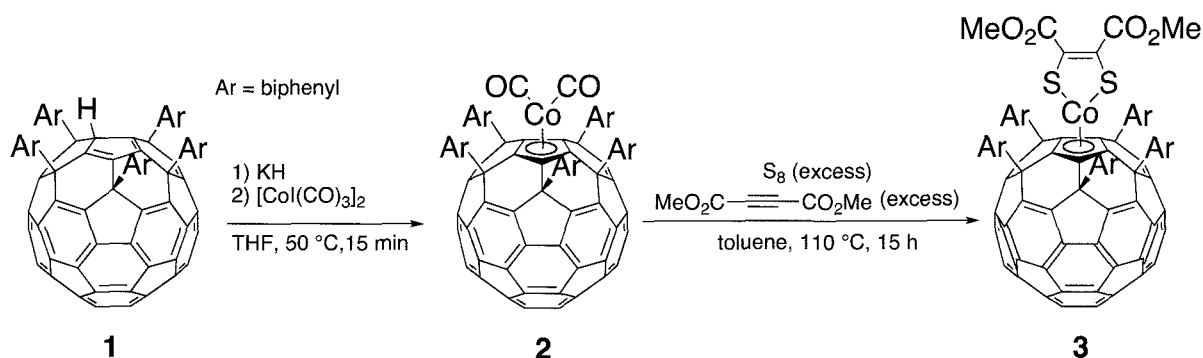
<sup>1</sup>Department of Chemistry, The University of Tokyo, Hongo, Bunkyo-ku, Tokyo 113-0033, Japan

<sup>2</sup>Japan Science and Technology Agency, ERATO, Nakamura Functional Carbon Cluster Project, Hongo, Bunkyo-ku, Tokyo 113-0033, Japan

$\eta^5$ -Fullerene metal complexes have been energetically studied in our group and a variety of organometallic compounds, both half-sandwich type and sandwich type, have been reported [1]. However,  $\eta^5$ -fullerene cobalt complexes were not reported yet.

This time, we report the synthesis and property of an  $\eta^5$ -fullerene cobalt complex **3**, a new class of half-sandwich type fullerene metal complexes. Cobalt dithiolene complexes are known to have unusual electronic structures, which is comprised of a metallacyclic conjugation of 6  $\pi$ -electrons in the 5-membered ring with charge transfer from p-orbital of the sulfur atom to the d-orbital of the cobalt atom. These unique conjugation systems give interesting chemical and physical properties, such as redox and absorption properties. In addition to those unusual electronic structures, the  $\eta^5$ -fullerene cobalt complex **3** has a fullerene moiety, which has an electron-withdrawing character. The  $\pi$ -electron systems between upper cyclopentadienyl and lower hemispherical substructures are partly overlapped through an endohedral homoconjugation.

To a solution of  $\text{KC}_{60}(\text{biph})_5$  in THF was added an excess amount of a mixture of  $\text{I}_2$  and  $\text{Co}_2(\text{CO})_8$  in THF to give a cobalt dicarbonyl complex **2** in 49% isolated yield. The dicarbonyl complex **2** was heated at 110 °C with excess amounts of elemental sulfur and an electron deficient alkyne to afford a cobalt dithiolene complex **3** in 83% isolated yield. The dithiolene complex **3** was characterized by UV-vis spectrum and cyclic voltammetry.



[1] (a) M. Sawamura, Y. Kuninobu, M. Toganoh, Y. Matsuo, M. Yamanaka, and E. Nakamura, *J. Am. Chem. Soc.*, **2002**, *124*, 9354. (b) Y. Matsuo and E. Nakamura, *Organometallics*, **2003**, *22*, 2554. (c) Y. Kuninobu, Y. Matsuo, M. Toganoh, M. Sawamura, and E. Nakamura, *Organometallics*, **2004**, *23*, 3259. (d) Y. Matsuo, A. Iwashita, and E. Nakamura, *Organometallics*, **2005**, *24*, 89. (e) Y. Matsuo, K. Tahara, and E. Nakamura, *J. Am. Chem. Soc.*, **2006**, *128*, 7154.

Corresponding Author: Yutaka Matsuo and Eiichi Nakamura

TEL/FAX: +81-3-5841-1476; E-mail: matsuo@chem.s.u-tokyo.ac.jp; nakamura@chem.s.u-tokyo.ac.jp

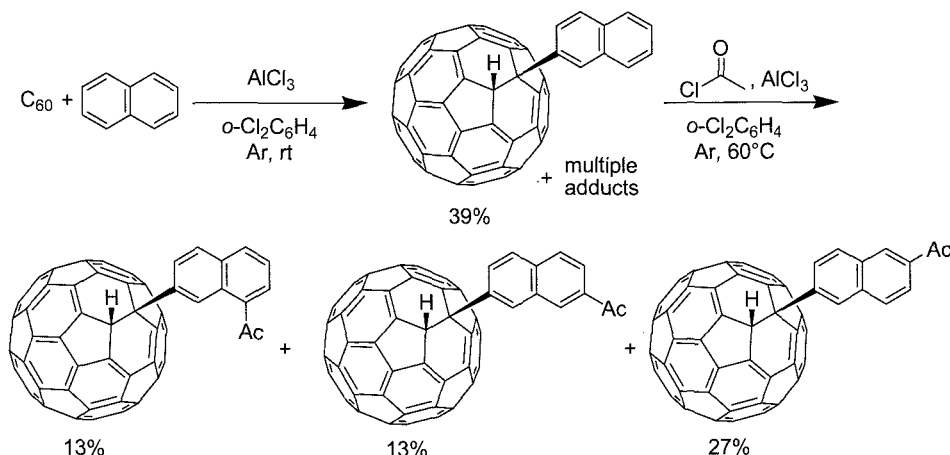
## Hydroarylation of Fullerene with Aromatic Compounds and Subsequent Friedel-Crafts Acetylation Reaction

○Shinya Tochika, Yui Sol, Mai Kato, Ken Kokubo and Takumi Oshima

*Division of Applied Chemistry, Graduate School of Engineering, Osaka University,  
Suita, Osaka 565-0871, Japan*

Elucidation of the regiochemistry in chemical modification of fullerene and fullerene derivatives has been one of the most significant subjects from both the mechanistic and the synthetic viewpoints. In 1991, Olah first reported a multiple hydroarylation of [60]fullerene catalyzed by  $\text{AlCl}_3$  without isolation of any adduct [1]. After 15 years, Nakamura's and our groups have independently isolated some these hydroarylation adducts and determined the structure and regiochemistry [2]. The regioselectively formed mono- or bisarylated adducts are of quite interest in a further chemical modification. In this study, we investigated the  $\text{AlCl}_3$ -catalyzed Friedel-Crafts acetylation of mono-hydroarylated fullerene adducts.

The reaction of  $\text{C}_{60}$  with various aromatic compounds (substituted benzenes, biphenyl, and naphthalene) in the presence of  $\text{AlCl}_3$  was terminated at the appropriate conversion in order to attain a higher yield of monoadduct. Subsequently, the acetylation of the pre-introduced aromatic rings with an excess amount of acetyl chloride was carried out to give the expected products along with some other products depending on the aryl rings. These results indicated that the fullerene cage behaves as a bulky electron withdrawing substituent.



**Scheme 1.**  $\text{AlCl}_3$ -catalyzed Friedel-Crafts fullereneation of naphthalene and subsequent acetylation.

[1] Olah, G. A.; Bucsi, I.; Lambert, C.; Aniszfeld, R.; Trivedi, N. J.; Sensharma, D. K.; Prakash, G. K. S. *J. Am. Chem. Soc.* **1991**, *113*, 9387.

[2] (a) Iwashita, A.; Matsuo, Y.; Nakamura, E. *Angew. Chem. Int. Ed.* **2007**, *46*, 3513. (b) Tochika, S.; Kato, M.; Kuang, C.; Kokubo, K.; Oshima, T. *The 31<sup>st</sup> Fullerene-Nanotubes General Symposium* **2006**, 1P-4.

Corresponding Author: Ken Kokubo

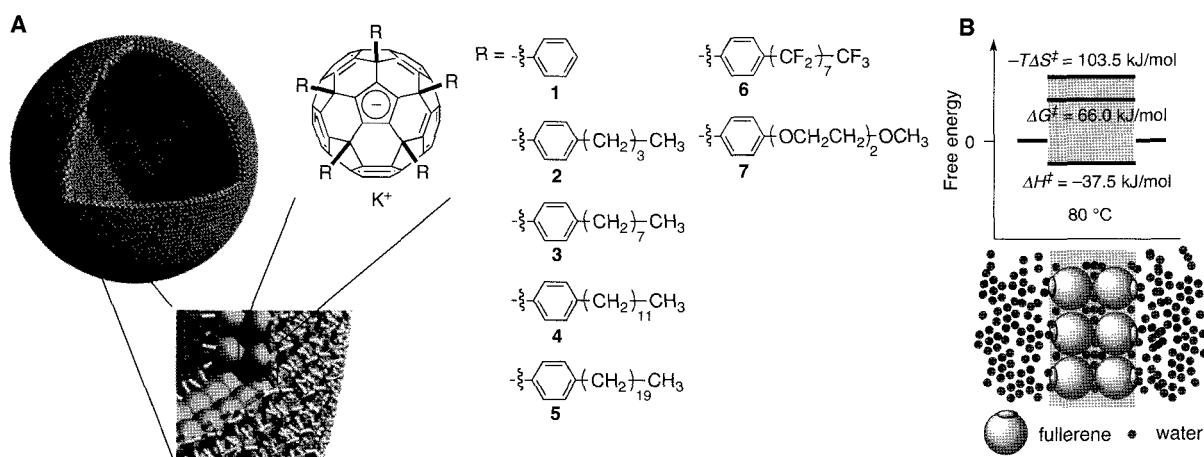
TEL: +81-6-6879-4592, FAX: +81-6-6879-4593, E-mail: kokubo@chem.eng.osaka-u.ac.jp

## Surface Functionalization of Fullerene Bilayer Vesicles and Study of Water Permeability

○Tatsuya Homma<sup>1</sup>, Koji Harano<sup>1</sup>, Hiroyuki Isobe<sup>1,†</sup>, Eiichi Nakamura<sup>1</sup>

<sup>1</sup>*Department of Chemistry and ERATO (JST),  
The University of Tokyo, Hongo, Bunkyo-ku, Tokyo 113-0033, Japan*

Bilayer membranes made of phospholipids are the fundamental structure in biology in that the membrane physically holds the biological machinery while keeping permeability to water at ambient temperature. Permeability of the membrane to water has therefore drawn much interest of scientists in various fields.



**Figure 1.** (A) A bilayer vesicle made of amphiphilic fullerene 1–7. (B) Thermodynamics and a schematic view of water permeation through fullerene bilayer made of 1.

In the present study, we found that a fullerene bilayer vesicle formed from amphiphilic fullerene, Ph<sub>5</sub>C<sub>60</sub>K (1), has extremely low permeability to water. The fullerene bilayer recorded permeability coefficient of  $5.43 \times 10^{-7}$  m/s (20 °C) which was 10000~100 times smaller than common lipid bilayers. The extremely low permeability originates from the entropy-controlled process in the water permeation mechanism.<sup>1</sup>

In addition, the surface of fullerene bilayer vesicles could be functionalized by introducing substituents on the periphery of the amphiphilic fullerenes (2–7). The study of water permeability of the fullerene membranes showed that the water permeability to fullerene bilayers could be controlled by changing the length of alkyl chains or the polarity of substituents attached on the vesicle surface.

† Present address: *Department of Chemistry, Tohoku University, Aoba-ku, Sendai 980-8578, Japan*

**Reference:** [1] Isobe, H.; Homma, T.; Nakamura, E. *Proc. Natl. Acad. Sci. U.S.A.* **2007**, *104*, 14895–14898.

**Corresponding Authors:** Hiroyuki Isobe and Eiichi Nakamura

**Tel&Fax:** 03-5841-4369, **E-mail:** isobe@mail.tains.tohoku.ac.jp, nakamura@chem.s.u-tokyo.ac.jp

### Singlet Oxygen Generation Efficiencies of Water-Soluble Fullerenes and Their Photo-Induced Cytotoxicity

○Yoko Iizumi<sup>1</sup>, Toshiya Okazaki<sup>1,2</sup>, Minfang Zhang<sup>3</sup>, Masako Yudasaka<sup>3</sup>  
and Sumio Iijima<sup>1</sup>

<sup>1</sup>*Research Center for Advanced Carbon Materials, AIST, Tsukuba 305-8565, Japan*

<sup>2</sup>*PRESTO, JST, 4-1-8 Honcho, Kawaguchi 332-0012, Japan*

<sup>3</sup>*SORST-JST, NEC Corporation, 34 Miyukigaoka, Tsukuba 305-8501, Japan*

Fullerenes are known to act as very strong photosensitizing agents due to their unique photophysical properties. For instance, C<sub>60</sub> efficiently generate singlet oxygen (<sup>1</sup>O<sub>2</sub>) under UV irradiation because the triplet energy of C<sub>60</sub> locates at about 1.6 eV which is approximately 0.7 eV higher than the <sup>1</sup>O<sub>2</sub> energy. The ability to produce <sup>1</sup>O<sub>2</sub> has been responsible for many biological actions of fullerenes such as DNA-cleavage and cell-toxicity. However, the quantitative evaluations of the singlet oxygen generation efficiencies of fullerenes have so far been limited.<sup>1</sup>

In this study, we have solubilized fullerenes into water using gamma-cyclodextrin<sup>2</sup> and poly(vinylpyrrolidone), and estimated their <sup>1</sup>O<sub>2</sub> generation efficiencies by detecting the near-infrared <sup>1</sup>O<sub>2</sub> emission at ~1275 nm. The obtained emission intensities were directly compared with those of typical photosensitizers (rose bengal and methylene blue) under the same experimental conditions. Furthermore, we also investigated the photo-induced cytotoxicity of the water-soluble fullerenes by WST-1 assay using rat fibroblast cell line (5RP7). We have compared with the results and assessed consistency of them.

[1] Nagano, T.; Arakane, K.; Ryu, A.; Masunaga, T.; Shinmoto, K.; Mashiko, S.; Hirobe, M. *Chem. Pharm. Bull.* **42**, 2291(1994).

[2] Komatsu, K.; Fjiwara, K.; Murata, Y.; Braum, T; *J. Chem. Perkin Trans. 1* 2963(1999).

**Corresponding Author:** Toshiya Okazaki

**E-mail:** toshi.okazaki@aist.go.jp **Tel:** +81-29-861-4173 **Fax:** +81-29-861-4851

## Synthesis of Fullerene Glycoconjugates via a Copper-Catalyzed Huisgen Cycloaddition Reaction

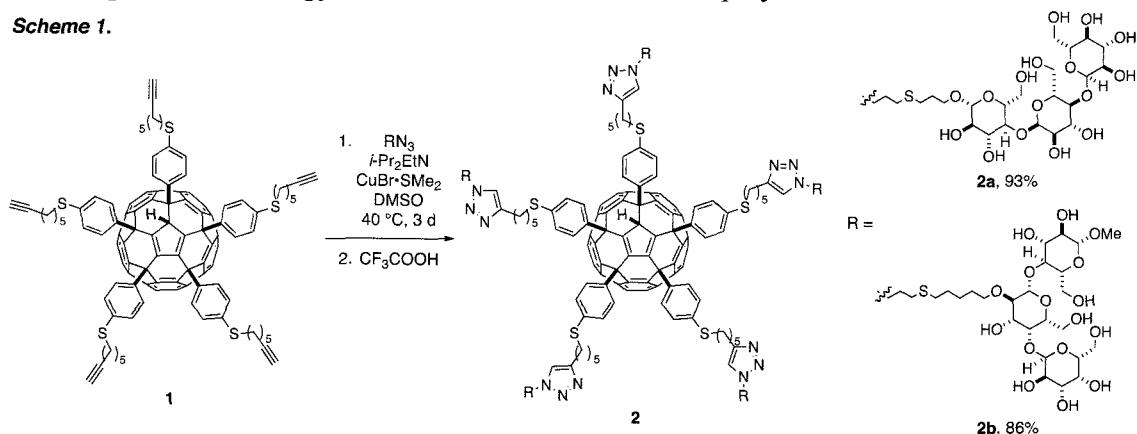
○Kaimei Cho<sup>1</sup>, Niclas Solin<sup>1</sup>, Daniel B. Werz<sup>2</sup>  
Hiroyuki Isobe<sup>1,†</sup>, Peter H. Seeberger<sup>2</sup>, Eiichi Nakamura<sup>1</sup>

<sup>1</sup>Department of Chemistry and ERATO (JST), The University of Tokyo, Hongo, Bunkyo-ku, Tokyo 113-0033, Japan; <sup>2</sup>Laboratory for Organic Chemistry, Swiss Federal Institute of Technology (ETH) Zürich, HCI F 315, Wolfgang-Pauli-Str. 10, 8093 Zürich, Switzerland

The multivalent display of saccharides is an important principle of molecular recognition in biological systems, and a number of tailor-made ligands for natural protein receptors have been synthesized. Among various low molecular weight displays, glycoconjugates possessing a number of carbohydrate units show promising phenomena of interaction with some important protein receptors. Here, we report the successful application of Cu-catalyzed Huisgen cycloaddition to the efficient and quick synthesis of fullerene glycoconjugates bearing as many as fifteen sugar moieties possessing a  $C_5$  symmetric framework [1].

The synthetic strategy of the five-fold Cu-catalyzed Huisgen cycloaddition approach is shown in Scheme 1. Penta-alkynyl fullerene **1** was treated with oligosaccharides, which bear a tether terminated with an azide group, in the presence of copper bromide and diisopropylethylamine in DMSO at 40 °C for 3 days. The reaction was so clean that the target molecules **2** were obtained in high yield and purity after washing excess azide and copper salts away. Compounds **2a** and **2b** are among the most densely functionalized organic molecules prepared using Cu-catalyzed Huisgen cycloaddition, and this new methodology provides a powerful strategy for multivalent saccharide displays.

**Scheme 1.**



† Present Address: Department of chemistry, Tohoku University, Aoba-ku, Sendai 980-8578, Japan.

**Reference:** [1] Isobe, H.; Cho, K.; Solin, N.; Werz, D. B.; Seeberger, P. H.; Nakamura, E. *Org. Lett.* **2007**, *9*, 4611-4614.

**Corresponding Authors:** Hiroyuki Isobe and Eiichi Nakamura

**E-mail:** isobe@mail.tains.tohoku.ac.jp, nakamura@chem.s.u-tokyo.ac.jp

**Tel&Fax:** 03-5800-6889

## Growth characteristics of single-walled carbon nanotubes at low temperature by low-pressure chemical vapor deposition

<sup>o</sup>Hiroshi Yoshida<sup>1,2</sup>, Masahiro Asakura<sup>1,2</sup>, Shu Watanabe<sup>1</sup>, Takao Shiokawa<sup>1,3</sup>,  
and Koji Ihibashi<sup>1,3</sup>

<sup>1</sup>Advanced Device Laboratory, RIKEN, Wako, Saitama 351-0198, Japan

<sup>2</sup>Department of Physics, Tokyo University of Science, Shinjuku, Tokyo 162-8601, Japan,

<sup>3</sup>CREST, JST, Kawaguchi, Saitama 332-0012, Japan

The low-pressure growth<sup>1,2)</sup> of single-wall carbon nanotubes (SWNTs) is a key technology in fabricating SWNT-based nanodevices, such as hybrids devices with a two-dimensional GaAs/AlGaAs system.<sup>3)</sup> This is because it is possible to grow them at temperatures as low as 350 °C in the low-pressure of 0.1- 1 Pa.<sup>1)</sup> In this paper, we report on the growth characteristic of the growth of SWNTs by the chemical vapor deposition (CVD) in the low-pressure of  $2 \times 10^{-3}$  Pa using in-situ catalyst deposition.

The low-pressure growth was performed with the ethanol gas of  $2 \times 10^{-3}$  Pa after the in-situ catalyst deposition (Co, 0.1 nm) in ultra-high vacuum (UHV). The detail processes are described in the reference.<sup>4)</sup> Raman spectroscopy with an excitation wavelength of 514.5 nm was carried out to characterize the grown SWNTs.

Figure 1 shows the Raman spectra of the radial breathing mode (RBM, the left panel) and the high energy mode (HEM, the right panel) for samples grown at different temperatures. The growth time was 1000 min for 380 °C and 350 °C, and 3000 min for 340 °C. For 380 °C, it is clearly seen that there is a peak at  $270 \text{ cm}^{-1}$  in the RBM region, and the peak at G-Band ( $\sim 1590 \text{ cm}^{-1}$ ) splits into two with one at  $1550 \text{ cm}^{-1}$  ( $G^-$ ) and the other at  $1590 \text{ cm}^{-1}$  ( $G^+$ ). These observations confirm the growth of SWNTs at 380 °C. For 350 °C, a peak in the RBM was not observed. In HEM, however, the splitting of the G-band peak was observed at  $1590 \text{ cm}^{-1}$  and  $1560 \text{ cm}^{-1}$ . Moreover, the Raman shift at  $1590 \text{ cm}^{-1}$  was equal to that for 380 °C. These observations confirm also the growth of SWNTs at 350 °C. For 340 °C, a peak in RBM and the split in G-band were not observed. It means that SWNTs growth may not occur at 340 °C.

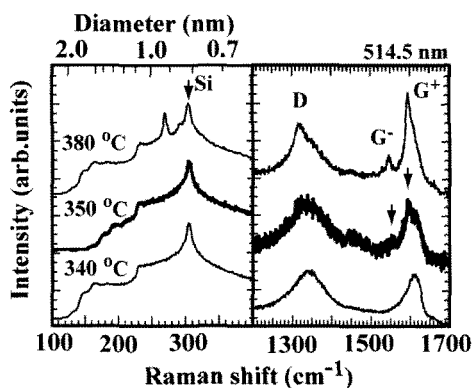


Figure 1

**References:** 1) M.Contoro et al., Nano Lett., **6**,(2006)1107. 2) T.Shiokawa et al., Jpn.J. Appl.Phys., **45**(2006)L605. 3) T.Tsukamoto et al., J.Appl.Phys. **98**, (2005) 076106. 4) H.Yoshida et al., presented at Ext. Abstr. (The 54<sup>th</sup> Spring Meeting,JSAP,2007), 27a-ZR-3 (in Japanese).

**Corresponding Author:** Takao Shiokawa **E-mail:**shiokawa@riken.jp

**Tel:**048-467-9368 **Fax:** 048-462-4659

## Effective catalyst diameter for extended growth duration of single-walled carbon nanotubes

○Takashi Uchida<sup>1,2</sup>, Hiroshi Sakai<sup>1,3</sup>, Akira Yamazaki<sup>1,4</sup>, and Yoshihiro Kobayashi<sup>1,2</sup>

<sup>1</sup>NTT Basic Research Laboratories, NTT Corporation, Atsugi 243-0198, Japan

<sup>2</sup>CREST/JST, Japan Science and Technology Corporation

<sup>3</sup>Department of Physics, Tokyo University of Science, Shinjuku, Tokyo 162-8601, Japan

<sup>4</sup>Department of Physics, Meiji University, Kawasaki 214-8571, Japan

*In-situ* Raman observation is very useful for investigating the growth mechanism of single-walled carbon nanotubes (SWCNTs) [1]. At the last meeting, we reported kinetic analyses of the time evolution of chirality-sensitive radial breathing mode (RBM) signals observed in *in-situ* Raman spectra during CVD growth [2]. Using Co-ferritin as a catalyst, we can rule out the effects of diffusion and aggregation of catalyst nanoparticles on SWCNT growth, which is significantly seen for thin film catalyst. In this work, we investigated the growth pressure-dependent behavior of CVD growth using Co-ferritin catalyst by *in-situ* Raman spectroscopy and AFM.

*In-situ* Raman spectra were obtained with a  $\mu$ -Raman system (633-nm excitation wavelength) combined with an ethanol-CVD system. Co-ferritin catalysts were prepared on a SiO<sub>2</sub> substrate [3]. The CVD was performed at 720 °C under the ethanol gas pressures of 80, 100, and 120 Pa. AFM observation was performed after the CVD growth.

Figure 1 shows growth duration  $\tau$  for each RBM peak, obtained by a kinetic analysis of the time evolution of the RBM intensity in *in-situ* Raman spectra. It is found that the  $\tau$  of specific RBM peaks for 100 Pa is significantly large. Figure 2 shows diameter distributions of Co catalyst nanoparticles before CVD and those of active Co catalyst nanoparticles (nanoparticles with SWCNTs) obtained at different ethanol gas pressures. The average diameter of active Co catalyst nanoparticles is larger than that of Co nanoparticles before CVD. For 100 Pa, the Co catalyst nanoparticles with a diameter of about 3 nm are effective for SWCNT growth. In addition, longer SWCNTs are grown from the 3 nm nanoparticles for 100 Pa. These results suggest that Co catalyst nanoparticles with a specific diameter extend the growth duration. This work was partly supported by JSPS Grant-in Aid for Scientific Research (B).

[1] S. Chiashi et al., CPL 386 (2004) 89.

[2] T. Uchida et al., 33rd F&NT General Symposium 2007, 1-15.

[3] G. -H. Jeong et al., JACS 127 (2005) 8328.

**Corresponding Author: Takashi Uchida**

**E-mail: uchida@will.brl.ntt.co.jp**

**Tel/Fax: +81-46-240-4319/+81-46-240-4718**

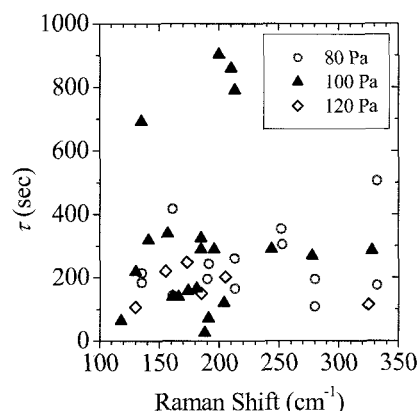


Fig. 1 Growth duration  $\tau$  for each RBM peak.

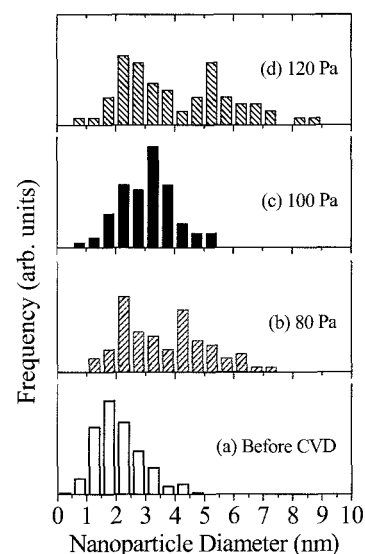


Fig. 2 Diameter distributions of (a) Co catalyst nanoparticles before CVD and (b-d) active Co catalyst nanoparticles obtained under ethanol gas pressures of 80, 100, and 120 Pa, respectively.



## RHEED Study on Growth Process of Carbon Nanotubes by Chemical Vapor Deposition

○Hidetoshi Nagatsu, Koji Asaka, Hitoshi Nakahara, Yahachi Saito

*Department of Quantum Engineering., Nagoya University, Furo-cho,  
Nagoya 464-8603, Japan*

Carbon nanotubes (CNTs) were synthesized by chemical vapor deposition (CVD) using an ethanol gas in ultrahigh vacuum chamber, and the growth process of CNTs was *in-situ* investigated by reflection high-energy electron diffraction (RHEED). Cobalt (Co) films of 1nm thickness were used as catalyst for the growth of CNTs. The films were prepared on a silicon substrate coated with silica films by high-vacuum electron beam deposition. A base pressure of  $5 \times 10^{-6}$  Pa was kept before CVD in order to minimize the effect of the residual gas on the CNT growth. The substrate was heated at 800 °C in a pressure of  $1 \times 10^2$  Pa for 2 hours during CVD. The morphology of CNTs was observed by scanning electron microscopy (SEM).

Figure 1(a) shows an ED pattern from the Co/SiO<sub>2</sub>/Si substrate before CVD. Figures 1(b) and 1(c) show ED patterns from the substrate after 1 hour CVD and 2 hour CVD, respectively. Figures 2(a)-2(c) show SEM images corresponding to Figs. 1(a)-1(c). The as-deposited Co film is composed of Co islands with diameter smaller than 10 nm, as seen in Fig. 2(a). The Co islands have a face-centered cubic structure, as indexed in Fig.1 (a). After CVD for 1 hour, Debye rings with d-spacings of ca. 0.2 and 0.3 nm, corresponding to the 10-0 and 00 2 reflections from graphite, appear, as shown in Fig. 1(b). In Fig. 2(b), CNTs with an average diameter of 8 nm is observed. After CVD for 2 hours, the average diameter of CNTs increases up to 10 nm, as shown in Fig. 2(c).

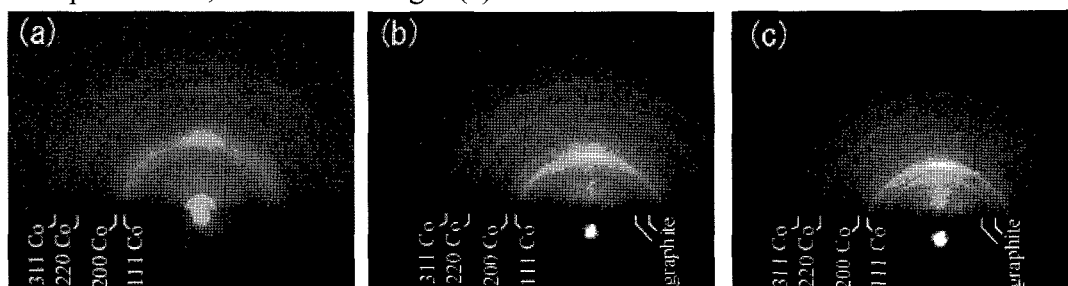


Fig.1 ED patterns taken from the substrate surface (a) as-deposited, (b) after 1 hour and (c) for 2 hours. The substrate is heated at 800 °C during CVD.

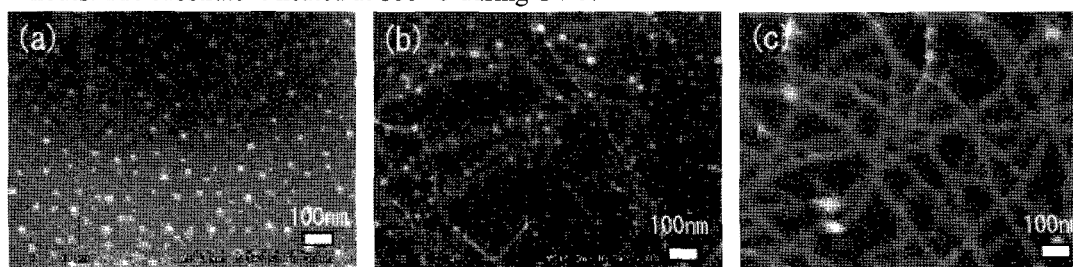


Fig.2 (a) -(c) SEM images of corresponding to Figs. 1(a)-1(c), respectively.

**Corresponding Author:** Hidetoshi Nagatsu

**E-mail:** nagatsu@surf.nuqe.nagoya-u.ac.jp

**Tel&Fax:** +81-52-789-3714 / +81-52-789-3703

## Carbon Nanotube Growth with Dipped (Fe,Co) Mo Catalysts by Chemical Vapor Deposition

○ Daisuke Ishizuka<sup>1</sup>, Takayuki Yanai<sup>2</sup>, Hiroki Okuyama<sup>1</sup>,  
Katsumi Uchida<sup>2</sup>, Nobuyuki Iwata<sup>1</sup>, Hirofumi Yajima<sup>2</sup>, Hiroshi Yamamoto<sup>1</sup>

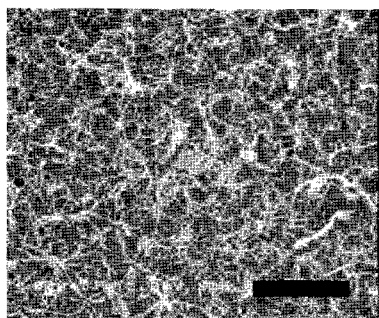
<sup>1</sup> Department of Electronics & Computer Science, College of Science & Technology, Nihon University, 7-24-1 Narashinodai, Funabashi, Chiba 274-8501, Japan

<sup>2</sup> Department of Applied Chemistry, Faculty of Science, Tokyo University of Science, 12-1 Funagawara-cho, Ichigaya, Shinjyuku-ku, Tokyo 162-0826, Japan

Single-Wall Carbon Nanotubes (SWNTs) are metals or semiconductors strongly depending on their diameter and chirality. For applying SWNTs to the nanoscale electronic devices, the diameter, the alignment and the chirality should be controlled. The diameter might be determined by the size of the catalysts, and the in-plane alignment was also reported in growth on sapphire or in “fast-heating” chemical vapor deposition (CVD) process and so on [1,2]. We propose a novel technique to control the chirality using free electron laser (FEL) irradiation.

As the first step of the chirality control, carbon nanotubes (CNTs) were grown on quartz substrates with dipped (Fe, Co) Mo catalysts. The quartz substrates were soaked for one min in HF solution and then ultrasonically cleaned for 10 min in Semico clean 23 (Furuuchi Chemical Corp.). The substrate was dipped in methanol dissolving Fe and Mo with the molar ratio of 94:6 using  $\text{Fe}(\text{NO}_3)_3 \cdot 9\text{H}_2\text{O}$  and  $\text{MoO}_2(\text{acac})_2$ . The dipping speed was 600  $\mu\text{m/s}$ . Dipped substrate was annealed for five min at 450 °C. The CNTs were grown using thermal chemical vapor deposition method with  $\text{C}_2\text{H}_4$  feeding gas.

From the result of the Raman spectrum, the G- and D- bands were clearly observed at  $1350\text{cm}^{-1}$  and  $1590\text{cm}^{-1}$ , however the radial breathing mode was not confirmed. Figure 1



(scale: 3  $\mu\text{m}$ )

Fig.1 SEM image  
of the specimen

shows the scanning electron microscopy (SEM) image of the specimen. Wires with 20 nm in diameter randomly grew all over on substrate. Those results indicated that the CNTs with 20 nm in diameter were produced. The growth of CNTs with CoMo catalyst, and growth using alcohol catalytic chemical vapor deposition (ACCVD) will be discussed.

### References:

- [1] Hiroki Ago et al., *Chem. Phys. Lett.*, **421** (2006) 399.
- [2] S. M. Huang et al., *Nano Lett.*, **4** (2004) 6.

## Sorting of double-walled carbon nanotubes using density-gradient ultracentrifugation

○S. Ina<sup>1,2,3</sup>, K. Yanagi<sup>2,3</sup>, Y. Miyata<sup>1,2,3</sup>, Y. Maniwa<sup>1,3</sup> and H. Kataura<sup>2,3</sup>

<sup>1</sup>Department of Physics, Tokyo Metropolitan University, Tokyo 192-0397, Japan

<sup>2</sup>Nanotechnology Research Institute, AIST, Tsukuba 305-8562, Japan

<sup>3</sup>JST-CREST

Recently, Arnold et al. have reported a new separation method of metallic and semiconducting single-wall carbon nanotubes (SWCNTs) by using a density-gradient ultracentrifugation.[1] Although they have succeeded high-quality separation of SWCNTs, no one has tried to separate the double-wall carbon nanotubes (DWCNTs) to date. Here we report the preliminary results of the separation of DWCNTs. In the case of SWCNT, the difference in the electronic types of the nanotube wall is thought to cause the difference in the micelle density in the mixed surfactant system. On the other hand, the formation of the micelle for DWCNTs is expected to be modified by the inner shell. One possible modification is the additional sorting by the electronic type of inner shell and the other possibility is the sorting by the degree of the interaction between inner and outer shell.

DWCNTs used in this work were synthesized by the ethanol-CVD method by using Fe/MgO catalysts. After the isolation process, DWCNT dispersion was separated into 9 fractions by the density-gradient ultracentrifugation. The diameter distribution of inner and outer shell for each fraction was characterized using optical absorption, Raman, and photoluminescence (PL) spectroscopy.

Figure 1 shows Raman spectra of each fraction and the starting material. Radial breathing mode peaks observed between 200 and 400  $\text{cm}^{-1}$  could be attributed to the inner CNTs. The spectra clearly indicate that the lower density fraction contains smaller diameter inner shell. The same tendency was also confirmed from the PL spectra. Interestingly, optical absorption spectra (not shown) show that the lower density fraction contains larger diameter outer shell. This result strongly suggests an additional sorting by the distance between inner and outer shell of the DWCNTs.

**References:** [1] M.S. Arnold et al. Nat. Nanotechnol. 1, 60 (2006)

**Corresponding Author:** H. Kataura

**E-mail:** [h-kataura@aist.go.jp](mailto:h-kataura@aist.go.jp)

**Tel:** +81-29-861-2551, **Fax:** +81-29-861-2786

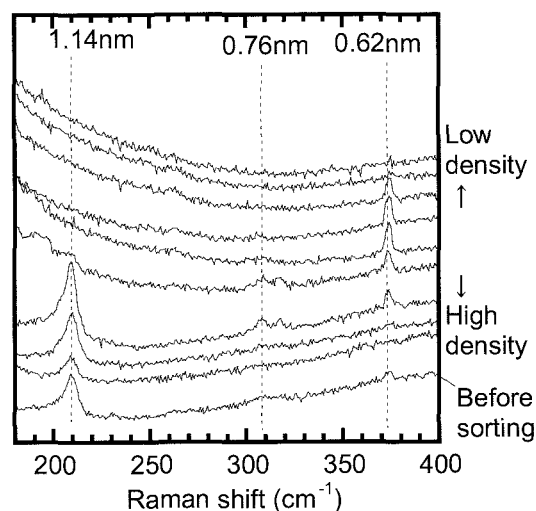


Fig. 1. Raman spectra of the starting material and each fraction after sorting.

## In-situ Monitoring and Kinetic Analysis of Millimeter-Thick Single-Walled Carbon Nanotube Growth

Kei Hasegawa<sup>1</sup>, Suguru Noda<sup>1</sup>, Shigeo Maruyama<sup>2</sup> and Yukio Yamaguchi<sup>1</sup>

<sup>1</sup> Dept. of Chemical System Engineering, The University of Tokyo, Tokyo 113-8656, Japan

<sup>2</sup> Dept. of Mechanical Engineering, The University of Tokyo, Tokyo 113-8656, Japan

Rapid growth of single-walled carbon nanotubes (SWNTs) was realized by the water-assisted growth method [1], and its growth kinetics was supposed as the exponential decay of the initial growth rate [2]. We reproduced such rapid growth by our combinatorial catalyst preparation method and proposed a novel mechanism of the growth rate enhancement by the Al<sub>2</sub>O<sub>3</sub> catalyst underlayer [3, 4]. In this study, we show the growth rate and the catalyst lifetime determined by the in-situ monitoring of growing SWNTs.

The growth condition was 8.0 kPa C<sub>2</sub>H<sub>4</sub>, 27 kPa H<sub>2</sub>, 5.0 Pa H<sub>2</sub>O, 67 kPa Ar at 1093 K. Figure 1a shows the nanotubes growing on the combinatorial catalyst library [5] of 0.2-3-nm Fe on Al<sub>2</sub>O<sub>3</sub>/SiO<sub>2</sub>/Si, and Fig. 1b shows the time profile of the SWNT thickness with 0.5 nm Fe. The nanotube forest grew up at an initial growth rate of 4.5 μm/s, kept growing at that rate for 6 minutes, and then suddenly stopped growing. Kinetics can be more precisely determined by this in-situ monitoring method than the conventional batch experiments, because the catalytic growth of nanotubes is not so reproducible among different experimental runs.

Figure 2 show the effect of temperature (a) and C<sub>2</sub>H<sub>4</sub> pressure (b) on the growth rate and the catalyst lifetime at the Fe thickness of 1.0 nm. Both the higher temperature and C<sub>2</sub>H<sub>4</sub> pressure caused the higher growth rate. Higher temperature shortened the catalyst lifetime. On the other hand, the effect of C<sub>2</sub>H<sub>4</sub> pressure for the lifetime was not significant. The underlying mechanism will be discussed considering the reaction both in the gas phase and on the Al<sub>2</sub>O<sub>3</sub> substrate and the structural change of Fe nanoparticles.

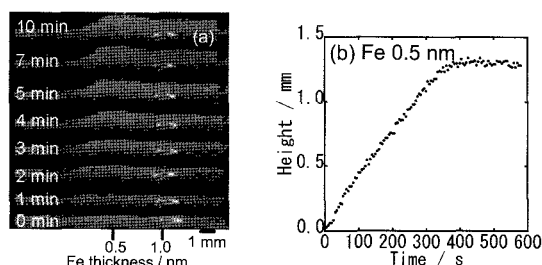


Fig. 1 (a) Photographs of growing CNTs.  
(b) Time profile of the growing CNTs

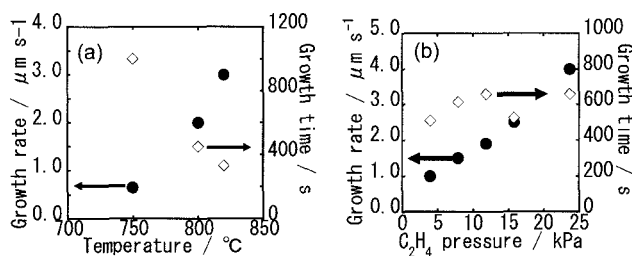


Fig. 2 Growth rate and lifetime at different temperatures (a) and C<sub>2</sub>H<sub>4</sub> pressures (b).

[1] K. Hata, et al., *Science*, **306**, 1362 (2004). [2] D. N. Futaba, et al., *Phys. Rev. Lett.*, **95**, 056104 (2005). [3] S. Noda, et al., *Jpn. J. Appl. Phys.*, **46**, L399 (2007). [4] K. Hasegawa et al., *J. Nanosci. Nanotech.* in press. [5] S. Noda et al., *Carbon*, **44**, 1414 (2006).

Corresponding Author: Suguru Noda

TEL: +81-3-5841-7330, FAX: +81-3-5841-7332, E-mail: noda@chemsys.t.u-tokyo.ac.jp

## Crucial Role of Gas-Phase Pyrolysis of Ethylene in Rapid Growth of Carbon Nanotubes

○Ryuhei Ito<sup>1</sup>, Suguru Noda<sup>1</sup>, Toshio Ohsawa<sup>1</sup>, Shigeo Maruyama<sup>2</sup>, Yukio Yamaguchi<sup>1</sup>

<sup>1</sup>Department of Chemical System Engineering,

<sup>2</sup>Department of Mechanical Engineering,

The University of Tokyo, 7-3-1 Hongo, Bunkyo-ku, Tokyo 113-8656, Japan

Rapid growth of millimeter-thick SWNT forests in a few minutes was realized by water-assisted ethylene CVD <sup>[1]</sup>. We previously reproduced such growth using C<sub>2</sub>H<sub>4</sub>/H<sub>2</sub>/H<sub>2</sub>O/Ar reactant gas and Fe/Al<sub>2</sub>O<sub>3</sub> catalyst, and found an essential role of Al<sub>2</sub>O<sub>3</sub> under layer <sup>[2]</sup>. In this work, we studied the effect of gas phase and substrate temperatures separately, and found a crucial role of gas phase reaction in forming actual precursor from ethylene.

Figure 1 shows the experimental apparatus used in this study. The reactant gas was once heated by flowing through an externally-heated quartz tube, cooled down, and then fed to a resistively-heated graphite substrate on which the catalyst was supported. The typical condition was 60 Torr C<sub>2</sub>H<sub>4</sub>/ 200 Torr H<sub>2</sub>/ 0.076 Torr H<sub>2</sub>O/ Ar for the reactant gas and 1 nm Fe/ 20 nm Al<sub>2</sub>O<sub>3</sub> for the catalyst.

Figure 2 shows the side-view images of the graphite substrates after CVD at 800 °C substrate temperature for 10 min. Nanotubes did not grow efficiently at preheating temperatures of 700 °C or below, but they grew efficiently to millimeter-thickness at higher preheating temperatures. CHEMKIN simulation showed the decomposition of C<sub>2</sub>H<sub>4</sub> and formation of C<sub>2</sub>H<sub>2</sub> in a residence time of a few seconds. Then, we mixed 4 Torr C<sub>2</sub>H<sub>2</sub> with 169 Torr H<sub>2</sub>/ 0.076 Torr H<sub>2</sub>O/ Ar instead of C<sub>2</sub>H<sub>4</sub>, and found that millimeter-thick nanotube forests actually grew without preheating. C<sub>2</sub>H<sub>2</sub> is the actual precursor for the rapid nanotube growth from C<sub>2</sub>H<sub>4</sub> feedstock.

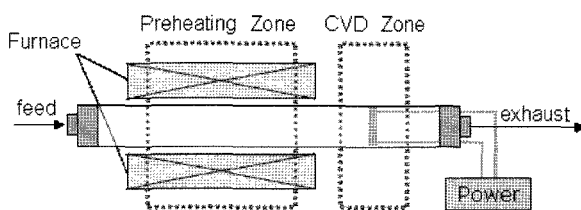


Fig.1 Experimental apparatus

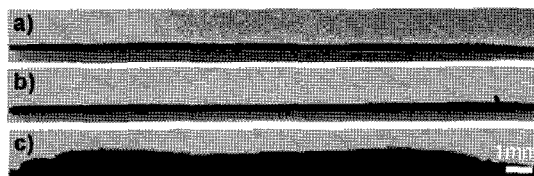


Fig.2 Images of SWNT forests (a) no preheating, (b)preheating: 700 °C, (c)preheating: 850 °C

<sup>[1]</sup>K. Hata, et al., *Science* **306**, 1362 (2004) <sup>[2]</sup>S. Noda, et al., *Jpn J. Appl. Phys.* **46**, L399 (2007)

Corresponding Author: Suguru Noda, [noda@chemsys.t.u-tokyo.ac.jp](mailto:noda@chemsys.t.u-tokyo.ac.jp) Tel&Fax: +81-3-5841-7332.

## Interaction of Amphiphilic Oligopeptides with Carbon Nanotubes

○Shin Ono<sup>1</sup>, Atsushi Yamamoto<sup>1</sup>, Shin-ya Masuhara<sup>1</sup>, Yosuke Miura<sup>1</sup>, Yasushi Maeda<sup>2</sup>,  
Kishio Hidaka<sup>3</sup>, and Hiromitsu Miyamoto<sup>4</sup>

<sup>1</sup>Graduate School of Science and Engineering, University of Toyama, Gofuku 3190,  
Toyama 930-8555, Japan

<sup>2</sup>Graduate School of Engineering, University of Fukui, Fukui 910-8507, Japan

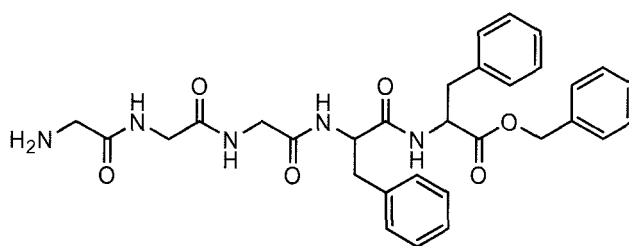
<sup>3</sup>Materials Research Laboratory, Hitachi Ltd., Hitachi-shi, Ibaraki 319-1292, Japan

<sup>4</sup>Analysis & Experiment Laboratory, Hitachi Kyowa Engineering Co. Ltd., Hitachinakai-shi,  
Ibaraki 312-8507, Japan

For the industrial applications of carbon nanotubes (CNTs), the development of a method for purification of CNTs is one of the important issues. We have proposed the use of amphiphilic peptides as a dispersant to purify CNTs. In this study, we designed and prepared some amphiphilic oligopeptides composed of Gly and Phe as the hydrophilic and hydrophobic residues, respectively, and examined the effects of their hydrophilic, hydrophobic, and ionic properties on the dispersion of CNTs in water by means of elemental analysis, Raman spectroscopy, scanning electron microscopy (SEM), thermogravimetric analysis (TGA), transmission electron microscopy (TEM), and UV/Vis/NIR spectroscopy.

The results of dispersion experiments showed that a pentapeptide, Gly<sub>3</sub>-Phe<sub>2</sub>-OBzl (pep-2), was useful for dispersion of SWNTs (Hipco). The C-terminal Bzl ester was found to be essential to the dispersion by UV/Vis/NIR spectroscopy. Upon addition of methanol to the SWNTs-dispersed solution using pep-2, nanotubes components came out in the solution and could be recovered by centrifugation. From the data of TG and elemental analyses, the content of remaining pep-2 in recovered SWNTs was calculated to be 16 wt%. TEM images of bundled SWNTs were observed.

Moreover, we examined whether pep-2 could be used for purification of CNTs. A raw CNT material containing amorphous carbons and metallic catalysts was once dispersed in water and then recovered by addition of methanol. Comparison of SEM images of the raw and recovered CNTs showed disappearance of most of the amorphous carbons. Increase in area ratios of the Raman peaks (G/D) was observed after treatment with pep-2. On the other hand, results of TG and elemental analyses indicated that removal of the impurities was incomplete. In conclusion, raw CNTs can be purified to some extent using pep-2 without damaging them.



Structure of amphiphilic oligopeptide pep-2.

Corresponding Author: Shin Ono

E-mail: shinono@eng.u-toyama.ac.jp

Tel&Fax: +81-76-445-6845

## Growth of super-long straight CNTs by highly dense catalyst particles

○Ryogo Kato, Tasuku Maki, Takayuki Iwasaki, Hiroshi Kawarada  
*School of Science and Engineering, Waseda university, Tokyo 169-8555, Japan*

We demonstrate synthesis of 7.4-mm long CNTs by dense catalyst particles obtained by adjusting thicknesses of sandwich-like catalyst films of Al/Fe/Al [1]. First, we investigated the effects of the film thickness of the top Al layer on the density of catalyst particles by annealing a substrate. When the Fe film was 0.5 nm in thickness, the densities of the catalyst particles measured from the SEM images were  $1.0 \times 10^{12} \text{ cm}^{-2}$  and  $1.3 \times 10^{12} \text{ cm}^{-2}$  for the top Al (0.5 nm) and the top Al (1.0 nm), respectively. The thicker top Al layer suppressed the diffusion of Fe atoms on a substrate, resulting in the denser catalyst particles from the 1.0-nm-thick Al layer. CNTs were synthesized on Si substrates coated with the catalyst films mentioned above. A mixture of hydrogen and methane and a remote-plasma CVD apparatus [1] were used for the CNT growth. Figure 1 shows SEM images of CNTs grown at 690°C for 30 h and schematic of the growth mechanism. CNTs obtained from the thicker top Al layer were higher for the same growth time. It is speculated that the density of CNTs also became higher for the thicker Al due to the dense catalyst particles and that the denser CNTs tend to be straightened by supporting one another even after long-time growth (Fig. 1). In the straight CNT mat, the diffusion length of carbon radicals to the catalyst particles at the bottom of CNTs [2] should be shortened, resulting in the higher growth rate.

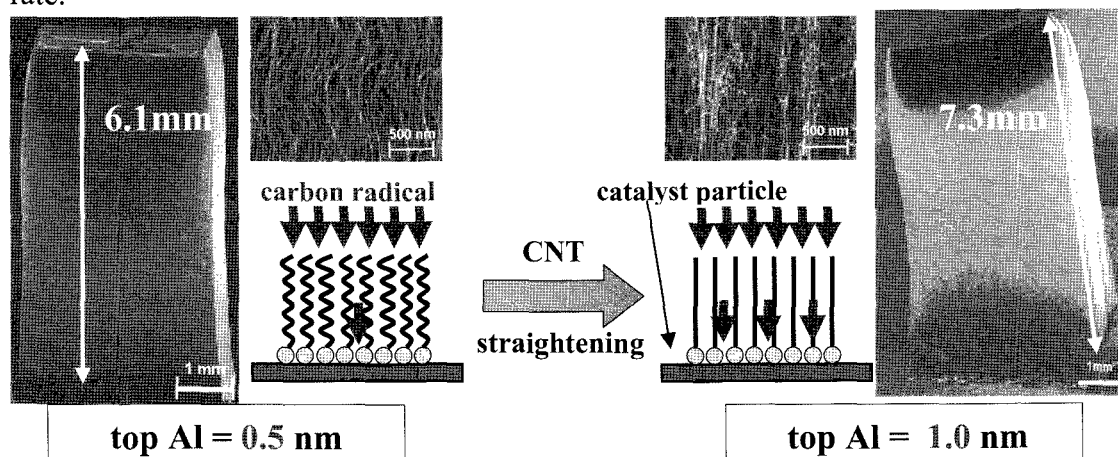


Figure 1. SEM images of super-long CNTs and the growth model.

[1] G. Zhong, *Jpn. J. Appl. Phys.*, 44, 1558 (2005). [2] T. Iwasaki, *J. Phys. Chem. B*, 109, 19556 (2005).

Corresponding Author: H. Kawarada E-mail : [kawarada@waseda.ac.jp](mailto:kawarada@waseda.ac.jp) Tel&Fax : +81-3-5286-3391

## Chemical Vapor Deposition of Carbon Nanotubes with dip-coated (Fe,Co)Pt catalysts

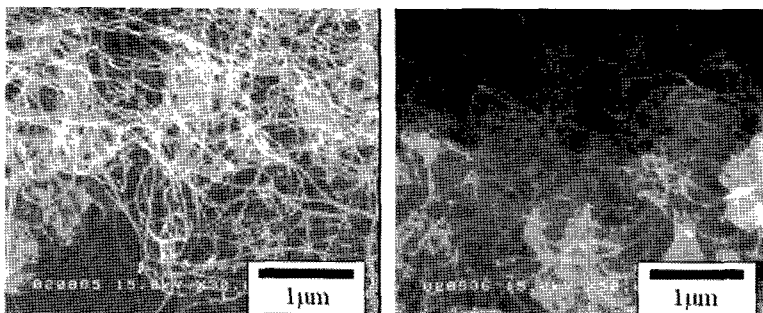
○Takuya Sonomura, Daisuke Ishizuka, Hiroki Okuyama,  
Nobuyuki Iwata and Hiroshi Yamamoto

*College of Science & Technology, Nihon University*

Carbon nanotubes (CNTs) are able to become the channel for the spin electronic devices because the spin of the electron is preserved over the long distance when the electron conducts in CNTs. The aim of our study is to apply CNTs to the spintronics with the ferromagnetic metals or alloys as catalysts. In addition to that, chirality control of the single wall carbon nanotubes (SWNTs) is expected irradiating free electron laser, the features of which are variable wave length and very short micro-pulse width less than 1 ps, during CNTs growth. In this report, as a first step, the SWNTs were tried to grow by thermal chemical vapor deposition (TCVD) method with dipped (Fe, Co)Pt catalysts.

The quartz substrate was ultrasonically cleaned in acetone and ethanol, Semico-Clean23(Furuuchi Chemical Corporation), and soaked in HF and HCl mixed acid solution. The  $0.05 \times 10^{-4}$  mol of Fe and Pt or Co and Pt was distributed in 1 mol methanol. The sources were  $\text{Fe}(\text{NO}_3)_3 \cdot 9\text{H}_2\text{O}$ ,  $\text{Co}(\text{NO}_3)_2 \cdot 6\text{H}_2\text{O}$ , and  $\text{Pt}(\text{acac})_2$ . The dipping speed was 60 or 600  $\mu\text{m/s}$ . The dipped specimens were annealed for 5 min at 450°C. The TCVD was carried out for 5 min on the annealed substrate at 800°C and 100 kPa with  $\text{Ar} : \text{H}_2 : \text{C}_2\text{H}_4 = 200 : 10 : 20$  ccm.

Figure 1(a) shows the scanning electron microscope (SEM) image after TCVD with FePt catalyst and 600  $\mu\text{m/s}$  dipping speed. The diameter of CNTs was between 20 and 40 nm. The Raman spectrum showed G-band peak. As shown in figure 1(b) the SEM image showed the diameter of CNTs was between 15 and 30 nm. However



(a) catalyst is FePt.

(b) Catalyst is CoPt.

Fig.1 SEM image of a difference in catalyst

the area where CNTs grew was limited. It is expected that the wetting property between catalytic solution and substrate is an important parameter.



## Effect of flow rate of ethanol on growth dynamics of VA-SWNT - Transition from no-flow CVD to normal ACCVD -

○Jun Okawa, Rong Xiang and Shigeo Maruyama

*Department of Mechanical Engineering, The University of Tokyo  
7-3-1 Hongo, Bunkyo-ku, Tokyo 113-8656, Japan*

Towards selective growth of SWNTs, it is important to know their growth mechanism. In previous studies, using optical absorbance technique, we have monitored the growth of vertically aligned single-walled carbon nanotubes (VA-SWNTs) [1] and obtained profiles of the VA-SWNT thickness with respect to the growth time, which was analyzed by suggesting a growth model [2].

In this study, the flow rate of ethanol during the CVD was controlled precisely. Figure 1 shows the growth curve of VA-SWNT film for various ethanol flow rates. In the figure, “No-flow” indicates that the supply of ethanol was stopped by sealing off the chamber during the reaction, when CVD was started. Normally, ACCVD is operated at flow rate of several hundred sccm. In that case, the growth rate of SWNT film decreases exponentially. On the other hand, for lower flow rate, the growth rate does not decrease with time and even increases in the case of 5sccm and 10sccm. However, after VA-SWNT film reaches certain thickness, the growth stops suddenly. The trend reflects the effect of ethanol decomposition in the growth mechanism of VA-SWNT using ACCVD method.

[1]. S. Maruyama, E. Einarsson, Y. Murakami and T. Edamura, Chem. Phys. Lett.403 (2005)320.

[2]. E. Einarsson, Y. Murakami, M. Kadowaki and S. Maruyama, Carbon, (2008).

Corresponding Author: Shigeo Maruyama E-mail: [maruyama@photon.t.u-tokyo.ac.jp](mailto:maruyama@photon.t.u-tokyo.ac.jp),

Tel/Fax: +81-3-5800-6983

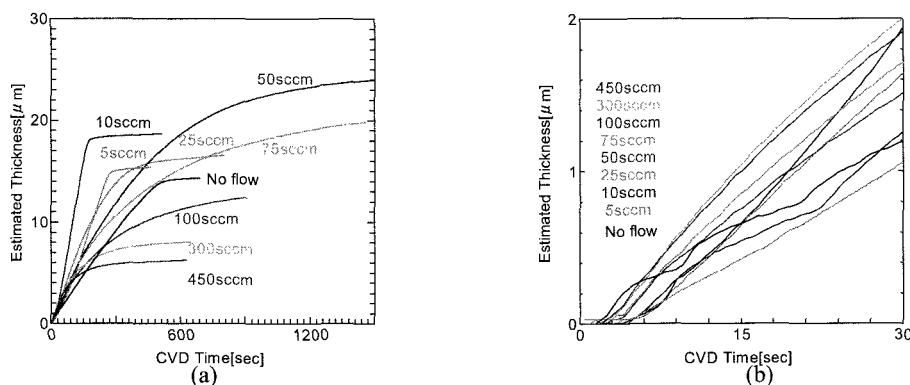


Fig. 1 Growth curve of VA-SWNT for different flow rate. (b) is a magnification of initial 30 s.

## Growth of Very-Thin Single-Wall Carbon Nanotubes by Catalyst-supported Chemical Vapor Deposition Using Surface-Treated Zeolites

○Keita Kobayashi<sup>1</sup>, Ryo Kitaura<sup>1</sup>, and Hisanori Shinohara<sup>1,2</sup>

<sup>1</sup>*Department of Chemistry, Nagoya University, Nagoya 464-8062, Japan*

<sup>2</sup>*Institute for Advanced Research, Nagoya University, and CREST/JST*

The catalyst-supported chemical vapor deposition (CCVD) by using nanometer-sized metal particles and porous catalyst supports such as zeolites has been extensively investigated as a promising method for growth of single-wall carbon nanotubes (SWNTs) [1]. In the CCVD growth of SWNTs, preparation of size-controlled metal catalyst nanoparticles is essential to realize diameter-controlled growth of SWNTs, in which the diameter of SWNTs depends primarily on the size of catalyst nanoparticles employed [2]. Ordered micropores of zeolites can provide us an ideal nano-space to prepare size-controlled metal catalyst nanoparticles. However, metal nanoparticles prepared using zeolites usually possess broad size distribution because of the formation of aggregates on the outer surface of zeolites. Thus, the SWNTs produced by the CCVD method have a large diameter distribution. Therefore, it is important to remove metal aggregates on the surface of zeolites for a diameter-controlled growth of SWNTs by CCVD. Here, we report SWNTs growth by CCVD using the zeolite which supports metal nanoparticles only within the micropores.

A zeolite supporting Rh or Co was prepared by H<sub>2</sub> reduction of the zeolites incorporating chlorides at 773 K Figure 1(a) shows a transmission electron microscopy (TEM) image of zeolite supporting Rh particles; The image shows many Rh particles aggregating on the surface. The zeolites supporting Rh or Co were refluxed at 353 K for 2 h with acetonitrile solution of Br<sub>2</sub>, and tetraethylammoniumbromide (TEAB) was used to remove the aggregates. Since, the molecular size of TEAB is larger than the diameter of the pore, the agent can remove only metals aggregating on the surface. Figure 1(b) shows zeolites supporting Rh, whose surface was similarly treated. The image indicates that no Rh aggregate exists on the surface. The CCVD was carried out at 973-1173 K for 10-60 s under an Ar gas flow. Figure 2 show SWNTs synthesized from Zeolite supporting Co. The SWNTs have diameter of ~0.75 nm corresponding size of the micropore.

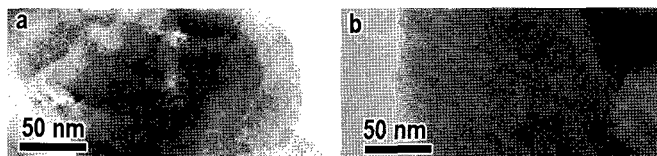


Fig.1 TEM image of zeolites supporting Rh (a) and surface-treated the zeolites (b)

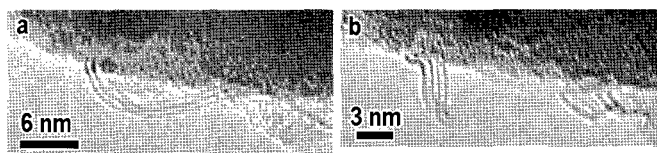


Fig.2 TEM image of SWNTs synthesized from zeolite supporting Co

[1] A. Okamoto et al., *Mol. Cryst. Liq. Cryst.*, **387**, 93 (2002).

[2] F. Ding et al., *J. Chem. Phys.*, **121**, 2775 (2004).

[3] A. Obuchi et al., Japan patent, P3049317 (2000).

Corresponding Author : Hisanori Shinohara

TEL: +81-52-789-2482, FAX:+81-52-789-1169, E-mail: noris@cc.nagoya-u.ac.jp

## Quantum response of carbon nanotube quantum dots to terahertz (THz) wave

<sup>o</sup>Seiko Toyokawa<sup>1,2</sup>, Tomoko Fuse<sup>1</sup>, Yukio Kawano<sup>1</sup>, Tomohiro Yamaguchi<sup>1</sup>,  
and Koji Ihibashi<sup>1,3</sup>

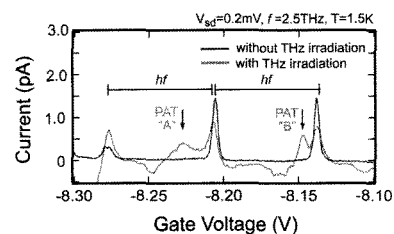
<sup>1</sup>Advanced Device Laboratory, RIKEN, Wako, Saitama 351-0198, Japan

<sup>2</sup>Department of Physics, Tokyo University of Science, Shinjuku, Tokyo 162-8601, Japan,

<sup>3</sup>CREST, JST, Kawaguchi, Saitama 332-0012, Japan

Single-wall carbon nanotubes (SWNTs) are attractive building blocks for quantum-dot based nanodevices<sup>1)</sup> because they have a very small diameter and an enough length to access with conventional electron beam lithography. Single quantum dots (QDs) are easily formed by depositing electrical contacts on top of an individual SWNT, and a whole SWNT in between the contacts behaves as a single quantum dot with a one-dimensional hard-wall potential. Important energy scales, associated with the QD, the single electron charging energy and the level spacing of confined states lie in a range from submillimeter to terahertz (THz) frequency, which is more than an order larger than those of conventional semiconductor QDs made with the electron beam lithography technique. These unique features have made us to expect a quantum response of the SWNT QD to the THz wave, a photon assisted tunneling. This may open up a new possibility for the ultra-sensitive THz detector.

Experiments were carried out by measuring low-temperature single electron transport under the irradiation of the THz wave to the SWNT QD, with changing THz frequency and power. Results with the 2.5THz irradiation at 1.5K is shown in the figure<sup>2)</sup>. Without the THz irradiation, typical Coulomb oscillations are observed with an alternate peak-to-peak distance, the even-odd effect. When the sample is irradiated, a complicated curve is observed with many features. Here, we focus on the new side peaks that do not appear when the sample is not irradiated. From the detailed analysis of the dot parameters, we conclude that the side peaks originate from the THz photon assisted tunneling (PAT) that occurs for an electron in a dot to tunnel out in the drain electrode. A frequency dependence is studied, and it was found that the distance between the main peak and the side peak varied linearly as the frequency was increased. A power dependence was also studied, and an indication of the Bessel-type behavior was observed<sup>3)</sup>. These observations confirm the THz wave was detected as a photon, not as a wave.



Figure

**References:** 1) K. Ihibashi et al., J. Vac. Sci. Technol. A **24** (4), 1349 (2006). 2) T. Fuse, et al., Nanotechnology **18**, 044001 (2007) 3) Y. Kawano, et al., J. Appl. Phys.

**Corresponding Author:** Koji Ihibashi **E-mail:** kishiba@riken.jp

**Tel:**048-462-1111 ext 8436 **Fax:** 048-462-4659

## Dispersion of Single-Wall Carbon Nanotubes by Thermostable Chitinases

○Takeshi Tanaka<sup>1</sup>, Hyekyeong Park<sup>1</sup>, Hehua Jin<sup>1</sup>, Tadayuki Imanaka<sup>2</sup>, Hiromichi Kataura<sup>1</sup>,

<sup>1</sup>Nanotechnology Research Institute, National Institute of Advanced Industrial Science and Technology (AIST), 1-1-1 Higashi, Tsukuba, Ibaraki 305-8562, Japan,

<sup>2</sup>Department of Synthetic Chemistry and Biological Chemistry, Graduate School of Engineering, Kyoto University, Katsura, Nishikyo-ku, Kyoto 615-8510, Japan

Besides applications of carbon nanotube (CNT) to electronics, medical applications attract a great deal of attention. When CNT is used as drug or drug carrier, CNTs modified by proteins which specifically bind the target molecules will be very useful. Although there were few reports that protein dispersed CNTs [1, 2], it was known that lysozyme disperse CNTs very well. Here we report a novel protein which can disperse CNTs. The protein is chitinase which degrades insoluble polysaccharides as well as lysozyme. In this study, we chose a chitinase from a hyperthermophilic microorganism which can grow even at 100°C, since the protein is very stable and suitable for applications. The chitinase (ChiA) has a unique domain structure comprising two catalytic domains (CD1 and CD2) and three chitin-binding domains (ChBD1~3) (Fig. 1). Various deletion mutants of ChiA (ChiA $\Delta$ 2~5, Fig. 1) were produced by conventional genetic engineering methods using *Escherichia coli* cells and then purified. The purified proteins and HiPco-CNT were used for CNT dispersion experiment. Among these mutants, ChiA $\Delta$ 2 composed of ChBD2, ChBD3 and CD2 showed the highest dispersibility of CNTs, suggesting that ChBD2 and/or ChBD3 play an important role in the dispersion. The details will be discussed at the presentation.

**References:** [1] D. Nepal and K. E. Geckeler, *Small*, 2006, **2**, 406, [2] K. Matsuura, T. Saito, T. Okazaki, S. Ohshima, M. Yumura and S. Iijima, *Chem. Phys. Lett.*, 2006, **429**, 497.

**Corresponding Author:** T. Tanaka, Tel: 029-861-2903, Fax: 029-861-2786, E-mail: tanaka-t@aist.go.jp

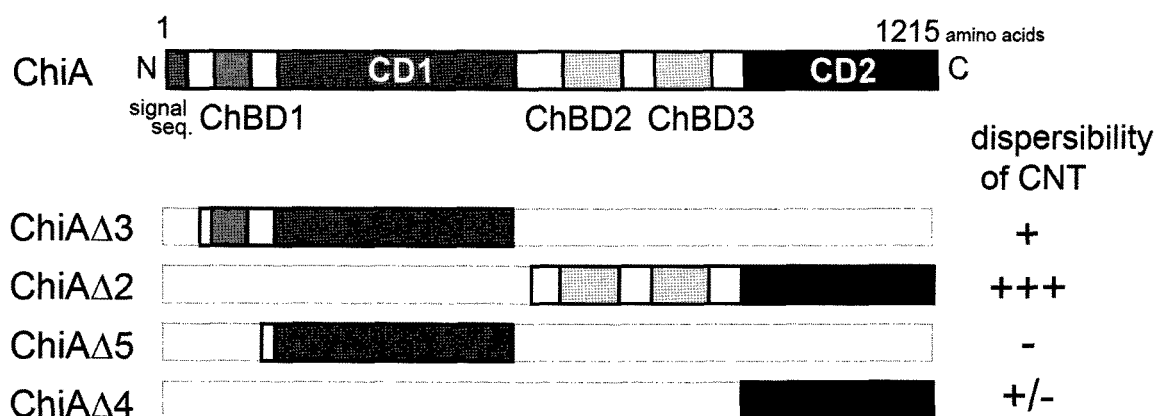


Fig. 1 Structural features of thermostable chitinase and its deletion mutants and their abilities of CNT dispersion.

## Carbon nanotube single electron transistors on a GaAs/AlGaAs 2-dimensional electron gas wafer

°Mitsutoshi Makihata<sup>1,2</sup>, Takahiro Mori<sup>1</sup>, Tomohiro Yamaguchi<sup>1</sup>, Yoshinobu Aoyagi<sup>1,2</sup>,  
and Koji Ihibashi<sup>1,3</sup>

<sup>1</sup>*Advanced Device Laboratory, RIKEN, Wako, Saitama 351-0198, Japan*

<sup>2</sup>*Interdisciplinary Graduate School of Science & Engineering, Tokyo Institute of  
Technology, 4259, Nagatsuta-cho, Midori-ku, Yokohama 226-8503, Japan*

<sup>3</sup>*CREST, JST, Kawaguchi, Saitama 332-0012, Japan*

Carbon nanotubes are attractive material for building blocks of nanodevices because of their extremely small diameter. So far, various nanodevices, such as single electron transistors (SETs) and field effect transistors (FETs), have been fabricated, and their basic operation has been demonstrated. When electronic systems with carbon-nanotube based nanodevices are considered, they may be combined with conventional semiconductor transistors. For example, essential parts of a circuit would be made of carbon nanotube, while interface parts to output would be consisting of conventional Si transistors. To explore the possibility of combining carbon nanotube nanodevices with conventional semiconductor devices, in this report, we fabricate SETs with single-wall carbon nanotubes (SWNTs) on a GaAs/AlGaAs wafer that contains the 2-dimensional electron gas (2DEG), widely used for the high electron mobility transistors (HEMTs).

SWNTs were dispersed on the 2DEG wafer from solution, and electrical contacts were fabricated to an individual SWNT<sup>1)</sup>. The surface gate and quantum point contact (QPC) were fabricated on the wafer (Fig). The transport measurements of the SWNT-SET were carried out at liquid helium temperatures, by changing either a potential of the 2DEG or the surface gate voltage.

We have succeeded in observing Coulomb oscillations as a function of the voltage on the 2DEG. The appearance of the oscillations were switched on and off by controlling the voltage on the QPC that depleted electrons underneath it. In this case, the role of the QPC is to electrically separate the 2DEG under the SWNT-SET and the 2DEG where the voltage is applied. The effect could be useful for coupled quantum-dot systems where a controlled coupling among dots may be needed.

We also measured Coulomb oscillations as a function of the surface gate, and have made clear the mechanism of the surface gating in association with the 2DEG.

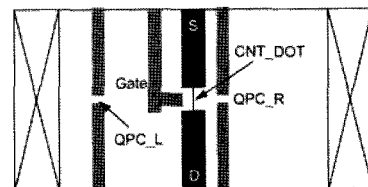


Figure: Schematic picture of the sample structure

**References:** 1) T. Tsukamoto, et al., J. Appl. Phys., **98**, 076106 (2005)

**Corresponding Author:** koji Ihibashi **E-mail:** kishiba@riken.jp

**Tel:**048-467-9366 **Fax:** 048-462-4659

### Inhibitory Effect of Carboxymethylcellulose Wrapping on the Oxidation of Single-walled Carbon Nanotubes Induced by Acidification

○Toru Ishii, Katsumi Uchida, Tadahiro Ishii and Hirofumi Yajima

*Department of Applied Chemistry, Faculty of Science, Tokyo University of Science  
12-1 Funagawara-machi, Shinjyuku-ku, Tokyo 162-0826, Japan*

A numerous of studies have been made with regard to extensive fundamentals and application of single-walled carbon nanotubes (SWNTs) because of high performance and multifunctional nanomaterials with unique and promising characteristics. For a basal aspect, the optical properties of dispersed SWNTs with some dispersants, such as sodium dodecylsulfate (SDS) and DNA, etc., in aqueous solutions have been well known to be significantly affected by acidification, depending on the chiralities of SWNTs.<sup>1,2)</sup> In particular, the acidification is observed to give rise to the diminution of the S<sub>11</sub> transition of the semiconducting SWNTs in the NIR wavelength range (1000-1600 nm). This behavior is interpreted in terms of the change in the electric transitions due to nanotube oxidation or hole-delocalization involving dissolved oxygen. However, definite information on the roles of dispersants in the pH effects has been not yet obtained. On the other hand, for an interesting biological application of SWNTs, N. W. S. Kam et al.<sup>3)</sup> proposed the utility of the NIR optical feature of SWNTs as multifunctional transporters for photodynamic therapy. Correlatively, the investigation of the pH effect is significantly involved in further development of biomaterials with SWNTs. The objective of this study is to probe the pH effect on the physicochemical characteristics of the dispersed SWNTs over a wide range of pH 1-14, using SDS and carboxymethylcellulose (CMC) as dispersants with alternately different adsorption structures.

#### Reference

- 1) Kristy Kelley, Pehr E. Pehrsson, Lars M. Ericson, and Wei Zhao, *J. Nanosci.. Nanotech.* **5** (2005) 1041-1044
- 2) M. S. Strano, C. A. Dyke, V. C. Moore, M. J. O'Connell, E. H. Haroz, J. Hubbard, M. Miller, K. Rialon, C. Kittrell, S. Ramesh, R. H. Hauge, R. E. Smally, *J. Phys. Chem. B* **107**, 6979 (2003)
- 3) Nadine Wong Shi Kam, Michael O'Connell, Jeffrey A. Wisdom, and Hongjie Dai, *PNAS* **102** (2005) 11600-11605

**Corresponding Author:** Hirofumi Yajima

TEL: +81-3-3260-4272(ext.5760), FAX: +81-3-5261-4631, E-mail: [yajima@rs.kagu.tus.ac.jp](mailto:yajima@rs.kagu.tus.ac.jp)

## Manipulation and Observation of Carbon Nanotubes in Microfluidic Chip Under Optical Microscope

○Naoki Inomata, Yoko Yamanishi, Fumihito Arai

*Department of Bioengineering and Robotics, Tohoku University*

**Abstract:** We demonstrate a visualization system of carbon nanotubes (CNTs) in water under the optical microscope using quenching phenomenon. Quenching phenomenon cause a decrease of fluorescent intensity around CNTs. With this method, we can observe CNTs continuously for a long time by supplying proper amount of fluorescent reagent. To get clear image of CNTs, we have to adjust the density of fluorescent reagent around CNTs precisely, however, it is extremely difficult to control proper condition of the reagent. Therefore, we propose a novel on-demand supplying system of fluorescent reagent in a microfluidic chip. CNTs are trapped around ITO (Indium Tin Oxide) electrodes by dielectrophoretic force. We have found that a porous structured PDMS support can adsorb fluorescent reagent as a carrier and supply reagent in high density and almost constantly for a long time. Moreover, we have mixed a couple of fluids in the chip using a micro-stirrer. With this method, we can mix different fluids uniformly and succeeded in controlling density of fluorescent reagent. Finally, we fixed CNTs around ITO electrodes by dielectrophoretic force, and observed CNTs in the solution on real time under the optical microscope. The fluorescent image of the CNTs was clearer than the bright-field image of them.

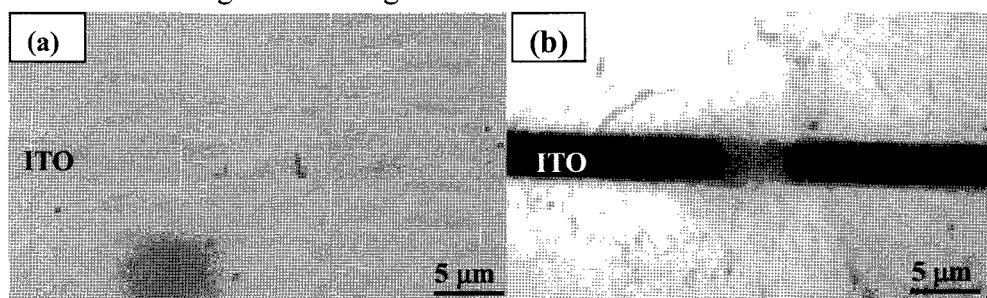


Fig. 3 (a) Bright-field image (b) fluorescent image. CNTs are attached around ITO electrodes by dielectrophoresis.

**References:** F. Arai et al., Observation of carbon nanotubes in water by supplying fluorescent reagent with porous structured PDMS support, Proc.MHS2007, IEEE, p43

**Corresponding Author:** Naoki Inomata, Tohoku University

**E-mail:** inomata@imech.mech.tohoku.ac.jp

**TEL:** +81-22-795-6968, **FAX:** +81-22-795-7035

### Purification and Physicochemical Properties of Double-Walled Carbon Nanotubes

○Noriko Maeda, Katsumi Uchida, Tadahiro Ishii, and Hirofumi Yajima

*Department of Applied Chemistry, Faculty of Science, Tokyo University of Science  
12-1 Funagawara-machi, Shinjyuku-ku, Tokyo 162-0826, Japan*

Recently, double-walled carbon nanotubes (DWNTs) have attracted a great deal of attention in their specific optical properties and possible technological applications in various fields of science because of the possession of advantageous features of both single- (SWNTs) and multi-walled carbon nanotubes (MWNTs), such as electric and thermal stabilities. However, the procedures of the isolation and purification of DWNTs has been not yet established, and thus, a definite information on the physicochemical characteristics of DWNTs has been not almost obtained. This study is concerned with the development of effective purification methods for DWNTs without few damage, and then, with the investigation of the physicochemical properties. We have proposed three kinds of treatment methods for the purification, that is, chemical oxidation, centrifugation, and heat treatment.

DWNTs from Carbon Nanotechnologies Inc. were used without further purification. The chemical oxidation was made for the DWNTs with 3:1 concentrated  $\text{H}_2\text{SO}_4/\text{HNO}_3$  mixtures (96 % and 69~70 % , respectively) under the sonication in a bath-type sonicator at 50 °C for appropriate time, giving rise to the carboxylation for the DWNTs. The centrifugation treatment was made for the dispersed DWNTs with carboxymethylcellulose (CMC) as a dispersant, adjusting an adequate condition of centrifugal forces and times for the separations of SWNTs and MWNTs. The heat treatment in air for 0.5h was made for the DWNTs annealing at several temperature in the range of 300-600 °C with electric muffle furnace. The samples were characterized by various spectroscopic techniques such as FT-IR, UV-vis near-infrared (NIR) absorption, photoluminescence (PL), resonance Raman spectroscopy, and transmission electron microscopy (TEM). The purity was evaluated by the TEM observations and quality parameters ( $= 1 - D/G$ ) determined from Raman measurements. We have obtained the results from TEM observations and Raman measurements that centrifugation procedures promoted the purity of DWNTs. The detailed results including those for the other treatment procedures will be presented and discussed in the symposium. At present, further studies of the physicochemical properties of the DWNTs are under the progress with structural characterization techniques such as AFM, DLS, and  $\zeta$ -potential measurements.

**References** : [1]T.Takahashi et al. *Jpn.J.Appl.Phys* **43** (2004) 3636

[2]J.Liu et al. *Science* **280** (1998) 1253

**Corresponding Author** : Hirofumi Yajima

**E-mail** : yajima@rs.kagu.tus.ac.jp

**Tel** : +81-3-3260-4272 (ext.5760) , **Fax** : +81-3-5261-4631



## Effects of the neutral Ar beam irradiation to the random-network single-walled carbon nanotube field effect transistors

Shunsuke Sato<sup>1,2,\*</sup>, Takahiro Mori<sup>1</sup>, Kazuo Omura<sup>1,3</sup>, and Koji Ishibashi<sup>1,4</sup>

- 1) Advanced Device Laboratory, RIKEN, Wako, Saitama, Japan
  - 2) Department of Physics, Tokyo University of Science, Shinjuku-ku, Tokyo, Japan
  - 3) Department of Applied Chemistry, Tokyo University of Science, Shinjuku-ku, Tokyo, Japan
  - 4) CREST, Japan Science and Technology (JST), Kawaguchi, Saitama, Japan
- \*) shunsuke917@riken.jp, phone:+81-(0)48-462-1111, fax:+81-(0)48-462-4659

Single-walled carbon nanotube field effect transistors (SWNT-FETs) have been attractive because they have the high potential in the field of electronics. There are three kinds of SWNT-FETs. One is an individual SWNT-FET, which demonstrated an extremely high mobility of  $79000 \text{ cm}^2\text{V}^{-1}\text{s}^{-1}$  [1]. Two is a so-called multi-channel SWNT-FET [2], which consists a number of parallel SWNTs between source and drain contacts to obtain high current, promising for the application of large scale integrated (LSI) circuits. Three is a random-network SWNT-FET [3], which consists a large number of SWNTs randomly distributed between source and drain contacts. The random-network SWNT-FET has a lower mobility than the individual SWNT-FET, however, it can be easily fabricated by a solution process, so promising for the lower cost application such as flexible devices like the organic FETs. One of important common problems in their SWNT-FETs is hysteresis caused from various charge traps induced by contaminations on the SWNT [4]. In this presentation we report effects of the neutral Ar beam irradiation to the random-network SWNT-FETs. The neutral Ar beam irradiation process can reduce hysteresis and enhance the n-type character of the random-network SWNT-FETs.

The random-network SWNT-FETs were fabricated on  $\text{SiO}_2/\text{Si}$  substrates by a solution process with a individually dispersed SWNT suspension using a surfactant, sodium dodecylsulfate. The suspension was sonicated and centrifuged. The oxide thickness was 200nm. The Pd source and drain contacts were fabricated on the random-network SWNTs by lift-off process and the channel length and width were  $1\mu\text{m}$  and  $3\mu\text{m}$ , respectively. The SWNTs outside the FET structure were burned out by oxygen plasma with the protection of the channel by resist. The neutral Ar irradiation was carried out with the low acceleration energy of 10eV.

Before the irradiation the SWNT-FET showed hysteresis of about 1.6V in gate characteristics in the range of -10V to 10V. After the irradiation the hysteresis was reduced up to about 0.6V in the same range. Furthermore, the enhancement of the n-type character was observed in the ambipolar SWNT-FET with the 10 times higher electron current than the one before the irradiation. These results suggest that the irradiation reduced contaminations on the SWNTs, such as organics like residual surfactant molecules or oxygen molecules which caused the p-type character of the SWNT-FETs.

- [1] S. Heinze et al., Phys. Rev. Lett. 89, 106801(2002).
- [2] R. Seidel et al., Nano Lett. 4, 831(2004).
- [3] E. S. Snow et al., Appl. Phys. Lett. 82, 2145(2003).
- [4] for example, W. Kim et al., Nano Lett. 3, 193(2003).

### Theoretical Analysis on Ion Permeation Mechanism through an Anion-Doped Carbon Nanotube

○Takashi Sumikama<sup>1</sup>, Shinji Saito<sup>2</sup>, and Iwao Ohmine<sup>1</sup>

<sup>1</sup> *Department of Chemistry, Faculty of Science, Nagoya University*

<sup>2</sup> *Department of Theoretical and Computational Molecular Science, Institute for  
Molecular Science, and The Graduate University for Advanced Studies*

The transport and storage of materials in confined space and nanopore have been extensively studied. In addition to the material science, biological pores, aquaporin and ion channels, have been extensively investigated. However, the dynamics of the transport of materials is still unclear.

We investigated the dynamics of ion permeation through an anion-doped carbon nanotube (ANT) by molecular dynamics simulation. The free energy, energy, and entropy profiles about ion permeation are calculated. The analysis of the free energy profile shows that there are two ions in ANT in the most stable state (S2 state). It is found that the entropy term stabilizes the S2 state. We analyzed the molecular origin of the entropy term in the S2 state in 2PT method.<sup>1</sup>

There is a high free energy barrier at the entrance of ANT, i.e., the rate-limiting step is the entering of an ion into ANT.<sup>2</sup> The present study shows that the free energy barrier mainly arises from the entropy. Therefore, the entire process of ion permeation is dominated by the entropy. We further analyzed the origin of high entropy at the entrance of ANT.

1. S.-T. Lin, M. Blanco, and W. A. Goddard III, *J. Chem. Phys.*, 119, 11792 (2003).

2. T. Sumikama, S. Saito, and I. Ohmine, *J. Phys. Chem. B*, 110, 20671 (2006).

**Corresponding Author:** Iwao Ohmine

**E-mail:** [ohmine@aquachem.nagoya-u.ac.jp](mailto:ohmine@aquachem.nagoya-u.ac.jp)

**Tel&Fax:** 052-789-2481 & 052-789-3551

## Recovery process of low-energy irradiation damage of SWNTs

○Kenji Yamaya<sup>1,3</sup>, Satoru Suzuki<sup>1,2</sup>, Yoshikazu Homma<sup>2,3</sup>, Yoshihiro Kobayashi<sup>1,2</sup>

<sup>1</sup>*NTT Basic Research Laboratories, Nippon Telegraph and Telephone Corporation, Atsugi, Kanagawa 243-0198, Japan*

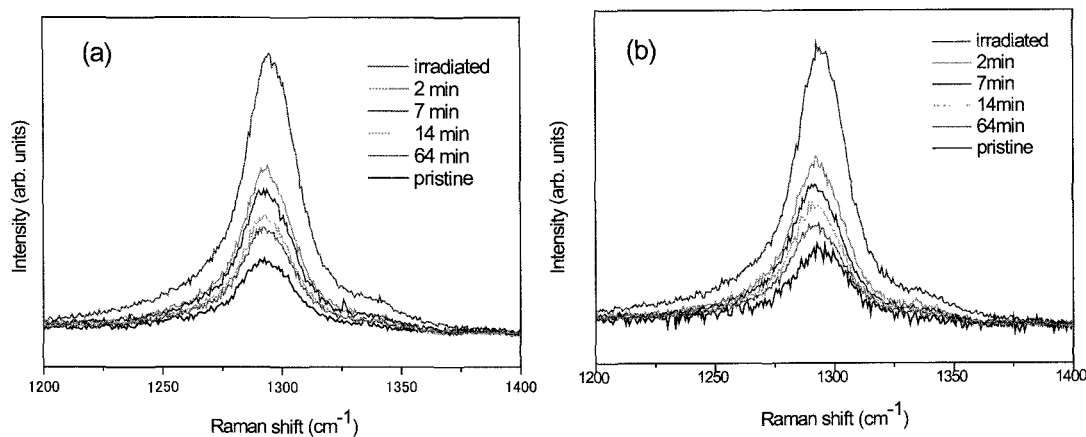
<sup>2</sup>*CREST/JST, Japan Science and Technology Corporation*

<sup>3</sup>*Department of Physics, Tokyo University of Science, Japan*

SWNTs are damaged by low-energy (6 eV [1]-20 keV) irradiation, and the damage and recovery are reversible [2,3]. In this work, we studied the recovery process of the low-energy irradiation-induced damage by means of Raman spectroscopy.

Two SWNT samples showing almost the same Raman spectra were grown by the ethanol CVD method. Both samples were irradiated by 20 keV-electrons to a dose of  $8 \times 10^{16} \text{ cm}^{-2}$ . After the irradiation, one sample was annealed for a certain time in Ar atmosphere at 220 °C and the other at 240 °C, respectively. Raman measurements were performed after the samples were cooled down to room temperature.

Figure 1 shows D-band spectra of pristine SWNTs and of SWNTs annealed at 220 and 240 °C following the irradiation. The annealing temperature difference of 20 K caused a substantial difference in the recovery speed. The activation energy of the defect healing can be evaluated from the results.



**Fig. 1.** D-band spectra of pristine SWNTs and of SWNTs annealed at (a) 220 and (b) 240 °C following the electron irradiation. The excitation wavelength was 785 nm.

### References:

- [1] S. Suzuki and Y. Kobayashi, submitted to Jpn. J. Appl. Phys. 47 (4B) (2008).
- [1] S. Suzuki and Y. Kobayashi, Mater. Soc. Symp. Proc. 994, F04-02 (2007).
- [2] S. Suzuki and Y. Kobayashi, J. Phys. Chem. C 111, 4524 (2007).

Corresponding Author: Satoru Suzuki (E-mail: ssuzuki@will.brl.ntt.co.jp)

Tel: +81-46-240-4711, Fax: +81-46-240-4711

## Synthesis of SWNTs by FH-arc method and Evaluation of SWNTs by Raman spectroscopy

○ B. Chen<sup>a</sup>, S. Inoue<sup>a</sup>, T. Hashimoto<sup>b</sup>, and Y. Ando<sup>a</sup>

<sup>a</sup>21<sup>st</sup> COE Program “Nano Factory”, Department of Material Science & Engineering,  
Meijo University, Tenpaku-ku, Nagoya 468-8502, Japan

<sup>b</sup>Meijo Nano Carbon Co., Ltd., Naka-ku, Nagoya 460-0002 Japan

Single-walled carbon nanotubes (SWNTs) with high crystallinity have been synthesized by a hydrogen DC arc discharge with evaporation of carbon anode containing 1at% Fe catalyst in H<sub>2</sub>-Ar mixture gas (FH-arc method) [1]. It is also very clear that some impurities such as metal particles and amorphous carbon coexist in the SWNTs soot. In order to obtain high quality of SWNTs, various purification methods such as annealing, oxidation by some oxidant have been attempted. As we concentrate on obtaining the high purity SWNT sample, unexpectedly, double-walled carbon nanotube (DWNTs) have been observed in these samples. However, it is necessary to make clear that whether DWNTs have been existed in the as-grown SWNTs soots.

In this study, we have precisely examined the preparation of SWNTs by changing synthesis conditions with FH-arc method. Synthesized SWNTs were characterized by Raman spectroscopy (Ar<sup>+</sup> laser, 514 nm) and by scanning probe microscopy (SPM). Fig. 1 shows the SPM image of purified SWNTs. Fig. 2 shows the Raman spectra of the as-grown SWNTs soot on a condition (Ar+H<sub>2</sub>: 200Torr, dc current: 70A).

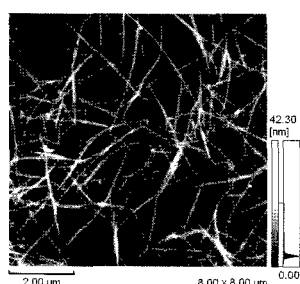


Fig. 1 SPM image of purified SWNTs

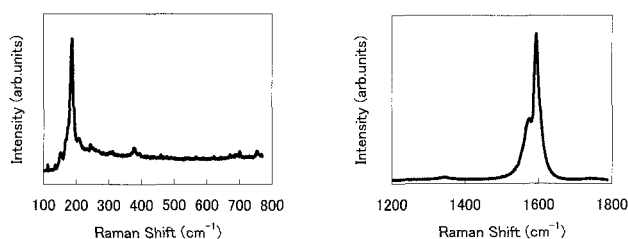


Fig. 2 Raman spectra of the as-grown SWNTs soot

Reference: [1] X. Zhao, et al., *Chem. Phys. Lett.*, **373**, 266-271 (2003)

Corresponding Author: Beibei Chen

Tel: +81-52-838-2409, Fax: +81-52-832-1170

E-mail: m0641507@ccmailg.meijo-u.ac.jp

## Long-range Electron Transfer through a Single-walled Carbon Nanotube Sheet

○Takeshi Saito<sup>1,2</sup>, Koji Matsuura<sup>3</sup>, Satoshi Ohshima<sup>1</sup>, Shigekazu Ohmori<sup>1</sup>,  
Motoo Yumura<sup>1</sup> and Sumio Iijima<sup>1,4</sup>

<sup>1</sup> *Research Center for Advanced Carbon Materials, AIST, Tsukuba 305-8565, Japan*

<sup>2</sup> *PRESTO, Japan Science and Technology Agency, Kawaguchi 332-0012, Japan*

<sup>3</sup> *Cardiovascular Physiology, Graduate School of Medicine, Dentistry and Pharmaceutical Sciences, Okayama Univ., Okayama 700-8558, Japan.*

<sup>4</sup> *Department of Materials Science and Engineering, Meijo Univ., Nagoya 468-8502, Japan*

In mitochondria, electron transfer (ET) is the mechanism by which chemical energy is produced in the form of ATP by the use of powerful reducing reagents such as NADH.<sup>[1]</sup> Simplified ET systems can function as redox-driven biomachines and/or compact bioreactors for the production of chemicals such as industrial materials and drugs.<sup>[1]</sup> This ET reaction in biological systems is often compared to that in a conductive nanowire. A single-walled carbon nanotube (SWNT) is one of the typical nanowires with an affinity for biomolecules such as proteins.<sup>[2]</sup> Recent reports suggest that the chemical oxidation and reduction of semiconductive SWNTs were observed by photobleaching of the bandgap transition.<sup>[3]</sup> The possibility of a SWNT-mediated ET between the reductant and the reduced material was also proposed on the basis of the redox properties of SWNTs.<sup>[3]</sup>

In this study, we have constructed an SWNT-mediated ET system (Fig. 1A) with an aim to realizing an effective bio-inspired reactor with large physical dimensions (several millimeters). Reductants supply electrons to the SWNTs that transfer and donate electrons to the acceptor molecules. Dithionite and cytochrome *c* (cyt *c*) were used as the reductant and acceptor, respectively. At this symposium, we will report on the reduction kinetics of cyt *c* in this system in detail by analyzing the optical absorption spectra parametrically.

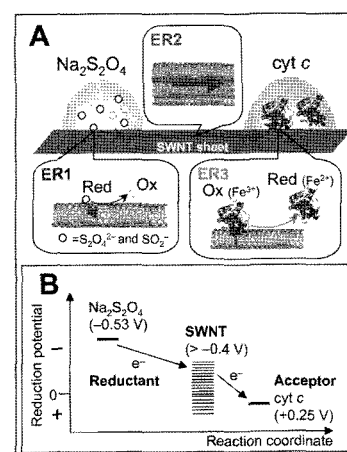
[1] M. Saraste, *Science* 1999, 283, 1488–1493.

[2] K. Matsuura, T. Saito, T. Okazaki, S. Ohshima, M. Yumura, S. Iijima, *Chem. Phys. Lett.* 2006, 429, 497–502.

[3] M. Zheng, B. A. Diner, *J. Am. Chem. Soc.* 2004, 126, 15490–15494.

Corresponding Author: Takeshi Saito

TEL: +81-29-861-4863, FAX: +81-29-861-3392, E-mail: takeshi-saito@aist.go.jp



**Figure 1. A:** The SWNT-mediated ET system showing reactions from dithionite to ferric cyt *c*. The green arrows indicate the direction of the ET. The numbers indicate the elementary reactions (ERs). **B:** Reduction potential of the acceptor, SWNT, and the reductant used in this study. The reaction coordinate is the ET process in the system.

## Diameter evaluation of multi-walled carbon nanotubes using SEM images

○Tohru Kawamoto, Hamazo Nakagawa, Takashi Muranaka,  
Atsuhiko Kunishige, and Yoshiyuki Sumiyama

*UBE Scientific Analysis Laboratory, Inc., Kogushi, Ube, Yamaguchi 755-8633, Japan*

In the multi-walled carbon nanotube (MWCNT) materials, the material properties such as electrical conductivity, thermal conductivity and strength have close relations to the geometrical properties of the tubes. Transmission electron microscopy (TEM) [1], X-ray diffraction (XRD) analysis[2] and scanning electron microscopy (SEM) have been used to evaluate the diameters of MWCNTs. SEM is widely used among them, and it allows to evaluate the distribution of tube diameters.

Figure 1 shows a SEM image of as-received MWCNTs produced by Shenzhen Nanotech Port Co., Ltd. The tubes have various diameters both throughout the sample and within the lengths of individual tubes. Because the tubes were not dispersed, it was difficult to evaluate the tube diameter by rule.

In this study, we have tried to evaluate the tube diameters from the SEM images of individually dispersed MWCNTs on a substrate. One of the SEM images is shown in Fig.2. Tubes having various diameters and lengths are observed.

We measured tube diameters at regular intervals of 0.5 microns along each tube length. Figure 3 shows the distribution of measured diameters. An average diameter and a standard deviation have been calculated to be 31nm and 11nm respectively.

**References:**[1]M. Endo et al.: J. Phys. Chem. Solids 58 (1997) 1707.

[2] A. Kunishige et al.: The 32<sup>nd</sup> Fullerene Nanotubes General Symposium, (2006) 167.

**Corresponding Author:** Tohru Kawamoto

**E-mail:** tooru.kawamoto@ube-ind.co.jp

**Tel&Fax:** +81-836-31-0987, +81-836-31-0956

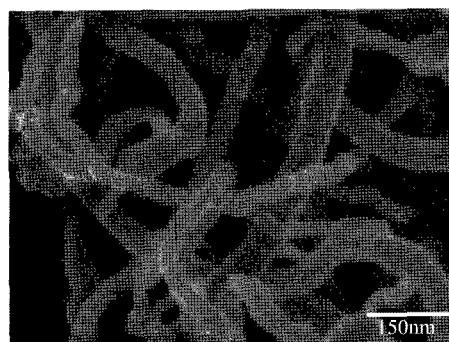


Fig.1 SEM image of as-received MWCNTs



Fig.2 SEM image of dispersed MWCNTs on a substrate

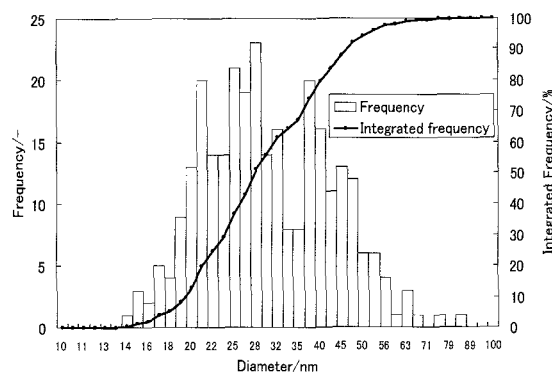


Fig.3 Diameter distribution of MWCNTs

## Saturation of Photoluminescence from Carbon Nanotubes at High Laser Intensities: Exciton-Exciton Annihilation near the Mott Density

○Yoichi Murakami, Junichiro Kono

Rice University, Dept. of Electrical and Computer Engineering,  
6100 Main St., Houston, TX 77005 USA

Nonlinear photoluminescence excitation (PLE) spectroscopy of individualized carbon nanotube ensembles has been carried out using wavelength-tunable femtosecond optical pulses. All the PL features we examined were seen to saturate at high laser fluence irrespective of the excitation wavelength. As the fluence was increased from the linear to the saturation regime, we found that excitation resonances at E22 energies gradually broadened and eventually became completely flat, where the PL intensity became independent of the excitation wavelength (Fig. 1).

Through absorption spectroscopy at high laser intensities, we demonstrated that *state-filling or strong scattering is not the cause of the observed flattening of the excitation spectra*. We developed a model to explain these observations by carefully taking into account the spatial overlap of excitons in the exciton-exciton annihilation process. The developed model shows an excellent agreement with the observed saturation behavior as shown by Fig. 2 up to near the Mott density, where the average inter-exciton distance approaches the Bohr radius. *Based on the saturation curve analysis, we estimated for the first time the density of excitons in carbon nanotubes for the nonlinear regime extended up to near the Mott density.*

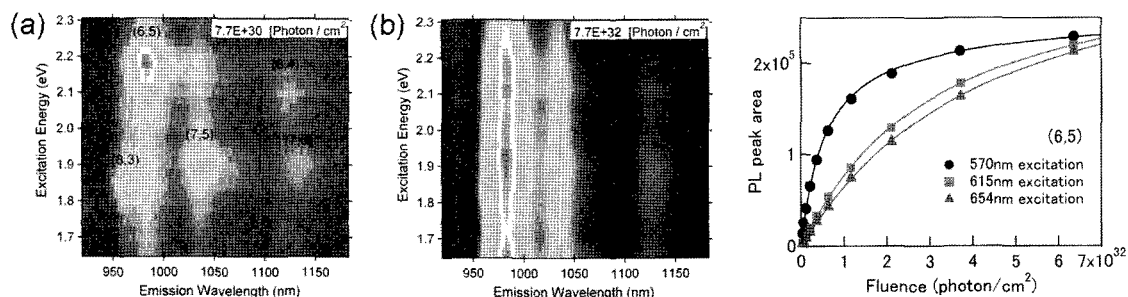


Fig. 1. PLE maps for the (a) linear ( $7.7E30$  photon/cm<sup>2</sup>) and (b) saturated ( $7.7E32$  photon/cm<sup>2</sup>) regimes. (Sample: micelle-suspended CoMoCAT in D<sub>2</sub>O)

Fig. 2. Dependence of the PL peak area of (6,5) tubes on the laser fluence at various excitation wavelengths. Solid lines are the behaviors fitted by the developed model.

Corresponding Author: Junichiro Kono

E-mail: kono@rice.edu

Tel: +1 (713) 348-2209 Fax: +1 (713) 348-5686

## Growth and characteristics of $^{13}\text{C}$ enriched carbon nanotubes

<sup>o</sup>Nobuyuki Yamazaki<sup>1,2</sup>, Ryo Hashiba<sup>1,2</sup>, Manabu Oie<sup>1,3</sup>, Yuichi Ochiai<sup>2</sup>,  
Tomohiro Yamaguchi<sup>1</sup>, and Koji Ihibashi<sup>1,4</sup>

<sup>1</sup>Advanced Device Laboratory, RIKEN, Wako, Saitama 351-0198, Japan

<sup>2</sup>Department of Nanomaterial Science, Chiba University, Inage, Chiba 263-8522, Japan

<sup>3</sup>Department of Physics, Tokyo University of Science, Shinjuku, Tokyo 162-8601, Japan,

<sup>4</sup>CREST, JST, Kawaguchi, Saitama 332-0012, Japan

Carbon nanotubes (CNTs) have been attracting considerable attentions as a building block of nanoscale devices. One of the most intriguing features of CNTs is their small size beyond a limit of conventional lithography techniques, which makes it possible to realize various small single-electron devices. CNTs are usually consists of  $^{12}\text{C}$  atoms which have no nuclear spins. To investigate the effect of nuclear spins on transport properties of CNT quantum dots, we grew  $^{13}\text{C}$ -enriched CNTs ( $^{13}\text{CNTs}$ ) and made Raman, NMR, and electronic transport measurement to characterize the  $^{13}\text{CNTs}$ .

$^{13}\text{CNT}$  was grown by the alcohol catalytic chemical vapor deposition (CVD) technique using cobalt as catalyst. We use commercial ethanol with natural abundance of  $^{13}\text{C}$  (1.1 %),  $1,2\text{-}^{13}\text{C}_2$  ethanol (99 %) and three kinds of their blends with different  $^{13}\text{C}$  contents (24 %, 48 % and 74 %) as carbon sources for CVD growth. From the Raman spectroscopy in the radial breathing mode region, these  $^{13}\text{CNT}$  samples are confirmed to be singles walled and the diameter is in range of 0.7 nm ~ 1.9 nm.

Figure 1 shows the Raman spectra from five different samples in the wave number range of the G-band and D-band peaks at room temperature. It is obvious that the peak positions of the both G- and D-band shift downwards with increasing  $^{13}\text{C}$  content in  $^{13}\text{CNTs}$ . The peak positions show a good agreement with the calculated Raman shift using the formula in Ref. 1 suggesting that the  $^{13}\text{C}$  content of  $^{13}\text{CNT}$  can be controlled by the  $^{13}\text{C}$  content of the ethanol.

The spin-lattice relaxation time  $T_1$  and the spin-spin relaxation time  $T_2$  are evaluated from magic angle spinning  $^{13}\text{C}$  NMR spectroscopy. For  $^{13}\text{CNT}(48\%)$ , we obtain  $T_{1\text{fast}} = 626\ \mu\text{s}$ ,  $T_{1\text{slow}} = 3.8\ \text{ms}$  and  $T_2 = 616\ \mu\text{s}$ .

Resently, we have succeeded to observe the quantum dot features of  $^{13}\text{CNT}(99\%)$  at low temperatures. Detailed studies of the effect of  $^{13}\text{C}$  nuclear spins on the transport properties of CNT quantum dots are now in progress.

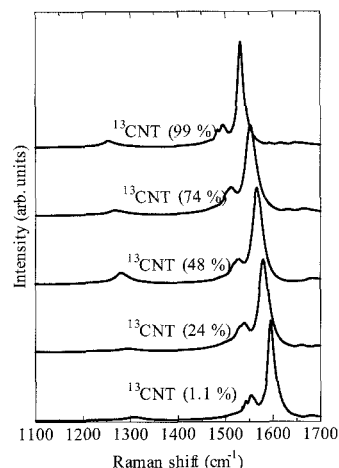


Figure 1  
Raman spectra for five  
kinds of  $^{13}\text{CNTs}$ .

**References:** 1) F. Simon, et al., Phys. Rev. Lett. **95** (2005) 017401.

**Corresponding Author:** Nobuyuki Yamazaki **E-mail:** nob-yamazaki@riken.jp

**Tel:**048-462-1111 ext 8437 **Fax:** 048-462-4659



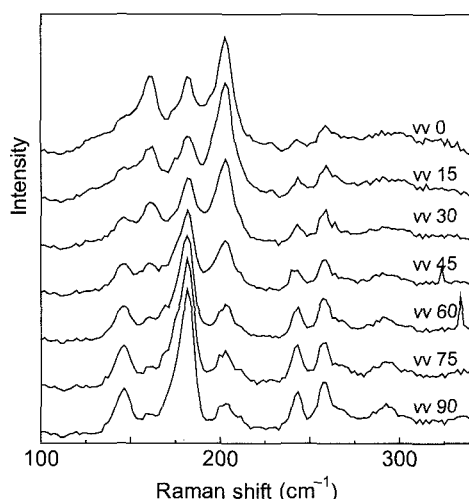
## Polarized Raman Spectroscopy of Vertically Aligned Single-walled Carbon Nanotubes

○ Zhengyi Zhang, Yuhei Miyauchi, Erik Einarsson, Shigeo Maruyama  
*Department of Mechanical Engineering, The University of Tokyo*

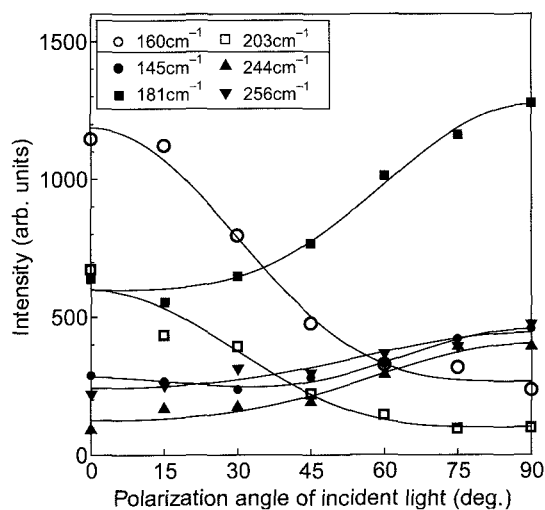
Recently, we have prepared up to 30  $\mu\text{m}$  thick vertically aligned single-walled carbon nanotube (VA-SWNT) films with high purity by the alcohol catalytic CVD method [1]. Previous polarized Raman spectroscopy studies [2] showed that the peak around  $180\text{ cm}^{-1}$  is very strong at 488 nm excitation for incident light polarized perpendicular to the tube growth direction, but diminishes for parallel polarization. Recent high-resolution Raman measurements revealed that this strong peak is composed of four separate sharp peaks and disappear when the VA-SWNT film is dispersed. Additionally, we found that the films are comprised primarily of small bundles, typically fewer than ten SWNTs [3], which inspired us to investigate the origin of the  $180\text{ cm}^{-1}$  peak.

Polarized Raman experiments were carried out with two configurations, where the orientation of the polarizer for inspecting the scattered light is parallel (VV) or perpendicular (VH) to the incident light polarization. By changing the angle of the incident light with respect to the VA-SWNT growth direction, two different polarization dependences were found for the RBM peaks (Fig. 1). The peaks at  $160\text{ cm}^{-1}$  and  $203\text{ cm}^{-1}$  behave consistently with the “antenna effect”, where optical spectra are dominated by absorption/emission of light polarized parallel to the tube axis. However, peaks at  $145\text{ cm}^{-1}$ ,  $181\text{ cm}^{-1}$ ,  $244\text{ cm}^{-1}$  and  $256\text{ cm}^{-1}$  exhibit the opposite behavior in the VV configuration (Fig. 2), which may due to the cross polarized excitation/emission process or the presence of isolated tubes within the array.

- [1] Y. Murakami, S. Chiashi, Y. Miyauchi, M. Hu, M. Ogura, T. Okubo, S. Maruyama: *Chem. Phys. Lett.* **385** (2004) 298.  
 [2] Y. Murakami, S. Chiashi, E. Einarsson, S. Maruyama: *Phys. Rev. B* **71** (2005) 085403.  
 [3] E. Einarsson, H. Shiozawa, C. Kramberger, M. H. R ummeli, et al.: *J. Phys. Chem. C* **111** (2007) 17861.  
 Corresponding author: Shigeo Maruyama E-mail: maruyama@photon.t.u-tokyo.ac.jp, Tel/Fax: +81-3-5800-6983



**Fig. 1.** Raman spectra of a VA-SWNT film in the VV configuration, and changing the incident polarization from  $0^\circ$  (along alignment direction) to  $90^\circ$  (perpendicular to the alignment direction).



**Fig. 2.** RBM Peak intensity changes for incident light polarization from  $0^\circ$  to  $90^\circ$  with respect to the VA-SWNT growth direction (VV configuration).

## Molecular dynamics of phonon relaxation of an SWNT

○Minetaka Nishimura, Junichiro Shiomi and Shigeo Maruyama\*

*Department of Mechanical Engineering, The University of Tokyo  
7-3-1 Hongo, Bunkyo-ku, Tokyo 113-8656, Japan*

SWNT is expected to have large thermal conductivity, therefore suggested for thermal devices. This has motivated extensive researches on thermal conductivity of SWNT using both experimental and numerical methods [1,2].

Generally, heat conduction of an SWNT strongly depends on the transport of acoustic phonons: LA, TA and TW. The aim of this research is to estimate the contribution of each acoustic phonon mode to heat conduction. The contribution of each acoustic phonon mode to heat conduction was quantified by exciting the mode and then monitoring the phonon relaxation process. The energy of a phonon mode is extracted by calculating the phonon energy spectra. Figures 1-2 demonstrate the case when a LA phonon mode is excited. Here, the spectra are calculated by taking two-dimensional Fourier transfer of atom velocity in the axial direction of SWNT. The dependence of the relaxation on the phonon branch, wave number, temperature of SWNT, kinetic energy of excited phonon and tube length will be discussed.

[1]. C. Yu et.al., Nano Lett. 5., (2005) 1842.

[2]. Maruyama, Physica B, 323 (2002)193.

Corresponding Author: Shigeo Maruyama

E-mail:maruyama@photon.t.u-tokyo.ac.jp

Tel/Fax: +81-3-5800-6983

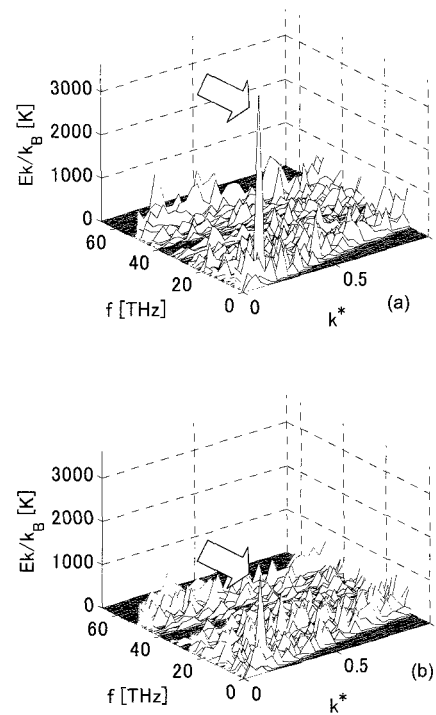


Fig.1 Excited phonon energy spectrum  $E_k(f, k^*)$  of an SWNT at (a)  $t=0.0$  and (b)  $t=0.21$  ns.

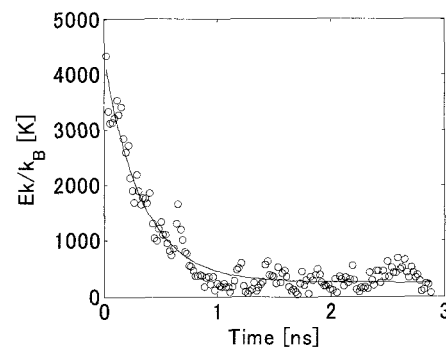


Fig. 2 Relaxation of excited LA phonon. The fitting line is denoted in solid.

**Surface Potential Investigations of Ballistic Conduction in SWNTs by Atomic Force Microscopy**

○Yuji Miyato<sup>1</sup>, Kei Kobayashi<sup>2</sup>, Kazumi Matsushige<sup>1</sup>, Hirofumi Yamada<sup>1</sup>

<sup>1)</sup> *Department of Electronic Science & Engineering, Kyoto University, Kyoto 615-8510*

<sup>2)</sup> *Innovative Collaboration Center, Kyoto University, Kyoto 615-8510, Japan*

A single wall carbon nanotube (SWNT) is known as an ideal one-dimensional quantum wire. In fact the ballistic transmission has been observed when its channel length is less than 300 nm<sup>1)</sup>. Since the transmission characteristics of the SWNT are strongly dominated by the electronic states at the interface between the SWNTs and the metal electrodes, sufficient understanding of these states of the SWNT is essentially important for quantum device applications. We have mapped surface potentials (SPs) on SWNTs by Kelvin probe force microscopy using the frequency-modulation detection method (FM-KFM), which is a powerful technique for investigating SP on a nanometer scale, as well as by AFM potentiometry (AFMP), which is a complementary method to measure the SP with a high-impedance voltmeter connected to an AFM tip. We have developed a new AFMP technique called “point-by-point AFMP” to improve the measurement accuracy<sup>2)</sup>. The AFMP measures the Fermi level at a place where the AFM tip is in contact while the KFM measures the contact potential difference between the AFM tip and sample by detecting the electrostatic force originating from the difference in their local work functions.

In this study the SPs of the SWNTs with applied bias voltages were investigated by both FM-KFM and point-by-point AFMP. We first fabricated nanogap electrodes on a highly doped Si substrate with a silicon oxide layer using the electron-beam (EB) lithography. The gap distance was less than 300 nm. Then, we deposited SWNTs between the nanogap electrodes by using the dielectrophoresis method. We compared the SP images obtained by FM-KFM with those obtained by point-by-point AFMP. We successfully observed a potential plateau region in the SP profile, which corresponds to the ballistic conduction in the SWNT channel.

[1] Y. Yaish, et al. *Phys. Rev. Lett.* **92** 046401 (2004), [2] Y. Miyato et al. *Nanotechnology* **18** 084008 (2007)

Corresponding Author: Hirofumi Yamada

TEL: +81-75-383-2307, FAX: +81-75-383-2308, E-mail: h-yamada@kuee.kyoto-u.ac.jp

## Raman Scattering Studies on Nanopeapod-Derived Double-Walled Carbon Nanotubes: Comparisons with Photoluminescence Spectra

○Soon-Kil Joung<sup>1</sup>, Toshiya Okazaki<sup>1,2</sup>, Naoki Kishi<sup>1</sup>, Takeshi Nakanishi<sup>1</sup>, Shunji Bandow<sup>3</sup>,  
Zujin Shi<sup>4</sup> and Sumio Iijima<sup>1,3</sup>

<sup>1</sup>Research Center for Advanced Carbon Materials, AIST, Tsukuba 305-8565, Japan

<sup>2</sup>PRESTO, JST, 4-1-8 Honcho, Kawaguchi 332-0012, Japan

<sup>3</sup>Department of Materials Science and Engineering, Meijo University, 1-501 Shiogamaguchi,  
Tenpaku-ku, Nagoya 468-8502, Japan

<sup>4</sup>Department of Chemistry, Peking University, Beijing 100871, P. R. China

Double-walled carbon nanotubes (DWCNTs) have been expected for nanocomposites, field emission sources, nanotube bi-cables and electronic devices because of their superior mechanical properties, thermal conductivity and structural stability [1]. Optical application of DWCNTs is also attractive because the inner core tube is protected from environment and its optical properties are preserved.

We have previously reported that photoluminescence (PL) of nanopeapod-derived DWCNTs presumably depend on the interlayer spacing between the outer and the inner tubes [2, 3]. Namely, PL quenching occurs in DWCNTs having smaller interlayer distance and the PL signals of the inner tubes are observable from DWCNTs having larger interlayer distance. However, the detailed mechanisms of the PL quenching are still controversial. We here carry out resonance Raman (RR) study of several nanopeapod-derived DWCNTs to quantitatively investigate the interlayer spacing dependence between the outer and the inner tubes on the PL quenching.

Using a contour plot of the Raman intensities of the radial breathing modes (RBMs) over the laser excitation wavelengths of 700-1070 nm, we found that the inner tubes of all DWCNTs studied here were mainly assigned to (6, 5) and (7, 3) tubes. It is very interesting that the diameter of the outer tubes was estimated to be 1.37–1.55 nm and 1.34–1.6 nm for DWCNTs which show faint PL signals from inner tubes, while that of DWCNTs with no PL from the inner tubes ranges 1.2–1.4 nm. These results strongly suggest that PL behaviors of DWCNTs are very sensitive to the interlayer distance between the outer and the inner tubes.

[1] M. Endo, H. Muramatsu, T. Hayashi, Y. A. Kim, M. Terrones, M. S. Dresselhaus., *Nature* **433**, 476 (2005).

[2] T. Okazaki, S. Bandow, G. Tamura, Y. Fujita, K. Iakoubovskii, S. Kazaoui, N. Minami, T. Saito, K. Suenaga, S. Iijima, *Phys. Rev. B*, **74**, 153404 (2006).

[3] T. Okazaki, Z. Shi, T. Saito, H. Wakabayashi, K. Suenaga, S. Iijima, *The 32<sup>nd</sup> Fullerene-Nanotube General Symposium*, 2P-2 (2007).

**Corresponding Author:** Toshiya Okazaki

**E-mail:** soonkil-joung@aist.go.jp; toshi.okazaki@aist.go.jp, **Tel:** 029-861-4173, **Fax:** 029-861-4851

## Behaviors of cells cultured on carbon nanotube-synthesized substrate surface

Masato Tominaga<sup>1</sup>, ○Shoichiro Nagaishi<sup>1</sup>, Nagisa Yoshizaka<sup>1</sup>, Etsuko Kumagai<sup>2</sup>,  
Shinji Harada<sup>2</sup> and Isao Taniguchi<sup>1</sup>

Graduate School of Science and Technology, Kumamoto University<sup>1</sup>, Kumamoto 860-8555,  
Japan. Faculty of Medical and Pharmaceutical Sciences, Kumamoto University<sup>2</sup>, Kumamoto  
860-8556, Japan

Carbon nanotube (CNT) structures have been attracting for applications such as scaffolds for cell seeding and growth, because of their nanosize and fabrication indented surface at nanoscale. In this study, we investigated behaviors of cells cultured on CNT-synthesized substrate surfaces.

CNTs with various surface density were synthesized on a quartz substrate surface. MAGI/CCR cells were used in this study, and were seeded on the CNT-synthesized substrates, quartz substrate and tissue culture dish.

Cell morphology cultured for 5 days did not depend on the surface density of CNTs, as shown in Fig.1. Fig.2 shows the proliferations of cells on CNTs with lower surface density, which was similar to quartz substrate and tissue culture dish. On the other hand, in case of CNTs with higher surface density, the proliferation was ca. half in comparison with the lower one. These cells were detached from CNTs with higher surface density, and seeded on tissue culture dish. The detached cells proliferated well.

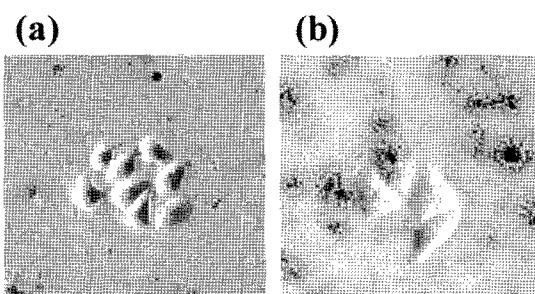


Fig. 1 (a) Cell morphology cultured on CNT-synthesized substrates ((a) lower and (b) higher densities).

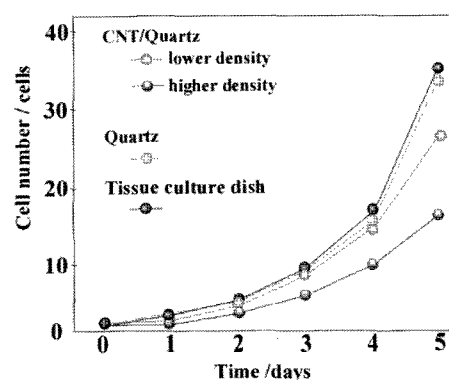


Fig. 2 Proliferation of cells cultured on various substrates.

Corresponding Author: Masato Tominaga

E-mail: masato@gpo.kumamoto-u.ac.jp

Tel&Fax: 096-342-3656

## Synthesis of Carbon Nanotube Particles from Used SiC Powder by SiC Surface Decomposition Method

○Takayuki Morishita<sup>a</sup>, Akihiro Ichikawa<sup>d</sup>, Motohiro Yamamoto<sup>e</sup>,  
Ryo Sasai<sup>b,c</sup>, and Michiko Kusunoki<sup>c</sup>

<sup>a</sup> School and <sup>b</sup> Graduate School of Engineering, and <sup>c</sup> EcoTopia Science Institute,  
Nagoya University, Nagoya 464-8603, Japan

<sup>d</sup> Sanwayuka Industry Corporation, Kariya 448-0002, Japan

<sup>e</sup> Electro and Material Department, Japan Fine Ceramics Center, Nagoya  
456-8587, Japan

The SiC surface decomposition method is one of the synthesizing methods of CNT. We have previously reported that this method gives the well-aligned and high-density CNTs on the SiC single crystal substrates[1]. However, SiC single crystals are rather expensive, and the synthesis of CNTs from cheaper SiC materials is desirable for encouraging the application of CNTs

Now, a large amount of SiC abrasives powder is discharged from the Si wafer manufacturing industry. However, most of such used SiC powder are discharged and reclaimed, since the used SiC powder cannot be reused as abrasives, because used SiC particles mostly become affable by repeat use. To realize the recycling of the used SiC powder, we attempted to synthesize CNT particles from the used SiC powder, which was much cheaper than pure SiC powder, in this study.

After the used SiC powder was rinsed by 5M HCl for removal of metal impurity, the powder was heated to 1900°C in vacuum. As results from TEM observation, it was revealed that dense CNTs layer could be synthesized on the used SiC particles, like the case of pure SiC particles. This indicates that not only the cost for synthesizing CNT particles but also the disposal amount of the used SiC powder can be reduced.

**References:**[1] M.Kusunoki, M.Rokkaku, T.Suzuki : Appl. Phys. Lett., 71, 2620 (1997)

**Corresponding Author :** Michiko Kusunoki

**E-mail :** [kusunoki@esi.nagoya-u.ac.jp](mailto:kusunoki@esi.nagoya-u.ac.jp)

**Tel :** +81-52-789-3920

**Fax :** +81-52-789-5849

## 3P-33

Carbon nanowalls as a negative electrode in lithium-ion secondary battery

Norihiro Kitada<sup>1</sup>, Hirofumi Yoshimura<sup>1</sup>, Osamu Tanaike<sup>2</sup>, Ken-ichi Kobayashi<sup>2</sup>,  
Kenichi Kojima<sup>1</sup>, Masaru Tachibana<sup>1</sup>

<sup>1</sup> International Graduate School of Arts and Sciences Yokohama City University

<sup>2</sup> National Institute of Advanced Industrial Science and Technology

<sup>3</sup> NISSAN ARC, LTD.

Contact e-mail: *tachiban@yokohama-cu.ac.jp*

Recently two-dimensional carbon nanostructures called carbon nanowalls (CNWs) have been fabricated at 700 °C by plasma-enhanced chemical vapor deposition. By means of Raman spectroscopy [1], transmission electron microscopy [2], and photoelectron spectroscopy [3], it was clarified that the CNWs are composed of small crystallites with a high degree of graphitization. Such structural feature can provide us for various applications such as electrodes, electric field emitters, hydrogen storages, etc.

The lithium-ion battery, that is one of the potential applications, has attracted much attention for electric vehicles. In commercial lithium-ion batteries, graphite is generally used as the negative electrodes. The high diffusivity of lithium ions in the active materials is one of important factors for the good performance. A practical way of enhancing the diffusivity of lithium ions is to decrease the particle size of the active materials. It is expected that CNWs composed of small crystallite with a high degree of graphitization is one of promising materials for electrodes in lithium-ion batteries.

In this paper, we report CNWs which serve as the negative electrode in lithium-ion batteries intended for high-rate use. We demonstrate that CNWs have promising electrochemical properties.

[1]S. Kurita, et al., *J. Appl. Phys.* **97**, 104320 (2005).

[2]K. Kobayashi et al., *J. Appl. Phys.* **101**, 094306 (2007).

[3]I. Kinoshita et al., *Chem. Phys. Lett.* (in press).

### Synthesis of Thin Graphite by Exfoliation Technique

○Satoshi Heguri, Nozomu Kimata, Mototada Kobayashi

*Department of Material Science, Graduate School of Material Science  
University of Hyogo, Ako, Hyogo 678-1297, Japan*

The discovery of fullerene and carbon nanotubes has raised interest in carbon-based material. Graphene is a form of graphite with only a single layer of carbon atoms. It is stable under ambient conditions and has been known for its peculiar electronic dispersion with massless two-dimensional Dirac fermions. Graphene is a new model system in condensed matter physics and is interesting subject to study in experimental and theoretical points. Recently, Novoselov et al. reported the observation of the electric field effect in few-layer graphene[1]. It has attracted further interest as new electronic device.

Several techniques have been reported for graphene preparation. However, the established techniques give rise to the variation of sample thickness and it is difficult to produce graphene in large quantities.

We adopted exfoliation technique for thin graphite preparation in order to improve homogeneity and thinness of the product. Our processes consist of the intercalation of the graphite by using various acids or halogen and the successive exfoliation by heat treatment. HOPG (highly oriented pyrolytic graphite) and natural graphite were used for starting graphite.

The photograph of the exfoliated graphite is shown in Fig.1. The x-ray diffraction profile and the magnetic susceptibility for the exfoliated graphite and the intercalation compounds synthesized from this exfoliated graphite will be presented at the meeting.

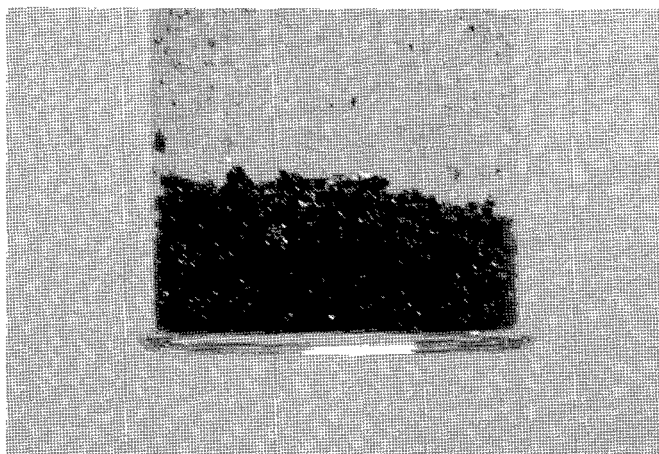


Fig. 1. The photograph of exfoliated graphite.

**References:** [1] K. S. Novoselov et al., Science 306, 666 (2004)

**Corresponding Author:** Satoshi Heguri

**E-mail:** rk07d004@stkt.u-hyogo.ac.jp

**Tel&Fax:** +81-791-58-0156/+81-791-58-0132



## Flattened Carbon Nanocoil and application to field emitter

○Y. Shinohara<sup>1</sup>, Y. Hosokawa<sup>1</sup>, M. Yokota<sup>1</sup>, S. Oke<sup>1</sup>, H. Takikawa<sup>1</sup>, Y. Fujimura<sup>2</sup>,  
T. Yamaura<sup>2</sup>, S. Itoh<sup>2</sup>, K. Miura<sup>3</sup>, K. Yoshikawa<sup>3</sup>, T. Ina<sup>4</sup>, F. Okada<sup>4</sup>

<sup>1</sup> *Department of Electrical and Electronic Engineering,  
Toyohashi University of Technology.*

<sup>2</sup> *Research and Development Center, Futaba Corporation.*

<sup>3</sup> *Fuji Research Laboratory, Tokai Carbon Co., Ltd.*

<sup>4</sup> *Fundamental Research Department, Toho Gas Co., Ltd.*

Helical carbon nanofiber (HCNF) is fibrilliform carbon nanofiber with helical shape. There are two kind of the HCNFs, carbon nanocoil (CNC) with the inside diameter and carbon nanotwist (CNTw) without the inside diameter. The mass production of HCNF was achieved with automatic-substrate-type CVD system [1]. These HCNFs are synthesized by Catalyst-CVD process. However these HCNF contains the catalyst. It is necessary to remove the catalyst by the acid treatment. In this work, the acid treatment was done by using the hydrogen peroxide solution according to the following procedures. 1) Powder of HCNF and hydrogen peroxide solution are put in the beaker. 2) The beaker is heated up to 100°C by a hot plate. 3) HCNF is filtered with the filter and washes by the pure water. 4) It was dried in an electric furnace. Fig.1 show the SEM image of the acid treated CNC. CNC is flattened by acid treatment. In this work, the field emission characteristic of CNC is measured. As a result, the emission characteristic has improved in CNC advanced by making flatly as shown in Fig. 2.

This work has been partly supported by the Outstanding Research Project of the Research Center for Future Technology, Toyohashi University of Technology; the Research Project of the Research Center for Future Vehicle, Toyohashi University of Technology; the Research Project of the Venture Business Laboratory, Toyohashi University of Technology; Global COE Program "Frontiers of Intelligent Sensing" from the Japanese Ministry of Education, Culture, Sports, Science and Technology (MEXT); The Japan Society for the Promotion of Science (JSPS), Core University Programs (JSPS-KOSEF program in the field of "R&D of Advanced Semiconductors.")

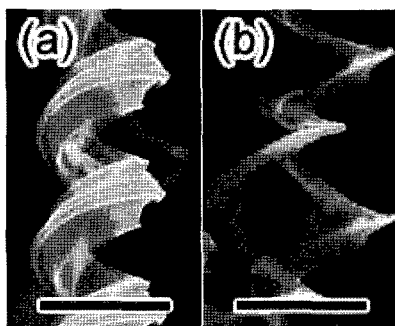


Fig. 1. SEM micrographs of CNC, (a) as-grown CNC and (b) after acid treat. Scale bar : 500 nm

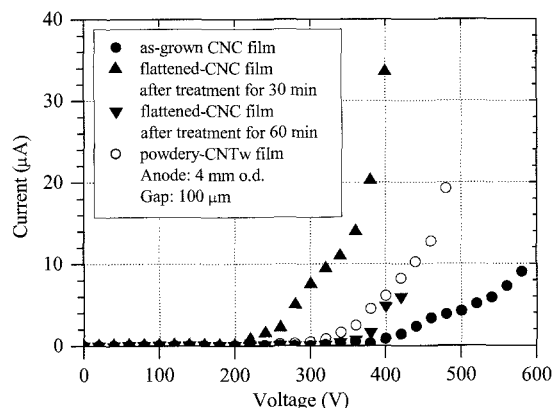


Fig. 2. Field emission characteristics of flattened CNC.

### References:

[1] Y. Hosokawa, H. Shiki, H. Takikawa, T. Ina, G. Xu, K. Shimizu, S. Itoh, T. Yamaura, *Abstracts of The 67<sup>th</sup> Japan Society of Applied Physics Annual Conference*, 30a-D-11 (2006)

Corresponding Author: Yuichiro Shinohara, Hirofumi Takikawa

E-mail: [yuichiro@arc.eee.tut.ac.jp](mailto:yuichiro@arc.eee.tut.ac.jp), Tel & Fax: +81-532-44-6644

E-mail: [takikawa@eee.tut.ac.jp](mailto:takikawa@eee.tut.ac.jp), Tel & Fax: +81-532-44-6727

## *Ab-initio* study on the electronic structure of few-layer graphene films connected to a titanium electrode under an electric field

○Mari Ohfuchi and Masakatsu Ito

*Nanotechnology Research Center, Fujitsu Laboratories Ltd.,  
10-1 Morinosato-Wakamiya, Atsugi 243-0197, Japan*

Since the successful fabrication of ultrathin graphite films [1], theoretical studies on few-layer graphene films have been actively reported. It has been shown [2] that a two-layer graphene film has a band gap under an electric field, but *ab-initio* study on contact with an electrode under an electric field has not been made despite its importance for electronics application. In this report, we carry out such calculations of graphene films up to four layers connected to titanium layers. The energy band for the innermost graphene layer falls by about 3 eV. For three-layer graphene, the energy bands similar to those of two-layer graphene without contact appear near the Fermi level. For the electric field  $E=0$ , they have a band gap unlike those without contact. For  $E=0.17$  V/nm, the band gap disappears and for a reverse electric field (not shown in Figs.), it opens wider.

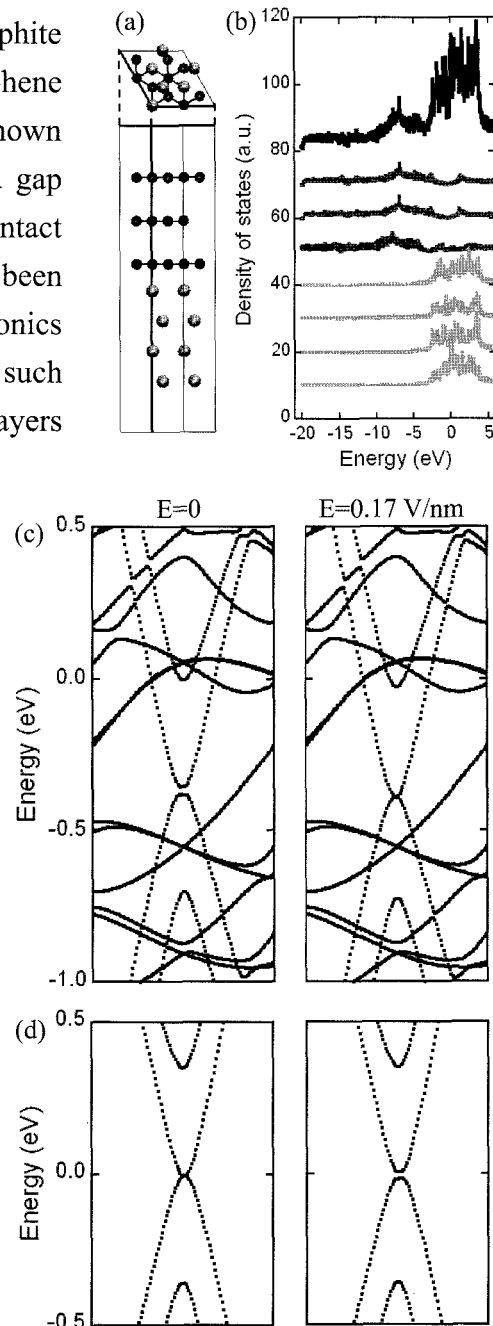
Figs. (a) Unit cell used for the calculations of three-layer graphene. White (black) spheres represent titanium (carbon) atoms. (b) Total density of states (Top) and those of each layer. (c) Energy band structures for  $E=0$ , 0.17 V/nm and (d) those of two-layer graphene without contact for comparison.

### References:

- [1] K.S. Novoselov *et al.*, Science 306, 666 (2004).
- [2] E. McCann, Phys. Rev. B 74, 161403 (2006).
- [3] T. Ozaki, Phys. Rev. B 67, 155108 (2003).

Corresponding Author: Mari Ohfuchi

E-mail: [mari.ohfuchi@jp.fujitsu.com](mailto:mari.ohfuchi@jp.fujitsu.com), Tel: +81-46-250-8234, Fax: +81-46-250-8844



### **Preparation of porous carbons composed of carbon nanotube and fullerene-like carbon by carbonization of Fe-containing phenol formaldehyde resin**

○Yuji Sakamoto, Katsuya Inomata, Yoshinobu Otake

*Department of Applied Chemistry, Meiji University  
1-1-1, Higashi-Mita, Tama-ku, Kawasaki, Kanagawa, Japan*

The aim in this study is to control the pore structures present in carbons by changing carbon nanostructure with various heat-treatment conditions after the addition of iron metal in polymeric substance.

Phenol formaldehyde resin is dissolved in methanol to finely disperse ferrocene(Fe), stirred continuously until the resin becomes dry and then is cured at 80°C for 10 days. The resulting resin blocks, containing 0.6 mmol of Fe, are carbonized under argon atmosphere at the final temperature of 1000°C for 1h to obtain Fe-containing carbons. In this study, the resins are heat-treated by two methods; one is called as method (i) and the other as method (ii). In the former method, the resins are heat-treated up to 1000°C by different heating rates ranging from 5 to 60000°C /min and held at this maximum for 1h. The latter case is focused on the temperatures of pre-heat treatment from 100 to 600°C prior to final heat-treatment, which is performed at 5 °C/min up to 1000°C and finally kept at this maximum for 1h.

The results of nitrogen adsorption/ desorption for the Fe-containing carbons indicates that the value of mesopore surface is constant to be about 120m<sup>2</sup>/g even if the heating rates are changed by method (i); however, the heating rates affect the development of micropores. The micropore and mesopores surface areas remain constant on the carbons which are prepared, by method (ii), with the pre-heat temperatures below 500°C. However, the micropore surface area increases suddenly when the pre-heat treatment is carried out at 600°C.

The crystalline structure and nanostructure of carbon nanotubes(CNTs) on the carbons are studied by X-ray diffraction, scanning electron microscopy and transmission electron microscopy. Nanostructures, composed of fullerene-like carbons (FLCs) and cup-stacked CNTs, are recognized in this study under a simple preparation process of the carbons. The results indicate that micropores exist as space surrounded by FLCs and mesopores as that by CNTs, thus implying the importance to control the nanostructures for the preparation of porous carbons.

#### **Corresponding Author**

E-mail:meiji\_file\_yuji@yahoo.co.jp

Tel: +81-44-934-7198

Fax: +81-44-934-7906

## Antimicrobial Activity of Fullerene and Its Derivatives

○Hisae Aoshima<sup>1</sup> Ken Kokubo<sup>2</sup>, Shogo Shirakawa<sup>2</sup>, Masayuki Ito<sup>1</sup>, Shuichi Yamana<sup>1</sup>, and Takumi Oshima<sup>2</sup>

<sup>1</sup>Vitamin C60 BioResearch Corporation, 1-8-7, Kyobashi, Chuo-ku, Tokyo 104-0031, Japan

<sup>2</sup>Division of Applied Chemistry, Graduate School of Engineering, Osaka University  
Suita, Osaka 565-0871, Japan

In order to find the novel functionality of fullerenes in cosmetic industry, we have assessed their antioxidant activities [1]. In this study, antimicrobial activities of fullerene C<sub>60</sub> and its derivatives against various bacteria and fungi were evaluated. The minimum inhibitory concentration (MIC) values were measured using an agar plate dilution method according to the Clinical and Laboratory Standard Institute. The fullerene samples tested were variously modified water-soluble C<sub>60</sub> (PVP/C<sub>60</sub>,  $\gamma$ -CD/C<sub>60</sub> [1], and Nano-C<sub>60</sub> [2]) and three fullerenols such as C<sub>60</sub>(OH)<sub>12</sub>, C<sub>60</sub>(OH)<sub>36</sub>•8H<sub>2</sub>O, and C<sub>60</sub>(OH)<sub>44</sub>•8H<sub>2</sub>O. Catechin was used as a reference material. Although pristine C<sub>60</sub> showed no antimicrobial activity, fullerenols exhibited a good antimicrobial activity against *P. acnes*, *S. epidermidis*, *C. albicans*, and *M. furfur*. In particular, C<sub>60</sub>(OH)<sub>44</sub> exhibited a strong and versatile antimicrobial activity comparable to catechin. These results indicate that the hydroxyl groups of fullerenes are responsible for the antimicrobial activity. It is expected that C<sub>60</sub>(OH)<sub>44</sub> has a possible wide-ranging application in the field of the household goods as well as the cosmetic ingredients.

Table 1. Antimicrobial activity of various fullerene derivatives

Strain	MIC ( $\mu\text{g/mL}$ )				
	C <sub>60</sub> (OH) <sub>44</sub>	C <sub>60</sub> (OH) <sub>36</sub>	C <sub>60</sub> (OH) <sub>12</sub>	C <sub>60</sub> <sup>a</sup>	(+)-Catechin
<i>Escherichia coli</i>	– <sup>b</sup>	–	–	–	5120
<i>Bacillus species</i>	–	–	–	–	5120
<i>Staphylococcus aureus</i> (MRSA)	2000	–	–	–	5120
<i>Staphylococcus aureus</i> (MSSA)	2000	–	–	–	5120
<i>Staphylococcus epidermidis</i>	2000	2000	–	–	2560
<i>Propionibacterium acnes</i>	1500	–	–	–	2560
<i>Candida albicans</i>	1200	600	3300	–	–
<i>Malassezia furfur</i>	900	1850	3750	–	37

<sup>a</sup> All PVP/C<sub>60</sub>,  $\gamma$ -CD/C<sub>60</sub>, and Nano-C<sub>60</sub> were tested. <sup>b</sup> No antimicrobial activity (–) was observed.

[1] H. Takada, K. Kokubo, and T. Oshima, *Biosci. Biotechnol. Biochem.* **2007**, *70*, 3088–3093.

[2] S. Deguchi, S. Mukai, M. Tsudome, and K. Horikoshi, *Adv. Mater.* **2006**, *18*, 729–732.

Corresponding Author: Hisae Aoshima

TEL: +81-3-3538-5917, FAX: +81-3-3538-5911, E-mail: hisae.aoshima@vc60.com

## Production of carbon clusters by collisional explosion-reaction of asteroids in space (model experiment)

○Tetsu Mieno<sup>1</sup>, Sunao Hasegawa<sup>2</sup>

<sup>1</sup>Dept. Physics, Shizuoka Univ., Oyo, Suruga-ku, Shizuoka-shi 422-8529, Japan

<sup>2</sup>Inst. Space & Astronautical Science, JAXA, Sagami-hara-shi, Kanagawa 229-8510, Japan

For more than 10 billion years, huge amount of carbon atoms are produced in space. Now, we want to know where and how these carbons are stored in space. It is informed that the Saturn explorer “Cassini” operated by NASA has arrived Saturn and it successfully sent astonishing IR images of surface of Titan satellite, where many huge methane seas are clearly visualized. We expect that this special satellite is reserving many kinds of carbon clusters and hydrocarbon molecules in the methane seas under dense nitrogen air. Because, many asteroids often hit the Titan’s surface in the past, which caused large-scale collisional explosions of methane under nitrogen atmosphere, and many kinds of carbon clusters, hydro-carbon molecules and amino-acids were produced. Main parts of these molecules would be stored in the methane seas under low temperature and UV-shielded atmosphere. Some parts of these molecules are diffused into space.

In order to simulate this process on Titan, we have carried out the gas-gun experiment. [1] By using a 2-stage light-gas gun, we can accelerate 3 mm $\phi$  stainless-steel ball to about 6 km/s and hit the ball to a stainless steel target without carbon contamination. We have developed a pressured target-chamber, where 1 atm of Nitrogen gas is stored and propanol target in a aluminum tank is set in front of the metal target. The accelerated ball penetrates into the target-chamber through aluminum thin window and causes the collisional explosion-reaction. [2] After the fire, produced carbon soot is carefully collected and analyzed.

From the laser-desorption time-of-flight mass spectrum (LD-TOF-MS) measurement, we can confirm many kinds of carbon clusters (C<sub>60</sub>, higher fullerenes etc.) in the soot. By extracting using toluene and the HPLC method, we could confirm extraction of small amount of C<sub>60</sub> and higher fullerenes.

From this model experiment we can insist that fullerenes can be produced by the explosion-reaction under nitrogen gas, though the scale is much smaller than that on Titan. This experiment was carried out by use of the ISAS/JAXA gas gun.

[1] T. Mieno S. Hasegawa, Abst. 33<sup>rd</sup> Fullerene-Nanotube Sympo., Fukuoka (2007) p.53.

[2] T. Mieno & A. Yamori, Jpn. J. Appl. Phys., **45** (2006) 2768.

E-mail (to T. M.): [piero@sannet.ne.jp](mailto:piero@sannet.ne.jp).

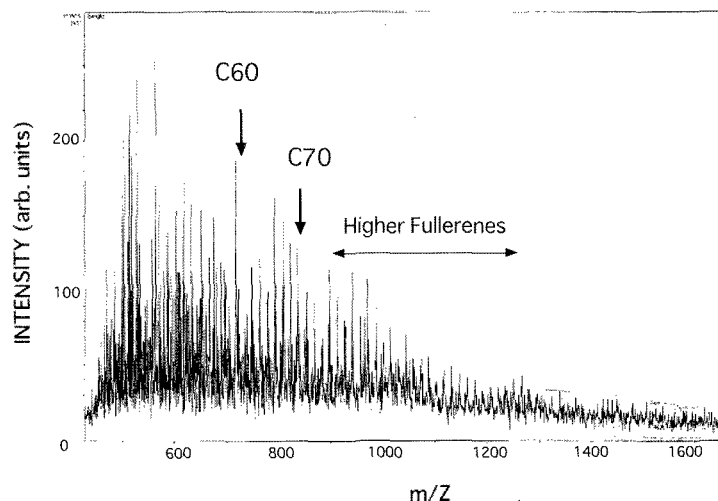


Fig. 1: A LD-TOD-MS spectrum of the sample by propanol explosion in N<sub>2</sub> gas (+ ion mode, 50 shots averaged).

### **Energetics and Electronic Structures of Fullerenes with Vacancies**

Susumu Okada○

*Center for Computational Sciences and Graduate School of Pure & Applied Sciences,  
University of Tsukuba, Tennodai, Tsukuba 305-8577*

Atomic imperfections in nanoscale carbon materials, such as nanotubes, fullerenes, and nanographites, are known to play crucial role to determine their stability and electronic properties near the Fermi level. The atomic defects (e.g. vacancies and interstitials) induces particular electron states of which wave functions are localized near the defects with lone pair character resulting in gap states at/near energy gap of the nanotubes.

In the present work, based on the density functional theory, we study the energetics and electronic structures of fullerene molecules with di-vacancies. We consider the fullerene molecules,  $C_n$  where  $n=60, 70, 80, 90, 100, 110, 120,$  and  $130$ , with five-fold symmetry axis to elucidate the difference and the similarity between the fullerene and carbon nanotubes. The di-vacancies introduced on the fullerenes are found to be spontaneously repaired by forming four-, five-, seven-, and eight-member rings. Our calculations clearly show the strong site dependence of the formation energy of the vacancies. The di-vacancies introduced at the atomic sites those shared by a hexagon and a pentagon give the smallest formation energy healed by two pentagons and a heptagon. In sharp contrast, healed structures containing the four-member ring give the largest formation energy indicating the unfavorable defect structure. On the other hand, the di-vacancies introduced in the hexagons give the moderate energy. Further, the energy strongly depends on the orientation of the C-C bond that is removed. Calculated electronic structures of fullerenes with di-vacancies exhibit the correlation with the energetics.

**Corresponding Author: Susumu Okada**

**E-mail: sokada@comas.frsc.tsukuba.ac.jp**

**Fax: 029-83-5924**

## Morphological Study of C<sub>60</sub> Thin Films for Electronic Device Application

○Hiroyuki Sagami<sup>3</sup>, Haruna Oizumi<sup>1</sup>, Morihiko Saida<sup>1</sup>, Kenji Omote<sup>1</sup>,  
Yuzo Mizobuchi<sup>1</sup>, Yasuhiko Kasama<sup>1</sup>, Kuniyoshi Yokoo<sup>1</sup>, Shoichi Ono<sup>1</sup>  
Hiroji Ohigashi<sup>1</sup>, Keiko Koga<sup>2</sup> and Takeo Furukawa<sup>3</sup>

<sup>1</sup>*Ideal Star Inc., Sendai 989-3204, Japan*

<sup>2</sup>*Advanced Instruments Center, Kyushu Sangyo University, Fukuoka 813-8503, Japan*

<sup>3</sup>*Graduate School of Faculty of Science, Tokyo University of Science, Tokyo 162-0826, Japan*

C<sub>60</sub> thin films are expected to be applicable to many organic electronic devices [1-3]. It is well known that the morphology of C<sub>60</sub> films influence strongly the operational characteristics of the devices. This paper describes the result of AFM and XRD studies on the morphological and structural properties of C<sub>60</sub> films deposited by different conditions.

The AFM results showed that the surface roughness and the size of crystal increased with increase in the substrate temperature for C<sub>60</sub> deposition (Fig.1 (a) and (b)). However, the morphology did not depend on deposition rate within the range of 3-10 Å/sec. Post-annealing does not affect the morphology of the deposited films (Fig.1(c)). The XRD study showed that the substrate temperature does not remarkably affect the crystallinity of the deposited films. These results suggest that C<sub>60</sub> should be deposited at low substrate temperature to form the reproducibly uniform films, which are most important for device application of C<sub>60</sub>.

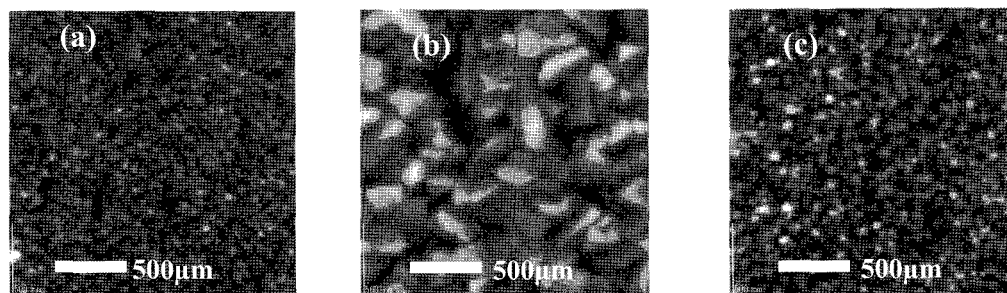


Fig.1 AFM images of 1- $\mu\text{m}$ -thick C<sub>60</sub> films deposited on quartz substrates at (a) 60°C, (b) 200°C, and (c) annealed at 200°C for 2 hours after deposition at 60°C.

[1] T. Nishikawa, S. Kobayashi, T. Nakanowatari, T. Mitani, T. Shimoda, Y. Kubozono, G. Yamamoto, H. Ishii, M. Niwano and Y. Iwasa, *J. Appl. Phys.*, **97**, 104509 (2005)

[2] K. Iwata, M. Yamashiro, J. Yamaguchi, M. Haemori, S. Yaginuma, Y. Matsumoto, M. Kondo and H. Koinuma, *Adv. Mater.*, **18**, 1713 (2006)

[3] T. Nagano, M. Tsutsui, R. Nouchi, N. Kawasaki, T. Ohta, Y. Kubozono, N. Takahashi and A. Fujiwara., *J. Phys. Chem. C*, **111**, 7211 (2007)

Corresponding Author: Kenji Omote

TEL: +81-22-303-7336, FAX: +81-22-303-7339, E-mail: [kenji.omote@idealstar-net.com](mailto:kenji.omote@idealstar-net.com)

Helium intercalated C<sub>60</sub> solid under high pressure

○S. Kawasaki, T. Hara, Y. Kanamori, A. Iwata

*Nagoya Institute of Technology,  
Gokiso, Showa, Nagoya 466-8555, Japan*

High pressure and high temperature (HPHT) treatments of solid C<sub>60</sub> (fcc-C<sub>60</sub>), in which C<sub>60</sub> molecules are bound together by weak van der Waals forces, produce a variety of polymerized C<sub>60</sub> phases known as "fullerene polymers". Recently, we reported [1] that C<sub>60</sub> molecules in peapods also polymerize by compression at room temperature and it has been attracting much interest [2, 3]. This work indicates that C<sub>60</sub> molecules are polymerized even at room temperature. In the course of the experiment to confirm the indication we found that solid C<sub>60</sub> absorb He gas under high pressure.

Fig. 1 shows the lattice constant  $a$  of fcc-C<sub>60</sub> under high pressure determined by the observed diffraction patterns of the two kinds of experiments (Exp-M+E and Exp-He using the alcohol mixture and He gas as pressure transmitting medium, respectively). The pressure dependence of the  $a$  values of Exp-M+E is in good agreement with previous reports. On the other hand, the pressure change of the lattice constant  $a$  derived from Exp-He is more gentle than that of Exp-M+E probably because of the penetration of He into the C<sub>60</sub> lattice.

[1] S. Kawasaki, et al, CPL, **418**, 260, (2006). [2] M. Chorro, et al., PRB, **74**, 205425 (2006). [3] M. Chorro, et al., Europhysics Lett. **79**, 56003, (2007).

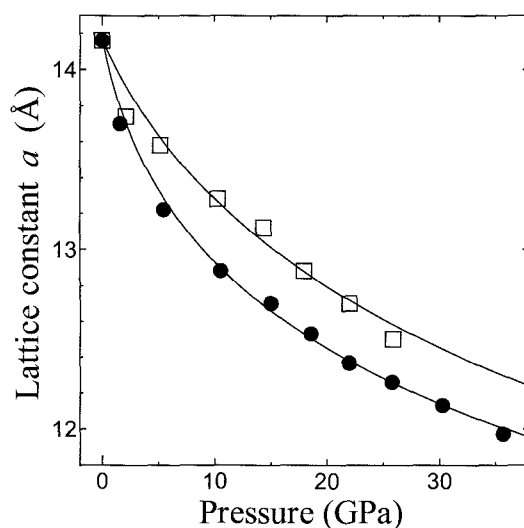


Fig. 1 Lattice constant  $a$  as a function of pressure. Solid circles and open squares correspond to Exp-M+E and Exp-He, respectively. Solid lines are fitting curves using Birch-Murnaghan's equation of state.



## Electric double-layer capacitances of the C<sub>60</sub> dispersed porous carbons

○S. Mori, T. Kawashita, S. Kawasaki

*Nagoya Institute of Technology,  
Gokiso, Showa, Nagoya 466-8555, Japan*

Electric double-layer capacitors (EDLCs) have attracted much interest as a new energy storage system. Recently, it was reported [1] that C<sub>60</sub> molecules improve the EDLC property of activated carbon fibers. However, the mechanism of the improvement has not been clarified yet. In this study, in order to elucidate the mechanism we have prepared several kinds of the C<sub>60</sub> dispersed porous carbons having different pore sizes and measured their EDLC capacitances.

Several kinds of mesoporous carbons have been prepared using mesoporous silicas having different pore sizes as templates. C<sub>60</sub> molecules were introduced into mesoporous carbons by immersing them in the toluene solution of C<sub>60</sub>. The immersed samples were dried with direct pumping to remove the adsorbed toluene. Figs. 1 and 2 show typical examples of the N<sub>2</sub> adsorption isotherms and the cyclic voltammograms of the pristine and C<sub>60</sub> dispersed mesoporous carbons. It was found that the BET surface area of the mesoporous carbon decreases from 2039 to 842 m<sup>2</sup>/g by the C<sub>60</sub> doping. On the contrary, it was found that the EDLC capacitance slightly increases by the doping.

We will also discuss the C<sub>60</sub> doping effect for the exfoliated graphite.

This study was supported partly by Iketani Science and Technology Foundation and partly by Tokai Foudation for Technology.

[1] K. Okajima, et al., *Electrochemica Acta*, **51**, 972, (2005).

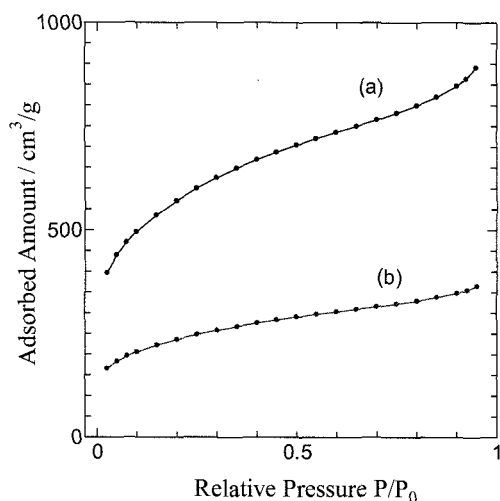


Fig. 1 N<sub>2</sub> adsorption isotherms at 77 K of (a) pristine and (b) C<sub>60</sub> dispersed mesoporous carbons.

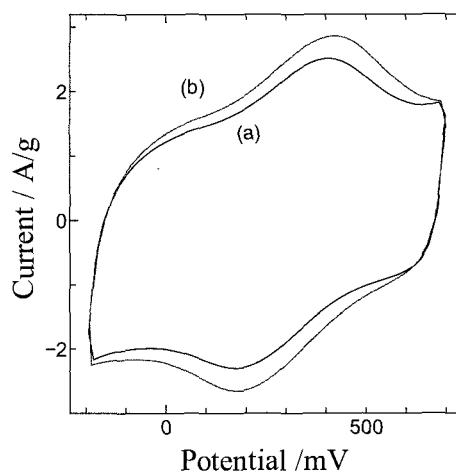


Fig. 2 Cyclic voltammograms of (a) pristine and (b) C<sub>60</sub> dispersed mesoporous carbons. 1 M H<sub>2</sub>SO<sub>4</sub> aqueous solution was used as electrolyte. Sweep rate was set at 10 mV/s.

## Electronic transport properties of photo- and electron-beam-irradiated C<sub>60</sub>

○Y.Tiba<sup>1</sup>, H.Tsuji<sup>1</sup>, M.Ueno<sup>1</sup>, N.Aoki<sup>1</sup>, J.Onoe<sup>2</sup>, and Y.Ochiai<sup>1</sup>

*1) Chiba University, Yayoi, Inage-Ku, Chiba 263-8522, Japan*

*2) Tokyo Institute of Technology, O-okayama, Meguro, Tokyo 152-8550 Japan*

Since the first report on C<sub>60</sub> polymerization by Rao et al.,<sup>1)</sup> there have been many kinds of C<sub>60</sub> polymerization methods. However, most of them have not examined the electronic transport properties of C<sub>60</sub> polymers so far.

We have hitherto investigated the electronic transport properties of the C<sub>60</sub> polymers irradiated with photo- and electron-beam. In this work, the field-effect transistor (FET) properties of photo-irradiated C<sub>60</sub> thin films were examined and compared with those of the electron-beam-irradiated C<sub>60</sub>.

Figure 1 shows the FET characteristics for the photo-irradiated C<sub>60</sub> polymers. As shown in Fig. 1, it was found that a current price fell by photo polymerization. When compared to our previous report, the current values rather increased by electron-beam-irradiation.

Figure 2 shows the SEM image of a photo-irradiated C<sub>60</sub> thin film. As shown in Fig. 2, crazing took place in the film, which was not confirmed for pristine C<sub>60</sub> films. This may make the current value reduced.

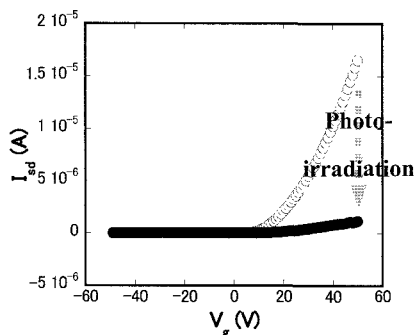


Fig. 1, Gate characteristics

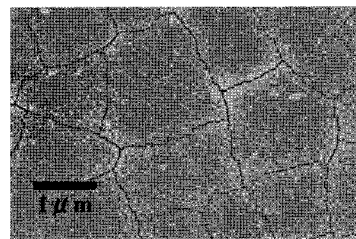


Fig. 2, SEM image

1) A.M.Rao, et al, Appl.phys.A, **64**, 231 (1993).

Corresponding Author: Y.Ochiai

E-mail: ochiai@faculty.chiba-u.ac.jp

Tel.043-290-3428, Fax.043-290-3427

## Modification of Hole-Transport Property of Fullerene Materials by Hydrogenation: A DFT Study on $C_{60}H_4$

○ Ken Tokunaga<sup>1</sup>, Hiroshi Kawabata<sup>2</sup>, and Kazumi Matsushige<sup>2</sup>

<sup>1</sup> *Research and Development Center for Higher Education  
Kyushu University, Fukuoka 810-8560*

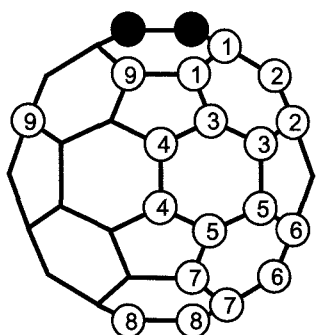
<sup>2</sup> *Department of Electronic Science and Engineering, Kyoto University, Kyoto 615-8510*

Fullerene derivatives are paid attention as one of the tendency to improve carbon materials. In our previous study [1, 2], we focused on the hydrogenation of  $C_{60}$ , which gives  $C_{60}H_2$ , and its effect on the hole-transport property. It was revealed that the hydrogenation is a novel and convenient method for modifying the hole-transport property of  $C_{60}$ .

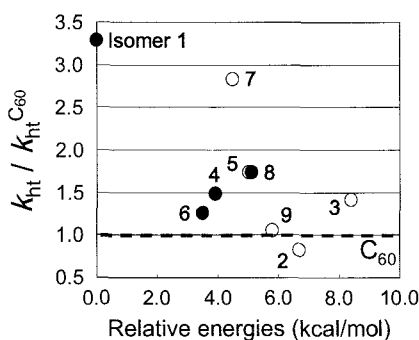
In the present study, this method is extended to the fullerene hydrides  $C_{60}H_4$ . On the basis of Marcus theory, reorganization energy ( $\lambda$ ) and hole-transfer rate constant ( $k_{ht}$ ) are calculated by density functional theory (B3LYP/6-311G(d)), assuming that the electronic coupling ( $H_{AB}$ ) are the same as that of  $C_{60}$ . Nine isomers are selected as shown in Fig. 1.

Isomer 1, the major product [3] of  $C_{60}H_4$ , has the largest  $k_{ht}$  which is more than 3 times as large as that of  $C_{60}$  (See Fig. 2). Thus,  $C_{60}H_4$  has an expectation of use as hole-transport material. It was also found that isomers with large  $\pi$ -conjugation tend to have large  $k_{ht}$  (See Fig. 3), so that the hydrogenation which leaves large  $\pi$ -conjugation of the original  $C_{60}$  is effective for the modification. It gives a clear guideline for the theoretical design of useful materials.

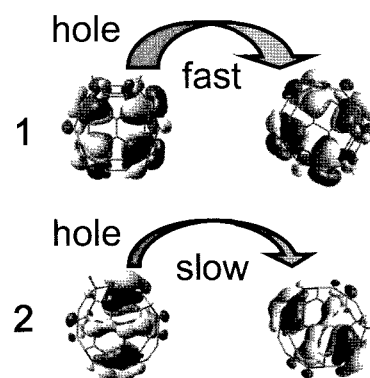
Details of the calculation and analysis [4] will be presented in the symposium.



**Figure 1.** Selected nine isomers. The initial two H atoms are placed at the carbon atoms represented by the filled circles, and the other two are at the carbon atoms labeled 1-9.



**Figure 2.** Relative energies and  $k_{ht}$  of nine  $C_{60}H_4$  isomers. Dashed line shows  $k_{ht}$  of the original  $C_{60}$ . Filled circles show those of synthesized isomers [3].



**Figure 3.** HOMOs of isomers 1 and 2, and schematic illustrations of hole-transport.

[1] **K. Tokunaga**, S. Ohmori, H. Kawabata, and K. Matsushige, *Jpn. J. Appl. Phys.*, **in press**.

[2] **K. Tokunaga**, S. Ohmori, H. Kawabata, and K. Matsushige, *The 33<sup>rd</sup> F-NT General Symp.*, 2P-14 (2007).

[3] C. C. Henderson, C. M. Rohlfing, R. A. Assink, and P. A. Cahill, *Angew. Chem. Int. Ed. Engl.*, **33** (1994).

[4] **K. Tokunaga**, T. Sato, and K. Tanaka, *J. Chem. Phys.*, **124**, 154303 (2006).

**Corresponding Author :** Ken Tokunaga

Tel : +81-92-726-4742, Fax : +81-92-726-4842, E-mail : tokunaga@rche.kyushu-u.ac.jp

## Fabrication of C60MC12 Films for Solution-Processed n-type Organic Thin Film Transistors

○K. Sakaguchi, M. Chikamatsu, A. Itakura, Y. Yoshida, R. Azumi, and K. Yase

*Photonics Research Institute, National Institute of Advanced Industrial Science and  
Technology (AIST), Central 5, 1-1-1 Higashi, Tsukuba, Ibaraki 305-8565, Japan*

We have reported high performance solution-processed n-type organic thin film transistors (TFTs) employing C<sub>60</sub>-fused *N*-methylpyrrolidine-*meta*-C<sub>12</sub> phenyl [C60MC12, see Fig.1 (a)] [1-2]. Generally, hydrophobic treatment on a gate insulator is effective for fabrication of a high performance organic thin-film transistor, since the surface treatment decreases electron trap sites and improves film crystallinity of an organic semiconductor on a gate insulator. However, uniform film fabrication on a hydrophobic surface is difficult compared to that on a hydrophilic surface by solution process, as a hydrophobic surface tends to shed organic solvents. In this study, we examine hydrophilic/hydrophobic patterning of the surface on an insulating layer as shown in Fig.1 (b), aiming at fabrication of uniform and high crystalline films on a hydrophobic surface.

The substrates with hydrophobic surface were prepared by hexamethyldisilazane (HMDS) treatment of highly doped silicon wafers covered with SiO<sub>2</sub>. The local hydrophilic surface was formed by vacuum deposition of SiO<sub>x</sub> using a shadow mask. Thin films of C60MC12 were fabricated by spin coating from a chloroform solution. Source and drain gold electrodes were deposited on the film. The TFT characteristics were measured at room temperature. The all processes after vacuum deposition of SiO<sub>x</sub> were carried out under an inert atmosphere.

Uniform C60MC12 films were easily formed by surrounding the hydrophobic part with a hydrophilic part. Moreover, various spin coating conditions were applied. As a result, the electron mobility and ON/OFF ratio were enhanced by waiting before spinning the substrate as shown in Table 1. The enhancement is interpreted by improvement of C60MC12 film crystallinity.

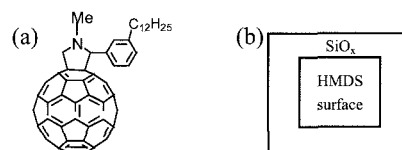


Fig.1. (a) Molecular structure of C60MC12 and (b) schematic view of the substrate

Table 1. FET characteristics of the device

Waiting time (s)	Mobility (cm <sup>2</sup> /Vs)	ON/OFF
0	0.037	>10 <sup>4</sup>
30	<b>0.078</b>	>10 <sup>5</sup>
45	<b>0.102</b>	>10 <sup>5</sup>
60	<b>0.085</b>	>10 <sup>5</sup>

This study was partly supported by Industrial Technology Research Grant Program from New Energy and Industrial Technology Development Organization (NEDO) of Japan.

[1] M. Chikamatsu et al., *Appl. Phys. Lett.* **87**, 203504 (2005).

[2] M. Chikamatsu et al., *J. Photoch. Photobio. A* **182**, 245 (2006).

Corresponding Author: Masayuki Chikamatsu

TEL: +81-29-861-6252, FAX: +81-29-861-6303, E-mail: m-chikamatsu@aist.go.jp

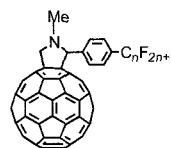
## High Performance N-Type Organic Thin-Film Transistors Based on Soluble C<sub>60</sub> Derivatives

○M. Chikamatsu, A. Itakura, K. Sakaguchi, Y. Yoshida, R. Azumi, K. Yase

*Photonics Research Institute, National Institute of Advanced Industrial Science and Technology (AIST), Central 5, 1-1-1 Higashi, Tsukuba, Ibaraki 305-8565, Japan*

We have reported that a solution-processed organic thin-film transistor (TFT) based on a perfluorooctyl substituted C<sub>60</sub> derivative, C<sub>60</sub>-fused *N*-methylpyrrolidine-*para*-perfluorooctyl phenyl (C60PC8F17), shows high electron mobility of 0.07 cm<sup>2</sup>/Vs and air-stability [1]. In this study, we have newly synthesized a long-chain perfluoroalkyl-substituted C<sub>60</sub> derivative, C<sub>60</sub>-fused *N*-methylpyrrolidine-*para*-perfluorododecyl phenyl (C60PC12F25), and fabricated the organic TFTs by solution process. Films of C<sub>60</sub> derivatives were fabricated on highly doped silicon wafers covered with SiO<sub>2</sub> by spin coating from chloroform solution under ambient condition. Source and drain gold electrodes were deposited on the films. The TFT characteristics were measured both in a vacuum and in air at room temperature.

The C60PC12F25-TFT exhibited high electron mobility of 0.24 cm<sup>2</sup>/Vs in a vacuum. After exposure to air for 24 hours the C60PC12F25-TFT showed good *n*-channel characteristics, whereas the TFTs employing C<sub>60</sub> derivatives with a hydrocarbon chain did not operate under the same condition. The field-effect electron mobility is calculated to be 0.05 cm<sup>2</sup>/Vs. This value is higher than that of C60PC8F17-TFT (0.004 cm<sup>2</sup>/Vs). We will discuss correlation of film structures and TFT performance using different perfluoroalkyl chain-length compounds.



**C60PC8F17** (n=8)

**C60PC12F25** (n=12)

Table 1. Electron mobilities of the TFTs

	Mobility (cm <sup>2</sup> /Vs)	
	Vacuum	Air (after 24h)
<b>PCBM</b>	0.02	-
<b>C60PC8F17</b>	0.07	0.004
<b>C60PC12F25</b>	0.24	0.05

This study was partly supported by Industrial Technology Research Grant Program from New Energy and Industrial Technology Development Organization (NEDO) of Japan.

[1] M. Chikamatsu et al., The 33<sup>th</sup> Fullerene-Nanotubes General Symposium, 2P-13 (2007).

Corresponding Author: Masayuki Chikamatsu

TEL: +81-29-861-6252, FAX: +81-29-861-6303, E-mail: [m-chikamatsu@aist.go.jp](mailto:m-chikamatsu@aist.go.jp)

## Effect of Free Electron Laser Irradiation on Pressed C<sub>60</sub> Powder at the Order of GPa

○Nobuyuki Iwata, Shingo Ando, Ryo Nokariya, Yasunari Iio and Hiroshi Yamamoto

*College of Science & Technology, Nihon University  
7-24-1 Narashinodai, Funabashi-shi, Chiba 274-8501, Japan.*

The aim of our study is to synthesize the amorphous C<sub>60</sub> polymer bulk by irradiating free electron laser (FEL). Characteristics of FEL were tunable wavelength (0.3~6μm) and few tens microsecond macro-pulse, which included few hundreds picosecond micro-pulse. Distinctive particles, which were C<sub>60</sub> polymer demonstrated by Raman spectrum, was obtained with approximately 5μm in diameter irradiating 3rd harmonics FEL 450 or 500 nm for four hours. It was possible to enlarge the size dissolving those particles in toluene and evaporating it to be approximately 0.1 mm-order. However, the size of polymer particle was limited to a few μm in diameter just after the FEL irradiation, although the irradiation diameter was 7mm[1]. In this report, we clarified the reason of the limitation

In this experiment, we used a unique anvil, the cross sectional view of which is a saw. The C<sub>60</sub> powder around the top of the saw is expected to be pressed at the order of GPa. The C<sub>60</sub> powder (99.5%) was pressed and FEL was irradiated (fundamental energy density was 5.5mJ/Pulse·cm<sup>2</sup>) in vacuum after annealed at 70°C

Figure 1 shows a typical Raman spectrum detected from the white line middle in the inset optical microscope (OM) image of the sample surface. The white line was the area pressed with the order of GPa. The intensity of the intrinsic Ag(2) mode at 1469 cm<sup>-1</sup> decreased extremely and the peak at 1455 cm<sup>-1</sup> appeared, indicating the polymerization. The similar OM image, meaning white line, was obtained just after pressing C<sub>60</sub> powder without FEL irradiation. However observed peak was only intrinsic Ag(2) mode. At the other area except for white line, the Ag(2) mode was clearly observed at 1469 cm<sup>-1</sup>. These results revealed that the most important key to produce polymer by irradiating the FEL was to press it at the order of GPa. From the width of the white line, calculated pressure was 7GPa.

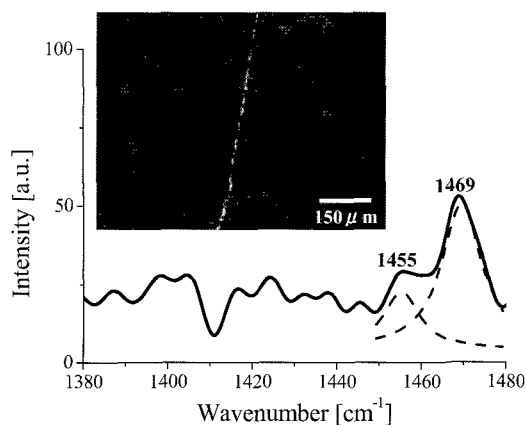


Figure 1. A Raman spectrum and an optical microscope image are illustrated. The 500 nm FEL was irradiated.

[1] The 33rd Fullerene-Nanotubes General Symposium 2P-15

## **C<sub>60</sub> Crystal Growth and Free Electron Laser Irradiation Effect on Pressed C<sub>60</sub> Powder in Solution**

○Yasunari Iio, Shingo Ando, Ryo Nokariya, Nobuyuki Iwata and Hiroshi Yamamoto

*College of Science & Technology, Nihon University  
7-24-1 Narashinodai, Funabashi-shi Chiba, Japan 274-8501*

The aim of our study is to synthesize amorphous C<sub>60</sub> bulk crystal with free electron laser (FEL) irradiation. In the last report we reported that polymerization degree of pillar C<sub>60</sub> crystal made by liquid-liquid interfacial precipitation (LLIP) method with m-xylene/IPA was higher than that of C<sub>60</sub> precipitate on the bottom in the supersaturated m-xylene from the result of Raman spectrum[1]. It is noted that the key for polymerization is shorter distance between C<sub>60</sub> molecules in a pillar C<sub>60</sub> crystal. By the way, the shape of C<sub>60</sub> crystal strongly depends on solvent. In this report, C<sub>60</sub> crystals were grown on substrate just by evaporating solvent, toluene, m-, o-, and p-xylene, from supersaturated solutions to obtain the shorter distance in crystal. The shorter distance was also obtained in a pressed C<sub>60</sub> powder.

Glass substrate (approximately 10×10mm<sup>2</sup>) was just immersed in the supersaturated solution and then evaporating the solvent at 12°C. The glass bottle filled with the solution and the substrate was tilted with 60° from the so-called z-axis, normal to the ground.

Figure 1 is an optical microscope image of C<sub>60</sub> crystal from the toluene supersaturated solution. The rectangular crystals with the size of mm-order were obtained. Needle-shaped grains with 10μm in diameter and 1mm in length from m-xylene supersaturated solution were obtained. Raman spectra showed that the crystal was C<sub>60</sub> monomer.

The crystal growth with different solvent and by LLIP method, and the FEL irradiation will be also discussed.

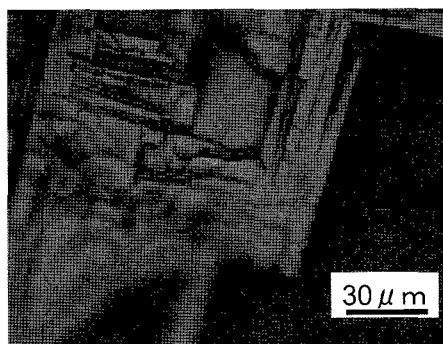


Fig.1 : Optical microscope image of the solution-grown C<sub>60</sub> with toluene.

[1] The 33rd Fullerene-Nanotubes General Symposium 2P-15

## Magnetic Properties of superconducting sodium fulleride $\text{Na}_x\text{C}_{60}$

○Nozomu Kimata, Satoshi Heguri, and Mototada Kobayashi

*Department of Material Science, Graduate School of Material Science,  
University of Hyogo, Ako, Hyogo 678-1297, Japan*

The structure and physical properties of sodium fullerenes  $\text{Na}_x\text{C}_{60}$  are very interesting because they are different from those of other alkali-doped  $\text{C}_{60}$ . Since the  $\text{Na}^+$  ion has a small ionic radius,  $\text{Na}_x\text{C}_{60}$  with large  $x$  value can be expected. Yildirim *et al.* reported the synthesis of  $\text{Na}_{9.7}\text{C}_{60}$  with a face-centered cubic (fcc) structure and suggested the Na-saturated phase to be  $\text{Na}_{11}\text{C}_{60}$  [1]. We reported structure, magnetic susceptibility and superconductivity for  $\text{Na}_x\text{C}_{60}$  at the last Symposium. Here we report physical properties of  $\text{Na}_x\text{C}_{60}$ , mainly on magnetic properties.

Sodium doped fullerenes were prepared from sublimed  $\text{C}_{60}$  powder with 99.95% purity (MTR Ltd.) and Na metal. The mixture of degassed  $\text{C}_{60}$  and Na metal was encapsulated into a stainless steel tube and sealed into a Pyrex glass tube after evacuating. Thermal treatments in a furnace were carried out at 573K for 672 hours. The molar composition  $x$  of products were determined by weight uptake measurement. We succeeded in preparing the samples with up to 11.

Figure 1 shows the applied magnetic field dependence of the molar magnetization for superconducting  $\text{Na}_{8.2}\text{C}_{60}$  by using SQUID magnetometer. Critical magnetic field of  $\text{Na}_{8.2}\text{C}_{60}$  are  $H_{c1}=1.6\text{mT}$ ,  $H_{c2}=2.5\text{T}$  at 2K and  $H_{c1}=1.0\text{mT}$ ,  $H_{c2}=1.6\text{T}$  at 8K. Ginzburg-Landau parameter estimates  $\kappa=13$ .

Details will be discussed at the meeting.

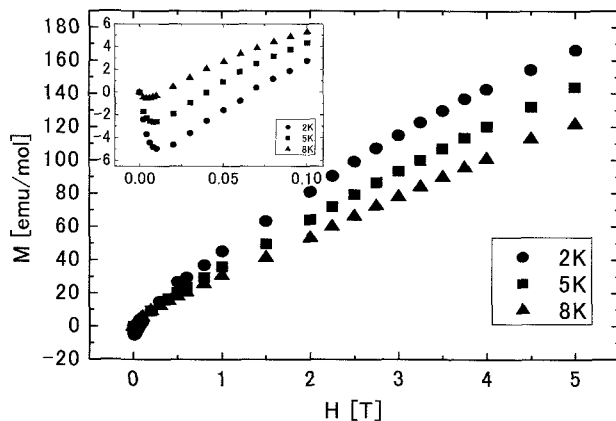


Fig.1 Applied magnetic field dependence of molar magnetization for  $\text{Na}_{8.2}\text{C}_{60}$ .

[1] T.Yildirim, O.Zhou, J.E.Fischer, N.Bykovetz, R.A.Strongin, M.A.Cichy, A.B.Smith III, C.L.Lin and R.Jelinek, *Nature*, **360**, 568(1992).

Corresponding Author: Nozomu Kimata

TEL: +81-791-58-0156, FAX:+81-791-58-0132, E-mail: [ri07v005@stkt.u-hyogo.ac.jp](mailto:ri07v005@stkt.u-hyogo.ac.jp)



発表索引  
**Author Index**

## Author Index

~A~

Abe, Masuhiro 2P-20  
 Abe, shigeaki 1P-17  
 Achiba, Yohji 1P-3, 2-3, 2P-9, 2P-10,  
 3-1  
 Adhikari, Sudip 2P-12  
 Afre, Rakesh 2P-12  
 Ago, Hiroki 1P-10  
 Ajima, Kumiko 1P-47  
 Akachi, Masahiro 1P-33, 1P-35  
 Akachi, Takao 1P-33  
 Akasaka, Takeshi 1P-30, 1P-31, 1P-32,  
 2-4, 2-6, 2-14, 2P-2,  
 2P-21, 2P-31, 2P-32,  
 2P-35  
 Akasaka, Tsukasa 1P-17  
 Akita, Seiji 2P-17, 2P-25  
 Ami, Yohei 2P-40  
 Ando, Hiroaki 2P-26  
 Ando, Shingo 3P-48, 3P-49  
 Ando, Yoshinori 2P-11, 3P-22  
 Aoki, Nobuyuki 3P-44  
 Aoki, Takaaki 1P-1  
 Aoshima, Hisae 2P-44, 3P-38  
 Aoyagi, Nobuyoshi 1P-48  
 Aoyagi, Shinobu 1P-39  
 Aoyagi, Yoshinobu 3P-15  
 Arai, Fumihito 3P-17  
 Arai, Toru 2P-16  
 Araki, Yasuyuki 2-12, 2P-35  
 Aryal, Hare Ram 2P-12  
 Asaka, Koji 1P-14, 1P-16, 1P-18,  
 1P-20, 3P-3  
 Asakura, Masahiro 3P-1  
 Ata, Masafumi 2P-35  
 Ataka, Tatsuaki 2P-20  
 Atake, Tooru 2-7  
 Awano, Yuji 1S-2, 3-4, 3-8  
 Azumi, Reiko 3P-46, 3P-47

~B~

Bando, Yoshio 1P-37  
 Bandow, Shunji 1P-46, 3P-30

~C~

Cecco, Alfonso Reina 1P-11  
 Chen, Beibei 3P-22  
 Chiba, Yasuto 3P-44  
 Chikamatsu, Masayuki 3P-46, 3P-47  
 Chiu, Chien-Chao 1P-7, 2-10  
 Cho, Kaimei 2P-50  
 Clair, Sylvain 1-9, 1-10

~D~

Dhawan, Nikhil 1P-5, 1P-25  
 Dinse, Klaus-Peter 2P-35  
 Dresselhaus, Gene 1P-11, 2P-23  
 Dresselhaus, Mildred S. 1P-11, 2P-23

~E~

Ehara, R. 1P-26  
 Einarsson, Erik 1P-28, 3-3, 3P-27  
 Enoki, Haruka 2P-31

~F~

Fan, Jing 1P-49  
 Fujigaya, Tsuyohiko 1P-15, 2P-14, 3-7  
 Fujihara, Hisashi 2P-32  
 Fujima, Nobuhisa 1P-27  
 Fujimura, Youhei 3P-35  
 Fukami, Shun 2P-17  
 Fukui, Nobuyuki 1P-33  
 Fukumaru, Takahiro 2P-14  
 Fukunaga, Yuhei 1P-46  
 Furuichi, Koji 1-12  
 Furukawa, Takeo 3P-41  
 Fuse, Tomoko 3P-13  
 Futaba, Don N. 1-15, 2P-4, 2P-15  
 Futami, Yoshisuke 1-5, 2P-24

~G~

Gao, Xingfa 2P-32  
 Golberg, Dmitri 1P-37  
 Goto, Tadashi 2P-44  
 Gotou, Jundai 1-15

~H~

Hara, Takeshi 3P-42  
 Harada, Manabu 1P-46  
 Harada, Shinji 3P-31  
 Harano, Koji 2P-48  
 Harima, Hiroshi 2P-6  
 Haruyama, Junji 1-8, 1P-28  
 Haseba, Takaki 2P-41, 2P-42  
 Hasebe, Yuki 2P-6  
 Hasegawa, Kei 3P-6  
 Hasegawa, Sunao 3P-39  
 Hasegawa, Tadashi 1P-32, 2P-2  
 Hashi, Tomofumi 2P-22  
 Hashiba, Ryo 3P-26  
 Hashimoto, Masahiro 2P-2  
 Hashimoto, Takeshi 1P-17, 3P-22  
 Hata, Kenji 1-5, 1-15, 2P-4, 2P-15  
 Hata, Koichi 1P-8  
 Hata, Kosuke 2P-25  
 Hatakeyama, Rikizo 1-3, 1P-24, 2P-13,  
 2P-33, 2P-36  
 Hatori, Hiroaki 2P-15  
 Hayashi, Kazuhiko 1P-1  
 Heguri, Satoshi 3P-34, 3P-50  
 Hibino, Hiroki 3-2  
 Hidaka, Kishio 3P-8  
 Hikata, Takeshi 1P-1  
 Hino, Shojun 2-2  
 Hiraoka, Tatsuki 2P-15  
 Ho, Dean 2S-3  
 Homma, Tatsuya 2P-48  
 Homma, Yoshikazu 3-2, 3P-21  
 Honda, Hiroyuki 1P-19  
 Horiguchi, Hirokazu 2P-19  
 Hosokawa, Yuji 3P-35  
 Hozumi, Yoko 1P-9  
 Huang, Houjin 2S-3

Huang, Yang 1P-37  
 Hyakushima, Takashi 3-8

~I~

Ichida, Masao 2P-26  
 Ichihashi, Toshinari 1P-45  
 Ichikawa, Akihiro 3P-32  
 Ichiki, Takahiko 2P-45  
 Iijima, Sumio 1-15, 1-17, 1P-36,  
 1P-44, 1P-45, 1P-46,  
 1P-47, 1P-49, 1P-50,  
 2-12, 2P-4, 2P-15,  
 2P-49, 3P-23, 3P-30  
 Iio, Yasunari 3P-48, 3P-49  
 Iizumi, Yoko 2P-49  
 Ikeda, Atsushi 1P-4  
 Imamura, Sadanobu 1-2  
 Imanaka, Tadayuki 3P-14  
 Imazu, Naoki 1P-40  
 Ina, Shingo 3P-5  
 Ina, Takashi 3P-35  
 Inaba, Sachio 2-15  
 Inada, Koji 1P-32  
 Inomata, Katsuya 3P-37  
 Inomata, Naoki 3P-17  
 Inoue, Noritaka 2P-34  
 Inoue, Sakae 2P-11, 3P-22  
 Inoue, Tadashi 1-4  
 Irle, Stephan 1P-21  
 Ishibashi, Koji 3P-1, 3P-13, 3P-15,  
 3P-19, 3P-26  
 Ishida, Takeo 2P-3  
 Ishigami, Itsuo 1P-1  
 Ishii, Fumiyuki 2-13  
 Ishii, Satoshi 1-7  
 Ishii, Tadahiro 3P-16, 3P-18  
 Ishii, Toru 3P-16  
 Ishimaru, Kentaro 3-8  
 Ishitsuka O., Midori 1P-32, 2P-31, 2P-32  
 Ishizuka, Daisuke 3P-4, 3P-10  
 Isobe, Hiroyuki 2-9, 2-12, 2P-48, 2P-50  
 Isshiki, Toshiyuki 2P-6  
 Itakura, Atsushi 3P-46, 3P-47

Ito, Manabu	2-3	Kato, Shigeki	1P-12
Ito, Masakatsu	3P-36	Kato, Tatsuhisa	1P-32, 2P-35
Ito, Masayuki	3P-38	Kato, Toshiaki	1-3, 2P-13
Ito, Osamu	1P-47, 2-12, 2P-35	Kato, Yuko	1P-39
Ito, Ryuhei	3P-7	Kawabata, Akio	3-4
Ito, Shigeo	1P-48	Kawabata, Hiroshi	3P-45
Ito, Yasuhiro	1P-33, 1P-35, 1P-39, 2-1	Kawabe, Masaaki	2-15
Ito, Y.	1P-26	Kawai, Maki	1-9, 1-10
Itoh, Shigeo	3P-35	Kawai, Takazumi	1-11, 1P-49, 2-13
Iwamoto, Masachika	2-1	Kawaji, Hitoshi	2-7
Iwasa, Yoshihiro	1-13	Kawamoto, Tohru	3P-24
Iwasaki, Takayuki	3-8, 3P-9	Kawano, Yukio	3P-13
Iwata, Atsushi	3P-42	Kawarada, Hiroshi	3-8, 3P-9
Iwata, Nobuyuki	3P-4, 3P-10, 3P-48, 3P-49	Kawasaki, Shinji	3P-42, 3P-43
Izadi-Najafabadi, Ali	2P-15	Kawashita, Takehiro	3P-43
Izard, N.	1-5	Kawata, Satoshi	2P-18
Izu, Yoshifumi	1P-43	Kazaoui, Said	1-5, 2P-24
Izumi, Yuuki	1P-48	Kertesz, Miklos	1P-29
Izumisawa, Satoru	2-7	Kikuchi, Koichi	2-3
~J~		Kim, Yousoo	1-9, 1-10
Jiang, Jie	2P-23	Kimata, Nozomu	3P-34, 3P-50
Jianxun, Xu	1P-44	Kimura, Takahide	2P-8
Jin, Hehua	3-6, 3P-14	Kishi, Naoki	3P-30
Joung, Soon-Kil	3P-30	Kishida, Hideo	1-2
~K~		Kishimoto, Shigeru	1P-19
Kajiwara, Kazuo	1P-8	Kisoda, Kenji	2P-6
Kakiuchi, Toru	2-7	Kitada, Norihiro	3P-33
Kalita, Golap	2P-12	Kitamura, Hiroshi	2P-43
Kanamori, Yusuke	3P-42	Kitaura, Ryo	1P-33, 1P-35, 1P-39, 1P-40, 1P-42, 3P-12
Kanda, Makoto	2P-2	Kito, Hironobu	1P-41
Kaneko, Toshiro	1P-24, 2P-36	Kiyohara, Yumie	2P-26
Kanemitsu, Yoshihiko	1-4	Kobayashi, Akiko	1P-22
Kasama, Yasuhiko	2P-33, 3P-41	Kobayashi, Kei	3P-29
Kashihara, Yoshihiko	2P-41, 2P-42	Kobayashi, Keita	1P-40, 1P-42, 3P-12
Kataura, Hiromichi	2P-3, 2P-26, 2P-30, 3-6, 3P-5, 3P-14	Kobayashi, Keita	1P-40, 1P-42, 3P-12
Kato, Haruo	1P-13	Kobayashi, Ken-Ichi	3P-33
Kato, Mai	2P-47	Kobayashi, Ken-Ichi	3P-33
Kato, Ryogo	3P-9	Kobayashi, Mototada	3P-34, 3P-50
		Kobayashi, Nagao	2P-21
		Kobayashi, Norihiro	2-1
		Kobayashi, Yoshihiro	2P-27, 3-2, 3P-2, 3P-21
		Kodama, Shin-Ichi	1P-4
		Kodama, Takeshi	2-3
		Koga, Keiko	3P-41

Kohama, Yoshimitsu	2-7	Maki, N.	1P-26
Kojima, Kenichi	1-18, 3P-33	Maki, Tasuku	3P-9
Kokai, Fumio	1P-41	Makihata, Mitsutoshi	3P-15
Kokubo, Ken	2P-43, 2P-44, 2P-47, 3P-38	Maniwa, Yutaka	2P-30, 3P-5
Komatsu, Koichi	2-7	Maruyama, Masashi	2P-46
Komatsu, Naoki	2P-8	Maruyama, Shigeo	1-4, 1-8, 1-12, 1-14, 1P-28, 1P-43, 2P-2, 2P-5, 3-3, 3P-6, 3P-7, 3P-11, 3P-27, 3P-28
Komatsu, Naoya	2P-21	Maruyama, Takahiro	1P-6, 1P-9, 2P-1
Kondo, Daiyu	3-4	Maruyama, Yusei	1P-22
Kondo, Y.	1P-26	Masuhara, Shinya	2P-7, 3P-8
Kong, Jing	1P-11	Masuo, Yuki	1P-4
Kono, Junichiro	3P-25	Matsuda, Kazunari	1-4
Kono, Keijiro	2-1	Matsudaira, Masaharu	1P-28
Kono, Takumi	1P-20	Matsumoto, K.	1P-26
Koretsune, Takashi	1-6	Matsumoto, Kazuhiko	2P-20
Koshino, Masanori	2-9	Matsunaga, Yoichiro	2P-35
Koshio, Akira	1P-41	Matsuo, Jiro	1P-1
Krishnamurthy, Raviprasad	1P-21	Matsuo, Yutaka	2P-45, 2P-46, 3S-6
Kumagai, Estuko	3P-31	Matsuoka, Makoto	1P-17
Kumar, Abhishek	1P-5, 1P-25	Matsushige, Kazumi	3P-29, 3P-45
Kumashiro, Ryotaro	2-7, 2P-21	Matsuura, Koji	3P-23
Kunishige, Atsuhiko	2P-29, 3P-24	Matsuura, T.	1P-26
Kuranoto, Tatsunori	2P-16	Mieno, Tetsu	2-5, 3P-39
Kusunoki, Michiko	1P-2, 1P-9, 1P-13, 3P-32	Minami, Nobutsugu	1-5, 2P-24
~L~		Minfang, Zhang	1P-44
Li, Y. F.	1P-24	Miura, Koji	3P-35
Li, Zhh.	2P-11	Miura, Mituharu	1P-48
Liu, Huarong	1P-12	Miura, Yosuke	2P-7, 3P-8
Liu, Michael T. H.	2P-31	Miyahara, Katsuya	2P-38
Liu, Zheng	2P-3	Miyake, Yoko	2-3
Lu, Jing	2P-2	Miyamoto, Hiromitsu	3P-8
Lu, Xing	2-6	Miyamoto, Yoshiyuki	1-11, 2P-37
~M~		Miyata, Yasumitsu	2P-3, 2P-26, 2P-30, 3-6, 3P-5
Maeda, Noriko	3P-18	Miyato, Yuji	3P-29
Maeda, Yasushi	2P-7, 3P-8	Miyauchi, Yuhei	2P-2, 3-3, 3P-27
Maeda, Yutaka	1P-30, 1P-31, 1P-32, 2-4, 2-6, 2P-2, 2P-21, 2P-32	Miyawaki, Jin	1P-45, 1P-49, 1P-50
Majima, Yutaka	2-1	Miyazaki, Takafumi	2-2
Maki, Hideyuki	2P-27	Mizobuchi, Yuzo	3P-41
		Mizorogi, Naomi	1P-30, 1P-31, 1P-32, 2-4, 2-6, 2P-31

Mizukoshi, Tomoyuki	1P-1	Nakashima, Yasuhiro	1P-19
Mizuno, Naoki	1P-41	Nakayama, Yoshikazu	2P-25
Mizuno, Tomoyuki	2P-27	Naritsuka, Shigeeya	1P-6, 1P-9, 2P-1
Mizusawa, Takashi	1P-3	Nihei, Mizuhisa	3-8
Mizutani, Takashi	1P-19, 1P-35	Nihsimura, Minetaka	3P-28
Mori, Midori	1P-9	Nii, Hiroyuki	2P-29
Mori, Shunsuke	3P-43	Nikawa, Hidefumi	2-6, 2P-35
Mori, Takahiro	3P-15, 3P-19	Nishi, Nobuyuki	2P-1
Moriguchi, Tetsuji	2P-16	Nishibori, Eiji	1P-39, 2S-4
Morishita, Takayuki	3P-32	Nishigaki, Shohei	1P-24, 2P-36
Morita, Hiroyuki	2P-32	Nishio, Koji	2P-6
Morokuma, Keiji	1P-21	Nobukuni, Shingo	2P-16
Motohashi, Satoru	1P-22	Noda, Suguru	1-12, 3P-6, 3P-7
Murakami, Tatsuya	1P-47	Nojiri, Hiroyuki	1-13
Murakami, Tetsushi	1P-4, 1P-38	Nokariya, Ryo	3P-48, 3P-49
Murakami, Toshiya	2P-6	Numao, Shigenori	2P-1
Murakami, Yoichi	1-4, 3-3, 3P-25		
Muranaka, Takashi	3P-24	~O~	
Murata, Katsuyuki	2P-20	Ochiai, Yuichi	3P-26, 3P-44
Murata, Naoyoshi	1P-28	Oda, Tatsuki	1-18, 1P-27
Murata, Yasujiro	2-7	Ogata, Hironori	1P-22
		Ogata, Teruhiko	2-5
~N~		Ogawa, Daisuke	1P-42
Nagaishi, Shouichiro	3P-31	Ohashi, Kazunori	1P-33
Nagaoka, Shiho	2-3	Ohfuchi, Mari	3P-36
Nagasawa, Hiroshi	2P-9	Ohigashi, Hiroji	3P-41
Nagasawa, Yoshiaki	1-2	Ohmine, Iwao	3P-20
Nagase, Shigeru	1P-30, 1P-31, 1P-32, 2-4, 2-6, 2P-2, 2P-31, 2P-32	Ohmori, Shigekazu	1-17, 3P-23
Nagatsu, Hidetoshi	3P-3	Ohno, Yutaka	1P-19, 1P-35
Naito, Ryoji	2P-6	Ohshima, Satoshi	1-17, 1P-42, 3P-23
Nakagawa, Hamazo	2P-29, 3P-24	Oie, Manabu	3P-26
Nakahara, Hitoshi	1P-14, 1P-16, 1P-20, 3P-3	Oishi, Osamu	2P-1
Nakahodo, Tsukasa	2P-32	Oizumi, Haruna	3P-41
Nakajima, Koji	1P-31, 2-4	Okada, Fumio	3P-35
Nakamura, Arao	1-2	Okada, Hiroshi	2P-33
Nakamura, Eiichi	2-9, 2-12, 2P-45, 2P-46, 2P-48, 2P-50	Okada, Mitsunori	2P-32
Nakanishi, Takeshi	3P-30	Okada, Susumu	2-13, 2P-28, 3P-40
Nakao, Kota	2P-38	Okamoto, Minoru	3-7
Nakashima, Naotoshi	1P-15, 2P-14, 3-7	Okamoto, Yasuharu	1S-1
		Okawa, Jun	3-3, 3P-11
		Okazaki, Toshiya	1-5, 1P-3, 1P-35, 1P-36, 2P-49, 3P-30
		Oke, Shinichiro	1P-48, 3P-35

Okimoto, Haruya	2-1, 2-2	Saito, Tatsuya	2P-21
Okochi, Mina	1P-19	Saito, Yahachi	1P-12, 1P-14, 1P-16,
Okubo, Shingo	1P-36		1P-18, 1P-20, 3P-3
Okumura, Kensuke	1P-18	Sakaguchi, Koichi	3P-46, 3P-47
Okuyama, Hiroki	3P-4, 3P-10	Sakai, Hiroshi	3P-2
Omote, Kenji	2P-33, 3P-41	Sakai, Takeshi	2P-33
Omura, Kazuo	3P-19	Sakakibara, Ikuo	1P-48
Onari, Seiichiro	1P-23	Sakamoto, Tomokazu	2-10
Ono, Shin	2P-7, 3P-8	Sakamoto, Yuji	3P-37
Ono, Shoichi	2P-33, 3P-41	Sakashita, Hirofumi	1P-27
Onoe, Jun	3P-44	Sakata, Makoto	1P-39
Oohara, Wataru	2P-13	Sakurai, Yoshiaki	1P-1
Ookawa, Takashi	1P-48	Sandanayaka, Atula	2-12
Osawa, Eiji	2-15, 2S-3	Sandanayaka, D. A.	1P-47
Osawa, Toshio	3P-7	Sano, Masahito	1-16, 2P-19
Oshima, Hisayoshi	2P-5	Sasai, Ryo	3P-32
Oshima, Takumi	2P-43, 2P-44, 2P-47, 3P-38	Sasaki, Kenichi	1-1, 1P-23
Oshima, Yugo	1-13	Sato, Hideki	1P-8
Osuka, Atsuhiro	2P-8	Sato, Kentaro	1-1, 2P-23
Otake, Yoshinobu	3P-37	Sato, Satoru	1P-32
~P~		Sato, Shintaro	3-4, 3-8
Park, Hyekyeong	3P-14	Sato, Shunsuke	3P-19
Park Sung, Jin	1-1, 1P-11	Sato, Tetsuya	2P-27
Peng, Xiaobin	2P-8	Sato, Yoshinori	1P-17
Pierstorff, Erik	2S-3	Sato, Yuta	1-5, 1P-36, 2P-3
~R~		Sawa, Hiroshi	2-7
Rachi, Takeshi	2-7	Sawada, Keisuke	2-13
Rodgers, Thomas	2P-18	Seeberger H., Peter	2P-50
~S~		Seki, Toshio	1P-1
Sagami, Hiroyuki	3P-41	Sharon, Maheshwar	2P-12
Saida, Morihiko	3P-41	Shi, Zujin	3P-30
Saito, Hiroshi	1-16	Shibata, Noriyoshi	1P-13
Saito, Mineo	2-13, 2P-22	Shibi, Yutaka	2-5
Saito, Riichiro	1-1, 1P-11, 1P-23, 2P-23	Shimazu, Tomohiro	2P-5
Saito, Shingo	2P-26	Shimote, Yoshikazu	2P-16
Saito, Shinji	3P-20	Shin, Hyung-Joon	1-9, 1-10
Saito, Susumu	1-6, 2-8	Shinohara, Hisanori	1-8, 1P-28, 1P-33, 1P-35, 1P-39, 1P-40, 1P-42, 2-1, 2-2, 3-5,
Saito, Takeshi	1-5, 1-17, 1P-42, 3P-23,		3P-12
		Shinohara, Kennzi	1P-48
		Shinohara, Yuichiro	3P-35
		Shiokawa, Takao	3P-1

Shiomi, Junichiro	1-14, 1P-43, 3P-28	Tanaka, Takeshi	3-6, 3P-14
Shiraiwa, Tomoyuki	1P-6, 2P-1	Tanaka, Yukio	1P-23
Shirakawa, Shogo	3P-38	Tang, Chengchun	1P-37
Shiratori, Yosuke	1-12	Tanigaki, Katsumi	2-7, 2P-21
Shishido, Jun	2P-13	Taniguchi, Isao	2P-38, 3P-31
Shoji, Satoru	2P-18	Tanioku, Kenji	1P-6
Slanina, Zdenek	2P-31	Tarao, Takashi	2-15
Soga, Tetsuo	2P-12	Tatamitani, Yoshio	2-5
Sol, Yui	2P-47	Terao, Takeshi	1P-37
Solin, Niclas	2-9, 2P-50	Tobita, Hiromi	2P-33
Sonomura, Takuya	3P-10	Tochika, Shinya	2P-47
Suenaga, Kazutomo	1-5, 1P-36, 2P-3	Toda, Masayuki	2P-33
Sugai, Toshiki	1P-28, 1P-33, 1P-35, 2-2, 3-5	Togaya, Kyoko	2P-44
Sugawara, Syuuichi	1P-48	Tohji, Kazuyuki	1P-17, 2P-13
Sugihara, Kunihiro	1P-13	Tokunaga, Ken	3P-45
Sugime, Hisashi	1-12	Tominaga, Masato	2P-38, 3P-31
Sugimoto, Shigeyuki	1P-13	Toyokawa, Seiko	3P-13
Sumii, Ryohei	2-2	Tsuchida, Kunihiro	1P-47
Sumikama, Takashi	3P-20	Tsuchiya, Takahiro	1P-30, 1P-31, 1P-32, 2-4, 2-6, 2P-2, 2P-31, 2P-32
Sumiyama, Yoshiyuki	2P-29, 3P-24		
Susami, Yasunori	2P-43	Tsuda, Shunsuke	1-7
Suzuki, Hirotaka	1-13	Tsuji, Hajime	3P-44
Suzuki, Masahiro	1P-23	Tsuji, Masaharu	1P-10
Suzuki, Satoru	2P-27, 3-2, 3P-21	Tsuji, Yoshiko	1-12
Suzuki, Shinzo	1P-3, 2-3, 2P-9	Tsuruoka, Yasuhiro	2P-10, 3-1
Suzuki, Shogo	1P-8		
Suzuki, Yoshinobu	2P-5	~U~	
		Uchida, Katsumi	3P-4, 3P-16, 3P-18
~T~		Uchida, Takashi	3P-2
Tachibana, Masaru	1-18, 3P-33	Ueda, Kazuyuki	1P-7, 2-10
Tagmatarchis, Nikos	3S-5	Ueno, Misaki	3P-44
Tahara, Shuichi	3S-7	Umemoto, Hisashi	1P-33, 2-1, 2-2
Taira, Y.	1P-26	Umeno, Masayoshi	2P-12
Takagi, Daisuke	3-2	Uo, Motohiro	1P-17
Takamori, Hisayoshi	1P-15	Urata, Keisuke	2P-9, 3-1
Takano, Yoshihiko	1-7	Usui, Shinji	2P-34
Takikawa, Hirofumi	1P-48, 3P-35		
Tamura, N.	1P-26	~W~	
Tanaike, Osamu	2P-15, 3P-33	Wada, Yoriko	2P-39
Tanaka, Kei	2-10	Waelchli, Markus	1P-31, 2-4
Tanaka, Masayuki	1P-22	Wakabayashi, Tomonari	1P-4, 1P-38, 2-11, 2P-39, 2P-40, 2P-41,
Tanaka, Takatsugu	2-9, 2-12		



	2P-42	Yanai, Takayuki	3P-4
Wakahara, Takatsugu	1P-30, 1P-31, 2-4, 2-14, 2P-2	Yase, Kiyoshi	3P-46, 3P-47
Wakamatsu, Nobuo	1P-15	Yasuda, Satoshi	1-15, 2P-4, 2P-15
Wako, Kei	1-18	Yasutake, Yuhsuke	2-1
Wang, Hf.	2P-11	Yokoo, Kuniyoshi	2P-33, 3P-41
Watanabe, Shu	3P-1	Yokota, Masashi	3P-35
Watanabe, Tohru	1-7	Yokoyama, Atsuro	1P-17
Watari, Fumio	1P-17	Yokoyama, Daisuke	3-8
Werz, Daniel B.	2P-50	Yoshida, Hiromichi	3-5
Williams, Oliver A.	2-15	Yoshida, Hiroshi	3P-1
		Yoshida, Yuji	3P-46, 3P-47
		Yoshihara, Naoki	1P-10
~X~		Yoshikawa, Kazuo	1P-2, 1P-48, 3P-35
Xiang, Rong	3-3, 3P-11	Yoshimura, Hirofumi	3P-33
Xu, Qian	1P-34	Yoshimura, Masamichi	1P-7, 2-10
		Yoshimura, Toshiaki	2P-32
~Y~		Yoshitake, Tsutomu	1P-45
Yagi, Yuko	1P-28	Yoshizaka, Nagisa	3P-31
Yajima, Hirofumi	3P-4, 3P-16, 3P-18	Yoza, Kenji	1P-30, 2-4
Yamada, Hirofumi	3P-29	Yudasaka, Masako	1P-44, 1P-45, 1P-47, 1P-49, 1P-50, 2-12, 2P-49
Yamada, Michio	1P-30, 1P-32		
Yamada, Takeo	1-15, 2P-15	Yuge, Ryota	1P-45, 1P-49
Yamagami, Yuichiro	2-8	Yumura, Motoo	1-15, 1-17, 2P-4, 2P-15, 3P-23
Yamaguchi, Takahide	1-7		
Yamaguchi, Tomohiro	3P-13, 3P-15, 3P-26	Yumura, Takashi	1P-29
Yamaguchi, Yukio	1-12, 3P-6, 3P-7		
Yamamoto, Atsushi	2P-7, 3P-8	~Z~	
Yamamoto, Hiroshi	3P-4, 3P-10, 3P-48, 3P-49	Zhang, Hong	2P-37
Yamamoto, Kazunori	2-14	Zhang, Minfang	1P-47, 1P-50, 2P-49
Yamamoto, Masanobu	1P-48	Zhang, Zhengyi	1-12, 3-3, 3P-27
Yamamoto, Motohiro	1P-2, 3P-32	Zhao, Xiang	1P-34
Yamamoto, Yo	1P-9	Zheng, Hong	1P-34
Yamana, Shuichi	3P-38	Zhi, Chunyi	1P-37
Yamanishi, Yoko	3P-17	Zhou, Biao	1P-22
Yamashita, Fuyuko	2P-33		
Yamashita, Tetsuya	1P-16		
Yamaura, Tatsuo	1P-48, 3P-35		
Yamaya, Kenji	3P-21		
Yamazaki, Akira	3P-2		
Yamazaki, Nobuyuki	3P-26		
Yamazaki, Yuko	1P-31, 2-4		
Yanagi, Kazuhiro	2P-3, 2P-30, 3P-5		

### 複写される方へ

フラーレン・ナノチューブ学会は、有限責任中間法人 学術著作権協会（学著協）に複写に関する権利委託をしていますので、本誌に掲載された著作物を複写したい方は、学著協より許諾を受けて複写して下さい。

但し、社団法人日本複写権センター（学著協より複写に関する権利を再委託）と包括複写許諾契約を締結されている企業の社員による社内利用目的の複写はその必要はありません。（※社外頒布用の複写は許諾が必要です。）

権利委託先：有限会社中間法人 学術著作権協会  
〒107-0052 東京都港区赤坂 9-6-41 乃木坂ビル 3 階  
電話：03-3475-5618 FAX：03-3475-5619 E-Mail：info@jaacc.jp

注意：複写以外の許諾（著作物転載・翻訳等）は、学著会では扱っていませんので、直接、フラーレン・ナノチューブ学会へご連絡下さい。

### Notice for Photocopying

If you wish to photocopy any work of this publication, you have to get permission from the following organization to which licensing of copyright clearance is delegated by the copyright owner.

<All users except those in USA>

Japan Academic Association for Copyright Clearance, Inc. (JAACC)  
6-41 Akasaka 9-chome, Minato-ku, Tokyo 107-0052 Japan  
TEL : 81-3-3475-5618  
FAX : 81-3-3475-5619 E-Mail : info@jaacc.jp

<Users e in USA>

Copyright Clearance Center, Inc.  
222 Rosewood Drive, Danvers, MA 01923 USA  
Phone : 1-978-750-8400 FAX : 1-978-646-8600

2008年3月3日発行

## 第34回フラーレン・ナノチューブ総合シンポジウム 講演要旨集

<フラーレン・ナノチューブ学会>

〒464-8602 愛知県名古屋市千種区不老町  
名古屋大学大学院理学研究科 物質理学専攻  
篠原研究室内  
Tel : 052-789-5948  
Fax : 052-789-1169

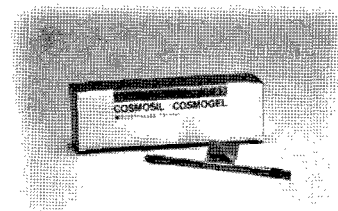
E-mail : fullerene@nano.chem.nagoya-u.ac.jp

URL : <http://fullerene-jp.org>

印刷 / 製本 名古屋大学消費生活協同組合印刷部

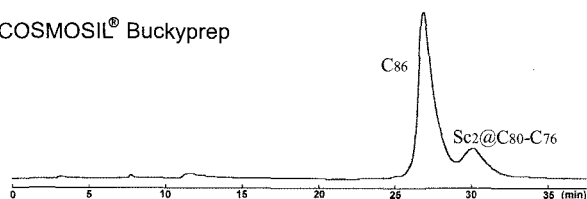
# COSMOSIL® Buckyprep-M

今まで分離できなかった  
金属内包フラーレンが分離可能！！

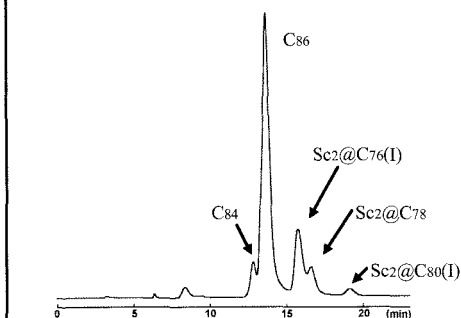


## ■分析例

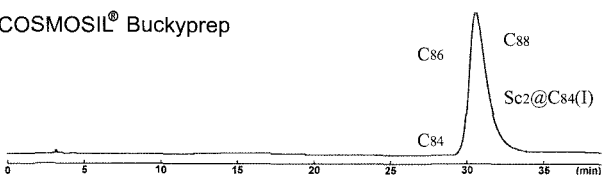
COSMOSIL® Buckyprep



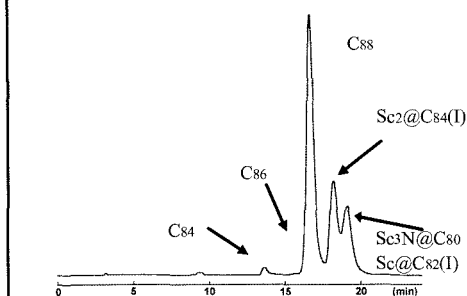
COSMOSIL® Buckyprep-M



COSMOSIL® Buckyprep



COSMOSIL® Buckyprep-M



分析条件

カラムサイズ: 4.6mm I.D. × 250mm, 移動相: トルエン, 流速: 1.0 ml/min, 温度: 30°C, 検出: UV312

資料提供: 名古屋大学 大学院理学研究科物質理学専攻 篠原 久典教授

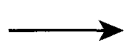
## ■その他COSMOSIL® フラーレン関連カラム

フラーレン分離のスタンダードカラム



COSMOSIL® Buckyprep

C<sub>60</sub>, C<sub>70</sub>等の大量分取に



COSMOSIL® PBB

詳しい情報はWeb siteをご覧ください。

ナカライテスク株式会社

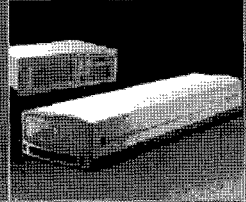
〒604-0855 京都市中京区二条通烏丸西入東五屋町498

価格・納期のご照会 フリーダイヤル 0120-489-552

製品に関するご照会 TEL: 075-211-2703 FAX: 075-211-2673

Web site: <http://www.nacalai.co.jp>

 Spectra-Physics



超短パルスレーザー  
 ランプ励起ナノ秒パルスレーザーシステム  
 フェーザルレーザー  
 LD励起Qスイッチ固体レーザー  
 LD励起CW/Q-CW固体レーザー  
 ガスレーザー  
 高出力半導体レーザー  
 光学部材

**信頼の製品ブランド**

Spire™ Tsunami™ Mai™ Tai™ Opal™ Navigator™  
 V-Xtreme™ HIPPO™ Vanguard™ ProLite™ Empower™  
 Millennia™ Quanta-Ray™ Excelsior™ Explorer™

レーザーで未来を創造するスペクトラ・フィジックス

**Creative Lasers for the Future**

**LabからIndustryまでの  
ソリューション・プロバイダー**

1960年にレーザーが発明された翌年、世界初のレーザー機器メーカーとして設立。常にレーザーの世界をリードし、長年におたりお客様の信頼と品質で高い評価をいただいております。  
 スペクトラ・フィジックスは、マーケットリーダーとして未来を見つめ、あらゆる最先端技術を提供いたします。

※1961年：世界初の商用レーザー機器メーカーとしてスペクトラ・フィジックス設立。1962-68年：世界初のガスレーザー及びイオンレーザーを発表。1983年：世界初の高出力半導体レーザー製造会社を設立。1986年：世界初のファイバーカップル半導体レーザー超短パルスレーザーを発表。1991年：世界初のモードロックテランサファイアレーザーを発表。1996年：世界初の連続発振高出力固体グリーンレーザーを発表。1999年：世界に先駆けてコンパクト1-BOX型フェーザルナノ秒パルスファイアレーザーを発表。2003年：イットリウムタンクスチウム結晶ベースの画期的な次世代フェムト秒レーザーを発表。2007年：画期的な次世代レーザー、モードロック高出力UVファイバーアンプレーザーを発表。2008年：What's Next...

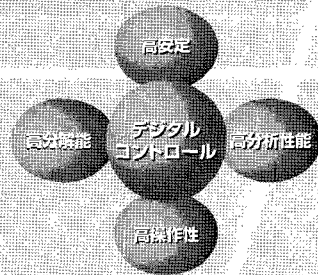
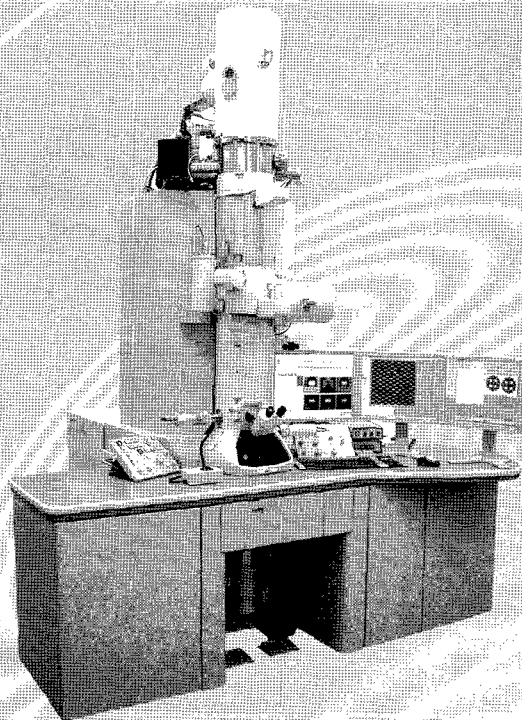
 Newport  
 Experience Solutions

 Spectra-Physics  
 A Division of Newport Corporation

**スペクトラ・フィジックス株式会社**

本社 〒153-0061 東京都目黒区中目黒4-6-1 大和中目黒ビル TEL: (03)3794-5511 FAX: (03)3794-5510  
 大阪支社 〒550-0005 大阪府大阪市西区西本町3-1-43 西本町ソーラービル TEL: (06)4390-6770 FAX: (06)4390-2760  
<http://www.spectra-physics.jp> E-mail: [spectra-physics@splasers.co.jp](mailto:spectra-physics@splasers.co.jp)

# 新時代インテグレーションTEM



## JEM-2100F

### フィールドエミッション電子顕微鏡

フィールドエミッションTEM JEM-2100Fは、簡単に原子レベルの構造解析や斬新な応用分野に利用できます。最小の電子プローブ、優れた点分解能、超高安定の試料ステージ、高耐久性などの特長にプラスして、理想的なクライオ、その場観察、電子線ホログラフィ、三次元観察など豊富なシステム構成が可能です。更に高い分解能のためには、球面収差(Cs)補正器を附加することができます。

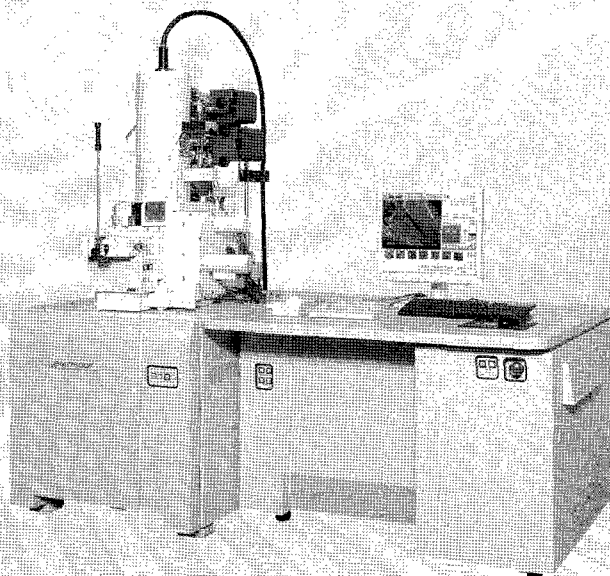
# 進化した新GUIで超高分解能を使いこなす

## JSM-7500F/7500FA

### フィールドエミッション走査電子顕微鏡

JSM-7500Fは、高輝度のコニカル形FE電子銃および低収差のコニカル形対物レンズ(セメインレンズ)を組み合わせた超高分解能フィールドエミッション走査電子顕微鏡です。日本電子開発によるNew r-filter(エネルギーフィルタ)を装備し、ナノ世界を切り開く試料最表面の超微形態観察が可能です。

JSM-7500FAは、FE SEM本体にEDSを組み込んだ一体化設計です。高倍率での形状観察に加えて、試料の材料に起因する組成コントラストによる組成像や試料に含まれる元素の分析を必要とする場合、像観察から瞬時に元素分析を行うことができます。



お問い合わせは、電子光学機器営業本部 (EO販促グループ) ☎042 (528) 3353

# JEOL

Serving Advanced Technology

日本電子株式会社

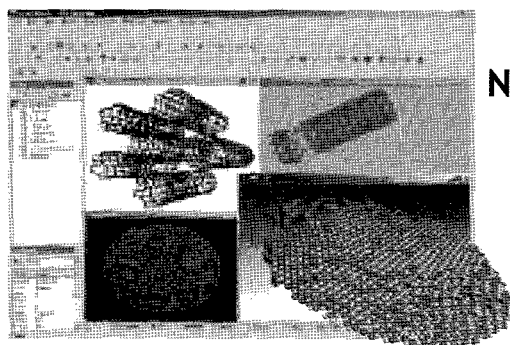
<http://www.jeol.co.jp/>

本社・昭島製作所 〒196-8558 東京都昭島市武蔵野 3-1-2 ☎(042)543-1111  
 営業統括本部 〒190-0012 東京都立川市曙町 2-8-3 新鈴香ビル 3F ☎(042)528-3381  
 札幌 (011) 726-9680・仙台 (022) 222-3324・京波 (029) 856-3220・東京 (042) 528-3211・横浜 (045) 474-2181  
 名古屋 (052) 581-1408・大阪 (06) 6304-3941・広島 (082) 221-2500・福岡 (092) 411-2381



# Nanotechnology Simulation

ナノシミュレーションの最新テクノロジー

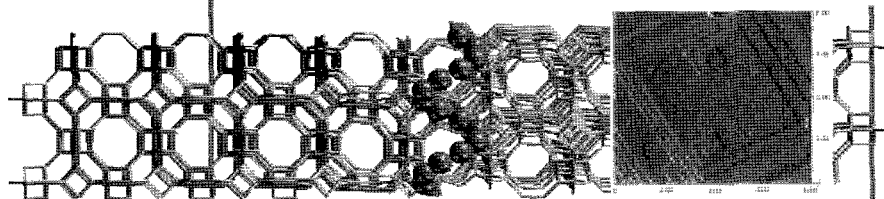


Nano Builder

ナノシミュレーションの基礎となるナノチューブ/ナノワイヤ/クラスター/AFMチップといった様々なナノ構造構築ツール

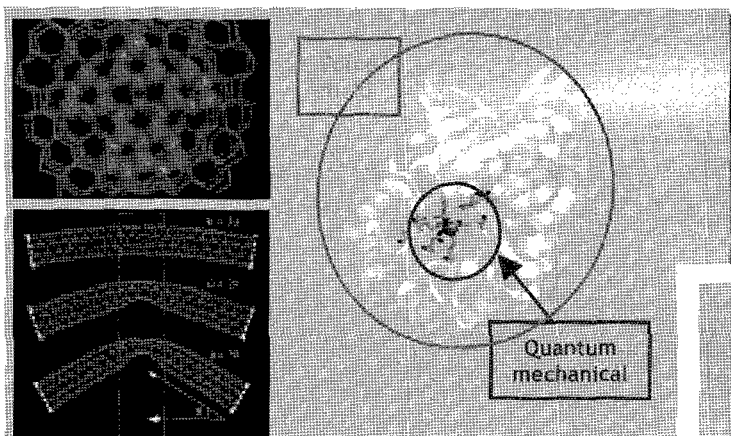
## ツール

- ・ Builder
- ・ QMERA
- ・ Adsorption
- ・ ONETEP
- ・ GULP



## GULP (無機カ場/格子ダイナミクス法)

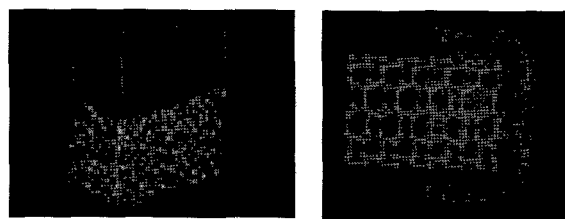
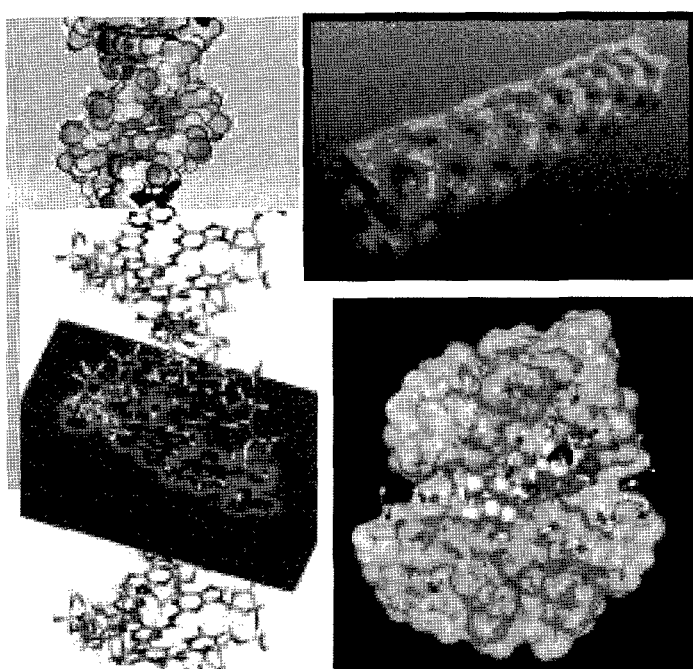
- ・ 構造最適化
- ・ 自由エネルギー最小化
- ・ 分子動力学
- ・ モンテカルロ法
- ・ 欠陥計算
- ・ カ場フィッティング
- ・ 遷移状態
- ・ 遺伝アルゴリズム
- ・ フォノン自由エネルギー
- ・ 弾性定数
- ・ バルク剛性
- ・ ズリ剛性
- ・ ヤング率
- ・ 誘電定数
- ・ ボルン有効電荷
- ・ フォノン振動数
- ・ 表面、付着エネルギー 等



MM QM MM

## QMERA (QM/MM法)

DMol3/GULP等による大きな系の効率的計算



## Adsorption Protocol

吸着サイトの同定

## ONETEP

数千原子レベルのDFT計算を高効率パラレル計算で実行

 MATERIALS  
STUDIO

 accelrys®

アクセルリス株式会社

〒105-0003 東京都港区西新橋3-3-1 西新橋Tビル11F

お問合せ先 TEL: 03-3578-3860 Email: info-japan@accelrys.com

ホームページ <http://accelrys.co.jp>

# BRANSON

SC 株式会社 セントラル科学貿易

〒243-0021 神奈川県厚木市岡田4-3-14  
TEL : 046-229-8323 FAX : 046-229-0262  
E-mail : info.bransonic@branson-jp.com  
URL : www.branson-jp.com

〒111-0052 東京都台東区柳橋1-8-1  
TEL : 03-5820-1500 FAX : 03-5820-1515  
E-mail : tokyo@cscjp.co.jp URL : http://cscjp.co.jp

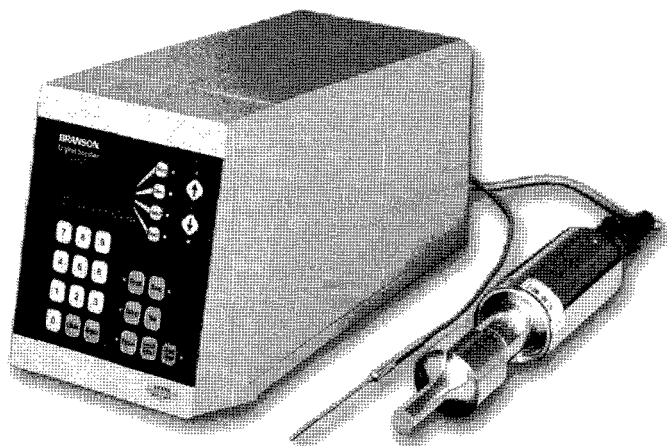
## 溶液中の粒子のナノレベル微細化・分散に BRANSON 超音波リキッドプロセッサ

ホーン先端部の振幅の安定性を、より高めたAdvanceタイプになりました。

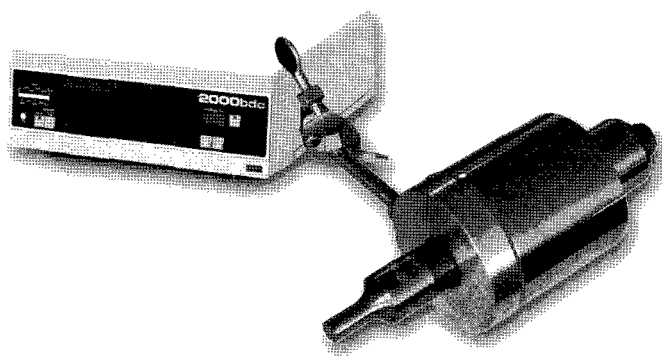
近年のナノテクノロジーの発展及び粉体関連技術の向上により微細な粒子に対する乳化分散処理の要望が増えてまいりました。超音波リキッドプロセッサを使用し、均質な乳化分散処理を行い安定させることにより製品の機能は向上します。

弊社では20kHz機と、40kHz機の2タイプを用意しております。1次粒子の凝集力にも拠りますが20kHz機では100nm程度までの分散力があります。40kHz機は、さらに細かいレベルで分散ができる可能性があります。

20kHz超音波ホモジナイザー  
BRANSON SONIFIERシリーズ



高周波40kHz超音波リキッドプロセッサ  
BRANSON 2000bdc



弊社の製品は、ホーン先端部の振幅の安定性が高く強力なキャビテーションが得られます。高効率で再現性の高い分散処理が行えます。

### 主なアプリケーション

#### 分散

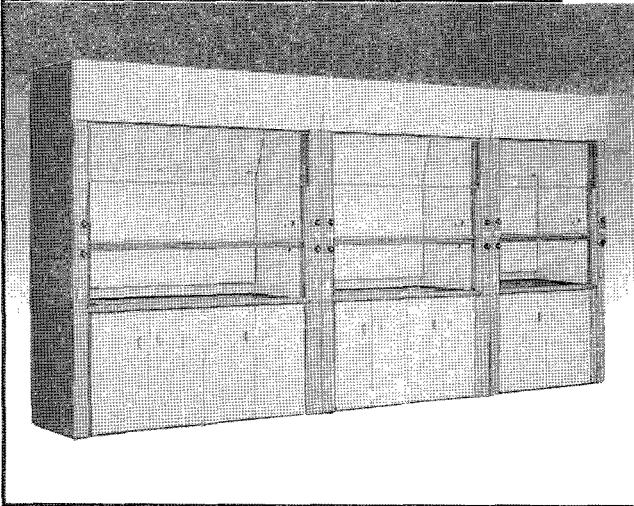
・カーボンナノチューブ ・有機顔料 ・無機顔料 ・セラミック  
・セメント ・感光体 ・記録材料 ・磁性粉 ・粉末冶金 ・酸化鉄  
・金属酸化物 ・シリカ ・アルミナ ・カーボンブラック  
・ポリマー ・ラテックス ・ファンデーション ・研磨剤 ・電池  
・フィラー ・光触媒 ・触媒 ・ワクチン ・体外診断薬  
・歯磨き粉 ・シャンプー ・製紙 ・半導体 ・電子基盤 ・液晶  
・貴金属 ・金属 ・タイヤ ・発酵菌類 ・その他

#### 乳化

・エマルジョン製剤 ・農薬 ・トナー ・ラテックス ・界面活性剤  
・クリーム ・乳液 ・等

# BREZZA

ヒュームフード[プレツツア]シリーズ



人間工学を取り入れた最新型のヒュームフード。研究者の安全性はもちろん、機能性と快適性をご提案します。

- **見やすい“大型の観察扉（ガラス）”**  
観察扉（ガラス）の占める割合を増やすことで、フードの内部が見やすくなりました。
- **使いやすい“大型のフード内サイズ”**  
作業面から邪魔なカランを取り除くことで、フードの内部がより一層広くなりました。
- **環境にやさしい“エコロジー設計”**  
塗装は耐薬性に優れ有機溶剤を使わない専用の粉体塗装を施しています。メンテナンスを考慮した分別設計はもちろんのこと、耐震設計まで考慮しています。

## オカムラの研究施設用家具

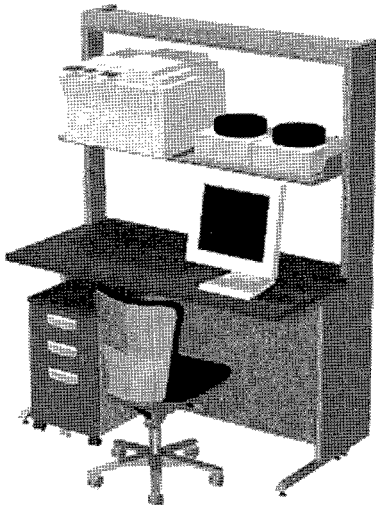
オカムラは、先進性とフレキシビリティを備えた設備機器の提供や、研究目的・人員に対応したスペースプランニングなど、研究者にとって快適な研究環境をご提案します。

オールスチールで設計された新しい形の実験台。研究目的に合わせて変化する実験・研究環境を柔軟にサポートします。

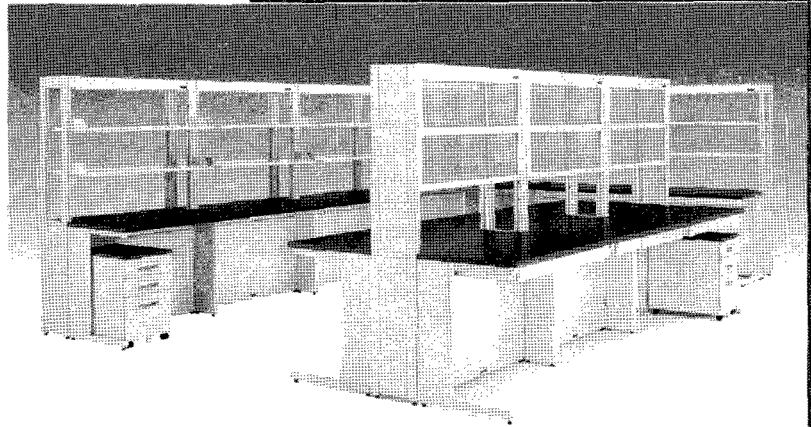
# LABO-AS series

オールスチール実験台[AS]シリーズ

※棚板1段（1800W）当たり、最大150Kgの積載が可能です。



(イメージ)



- **棚が使える“機能性”**  
作業面に載せていた計測機器を棚に設置することで、作業面を確保できます。また、機器のサイズに合わせて棚板高さを調整できます。
- **組替え自由な“拡張性”**  
研究の目的にあわせてレイアウト変更が簡単にできます。

[名古屋支店]

〒450-6020 名古屋市中村区名駅1-1-4 JRセントラルタワーズ20階 TEL:052(551)3180 FAX:052(551)3185

お問い合わせは「お客様サービスセンター」へ… ☎ 0120-81-9060 月曜～金曜(祝日を除く)9:00～18:00

○オカムラの最新情報をご覧下さい。【ホームページアドレス】 <http://www.okamura.co.jp/>

よい品は結局おトクです

**オカムラ**  
株式会社 岡村製作所



# 超遠心機による単層CNTの分離

※CNT:Carbon Nano Tube

CNTは炭素でできた円筒状の物質で、半導体材料・燃料電池の電極などで“驚異の新素材”として注目を集めています。また、種々の異なった構造(単層、二層など)が存在し、構造の違いによって性質が異なるため、詳細な研究には分離精製が欠かせません。

1996年、Robert F. Curl, Harold W. Krotoと共に「フラーレンと呼ばれる新しい立体構造を持つ化合物の合成研究」によりノーベル化学賞を受賞した米国テキサス州ヒューストン、ライス大学のRichard E. Smalley博士のグループは、超遠心機を用いた単層カーボンナノチューブの分離について報告致しました<sup>1)</sup>。

この分離を日立工機(株)製小形超遠心機CS-GXLシリーズで行うこともできます。大形の超遠心機よりも簡便で少量試料の場合には最適ですので皆様のご研究にお役立て下さい。

## 単層CNT分離システム



<sup>1)</sup>引用文献: Band Gap Fluorescence from Individual Single-Walled Carbon Nanotubes, Michael J. O'Connell I, et al., Science, vol.297,593-596 (2002).

## 遠心分離条件

使用ロータ: S52ST(文献と同じスイングロータ)  
回転速度 : 52,000rpm(文献: 30,000rpm)  
時間 : 1時間30分(文献: 4時間)  
試料量 : チューブ1本あたり約5ml  
試料 : 1%SDSを含むD<sub>2</sub>Oに懸濁させたCNT(20~25mg/l)

使用ロータ: S100AT6(アングルロータ)  
回転速度 : 100,000rpm  
時間 : 20分  
試料量 : チューブ1本あたり約3.4ml  
試料 : 1%SDSを含むD<sub>2</sub>Oに懸濁させたCNT(20~25mg/l)

製造・保守

**日立工機株式会社**

茨城県ひたちなか市武田1060番地

電話: 029-276-7384

販売店

**オザワ科学株式会社**

本社: 〒460-0003名古屋市中区錦三丁目9-22

電話: 052-951-5331

FAX: 052-962-7358

# 米国・MTR社 フラーレン・ナノチューブ

株式会社マツボー  
東京都港区虎ノ門3-8-21  
電話 03-5472-1722  
FAX 03-5472-1720  
email: fulen@matsubo.co.jp

1. フラーレン混合物 (C60:70%, C70:25%, High Fullerenes:5%)

2. フラーレンC60

純度 >99%  
>99.5%  
>99.98%  
Sublimed

3. フラーレンC70

純度 >99%  
>99%  
>99.5%  
Sublimed

4. SWナノチューブ(20-40%) クローズドエンド

5. SWナノチューブ(50%-70%) クローズドエンド

6. SWナノチューブ(70~80%)  
50~60%がオープンエンド

7. MWナノチューブ(95%) クローズドエンド

8. MWナノチューブ(70~80%)  
50~60%がオープンエンド

9. MWナノチューブ(85~90%)  
95%以上がオープンエンド

\*High Fullerenes 95%

C76

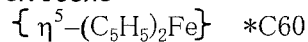
C78

C84>95%

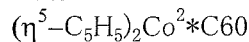
C6099.9%(OH)<sub>n</sub> n=22-26

C6099.9%(OH)<sub>n</sub> n=22-26

\*Bucky Ferrocene-molecular hybrid C60 w/ Ferrocene



\*Bucky Cobaltocene-ionic hybrid C60 w/ Cobaltocene



\*Complex C60 w/ Pt: (h2-C60)Pt(PPh<sub>3</sub>)<sub>2</sub>

\*Complex C60 w/ Fe: (h2-C60)Fe(Co)<sub>4</sub>

\*Complex C60 w/ Ni: C60 (h3-C<sub>5</sub>H<sub>5</sub>)Ni(h5-C<sub>5</sub>H<sub>5</sub>)<sub>2</sub>

\*Mixture of isomers C60F36

\*20-30%C13enrichedC60=99.0%

\*Higher Order Mixed Fullerenes(C76,78,84)

\*New Endohedral Metallofullerene Gd@C82

\*Halogenated Fullerenes

1.C60Br<sub>24</sub>

2.C60C16

3.C60Br<sub>8</sub>Br<sub>2</sub>

4.Mixtures of isomers of C60F36

## \*水溶性 Amino Acids complexes of C60

(w/Aminocaproic(A) and w/Aminobutyric(B) acids)w/unique solubility in water  
(50mg/ml)

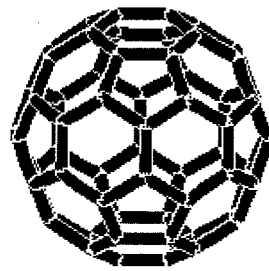
(A)C60(H)NH(CH<sub>2</sub>)<sub>5</sub>COO<sup>-</sup>Na<sup>+</sup>

(B)C60(H)NH(CH<sub>2</sub>)<sub>3</sub>COO<sup>-</sup>Na<sup>+</sup>

\*PCBM(6,6-Phenyl-C61-Butyl acid-Methylester)

本ページ未掲載の種類のフラーレン・ナノチューブをご希望の場合はメーカーに問い合わせますのでお申し付け下さい。

\*C60, 70の純度はHPLCにより測定されています。



# SOGO 株式会社 十 合

**物**質の状態は、固体と液体を除くと「ガス」です。

ガスは入れ物と配管がなければ、使うことができません。  
また、「都市ガス」や「プロパンガス」だけが「ガス」ではありません。

現代社会の最先端を行く研究分野の中で、分析装置、レーザー設備、半導体設備、燃料電池、触媒設備で「ガス」を使用しないものはほとんどありません。

お客様から要求されるガスの純度、安全管理、供給管理は年々高度化してきています

私どもの会社は、工業用や医療用、研究用に使用されるガス、および関連機器の販売商社でしたが、それだけでは、お客様のニーズを満足させることはできません。そこで、先端研究設備で要求される仕様を十分満たす「ガス供給設備」の設計施工を手がけてまいりました。

これからも、常に知識技術の向上に努め、新世紀を生き抜ける企業を目指し、なおかつお客様の成功に貢献していきたいと考えています。

今後とも、末永いお付き合いのほど、よろしくお願い申し上げます

- ◇ 一般高圧ガス
- ◇ 分析用標準ガス
- ◇ 半導体製造用ガス
- ◇ 特殊配管用弁類及び継手
- ◇ 各種ガス供給システムの設計施工
- ◇ 半導体製造ガス供給システムの設計施工

株式会社 十 合

お客様第一主義に徹します

本社 〒464-0075


名古屋氏千種区内山一丁目24番9号 (第2ダイワビル 3F)

TEL (052) 741-0288 FAX (052) 731-6617

営業所 〒470-0213

西加茂郡三好町大字打越字三本松30-30

TEL (052) 32-0621 FAX (052) 32-0623

 Eメールは、[sogomail@sogo-inc.jp](mailto:sogomail@sogo-inc.jp) までお願いします。



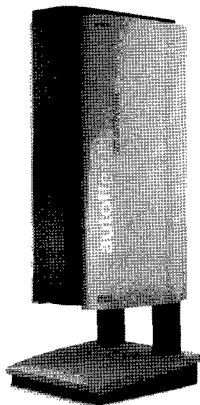
# Bruker Daltonics プロテオミクス・イメージングMS・細菌同定システム

## MALDI-TOF/TOF-MS

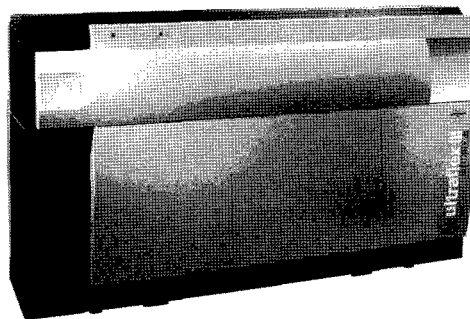
### ultraflex III, autoflex III, ベンチトップ型 microflex

FlexシリーズにautoflexIII、ultraflexIIIが新登場。ラインナップがautoflex III TOF、autoflex III TOF/TOF、ultraflex III TOF、ultraflex III TOF/TOF、microflex TOFになりました。

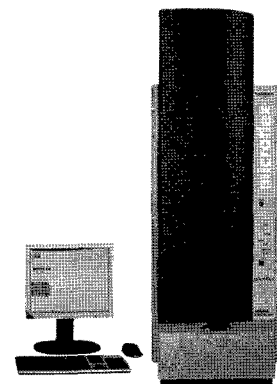
特許LIFT技術により、極微量サンプルから超高速・超高感度で卓越したMS/MSデータを得ることが可能です。また、バイオマーカー探索用ソフトウェア ClinProTools、Imaging MS用ソフトウェアflexImaging、細菌同定用ソフトウェアBioTyperもリリースされ、研究に合ったシステムをご選択いただけます。



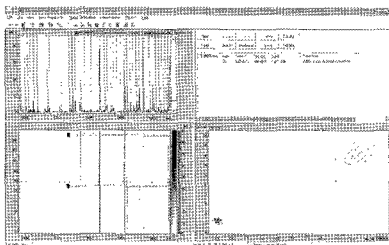
autoflex III TOF/TOF



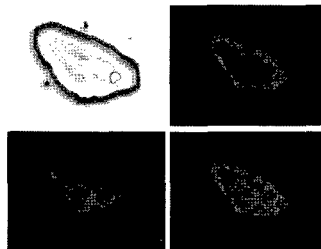
ultraflex III TOF/TOF



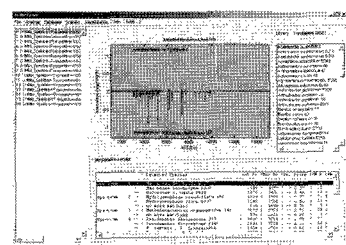
microflex TOF



バイオマーカー探索用ソフトウェア  
ClinProTools 2.0



flexImaging 1.0による  
ゼブラフィッシュ切片のImaging MS



細菌同定用ソフトウェア  
BioTyper 1.0

## ブルカー・ダルトニクス株式会社

■ 営業本部・テクニカルサポートセンター  
〒221-0022  
横浜市神奈川区守屋町3-9  
A棟6F  
TEL: 045-440-0471  
FAX: 045-440-0472

■ 大阪営業所  
〒532-0004  
大阪市淀川区西宮原1-8-29  
テラサキ第2ビル2F  
TEL: 06-6369-8211  
FAX: 06-6369-1118

■ 本社  
〒305-0051  
茨城県つくば市二の宮3-21-5  
TEL: 029-852-3510  
FAX: 029-852-6729

## 分析・試験装置のエキスパート

お客様の研究開発、品質管理、製造工程等、色々な分野におけるご要望に対し、総合的なご提案が出来るように努めております。そして、新しい技術や内外の幅広い商品に関する知識情報を生かし、皆様の発展に貢献出来る事を希望しております。

### ●企業活動の基本方針

弊社の方針と致しまして“企業のコンプライアンスの遵守”“地球環境に配慮した経営の推進”“地域社会に貢献し相互繁栄を考えた施策”などを重視してまいります。

### ●お客様の満足度を第一に考えた営業活動

装置の導入目的、技術評価、コスト、納期、アフターサービス等のお客様のニーズに貢献できるよう、迅速な対応に努力し、お客様との信頼関係を大切に致します。

### ●取扱商品の充実

新しい技術や内外の幅広い商品に関する情報収集と共に知識の向上に努め、お客様の立場に立ったご相談相手としてお役に立てる事を目標にしております。

### 取扱品目

分析測定器・試験検査器・バイオ機器・理化学機器・実験用器具・実験室設備  
環境計測測定機器・粉粒体測定装置・真空機器・その他専用機器

## 株式会社 三洋商事 名古屋支店

Analytical Instrument Sales Agency

<http://www.sanyo-shoji.co.jp>

〒450-0002 名古屋市中村区名駅三丁目28番12号 大名古屋ビル12F

TEL 052-583-7070 FAX 052-583-7110

E-mail: [nago@sanyo-shoji.co.jp](mailto:nago@sanyo-shoji.co.jp)

大阪・神戸・四日市・名古屋

生命を構成するDNA。それは宇宙の誕生から現在まで途切れることなく、全ての生命に受け継がれてきました。しかし、もとをたどれば全宇宙に存在する虫も、動物も、そしてヒトも、全て同じものから創られているのです。

そこにはまだ、未知なる宇宙の神秘として医療・研究・開発者の前に立ちはだかり、  
様々な難問を解かれることを待っています。

私たち「理科研」が、この問題へ向かう人々を真心でお手伝い出来るのは、  
設立当初から受け継がれてきた社訓、「誠意」が遺伝子として組み込まれているから。

理科研は、「バイオ研究」に欠かすことのできない機器・試薬の販売を通じ、  
人類の幸せと豊かな社会の実現を願っています。

体内宇宙への挑戦。

## 理科研株式会社

<http://www.rikaken.co.jp>

- 本社 名古屋市守山区元郷二丁目107番地  
〒463-8528 TEL 052-798-6151(代) FAX 052-798-6157
- 岐阜営業所 岐阜県岐阜市岩地2丁目25番2号  
〒500-8225 TEL 058-240-0721(代) FAX 058-240-1082
- 津営業所 三重県津市丸之内養正町20番地14号  
〒514-0036 TEL 059-224-6661(代) FAX 059-224-6671
- 四日市営業所 三重県四日市市桜町2129番の1  
〒512-1211 TEL 059-326-0231(代) FAX 059-326-3577
- 静岡営業所 静岡県駿河区広野3丁目29番8号  
〒421-0121 TEL 054-256-3751(代) FAX 054-256-3755

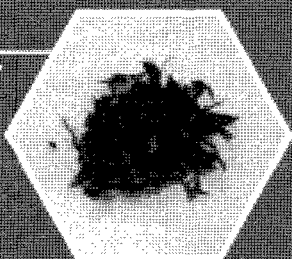
- 東京支店 東京都文京区本郷七丁目2番1号  
〒113-0033 TEL 03-3815-8951(代) FAX 03-3818-0889
- つくば営業所 茨城県つくば市高野台三丁目16-2  
〒305-0074 TEL 029-856-2151(代) FAX 029-856-5071
- 柏営業所 千葉県柏市若柴197番地17  
〒277-0871 TEL 04-7135-6651(代) FAX 04-7135-6751
- 神奈川営業所 横浜市緑区十日市場町901-31  
〒226-0025 TEL 045-989-6551(代) FAX 045-989-6701
- 鶴見営業所 横浜市鶴見区朝日町一丁目49番地  
〒230-0033 TEL 045-500-4551(代) FAX 045-500-4571
- 三島営業所 静岡県駿東郡長泉町下土狩217番地1  
〒411-0943 TEL 055-980-1101(代) FAX 055-980-1105

# Lab set CNT10

## 1.SWNT(FH-P)

単層カーボンナノチューブ  
FH精製タイプ

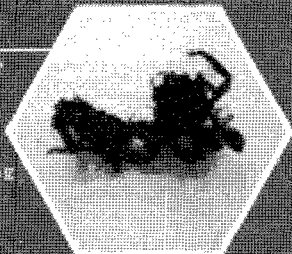
■アーク放電法  
carbon contents >90% 数量50mg



## 2.SWNT(FH-A)

単層カーボンナノチューブ  
FHタイプ

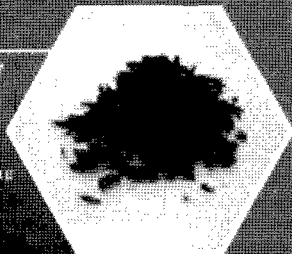
■アーク放電法  
carbon contents >40% 数量100mg



## 3.SWNT(APJ)

単層カーボンナノチューブ  
APJタイプ

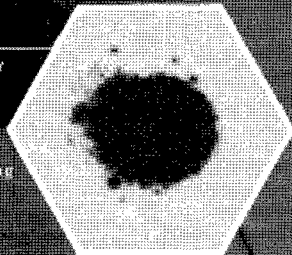
■アーク放電法  
carbon contents >90% 数量300mg



## 4.MWNT

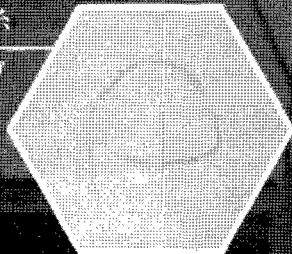
多層カーボンナノチューブ

■CVD法  
carbon contents >85% 数量300mg



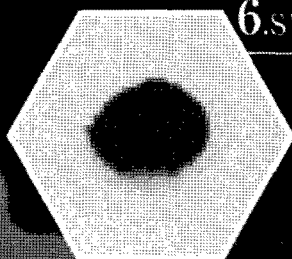
## 5.SWNT(FH-A)系

単層カーボンナノチューブ  
FHタイプの糸



## 6.SWNT(FH-P)ペーパー

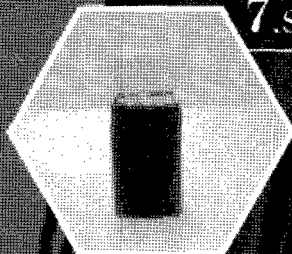
単層カーボンナノチューブ  
FH精製タイプのペーパー



## 7.SWNT(FH-P)分散液

単層カーボンナノチューブ  
FH精製タイプ

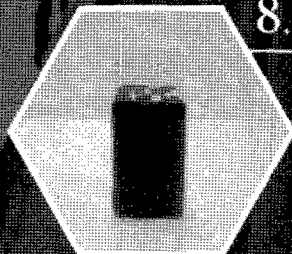
■溶媒:  
H<sub>2</sub>Oベース、数量10ml



## 8.SWNT(FH-A)分散液

単層カーボンナノチューブ  
FHタイプ

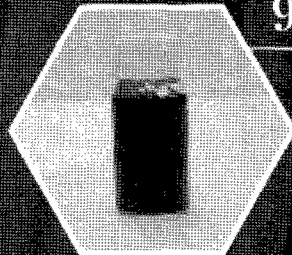
■溶媒:  
H<sub>2</sub>Oベース、数量10ml



## 9.SWNT(APJ)分散液

単層カーボンナノチューブ  
APJタイプ

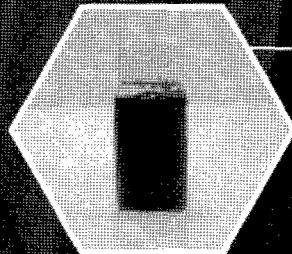
■溶媒:  
H<sub>2</sub>Oベース、数量10ml



## 10.MWNT分散液

多層カーボンナノチューブ

■溶媒:  
H<sub>2</sub>Oベース、数量10ml



※各製品単独でご購入希望の場合は、別途お問い合わせください。

価格 **95,000**円(税別)

◎本製品は、大学・企業・公的機関等の研究・開発向けに企画された素材・材料です。 ◎本製品の使用にあたっては、相応に熟達した使用者を想定いたしております。 ◎人体への影響など明らかでない点もあることから、ご使用にあたっては製造安全データシート等をよくお読みいただき、慎重にお取り扱い下さいようお願い申し上げます。

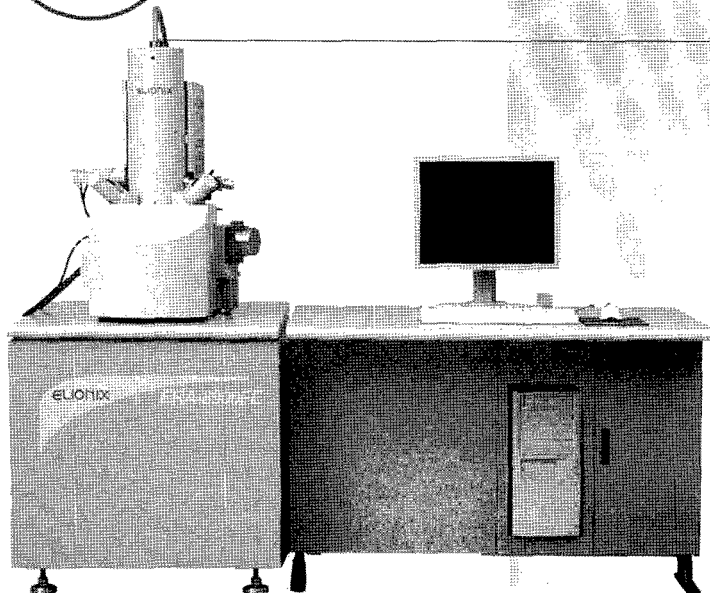


〒460-0002  
愛知県名古屋市中区丸の内 3-4-10  
TEL:052-971-2408・FAX:052-955-3257

HP: <http://www.meijo-nano.com> ✉ [hashimo@ccmfs.meijo-u.ac.jp](mailto:hashimo@ccmfs.meijo-u.ac.jp)

# ELIONIX

精密工学会  
技術賞 受賞



## Electron Probe Surface Roughness Analyzer

3D-SEMフィールドエミッション電子線三次元粗さ解析装置

### ERA-8900FE

**低加速でSEM観察しながら試料表面の粗さ解析が可能。**

低加速領域においても簡単に高性能を発揮する新設計の TFE 電子銃を搭載しました。横方向、縦方向ともに分解能が極めて高く、SEM 観察視野をリアルタイムで CRT に三次元表示します。

**4本の二次電子検出器を搭載。**

マルチ方向から凹凸 (TOPO)、組成 (COMPO)、通常の SEI の 3 タイプの画像が高分解能で得られます。従来の SEM では困難とされた低倍率での無影照明像、微細凹凸像、緩やかなうねりなどの観察を可能としました。

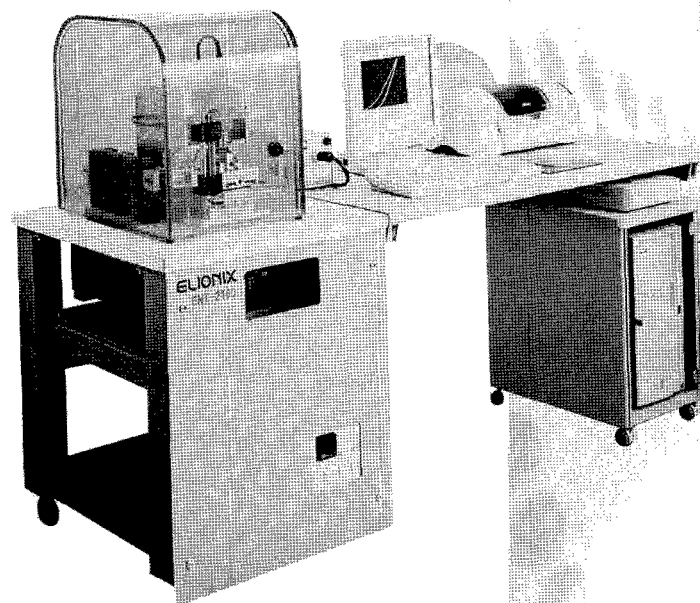
## Nano Indentation Tester

超微小押し込み硬さ試験機 (超軽荷重型)

### ENT-2100

**数ナノの押し込み深さで、優れた再現性と安定性。**

当社が独自に開発した定点荷重方式の採用により、サンプルに圧子を垂直に押し込むことができます。これにより正確な荷重負荷と表面検出精度を飛躍的に向上させ、最小  $1\mu\text{N}$  という超軽荷重領域での試験を可能にしました。押し込み深さ数 nm でも安定した測定ができます。



## 株式会社 エリオニクス

本社 〒192-0063 東京都八王子市元横山町3-7-6

TEL.042-626-0611 (代表) FAX.042-626-6136

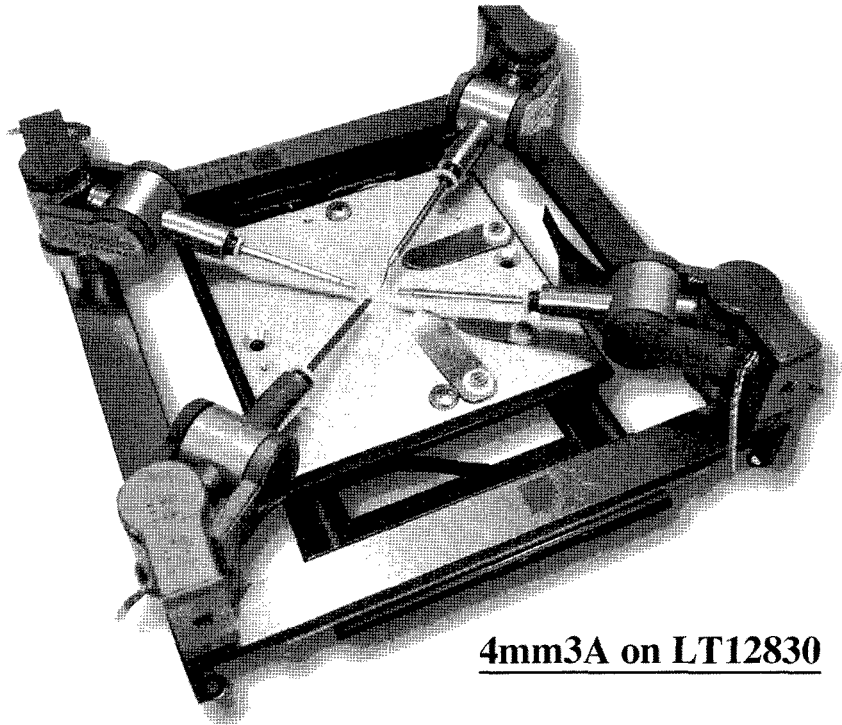
大阪営業所 〒563-0025 大阪府池田市城南1-9-22 グリーンプラザ2F TEL.072-754-6999 (代表) FAX.072-754-6990

<http://www.elionix.co.jp/>



for Electron microscope

# Micromanipulator Linear table



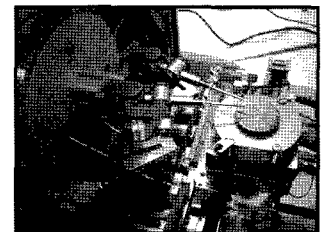
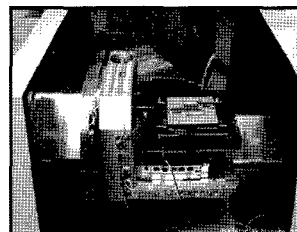
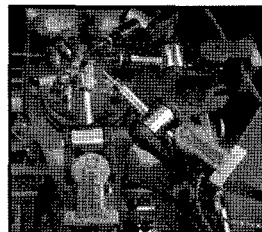
4mm3A on LT12830

## Semiconductor/MEMS/NEWS

- Electrical probing
- Failure analysis
- IC test&repair
- TEM samplepreparation
- eBeam lithography
- Cell counting

## Material science

- Manipulation
- Electrical/Mechanical/ characterisation
- Microinjection in ESEM
- Force measurement
- Nanoindentation
- STEM
- Scanning probe microscopy



**ADS** 株式会社 **アド・サイエンス**

## 地球の一員として私たちの責任

私たちは無限の可能性を秘めた炭素に魅せられ、理想の品質を追求し研究開発を重ねてきました。今や炭素の可能性は飛躍的に拡がり、エネルギー、環境など最先端テクノロジー分野にも幅広く採用されています。

これからも想像力を磨き続け、画期的な製品開発により社会に貢献できる企業を目指して、私たちの挑戦は続きます。

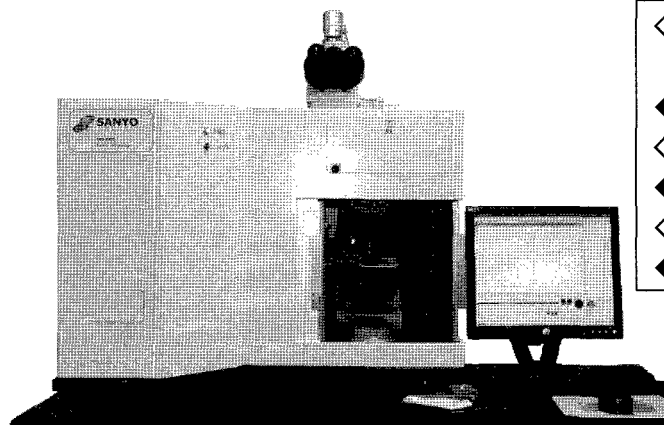


**TOYO TANSO**  
Inspiration for Innovation

東洋炭素株式会社

本社 〒530-0001 大阪市北区梅田3-3-10 梅田ダイビル10F Tel 06-6451-2114 Fax 06-6451-2186 [www.toyotanso.co.jp](http://www.toyotanso.co.jp)

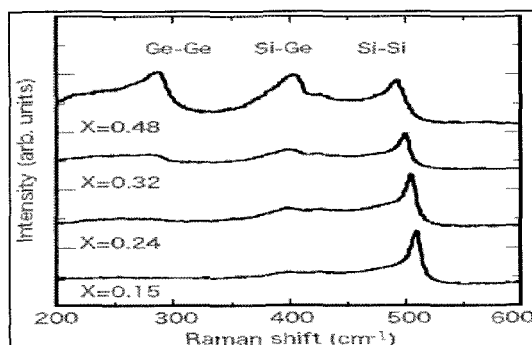
# 顕微ラマン散乱分光装置



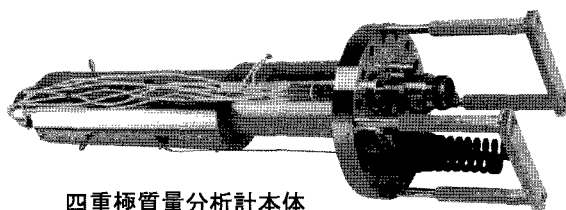
## SNR-6001

測定条件: スパッタ法 H<sub>2</sub>, 基板温度 200°C, 圧力 25Pa,  
膜厚 300~400nm, 基板コーニング#7059  
(東海大学 工学部 電気電子工学科 磯村雅夫教授 ご提供)

- ◇ 独自技術の光学システム(特許出願中)により、従来の機種に比べて感度が大幅にUP
- ◆ 独自の光学システムにより熱損傷の大幅軽減
- ◇ アプリケーションに応じて、カスタマイズ可能
- ◆ 深さ分解能 0.5 μm
- ◇ 装置の小型化実現
- ◆ 低価格

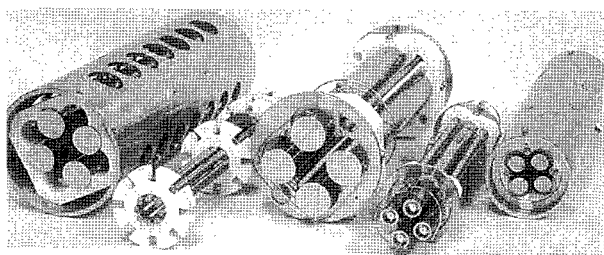


# 研究用四重極質量分析計コンポーネント



四重極質量分析計本体

Extrel CMS社は40年以上の経験を持ち、質量分析においては「高質量」、「高分解能」を得意としております。また、ユーザの分析目的に応じてシステムを自由に構成することができ、様々なアプリケーション・ソリューションに対応可能です。



四重極マスフィルタ

### <アプリケーション>

- カーボンクラスター・水クラスター等のクラスター分析
- 2次イオン質量分析 (SIMS)
- He と D<sub>2</sub> の分離等の超高分解能質量分析
- 最大 9,000amu までの高質量分析
- 分子ビーム源・プラズマ源による質量分析
- サーマルディソープション・レーザディソープション等の表面脱離質量分析

詳細については、下記にお気格にお問い合わせ下さい。



三洋貿易株式会社 科学機器事業部

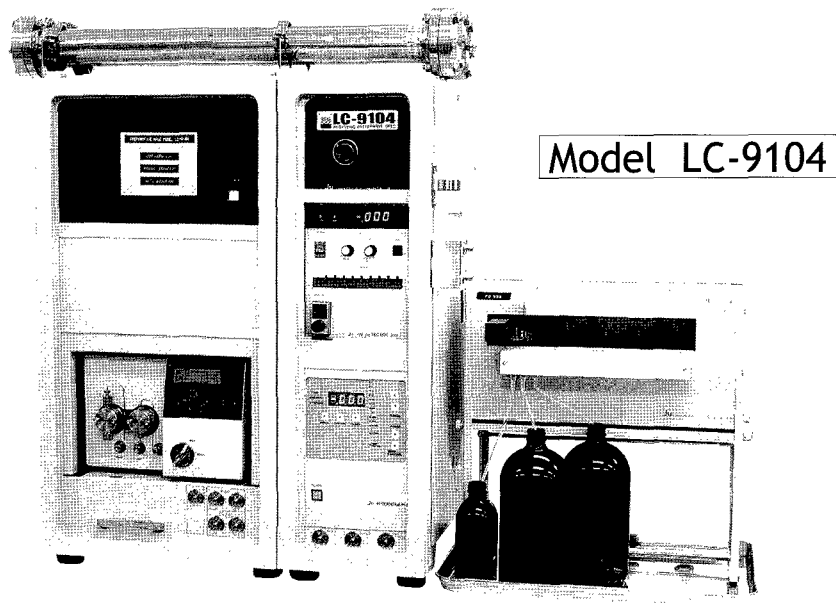
〒101-0062 東京都千代田区神田駿河台4丁目2番5号  
トライエッジ御茶ノ水

TEL 03-5296-9570 FAX 03-3252-2882

URL: <http://www.sanyo-si.com/> e-mail: [info-si@sanyo-trading.co.jp](mailto:info-si@sanyo-trading.co.jp)

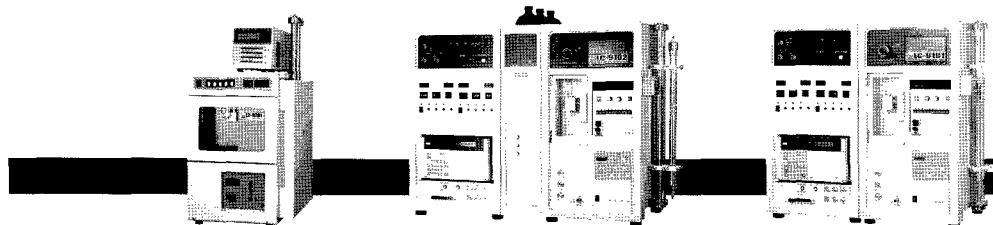
リサイクル分取 HPLC は JAI の LC-9000 シリーズ!

## Recycling Preparative HPLC



### ◆LC-9104 大量分取モデル

専用のGPCカラム (40 φ×600 mm) を装着すれば、試料処理量は、LC-9101型の約4倍。試料注入から分取まで自動化されています。また、ODS・シリカカラムなど、大量分取用カラムの性能を最大限に引き出す装置設計がなされています。



### ◆LC-9201/LC-9204 コンパクトモデル

分離分取に定評のあるLC-9101型の高い性能を受継ぎながら、サイズをコンパクトにし、省スペース化と低価格化を実現しました。

### ◆LC-9102/9103 グラジエントモデル

グラジエントとリサイクルがワンタッチで切替えられます。

### ◆LC-9101 標準モデル

専用のGPCカラム (20 φ×600 mm) を装着すれば、分離能を落とすことなく、常時300 mgを注入することができます。

—— 高分子分析の未来と取り組む! ——

分取LCに関する  
新連携認定企業

**Jai** 日本分析工業株式会社

ISO9001/14001取得

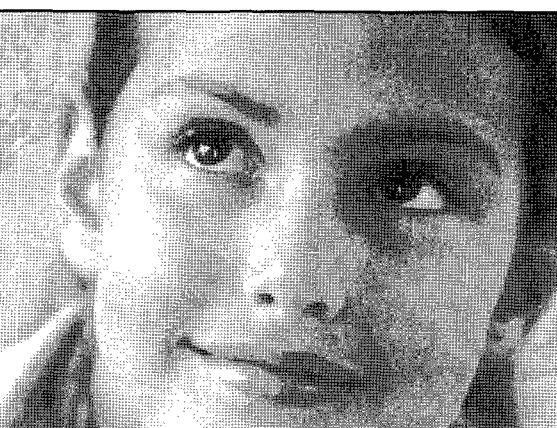
URL : <http://www.jai.co.jp/> E-mail : [sales-1@jai.co.jp](mailto:sales-1@jai.co.jp)

□本社・工場 : 〒190-1213 東京都西多摩郡瑞穂町武蔵208 TEL 042-557-2331 FAX 042-557-1892  
□大阪営業所 : 〒532-0002 大阪市淀川区東三国5-13-8-303 TEL 06-6393-8511 FAX 06-6393-8525

# Best for Our Customers

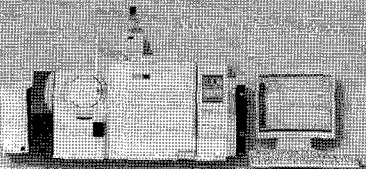
～すべてはお客様のために～

を合言葉にナノテク新材料における最高のソリューションを提供します。

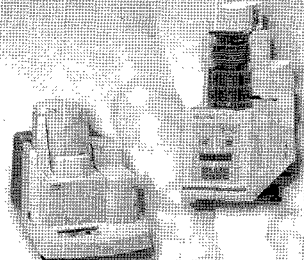


- ① 微量測定
- ② 純度
- ③ 直径
- ④ 観察
- ⑤ カイラリティ
- ⑥ 凝集分散

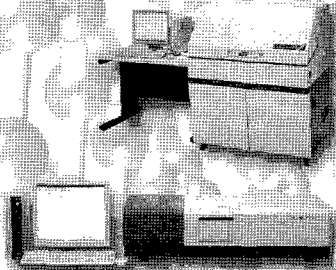
① 熱分解生成物・発生ガスの分析  
 ガスクロマトグラフ質量分析計  
 GCMS-QP2070 Plus



① 微量CNTの純度・熱特性評価  
 ① CNTの結晶性と耐熱性の評価  
 ミクロ熱量測定装置  
 TGA-50  
 TG/DTA同時測定装置  
 DTG-60/60H



① ② CNTの紫外可視近赤外吸収スペクトル測定  
 紫外可視近赤外分光光度計  
 SolidSpec-3700  
 紫外可視近赤外分光光度計  
 UV-3600



② CNTの密度測定  
 乾式自動密度計  
 アキュピック1330



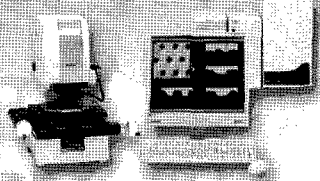
② 触媒元素の測定  
 ソインジャーケンシャル形ICP発光分析装置  
 ICPS-8100



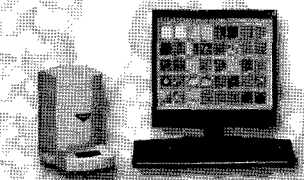
② ③ 直径測定  
 ② ③ 結晶性と耐熱性の評価  
 ラマン分光光度計  
 Holo-Probe モニタリングシステム



③ ④ あらゆるナノテク材料を  
 観察・測定  
 ナノサーチ顕微鏡  
 SFT-3500



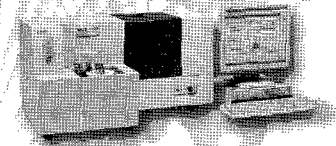
③ ④ 直径測定  
 ③ ④ 精製前後の観察  
 ③ ④ CNTとポリマーコンポジット  
 試料の観察  
 走査型プローブ顕微鏡  
 SPM-9600



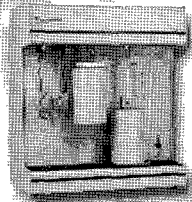
⑥ SWNTの近赤外PL  
 3次元分布測定  
 近赤外フォトルミネッセンス測定システム  
 NIR-PL System



⑥ 分散・凝集過程評価  
 ナノ粒子径分布測定装置  
 SALD-7100



⑥ 比表面積と吸着特性  
 マイクロメリテックス  
 高速比表面積/細孔分布測定装置  
 アサップ2020シリーズ



**nanotech**  
 SHIMADZU

## Total solutions for the future of nanotechnology

株式会社 **島津製作所**

東京支社：分析計測事業部事業戦略室マーケティングG TEL03-3219-5633 FAX03-3219-5557  
 東京都千代田区神田錦町1-3 <http://www.shimadzu.co.jp>

# 季刊 ナノテク読本 広告企画のご案内

ナノテクノロジーを活用した製品は日進月歩で開発が進み、続々と市場に登場しています。さらに、これからのナノテク実用化を目指す各分野の研究開発も着実な進歩を見せており、産業界や自治体からの期待は高まる一方です。

08年初頭より、半導体産業新聞は「週刊ナノテク」と統合し、各方面からの大きな期待を背負うナノテクノロジーを精力的に追いかけていますが、今回、「週刊ナノテク」の魂を継承し、当社がこれまで

培ってきたナノテクの取材ノウハウをフル活用した新媒体として、『季刊 ナノテク読本』を企画いたしました。この媒体は、エレクトロニクス、エネルギー、環境、ライフサイエンスなど様々な分野で芽吹いているナノテクノロジーの現在を、豊富な取材データをもとに俯瞰し、その将来像を展望することを主眼にしています。また、ナノテクノロジーに関連性の深い国内展示会・学会ともタイアップし、その見どころをご紹介します。年4回の発行を予定しております。

## 2008年発刊スケジュール

- Vol.1: 2008年2月8日発行**  
**「nano tech 2008」「FC EXPO / PV EXPO」特集号**
- Vol.2: 2008年6月下旬発行予定**  
**「国際バイオEXPO」「マイクロマシン/MEMS展」特集号**
- Vol.3: 2008年8月下旬発行予定**  
**「2008分析展」特集号**
- Vol.4: 2008年11月下旬発行予定**  
**「セミコン・ジャパン 2008」特集号**

## ■広告料金

スペース	普通版
4色1ページ	¥350,000(税込: ¥367,500)
2色1ページ	¥250,000(税込: ¥262,500)
1色1ページ	¥200,000(税込: ¥210,000)
2色1/2ページ	¥150,000(税込: ¥157,500)
1色1/2ページ	¥120,000(税込: ¥126,000)
1色1/3ページ	¥80,000(税込: ¥84,000)

## ■広告原稿サイズ(天地mm×左右mm)

スペース	普通版	断切版
1ページ	255×180	280×208
ヨコ1/2ページ	120×180	—
ヨコ1/3ページ	80×180	—

## 媒体概要

- 媒体名: 季刊 ナノテク読本
- 体裁・頁数: A4変形判、オフセット印刷、平綴じ、70ページ
- 価格: 2,650円(本体:2,500円)
- 発行予定部数: 15,000部
- 特典: 各展示会にて会場無料配布

株式会社 産業タイムズ社 広告部 〒101-0021 東京都千代田区外神田5-5-4 第二日昌ビル TEL: 03-3834-5133  
 E-Mail: ad@sangyo-times.co.jp FAX: 03-3834-5140

〒101-0021 東京都千代田区外神田5-5-4  
 第二日昌ビル  
 Tel.03-3834-5131(代)/Fax.03-3834-5188

## 産業タイムズ社の出版案内

## 詳細カタログ呈

Fax.での注文も承ります。定価は税・送料込み。

- 好評発売中!** **半導体工場ハンドブック2008** グローバリゼーションに突入した次世代ラインの全貌  
 A4変形判・145頁・定価4,200円(本体4,000円)
- 好評発売中!** **アジア半導体/液晶ハンドブック2007** 台湾・韓国・中国・東南アジアのメーカー別プロフィール・設備投資を一覧  
 A4変形判・108頁・定価4,200円(本体4,000円)
- 2008年3月下旬発刊予定** **半導体産業会社録2008年度版** 日本で唯一の半導体産業ダイレクトリ“最新・大改訂版”  
 A4変形判・約500頁・定価15,750円(本体15,000円)
- 2008年2月下旬発刊予定** **液晶・PDP・ELメーカー計画総覧2008年度版** 大画面/極薄/有機EL化競争が始まった薄型テレビへ搭載されるFPD  
 B5判・約390頁・定価14,700円(本体14,000円)
- 好評発売中!** **半導体産業計画総覧2007-2008年度版** グローバル時代の必勝パターンを探る  
 A4変形判・556頁・定価19,950円(本体19,000円)
- 好評発売中!** **プリント回路メーカー総覧2007年度版** 得意分野でさらなる飛躍に挑戦!!  
 B5判・292頁・定価16,800円(本体16,000円)
- 好評発売中!** **太陽電池産業総覧2007** リニューアブルエネルギーの切り札 太陽電池ビジネスに取り組む企業60社の全貌  
 B5判・339頁・定価18,900円(本体18,000円)
- 好評発売中!** **燃料電池産業総覧2008** 主要100社の最新事業計画と、大学・研究機関の研究開発動向を網羅  
 B5判・303頁・定価18,900円(本体18,000円)
- 好評発売中!** **ナノテク産業総覧** ナノテクキーカンパニー700社収録 キーパーソン300人網羅  
 A4変形判・540頁・定価25,200円(本体24,000円)



Sepax Technologies



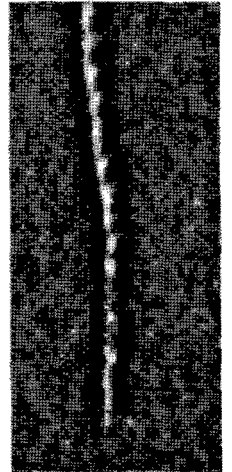
工ム工ス機器

## ナノ粒子の分離用 HPLC カラム

### ・・・カーボンナノチューブ(CNT)、金属コロイド粒子・・・

#### 世界初の SEPAX 社が独自開発したカーボンナノチューブ用カラム CNTSEC

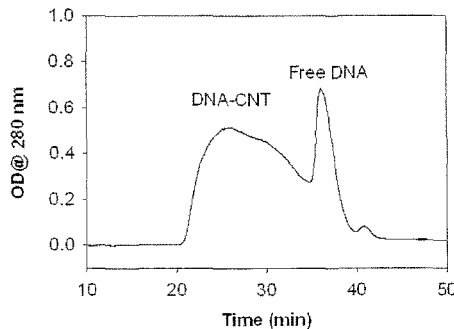
- ・ **長さ、チューブの内径による分離**・・・カーボンナノチューブ専用ゲルろ過カラム
  - ☆ 可溶化されたカーボンナノチューブを長さ/直径で分離することの出来るカラムです。
  - ☆ 充填剤は、SEPAX 社独自の技術により表面加工を施しており、可溶化されたカーボンナノチューブがカラム内に吸着しません。(高回収率 95%以上)
  - ☆ カーボンナノチューブの長さ、直径に応じて、4種類の細孔直径の充填剤(300~2000Å)が用意されています。また、分析レベル(数百 ng レベル)から分取・精製レベル(数 mg またはそれ以上)までカラムの内径(4.6~21.2mm)、長さ(30~250mm)などをそろえています。



商品	細孔直径	粒径	対象 CNT サイズ
CNT SEC-300	300Å	5, 10 μm	長さ 1~100nm、直径 1~5nm
CNT SEC-500	500Å	5, 10 μm	長さ 25~250nm、直径 1~10nm
CNT SEC-1000	1000Å	5, 10 μm	長さ 100~500nm、直径 1~25nm
CNT SEC-2000	2000Å	5, 10 μm	長さ 300~1000nm、直径 1~50nm

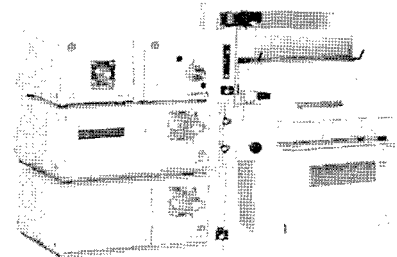
ssDNA で可溶化されたカーボンナノチューブ (AFM 画像, Dr.Ming Zheng et al, Science 2004)

ssDNA により可溶化された DNA-wrapped CNT を Sepax 社 CNT SEC-300、CNT SEC-1000、CNT SEC-2000、(各 4.6x250 mm, 5mm) の 3 本連結により分離・分取 (移動相条件: 0.1 M Tris + 0.2 M NaCl, pH 7.0、流速: 0.25mL/min) (Huang et al, Anal Chem. 2005, 77, 6225)



カラムの価格につきましては、弊社 Web サイトをご覧ください。

[http://www.technosaurus.co.jp/product/sepax\\_SEC.htm](http://www.technosaurus.co.jp/product/sepax_SEC.htm)



工ム工ス機器株式会社



[www.technosaurus.co.jp](http://www.technosaurus.co.jp)

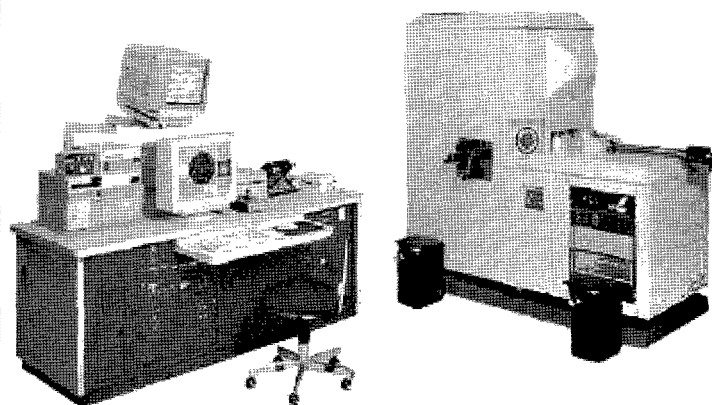
□東京  
〒162-0805  
東京都新宿区矢来町 113 番地  
TEL:03-3235-0661/FAX:03-3235-0669

□大阪  
〒532-0005  
大阪市淀川区三国本町 2 丁目 12 番 4 号  
TEL:06-6396-0501/FAX:06-6395-2588

□福岡  
〒812-0054  
福岡市東区馬出 1 丁目 2 番 23 号  
TEL:092-631-1012 / FAX:092-641-1285

# UBE

## 迅速に 精緻に 確実に



8インチウェハ対応オージェ分析装置  
アルバック・ファイ (株) 製 SMART-200

- 透過型電子顕微鏡 (TEM)
  - ・半導体デバイスの断面・界面・平面分析
  - ・マイクロサンプリングFIBによる特定微小領域の分析
  - ・FPD (フラットパネルディスプレイ) の断面観察
- 表面構造評価用多機能X線回折 (XRD・XRR・XDS)
  - ・多層薄膜の面内および深さ方向の結晶構造評価
  - ・多層薄膜の膜厚、ラフネス、密度測定および配向性評価
  - ・空孔径分布解析
- 誘導結合プラズマ質量分析 (ICP-MS)
  - ・ウェーハ表面の微量金属汚染評価
  - ・電子材料中の微量元素分析
- WEEE・RoHS関連無機物質分析
- 昇温脱離ガス分析 (TDS)
  - ・8インチ、12インチウェーハ表面の有機物汚染
  - ・脱離ガス分析
  - ・ボックス保存ウェーハ表面有機物の分析
- 二次イオン質量分析 (SIMS)
  - ・ドーパントのデプスプロファイル分析
  - ・半導体デバイスの層構造・不純物の分析
  - ・極浅領域の分析
- 飛行時間型二次イオン質量分析 (TOF-SIMS)
  - ・ウェーハ表面の汚染の分析
  - ・有機EL材料の分析
  - ・有機膜・レジスト残りの分析
- オージェ電子分光分析 (FE-SAM)
  - ・8インチウェーハ表面の微小異物元素分析
  - ・多層薄膜の構造・組成分析
  - ・FIB-オージェ測定によるデバイスの欠陥解析
- X線光電子分光分析 (XPS・ESCA)
  - ・半導体デバイス表面の状態分析
  - ・光触媒表面の分析
  - ・有機膜・ポリマー表面の官能基濃度定量
- 走査型プローブ顕微鏡 (SPM)
  - ・各種ウェーハ、半導体材料表面の凹凸形状観察
  - ・複合材料、ポリマーアロイ等の相構造マッピング
  - ・電気力、摩擦力、磁気力イメージ測定

[お問い合わせ先]

株式会社 UBE 科学分析センター

UBE SCIENTIFIC ANALYSIS LABORATORY, INC

ホームページ: <http://www.ube.co.jp/usal/>

ISO 9001 & 14001 認証取得済

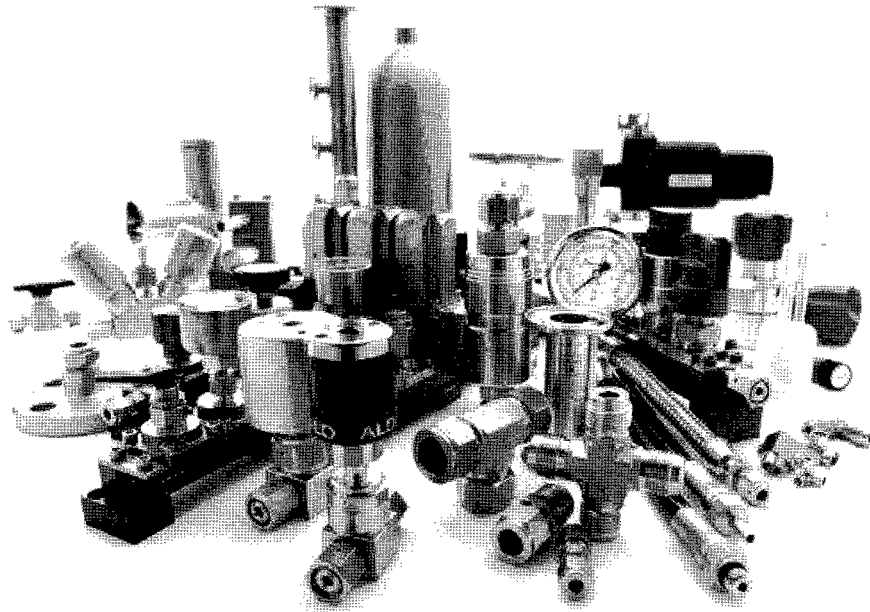
東京営業部 〒105-6791 東京都港区芝浦一丁目2番1号シーパンスN館 20F  
TEL 03-5419-6333 FAX 03-5419-6334

大阪営業部 〒530-0002 大阪市北区曽根崎新地二丁目2番16号桜橋東洋ビル7F  
TEL 06-6346-2853 FAX 06-6346-1763

西部営業部 〒755-8633 山口県宇部市大字小串1978-5  
TEL 0836-31-6568 FAX 0836-31-6601

千葉営業所 〒290-0045 千葉県市原市五井南海岸8番1号  
TEL 0436-23-5155 FAX 0436-23-5449





## スウェージロックの流体システム・トータル・ソリューション

### 継手・バルブ以外のスウェージロック製品をご存知ですか？

チューブ継手や各種バルブ、皆様にご存知頂いているスウェージロック社製品。実はそれら以外にも様々なラインナップがあります。圧力計、圧カトランスデューサー、圧力レギュレーターなどの圧力制御機器類。集積化システム、プラスチック製品など。様々な産業界に何千もの流体に関わるコンポーネントとシステムを提供しています。また、特注品の対応、製品の加工サービス、各種セミナーや技術トレーニングなどソリューション・プロバイダーとしての体制も万全です。流体システムに関するご相談を是非、名古屋バルブ・フィッティング株式会社にお問い合わせください。

名古屋バルブ・フィッティング株式会社

【本社】〒467-0811 名古屋市瑞穂区北原町 1-33-2

TEL:052-853-7511 FAX:052-853-7522 E-mail:nagoyavf@quartz.ocn.ne.jp

【四日市営業所】〒510-0891 四日市市日永西 3-2-8

TEL:0593-45-5550 FAX:0593-45-9258 E-mail:navfyokk@fine.ocn.ne.jp

URL:<http://www.swagelok.co.jp>

# Swagelok®

MEET THE CHALLENGE<sup>SM</sup>

# Nanomaterials

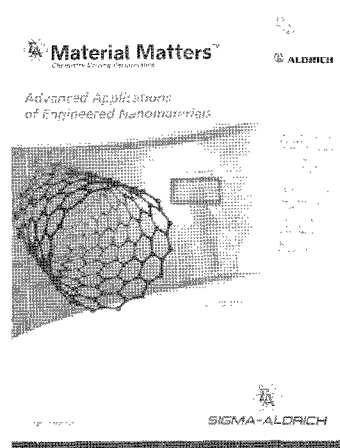
製品番号	製品名	容量	価格(円)	構造式
684430	Phenyl-C <sub>61</sub> -Butyric-Acid-Methyl Ester, [60] PCBM, 99% (scale-up grade)	1g	103,600	
684449	Phenyl-C <sub>61</sub> -Butyric-Acid-Methyl Ester, [60] PCBM, 99.5% (research grade)	100mg 500mg	29,800 118,000	
684457	Phenyl-C <sub>61</sub> -Butyric-Acid-Methyl Ester, [60] PCBM, 99.9% (for exploratory work)	100mg	119,000	
684465	Phenyl-C <sub>71</sub> -Butyric-Acid-Methyl Ester, [70] PCBM, 99%	100mg	57,000	
684473	Phenyl-C <sub>85</sub> -Butyric-Acid-Methyl Ester, [84] PCBM, 99%	100mg	185,800	
685321	Phenyl-C <sub>61</sub> -Butyric-Acid-Butyl Ester, PCBB, [60] PCB-C <sub>4</sub> > 97%	100mg	42,300	
684481	Phenyl-C <sub>61</sub> -Butyric-Acid-Octyl Ester, PCBO, [60] PCB-C <sub>8</sub> , 99%	100mg	77,800	
688215	Thienyl-C <sub>61</sub> -Butyric-Acid-Methyl Ester, [60] ThCBM, 99%	100mg	98,000	
684503	Pentadeuterophenyl-C <sub>61</sub> -Butyric-Acid-Methyl Ester, d5-PCBM, 99%	100mg	103,200	

フラーレン、カーボンナノチューブ等の  
ナノ材料を特集した、

**Material Matters™ Vol.2 No.1 Advanced Applications of Engineered Nanomaterials (英語版)** が発行になりました。

[sigma-aldrich.com/matsci](http://sigma-aldrich.com/matsci) から PDF をダウンロードいただけます。

**日本語版印刷物配布中!**



**Material Matters™**  
Chemistry Driving Performance

日本語版既刊  
好評配布中!

第一線の研究者による、  
テクニカルレビュー、  
アプリケーションノートを紹介した  
ニュースレターです!

日本語版既刊:

- Vol.1 No.1 高分子材料
- Vol.1 No.2 分子自己組織化
- Vol.1 No.3 セラミックおよびハイブリッド材料の堆積/成長
- Vol.2 No.1 ナノ材料の応用最前線 (08年2月発行)
- Vol.2 No.2 水素貯蔵材料 (08年2月発行)
- Vol.2 No.3 有機エレクトロニクス (08年2月発行)

発行予定:

- Vol.2 No.4 Advanced Metals and Alloys

以下続刊

新規登録および既存カタログのご請求は、  
日本サイトから!

材料関連の詳細情報は、[sigma-aldrich.com/matsci](http://sigma-aldrich.com/matsci) (USサイト)  
および [sigma-aldrich.com/japan](http://sigma-aldrich.com/japan) (日本サイト) をご覧ください!

**SIGMA-ALDRICH™**

シグマ アルドリッチ ジャパン株式会社

〒140-0002 東京都品川区東品川2-2-24  
天王洲セントラルタワー4階

■製品に関するお問い合わせは、弊社テクニカルサポートへ  
TEL: 03-5796-7330 FAX: 03-5796-7335  
E-mail: [sialjpts@sial.com](mailto:sialjpts@sial.com)

■在庫照会・ご注文方法に関するお問い合わせは、弊社カスタマーサービスへ  
TEL: 03-5796-7320 FAX: 03-5796-7325

<http://www.sigma-aldrich.com/japan>

# 住友商事のカーボンナノチューブ

Produced by Unidym, Inc. (旧Carbon Nanotechnologies Inc.)

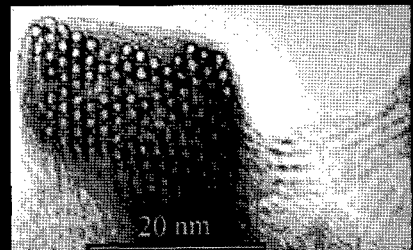
住友商事はUnidym社の日本・アジア地域での総代理店として、学術研究用途から事業化・応用開発用途まで、各種用途に適した製品のご提供に加え、共同開発の推進や事業化支援プロジェクトの実施など、カーボンナノチューブの応用製品開発を総合的に支援しています。

## ● HiPco® 単層カーボンナノチューブ

直径約1nmの単層カーボンナノチューブです。基礎研究や高機能用途向けに、触媒残留率の異なる下記3製品をご提供しております。

製品名	触媒残留率
HiPco® As Produced (未精製品)	< 35 wt%
HiPco® Purified (精製品)	< 15 wt%
HiPco® Super Pure (超高純度品)	< 5 wt%

\* Bucky Plus™(フッ化カーボンナノチューブ)など、修飾品についてもご相談ください。



■ 単層カーボンナノチューブ TEM像 ■

## ● CNI® Xシリーズ

Unidym社独自の製法で製造された、用途別産業応用向けカーボンナノチューブです。量産性に優れ、導電性付与/複合材(EMI, ESD, Anti-Static)、ディスプレイ光源、燃料電池の電極用途などに、安定した製品供給が可能です。詳細につきましては、下記連絡先までお問合せください。



■ 二層カーボンナノチューブ TEM像 ■

## ● 二層カーボンナノチューブ

Unidym社独自の製法で製造された、直径約2nmの二層カーボンナノチューブです。

上記製品群を中心に、研究用から量産対応品、共同開発によるカスタマイズ対応など、用途に応じたカーボンナノチューブの開発を進めています。弊社までお気軽にお問合せ下さい。

本件に関するお問合せ先

住友商事株式会社 電子材事業部 (担当:河本/宮川)

E-mail : nano@sumitomocorp.co.jp

TEL : 03-5166-4546 FAX : 03-5166-6234

住所 : 〒104-8610 東京都中央区晴海1-8-11

URL : www.sumitomocorp.co.jp/section/joho/nanotube.shtml





**1/1,000,000,000メートルの世界。  
そこが、東レのフィールド。**

物質を原子レベルの大きさと正確にコントロールする技術。東レは  
ナノテクを使い、様々な分野で新しい価値を生み出しています。

**未来を変える先端材料を創る。  
それが、東レのナノテク。**

**TORAY**  
Innovation by Chemistry

JASCO Corporation

# 高機能、簡単操作がかつてない 測定環境を実現 多目的な Raman series です。

**NRS-3000**シリーズは、操作性の向上を実現しました。試料のセットからオートアライメントなどの装置の最適化、測定までをスピーディーに行えます。また、低波数測定ユニットへの切替えもボタンひとつで行えます。測定結果の解析には、データベース機能を用い簡単検索、ジャスコキャンバスを用いた簡単レポート作成機能があります。ラマン分析の可能性を大幅に広げました。



Laser Raman Spectrophotometer

レーザラマン分光光度計

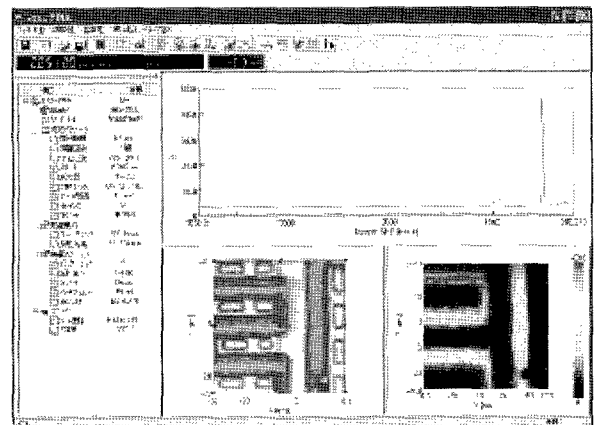
## NRS-3000 series

NRS-3100/3200/3300

### ● 特長

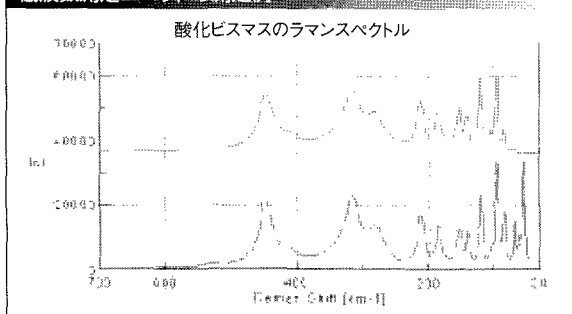
- ▶ ユーザーフレンドリーな操作性を実現
- ▶ ダイレクトドライブ方式のモノクロメータと高性能ノッチフィルタの組み合わせにより、高い波数精度・再現性と高感度化を実現
- ▶ グレーティングを最大3枚搭載でき、多様な測定に対応
- ▶ レーザを最大6台まで搭載可能
- ▶ 日本分光独自のSRI機能 (SRI: Spatial Resolution Image) によりPCモニタ上で試料像とアパーチャ像およびレーザービームを同時観測
- ▶ コンフォーカル光学系により深さ方向の測定が可能
- ▶ イメージング測定に対応可能
- ▶ オートアライメント機能によりシステムの安定性を追及
- ▶ レーザ放射安全基準Class1の安全性を確保
- ▶ スペクトル検索プログラムおよびデータベースを標準搭載

### ● シリコンパターンのマッピング測定例



マッピング測定で機能と操作性が向上しました。画像情報をもとに測定者が画面上でマウスを使って、測定エリアを指定できます。また、測定中のデータを色分け図で表示することで測定結果をリアルタイムで確認することができます。

### 低波数測定ユニットの測定例



低波数測定ユニットは、無機物などの格子振動低波数域を精度よく測定する場合に有効になります。

JASCO は日本分光株式会社の登録商標です。

光と技術で未来を見つめる

# 日本分光

JASCO 日本分光株式会社

〒192-8537 東京都八王子市石川町2967-5  
PHONE 042 (646) 4111 (代表)  
FAX 042 (646) 4120 <http://www.jasco.co.jp/>

北海道S-C 011(741)5285  
北日本S-C 022(748)1040  
筑波S-C 029(857)5721  
東京S-C 03(3294)0341  
西東京S-C 042(646)7001

神奈川S-C 045(989)1711  
名古屋S-C 052(452)2671  
大阪S-C 06(6312)9173  
広島S-C 082(238)4011  
九州S-C 092(588)1931

JSA  
EMS  
ISO14001 ISO9001  
JSAE 024 JQA-0777

## フラーレンの化学と物理

篠原久典／齋藤弥八著 わが国でこの分野をリードする著者による、最も基礎となる概説書。発見までの背景や、物理・化学の基礎、バラエティ豊かな性質を、フラーレンを中心にカーボンナノチューブまで解説する。 5775円

## 物理仮想実験室

—3Dシミュレーションで見る、試す、発見する—  
土井正男／滝本淳一編 付属のCDを使って、振り子の運動や光の屈折などの問題を、条件を変えながらコンピュータの中で「実験」できる、新しい形の教科書。 4410円

## やさしい有機光化学

伊澤康司著 物質が光を吸収すると何が起きるのか。近年大きく発展を遂げた光化学の基礎から、ベンゼン類などの有機化合物が光特有の反応を起こす仕組みまで丁寧に解説、有機光化学の入門として最適の書。 2940円

## 放射線安全取扱の基礎[第三版]

—アイソトープからX線・放射光まで—  
西澤邦秀／飯田孝夫編 人体への影響や放射線計測手法、諸法令など、放射線を扱う上で必要な知識を、図・写真を多用し幅広く解説。最新の障害防止法に全面対応。 2520円

## 疑似科学と科学の哲学

伊勢田哲治著 占星術、超能力研究、中国医学、創造科学……これらはなぜ「疑似科学」と言われるのだろうか。科学のようで科学でない疑似科学を通して、科学とは何かを解き明かしていくユニークな科学哲学入門。 2940円

## 誰が科学技術について考えるのか

—コンセンサス会議という実験—  
小林傳司著 社会の中の科学技術のあり方をめぐって専門家と市民が対話を行う「コンセンサス会議」。その実際を紹介し、科学をめぐる公共空間について考える。 3780円

## 誇り高い技術者になろう

—工学倫理ノスメー—  
黒田光太郎／戸田山和久／伊勢田哲治編 プロとして責任ある仕事をするために、何に配慮し、日々の仕事でどう行動すべきか。指針を示し、判断のスキルを高める。 2940円

## サナギから蛾へ

—カイコの脳ホルモンを究める—  
石崎宏矩著 延べ三千万個の蛾頭をすり潰し、昆虫の変態を司るホルモンの本体をついに解明——研究者本人にしか書けない、波瀾万丈の科学ドキュメント。 3360円

〒464-0814 名古屋市千種区不老町名大構内

名古屋大学出版会

☎(052)781-5353/FAX(052)781-0697  
http://www.unp.or.jp 宅配可

### Nano & Bio

## — フロンティア出版のナノテクノロジー・ナノマテリアルシリーズ —

### 自己組織化ナノマテリアル

—フロントランナー85人が語るナノテクノロジーの新潮流—  
企画：理化学研究所 フロンティア研究システム  
時空間機能材料研究グループ  
監修：国武豊喜(北九州市立大学/理化学研究所)  
編集幹事：下村政嗣(北海道大学/理化学研究所)  
山口智彦(産業技術総合研究所)  
■体裁/B5判・392頁 ■価格/57,750円(税込)

### 有機・無機・金属ナノチューブ

—非カーボンナノチューブ系の最新技術と応用展開—  
編集：清水敏美(産業技術総合研究所)  
木島 剛(宮崎大学)  
■体裁/B5判・330頁 ■価格/57,750円(税込)

### ナノ粒子の創製と応用展開

編集：米澤 徹(東京大学)  
■体裁/B5判・322頁 ■価格/57,750円(税込)

### ナノコンポジットマテリアル

—金属・セラミック・ポリマー3大物質のナノコンポジット—  
編集：井上明久(東北大学)  
■体裁/B5判・363頁 ■価格/52,500円(税込)

### ナノオプティクス・ナノフォトニクスすべて

—ナノ光技術の基礎から実用まで—  
監修：河田 聡(大阪大学/理化学研究所)  
編集：梅田倫弘(東京農工大学)  
川田善正(静岡大学)  
羽根一博(東北大学)  
■体裁/B5判・352頁 ■価格/57,750円(税込)

### MEMS/NEMSの最先端技術と応用展開

編集：前田龍太郎(産業技術総合研究所)  
澤田廉士(九州大学)  
青柳桂一(マイクロマシンセンター)  
■体裁/B5判・285頁 ■価格/52,500円(税込)

### ナノインプリントの基礎と技術開発・応用展開

—ナノインプリントの基盤技術と最新の技術展開—  
編集：平井義彦(大阪府立大学)  
■体裁/B5判・281頁 ■価格/52,500円(税込)

### ナノバイオエンジニアリングマテリアル

—バイオインターフェイス・ナノバイオプロセッシング  
・バイオコンジュゲーション・バイオマトリックス—  
監修：石原一彦(東京大学)  
■体裁/B5判・350頁 ■価格/52,500円(税込)



フロンティア出版

〒110-0012 東京都台東区竜泉1-21-18 TEL:03-6802-1640 FAX:03-6802-1641 E-mail: info@frontier-books.com

http://www.frontier-books.com

# 株式会社 マシナックス

代表取締役 佐野隆治

〒454-0856 名古屋市中川区小碓通 2-6

TEL 052-654-5021(代) FAX 052-654-5125

HP <http://www.mashinax.jp/>

メール [mashinax@sf.starcat.ne.jp](mailto:mashinax@sf.starcat.ne.jp)

## 菱田商店会社案内

### オフィス家具

メーカー(既製品) オカムラ・コクヨ・プラス等  
木製家具 好みにあわせて作ります

### 室内装飾

ブラインド 立川・日米  
カーテン・カーペット スミノエ・サンゲツ・タジマ等  
床仕上げ フリーアクセス・Pタイル・ロンリウム等  
クロス ルノン・サンゲツ等  
間仕切り 各種パパーティション

### 学校関連



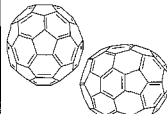
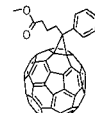
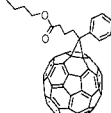
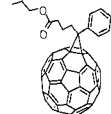

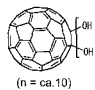
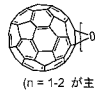
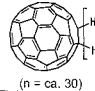
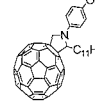
黒板・ホワイトボード・掲示板  
実験台・薬品棚・吊棚  
既製品から特注品まで、もちろん取り付けます。

(有)菱田 商店

名古屋市緑区浦里4-207

Tel 891-8125

Fax 891-3957

銘柄	分子構造	純度(HPLC面積%、代表値)	取扱数量
<b>nanom purple</b> フラーレンC60		99	10g以上
		99.5	5g以上
		99.5/昇華精製品	2g以上
		99.9/昇華精製品	1g以上
<b>nanom orange</b> フラーレンC70		97	1g以上
		98/昇華精製品	0.5g以上
<b>nanom mix</b> フラーレン混合物		C60:約60、C70:約25 (その他:高次フラーレン)	50g以上
<b>nanom spectra E100</b> PCBM (phenyl C61-butyl acid methyl ester)		99	1g以上
<b>nanom spectra E200</b> PCBNB (phenyl C61-butyl acid n-butyl ester)		99	1g以上
<b>nanom spectra E210</b> PCBIB (phenyl C61-butyl acid i-butyl ester)		99	1g以上
<b>nanom spectra E110</b> C70PCBM (phenyl C71-butyl acid methyl ester)	 主成分	99 (異性体トータル) 位置異性体の混合物	0.5g以上
銘柄	分子構造	内容	取扱数量
<b>nanom spectra D100</b> 水酸化フラーレン	 (n = ca. 10)	C <sub>60</sub> OH <sub>n</sub> n=10を主成分とする 混合物	2g以上
<b>nanom spectra B100</b> 酸化フラーレン	 (n = 1-2 が主成分)	C <sub>60</sub> O <sub>n</sub> n=1および2を主成分 とする混合物	2g以上
<b>nanom spectra A100</b> 水素化フラーレン	 (n = ca. 30)	C <sub>60</sub> H <sub>n</sub> n=30を主成分とする 混合物	2g以上
<b>nanom spectra G100</b>		純度 (HPLC面積%, 代表値) 99	1g以上

銘柄、取扱数量等は予告無く変更する場合がございます。予めご了承下さい。

試験研究用として2008年4月以降、関東化学(株)からも上記フラーレンおよびフラーレン誘導体をご購入いただけます。取扱銘柄等の詳細は下記にお問い合わせ下さい。

関東化学株式会社 試薬事業本部

〒103-0023 東京都中央区日本橋本町3-11-5 TEL:03-3663-7631 FAX:03-3667-8277

http://www.kanto.co.jp E-mail:reag-info@gms.kanto.co.jp

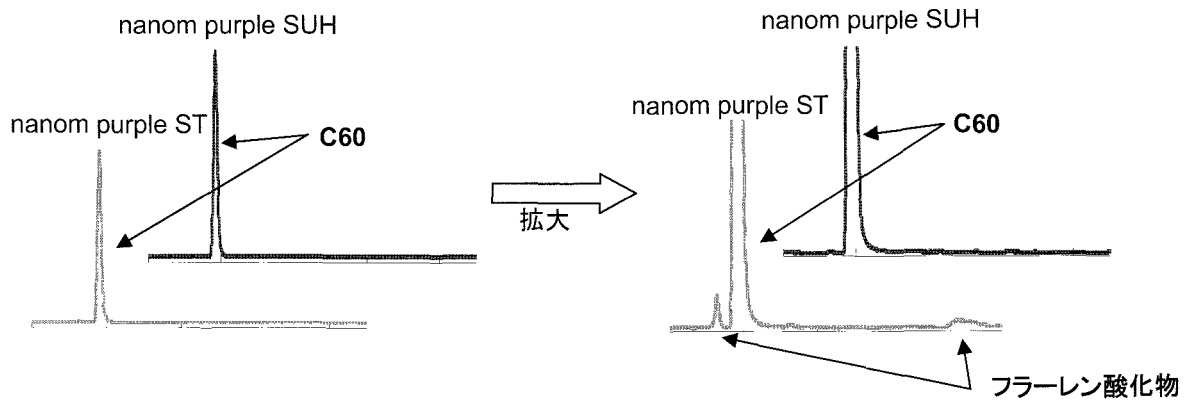
尚、従来同様、第一実業(株)、他からもご購入いただけます。



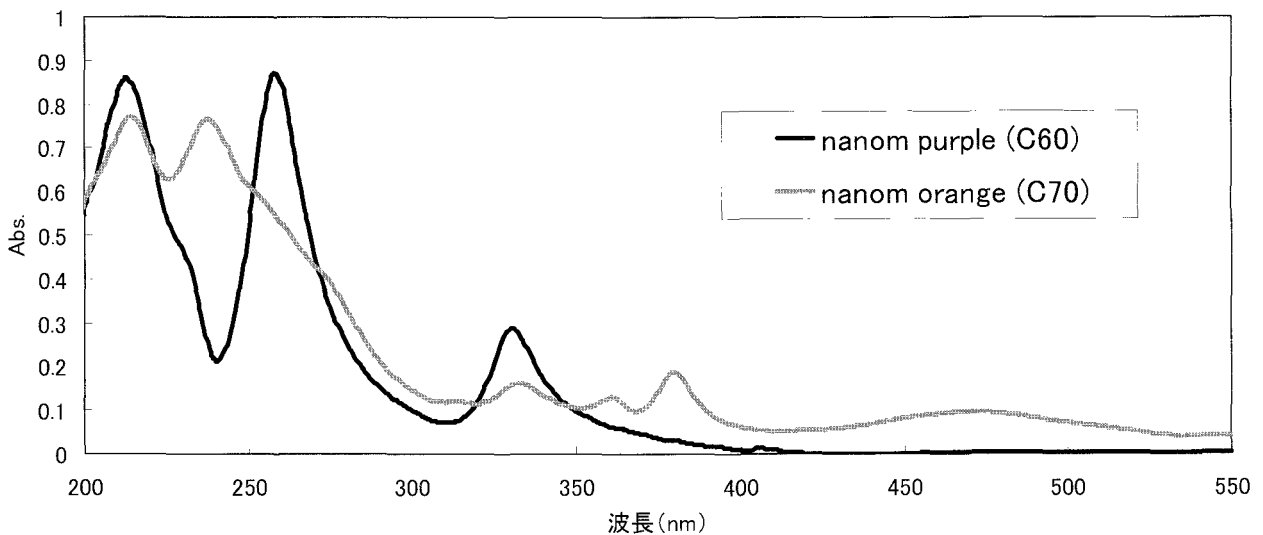
●nanom purple(C60)およびnanom orange(C70)各グレードの分析値

銘柄	nanom purple (C60)				nanom orange(C70)	
	ST	TL	SU	SUH	ST	SU
C60(HPLC面積%)	99.4	99.8	99.9	>99.9	0.3	0.1
C70(HPLC面積%)	<0.1	ND	0.1	ND	99.4	99.9
フラーレン酸化物(HPLC面積%)	0.6	0.2	ND	ND	0.3	ND
残溶媒(GCwt%)	0.8	ND	ND	ND	0.4	ND

●nanom purple STおよびnanom purple SUHのHPLC



●nanom purple ST(C60)およびnanom orange ST(C70)のUV / VIS スペクトル



<お問い合わせ先>

フロンティアカーボン株式会社 営業販売センター

<http://www.f-carbon.com> E-mail:[fcc-ho-contact@f-carbon.com](mailto:fcc-ho-contact@f-carbon.com)



Frontier Carbon Corporation

# 進化する売れ筋ナノテク材料

## 弊社取り扱いナノテク材料群

### フラーレン材料群

【60】【70】【84】PCBMフラーレン

高次フラーレン(C76,C78,C84)

水溶性フラーレン

C60(OH)<sub>6</sub>, C60(OH)<sub>22-26</sub>, C60(OH)<sub>24</sub>,

C60(OH)<sub>18-22</sub>(O<sup>-</sup>K<sup>+</sup>)<sub>4</sub>フラーノール

アミノ酪酸フラーレン誘導体

アミノカプロン酸フラーレン

ビスマロン酸エチルフラーレン

C13安定同位体置換フラーレン

Gd@C82金属内包フラーレン

La@C82金属内包フラーレン

Anti-HIVフラーレン

C60F<sub>36</sub>, C60F<sub>48</sub>, C60Br<sub>24</sub>フラーレン

### カーボンナノチューブ

高純度多層カーボンナノチューブ

高純度単層カーボンナノチューブ

水溶性ナノチューブ

SWNT-COOH, SWNT-NH<sub>2</sub>, SWNT-PEG, SWNT-SH

MWNT-COOH, MWNT-NH<sub>2</sub>, MWNT-PEG, MWNT-SH

大口径カーボンナノチューブ

2層構造カーボンナノチューブ

カーボンナノチューブ・フィルム【Cu, Si, Ni, Graphite】

カーボンナノチューブ・カソード【Cu, Si】

### 金ナノ微粒子

金ナノ微粒子, 0.01%金, 2~50nm

Dextranコート, 0.01%金, 10~50nm

PEGコート, 0.01%金, 10~50nm

Biotinラベル, 0.01%金, 5~50nm

Streptavidinラベル, 0.01%金, 5~50nm

その他銀ナノ微粒子

### 希少価値金属(レアメタル)

ニッケル, コバルト, フェロクロム, フェロマンガ, フェロバナジウム, 亜鉛, チタン, スズ, アンチモン, タングステン

### 電気鋳造精密メッシュ

金, 銅, ニッケル, 透過率(36~98%), 標準サイズ279x279mm

### ナノ微粒子群

1. 元素材料

Au, Ag, Al, Cu, Fe, In, Mo, Ni, Si, Ti, W, Zn

2. 非酸化物ナノ化合物

BN, GaP, InP, SiC, TaN, TiC, TiN, WC, WC/Co

3. 酸化物

Al<sub>2</sub>O<sub>3</sub>, Al<sub>2</sub>(OH)<sub>3</sub>, B<sub>2</sub>O<sub>3</sub>, BaCO<sub>3</sub>, BaFe<sub>12</sub>O<sub>19</sub>, BaSO<sub>4</sub>, BaTiO<sub>3</sub>, Bi<sub>2</sub>O<sub>3</sub>, CeO<sub>2</sub>, CoFe<sub>2</sub>O<sub>4</sub>, Co<sub>0.5</sub>Zn<sub>0.5</sub>Fe<sub>2</sub>O<sub>4</sub>

CoO, Co<sub>3</sub>O<sub>4</sub>, CrO<sub>3</sub>, Cr<sub>2</sub>O<sub>3</sub>, CuO, Dy<sub>2</sub>O<sub>3</sub>, Er<sub>2</sub>O<sub>3</sub>, Eu<sub>2</sub>O<sub>3</sub>, Fe<sub>2</sub>O<sub>3</sub>, Fe<sub>3</sub>O<sub>4</sub>, Gd<sub>2</sub>O<sub>3</sub>, HfO<sub>2</sub>, In<sub>2</sub>O<sub>3</sub>, In(OH)<sub>3</sub>

In<sub>2</sub>O<sub>3</sub>:SnO<sub>2</sub>, Li<sub>4</sub>Ti<sub>5</sub>O<sub>12</sub>, MgAl<sub>2</sub>O<sub>4</sub>, MgO, Mg(OH)<sub>2</sub>, Mn<sub>2</sub>O<sub>3</sub>, MoO<sub>3</sub>, Nd<sub>2</sub>O<sub>3</sub>, NiFe<sub>2</sub>O<sub>4</sub>, Ni<sub>0.5</sub>Zn<sub>0.5</sub>Fe<sub>2</sub>O<sub>4</sub>

NiO, Ni<sub>2</sub>O<sub>3</sub>, Pr<sub>6</sub>O<sub>11</sub>, Sb<sub>2</sub>O<sub>3</sub>, SiO<sub>2</sub>Sm<sub>2</sub>O<sub>3</sub>, SnO<sub>2</sub>, SrAl<sub>12</sub>O<sub>19</sub>, SrCO<sub>3</sub>, SrFe<sub>12</sub>O<sub>19</sub>, SrTiO<sub>3</sub>, Tb<sub>4</sub>O<sub>7</sub>, TiO<sub>2</sub>

VO, V<sub>2</sub>O<sub>3</sub>, V<sub>2</sub>O<sub>5</sub>, WO<sub>3</sub>, Y<sub>2</sub>.98Ce<sub>0.02</sub>AlO<sub>12</sub>, Y<sub>3</sub>Al<sub>5</sub>O<sub>12</sub>, Y<sub>2</sub>O<sub>3</sub>, ZnFe<sub>2</sub>O<sub>4</sub>, ZnO, ZrO<sub>2</sub>, ZrO<sub>2</sub>+

詳しいお問合せはこちら <http://atr-atr.co.jp>

次世代ナノテク技術で新時代を築く



株式会社 ATR

Advanced Technology Research

〒270-0021 千葉県松戸市小金原 7-10-25

TEL : 047-394-2112 FAX : 047-394-2100

E-mail : sales@atr-atr.co.jp

# 2007年10月より販売開始

## 高純度 PCBМ フラーレン

弊社では2007年10月より【60】PCBM 純度99.9%及び  
d5-【60】PCBMの製品を追加登録致しました。

高純度 PCBМ フラーレン  
【60】PCBM 純度99.9%  
販売最小単位 100mg～

新型 PCBМ フラーレン  
d5-【60】PCBM 純度99.5%  
販売最小単位 100mg～

### その他取扱い PCBM フラーレン

【60】PCBM フラーレン純度99%  
【60】PCBM フラーレン純度99.5%  
【70】PCBM フラーレン純度99%  
【84】PCBM フラーレン純度99%

尚、納期につきましては若干のお時間を頂く場合がございます。

詳しいお問合せはこちら <http://www.atr-atr.co.jp>

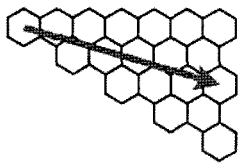
次世代ナノテク技術で新時代を築く



株式会社 ATR

Advanced Technology Research

〒270-0021 千葉県松戸市小金原 7-10-25  
TEL : 047-394-2112 FAX : 047-394-2100  
E-mail : sales@atr-atr.co.jp



Applied  
NanoFluorescence

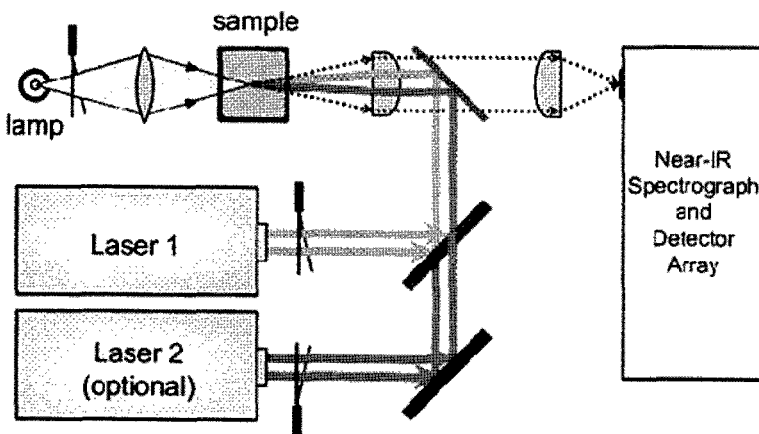
# NS1 NanoSpectralyzer

ライス大学ワイズマン教授グループが開発した新技術

## 近赤外蛍光吸収分光法による単層カーボンナノチューブを分析する最新のラボツール

### 製品概要

ナノスペクトライザ™ (特許申請中) は顧客の皆様のご要望に応じて設計が可能なユニークで使い易い分光計で、水性懸濁剤により単層カーボン・ナノチューブ (SWNT) の組成を詳細に分析します。光学系はコンパクトで、専用ソフトウェアにより装置の調節、データ分析、研究結果の報告が可能です。ナノチューブ分光計に関する最先端の研究結果を土台にし、サンプルを数秒間で自動的に分析します。



各半導性 SWNT 種には近赤外線蛍光周波数として知られる特徴があり、励起波長を選択し、多チャンネル検出器列によりサンプルの発光スペクトルを高精度で迅速に取り込みます。そして、測定済みのスペクトルを自動的に分析し、基礎をなす特殊成分を明らかにし、半導性 SWNT 種の (n, m) 組成をサンプル中に提供します。さらに、相対的に明らかにされた SWNT 種の濃度を推定し、グラフェンシート図や直径ヒストグラムといったデータを表やグラフに表示します。また、ナノスペクトライザは迅速近赤外線吸収分光計であり、吸収特性と発光特性との比較により分散状態を質的、量的に評価し、ナノチューブの完成度を判定します。

ナノスペクトライザは、以下の方々には是非、使用して頂きたい製品です。

#### ■ ナノチューブ製造技術者

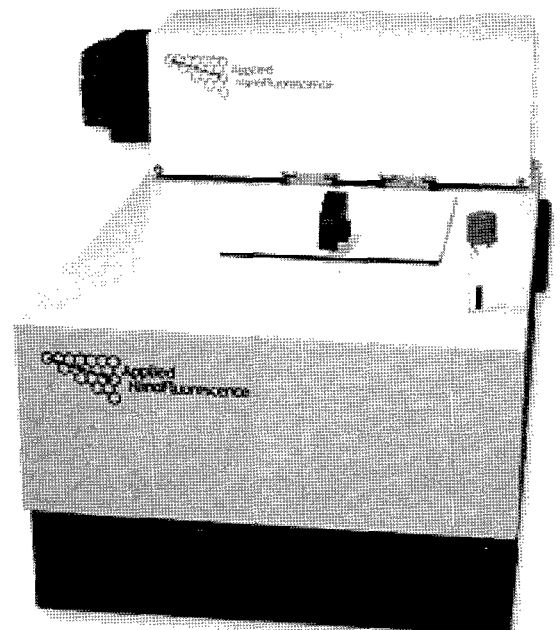
- ・ 製造工程の一貫性を監視。
- ・ 加工条件を調整し、製品の組成を制御。

#### ■ ナノチューブのユーザ

- ・ 受け入れた SWNT 材料の特性と品質を評価。
- ・ SWNT の分散を質的に評価。

#### ■ ナノチューブ研究者

- ・ SWNT サンプルの組成を判定。
- ・ SWNT の構造的な分類方法の考案。
- ・ 構造中心にプロセスを研究。



次世代技術知識集団

**SCIENCE LABORATORIES**  
株式会社サイエンスラボラトリーズ

〒270-0021 千葉県松戸市小金原 7-10-25  
TEL: 047-309-8311 FAX: 047-309-8310  
MAIL: sales@scilab.co.jp WEB: scilab.co.jp